

NORTHWESTERN UNIVERSITY

The Total Synthesis of (-)-Isosilybin A and the Development of Novel Strategies Towards
Inverse Polarity Operators

A DISSERTATION

SUBMITTED TO THE GRADUATE SCHOOL
IN PARTIAL FULFILLMENT OF THE REQUIREMENTS

for the degree

DOCTOR OF PHILOSOPHY

Field of Chemistry

By

Benjamin Rebbeck McDonald

EVANSTON, ILLINOIS

September 2018

© Copyright by Benjamin Rebbeck McDonald 2018

All Rights Reserved

Abstract

The Total Synthesis of (–)-Isosilybin A and the Development of Novel Strategies Towards Inverse Polarity Operators

Ben McDonald

Synthetic organic chemistry continues to be a driver in the discovery and development of new molecules for applications in biology, medicine, crop science, polymer science, and materials science. Central to the continued development of this field is the pursuit of new strategies and methods for the efficient construction of molecules with precise chemical and structural control. Towards this end, a major focus is the development of catalytic systems to enhance efficiency and specificity. This thesis describes the total synthesis of the complex flavanolignan natural product isosilybin A and the development of new inverse polarity operators. The first Chapter overviews approaches to the synthesis of pyran natural products and details the first stereoselective synthesis of a member of the silybin natural product family, (–)-isosilybin A using a nature-inspired catalytic cyclization. The second Chapter details our efforts towards new open-shell inverse polarity operators. Described is the use of photoredox catalysis to reductively turn electron acceptors, enones and carbonyls, into stabilized radical anions for carbon-carbon bond-forming reactions. Finally, Chapter Three describes our investigation of the 1,2-Brook rearrangement as an approach towards carbonyl nucleophile equivalents by harnessing the unique reactivity of organosilicon compounds.

Thesis Advisor: Professor Karl A. Scheidt

Acknowledgements

I'd first like to thank my loving family and partner Laura Alagna. Without your unwavering love, belief, and support this document could not exist. Second, I'd like to thank my advisor Prof. Karl Scheidt for standing as an example of what drive and sacrifice can achieve. I am fortunate to have received my education in one of the most beautiful and well-equipped labs in the world and have learned more chemistry and life-lessons than I could have imagined. I am further indebted to Prof. Reagan Thomson for lending an ear and taking time to talk with me when I needed it most. Your support has been indispensable. To my labmates from years past, laboratories are hidden focal points that reveal the idiosyncrasies and brilliance of humanity. I've relished my time spent sharing and learning with each and every one of you and am glad to have made some lifelong friends.

To the younger students: If I were to leave you with a few bits of wisdom I've panned over the years, it's that no matter the current state of affairs, you have to believe (to a borderline quixotic degree) that by doing your best, you *will* achieve your goals; your best work is work that you are proud of, so dedicate some time to self-reflection and be true to yourself.

List of Abbreviations

4 Å MS	4 angstrom molecular sieves
AcOH	Acetic acid
Ar	aryl
Ac	acetyl
BCE	before common era, equivalent to BC (before Christ)
Bp	boiling point
BINAP	2,2'-bis(diphenylphosphino)-1,1'-binaphthyl
BINOL	1,1'-bi(2-naphthol)
Boc	<i>tert</i> -butyloxycarbonyl
Bu	butyl
<i>n</i> -BuLi	<i>n</i> -butyl lithium
Bz	benzoyl
δ	chemical shift (parts per million)
CHI	chalcone isomerase
CD	circular dichroism
CE	common era, equivalent to AD (Anno Domini, in the year of our Lord)
COSY	correlation spectroscopy
CRPC	castration-refractory prostate cancer
dba	dibenzylidene acetone
DBN	1,5-diazabicyclo[4.3.0]non-5-ene
DBU	1,8-diazabicyclo[5.4.0]undec-7-ene

DCAD	Di- <i>p</i> -chlorobenzylazodicarboxylate
DCE	1,2-dichloroethane
DCM	dichloromethane
DEAD	diethylazodicarboxylate
DFT	density functional theory
DIAD	diisopropylazodicarboxylate
DIBAL-H	diisobutyl aluminum hydride
DIPEA	diisopropylethylamine
DKR	dynamic kinetic resolution
DMAP	4-(Dimethylamino)pyridine
DMDO	dimethyldioxirane
DMP	Dess-Martin periodane
DMSO	dimethylsulfoxide
dr	diastereomeric ratio
DTBM	di- <i>tert</i> -butyl-4-methoxy-phenyl
ECD	electronic circular dichroism
ee	enantiomeric excess
er	enantiomeric ratio
eq	equation
equiv	equivalents
er	enantiomeric ratio
EI	electron impact

ESI	electrospray ionization mass spectrometry
EtOAc	ethyl acetate
GC	gas chromatography
HBD	hydrogen bond donor
HMPA	hexamethylphosphoramide
HOMO	highest occupied molecular orbital
HPLC	high-performance liquid chromatography
HRMS	high-resolution mass spectrometry
HWE	Horner-Wadsworth-Emmons
IMES	2,4,6-trimethylphenylimidazole
IPA	isopropanol
IR	infrared
<i>J</i>	coupling constant
KHMDS	potassium hexamethyldisilazane
KOtBu	potassium <i>tert</i> -butoxide
LA	Lewis acid
LiHMDS	lithium hexamethyldisilazane
LDA	lithium diisopropylamide
LRMS	low-resolution mass spectroscopy
LUMO	lowest unoccupied molecular orbital
MALDI-TOF	matrix-assisted laser desorption ionization time-of-flight
Me	methyl

MeOH	methanol
Mes	2,4,6-trimethylphenyl
MOM	methoxyethyl ether
mg	milligram
Mp	melting point
Ms	mesylate, methanesulfonate
NHC	<i>N</i> -heterocyclic carbene
NMR	nuclear magnetic resonance
NOE	nuclear Overhauser effect
NR	no reaction
ORTEP	Oak Ridge thermal ellipsoid plot
PCa	prostate cancer
PhCH ₃	toluene
PCC	pyridinium chlorochromate
Ph	phenyl
PPTS	pyridinium <i>p</i> -toluenesulfonate
R _f	response factor
Rt	room temperature
<i>s</i> factor	selectivity factor
SEGPPOS	4,4'-Bi-1,3-benzodioxole-5,5'-diylbis(diphenylphosphane)
SDS	solvent delivery system
TADDOL	$\alpha,\alpha,\alpha',\alpha'$ -tetraaryl-2,2-disubstituted 1,3-dioxolane-4,5-dimethanol

TIPS	triisopropylsilyl
TBS	<i>tert</i> -butyldimethylsilyl
TBDPS	<i>tert</i> -butyldiphenylsilyl
TEA	triethylamine
TES	triethylsilyl
TEP	Tolman electronic parameter
THF	tetrahydrofuran
TLC	thin layer chromatography
TMS	trimethylsilyl
Ts	<i>p</i> -toluene sulfonyl
<i>p</i> -TsOH	<i>para</i> -toluenesulfonic acid
UV	ultraviolet

Dedication

To my Aunt Corny, the world is not the same without you.

Table of Contents

Abstract.....	3
Acknowledgements.....	4
List of Abbreviations.....	5
List of Figures.....	13
List of Schemes.....	15
List of Tables.....	17
Chapter 1: Total Synthesis of (+)-Isosilybin A.....	18
1.1 Introduction to Natural Products.....	19
1.1.1 Natural Products as a Privileged Source of Molecular Therapeutics.....	20
1.1.2 Pyran Natural Products.....	22
1.2 Approaches Towards the Synthesis of Pyran Natural Products.....	22
1.2.1 Utilization of the Prins Reaction Towards the Stereoselective Synthesis of Substituted Pyrans.....	24
1.2.2 Conjugate Addition Approaches to Benzopyranones.....	27
1.3 The Silybin Natural Product Family.....	30
1.3.1 Introduction.....	30
1.3.2 Bioactivity of Silybin Natural Products.....	34
1.3.3 Previous Syntheses of Silybin Natural Products.....	36
1.4 Retrosynthetic Analysis towards Isosilybin B.....	38
1.5 Previous Efforts Towards Isosilybin B Total Synthesis.....	39
1.5.1 Synthesis of Benzodioxane Aldehyde.....	39
1.5.2 Biomimetic Cyclization to Yield Flavanone Core.....	43
1.5.3 Attempted α -Oxygenation of Flavanone.....	46
1.6 Revision of Route to Isosilybin B.....	47
1.7 Development of Global Protection Conditions.....	47
1.8 Synthesis Endgame.....	49
1.8.1 Rubottom Oxidation Sequence of MOM protected Flavanone.....	49
1.8.2 Investigation of Soft Enolization Conditions.....	52
1.8.3 Completion of the Synthesis.....	53
1.9 Confirmation of Absolute Stereochemistry.....	54
1.10 Future Directions.....	57
1.11 Conclusion.....	61
1.12 Experimental Section.....	61
1.12.1 Experimental Procedures and Characterization Data.....	63
1.12.2 Comparison of ^1H NMR Spectral Data of Isosilybin A.....	89
1.12.3 Comparison of ^{13}C NMR Spectral Data of Isosilybin A.....	91
1.12.4 Silybin Electronic Circular Dichroism Data.....	93
1.12.5 CD Spectra of Synthetic (-)-Isosilybin A (1).....	95
1.12.6 High Resolution Mass Spectrometry Data of Synthetic (-)-Isosilybin A.....	98
1.12.7 Selected NMR Spectra.....	99

1.12.8 HPLC Traces of Selected Compounds.....	120
1.12.9 Preparative Separation of Protected Flavanolignan SI-VIII Diastereomers.....	123
1.12.10 Preparative Separation of α -hydroxyflavanolignan SI-X Diastereomers.....	124
Chapter 2: Single-Electron Approaches to New Inverse Polarity Operators.....	126
2.1 Introduction.....	127
2.1.1 Polarity Based-Bond Disconnections.....	127
2.1.2 Open-Shell Reactive Intermediates.....	135
2.1.3 Principles Governing the Reactivity of Radicals.....	136
2.1.4 Photocatalysis for the Generation of Open-Shell Intermediates.....	139
2.1.5 β -Radical Enolates in Chemistry.....	146
2.2 The Design of a New β -Radical Enolate.....	148
2.2.1 Hypothesis Towards Stabilized β -Radical Enolate.....	150
2.2.2 Redox Properties of Arylidene Malonates.....	151
2.3 Transfer Hydrogenation of Arylidene Malonates.....	152
2.3.1 Initial Screening to Define Reaction Parameters.....	153
2.3.2 Design of a One-Pot Homologation Reaction.....	155
2.4 Intramolecular Cyclization Reactions of Arylidene Maloantes.....	158
2.4.1 Approaches towards δ -Lactones.....	158
2.4.2 Preparation of New Chroman Derivatives.....	160
2.5 Intermolecular Radical Cross-coupling Malonate Derived Radical Enolates.....	163
2.5.1 Reaction Design.....	164
2.5.2 Reaction Optimization.....	166
2.5.3 Scope of Malonate Coupling Partners.....	170
2.5.4 Scope of Benzylic Radicals.....	173
2.5.5 Proposed Mechanism For Radical Cross-Coupling Reaction.....	174
2.6 Discovery of the Reductive Dimerization of Arylidene Malonates.....	176
2.6.1 Reaction Optimization.....	177
2.6.2 Scope of Malonates.....	179
2.7 Conclusion to Reductive Couplings of Arylidene Malonates.....	180
2.8 Future Work.....	181
2.8.1 Future Work on Reductive Arylidene Malonate Chemistry.....	181
2.9 Summary.....	183
2.10 Experimental Section.....	185
2.10.1 Preparation of Substituted Malonates.....	186
2.10.2 Preparation of Benzylidene Malonates and Ketoester Substrates.....	187
2.10.3 General Procedure for Transfer Hydrogenation.....	191
2.10.4 General Procedure for Reductive Cyclization.....	192
2.10.5 Preparation of Nitrile Hantzsch Ester Derivatives.....	193
2.10.6 General Procedure for Radical-Radical Coupling Reaction.....	194
2.10.7 General Procedure for Radical Dimerization.....	211
2.10.8 Procedure for Determination of Quantum Yield of Cross-Coupling Reaction..	218
2.10.9 Procedure for Coupling of Arylidene Malonate and Enamine.....	220
2.10.10 Electrochemical Measurements.....	222

2.10.11 Selected NMR Spectra.....	224
2.10.12 SFC Traces of Racemic and Enantioenriched Radical Coupling Products (Table 2-6).....	271
2.10.13 ORTEPS of Crystallographic Structures.....	277
Chapter 3: The Application of the 1,2-Brook Rearrangement Towards Inverse Polarity Carbonyl Operators	281
3.1 The Brook Rearrangement.....	282
3.2 Applications of the Brook Rearrangement in Carbon-Carbon Bond Forming Reactions	285
3.3 New Brønsted Base Mediated 1,2-Brook Rearrangement Coupling Reactions	288
3.4 Lewis Base Mediated 1,2-Brook Coupling Reactions	290
3.4.1 Addition to Imines.....	291
3.4.2 Addition to Arylidene Malonates	293
3.4.3 Studies Towards Acyl Transfer Initiated 1,2-Brook.....	296
3.5 Photo-triggered 1,2-Brook Rearrangement of Acyl Silanes	302
3.5.1 Lewis Acid Mediated Cyclopropanation of Arylidene Malonates	304
3.5.2 Cyclopropanation of Maleimides	307
3.6 Future Work	309
3.7 Conclusion.....	311
3.8 Experimental Section.....	312
3.8.1 General Information	312
3.8.2 Preparation of α -Silyl, Silyl Alcohols	313
3.8.3 General Procedure for the Fluoride Triggered Addition to Imines.....	315
3.8.4 General Procedure for the Fluoride Triggered Addition to Arylidene Malonate.....	316
3.8.5 General Procedure Preparation of α -Silyl Carbonates	318
3.8.6 General Procedure Preparation of α -Silyl Esters.....	320
3.8.7 General Procedure for the Acyl Transfer Mediated Addition to Aldehydes.....	321
3.8.8 General Procedure for the Photoaddition of Acyl Silanes to Arylidene Malonates	322
3.8.9 General Procedure for the Photoaddition of Acyl Silanes to Maleimides.....	323
3.8.10 General Procedure for the Photoaddition of Acyl Silanes to Maleimides.....	324
3.8.11 General Procedure for Preparation of Morpholinyl Carbamoyl Silane.....	324
3.8.12 Selected NMR Spectra	326
References:	343

List of Figures

Figure 1-1 Original Approach to Okilactomycin.....	23
Figure 1-2 Design of a New Prins-like Reaction	26
Figure 1-3 General Scope of Lewis Acid Mediated Dioxinone Prins-type Reaction.....	27
Figure 1-4 Biomimetic Conjugate Addition Approaches to Benzopyranones.....	28

Figure 1-5. Constituents of Silymarin.....	32
Figure 1-6. Proposed Biosynthesis of Silybin Natural Products.....	33
Figure 1-7. Proposed Mechanism of the Biomimetic Preparation of Silybins.....	37
Figure 1-8. Divergent Cyclization Pattern.....	42
Figure 1-9. Attempted Knoevenagel Condensation.....	43
Figure 1-10. Aldol Condensation and Deprotection To Yield Chalcone Cyclization Substrate.....	43
Figure 1-11. Hintermann's Asymmetric Chalcone Cyclization.....	44
Figure 1-12. Cyclization Sequence to Yield Protected Flavanone.....	46
Figure 1-13. Attempted α -Oxidation of Boc-Protected Flavanone Silyl Enol Ether.....	47
Figure 1-14. Cyclization Sequence to Yield MOM-Protected Flavanone.....	49
Figure 1-15. Rubottom Oxidation of MOM-Protected Flavanone.....	50
Figure 1-16. Rubottom Oxidation of Unsubstituted Flavanone.....	51
Figure 1-17. 1,3 Allylic Strain as Potential Driver of Flavanone Enolate Ring Opening.....	52
Figure 1-18. Investigation of Soft Enolization Conditions.....	53
Figure 1-19. Rubottom Sequence on a Single MOM-Flavanone Stereoisomer.....	53
Figure 1-20. Global Deprotection to Yield Final Product.....	54
Figure 1-21. CD Spectra of Silybin Natural Products ⁹⁷	55
Figure 1-22. CD Spectra of Major Synthetic Silybin Product, Assigned (-)-Isosilybin A.....	56
Figure 1-23. CD Spectra of Minor Synthetic Silybin Product, Assigned MOM-(-)-Isosilybin B.....	57
Figure 2-1. Selected Tropane Alkaloids.....	127
Figure 2-2. Polarity Analysis of Robinson's Tropinone Synthesis.....	131
Figure 2-3. Gomburg's Trityl Radical Synthesis.....	135
Figure 2-4. Competing Radical Reactions Depend on Radical Concentration.....	137
Figure 2-5. Radical-Alkene Addition Competition Experiment.....	138
Figure 2-6. Commonly Employed Photoredox Catalysts.....	143
Figure 2-7. Location of Frontier Molecular Orbitals on Excited States of Homoleptic and Heteroleptic Polypyridyl Complexes.....	144
Figure 2-8. Lewis Acid Mediated Enone Reduction.....	146
Figure 2-9. Hypothesis for Stabilization of β -Radical Enolate.....	150
Figure 2-10. Effect of Scandium Triflate on the Reduction Potential of Ph Arylidene Malonate.....	152
Figure 2-11. Transfer Hydrogenation of Arylidene Malonates with Tertiary Amines.....	153
Figure 2-12. Transfer Hydrogenation of Arylidene Malonates with Lewis acids and Hantzsch Ester.....	154
Figure 2-13. Knoevenagel condensation of <i>t</i> butyl ethyl malonate with <i>p</i> -tolylaldehyde.....	156
Figure 2-14. Organo-photocatalysis in Transfer Hydrogenation of Arylidene Malonates.....	157
Figure 2-15. One-Pot Organocatalyzed Transfer Hydrogenation of Arylidene Malonates.....	158
Figure 2-16. Design of a New Intramolecular Cyclization Substrate.....	160
Figure 2-17. Optimization of Cyclization Reaction.....	161
Figure 2-18. Attempted Reductive Enone Cross-Coupling.....	163
Figure 2-19. Preparation of HE-derivative Radical donor.....	165

Figure 2-20. Scope of Malonate Coupling Partners.....	171
Figure 2-21. Scope of Malonate Coupling Partners with Primary Benzylic Radical.....	173
Figure 2-22. Scope of Malonate Coupling Partners with Primary Benzylic Radical.....	174
Figure 2-23. Proposed Mechanism for the Coupling of Arylidene Malonates with Benzylic Radicals.....	176
Figure 2-24. Reductive Dimerization of Arylidene Malonate through Oxidative Quenching..	177
Figure 2-25. Possible Structure of Isolated Trimeric Species.....	178
Figure 2-26. Optimization of Reductive Dimerization Conditions.....	178
Figure 2-27. Scope of Malonate Dimerization.....	180
Figure 2-28. Initial Hit in β - β coupling of Enamine and Arylidene Malonate.....	181
Figure 2-29. Initial Exploration of Merger with Mes-Acr Oxidative Pathway.....	183
Figure 3-1. Substituent Effects on the Rate of the 1,2-Brook Rearrangement.....	283
Figure 3-2. Inversion Process in the 1,2-Brook Rearrangement.....	284
Figure 3-3. Hybridization and Molecular Orbital Schemes of Silicon Complexes.....	285
Figure 3-4. Cyclopentenone Synthesis By 1,2-Brook Cascade.....	286
Figure 3-5. Cycloheptanone Synthesis By 1,2-Brook/Oxy-Cope Cascade.....	287
Figure 3-6. Diastereoselective Homoenate Alkylation via Enolate Addition to Acyl Silanes.....	287
Figure 3-7. 1,2-Brook Mediated Stereoselective Synthesis of 1,2-Aminoalcohols Initially Reported by Dr. Dmitrijs Cernaks.....	289
Figure 3-8. Testing Stabilized Carbanions in the Imine Addition Reaction.....	289
Figure 3-9. Lewis Base Enhanced 1,2-Brook Rearrangement.....	290
Figure 3-10. Investigation of Addition to Arylidene Malonates.....	293
Figure 3-11. Investigation of Stereochemical Transfer in Fluoride Mediated 1,2-Brook..	294
Figure 3-12. Screen of Lewis Acids as Additives in Addition to Arylidene Malonates.....	294
Figure 3-13. Product Distribution in Addition to Arylidene Malonate.....	295
Figure 3-14. Investigation of Radical Traps on the Addition to Arylidene Malonates.....	295
Figure 3-15. Investigation of Brønsted Base Mediated Addition to Arylidene Malonates	296
Figure 3-16. Preparation of Acylated α -Silyl Alcohols.....	299
Figure 3-17. Investigation of 1,2-Brook Rearrangement of Acylated α -Silyl Alcohols.....	300
Figure 3-18. NHC Transesterification Catalyzed Addition to an Aryl Aldehyde.....	300
Figure 3-19. Acyl Cross-Over Experiment.....	302
Figure 3-20. NHC Transesterification Catalyzed Addition to Aryl Aldimines.....	302
Figure 3-21. Initial Investigation of Lewis Acid Mediated Photoaddition of Acyl Silanes.	305
Figure 3-22. Initial Investigation of Lewis Acid Mediate Photoaddition of Acyl Silanes..	308
Figure 3-23. Photoaddition to Substituted Maleimides.....	308
Figure 3-24. Application of LUMO Lowering Catalysts to Photoaddition to Maleimides..	309

List of Schemes

Scheme 1-1 General Approaches to Substituted Pyrans.....	22
---	----

Scheme 1-2 Challenges Associated with the Prins Reaction.....	25
Scheme 1-3 Approach to the Synthesis of Isosilybin B.....	38
Scheme 1-4 Pan et al.'s Approach to Benzodioxane Aldehyde.....	39
Scheme 1-5 Modified Approach to Epoxy Alcohol.....	40
Scheme 1-6 Attempted Completion Benzodioxane Aldehyde.....	41
Scheme 1-7 Completion of Benzodioxane Aldehyde Fragment.....	42
Scheme 1-8 Second Generation, Stereodivergent Approach to Benzodioxane Aldehyde....	58
Scheme 1-9 Unified Approach to Silybin Benzodioxane Subunits.....	59
Scheme 1-10 Alternate Approach to Biomimetic Cyclization Precursor.....	60
Scheme 1-11 Alternate Cyclization Approach.....	60
Scheme 2-1 The First Synthesis of Tropinone by Willstätter, 1901.....	128
Scheme 2-2 Robinson's Biomimetic Synthesis of Tropinone.....	129
Scheme 2-3 Overview of Polarity-based Bond Disconnections.....	130
Scheme 2-4. Approaches to Acyl Anion Operators.....	132
Scheme 2-5. Approaches to Homoenolate Operators.....	134
Scheme 2-6. Elementary Steps in Radical Reactions.....	136
Scheme 2-7. Simplified Molecular Orbital Description of Photoredox Catalysis with Transition Metals.....	140
Scheme 2-8. Effect of Photoexcitation on the Molecular Orbitals of Small Molecules.....	142
Scheme 2-9. Photoredox Catalyst Quenching Cycles.....	142
Scheme 2-10. Scale of Electrochemical Data of Some Photocatalysts and Organic Compounds.....	145
Scheme 2-11. Stoichiometric Approaches to Enone Reduction.....	147
Scheme 2-12. Approaches to Enone Reductive Cyclization.....	148
Scheme 2-13. Approaches to Intermolecular Enone Reductive Reactivity.....	149
Scheme 2-14. Design of a One-Pot Reductive Homologation Reaction.....	157
Scheme 2-15. Efforts Towards the Cyclization of Arylidene Malonate to δ -Lactones.....	159
Scheme 2-16. Two Possible Rationales for the Lack of Cyclization.....	159
Scheme 2-17. Observed Trends in Radical Termination in this Work.....	162
Scheme 2-18. Design of Radical-Radical Coupling Reaction.....	164
Scheme 2-19. Considerations of a Radical-Radical Coupling Reaction.....	166
Scheme 2-20. New Multi-Component Alkene Difunctionalizations.....	182
Scheme 3-1. The Brook Rearrangement.....	282
Scheme 3-2. Addition of Unsaturated Nucleophiles to Acyl Silanes.....	285
Scheme 3-3. Integration of 1,2-Brook Rearrangement into NHC Catalysis.....	288
Scheme 3-4. Use of α -Silyl, Silyl Ethers as Nucleophiles.....	291
Scheme 3-5. Acyl Transfer Initiated 1,2-Brook Rearrangement.....	297
Scheme 3-6. Investigation of Acyl Transfer Driven 1,2-Brook Rearrangement.....	298
Scheme 3-7. 1,2-Brook Rearrangement of Acyl Silanes.....	303
Scheme 3-8. Proposed Mechanism of Photo-Cyclopropanation of Activated Alkenes.....	304
Scheme 3-9. 1,2-Brook Rearrangement of Carbamoyl Silanes.....	310

List of Tables

Table 1-1. Optimization of Biomimetic Arylidene Malonate Cyclization.....	29
Table 1-2. Optimization of Biomimetic Chalcone Cyclization.....	45
Table 1-3. Optimization of Global MOM Protection of Narigenin.....	48
Table 2-1. Cursory Survey of Compatible Arylidene Malonates.....	155
Table 2-2. Survey of Compatible Arylidene Malonates.....	163
Table 2-3. Deviation from Optimal Conditions for Radical Cross-Coupling.....	167
Table 2-4. Effect of Modulation of Reaction Conditions.....	168
Table 2-5. Effect of Concentration and Catalyst Loading on Coupling Reaction.....	169
Table 2-6. Studies Towards Asymmetric Cross-Coupling Reaction.....	170
Table 3-1. Effect of Silicon Group on Addition to Diphenyl Phosphoryl Aldimine.....	291
Table 3-2. Effect of Solvent Upon Addition to Diphenyl Phosphoryl Aldimine.....	292
Table 3-3. Optimization of Biomimetic Arylidene Malonate Cyclization.....	293
Table 3-4. Optimization of Lewis Acid Mediated Photoaddition of Acyl Silanes.....	306
Table 3-5. Investigation of Magnesium Lewis Acids in Photoaddition of Acyl Silanes.....	306
Table 3-6. Investigation of Operational Parameters of Lewis Acid Mediated Photoaddition.	307

Chapter 1: Total Synthesis of (+)-Isosilybin A

Portions of this chapter appear in the following publications:

McDonald, B. R.; Nibbs, A. E.; Scheidt, K. A. "A Biomimetic Strategy to Access the Silybins:

Total Synthesis of (–)-Isosilybin A," *Org. Lett.* **2015**, *17*, 98-101.

McDonald, B. R.; Scheidt, K. A. "Pyranone Natural Products as Inspirations for Catalytic

Reaction Discovery and Development," *Acc. Chem. Res.* **2015**, *48*, 1172-1183.

1.1 Introduction to Natural Products

Humans have relied on nature for the fulfillment of basic needs like foodstuffs, clothing and shelter, transportation, and importantly medicine throughout their existence. The active compounds in these natural substances are typically secondary metabolites, termed natural products. The first written collections of such remedies were found in Mesopotamia on clay tablets in cuneiform, dating from approximately 2600 BCE. Described are approximately 1000 plant derived substances, many of which are still in current use.^{1,2} Encyclopedic compilations of medicines, i.e. pharmacopoeias, from the ancient societies of Egypt, India, China, and Greece have also been discovered and preserved. From Egypt, the “Ebers Papyrus”, believed to have originated around 1500 BCE, documents over 700 therapeutics derived from plant, mineral, and animal sources.³ This 20 meter long document is notably the first thorough description of delivery mechanisms for medicines. The Chinese *Materia Medica* which has been extensively documented and updated over the centuries (1100 BCE to ~700 CE) and contains over a thousand entries of plant based medicines.^{4,5} Likewise, documentation of the Indian Ayurvedic system dates from about 1000 BCE (Charaka, Sushruta and Samhitas reporting 341 and 516 therapies respectively).⁶ Centuries later, Greek philosophers and physicians began to contribute to the systematic and rational development of herbal remedies. Theophrastus’s “History of Plants” (~300 BCE) addressed the medicinal quality of herbs and noted modulation of characteristics based on cultivation. Dioscorides, a Greek physician (~100 CE), travelled extensively with the Roman army and thoroughly recorded the collection, storage, use of and effects of medicinal herbs. His five volume treatise “De Materia Medica” covered 600 plants, over 1000 herbal drugs, 4740 medicinal uses of these therapeutics, as well as 360 medical

properties, i.e. antiseptic, anti-inflammatory, stimulant, etc.⁷ Additionally, ethnomedicines preserved through oral history have served as repositories of medicinal knowledge and are rich sources for the discovery of natural products.⁸⁻¹⁰ This tradition of compiling and preserving knowledge has been maintained as medicine has evolved. The Merck Index, first published in 1888, is a leading example of a modern pharmacopoeia.¹¹ Nature remains the foundation of traditional medicine systems in cultures around the world,¹² as the WHO has estimated that up to 80% of the world population rely primarily on these systems for health care.¹³ Historic and traditional remedies are a vast repository of biologically active natural products. The isolation, characterization, and modification of these compounds has propelled medicine into the age of modern molecular medicine and continues to sustain new advancements.¹⁴

1.1.1 Natural Products as a Privileged Source of Molecular Therapeutics

Natural products, have been the most successful source of potential drug leads. At least 119 chemical substances, derived from 90 plant species, are considered important drugs in use in one or more countries.¹⁵ While plants have been used as sources of remedies to human ailments for millennia, it was only ~200 years ago that a 21-year old pharmacist's apprentice, Freidrich Sertürner, isolated the first pharmacologically active, pure compound from a plant, morphine.¹⁶ This marked the beginning of the modern era of drug discovery, wherein biologically active compounds from plants were purified, studied, and administered in a precise, controlled fashion. World War II served as a proving ground for the value of the pharmaceutical sciences with the development of penicillin and served as an impetus to drive intensive efforts towards the development of molecular medicine.¹⁵ These efforts continued, expanding to global effort that began to yield new drugs at a breathtaking pace.¹⁷ This expansive effort led to 1950-1960 being

dubbed the “golden age of antibiotics”, as one-half of the drugs commonly used today were discovered in this period.¹⁸ By 1990, 80% of approved drugs in the United States were either natural products or derivatives of natural products. Recently, the expansion of synthetic medicinal chemistry, particularly fragment-based drug discovery, has lowered this percentage, but natural products and their derivatives remain a central source of new entries into small-molecule based therapies.¹⁹

The development of synthetic organic chemistry has closely mirrored the progress of molecular medicine, as it is uniquely positioned to support this endeavor. The ability to synthetically access natural products provides a source that can supplement and often outstrip natural sources.²⁰⁻²² This activity, known as “total synthesis”, enables the comparison of synthetic and therefore structurally defined material to natural sources, thus enabling the unequivocal validation of molecular structure. Even more importantly this total synthesis provides a blueprint towards the construction of analogs. This is vital as the structural complexity of natural products may hamper or even prevent the sourcing of quantities required to meet clinical evaluation as well as serve patients. Furthermore, this blueprint enables the synthesis of truncated analogs that are more synthetically tractable and perhaps even more importantly, are more potent and show improved pharmacological properties, thus improving patient outcomes. As we move into the age of precision medicine, synthetic organic chemistry enables the exploration of biological signaling pathways, i.e. chemical biology, providing precise understanding of the molecular biology associated with disease states, in general and patient-specific cases.

In addition to making broad impacts on human health, natural products have synergistically supported and stimulated the field of synthetic organic chemistry. These complex

structures are effective measuring sticks for the current state of chemical synthesis as a field and are a source of inspiration to new synthetic approaches and strategies that in turn support fundamental understanding of biology and medicine.

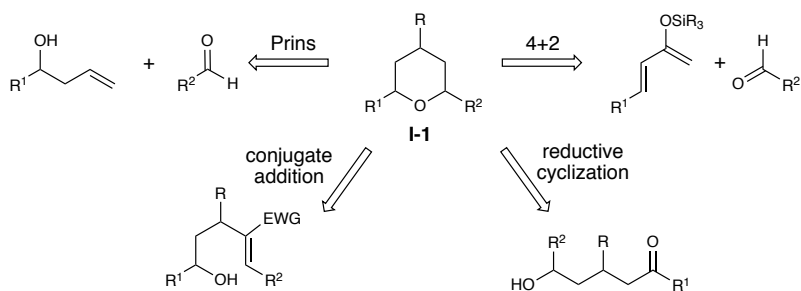
1.1.2 Pyran Natural Products

Pyrans and pyran-4-ones are ubiquitous motifs found in numerous bioactive natural products²³ and medicinal compounds.²⁴ This broad family of heterocycles spans a variety of substitution patterns and oxidation states. Compound classes included in this family are glycosides, δ -lactones, pyrenes, chroman, coumarin, flavanones, polycyclic ethers, among others. This prevalence and diversity has driven the development of a variety of strategies to construct these six-membered heterocycles over the past century.²⁵⁻²⁷

1.2 Approaches Towards the Synthesis of Pyran Natural Products

Given the variety of substitution patterns possible around a pyrans (**I-1**) and pyranones, a myriad of methods have been developed for their construction. Generally, Prins cyclizations,²⁸⁻³³ hetero-Diels-Alder reactions,³⁴ and intramolecular nucleophilic reactions^{35,36} have been the primary approaches developed towards the construction of these structures (**Scheme 1-1**).

Scheme 1-1 General Approaches to Substituted Pyrans.



The tetrahydropyran-4-one containing natural product okilactomycin (**I-2**) spurred the Scheidt laboratory's interest in the addressing synthetic challenges to pyranone synthesis in 2002

(**Figure 1-1**). Okilactomycin is a antitumor antibiotic isolated from *Sterptomyces griseoflavus* in 1987.^{37,38} *In vitro* studies have demonstrated that **I-2** exhibits significant antitumor and antiproliferative activity against both lymphoid leukemia L1210 cells and P388 leukemia cells, with promising IC₅₀ values of 216 nm and 89 nm, respectively.³⁷ A closely related compound, chrolactomycin (**I-3**), differs only in structure by the replacement of a methyl group with a methoxy moiety at the pyranone/lactone ring fusion (**Figure 1-1**).³⁹

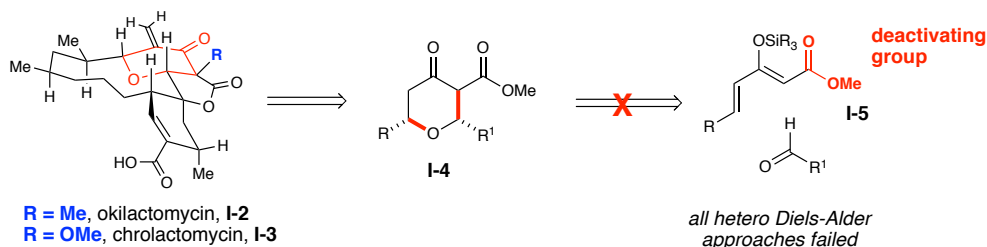


Figure 1-1 Original Approach to Okilactomycin.

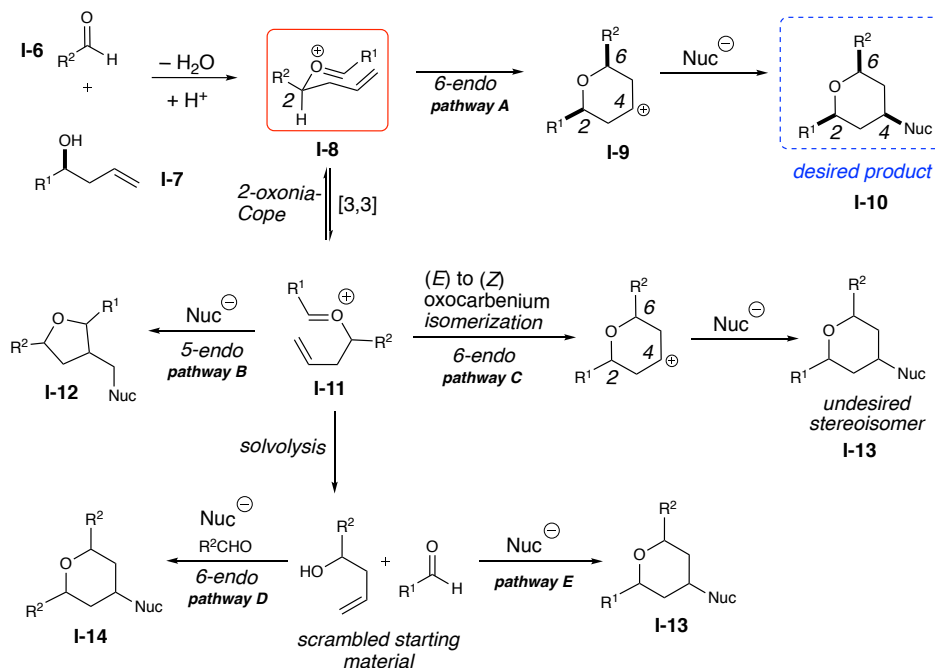
Notably, chrolactomycin has shown promising inhibition of the telomerase enzyme.⁴⁰ Telomerase is a target of intense interest for which there is a dearth of efficacious small molecule inhibitors.⁴¹ In addition to potent biological activity, these compounds possess an intriguing polycyclic architecture. The tricyclic core is characterized by a unique 6,5-fused tetrahydropyranone δ -lactone bicycle with fused with a highly substituted cyclohexene. A strained deoxygenated dipropionate segment spans this unusual tricycle to generate a highly rigid tetracyclic topology. Despite the biological activity and structural complexity, only the synthesis of **I-2** has only been reported by Takeda,⁴² Paquette,^{43,44} and Smith.⁴⁵ These efforts have resulted in the synthesis of unnatural enantiomer of **I-2** and the determination of the absolute configuration of the natural product by Smith et al. in 2007. There are no syntheses of chrolactomycin (**I-3**) reported to date. The Scheidt laboratory's original retrosynthesis of

okilactomycin utilized a Diels-Alder strategy to generate a 3-carboxy substituted tetrahydropyran-4-one (**I-4**) (**Figure 1-1**). While the 3-carboxy handle was a seemingly small requirement, it had significant consequences, ultimately precipitating a completely new approach. This added substituent precluded the use of a hetero-Diels–Alder strategy. After exhaustive screening of reaction conditions, a new strategy was sought.

1.2.1 Utilization of the Prins Reaction Towards the Stereoselective Synthesis of Substituted Pyrans

The Prins reaction stereospecifically provides the 2,6-*cis* relationship required to access okilactomycin. Condensation of an allylic alcohol and aldehyde yields an oxocarbenium (**I-8**) that then undergoes addition from the allylic alkene, yielding oxocarbenium **I-9**. Since the C–C bond forming event is believed to occur via a chair-like transition state, with the C-2 substituent located equatorially and an *E* configuration about the oxocarbenium, the desired 2,6-*cis* relationship is provided with exquisite selectivity (**Scheme 1-2**).^{46,32} This high degree of organization further enables transfer of chirality from the C-2 position to the newly formed chiral center at C-6.⁴⁷ Nucleophilic attack at the C-4 carbocation (**I-8**) (**Scheme 1-2**, pathway A) terminates the reaction. A significant pitfall of the Prins reaction is the array of unproductive pathways accessible from the high-energy oxocarbenium intermediates (**Scheme 1-2**, pathways B–E).

Scheme 1-2 Challenges Associated with the Prins Reaction.



Racemic products are sometimes observed, as there are a number of possible pathways that enable scrambling of the C-2 stereocenter. Of primary concern is the erosion of stereochemical information at the C-2 position via a tandem oxonia-Cope/oxocarbenium isomerization process (**Scheme 1-2**, pathway C).⁴⁸⁻⁵⁰ However, this undesired pathway can be avoided through prudent substrate design. Destabilization of the oxocarbenium intermediate **I-8** or stabilization of the C-4 carbocation species **I-9**, makes the desired Prins pathway the kinetically favored outcome.⁵¹⁻⁵³ With these design parameters and challenges in mind, dioxinones were envisioned as a novel substrate to execute the desired Prins transformation as it would provide the desired 3-carboxy handle. Dioxinones have been used as masked β -ketoesters and as precursors to extended enolates,^{54,55} however, their use as nucleophiles is quite uncommon, with only a single example preceding this application.⁵⁶ This new strategy was

designed to leverage two structural features of dioxinones: first, the embedded enol ether functionality, which would provide a nucleophilic handle at the α -position; second, the entire dioxinone framework, as it should provide a rigid platform to engender high stereoselectivity (**Figure 1-2**). Furthermore, the requisite enol character is essentially “locked” in dioxinones, and the expected tautomeric-related issues of related β -ketoesters are conveniently sidestepped. Finally, chiral dioxinones substrates are easily accessed from catalytic asymmetric reactions, thus enabling facile access to diverse functionality.⁵⁷

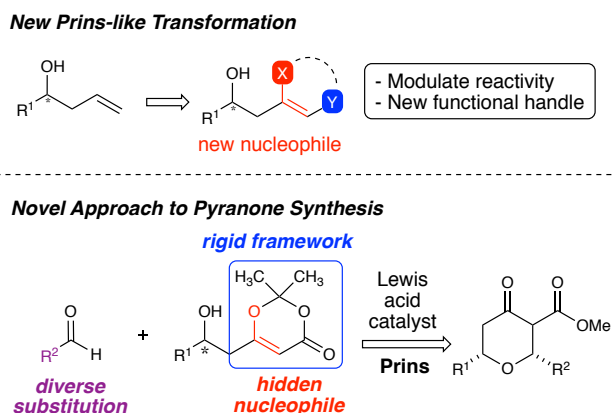


Figure 1-2 Design of a New Prins-like Reaction

A brief survey of Lewis acids revealed that scandium(III) triflate afforded the desired pyran–dioxinone at loadings as low as 10 mol %, while other metal triflate salts failed to yield significant amounts of product.⁵⁸ Notably, selection of dehydrating reagent is crucial as calcium sulfate (specifically Drierite[®]) exclusively enables formation of the desired pyranone product in high yield.

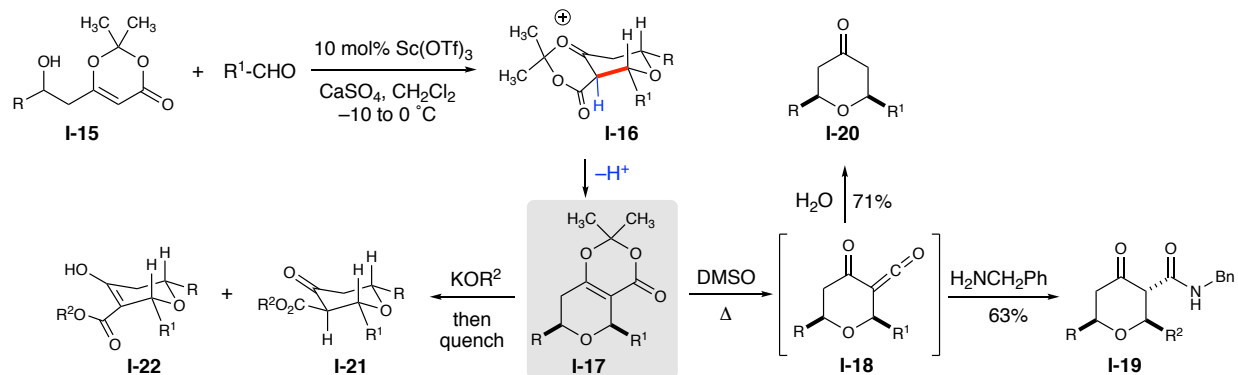


Figure 1-3 General Scope of Lewis Acid Mediated Dioxinone Prins-type Reaction

While the parent pyran–dioxinones **I-17** can be isolated in good yield, the related β -keto carboxy derivatives can be obtained with excellent diastereoselectivity in a single-pot operation. Upon exposure to heat, a highly reactive acylketene (**I-18**) is likely formed. This can be trapped with an amine to yield the corresponding β -keto amide (**I-19**), or the use of wet DMSO promotes decarboxylation, affording disubstituted tetrahydropyran-4-ones (**I-20**) with complete retention of stereochemistry. This chemistry has paved the way for the completion of okilactomycin⁵⁹ as well as the complex, macrocyclic natural products neopeltolide^{60,61} and exiguolide.⁶² This chemistry has further enabled the preparation of a diverse array of enantio-enriched pyranone scaffolds, which supports the Scheidt laboratory program in the development of truncated chrolactomycin analogs. Finally, access to these pyranone-containing natural products drove interest in the further exploration of pyranone natural products.

1.2.2 Conjugate Addition Approaches to Benzopyranones

Benzopyranones are a sub-class of pyranones that make up the core of flavonoids, a vast class of plant secondary metabolites that possess a diverse array of biological activity and medicinal applications.⁶³ The biosynthetic origins of these compounds lies in an enzyme-

mediated annulation of 2'-OH chalcones to a 2-aryl benzopyranones, known as flavanones.^{64,65} This enzyme, chalcone isomerase enzyme, (CHI) performs the isomerization in an amazing S/R ratio of 100,000:1 (ee = 99.998%) (estimated by kinetic analysis as conventional HPLC methods can only detect a single stereoisomer).⁶⁶ A series of oxidations and other transformations turn this simple flavanone product into the abundant variety of flavonoids isolated from plants. We sought to mimic this impressive biosynthetic transformation via a bifunctional H-bonding/Brønsted base catalyst in direct analogy to CHI (**Figure 1-4**). For a review detailing the general landscape of the asymmetric synthesis of flavonones, see Nibbs and Scheidt.⁶⁷

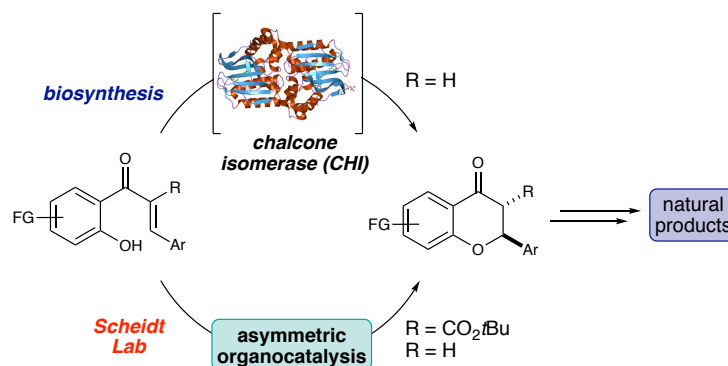
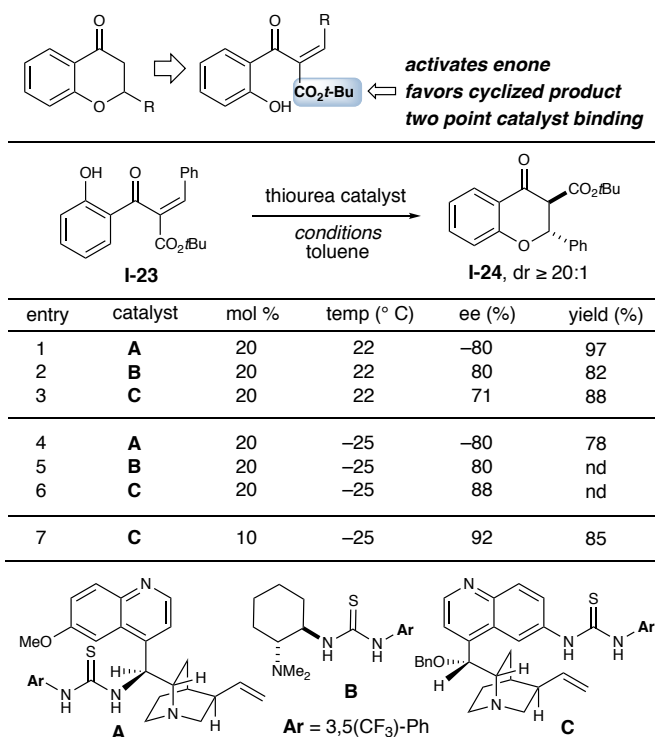


Figure 1-4 Biomimetic Conjugate Addition Approaches to Benzopyranones

The preparation of chalcones and the related alkylidene β -ketoesters, is generally facile and robust, and thus spurred further interest in the development of a biomimetic synthetic approach. *A significant challenge with reconstituting the chalcone cyclization under laboratory settings is the ease of which the flavanone undergoes the reverse reaction, phenoxide elimination.*⁶⁸ Mild conditions, analogous to physiological conditions, are therefore required. With this requirement in mind, neutral hydrogen-bonding organocatalysis seemed an ideal solution. It was hypothesized that this undesired retro-cyclization could be prevented by

employing activated unsaturated ketones (**I-23**) (e.g., alkylidene β -ketoesters). This functionality would further gear the system toward cyclization, while being easily cleavable. Furthermore, this second electron-withdrawing group would provide an additional point of interaction with a hydrogen bonding catalyst, strengthening the substrate/catalyst interaction and potentially enhancing stereocontrol (**Table 1–1**).⁶⁹ Cinchona alkaloid thioureas have been highly explored as bifunctional catalysts⁷⁰ and were chosen as the point of entry due to their relative ease of preparation. Surveying three such catalysts (**Table 1–1**) demonstrated that these were promising catalysts, particularly due to the fact that the catalysts yielding equivalent and complementary stereocontrol were identified (**Table 1–1**, entries 1–3).

Table 1–1. Optimization of Biomimetic Arylidene Malonate Cyclization



Interestingly, only catalyst **C** showed an enhancement of selectivity when the temperature was lowered (**Table 1–1**, entries 4–6). Further investigation revealed a dependence on concentration, with 10 mol % loading of **C** at –25 °C yield the isomerization product **I-24** in a yield of 85% and 92% ee. This sensitivity to concentration in thiourea HBD catalysis has been previously observed.^{71,72} Notably, the corresponding chalcone substrate does not react when exposed to catalysts **A**, **B**, or **C** under these conditions. With a highly selective and efficient biomimetic reaction established, the application to the synthesis of complex flavanones was sought.

1.3 The Silybin Natural Product Family

1.3.1 Introduction

The milk thistle, *silybum marianum*, is an edible thistle native to southern Europe, southern Russia, Turkey, and northern Africa. It has been further naturalized to North and South America. ‘Silybum’ is the name Dioscorides gave to edible thistles (derived from the Greek sillybon or silybos, meaning 'tassel' or 'tuft'), while ‘marianum’ originates from the legend that the white veins running through the plant’s leaves were caused by a drop of the Virgin Mary’s milk.⁷³ Milk thistle has been used as a for centuries for the treatment of liver disorders and as a hepatoprotectant. The extracts of the fruit (achenes) are known as silymarin and consist of a complex mixture of flavonolignans and flavonoids including silybin A (**I-25**) (16%), silybin B, (**I-26**) (23.8%), isosilybin A, **I-27** (6.4%), isosilybin B, **I-28** (4.4%), silychristin, **I-31** (11%), isosilychristin (**I-32**) (2.2%), silydianin (**I-33**) (16.7%) and dihydroquercetin (**I-34**) also known as taxifolin (1.6%) (% by mass of silymarin) (**Figure 1-5**).⁷⁴ Isosilybins **C** (**I-29**) and **D** (**I-30**) are recent additions to the silybin family, having recently been isolated in minute quantities (3 mg

and 32 mg from 1 kg of extracts respectively).⁷⁵ Silymarin has been studied for over 60 years and due to this long history, there are some nomenclature issues.⁷⁶ The mixture of silybins A (**I-25**) and B (**I-26**) is known as silibinin, while the mixture of isosilybins A (**I-27**) and B (**I-28**) is known as isosilibinin. There is often conflation of this terminology, which has led to confusion regarding the exact composition of extracts used in biological studies (*vide infra*). This issue arises from the structural similarity among the silybin compounds. The silybins are composed of a flavanone system, derived from taxifolin (**I-34**) and a phenyl propane unit derived from coniferyl alcohol (**I-35**) (**Figure 1-5**).

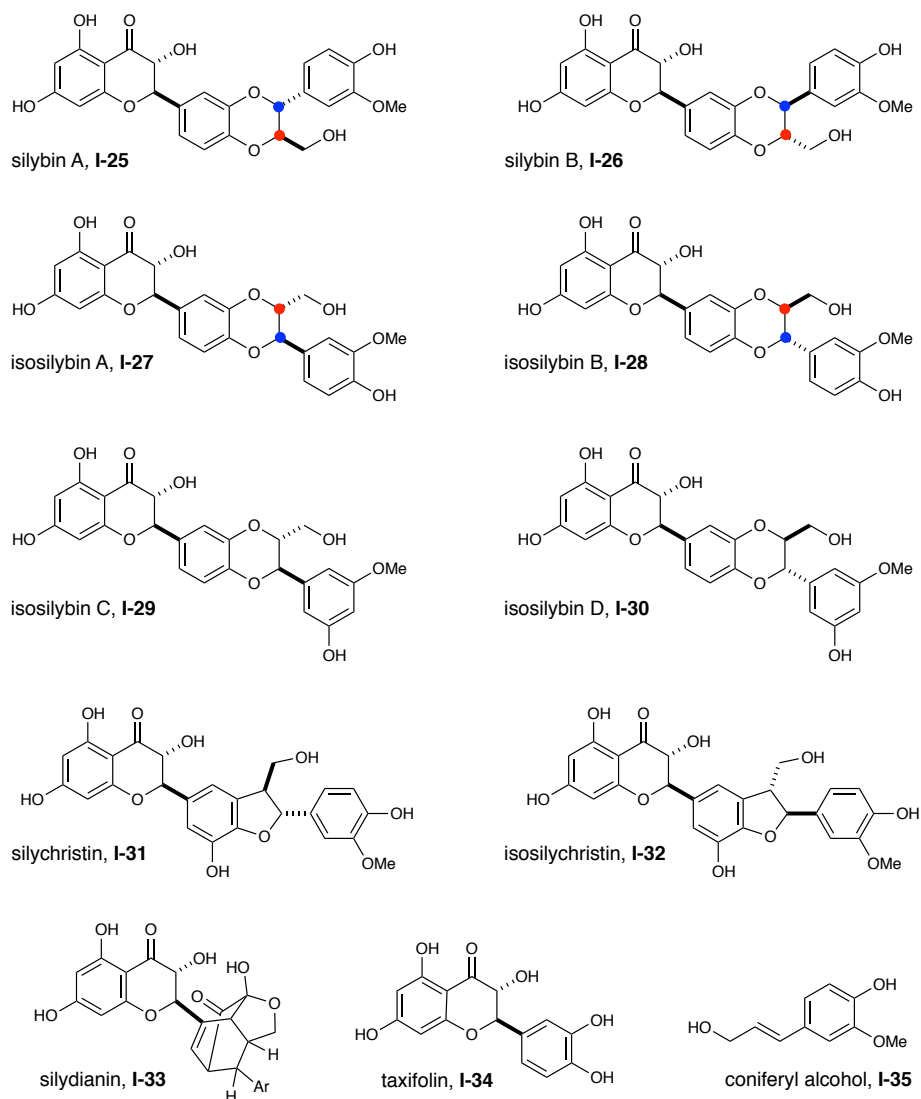


Figure 1-5. Constituents of Silymarin.

Silibinin and isosilibinin each exist as a pair of *trans* diastereoisomers with respect to the relative configuration at positions C7'' and C8'' in the 1,4-benzodioxane ring. Silychristin (**I-31**) and isosilychristin (**I-32**) are distinguished by the related dihydrobenzofuran bicycles. The position of this bicycle differs by being joined at either the C4' and C5' positions in silychristin or the C2' and C3' positions in isosilychristin (**I-32**). Silydianin (**I-33**) is the most structurally

complex of the flavonolignans in silymarin as it is characterized by a bicyclo[2.2.2]octenone with a transannular hemiketal. Since this family of isomeric compounds are derived from taxifolin, the stereochemistry about the flavanone system is conserved since chalcone isomerase only produces a single stereoisomer that is elaborated to taxifolin. Additionally, the regio- and stereochemical diversity about the originates from the peroxidase-mediated radical addition to coniferyl alcohol of taxifolin (**Figure 1-6**).⁷⁷ It has been postulated that the peroxidase enzyme simultaneously oxidizes taxifolin and coniferyl alcohol to generate two radical that combine to provide *ortho*-quinone methide species **I-36**. The divergence between isosilibinin and silibinin is believed to originate from the non-regiospecific oxidization of taxifolin. A diastereoselective intramolecular conjugate addition is then believed to furnish the natural product (**Figure 1-6**).

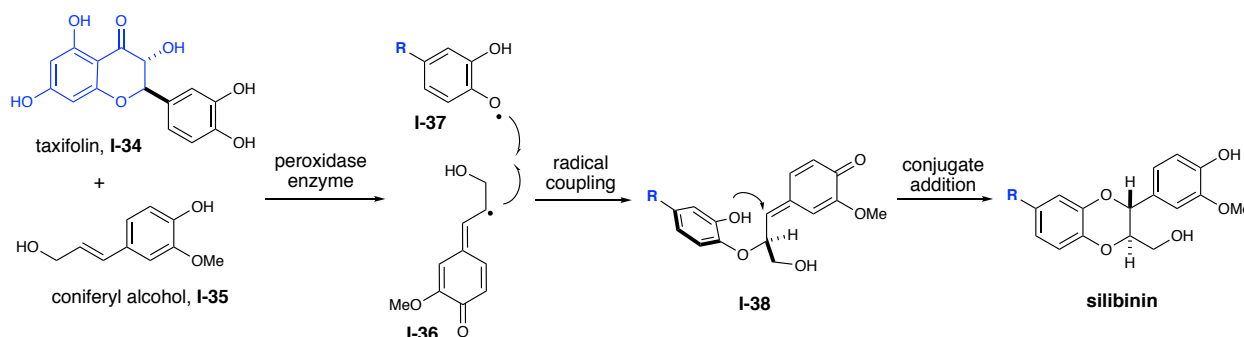


Figure 1-6. Proposed Biosynthesis of Silybin Natural Products.

Concerns have been raised about this proposed mechanism, namely the likelihood of radical-radical coupling being the initial C-O bond forming step, due to kinetic issues associated with radical-radical couplings.⁷⁸ An alternate mechanism for biomimetic oxidative cyclization can be found in **Figure 1-7** (see page 37) that does not invoke an intermolecular radical-radical coupling.

1.3.2 Bioactivity of Silybin Natural Products

Milk thistle has been employed for thousands of years as a traditional herbal remedy to treat a range of liver and gallbladder disorders, including hepatitis viral infection, liver cirrhosis and jaundice. In traditional medicine, Milk thistle has been further employed as a hepatoprotectant from chemical and environmental toxins such as snakebites, insect stings, as well as mushroom and alcohol poisoning.^{79,80} Some of these functions, such as supportive therapy in liver disease⁸¹ and protection from toxins have been validated by clinical trials.⁸² In the US and Europe, about 65% of patients with liver disease take herbal preparations; in Europe, expenditures on silymarin therapy has reached \$180 million in Germany alone.⁸³ In the United States silymarin is available as an over-the-counter dietary supplement. Given the ubiquity and importance of silymarin in the support of liver health, it has come under intense investigation to elucidate the mechanism(s) of this bioactivity. Studies have shown that silymarin has a broad profile of biological activity, with *in vitro* studies revealing that silymarin has a complex polypharmacological profile, interacting with a wide variety of cellular pathways (modulation of the activity/expression of >100 proteins has been reported).⁸⁴ In consideration of this information, it is vital to note that *only a small fraction of the biological studies performed were conducted with isomerically pure silybin compounds*. The material employed in these studies varied from bulk silymarin to mixtures of silybin diastereomers (silibinin/isosilibinin).

In addition to the important hepatoprotectant activities, focus on the silybins has shifted towards investigation of cancer as a phytoprotective and phytotherapeutic.^{85,84,86} Promising anti-cancer activity *in vitro* and *in vivo* has been observed,^{87,85,74,88-91} with particularly interesting

results in the area of prostate cancer (PCa), the second most frequently diagnosed cancer and the sixth leading cause of cancer-related deaths in men worldwide.⁹²

Regulation of prostate development and homeostasis occurs through androgen and androgen receptor (AR)-mediated signaling pathways.^{93,92} As such, the development and progression of prostate cancer is driven through the dysregulation and malfunction of these pathways.⁹⁴ Specifically, the transition from AR-guiding cytodifferentiation of luminal epithelial cells to AR driving the uncontrolled proliferation has been identified as a key event by which prostate cancer arises (this shift is believed to be triggered by lowered testosterone levels).⁹² The initial options for therapeutic intervention are hormone therapy, combined-androgen blockade surgery, and radio/chemotherapy. Advanced progression of the disease is marked by a hormone-refractory state, known as castration-refractory prostate cancer (CRPC). Androgen receptor overexpression, mutations, or post-translational activation of the receptor are believed to be the origin of CRPC. This advanced disease state is characterized by promiscuous AR function, with low levels of adrenal androgens, other steroids, even anti-androgens able to act as AR agonists. This effectively renders treatments that target circulating androgens ineffective, the consequence of which is metastasis.⁹⁵ Local and regional stage prostate cancers have nearly 100% 5-year relative survival rates, while distant stage cancers (metastasis to bones, lymph nodes, or other organs) have a 29% 5-year relative survival rate. Approximately 40-50% of prostate cancers are recurrent and often lead to metathesis. Based on these data, new mechanisms for targeting the AR are required. Excitingly, the phytochemicals found in silymarin are leads for the ablation of androgen receptors from prostate cancer cells, which could ultimately lead to improved outcomes for cases of CRPC.

The effects of individual constituents of silymarin on prostate carcinoma cells have been evaluated. The silybins (**I-25-I-28**) have been evaluated for anti-proliferative activity against androgen-dependent LNCaP cells, and androgen-independent DU145, and PC3 human prostate carcinoma cell lines.⁷⁴ Interestingly, isosilybin B (**I-28**) consistently out-performed other isomers (individually and as mixtures) in the inhibition of cellular proliferation in tested PCa cell lines. Additionally, **I-28** was the most effective inhibitor of prostate specific antigen, a key biomarker of PCa, in androgen-dependant LNCaP cells. Further work demonstrated that the isosilybins (**I-27-I-28**) inhibit growth, induce G1 arrest, and cause apoptosis in human prostate cancer LNCaP and 22Rv1 cells.⁹⁶ A direct connection to the AR and the silybins was demonstrated by Agarwal et al wherein they showed that isosilybin B strongly decreased AR levels in both androgen-dependent (LNCaP and LAPC4) and androgen-independent (22Rv1) PCa cells.⁹³

Despite the considerable effort invested in cataloging the myriad of effects of the silybins, *a specific molecular target has never been reported*. Thus, we believed that this considerable knowledge gap could be addressed by synthetic chemistry, as it stands uniquely poised to drive structure-function studies as well as enable chemical biology studies to elucidate the molecular target.

1.3.3 Previous Syntheses of Silybin Natural Products

There have been no selective (regio- and stereoselective) syntheses of a constituent of the silybin family to date. Efforts have largely focused on the purification of constituent isomers and their chemical modification, which has been limited to simple derivatization such as phosphorylation and alkylation.⁹⁷⁻⁹⁹ All reported syntheses have been biomimetic oxidative cyclizations that produce mixtures of regioisomers, diastereomers, and enantiomers.^{100,101,78} The

first synthesis was reported by Merlini and employed Ag_2O as oxidant to drive the coupling of coniferyl alcohol with taxifolin to provide a mixture of silibinin and isosilibinin (57:43) in 76% yield (**Figure 1-7**).¹⁰⁰ Zhao reported that substituting Ag_2O with Ag_2CO_3 changes the silibinin/isosilibinin ratio to slightly favor silibinin (69:31), in an unreported yield.¹⁰¹ Oberlies and co-workers conducted a mechanistic investigation of the possible mechanisms by which these oxidative biomimetic cyclizations could be occurring. Based upon the very slow oxidation of taxifolin (**I-34**), they concluded that these reactions were likely proceeding by oxidation of coniferyl alcohol (**I-35**) to *para*-quinone methide **I-36**. Conjugate addition of taxifolin at either phenol would then radicals **I-39** and **I-40** which upon a successive oxidation would yield a carbocation that is trapped by the remaining phenol, thus yielding mixtures of silibinin and isosilibinin.

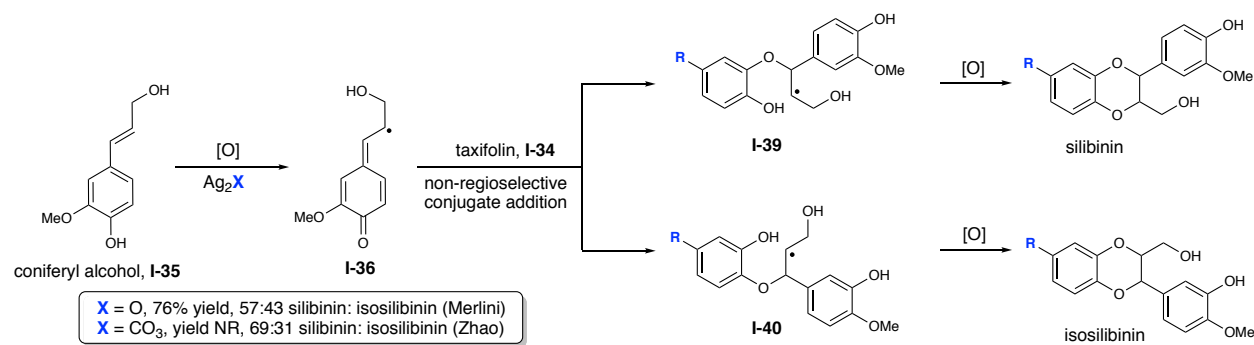


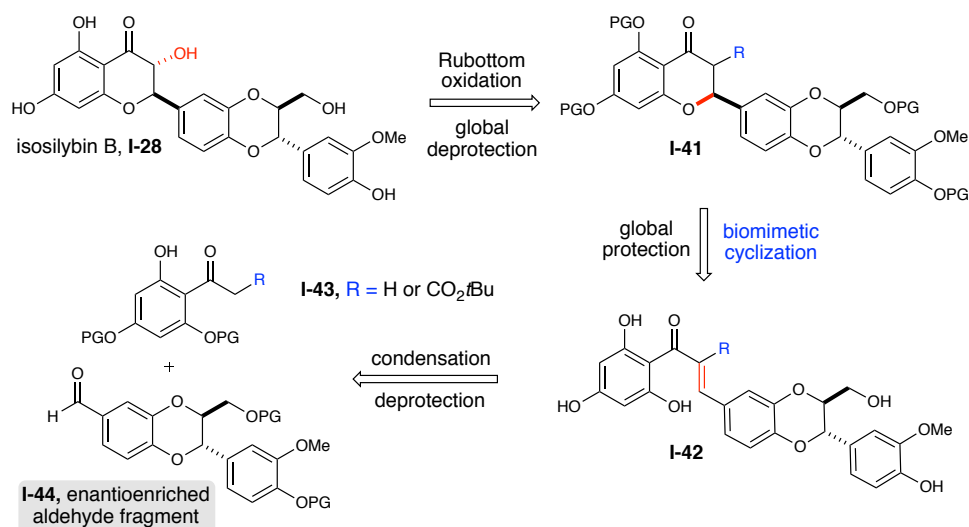
Figure 1-7. Proposed Mechanism of the Biomimetic Preparation of Silybins.

Notably, the biological studies outlined above have demonstrated differential activity based on stereoisomerism and therefore the preparation of isomerically pure compounds would be of the utmost importance for the collection of meaningful chemical biological data. With our work on the biomimetic synthesis of flavanones, we felt well-positioned to address this gap in the knowledge.

1.4 Retrosynthetic Analysis towards Isosilybin B

Since the reported biological activity data showed that isosilybin B was the most efficacious of the silybin compounds, this was targeted for the first selective synthesis of a silybin constituent. We sought to build upon the biomimetic cyclization previously developed in the Scheidt laboratory (**Table 1–1**). The requisite cyclization substrate would be obtained from the robust condensation of a keto-ester or acetophenone (**I-43**) with the corresponding aryl aldehyde **I-44** (**Scheme 1-3**). The β -keto ester or acetophenones (**I-43**) required for the condensation are simple to prepare and approaches to the enantioenriched aldehyde **I-44** from ferulic acid had previously been disclosed by Pan (**Scheme 1-4**).^{102,103} Oxidation and global deprotection of **I-41** would provide isosilybin B. This flexible route was needed as the Knoevenagel condensation of 2,4,6-substituted keto-esters with aldehydes was anticipated to be challenging.

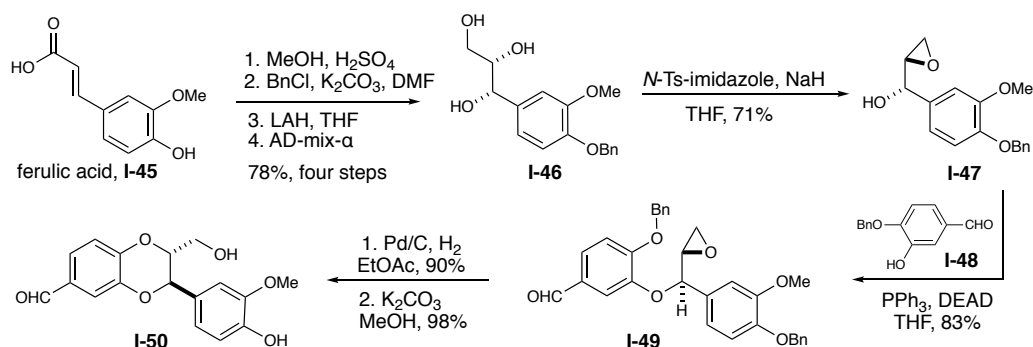
Scheme 1-3 Approach to the Synthesis of Isosilybin B



An additional consideration is the high degree of oxygenation of the silybins, possessing five different alcohols and total of 10 oxygen atoms. Judicious choice of protecting group would

be required so that nucleophilic alcohols can be selectively masked and released, thus allowing the regioselective formation of carbon-oxygen.

Scheme 1-4 Pan et al.'s Approach to Benzodioxane Aldehyde



1.5 Previous Efforts Towards Isosilybin B Total Synthesis

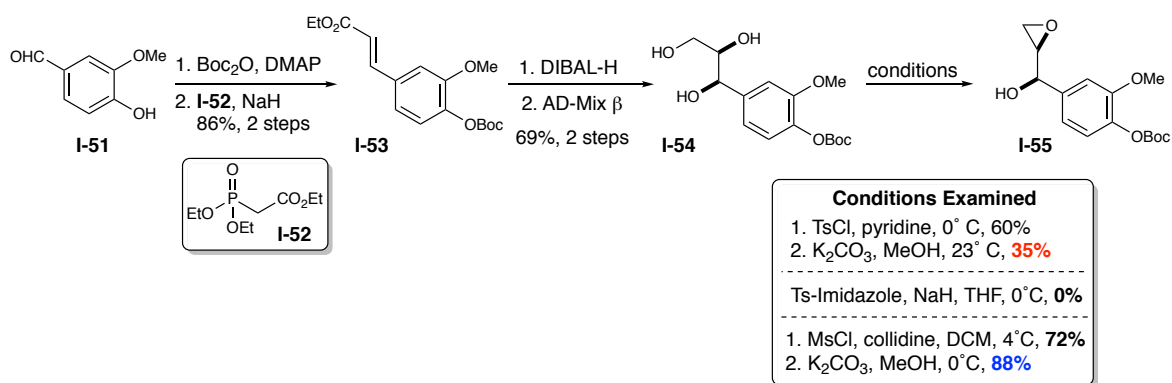
The groundwork for the completion of the first total synthesis of a silybin natural product was laid by previous graduate student Antoinette Nibbs.

1.5.1 Synthesis of Benzodioxane Aldehyde

Applying general route to aldehyde **I-44** disclosed by Pan et al. proved to require considerable revisions (**Scheme 1-5**). Vanillin (**I-51**) was chosen a cheaper starting material and elaborated to the protected ferulic ester derivative **I-53** with Boc protection and a subsequent HWE reaction with phosphonate **I-52** in 86% yield over two steps. Enantioenriched triol **I-54** was obtained in 69% yield over two steps by DIBAL-H reduction and dihydroxylation with AD-mix- β . New conditions to enable the regioselective alcohol activation and epoxide ring-closure were developed. The one-pot tosylation/ring-closure conditions to provide epoxy alcohol **I-55** reported by Pan proved to be unreproducible and a stepwise procedure was required. Nibbs developed step-wise regioselective tosylation followed by ring-closure in methanol with potassium carbonate, but in my efforts, this sequence proved to be inconsistent, typically

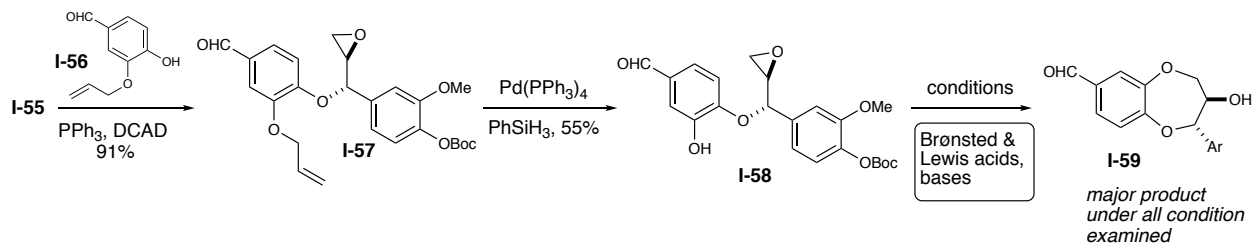
yielding **I-55** in approximately 35% yield. Re-examining Chan's one-pot procedure yielded no product (**Scheme 1-5**). Alternate tosylation conditions using dibutyltin oxide as a regioselective catalyst only provided complex mixtures of products.¹⁰⁴ While this system is designed to regioselectively sulfonate the terminal alcohol of vicinal diols, its application to a triol was likely plagued by competing coordination modes.

Scheme 1-5 Modified Approach to Epoxy Alcohol



Replacement of the tosyl group with a methanesulfonate group enabled this procedure to be carried out consistently in nearly 60% yield over the two steps.¹⁰⁵ Mitsunobu reaction between allylated isovanillin derivative **I-56** and the epoxy alcohol **I-55**, yielded the etheric product **I-57** in 91% yield as a single diastereomer (**Scheme 1-6**). The use of the Boc protecting group and DCAD¹⁰⁶ as activating group in this Mitsunobu reaction were key to the observed efficiency and stereoselectivity.

Scheme 1-6 Attempted Completion Benzodioxane Aldehyde



It was hypothesized that in analogous fashion to biosynthesis (**Figure 1-6**, **Figure 1-7**), *para*-quinone methide intermediates were the cause of the observed erosion of stereochemistry. The use of Boc as an electron-withdrawing group is believed to have suppressed this pathway. The most significant synthetic challenge was encountered upon the attempted nucleophilic epoxide ring opening. De-allylation under reductive palladium conditions provided phenol **I-58** in modest yield. In a significant departure from the results reported by Chan, the regiochemistry of the attack by the phenol was dictated by whether the phenol was in conjugation with the aldehyde (**Figure 1-8**). Under all conditions screened, the *meta* relationship between aldehyde or other electron-withdrawing groups provided the seven-member product. Even reduction of the aldehyde to benzyl alcohol and subjection to cyclization conditions provided the undesired seven-member product as the major product. Interestingly, with a *para* relationship between aldehyde and phenol, the cyclization smoothly provided the desired six-membered product, validating this approach towards the silybin isomeric series.

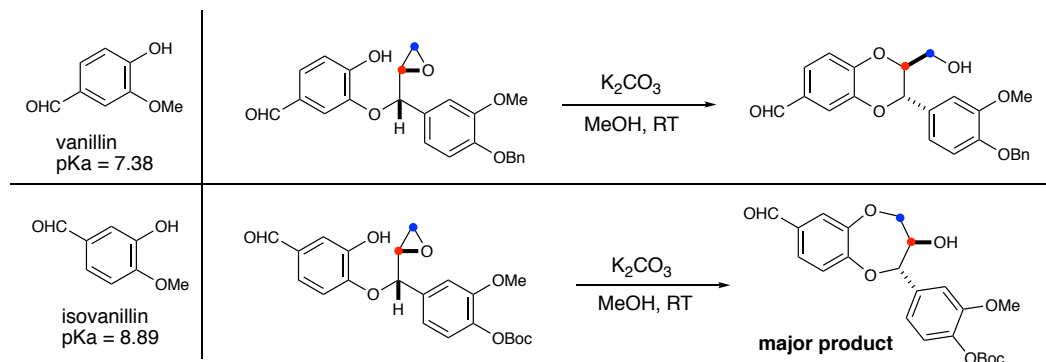
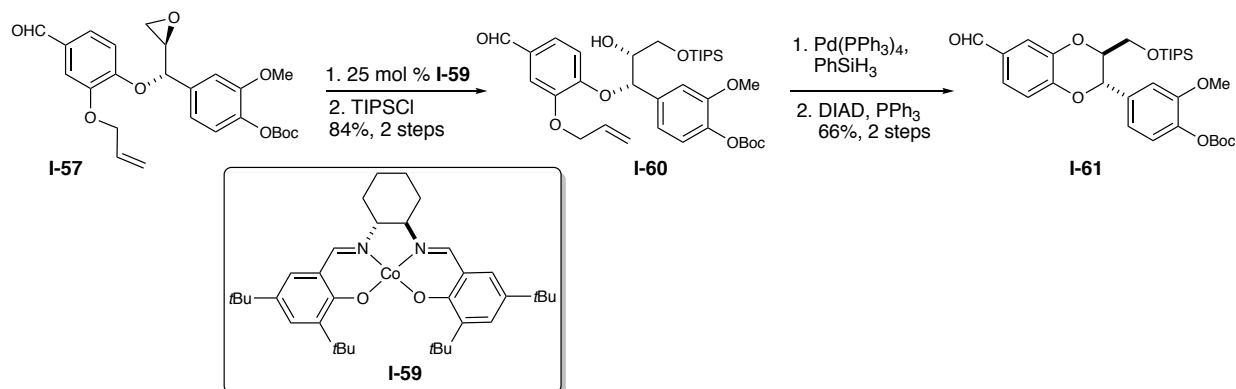


Figure 1-8. Divergent Cyclization Pattern.

In order to access the desired regiochemistry required for the isosilybin series, an alternate strategy was devised (**Scheme 1-7**). Instead of de-allylation, the epoxide **I-56** was opened by Jacobsen's chiral cobalt salen complex¹⁰⁷ **I-59** to provide a diol that was regioselectively silylated, yielding alcohol **I-60** in 84% yield over two steps. De-allylation yielded a diol that upon exposure to DIAD and triphenyl phosphine yield the completed benzodioxane aldehyde fragment **I-61** in 66% yield over the two steps. It is worth noting that DIAD is surprisingly hygroscopic and should be dried over 4 Å molecular sieves before performing this Mitsunobu reaction. This simple precaution nearly doubled the yield of the Mitsunobu reaction from 43% to 74% yield.

Scheme 1-7 Completion of Benzodioxane Aldehyde Fragment



1.5.2 Biomimetic Cyclization to Yield Flavanone Core

At this point, the Knoevenagel condensation to provide cyclization precursor could be explored. Frustratingly, the attempted Knoevenagel condensation with the 2,4,6-substituted β -keto ester never yielded any of the desired arylidene malonate after an exhaustive examination of conditions and aldehyde equivalents (**Figure 1-9**).

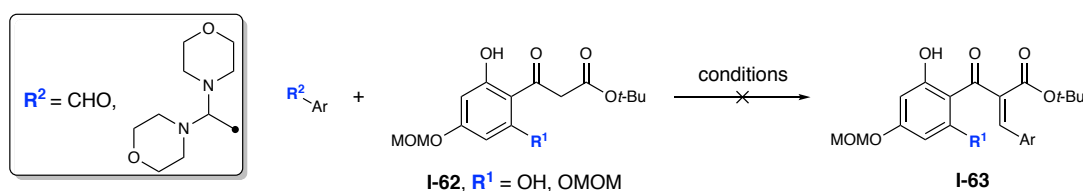


Figure 1-9. Attempted Knoevenagel Condensation.

Simple condensation conditions employing sodium hydroxide followed by global deprotection with *p*-TsOH and neopentyl glycol afforded the pentahydroxy chalcone cyclization substrate (**I-65**) in 49% yield from acetophenone **I-64** and **I-60** over two steps (**Figure 1-10**). With the aldol condensation smoothly providing an alternative cyclization substrate, a new biomimetic cyclization was required.

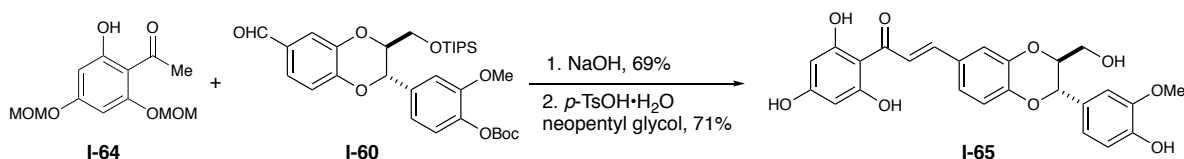


Figure 1-10. Aldol Condensation and Deprotection To Yield Chalcone Cyclization Substrate.

Hintermann et al. previously disclosed the cinchona alkaloid catalyzed asymmetric cyclization of 2',6'-dihydroxychalcones.¹⁰⁸ In the cyclization of narigenin derivative **I-66**, Hintermann's best results, 81% conversion, 64% ee, were obtained with quinine in

chlorobenzene (**Figure 1-11**). Unfortunately, 70 hours were required to observe this level of conversion.

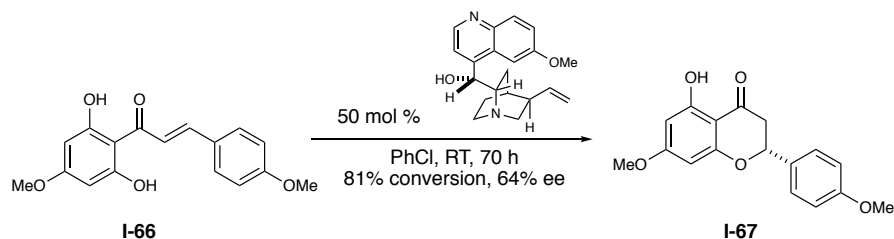
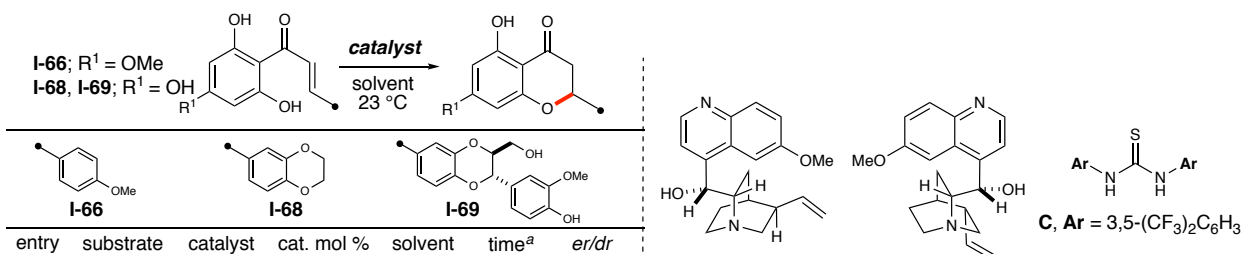


Figure 1-11. Hintermann's Asymmetric Chalcone Cyclization

Given these promising preliminary results and we believed that the bifunctional catalysts employed in our cyclization of the arylidene malonates could improve this cyclization. Summarized in **Table 1-2** is the optimization of the biomimetic chalcone isomerization. Preliminary studies were carried out on the cyclization of naringenin dimethyl ether chalcone **I-66** (**Table 1-2**). The 2'- and 6'-phenolic oxygens must remain unprotected for successful cyclizations under these conditions, as hydrogen bonding of one phenol with the ketone planarizes the aryl and ketone systems, effectively gearing the chalcone for cyclization.^{68,108} Quinine and quinidine stereodivergently produced the desired flavanone with good stereoselectivity, but the overall process was extremely slow, even at 50 mol % loading (**Table 1-2**, entries 1-2). The addition of an equimolar amount of Schreiner's thiourea¹⁰⁹ (**C**) greatly accelerated the cyclization, but resulted in lowered stereoselectivities (**Table 1-2**, entries 3-4). Merging the HBD thiourea functionality and the Brønsted base cinchona alkaloid moiety into a single compound based (catalysts **D** and **E**) improved reaction times (<6 h).^{72,70} These pseudoenantiomeric catalysts led to good diastereoselectivity (85:15) for the desired (*R*)-flavanolignan (with **F**) yet almost racemic product (56:44) with **D** (**Table 1-2**, entries 5-6).

Further studies to understand the stereochemical complexities of this cyclization (i.e., matched vs. mismatched)¹¹⁰ and the investigation of new catalysts to favor the (*S*) antipode in a manner that is complimentary to selectivities observed with catalyst **F** are required.

Table 1–2. Optimization of Biomimetic Chalcone Cyclization



entry	substrate	catalyst	cat. mol %	solvent	time ^a	er/dr
1	I-66	A	50	PhCl	9 d	80:20
2	I-66	B	50	PhCl	9 d	20:80
3 ^b	I-66	A + C	50	PhCl	2 d	60:40
4 ^b	I-66	B + C	50	PhCl	2 d	40:60
5	I-66	D	50	PhCl	<6 h	56:44
6	I-66	E	50	MeCN	<6 h	75:25
7	I-68	D	15	MeCN	48 h	65:35
8	I-68	E	15	MeCN	48 h	79:21
10	I-69	C	30	MeCN	–	50:50
11	I-69	D	30	MeCN	48 h	56:44
12	I-69	E	30	MeCN	48 h	83:17
13	I-69	F	30	MeCN	36 h	85:15

^aTime required for complete consumption of starting material; yield not determined. ^b1:1 ratio of catalysts (50 mol % each).

A, quinine
B, quinidine
C, Ar = 3,5-(CF₃)₂C₆H₃
D
E, X = S
F, X = O
Ar = 3,5-(CF₃)₂C₆H₃

Chalcone **I-68**, possessing an unsubstituted benzodioxane ring and unprotected 4'-phenol, was then explored as a simplified analog of the natural product system. Switching the solvent to acetonitrile allowed for lower catalyst loading (15 mol %) without significant loss of stereoselectivity. Subjection of the fully elaborated substrate **I-69** to the optimized conditions necessitated the increase of catalyst loading to 30 mol %, but afforded the product with 83:17 d.r with catalyst **E**. It is likely that the additional hydroxyl group promotes non-productive substrate catalyst interactions. Notably, the use of achiral thiourea **C** with chalcone **I-69** led to a 50:50 mixture of diastereomers, indicating the existing stereocenters in the benzodioxane portion do not exert stereocontrol over ring closure (**Table 1–2**, entry 10). Ultimately, urea analog **F** was

determined to be the optimal catalyst with reduced reaction times (36 h vs. 48 h) and a small improvement in stereoselectivity. Nibbs found isolation of the tetrahydroxy flavanone challenging, with poor mass recovery. The sequence of cyclization followed by global Boc protection of the unpurified material yielded the desired flavanone in good yield (63%, 75:25 dr), with hydroxyl groups protected for further elaboration (**Figure 1-12**). With the desired flavanone in hand, all that was required was the installation of an α -hydroxyl group on the ketone.

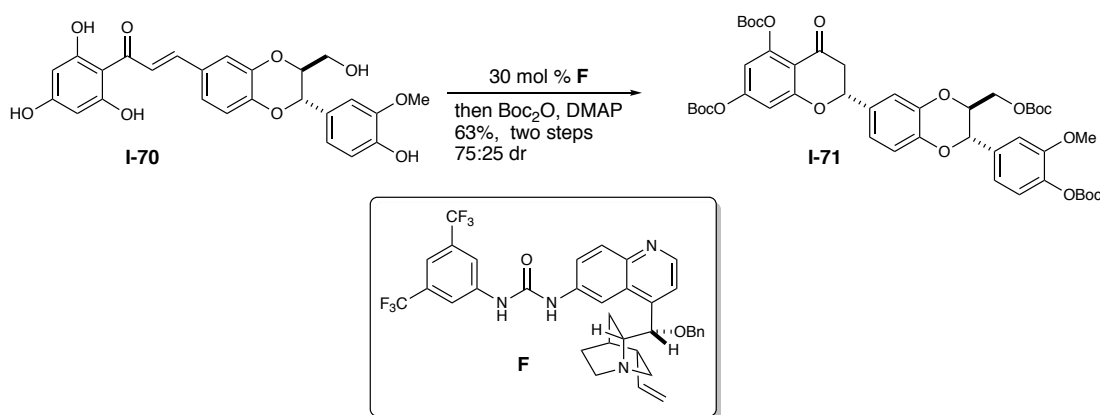


Figure 1-12. Cyclization Sequence to Yield Protected Flavanone

1.5.3 Attempted α -Oxygenation of Flavanone

The primary method for the α -hydroxylation of carbonyls is the oxygenation of silyl enol ethers. Silyl enol ethers of **I-70** could be formed and isolated, but after an exhaustive survey of conditions to oxidize this silyl enol ether, no oxygenated product was obtained, thus providing a significant hurdle towards the completion of the total synthesis (**Figure 1-13**).

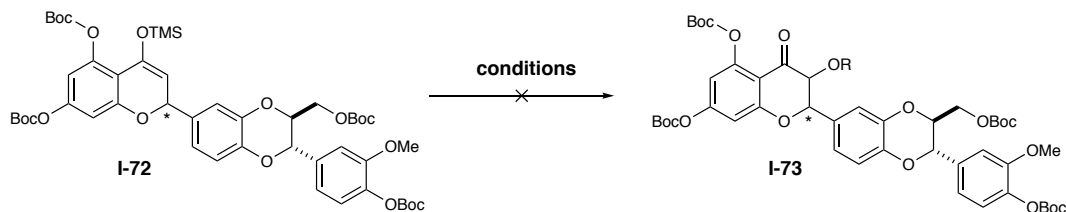


Figure 1-13. Attempted α -Oxidation of Boc-Protected Flavanone Silyl Enol Ether

1.6 Revision of Route to Isosilybin B

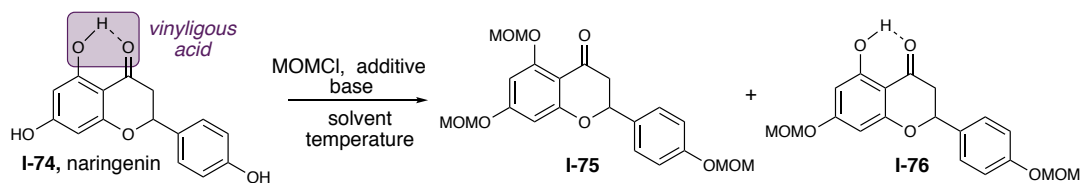
After the exhaustive efforts to oxidize the Boc-protected silyl enol ether (**I-72**), it was hypothesized that simply changing the protecting groups to electron neutral groups would enable the desired oxidation to take place. This change in protecting group scheme would require global alkylation conditions rather than the previously used acylation conditions. Considering that the parent flavanone contains four different hydroxyl groups, this transformation was not expected to be a trivial task.

1.7 Development of Global Protection Conditions

Methoxy methyl ethers (MOM) were chosen as the replacement protecting group due their tolerance of the strongly basic conditions required to effect enolization, as well as the mild acidic conditions required to cleave the acetals. An examination of the literature revealed that the MOM protecting group had not been used in a global protection. Narigenin (**I-74**) was chosen as a model system as it possessed similar hydroxylation pattern as the parent substrate. Compatibility with base was first evaluated. Sodium hydride in DMF, standard conditions for the alkylation of phenols, yielded no product, and instead gave the retro-cyclization to the chalcone (**Table 1-3**, entry 1). Mild bases like potassium carbonate and Hunig's base yielded minimal conversion, even being allowed to stir for several days. Tracking these reactions indicated that the first two alkylation events occurred rapidly, with the third being quite slow. Isolation of the

bis-MOM protected product **I-76** revealed that the phenol in the 5-position was the recalcitrant hydroxyl group. This is unsurprising since this position is a vinylic acid, with the phenol proton appearing as a broad singlet in the 12 ppm region typically associated with carboxylic acids in ^1H NMR spectra. Given the limited selection of bases, as well as low nucleophilicity of the 5-phenol, activation of the electrophile seemed a prudent area of investigation. The addition of iodide additives, sodium iodide and the more soluble tetrabutylammonium bromide began to yield appreciable amounts of **I-75** with heating to 40 °C. Despite these encouraging results, further improvements were not realized by substituting in other mild bases. However, Mander and co-workers previously reported the use of DMAP as a base to facilitate MOM protection of a tertiary alcohol on a complex intermediate. The addition of DMAP to the established conditions yielded a greatly improved conversion to **I-75**, obviating the need for heat and thus allowing the isolation of **I-75** in 70% yield (Table 1–3, entry 7).

Table 1–3. Optimization of Global MOM Protection of Narigenin



Entry	Base	Additive	Solvent	Temp.	Isolated Yield
1	NaH	–	DMF	0 °C	–
2	K ₂ CO ₃	–	DMF	23 °C	Mixture
3	DIPEA	–	DCM	23 °C	Mixture
4	DIPEA	NaI	DCM	40 °C	20%
5	DIPEA	TBAI	DCM	40 °C	24.5%
6	DIPEA	NaI, DMAP	DCM	23 °C	65%
7	DIPEA	TBAI, DMAP	DCM	23 °C	70%

With these conditions in hand, they were applied to the target system. The entire cyclization sequence was re-worked to provide the most efficient mass recovery and throughput. Purification of the unprotected pentahydroxy chalcone was challenging, with mass recovery inconsistent. Gratifyingly, this material could be used without purification in the biomimetic cyclization, enabling a greatly improved 72% yield over two steps. Conditions were found to enable purification of tetrahydroxy flavanone, thus positioning us to test the developed global protection conditions.

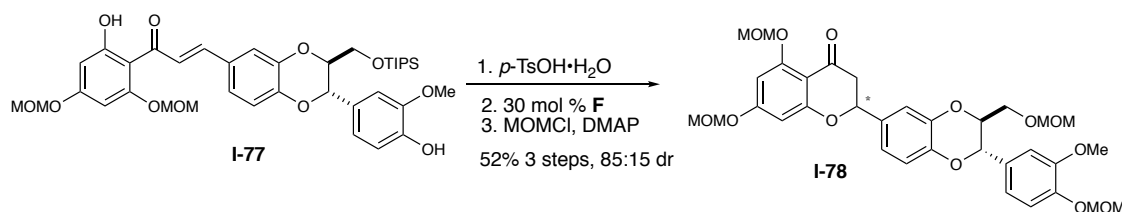


Figure 1-14. Cyclization Sequence to Yield MOM-Protected Flavanone

With some small modifications, the globally protected flavanone **I-78** could be isolated in 72% yield, 85:15 dr on ~150 mg scale. With a scalable route to our desired protected flavanone, we were positioned to test the α -hydroxylation hypothesis.

1.8 Synthesis Endgame

1.8.1 Rubottom Oxidation Sequence of MOM protected Flavanone

Subjecting **I-78** to lithium hexamethyldisilane in the presence of a TMSCl-TEA adduct yielded the silyl enol ether (**Figure 1-15**).¹¹¹ **I-78** proved to be quite sensitive to the concentration of base present, often ring opening to the 2' hydroxyl chalcone, particularly if base was added too rapidly. Adding base as dilute solution (0.1 M) to a mixture of the flavanone and TMSCl-TEA adduct mitigated this issue. Due to the instability of the TMS silyl enol ether, it was not purified and subjected to DMDO (**Figure 1-15**).

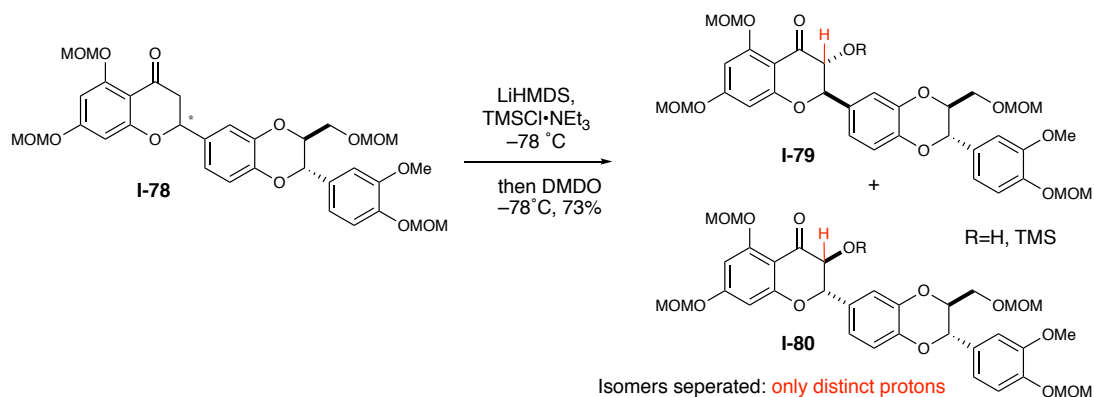


Figure 1-15. Rubottom Oxidation of MOM-Protected Flavanone

Gratifyingly, the product was furnished in 73% total yield, as a mixture of hydroxyl and trimethyl silyl ether product. Upon evaluation by chiral HPLC, the product was revealed to be 3:2 of diastereomers. Since the diastereomers now differed by multiple stereogenic centers, we believed that UV absorption properties could differ more significantly, as compared to the previous diastereomers. Unfortunately, as with the silybin isomers, these diastereomers were difficult to differentiate by ¹H and ¹³C NMR spectroscopy.¹¹² Using a semi-preparative (S,S)-Whelk-O column, the diastereomers were separated and compared. Mass recovery supported the 3:2 ratio and it was further observed that the chemical shift of the C-2 proton of each diastereomer was distinct. Analysis of the mixture confirmed the 3:2 ratio and with *J*-values of ~12.2 Hertz, it was confirmed that these were both *trans* diastereomers. Quenching conditions at cryogenic conditions were surveyed as remaining base could have been acting upon the silyl enol ether product, with no change reaction outcome. To investigate if the enolate species was not being trapped quickly enough, additional equivalents of TMSCl-TEA adduct were employed, which only prevented enolization from occurring. Additionally, the use of TMS-Br as a potentially more reactive silylating agent was unsuccessful. Finally, HMPA was added to

potentially disrupt aggregation of the lithium enolate species, again with the same outcome of 3:2 dr.

The sensitivity of flavanone **I-78** to the hard enolization conditions was unexpected given literature reports of the Rubottom oxidations sequence on unsubstituted flavanones. The procedure for the formation of the silyl enol ether was reported as LDA being added to unsubstituted flavanone **I-81**, allowing enolization to take place, *followed by addition of TMS-Cl*.

(**Figure 1-16**).¹¹³

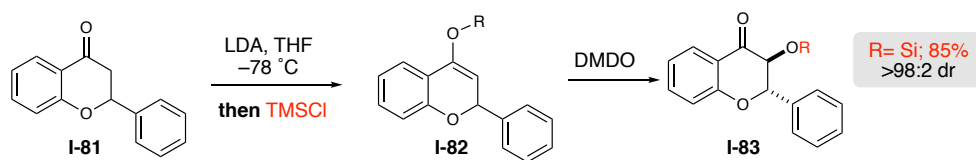


Figure 1-16. Rubottom Oxidation of Unsubstituted Flavanone

This is in stark contrast to observations on both the global MOM protection of narigenin as well studies towards the enolization of **I-78** that upon subjection to strongly basic conditions at temperatures ranging from RT to $0\text{ }^{\circ}\text{C}$ to $-78\text{ }^{\circ}\text{C}$, flavanones with the 5-hydroxyl or 5-MOM ether rapidly ring opened to the chalcone. This striking difference in reactivity is attributed to the planar, allylic 1,3 relationship imposed by the fused ring system. We hypothesize that upon enolization the electronic repulsion of the 5-MOM ether and the enolate lead to strain that is analogous to the 1,3-allylic strain seen in 1,8-dimethyl naphthalene (**Figure 1-17**).¹¹⁴

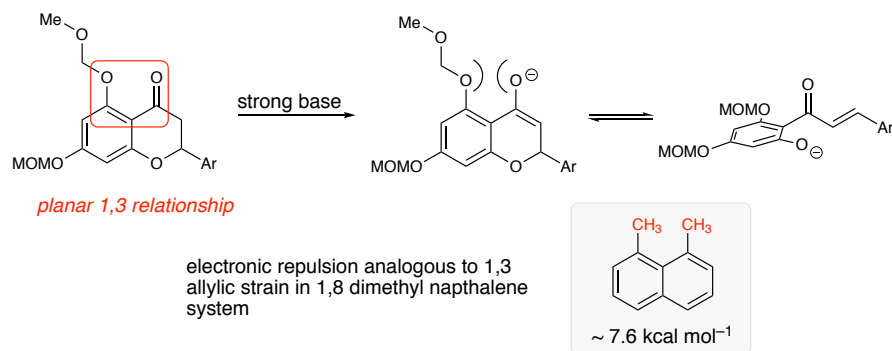


Figure 1-17. 1,3 Allylic Strain as Potential Driver of Flavanone Enolate Ring Opening

With this analysis, we hypothesized that this erosion of stereochemistry was likely taking place during the enolization step, and therefore alternate methods to access the necessary silyl enol ether could ameliorate these isomerization issues.

1.8.2 Investigation of Soft Enolization Conditions

Based on the hypothesis that the undesired ring-opening was occurring under anionic conditions, soft enolization methods presented an alternative route to the desired silyl enol ether. A variety of silicon Lewis acids with trimethylamine base were evaluated (**Figure 1-18**). Trimethylsilyl iodide was generated *in situ* using TMSCl and iodide sources and evaluated on MOM protected narigenin.¹¹⁵ This system provided mixtures of silyl enol ether and predominantly silylated chalcone **I-86**. The use of stronger Lewis acids like TMSOTf required the use of THF to attenuate its reactivity, as even at cryogenic conditions, silylated chalcone **I-86** was the primary product. TMS-Br proved the most promising, with the reactivity proving tunable by ratio of DCM/THF. However using these conditions on the elaborate system yielded the desired oxygenated product, in low yield in the same 3:2 ratio. Further investigation of enolization with titanium Lewis acids yielded no observed product upon subjection to DMDO.

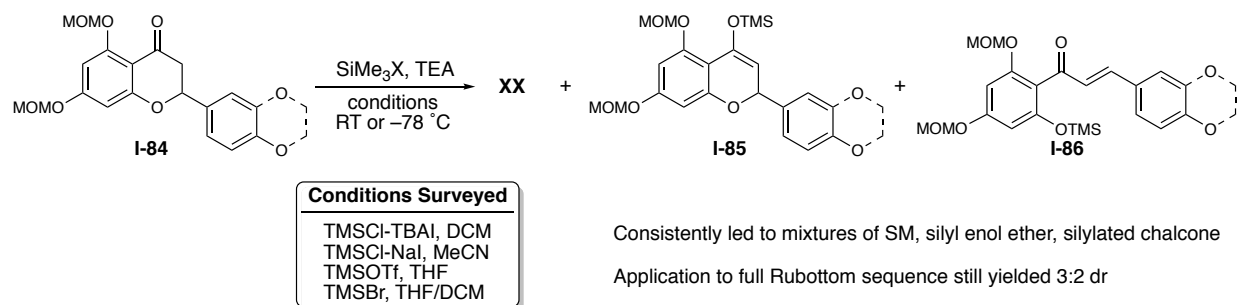


Figure 1-18. Investigation of Soft Enolization Conditions

1.8.3 Completion of the Synthesis

With these efforts unsuccessful, attention was turned towards quantifying the amount of epimerization occurring under the hard enolization/Rubottom sequence. Using a Regispack semi-preparative column, the diastereomers of the MOM-protected flavanone **I-78** were separated. Subjection of the stereochemically pure MOM-flavanone yielded a 9:1 ratio of diastereomers (**Figure 1-19**). With the goal of completing the first selective synthesis of a silybin isomer, it was decided that this minor amount of epimerization was acceptable. In order to produce stereochemically pure final product, the 9:1 ratio of diastereomers was resolved using a semi-preparative Whelko column.

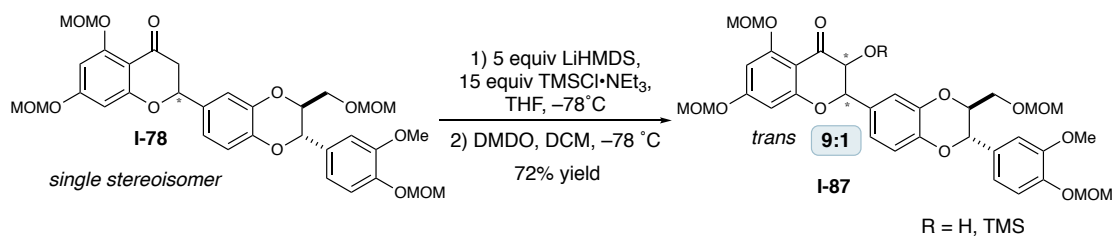


Figure 1-19. Rubottom Sequence on a Single MOM-Flavanone Stereoisomer

The final step that remained was the global deprotection of the MOM-protected hydroxyl flavanone (**I-87**). The previously used acetal metathesis conditions of *p*-TsOH•H₂O, neopentyl glycol proved mild, providing the fully deprotected product with gentle heating at 40 °C over 30

hours (**Figure 1-20**). Characterization of the material by ^1H and ^{13}C NMR spectroscopy showed a match to isosilybin B, but as previously noted, the differentiation of these isomeric compounds is extremely difficult with standard NMR techniques.

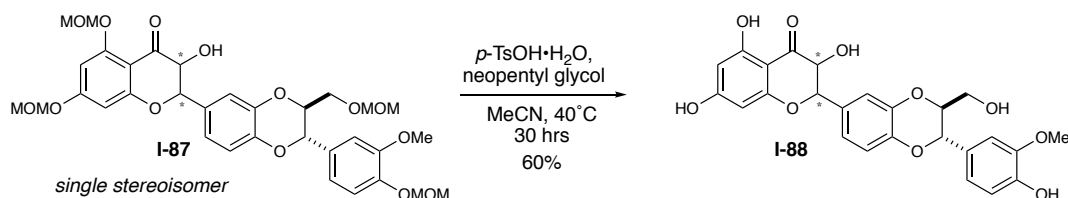


Figure 1-20. Global Deprotection to Yield Final Product

1.9 Confirmation of Absolute Stereochemistry

Electronic circular dichroism (ECD) is a powerful tool for the interrogation of the chiral compounds that interact with light.¹¹⁶ ECD has been used extensively in the assignment of absolute stereochemistry of flavanones,^{117,118} including the silybin natural products.⁹⁷ Oberlies and co-workers have further employed this technique in conjunction with single-crystal X-ray crystallography of a heavy-atom containing isosilybin A derivative to unambiguously assign the absolute stereochemistry of silybin natural products.⁹⁹

Based on the work of Gaffield,¹¹⁷ Cotton effects around the wavelengths of 320 nm and 290 nm indicates the absolute stereochemistry at C-2 and C-3 (a negative Cotton effect at approx. 320 nm and positive value at approx. 290 nm indicates 2S, 3S and vice-versa), while a Cotton effect in the area of 220-240 nm imparts the absolute stereochemistry at the C-7' & C-8'. A positive value in this area indicates 7S', 8'S while a negative value indicates 7R', 8'R.¹⁴ By these rules, the absolute configurations of (–)-isosilybin A is 2S, 3S, 7'S, 8'S (**Figure 1-21**).⁹⁷

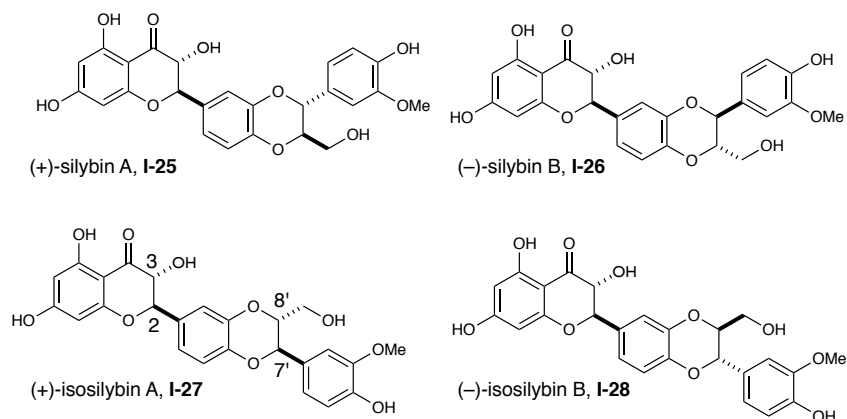
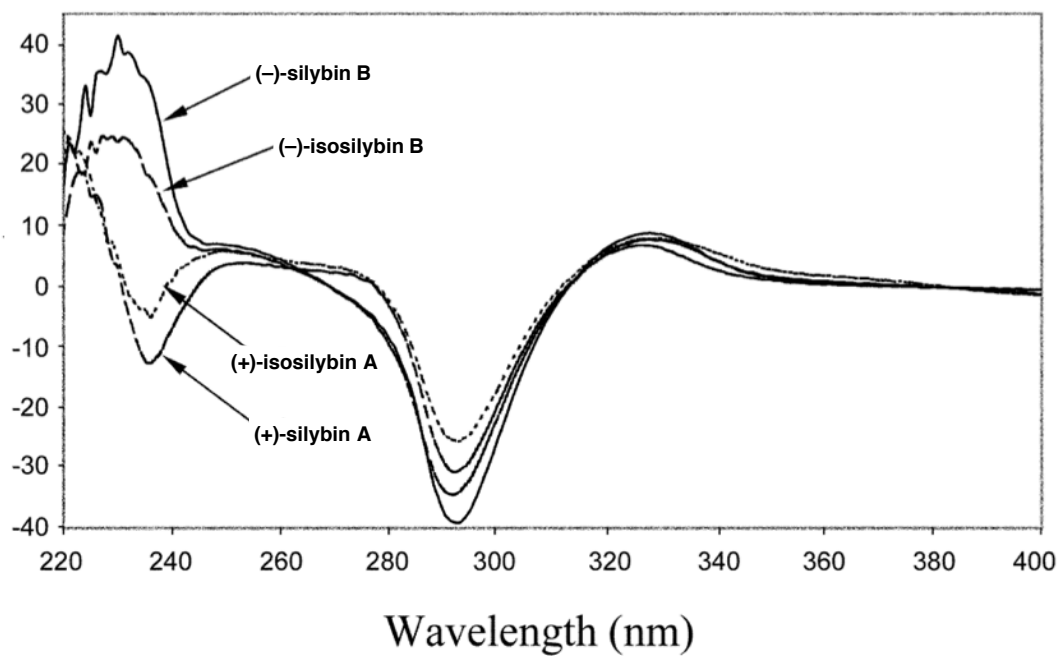


Figure 1-21. CD Spectra of Silybin Natural Products⁹⁷

The CD spectra of our synthetic material, both the final isolated product as well as the MOM minor protected minor diastereomer **I-90**, were collected in methanol. **It is important to note that the source of methanol is crucial.** HPLC grade methanol was found to be required for the characterization of these compounds. Use of methanol from an SDS system repeatedly lead

to decomposition of samples. This is likely due to alumina from the drying column or mild basification of the methanol as result of the drying process.

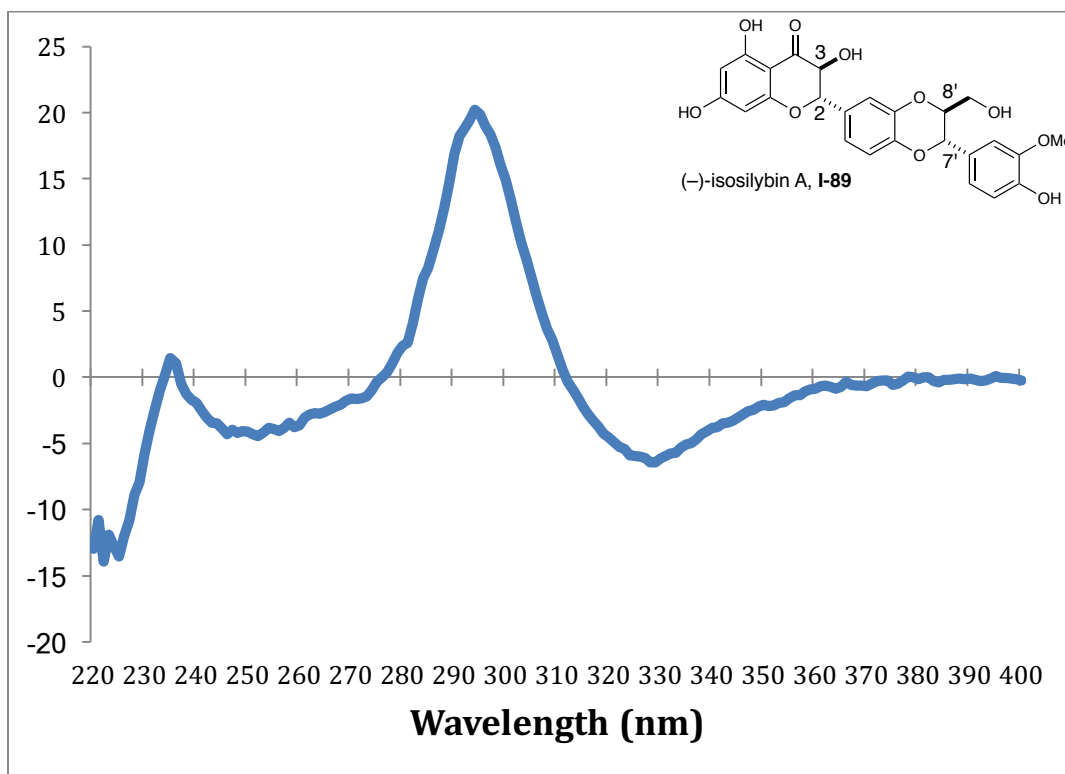


Figure 1-22. CD Spectra of Major Synthetic Silybin Product, Assigned (-)-Isosilybin A

The CD spectra of the final product derived from the major cyclization diastereomer revealed it to be the antipode of isosilybin A (**Figure 1-22**). The Cotton effects around 320 nm and 290 nm indicates the absolute stereochemistry at C-2 and C-3 is inverted with respect to the natural material. However, the positive Cotton effect in the area of 230 nm indicates that absolute stereochemistry at C-7' & C-8' is correct in relation to the natural configuration. Inversion of the entire spectra shows it to match isosilybin A, thus confirming this material to be the enantiomer of isosilybin A.

Examination of the CD spectra of the minor diastereomer shows a negative Cotton effect at 290 nm confirming the natural configuration at C-2 and C-3. The positive Cotton effect in the area of 230 nm indicates that absolute stereochemistry at C-7' & C-8' is correct in relation to the natural configuration. Thus the minor diastereomer can be assigned as MOM-(–)-isosilybin B (Figure 1-23).

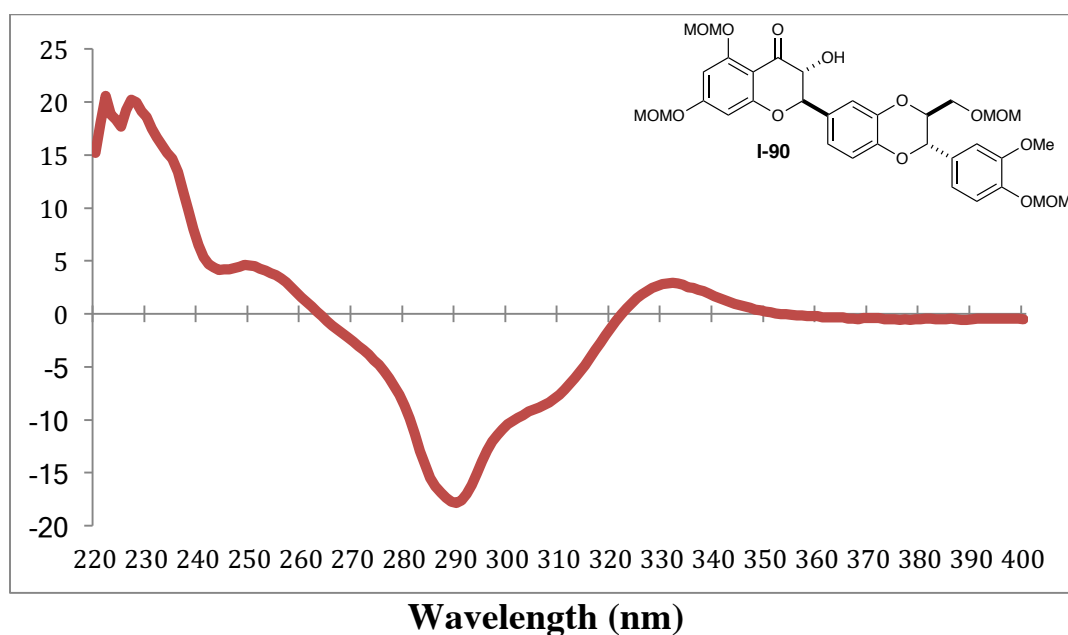


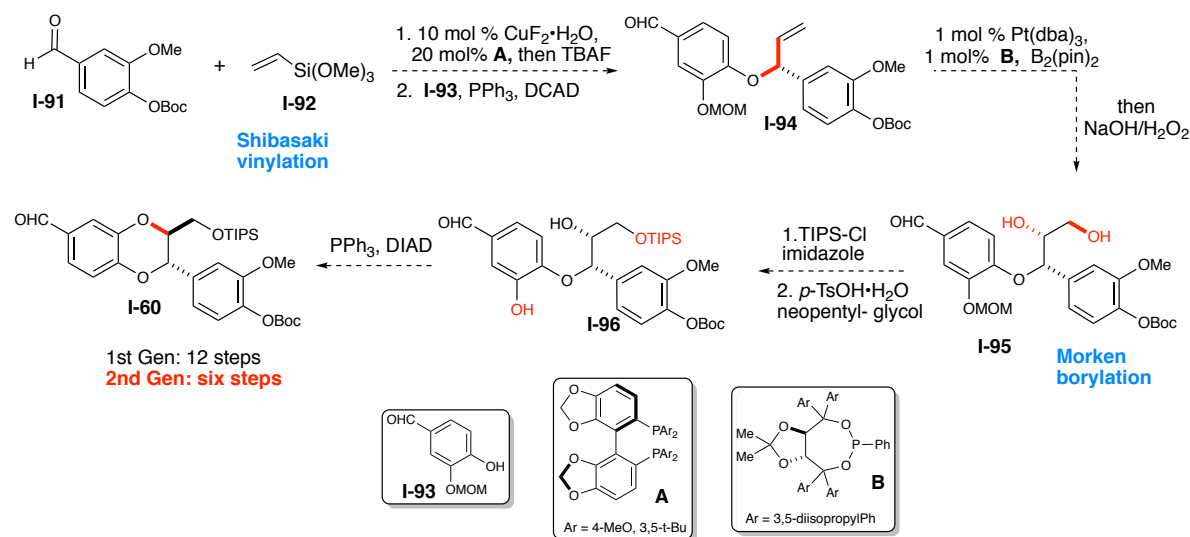
Figure 1-23. CD Spectra of Minor Synthetic Silybin Product, Assigned MOM-(–)-Isosilybin B

1.10 Future Directions

Given that this is the first selective total synthesis of a silybin natural product, there is room for significant improvements to the synthetic route. Without changing the overall strategy to the benzodioxane aldehyde system, a second generation approach that requires half the number of synthetic steps can be designed (Scheme 1-8). Rapid access to the corresponding allylic alcohol can be achieved using a robust copper-catalyzed Shibasaki vinylation reaction.¹¹⁹ This reaction works well with electron rich aldehydes (99% yield, 92% ee on 4-methoxy-

benzaldehyde), employing commercially available DTBM-SEGPHOS **A** as a ligand. As such, either antipode could be accessed. A Mitsunobu similar to that already used would furnish allylic ether **I-94**. A diastereoselective platinum-catalyzed diboration-oxidation sequence would then provide diol **I-95**. This robust methodology developed by Morken is highly stereoselective for a wide variety of substrates, including chiral allylic ethers.¹²⁰

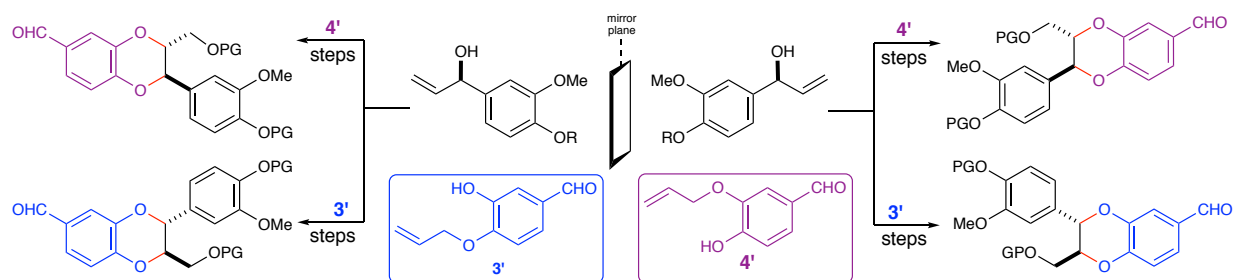
Scheme 1-8 Second Generation, Stereodivergent Approach to Benzodioxane Aldehyde



For the diborylation of **I-94**, enantioenriched TADDOL ligand **B** will still be required for excellent stereoselectivity, but the low loading and ready availability of the ligand mitigates this diastereoselective transformation. Importantly, use of a chiral ligand will enable catalyst control, enabling stereodivergent preparation of the natural and unnatural silybin analogs. *Importantly, Morken and co-workers have demonstrated that the chiral catalyst generally overrides adjacent stereocenters and only minor match, mis-match issues were observed.* Additionally the use of the TADDOL-derived phosphonite ligand allows for further ligand tailoring to this specific system if

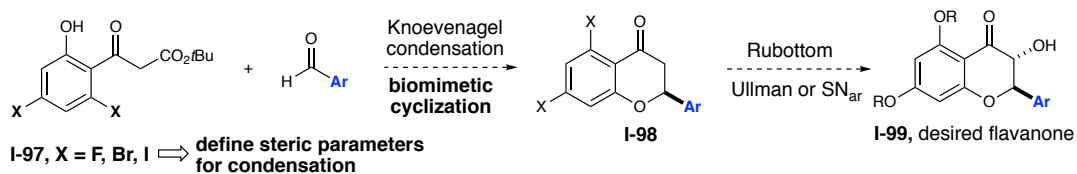
necessary.¹²¹ This then enables the unified synthesis of every benzodioxane unit, natural and unnatural of the silybin natural products (**Scheme 1-9**).

Scheme 1-9 Unified Approach to Silybin Benzodioxane Subunits



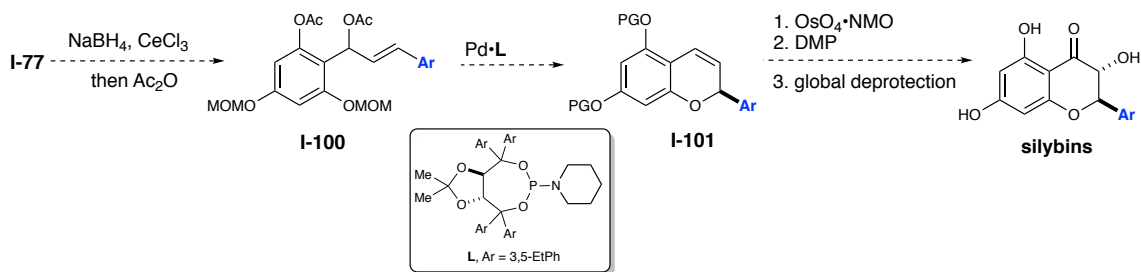
While streamlining and unification of the synthesis of the benzodioxane subunits would be an important advance, a serious challenge remains to be addressed, namely the construction of the flavanone core with the complete stereocontrol. Given that the current route would require the unnatural enantiomer of quinidine, alternatives are required. Two alternative approaches are proposed. The first builds upon our existing cyclization of arylidene malonates. Given that the 2,6-hydroxy β -keto esters proved unable to undergo Knoevenagel condensation, a work-around strategy could be devised. While Nibbs investigated late-stage C-H oxidation approaches, a simpler approach may be within reach. Using halogens as placeholders for later installation of hydroxyl groups is an unexplored strategy (**Scheme 1-10**). The stereochemical limitations for condensation could be rapidly delineated on a model system. Fluorine is likely to be tolerated, but it would be interesting to investigate the size limitations of other halogens. Metal couplings or nucleophilic aromatic substitution could be used following successful cyclization and Rubottom oxidation.

Scheme 1-10 Alternate Approach to Biomimetic Cyclization Precursor



A different approach would build upon a palladium-mediated cyclization to yield chromenes developed in the Scheidt laboratory (Scheme 1-11).¹²² Upon reduction and acetylation, chalcone **I-77** could be diverted to the required cyclization precursor. The palladium catalyzed reaction using phosphoramidite ligand **L** would then provide the chromene precursor **I-100**. This chromene should be easily oxidized to the desired hydroxy-flavanone by diastereoselective dihydroxylation and regiospecific benzylic oxidation as demonstrated in the initial disclosure of this methodology.

Scheme 1-11 Alternate Cyclization Approach



Finally, the greatest challenge remaining in the realm of silybin natural products is the lack of a fundamental understanding of the mechanism of action of these compounds. Despite decades of work invested in categorizing the effects of these compounds *in vivo* and *in vitro* **there is no known molecular target**. The broad polypharmacology of these compounds, able to affect disparate biological pathways, has remained a puzzle. This profile of bioactivity is not unique, as many polyphenols display this sort of polypharmacology on unrelated signaling

pathways. On such rational is that these compounds are typically localized in membranes rather than binding with a specific protein of interest and are thus positioned to interact with a broad variety of biological pathways.¹²³ Ultimately, future work should focus on the pinpointing a molecular target or mechanism of action. The synthetic tools developed in this work are poised to drive chemical biology efforts to unravel this mystery.

1.11 Conclusion

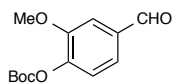
In summary, the first selective total synthesis of a member of the complex flavanolignan family, the silybins, has been completed in 16 steps (longest linear). The significant challenge of preparing polyphenolic flavanones has been highlighted, with the polyphenolic functionality the source of many synthetic issues. Our synthetic strategy employed a late-stage biomimetic cyclization of a chalcone to install the benzopyranone ring, which was inspired by the biosynthesis route employing chalcone isomerase (CHI). The applications of an asymmetric Sharpless dihydroxylation and Mitsunobu inversion transformations further provide a robust and flexible approach to selectively synthesize the benzodioxane ring systems of the silybin isomers. These stereoselective operations combined with our biomimetic cyclization to install the flavanone core ring system have provided a general platform to access all silybins. Future work should focus on incorporating program of synthesis supported chemical biological investigation of these compounds unlock their full potential in the realm of prostate cancer and beyond.

1.12 Experimental Section

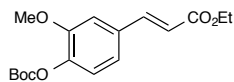
All reactions were carried out under a nitrogen atmosphere in oven-dried glassware with magnetic stirring. THF, toluene, and DMF were purified by passage through a bed of activated alumina.¹²⁴ Reagents were purified prior to use unless otherwise stated following the guidelines of

Perrin and Armarego.¹²⁵ Silica gel used in flash chromatography using Silicycle SiliaFlash P60 silica gel 60 (230-400 mesh). Analytical thin layer chromatography was performed on EM Reagent 0.25 mm silica gel 60-F plates. Visualization was accomplished with UV light and ceric ammonium nitrate stain or potassium permanganate stain followed by heating. Infrared spectra were recorded on a Bruker Tensor 37 FT-IR spectrometer. ¹H NMR spectra were recorded on AVANCE III 500 MHz w/ direct cryoprobe (500 MHz) spectrometer and are reported in ppm using solvent as an internal standard (CDCl₃ at 7.26 ppm, (CD₃)₂SO at 2.50 ppm). Data are reported as (ap = apparent, s = singlet, d = doublet, t = apparent triplet, q = quartet, m = multiplet, b = broad; coupling constant(s) in Hz; integration.) Proton-decoupled ¹³C NMR spectra were recorded on an AVANCE III 500 MHz w/ direct cryoprobe (125 MHz) spectrometer and are reported in ppm using solvent as an internal standard (CDCl₃ at 77.16 ppm, (CD₃)₂SO at 39.52 ppm). ⁷⁷Se spectra were acquired at 26 °C on a 400 MHz Agilent 400MR-DD2 spectrometer equipped with a OneNMR probe and a 7600AS autosampler; this system was funded by NSF CRIF grant CHE-104873. Optical rotations were measured on a Perkin Elmer Model 341 Polarimeter with a sodium lamp. Mass spectra were obtained on a WATERS Acquity-H UPLC-MS with a single quad detector (ESI) or an Agilent 7890 gas chromatograph equipped with a 5975C single quadrupole EI-MS detector.

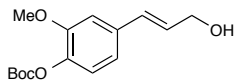
1.12.1 Experimental Procedures and Characterization Data



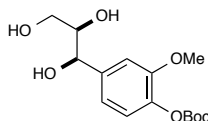
tert-butyl (4-formyl-2-methoxyphenyl) carbonate (SI-1): To a 500 mL round bottom flask was added vanillin (15.2 g, 100 mmol), CH_2Cl_2 (200 mL), and DMAP (2.44 g, 20 mmol). Boc_2O (24 g, 110 mmol) was added portionwise over the course of 5 min to the uncapped round bottom flask. Light effervescence occurred as the reaction became a bright yellow-green color. After 15 min, the reaction became colorless and TLC analysis indicated complete consumption of the starting material. The reaction mixture was poured into a separatory funnel, washed three times with 1.0 M HCl, and dried over anhydrous Na_2SO_4 to afford aldehyde **SI-1** (23.6 g, 94%) as a white powder. The material was carried on without further purification. Analytical data for **SI-1**: IR (film) 3075, 2982, 2940, 2840, 2735, 1764, 1701, 1603, 1507, 1466, 1424, 1393, 1371, 1322, 1277, 1255, 1142, 1122, 1071, 1032, 959, 888, 780, 733, 637, cm^{-1} ; ^1H NMR (500 MHz, CDCl_3) δ 9.95 (s, 1H), 7.50 (d, $J = 1.7$ Hz, 1H), 7.47 (dd, $J = 8.0, 1.8$ Hz, 1H), 7.31 (d, $J = 8.0$ Hz, 1H), 3.93 (s, 3H), 1.56 (s, 9H); ^{13}C (125 MHz, CDCl_3) δ 191.1, 152.0, 150.6, 145.1, 135.0, 124.8, 123.0, 110.7, 84.2, 56.1, 27.5; LRMS (ESI): Mass calcd for $\text{C}_{13}\text{H}_{16}\text{O}_3$ $[\text{M}+\text{Na}]^+$, 275. Found $[\text{M}+\text{Na}]^+$, 275.



(E)-ethyl 3-(4-((*tert*-butoxycarbonyl)oxy)-3-methoxyphenyl)acrylate (I-53): To a 500 mL round bottom flask was added THF (200 mL) and triethylphosphonoacetate (10.2 mL, 50.7 mmol, 1.28 equiv). The mixture was cooled to 0 °C, and NaH (2.06 g, 51.5 mmol, 1.3 equiv) was added in three portions. The reaction mixture was allowed to stir until homogenous (~30 min), and then aldehyde **SI-1** (7.73 g, 30.6 mmol) in THF (50 mL) was added dropwise via cannula over 15 min. The reaction mixture was allowed to warm to ambient temperature overnight. After 12 h, the yellowish-green mixture was quenched with H₂O (150 mL), poured into a separatory funnel, and extracted with EtOAc (3 x 100 mL). The combined organic layers were washed twice with sat. brine solution and dried over anhydrous MgSO₄, filtered and concentrated under reduced pressure. The residue recrystallized from hexanes to afford enoate **I-53** (12.01 g, 94%) as large, white crystalline chunks. Analytical data for **I-53**: IR (film) 2981, 2937, 2847, 1762, 1711, 1639, 1511, 1370, 1255, 1176, 1144, 1125, 1035 cm⁻¹; ¹H NMR (500 MHz, CDCl₃) δ 7.64 (d, *J* = 16.0 Hz, 1H), 7.15 – 7.09 (m, 3H), 6.38 (d, *J* = 16.0 Hz, 1H), 4.27 (q, *J* = 7.1 Hz, 2H), 3.88 (s, 3H), 1.55 (s, 9H), 1.34 (t, *J* = 7.1 Hz, 3H); ¹³C (125 MHz, CDCl₃) δ 166.8, 151.5, 151.1, 143.9, 141.7, 133.3, 122.9, 121.2, 118.4, 111.2, 83.8, 60.6, 55.9, 27.6, 14.3; LRMS (ESI): Mass calcd for C₁₇H₂₂O₆ [M+H]⁺, 323. Found [M+H]⁺, 323.



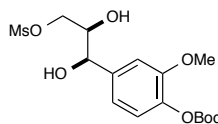
(E)-tert-butyl (4-(3-hydroxyprop-1-en-1-yl)-2-methoxyphenyl) carbonate (SI-2): To a 1 L round bottom flask was added enoate **I-53** (15 g, 46.5 mmol). The flask was charged with THF (120 mL) and the mixture was cooled to $-78\text{ }^{\circ}\text{C}$. DIBAL-H (116 mL, 1.0 M solution in hexanes, 2.5 equiv) was added to the reaction via cannula. After 2 h, TLC indicated complete consumption of starting material. The reaction was quenched at $0\text{ }^{\circ}\text{C}$ with a saturated solution of potassium sodium tartrate (cautious addition of 100 mL) and allowed to warm to ambient temperature overnight. Once a bi-phasic mixture was observed, the mixture was poured into a separatory funnel and extracted with EtOAc (3 x 100 mL). The combined organic layers were washed once with sat. brine solution, and dried over anhydrous MgSO_4 to afford allylic alcohol **SI-2** as a yellow oil. The material was carried on without further purification. $^1\text{H NMR}$ (500 MHz, $(\text{CD}_3)_2\text{CO}$) δ 7.11 (d, $J = 8.2$ Hz, 1H), 7.06 (dd, $J = 8.2, 2.0$ Hz, 1H), 6.68 (dt, $J = 16.1, 1.8$ Hz, 1H), 6.48 (dt, $J = 15.9, 5.2$ Hz, 1H), 4.31 (td, $J = 5.4, 1.9$ Hz, 2H), 3.95 (s, 3H), 1.58 (s, 9H).



tert-butyl (2-methoxy-4-((1R,2R)-1,2,3-trihydroxypropyl)phenyl) carbonate (I-54):

A 1 L round bottom flask containing allylic alcohol **SI-2** (10.1 g, 36 mmol) was charged with 150 mL *tert*-butanol and 150 mL of H_2O . The mixture was stirred until homogeneous. AD-Mix β

(50 g, 1.4 g/mmol **SI-2**) and methanesulfonamide (3.77 g, 30.6 mmol, 1.1 equiv) was then added. The brownish-orange mixture was allowed to stir for 24 h and upon consumption of starting material (determined via $^1\text{H NMR}$), sodium sulfite (5 g, 39.6 mmol) was added and the mixture stirred for 2 h. The tan, heterogeneous mixture was filtered and rinsed with CH_2Cl_2 (2 x 400 mL). The aqueous layer was extracted with CH_2Cl_2 (3 x 400 mL). The combined organic extracts were washed with sat. brine solution (200 mL), dried over anhydrous Na_2SO_4 and concentrated under reduced pressure. The resulting residue was dissolved in benzene and concentrated (3x) to remove residual *tert*-butanol, then subjected to flash column chromatography (SiO_2 , 5 \rightarrow 10% $\text{MeOH}/\text{CH}_2\text{Cl}_2$) to yield triol **I-54** (7.8 g, 69% yield over two steps) as a white, hygroscopic foam. Analytical data for **I-54** $[\alpha]_D^{25} = -19.0$ (CHCl_3 , $c = 0.42$); IR (film) 3374, 2982, 1758, 1608, 1511, 1370, 1256, 1142, 1031, 889, 739 cm^{-1} ; $^1\text{H NMR}$ (500 MHz, CDCl_3) δ 7.10 (d, $J = 8.1$ Hz, 1H), 7.03 (d, $J = 1.9$ Hz, 1H), 6.92 (dd, $J = 8.2, 1.9$ Hz, 1H), 4.70 (d, $J = 6.4$ Hz, 1H), 3.86 (s, 3H), 3.79 – 3.70 (m, 1H), 3.65 (dd, $J = 11.5, 3.4$ Hz, 1H), 3.54 (dd, $J = 11.5, 4.9$ Hz, 1H), 1.55 (s, 9H); $^{13}\text{C NMR}$ (125 MHz, CDCl_3) δ 151.6, 151.4, 139.9, 139.5, 122.5, 118.8, 110.6, 83.7, 75.6, 74.6, 63.3, 56.0, 27.6; LRMS (ESI): Mass calcd for $\text{C}_{15}\text{H}_{22}\text{O}_7$ $[\text{M}+\text{H}]^+$, 315. Found $[\text{M}+\text{H}]^+$, 315.

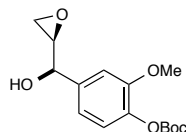


(2*R*,3*R*)-3-(4-((*tert*-butoxycarbonyl)oxy)-3-methoxyphenyl)-2,3-dihydroxypropyl 4-

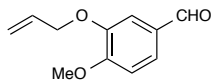
methanesulfonate (SI-3): To a 1 L round bottom flask containing triol **I-54** (8.0 g, 25.5 mmol)

was added CH_2Cl_2 (500 mL), 2,4,6-trimethylpyridine¹ (33.9 mL, 255 mmol, 10 equiv). The resulting solution was stirred until homogenous and subsequently cooled to 0 °C. MsCl (2.2 mL, 28.0 mmol, 1.1 equiv) was then added in a single portion. The solution was stirred for 2 h at 0 °C then transferred to a fridge (4 °C). After 21 h, the reaction was poured over H_2O (300 mL) and diluted with CH_2Cl_2 . The water layer was extracted with CH_2Cl_2 (3 x 150 mL). The pooled organic extracts were washed with sat. citric acid solution (3 x 300 mL), dried over anhydrous Na_2SO_4 , and concentrated under reduced pressure. The resulting residue was purified via flash column chromatography (SiO_2 , 2.5→8% MeOH/ CH_2Cl_2) to yield mesylate **I-54** (7.4 g, 74% yield) as a white, hygroscopic foam. (*NOTE: It is recommended that this material be used immediately or stored at -78 °C frozen in a benzene matrix due to water sensitivity.*) Analytical data for **I-54**: $[\alpha]_D^{25} = -5.1$ (CHCl_3 , $c = 0.91$) IR (film) 3404, 2983, 2939, 1758, 1351, 1256, 1112, 1035, 964, 813, 737, 679 cm^{-1} ; ^1H NMR (500 MHz, CDCl_3) δ 7.13 (d, $J = 8.1$ Hz, 1H), 7.03 (d, $J = 1.9$ Hz, 1H), 6.95 (dd, $J = 8.2, 1.9$ Hz, 1H), 4.74 (dd, $J = 6.5, 3.7$ Hz, 1H), 4.29 (dd, $J = 11.1, 3.6$ Hz, 1H), 4.15 (dd, $J = 11.1, 5.3$ Hz, 1H), 3.99 – 3.95 (m, 1H), 3.88 (s, 3H), 3.07 (s, 3H), 2.77 (d, $J = 4.3$ Hz, 1H), 2.58 (d, $J = 3.6$ Hz, 1H), 1.55 (s, 9H); ^{13}C NMR (125 MHz, CDCl_3) δ 151.5, 140.1, 138.6, 122.7, 118.7, 110.6, 83.8, 73.7, 73.4, 70.0, 56.1, 37.6, 27.6; LRMS (ESI): Mass calcd for $\text{C}_{16}\text{H}_{24}\text{O}_5\text{S}$ $[\text{M}+\text{H}]^+$, 393. Found 393.

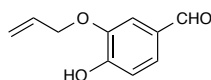
¹ Freshly distilled from CaH_2 .



tert-butyl (4-((R)-hydroxy((R)-oxiran-2-yl)methyl)-2-methoxyphenyl) carbonate (I-55): To a 1 L round bottom flask was added mesylate **SI-3** (6.2 g, 15.8 mmol) and MeOH (200 mL). The mixture was cooled to 0 °C and allowed to stir until the homogenous (~10 min). K_2CO_3 (6.55 g, 47.4 mmol, 3 equiv) was added to the mixture. After 1 h, the reaction was quenched with sat. aq. NH_4Cl (100 mL). The mixture was extracted with CH_2Cl_2 (3 x 150 mL), and the combined organics were washed with sat. brine solution and dried over anhydrous $MgSO_4$. Purified by flash column chromatography (SiO_2 , 30% EtOAc/hexanes) to afford epoxide **I-55** (4.1 g, 88%) as a white solid. Analytical data for **7**: $[\alpha]_D^{25} = -2.2$ ($CHCl_3$, $c = 1.09$, er = 99:1); IR (film) 3437, 3064, 2982, 2938, 2882, 2848, 1760, 1608, 1512, 1465, 1419, 1396, 1371, 1276, 1258, 1212, 1145, 1126, 1034, 919, 890, 781, 742 cm^{-1} ; 1H NMR (500 MHz, $CDCl_3$) δ 7.12 (d, $J = 8.1$ Hz, 1H), 7.09 (d, $J = 1.8$ Hz, 1H), 6.94 (dd, $J = 8.1, 1.9$ Hz, 1H), 4.49 – 4.43 (m, 1H), 3.88 (s, 3H), 3.21 (ddd, $J = 5.3, 4.0, 2.8$ Hz, 1H), 2.89 – 2.85 (m, 1H), 2.83 (dd, $J = 4.8, 2.7$ Hz, 1H), 2.35 (d, $J = 3.9$ Hz, 1H), 1.55 (s, 9H); ^{13}C (125 MHz, $CDCl_3$) δ 151.5, 139.9, 139.0, 122.6, 118.4, 110.4, 83.6, 74.1, 56.0, 55.8, 45.4, 27.6; LRMS (ESI): Mass calcd for $C_{15}H_{20}O_6$ $[M+H_3O]^+$, 315. Found $[M+H_3O]^+$, 315. Enantiomeric ratio was measured by chiral HPLC (Chiralcel OD-H, 10% *i*-PrOH/hexanes, 1 mL/min, $Rt_{major} = 13.49$, $Rt_{minor} = 18.68$).



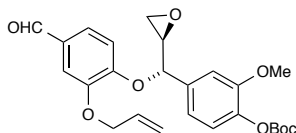
3-(allyloxy)-4-methoxybenzaldehyde (SI-4): To a 500 mL round bottom flask was added isovanillin (10 g, 65.7 mmol), K_2CO_3 (11.3 g, 82.1 mmol), acetone (130 mL), and allyl bromide (7.1 mL, 82.1 mol). The mixture was heated to reflux. After 3.5 h KBr was filtered from the reaction and the filtrate was collected and concentrated. The residue was diluted with water and extracted three times with EtOAc. The combined organics were washed once with sat. brine solution and dried to afford aldehyde **SI-4** (11.9 g, 94%) as a yellow oil. The material was carried on without further purification. Analytical data matched those reported in the literature.²



3-(allyloxy)-4-hydroxybenzaldehyde (I-56): To a flame-dried 250 mL round bottom flask containing aldehyde **SI-4** (10.6 g, 55.1 mmol) was added DMF (162 mL). Sodium ethanethiolate (5.8 g, 68.9 mmol) was added and the mixture was heated to 110 °C. After 1.5 h the reaction was cooled to ambient temperature. To the reaction mixture was added sat. aq. NH_4Cl (200 mL) then 1.0 M HCl (50 mL). The mixture was extracted with Et_2O (4 x 100 mL). The combined organics were washed with H_2O (4 x 100 mL) washed with sat. brine solution (1 x 100 mL), and dried over anhydrous $MgSO_4$ and concentrated under reduced pressure. Purified by flash column

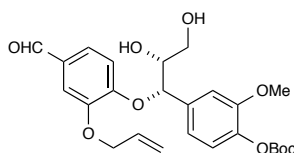
²M. Hayashida; M. Ishizaki; H. Hara *Chem. Pharm. Bull.* **2006**, *54*, 1299-1303.

chromatography (SiO₂, 20→25% EtOAc/hexanes) to afford phenol **I-56** (6.85 g, 59%) as a pale yellow solid. Analytical data for **I-56**: IR (film) 3354, 3081, 2929, 2838, 2734, 1678, 1592, 1510, 1443, 1426, 1407, 1289, 1273, 1197, 1162, 1121, 1016, 933, 867, 822, 766, 732 cm⁻¹; ¹H NMR (500 MHz, CDCl₃) δ 9.82 (s, 1H), 7.43 (m, 2H), 7.06 (d, *J* = 7.9 Hz, 1H), 6.22 (s, 1H), 6.07 (ddt, *J* = 16.1, 10.9, 5.6 Hz, 1H), 5.44 (d, *J* = 17.2, 1.1 Hz, 1H), 5.36 (m, *J* = 10.5, 1.0 Hz, 1H), 4.69 (d, *J* = 5.5 Hz, 2H); ¹³C (125 MHz, CDCl₃) δ 190.8, 151.8, 146.0, 131.9, 129.8, 127.5, 119.2, 114.5, 110.1, 69.9; LRMS (ESI): Mass calcd for C₁₀H₁₀O₃ [M+H]⁺, 179. Found [M+H]⁺, 179.



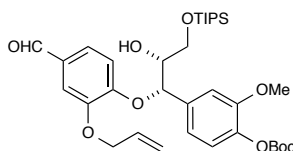
4-((S)-2-(allyloxy)-4-formylphenoxy)((R)-oxiran-2-yl)methyl-2-methoxyphenyl *tert*-butyl carbonate (I-57**):** To a 50 mL round bottom flask was added phenol **I-56** (728 mg, 4.08 mmol, 1.1 equiv) and DCAD (1.5 g, 4.08 mmol, 1.1 equiv). The flask was capped, equipped with a N₂ inlet, and purged with N₂. CH₂Cl₂ (20 mL) was added, and the mixture was cooled to 0 °C. Into this mixture was cannulated a mixture of epoxide **I-55** (1.1 g, 3.71 mmol) and PPh₃ (1.07 g, 4.08 mmol, 1.1 equiv) in CH₂Cl₂ (25 mL). After stirring for 30 min, the ice/water bath was removed. After 3 h the reaction was vacuum filtered to remove the hydrazine carboxylate and the solid was washed with hexanes. The filtrate was washed with 1 M NaOH (3 x 50 mL), then once with sat. brine solution, dried over anhydrous Na₂SO₄, and concentrated under reduced pressure. The resulting residue was purified by flash column chromatography (SiO₂, 20→35% EtOAc/hexanes)

to afford aldehyde **I-57** (1.60 g, 94%) as a white semi-solid. Analytical data for **I-57**: $[\alpha]_D^{25} = -0.92$ (CHCl₃, $c = 1.2$, $dr = 20:1$); IR (film) 3493, 3354, 3072, 2982, 2935, 2873, 2854, 2730, 1761, 1689, 1587, 1506, 1464, 1435, 1422, 1395, 1370, 1272, 1230, 1214, 1145, 1033, 1016, 889, 812, 780, 760, 740 cm⁻¹; ¹H NMR (500 MHz, CDCl₃) δ 9.79 (s, 1H), 7.39 (d, $J = 1.9$ Hz, 1H), 7.29 (dd, $J = 8.2, 1.9$ Hz, 1H), 7.12 (d, $J = 8.1$ Hz, 1H), 7.06 (d, $J = 1.9$ Hz, 1H), 6.99 (dd, $J = 8.2, 1.9$ Hz, 1H), 6.88 (d, $J = 8.2$ Hz, 1H), 6.09 (ddt, $J = 17.3, 10.4, 5.1$ Hz, 1H), 5.47 (dq, $J = 17.2, 1.6$ Hz, 1H), 5.32 (dq, $J = 10.6, 1.5$ Hz, 1H), 5.25 (d, $J = 3.9$ Hz, 1H), 4.65 (dt, $J = 4.5, 1.4$ Hz, 2H), 3.84 (s, 3H), 3.37 (td, $J = 3.9, 2.5$ Hz, 1H), 2.95 (dd, $J = 5.2, 2.5$ Hz, 1H), 2.86 (dd, $J = 5.2, 3.9$ Hz, 1H), 1.54 (s, 9H); ¹³C (125 MHz, CDCl₃) δ 190.8, 152.6, 151.6, 151.4, 149.5, 140.2, 135.7, 132.6, 130.9, 126.3, 122.8, 118.8, 117.8, 115.4, 111.7, 110.5, 83.7, 79.6, 69.6, 56.0, 54.3, 45.0, 27.6; LRMS (ESI): Mass calcd for C₂₅H₂₈O₈ [M+Na]⁺, 479. Found [M+Na]⁺, 479.



4-((1S,2R)-1-(2-(allyloxy)-4-formylphenoxy)-2,3-dihydroxypropyl)-2-methoxyphenyl tert-butyl carbonate (SI-6): To a 50 mL round bottom flask was added (*R,R*)-*N,N'*-bis(3,5-di-*tert*-butylsalicylidene)-1,2-cyclohexanediamino-cobalt(II) (800 mg, 1.33 mmol, 0.25 equiv. This was dissolved in toluene (14 mL) and AcOH (180 μ L, 3.15 mmol, 0.6 equiv was added to the bright red mixture. Upon addition of AcOH, the mixture turned a dark brown color. The reaction mixture was allowed to stir at ambient temperature open to air for 1 h. At this point, the solvent

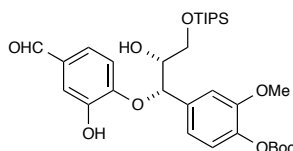
was removed under reduced pressure. To the deep reddish-brown residue was added aldehyde **I-57** (2.4 g, 5.26 mmol) in THF (20 mL) and H₂O (100 μ L, 5.78 mmol, 1.1 equiv. The mixture was allowed to stir 26 h and the solvent removed under reduced pressure. Purified by flash column chromatography (SiO₂, 30% \rightarrow 100% EtOAc/hexanes, followed by 0 \rightarrow 5% MeOH/CH₂Cl₂) to afford diol **SI-6** (2.2 g, 88%) as a brown solid foam. Analytical data for **SI-6**: CD (*c* 0.123 mM, MeOH) $\Delta\epsilon_{337}$ -8.8, $\Delta\epsilon_{272}$ -1.5, $\Delta\epsilon_{226}$ +2.5, $\Delta\epsilon_{207}$ -4.8; IR (film) 3468, 3079, 2938, 1761, 1687, 1586, 1506, 1463, 1436, 1422, 1370, 1261, 1145, 1127, 1034 cm⁻¹; ¹H NMR (500 MHz, CDCl₃) δ 9.79 (s, 1H), 7.41 (d, *J* = 1.9 Hz, 1H), 7.28 (dd, *J* = 8.3, 1.8 Hz, 1H), 7.13 (d, *J* = 8.1 Hz, 1H), 6.97 (d, *J* = 1.9 Hz, 1H), 6.94 (dd, *J* = 8.1, 1.9 Hz, 1H), 6.75 (d, *J* = 8.2 Hz, 1H), 6.12 (ddt, *J* = 17.4, 10.7, 5.5 Hz, 1H), 5.48 (dd, *J* = 17.3, 1.5 Hz, 1H), 5.39 (d, *J* = 1.3 Hz, 2H), 5.39 – 5.36 (m, 1H), 4.68 (dt, *J* = 5.4, 1.5 Hz, 2H), 4.01 (dt, *J* = 11.8, 3.7 Hz, 1H), 3.95 – 3.90 (m, 1H), 3.83 (s, 3H), 3.72 (ddd, *J* = 11.8, 9.3, 4.5 Hz, 1H), 3.03 (d, *J* = 7.6 Hz, 1H), 2.90 (dd, *J* = 9.3, 4.2 Hz, 1H), 1.55 (s, 9H); ¹³C (125 MHz, CDCl₃) δ 190.7, 152.2, 151.7, 151.3, 148.8, 140.0, 135.6, 132.1, 130.7, 126.6, 123.0, 118.9, 118.3, 114.1, 110.4, 110.0, 84.8, 83.7, 74.0, 69.6, 61.8, 56.0, 27.5; LRMS (ESI): Mass calcd for C₂₅H₃₀O₉, [M+Na]⁺, 497. Found [M+Na]⁺, 497.



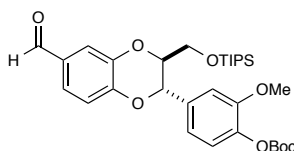
4-((1*S*,2*R*)-1-(2-(allyloxy)-4-formylphenoxy)-2-hydroxy-3-((triisopropylsilyl)oxy)propyl)-2-methoxyphenyl *tert*-butyl carbonate (I-60**):** To a 100 mL round bottom flask containing diol

SI-6 (2.4 g, 5.1 mmol), under atmosphere of N₂, was added CH₂Cl₂ (40 mL) and imidazole (860 mg, 12.6 mmol, 2.5 equiv). The mixture was cooled to 0 °C and TIPSCl (2.1 mL, 10.1 mmol, 2 equiv) was added. The reaction mixture was allowed to warm to ambient temperature and monitored by TLC. After 18 h the reaction was diluted with H₂O (50 mL) and CH₂Cl₂ (25 mL) and passed through a Biotage ISOLUTE® phase separator. The organic extracts were concentrated under reduced pressure and the residue purified by flash column chromatography (SiO₂, 20→30% EtOAc/hexanes) to afford alcohol **I-60** (2.74 g, 86%) as a clear yellow oil.

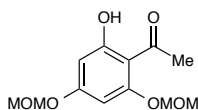
Analytical data for **13**: $[\alpha]_D^{25} = -15.4$ (CHCl₃, $c = 1.23$); 3502, 3080, 2942, 2891, 2726, 1762, 1690, 1594, 1506, 1463, 1260, 1146, 1125, 1034, 884 cm⁻¹; ¹H NMR (500 MHz, CDCl₃) δ 9.77 (s, 1H), 7.37 (d, $J = 1.9$ Hz, 1H), 7.26-24 (m, 1H), 7.11 (d, $J = 8.1$ Hz, 1H), 7.06 (d, $J = 1.9$ Hz, 1H), 7.00 (dd, $J = 8.2, 1.9$ Hz, 1H), 6.82 (d, $J = 8.3$ Hz, 1H), 6.08 (ddt, $J = 17.2, 10.4, 5.1$ Hz, 1H), 5.47 (dq, $J = 17.3, 1.6$ Hz, 1H), 5.31 (dq, $J = 10.5, 1.4$ Hz, 1H), 5.22 (d, $J = 6.4$ Hz, 1H), 4.64 (m, 2H), 4.08 – 3.99 (m, 2H), 3.91 (dd, $J = 9.8, 4.1$ Hz, 1H), 3.82 (s, 3H), 2.66 (d, $J = 5.0$ Hz, 1H), 1.53 (s, 9H), 1.14 – 1.05 (m, 3H), 1.03 (d, $J = 6.1$ Hz, 21H); ¹³C (125 MHz, CDCl₃) δ 190.8, 152.8, 151.3, 149.1, 139.9, 136.3, 132.6, 130.3, 126.5, 122.3, 119.3, 117.7, 114.5, 111.0, 110.7, 83.4, 80.7, 74.4, 69.4, 63.4, 55.9, 27.5, 17.8, 11.7; LRMS (ESI): Mass calcd for C₃₄H₅₀O₉Si [M+Na]⁺, 653. Found [M+Na]⁺, 653.



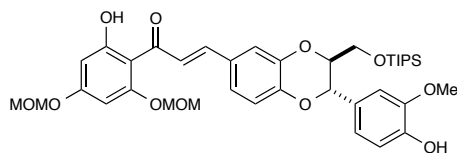
***tert*-butyl(4-((1*S*,2*R*)-1-(4-formyl-2-hydroxyphenoxy)-2-hydroxy-3-((triisopropylsilyl)oxy)propyl)-2-methoxyphenyl) carbonate (SI-7):** To a flame-dried 100 mL round bottom flask was added alcohol **I-60** (2.0 g, 3.2 mmol), followed by CH₂Cl₂ (30 mL). The flask was equipped with a N₂ inlet, purged with N₂, and cooled to 0 °C. Pd(PPh₃)₄ (183 mg, 0.160 mmol, 0.05 equiv) was added. The reaction was allowed to stir for five min and removed from the ice bath. PhSiH₃ (490 μL, 4 mmol, 1.25 equiv) was then added. After 1.5 h, the reaction mixture was filtered through a plug of Celite using CH₂Cl₂ as the eluent. The solvent was removed under reduced pressure and the residue purified by flash column chromatography (SiO₂, 25→40% EtOAc/hexanes) to afford diol **SI-7** (1.66 g, 89%) as a rose-colored solid foam. Analytical data for **SI-7**: [α]_D²⁵ = +55.7 (CHCl₃, *c* = 0.53); IR (film) 3366, 2942, 2891, 2867, 1763, 1691, 1609, 1587, 1507, 1463, 1370, 1276, 1255, 1147, 1125, 1039, 883, 787 cm⁻¹; ¹H NMR (500 MHz, CDCl₃) δ 9.82 (s, 1H), 7.46 (d, *J* = 2.0 Hz, 1H), 7.23 (dd, *J* = 8.3, 2.0 Hz, 1H), 7.20 (bs, 1H), 7.16 (d, *J* = 7.9 Hz, 1H), 7.01–6.97 (m, 2H), 6.82 (d, *J* = 8.3 Hz, 1H), 5.24 (d, *J* = 4.6 Hz, 1H), 4.10 – 4.04 (m, 1H), 3.96 (dd, *J* = 10.1, 6.5 Hz, 1H), 3.84 (s, 3H), 3.73 (dd, *J* = 10.1, 4.6 Hz, 1H), 3.07 (bs, 1H), 1.55 (s, 9H), 1.18–1.07 (m, 3H), 1.05 (m, 21H); ¹³C (125 MHz, CDCl₃) δ 191.1, 151.6, 151.3, 150.4, 148.0, 140.2, 135.0, 132.1, 123.5, 122.8, 118.9, 116.4, 115.7, 110.5, 83.7, 82.9, 74.3, 62.3, 56.0, 27.6, 17.9, 11.8; LRMS (ESI): Mass calcd for C₃₁H₄₆O₉Si [M–H]⁻, 589. Found [M–H]⁻, 589.



***tert*-butyl(4-((2*S*,3*S*)-6-formyl-3-(((triisopropylsilyl)oxy)methyl)-2,3-dihydrobenzo[*b*][1,4]dioxin-2-yl)-2-methoxyphenyl) carbonate (**I-61**):** To a 100 mL round bottom flask was added (**SI-7**) (1.35 g, 2.29 mmol). The flask was equipped with a N₂ inlet, purged with N₂, and THF (50 mL) was added. The mixture was cooled to 0 °C and DIAD (555 μL, 2.86 mmol, 1.25 equiv) was added. PPh₃ (750 mg, 2.68 mmol, 1.25 equiv in THF (10 mL)) was then added dropwise via syringe over 5 min. The vial was rinsed with THF (2 mL). After 20 min, TLC indicated that all of the starting material was consumed. The solvent was concentrated under reduced pressure. Purified by flash column chromatography (SiO₂, 10% EtOAc/hexanes) to afford aldehyde **I-61** (964 mg, 74%) as a solid white foam. Analytical data for **I-61**: [α]_D²⁵ = -7.6 (CHCl₃, *c* = 0.41); IR (film) 3070, 2942, 2891, 2867, 2732, 1764, 1695, 1607, 1586, 1504, 1464, 1443, 1369, 1277, 1257, 1146, 1125, 1016, 890 cm⁻¹; ¹H NMR (500 MHz, CDCl₃) δ 9.87 (s, 1H), 7.49 (d, *J* = 1.9 Hz, 1H), 7.44 (dd, *J* = 8.3, 1.9 Hz, 1H), 7.18 (d, *J* = 8.6 Hz, 1H), 7.08 (m, 3H), 5.24 (d, *J* = 7.9 Hz, 1H), 4.05 (dd, *J* = 11.8, 2.3 Hz, 1H), 3.99 (dt, *J* = 7.9, 2.3 Hz, 1H), 3.87 (s, 3H), 3.68 (dd, *J* = 11.7, 2.4 Hz, 1H), 1.57 (s, 8H), 1.16-1.10 (m, 3H), 1.08 (m, 21H); ¹³C (125 MHz, CDCl₃) δ 190.9, 151.4, 151.2, 149.2, 144.1, 140.6, 134.7, 130.8, 124.2, 122.7, 119.8, 117.8, 117.6, 111.4, 83.6, 78.4, 76.2, 62.2, 56.0, 27.6, 17.9, 11.9; LRMS (ESI): Mass calcd for C₃₁H₄₄O₈Si [M+H]⁺, 595. Found [M+H]⁺, 595.



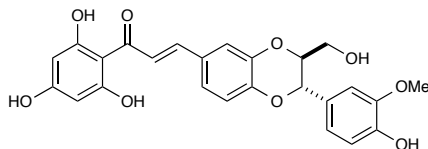
1-(2-hydroxy-4,6-bis(methoxymethoxy)phenyl)ethanone (I-64): To a 250 mL round bottom flask was added 2,4,6-trihydroxyacetophenone (2.33 g, 25 mmol). The flask was equipped with a N₂ inlet, purged with N₂, and CH₂Cl₂ (50 mL) was added. DIPEA (4.8 mL, 55 mmol) was added and the mixture was cooled to 0 °C. MOMCl was added dropwise, and the reaction mixture was allowed to warm to ambient temperature. After 16 h 1.0 M HCl was added to the reaction. The contents of the flask were poured into a separatory funnel and the aqueous layer was separated. The organic layer was washed two additional times with 1.0 M HCl, and once with sat. brine solution. The organic layer was dried over Na₂SO₄ and concentrated to afford a yellow residue. Purified by flash column chromatography (SiO₂, 15→25% EtOAc/hexanes) to afford acetophenone **I-64** (1.54 g, 48%) as a white solid. Analytical data matched those reported in the literature.³



(E)-3-(((2S,3S)-2-(4-hydroxy-3-methoxyphenyl)-3-(((triisopropylsilyl)oxy)methyl)-2,3-dihydrobenzo[b][1,4]dioxin-6-yl)-1-(2-hydroxy-4,6-bis(methoxymethoxy)phenyl)prop-2-en-1-one (I-77): To a 1-dram vial was added aldehyde **I-61** (245 mg, 0.428 mmol) and acetophenone **I-64** (121 mg, 0.471 mmol, 1.1 equiv). The solids were dissolved in EtOH (1.5

³ S. Urgaonkar; H. S. La Pierre; I. Meir; H. Lund; D. RayChaudhuri; J. T. Shaw *Org. Lett.* **2005**, *7*, 5609-5612.

mL), and 40 wt. % aq. NaOH solution (1.5 mL) was added. The mixture was allowed to stir at ambient temperature overnight. After 17 h the bright orange homogeneous reaction was neutralized with 1.0 M HCl, diluted with CH₂Cl₂ (20 mL), and passed through a Biotage ISOLUTE® phase separator. The organic extracts were concentrated under reduced pressure and the orangish residue purified by flash column chromatography (SiO₂, 10→20% EtOAc/hexanes) to afford chalcone **15** (199 mg, 65%) as a bright yellow solid foam. Analytical data for **I-77**: CD (*c* 0.469 mM, MeOH) $\Delta\epsilon_{232} +2.8$, $\Delta\epsilon_{211} -2.1$, $\Delta\epsilon_{203} +10.3$; IR (film) 3431, 2942, 2866, 1623, 1580, 1561, 1517, 1505, 1465, 1438, 1347, 1271, 1248, 1221, 1201, 1150, 1110, 1082, 1059, 1021, 961, 927 cm⁻¹; ¹H NMR (500 MHz, CDCl₃) δ 7.83 (d, *J* = 15.5 Hz, 1H), 7.75 (d, *J* = 15.5 Hz, 1H), 7.21 (d, *J* = 1.9 Hz, 1H), 7.14 (dd, *J* = 8.4, 1.9 Hz, 1H), 7.02 – 6.91 (m, 4H), 6.32 (d, *J* = 2.3 Hz, 1H), 6.27 (d, *J* = 2.3 Hz, 1H), 5.71 (bs, 1H), 5.30 (s, 2H), 5.19 (s, 2H), 5.11 (d, *J* = 7.7 Hz, 1H), 4.03-3.94 (m, 2H), 3.91 (s, 3H), 3.63 (dd, *J* = 12.1, 3.1 Hz, 1H), 3.55 (s, 3H), 3.49 (s, 3H), 1.17 – 0.94 (m, 24H); ¹³C (125 MHz, CDCl₃) δ 192.8, 167.3, 163.3, 159.8, 146.6, 146.2 (x2), 144.0, 142.7, 129.2, 128.2, 125.4, 122.3, 120.9, 117.6, 116.4, 114.5, 109.7, 107.5, 97.5, 95.0, 94.7, 94.0, 78.6, 76.4, 62.5, 56.8, 56.5, 55.9, 17.9, 11.8; LRMS (ESI): Mass calcd for C₃₈H₅₀O₁₁Si [M+H]⁺, 711. Found [M+H]⁺, 711.



(E)-3-((2S,3S)-2-(4-hydroxy-3-methoxyphenyl)-3-(hydroxymethyl)-2,3-

dihydrobenzo[*b*][1,4]dioxin-6-yl)-1-(2,4,6-trihydroxyphenyl)prop-2-en-1-one (I-65): To a 2-

dram vial containing chalcone **I-77** (480 mg, 0.592 mmol) was added 2,2-dimethylpropane-1,3-

diol (250 mg, 2.4 mmol, 4 equiv) and *p*-TsOH·H₂O (17 mg, 0.089 mmol, 0.15 equiv). The solids

were diluted with MeCN (8.5 mL) and the reaction mixture was heated to 55 °C. After 4.5 h, the deep red reaction was cooled to ambient temperature and concentrated under reduced pressure.

The residue was dissolved in EtOAc (10 mL) and washed with H₂O (2 x 10 mL). The organic

extracts were dried over anhydrous Na₂SO₄ and concentrated under reduced pressure. The

unpurified material was carried forward to the biomimetic cyclization without further

purification. (*NOTE: Material can be purified by flash column chromatography (SiO₂, 5 → 7.5*

MeOH/CH₂Cl₂) to yield an orange solid, but mass recovery is inconsistent.) Analytical data for **I-**

77: CD (*c* 0.0441 mM, MeOH) Δε₂₃₃ +3.0, Δε₂₁₃ -4.3, Δε₂₁₂ -3.4, Δε₂₀₇ -6.8; IR (film) 3307, 2959,

2920, 2851, 1700, 1626, 1604, 1562, 1503, 1462, 1438, 1350, 1269, 1221, 1162, 1124, 1082,

1030 cm⁻¹; ¹H NMR (500 MHz, (CD₃)₂CO) δ 12.13 (s, 1H), 9.45 (s, 1H), 8.15 (d, *J* = 15.5 Hz,

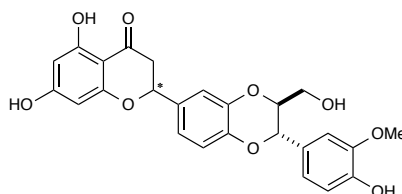
1H), 7.90 (bs, 1H), 7.73 (d, *J* = 15.6 Hz, 1H), 7.26 (d, *J* = 2.0 Hz, 1H), 7.22 (dd, *J* = 8.3, 2.1 Hz,

1H), 7.13 (d, *J* = 2.0 Hz, 1H), 7.00 – 6.94 (m, 2H), 6.89 (d, *J* = 8.0 Hz, 1H), 5.97 (s, 2H), 5.04 (d,

J = 8.1 Hz, 1H), 4.17 (ddd, *J* = 8.2, 4.2, 2.5 Hz, 2H), 3.87 (s, 3H), 3.79-3.72 (m, 1H), 3.56 – 3.49

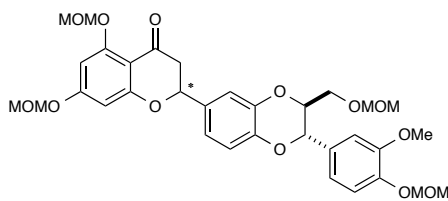
(m, 1H); ¹³C (125 MHz, (CD₃)₂CO) δ 193.0, 165.7, 165.5, 148.4, 148.0, 147.0, 144.8, 142.7,

130.0, 128.7, 126.4, 122.9, 121.5, 118.2, 117.1, 115.7, 111.8, 105.6, 96.0, 79.4, 77.5, 61.7, 56.2;
LRMS (ESI): Mass calcd for C₂₅H₂₂O₆ [M-H]⁻, 465. Found [M-H]⁻, 465.



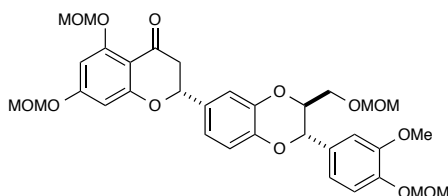
Flavanolignan SI-8: To a flame-dried two-dram vial containing unpurified chalcone **I-65** (~270 mg, 0.592 mmol), was added urea catalyst **F** (116 mg, 0.178 mmol, 0.3 equiv). The vial was capped and purged with dry N₂. Acetonitrile (12 mL) was added and the mixture was allowed to stir at ambient temperature. After 48 h, TLC analysis indicated complete consumption of starting material. Solvent was removed via reduced pressure and the residue was dissolved in a minimal amount of EtOAc. Silica gel (~2 mL) was added and solvent was removed again under reduced pressure. The resulting silica-adsorbed flavanolignan was loaded onto a silica column and purified via flash column chromatography (SiO₂, 4:1 CH₂Cl₂/ acetone) to yield flavanolignan **SI-8** (201 mg, 72% yield over two steps) as a white powder. Analytical data for **SI-8**: IR (film) 2922, 1636, 1510, 1215, 1163, 1128, 818; ¹H NMR (500 MHz, Acetone-*d*₆) δ 12.19 (s, 1H), 7.15 (dd, *J* = 3.2, 2.0 Hz, 2H), 7.07 (dd, *J* = 8.4, 2.2 Hz, 1H), 7.00 (dd, *J* = 8.0, 1.9 Hz, 1H), 6.98 (d, *J* = 8.3 Hz, 1H), 6.91 (d, *J* = 8.1 Hz, 1H), 6.02 (d, *J* = 2.1 Hz, 1H), 5.99 (d, *J* = 2.2 Hz, 1H), 5.52 (dd, *J* = 12.4, 3.1 Hz, 1H), 5.03 (d, *J* = 8.0 Hz, 1H), 4.17 (ddd, *J* = 8.1, 4.3, 2.5 Hz, 1H), 3.90 (s, 3H), 3.77 (dd, *J* = 12.5, 2.5 Hz, 1H), 3.54 (dd, *J* = 12.4, 4.1 Hz, 1H), 3.20 (dd, *J* = 17.0, 12.5 Hz, 1H), 2.83 (dd, *J* = 17.0, 3.1 Hz, 1H); ¹³C NMR (125 MHz, Acetone) δ 196.8, 166.5, 164.4, 163.3,

147.6, 147.1, 144.3, 143.7, 132.2, 128.2, 120.7, 119.4, 116.9, 115.2, 115.1, 114.8, 111.0, 102.4, 96.0, 95.0, 78.7, 76.4, 60.9, 55.5, 42.6; LRMS (ESI): Mass calcd for $C_{25}H_{22}O_9$ [M-H]⁻, 465. Found [M-H]⁻, 465.

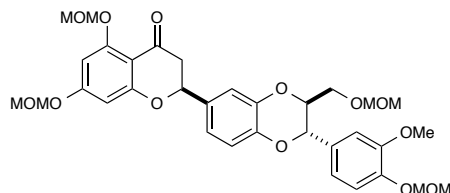


Protected flavanolignan I-78: To a flame-dried vial was added unprotected flavanolignan **SI-8** (155 mg, 0.332 mmol), DMAP (122 mg, 1 mmol, 3 equiv), and *n*-Bu₄NI (368 mg, 1 mmol, 3 equiv). The vial was capped and purged with dry N₂. CH₂Cl₂ (2.5 mL) was added, followed by DIPEA (1.7 mL, 10 mmol, 30 equiv). The heterogenous mixture was allowed to stir until homogeneous (~5 min) and cooled to 0 °C. Freshly distilled MOMCl was added (0.38 mL, 5 mmol, 15 equiv) was added and the mixture allowed to warm to ambient temperature. After stirring for 12 h, the reaction mixture was diluted with CH₂Cl₂ (5 mL) and stirred over pH 7 buffer solution (10 mL) for 10 min. The organic layer was collected and washed with 1.0 M HCl (10 mL). The organic layer was dried with over anhydrous Na₂SO₄ and concentrated under reduced pressure. The residue was purified by flash column chromatography (SiO₂, 50% EtOAc/hexanes) to afford flavanolignan **I-78** (154 mg, 72% yield) as a white powder. The two diastereomers were separated by semi-preparative HPLC (RegisPack, 250 mm X 10 mm column, 5 μm, 90% EtOH/hexanes, 4 mL/min, Rt_{major} = 10.8 min, Rt_{minor} = 9.1 min) Diastereomeric ratio was

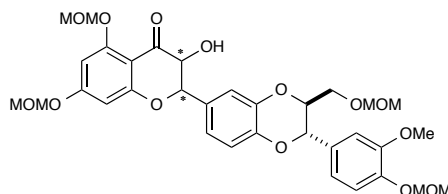
determined to be 85:15 via analytical HPLC (Chiracel AD-H, 70% isopropanol/hexanes, 1 mL/min, $R_{t_{\text{major}}} = 17.54$ min, $R_{t_{\text{minor}}} = 15.89$ min).



Analytical data for major isomer (**SI-9**): $[\alpha]_D^{25} = -32.5$ (CHCl_3 , $c = 0.59$); IR (film) 2929, 1678, 1510, 1435, 1262, 1148, 1108, 1025, 921, 817 cm^{-1} ; ^1H NMR (500 MHz, CDCl_3) δ 7.21 – 7.17 (m, 1H), 7.13 (d, $J = 2.0$ Hz, 1H), 6.97 (td, $J = 11.0, 10.3, 7.4$ Hz, 5H), 6.43 (d, $J = 2.3$ Hz, 1H), 6.39 (d, $J = 2.3$ Hz, 1H), 5.34 (dd, $J = 13.2, 2.8$ Hz, 1H), 5.28 (s, 2H), 5.26 (s, 2H), 5.17 (d, $J = 2.6$ Hz, 2H), 4.99 (d, $J = 8.0$ Hz, 1H), 4.66 (d, $J = 6.5$ Hz, 1H), 4.62 (d, $J = 6.5$ Hz, 1H), 4.22 – 4.16 (m, 1H), 3.90 (s, 3H), 3.72 (dd, $J = 11.6, 2.5$ Hz, 1H), 3.54 (s, 3H), 3.53 (s, 3H), 3.48 (s, 3H), 3.35 (s, 3H), 3.00 (dd, $J = 16.5, 13.2$ Hz, 1H), 2.77 (dd, $J = 16.5, 2.9$ Hz, 1H); ^{13}C NMR (125 MHz, CDCl_3) δ 189.3, 164.5, 163.3, 159.6, 150.1, 147.2, 144.1, 143.5, 132.2, 130.3, 120.4, 120.3, 119.4, 117.4, 116.3, 115.3, 110.8, 98.1, 97.5, 97.0, 95.5, 95.1, 94.2, 78.8, 77.5, 76.4, 66.4, 56.6, 56.5, 56.3, 56.1, 55.5, 45.7; LRMS (ESI): Mass calcd for $\text{C}_{33}\text{H}_{38}\text{O}_{13}$ $[\text{M}+\text{H}]^+$, 643. Found $[\text{M}+\text{H}]^+$, 643.



Analytical data for minor isomer of **SI-10**: $[\alpha]_D^{25} = -16.4$ (CHCl_3 , $c = 0.61$) IR (film) 2927, 1678, 1510, 1436, 1264, 1150, 1108, 1026, 921, 818 cm^{-1} ; ^1H NMR (500 MHz, CDCl_3) δ 7.19 (d, $J = 8.1$ Hz, 1H), 7.13 (s, 1H), 7.01 – 6.92 (m, 5H), 6.43 (s, 1H), 6.39 (s, 1H), 5.37 – 5.31 (m, 1H), 5.28 (s, 2H), 5.25 (s, 2H), 5.17 (d, $J = 2.6$ Hz, 2H), 4.99 (d, $J = 8.0$ Hz, 1H), 4.70 – 4.58 (m, 2H), 4.25 – 4.11 (m, 1H), 3.90 (s, 3H), 3.73 (dd, $J = 11.9, 3.2$ Hz, 1H), 3.54 (s, 3H), 3.53 (s, 3H), 3.48 (s, 3H), 3.35 (s, 3H), 3.00 (dd, $J = 16.4, 13.1$ Hz, 1H), 2.77 (dd, $J = 16.5, 2.9$ Hz, 1H); ^{13}C NMR (125 MHz, CDCl_3) δ 189.3, 164.5, 163.3, 159.6, 150.1, 147.2, 144.1, 143.5, 132.2, 130.3, 120.4, 120.3, 119.4, 117.4, 116.3, 115.3, 110.8, 98.1, 97.5, 97.0, 95.5, 95.1, 94.2, 78.8, 77.5, 76.4, 66.4, 56.6, 56.5, 56.3, 56.1, 55.5, 45.7; LRMS (ESI): Mass calcd for $\text{C}_{33}\text{H}_{38}\text{O}_{13}$ $[\text{M}+\text{H}]^+$, 643. Found $[\text{M}+\text{H}]^+$, 643.

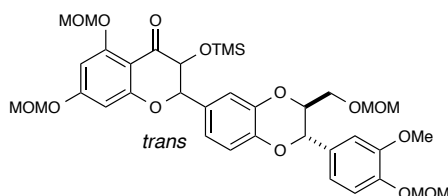


α -hydroxyflavanolignan SI-11: Silyl enol ether formation: A flame-dried, 2-dram vial containing the major isomer (**21**) (20 mg, 0.031 mmol) was charged with 600 μL of THF and cooled to -78 $^\circ\text{C}$. In a separate flame-dried vial, freshly distilled TMSCl (200 μL , 1.56 mmol, 50

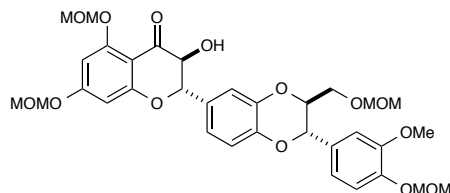
equiv) was mixed with triethylamine (200 μL , 1.44 mmol, 46 equiv) to form a milky-white, heterogeneous solution. Of this solution 120 μL was removed and added via syringe (passed through filter needle, 5 micron) to the solution of **21**. This solution was allowed to stir for five min, then freshly prepared 0.15 M LiHMDS (1 mL, 0.16 mmol, 5 equiv) was added down the side of the vial over 10 min. After stirring for 1 h at $-78\text{ }^\circ\text{C}$, TLC analysis indicated complete conversion of the starting material. An AcOH/MeOH mixture (10% (v/v), 50 μL) were added and the now white, heterogeneous mixture was allowed to stir for one min. The vial was then removed from the dry ice bath and pentanes (2 mL), followed by pH 7 buffer solution (1 mL) was added. The vial was shaken until a homogeneous, bi-layered solution was obtained (~30 seconds). Then organic layer was then removed and the aqueous layer washed with pentanes (0.5 mL x 2). The combined organic extracts were dried over anhydrous Na_2SO_4 and rapidly concentrated under vacuum. (*NOTE: The silyl enol ether is unstable at room temperature and as a result, the work-up process was executed swiftly. The material was not be subjected to temperatures greater than $25\text{ }^\circ\text{C}$.*)

Oxidation: The resulting yellow residue was dissolved in 1.5 mL of CH_2Cl_2 and cooled to $-78\text{ }^\circ\text{C}$. DMDO (520 μL , 0.09 M, 1.5 equiv) is added in a single portion. The mixture is allowed to stir for 10 min and rapidly concentrated under vacuum. The yellow residue was then purified by flash column chromatography (SiO_2 , 50% EtOAc/hexanes) to yield **α -hydroxyflavanolignan SI-11** as a white foam (12 mg, 9:1 dr, 60% yield) and **α -siloxyflavanolignan SI-12** (3 mg, 13% yield) as a yellow oil. Diastereomers of **SI-X** were separated by semi-preparative HPLC (Regis (*S,S*)-Whelk-O 1, 250 mm X 10 mm column, 5 μm , 90% EtOH/hexanes, 10 mL/min, $\text{Rt}_{\text{major}} = 3.3$

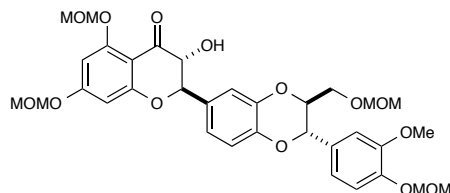
min, $R_{t_{\text{minor}}} = 3.8$ min). Diastereomeric ratio was determined to be 9:1 by 500 MHz ^1H NMR spectroscopy.



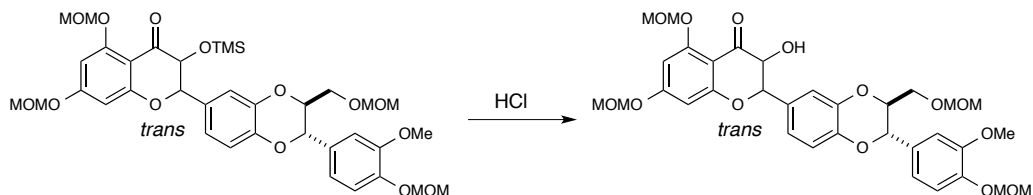
α -siloxyflavanolignan SI-12: IR (film) 2922, 2851, 1609, 1509, 1464, 1261, 1147, 1079, 802 cm^{-1} ; ^1H NMR (500 MHz, CDCl_3) δ 7.19 (d, $J = 8.4$ Hz, 1H), 7.15 (d, $J = 13.1$ Hz, 1H), 7.00 – 6.94 (m, 4H), 6.47 (d, $J = 2.3$ Hz, 1H), 6.36 (d, $J = 2.2$ Hz, 1H), 5.29 (q, $J = 7.0$ Hz, 3H), 5.26 (s, 2H), 5.17 (d, $J = 1.8$ Hz, 2H), 5.06 (d, $J = 11.3$ Hz, 1H), 4.98 (dd, $J = 10.5, 7.8$ Hz, 1H), 4.66 (dd, $J = 6.5, 2.9$ Hz, 1H), 4.62 (d, $J = 6.5$ Hz, 1H), 4.29 (dd, $J = 11.2, 3.4$ Hz, 1H), 4.20 (ddd, $J = 10.2, 4.5, 2.3$ Hz, 1H), 3.91 (s, 3H), 3.73 (d, $J = 11.6$ Hz, 1H), 3.52 (s, 6H), 3.47 (s, 3H), 3.35 (d, $J = 2.9$ Hz, 3H), -0.06 (d, $J = 1.6$ Hz, 9H). ^{13}C NMR (126 MHz, CDCl_3) δ 189.9, 164.0, 163.4, 159.8, 150.1, 147.3, 144.1, 143.3, 131.2, 130.5, 120.9, 120.7, 120.4, 117.1, 117.0, 116.3, 110.8, 106.0, 98.4, 97.5, 97.1, 95.5, 95.0, 94.2, 83.2, 83.1, 76.5, 75.9, 66.5, 56.7, 56.6, 56.4, 56.2, 55.6, 0.0; LRMS (ESI): Mass calcd for $\text{C}_{36}\text{H}_{46}\text{O}_{14}\text{Si}$ $[\text{M}+\text{H}]^+$ 731. Found $[\text{M}+\text{H}]^+$ 731.



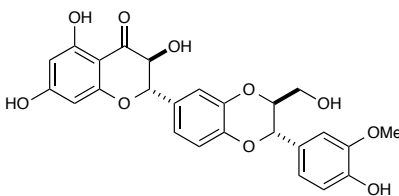
Analytical data for major isomer of **I-80**: $[\alpha]_D^{25} = -28.4$ (CHCl_3 , $c = 0.25$); CD (c 0.00611 mM, MeOH) $\Delta\epsilon_{332} -1.2$, $\Delta\epsilon_{291} +3.8$, $\Delta\epsilon_{239} -0.66$; IR (film) 2927, 2160, 1609, 1574, 1510, 1438, 1208, 1153, 1076, 1030, 922, 820 cm^{-1} ; ^1H NMR (500 MHz, CDCl_3) δ 7.23 (d, $J = 2.0$ Hz, 1H), 7.21 – 7.17 (m, 1H), 7.06 (dd, $J = 8.4, 2.0$ Hz, 1H), 7.02 (d, $J = 8.3$ Hz, 1H), 6.97 (d, $J = 7.3$ Hz, 2H), 6.46 (d, $J = 2.2$ Hz, 1H), 6.36 (d, $J = 2.2$ Hz, 1H), 5.34 – 5.27 (m, 2H), 5.25 (s, 2H), 5.18 (d, $J = 1.3$ Hz, 2H), 5.06 – 4.90 (m, 2H), 4.66 (d, $J = 6.5$ Hz, 1H), 4.61 (d, $J = 6.5$ Hz, 1H), 4.42 (d, $J = 12.2$ Hz, 1H), 4.18 (ddd, $J = 8.1, 4.2, 2.5$ Hz, 1H), 4.01 (d, $J = 1.8$ Hz, 1H), 3.91 (s, 3H), 3.73 (dd, $J = 11.5, 2.5$ Hz, 1H), 3.55 (s, 3H), 3.52 (s, 3H), 3.48 (s, 3H), 3.34 (s, 3H); ^{13}C NMR (125 MHz, CDCl_3) δ 191.0, 164.4, 164.3, 159.5, 150.0, 147.2, 144.5, 143.4, 130.4, 129.9, 120.8, 120.3, 117.4, 116.4, 116.3, 110.8, 104.25, 97.7, 97.4, 97.0, 95.5, 95.0, 94.2, 82.9, 77.2, 76.4, 73.0, 66.4, 56.7, 56.56, 56.3, 56.0, 55.5; LRMS (ESI): Mass calcd for $\text{C}_{33}\text{H}_{38}\text{O}_{14}$ $[\text{M}+\text{H}]^+$, 659. Found $[\text{M}+\text{H}]^+$, 659.



Analytical data for minor isomer of **I-79**: $[\alpha]_D^{25} = -19.7$ (CHCl_3 , $c = 0.31$); CD (c 0.00604 mM, MeOH) $\Delta\epsilon_{332} +1.4$, $\Delta\epsilon_{290} - 8.7$, $\Delta\epsilon_{227} +9.8$; IR (film) 2920, 1680, 1607, 1573, 1509, 1438, 1266, 1134, 1017, 919 cm^{-1} ; ^1H NMR (500 MHz, CDCl_3) δ 7.23 (d, $J = 1.9$ Hz, 1H), 7.21 – 7.17 (m, 1H), 7.05 (dd, $J = 8.3, 2.0$ Hz, 1H), 7.02 (d, $J = 8.3$ Hz, 1H), 6.99 – 6.95 (m, 2H), 6.46 (d, $J = 2.2$ Hz, 1H), 6.36 (d, $J = 2.2$ Hz, 1H), 5.33 – 5.28 (m, 2H), 5.25 (s, 2H), 5.18 (d, $J = 1.2$ Hz, 2H), 5.03 – 4.93 (m, 2H), 4.66 (d, $J = 6.5$ Hz, 1H), 4.61 (d, $J = 6.5$ Hz, 1H), 4.44 (dd, $J = 12.2, 1.5$ Hz, 1H), 4.18 (ddd, $J = 8.1, 4.2, 2.4$ Hz, 1H), 4.01 (d, $J = 1.8$ Hz, 1H), 3.90 (s, 3H), 3.72 (dd, $J = 11.5, 2.5$ Hz, 1H), 3.55 (s, 3H), 3.52 (s, 3H), 3.48 (s, 3H), 3.35 (s, 3H). ^{13}C NMR (125 MHz, CDCl_3) δ 191.0, 164.4, 164.3, 159.5, 150.0, 147.2, 144.5, 143.4, 130.4, 129.9, 120.9, 120.3, 117.4, 116.4, 116.3, 110.78, 104.3, 97.8, 97.4, 97.0, 95.5, 95.0, 94.2, 82.9, 77.3, 76.4, 72.9, 66.4, 56.7, 56.6, 56.3, 56.0, 55.5; LRMS (ESI): Mass calcd for $\text{C}_{33}\text{H}_{38}\text{O}_{14}$ $[\text{M}+\text{H}]^+$, 659. Found $[\text{M}+\text{H}]^+$, 659.



α -hydroxyflavanolignan SI-11: A two-dram vial containing α -silyoxyflavanolignan **SI-12** was charged with EtOAc (1.4 mL). HCl (0.2 M, 1.4 mL) was added and the mixture was vigorously stirred at room temperature for 2 h. Upon completion of the reaction (as determined by TLC analysis) the organic layer was removed and dried over anhydrous Na_2SO_4 . The mixture was concentrated under vacuum and purified by flash column chromatography (SiO_2 , 50% EtOAc/hexanes) to yield **SI-11** (15.5 mg, 82% yield) as a white foam. The mixture of diastereomers was further purified by preparative HPLC as described above.



(-)-isosilybin A (I-89): To a flame-dried, two-dram vial containing α -hydroxyflavanolignan **I-80** (7.5 mg, 0.011 mmol) and a magnetic stir bar was added 2,2-dimethylpropane (6 mg, 0.058 mmol, 5 equiv) and *p*-TsOH·H₂O (0.7 mg, 3.7 μmol , 0.3 equiv). The vial was capped and purged with dry N_2 . Acetonitrile (200 μL) was added and the reaction heated to 40 °C. After stirring for 20 h, the pale yellow mixture was concentrated under vacuum. The residue was dissolved in

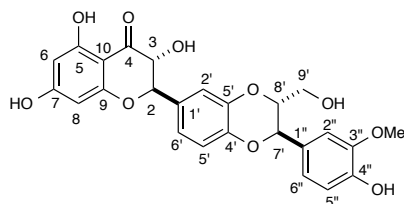
EtOAc (2 mL) and washed with water (2 mL x 2). The solution was dried over anhydrous Na_2SO_4 and concentrated under vacuum. The unpurified material was then purified by reverse-phase HPLC (Phenomenex Luna CN 5μ C18 100 Å, (150 x 21.2 mm) column, 10-30% acetonitrile/water, 20 mL/min, Rt = 14.4 min, mass directed fraction collection) to afford a white solid (3.0 mg, 55% yield). Analysis via electronic circular dichroism confirmed that this material was (-)-isosilybin A. Analytical data for (-)-isosilybin A (**I-89**): IR (film)⁴ 3357, 2925, 2850, 2359, 1640, 1512, 1276, 1165, 1129, 1089, 1032, 618 cm^{-1} ; $[\alpha]_{\text{D}}^{25} = -37.8^{\text{s}}$ (MeOH, $c = 0.09$); CD ($c = 0.0622$ mM, MeOH) $\Delta\epsilon_{328} -3.1$, $\Delta\epsilon_{294} +9.2$, $\Delta\epsilon_{235} +0.7^{\text{s}}$; $^1\text{H NMR}$ (500 MHz, Acetone- d_6) δ 11.70 (s, 1H), 7.16 (t, $J = 1.7$ Hz, 1H), 7.14 (t, $J = 1.6$ Hz, 1H), 7.09 (dt, $J = 8.2, 1.8$ Hz, 1H), 6.99 (d, $J = 8.1$ Hz, 1H), 6.95 (d, $J = 8.3$ Hz, 1H), 6.89 (d, $J = 8.2$ Hz, 1H), 6.01 (d, $J = 8.2$ Hz, 1H), 5.98 (d, $J = 1.9$ Hz, 1H), 5.11 (d, $J = 11.4$ Hz, 1H), 5.02 (d, $J = 8.0$ Hz, 1H), 4.66 (d, $J = 11.4$ Hz, 1H), 4.15 (ddd, $J = 6.4, 4.0, 1.9$ Hz, 1H), 3.88 (d, $J = 1.5$ Hz, 3H), 3.76 (d, $J = 12.3$ Hz, 1H), 3.53 (dd, $J = 12.4, 4.0$ Hz, 1H). $^{13}\text{C NMR}$ (125 MHz, Acetone) δ 197.5, 167.9, 164.6, 163.6, 148.1, 147.6, 145.0, 143.9, 130.9, 128.7, 121.3, 121.2, 117.1, 116.9, 115.3, 111.5, 101.0, 96.8, 95.8, 83.7, 79.1, 76.8, 72.7, 61.4, 55.9; HRMS (ESI): Mass calcd for $\text{C}_{25}\text{H}_{22}\text{O}_{10}$ $[\text{M}+\text{H}]^+$, 483.12857. Found 483.12897.

⁴ Reported characterization data for naturally isolated (+)-isosilybin A: IR (KBr) 3424, 2939, 1640, 1595, 1510, 1468, 1365, 1271, 1163, 1085, 1027 cm^{-1} . Kim, N.-C.; Graf, T. N.; Sparacino, C. M.; Wani, M. C.; Wall, M. E. *Org. Biomol. Chem.* **2003**, *1*, 1684.

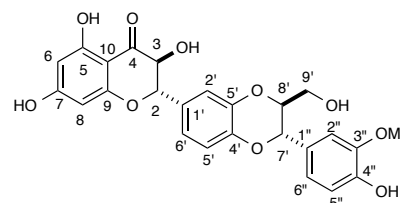
⁵ Reported literature value for (+)-isosilybin A: $[\alpha]_{\text{D}} = +30.4$ ($c = 0.3$, MeOH). Kim, N.-C.; Graf, T. N.; Sparacino, C. M.; Wani, M. C.; Wall, M. E. *Org. Biomol. Chem.* **2003**, *1*, 1684.

⁶ Reported literature values for naturally isolated (+)-isosilybin A: CD (MeOH) $\Delta\epsilon_{326} +2.9$, $\Delta\epsilon_{298} -9.3$, $\Delta\epsilon_{226} -1.9$. Kim, N.-C.; Graf, T. N.; Sparacino, C. M.; Wani, M. C.; Wall, M. E. *Org. Biomol. Chem.* **2003**, *1*, 1684.

1.12.2 Comparison of ^1H NMR Spectral Data of Isosilybin A



Natural (+)-Isosilybin A (300)



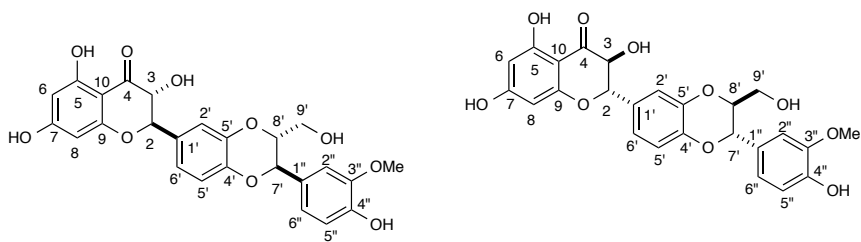
Synthetic (-)-Isosilybin A (500)

Position	Natural (+)-Isosilybin A (300) MHz, (CD ₃) ₂ CO ⁷	Synthetic (-)-Isosilybin A (500) MHz, (CD ₃) ₂ CO
2'	7.15 (d, $J = 1.8$ Hz, 1H)	7.16 (appt, $J = 1.9$ Hz, 1H)
2''	7.12 (d, $J = 1.8$ Hz, 1H)	7.14 (appt, $J = 1.8$ Hz, 1H)
6'	7.07 (dd, $J = 8.7, 1.8$ Hz, 1H)	7.09 (d appt, $J = 8.2, 1.8, 1.8$ Hz, 1H)
6''	6.97 (dd, $J = 8.4, 1.8$ Hz, 1H)	6.99 (dd, $J = 8.1, 1.8$ Hz, 1H)
5'	6.94 (d, $J = 8.7$ Hz, 1H)	6.95 (d, $J = 8.3$ Hz, 1H)
5''	6.87 (d, $J = 8.1$, 1H)	6.90 (d, $J = 8.2$ Hz, 1H)
8	5.97 (d, $J = 2.1$ Hz, 1H)	6.01 (d, $J = 1.8$, Hz, 1H)
6	5.94 (d, $J=2.1$ 1H)	5.98 (d, $J = 1.8$, Hz, 1H)
2	5.08 (d, $J = 11.4$ Hz, 1H)	5.11 (d, $J = 11.5$ Hz, 1H)
7'	5.01 (d, $J = 7.8$ Hz, 1H)	5.02 (d, $J=8.0$ Hz, 1 H)
3	4.60 (d, $J= 11.4$ Hz, 1H)	4.66 (d, $J = 11.4$ Hz, 1H)

⁷ Lee, D. Y.-W.; Liu. *J. Nat. Prod.* **2003**, 66, 1171.

8'	4.10 (ddd, $J = 6.0, 3.9, 2.4$ Hz, 1H)	4.15 (ddd, $J = 6.4, 3.9, 1.9$ Hz, 1H)
OMe	3.88 (s, 3H)	3.88 (s, 3H)
9'	3.74 (dd, $J=12.3, 2.4$ Hz 1H)	3.76 (d, $J=12.3$ Hz, 1H)
9'	3.50 (dd, $J = 12.3, 4.2$ Hz, 1H)	3.53 (dd, $J = 12.4, 4.0$ Hz, 1H)

1.12.3 Comparison of ^{13}C NMR Spectral Data of Isosilybin A



Natural (+)-Isosilybin A (75)

Synthetic (-)-Isosilybin A

carbon

MHz, $(\text{CD}_3)_2\text{CO})^a$

(125 MHz $(\text{CD}_3)_2\text{CO})$

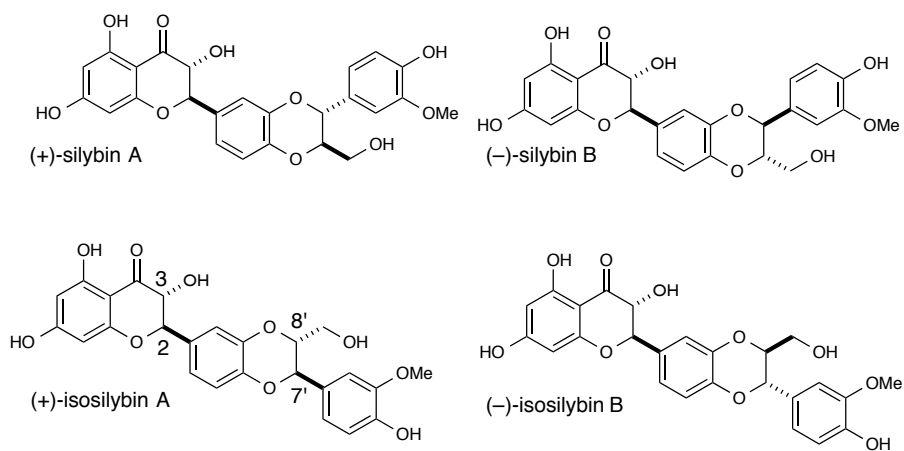
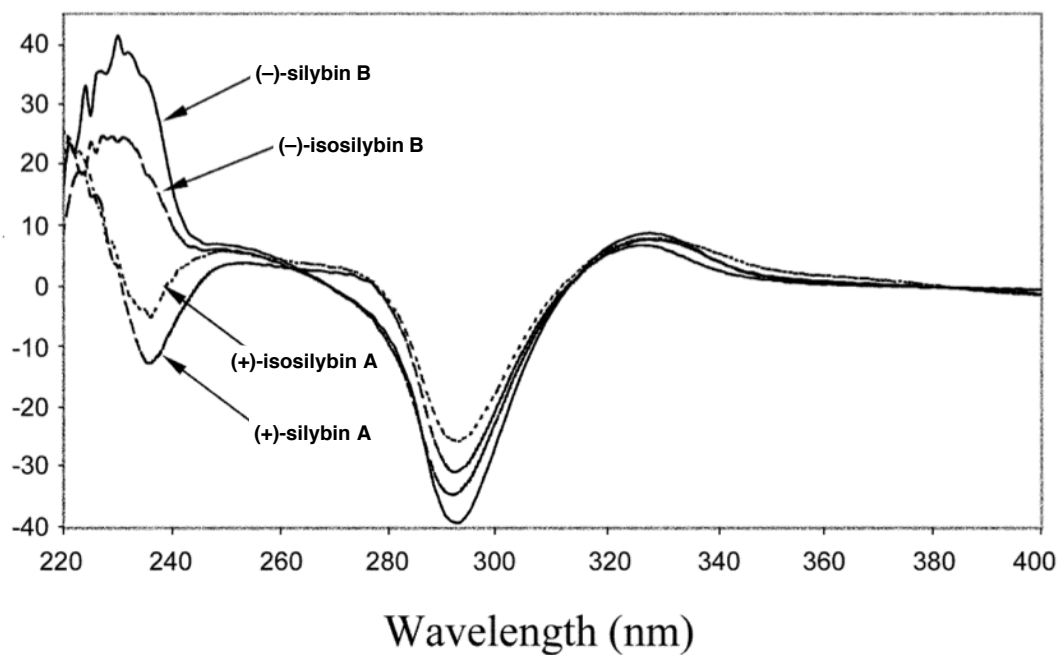
carbon	MHz, $(\text{CD}_3)_2\text{CO})^a$	(125 MHz $(\text{CD}_3)_2\text{CO})$
4	197.4	197.5
7	167.2	167.9
5	164.3	164.6
9	163.4	163.6
3''	147.8	148.1
4''	147.4	147.6
3'	144.8	145.0
4'	143.7	143.9
1'	130.6	130.9
1''	128.5	128.7
6'	121.1	121.3
6''	120.9	121.2

^a Lee, D. Y.-W.; Liu. *J. Nat. Prod.* **2003**, 66, 1171.

2'	116.8	117.1
5'	116.7	116.9
5"	115.1	115.3
2"	111.3	111.5
10	100.9	101.0
8	96.5	96.8
6	95.4	95.8
2	83.4	83.7
8'	78.9	79.1
7'	76.6	76.8
3	72.5	72.7
9'	61.2	61.4
OMe	55.7	55.9

1.12.4 Silybin Electronic Circular Dichroism Data

Authentic spectra from Kim et al.⁹



⁹ Kim, N.-C.; Graf, T. N.; Sparacino, C. M.; Wani, M. C.; Wall, M. E. *Org. Biomol. Chem.* **2003**, *1*, 1684

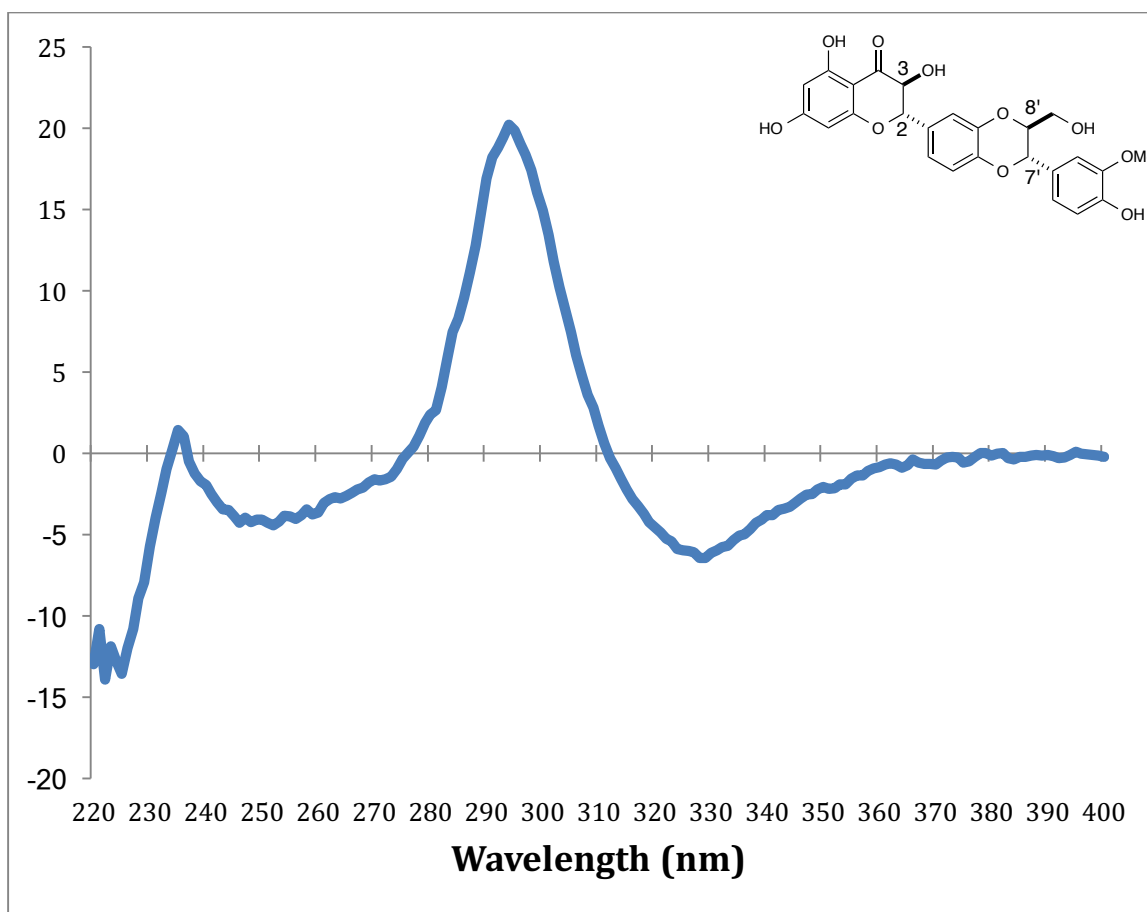
The use of electronic circular dichroism to establish absolute stereochemistry at the C-2, C-3, C-7', C-8' stereocenters of the silybins has been developed by comparison to stereodefined model compounds.¹⁰ This method has been further validated by crystal structure of a heavy-atom analog of (+)-isosilybin A by Oberlies and co-workers.¹¹ Based on the work of Gaffield, Cotton effects around the wavelengths of 320 nm and 290 nm indicates the absolute stereochemistry at C-2 and C-3 (a negative Cotton effect at approx. 320 nm and positive value at approx. 290 nm indicates 2S, 3S and vice-versa), while a Cotton effect in the area of 220-240 nm imparts the absolute stereochemistry at the C-7' & C-8'. A positive value in this area indicates 7S', 8'S while a negative value indicates 7R', 8'R.¹² By these rules, the absolute configurations of (-)-isosilybin A is 2S, 3S, 7'S, 8'S.

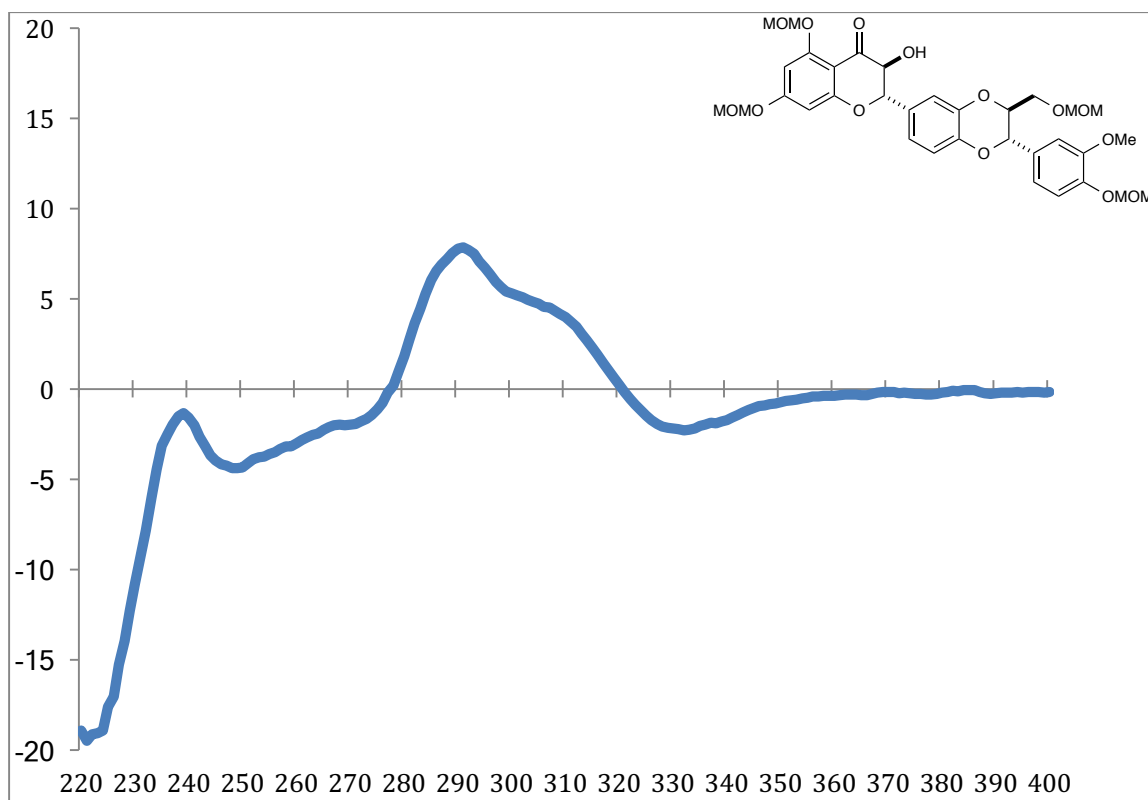
¹⁰ Gaffield, W. *Tetrahedron*, **1970**, *26*, 4093; Arnoldi, A; Merlini, L; *J. Chem. Soc., Perkin Trans. 1* **1985**, 2555. Da Silva, M. S.; Barbosa-Filho, J. M.; Yoshida, M.; Gottlieb, O. R. *Phytochemistry* **1989**, *28*, 3477. Fang, J.-M.; Lee, C.-K.; Cheng, Y.-S. *Phytochemistry* **1992**, *31*, 3659.

¹¹ Sy-Cordero, A. A.; Day, C. S.; Oberlies, N. H. *J. Nat. Prod.* **2012**, *75*, 1879.

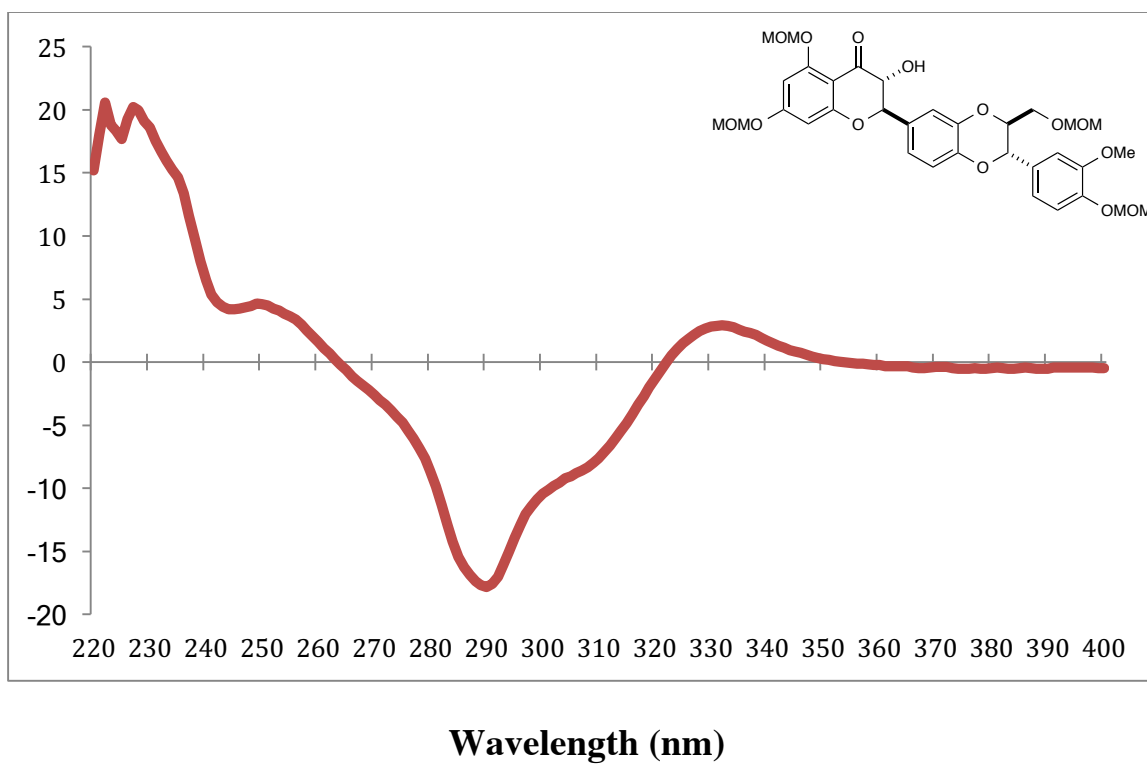
¹² It should be noted that these rules for determining absolute stereochemistry apply to *trans* configured substituents. Slade and co-workers provide an excellent comprehensive review of the use of CD to determine stereochemistry of flavonoids: Slade, D.; Ferreira, D.; Marais, J. P. J. *Phytochemistry* **2005**, *66*, 2177.

1.12.5 CD Spectra of Synthetic (-)-Isosilybin A (1)



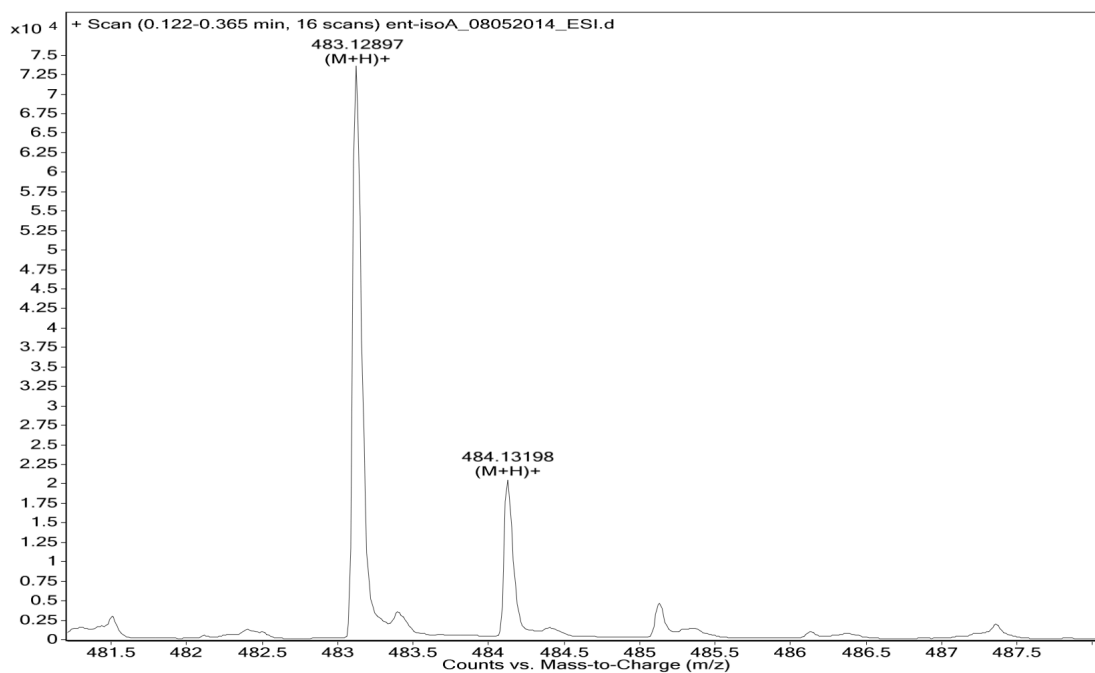
CD Spectra of α -Hydroxyflavanolignan Major Isomer **20**

Wavelength (nm)

CD Spectra of α -Hydroxyflavanolignan Minor Isomer **SI-XI**

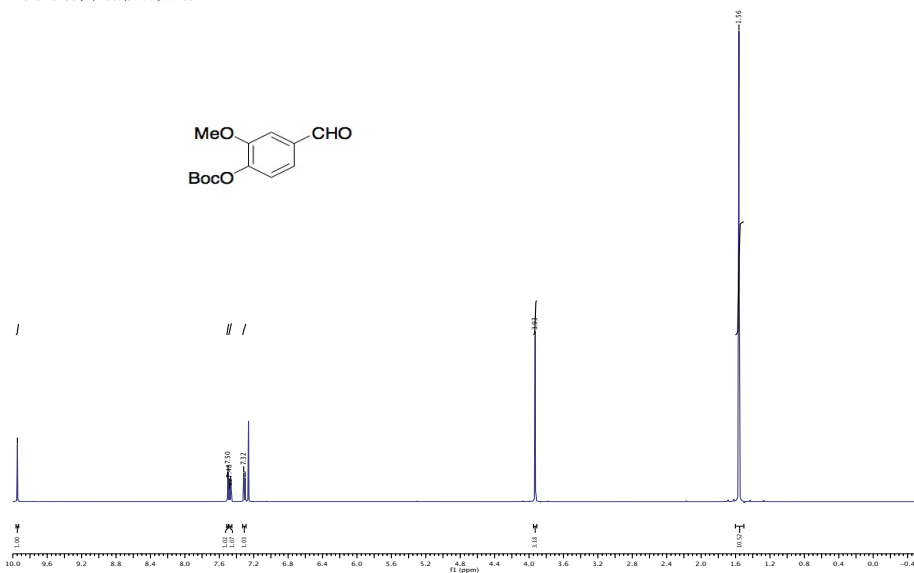
1.12.6 High Resolution Mass Spectrometry Data of Synthetic (-)-Isosilybin A

Sample Name	ent-isoA	Position	P1-D9	Instrument Name	Instrument 1	User Name	
Inj Vol	3	InjPosition		SampleType	Sample	IRM Calibration Status	Success
Data Filename	ent-isoA_08052014_ES	ACQ Method	ESI_ASL_Pos_Main_051	Comment		Acquired Time	8/5/2014 5:38:25 PM

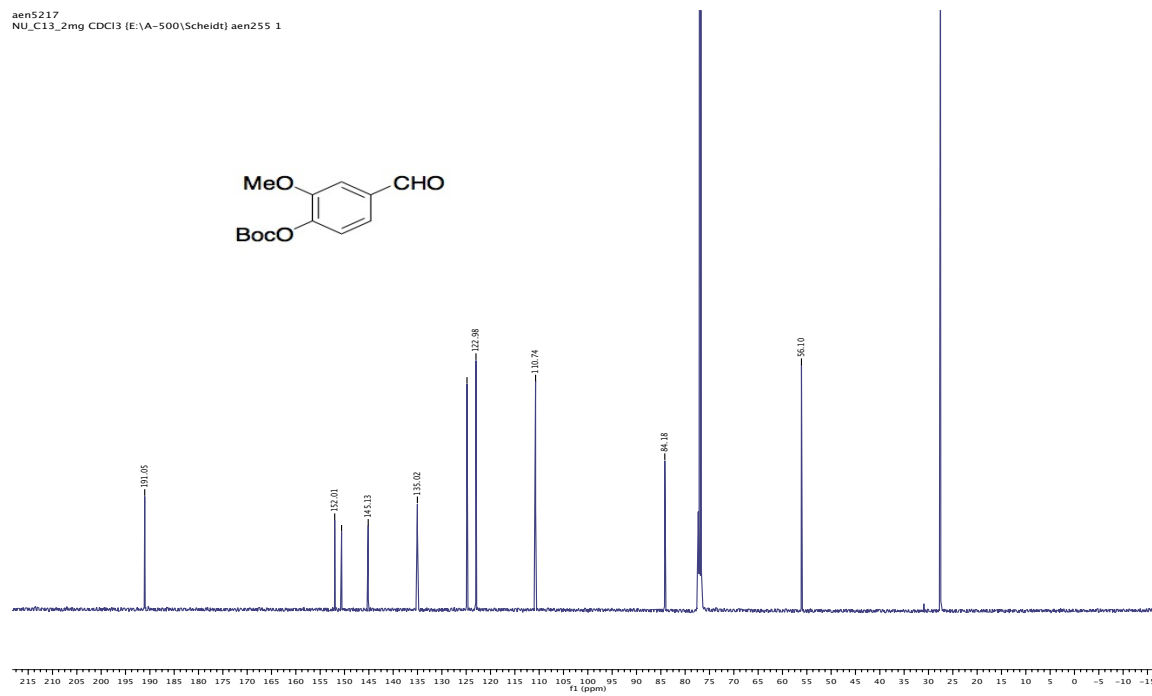


1.12.7 Selected NMR Spectra

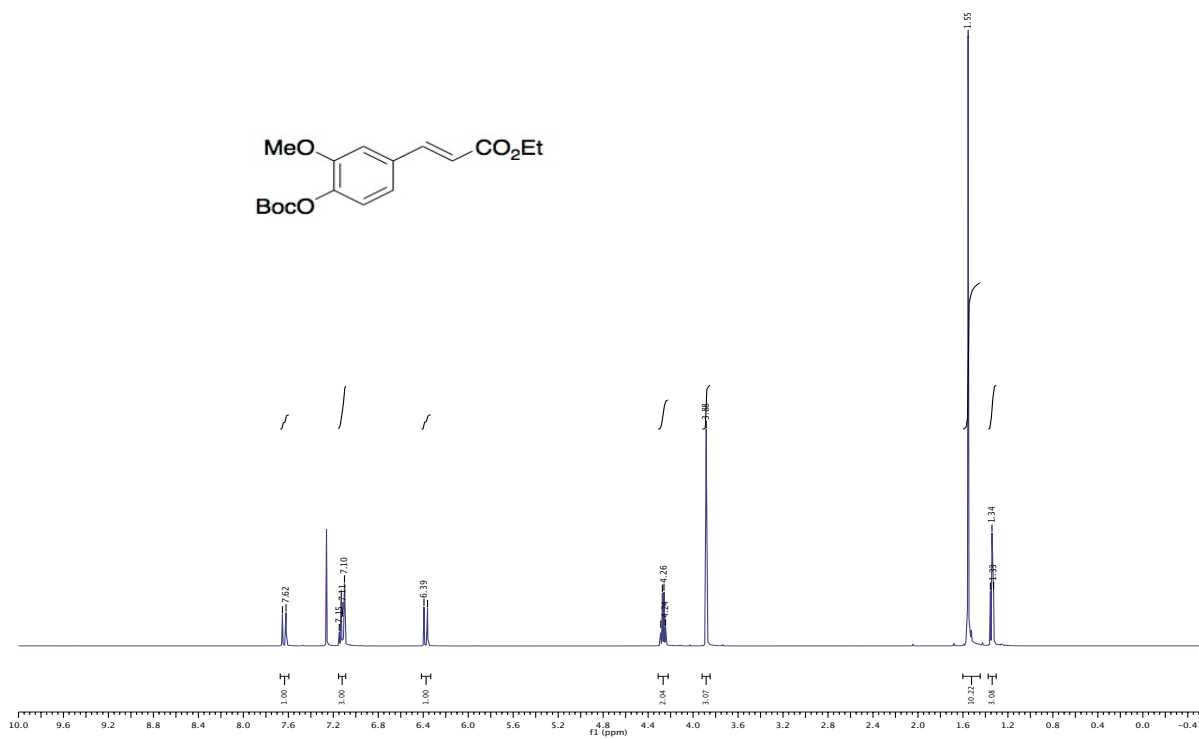
aen5217
PROTON CDCl3 (E:\A-500\Scheidt) aen255 1



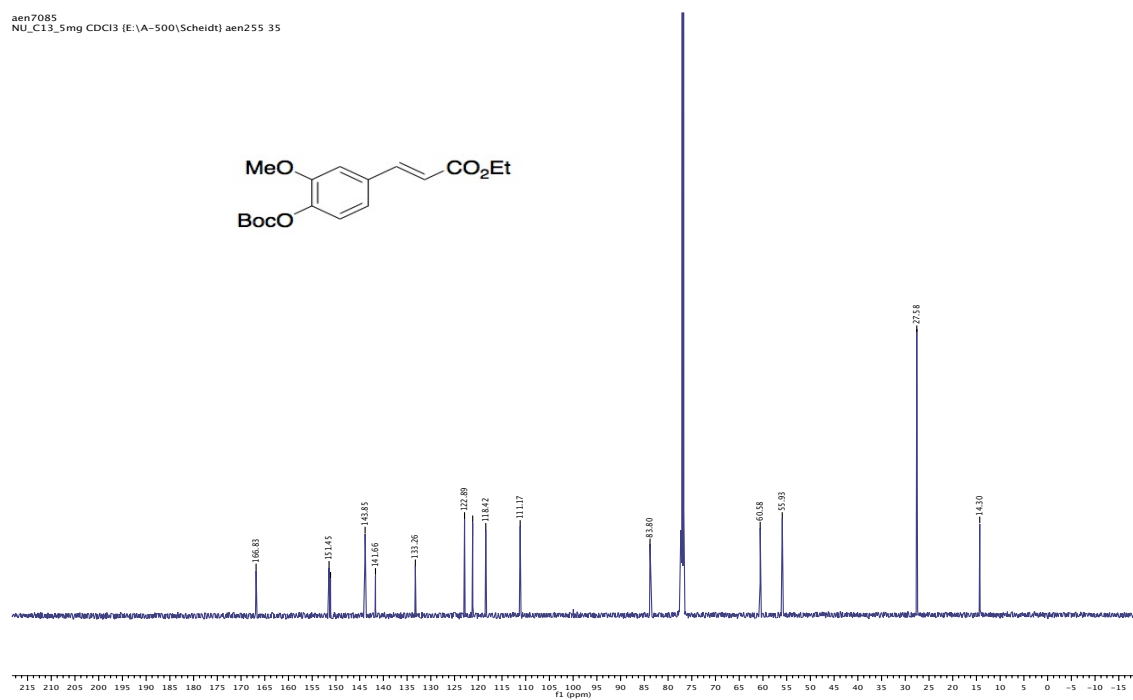
aen5217
NU_C13_2mg CDCl3 (E:\A-500\Scheidt) aen255 1



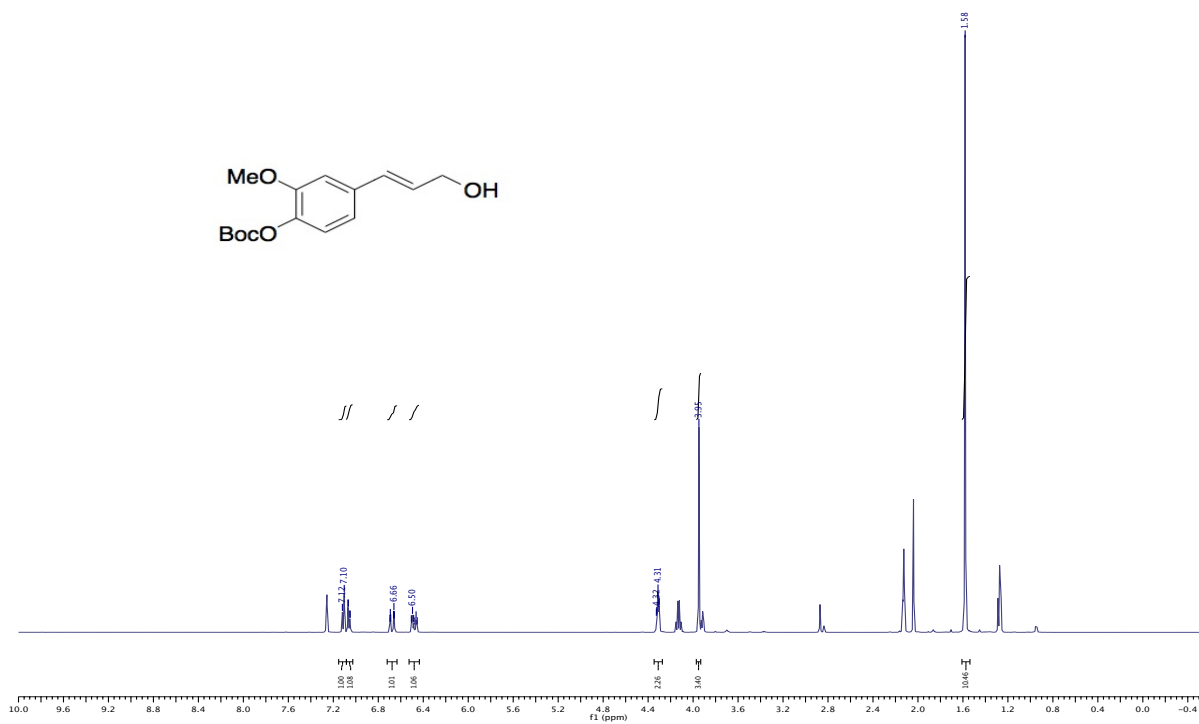
aen7085
PROTON CDCl3 (E:\A-500\Scheidt) aen255 35



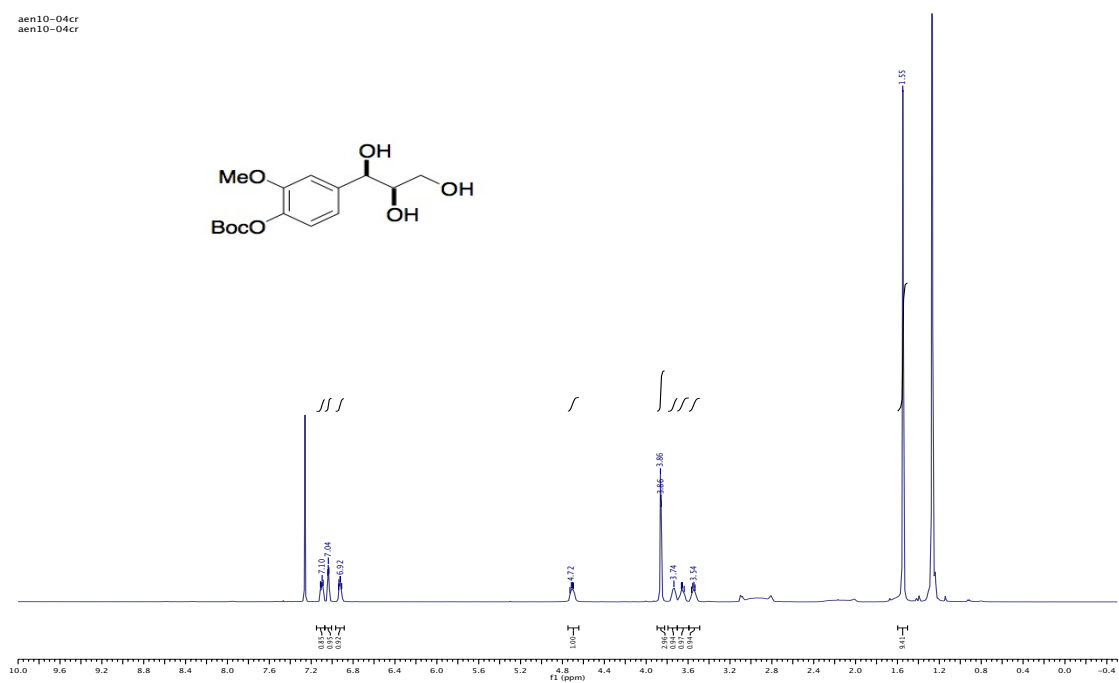
aen7085
NU_C13_5mg CDCl3 (E:\A-500\Scheidt) aen255 35



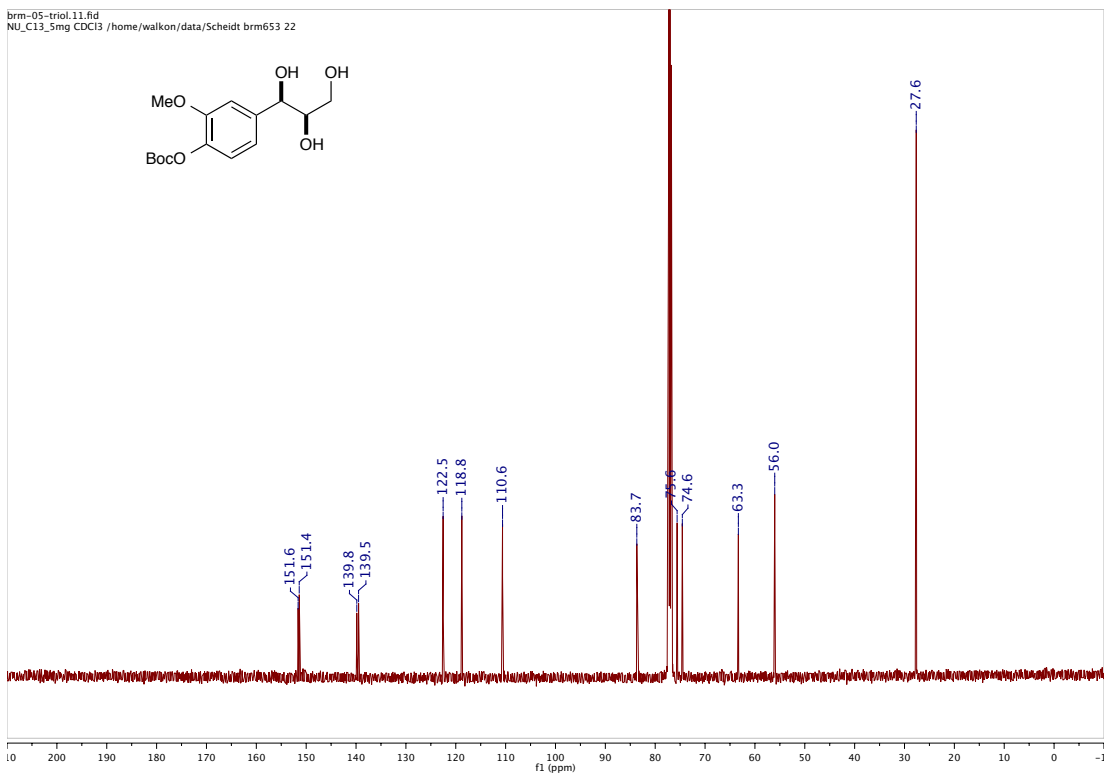
aen10-03cr
aen10-03cr

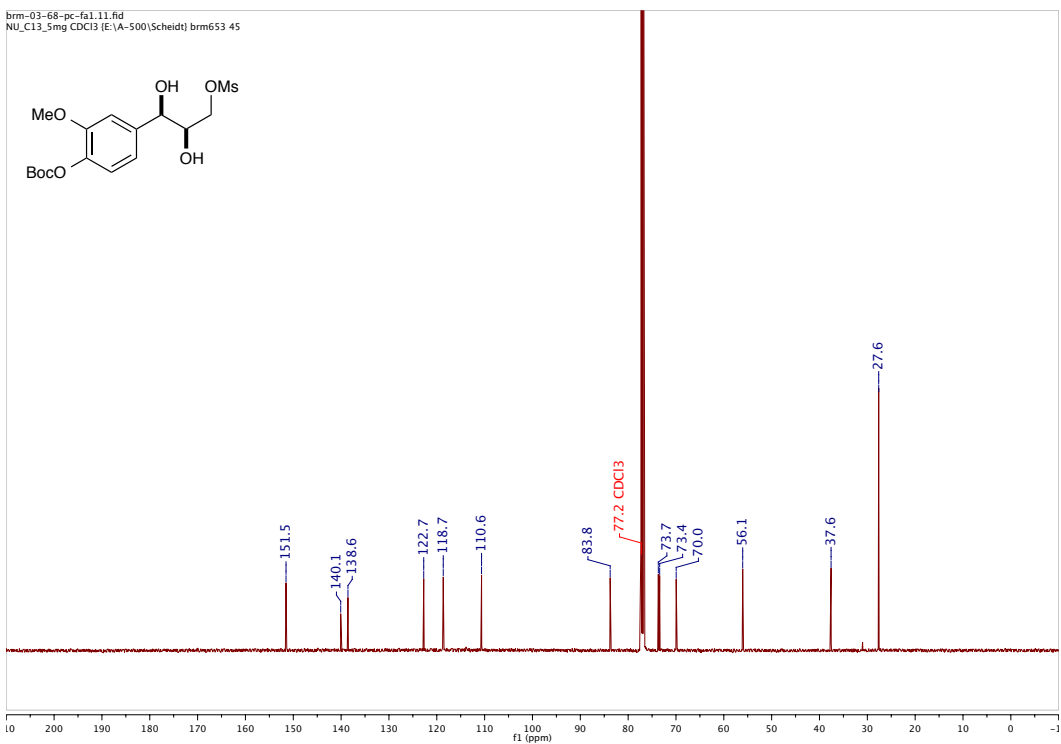
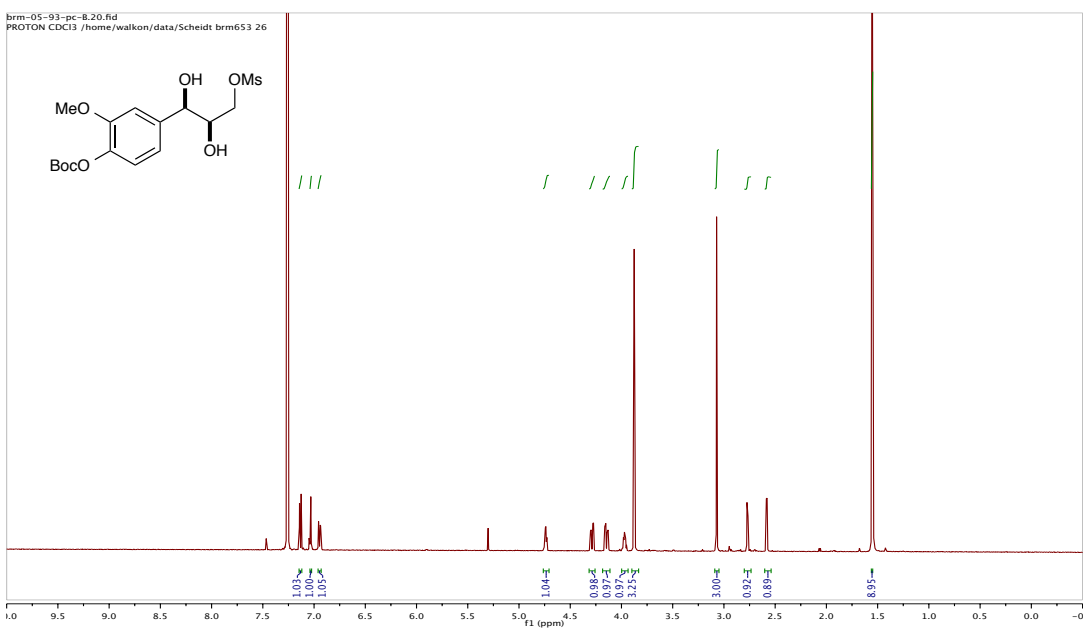


aen10-04cr
aen10-04cr

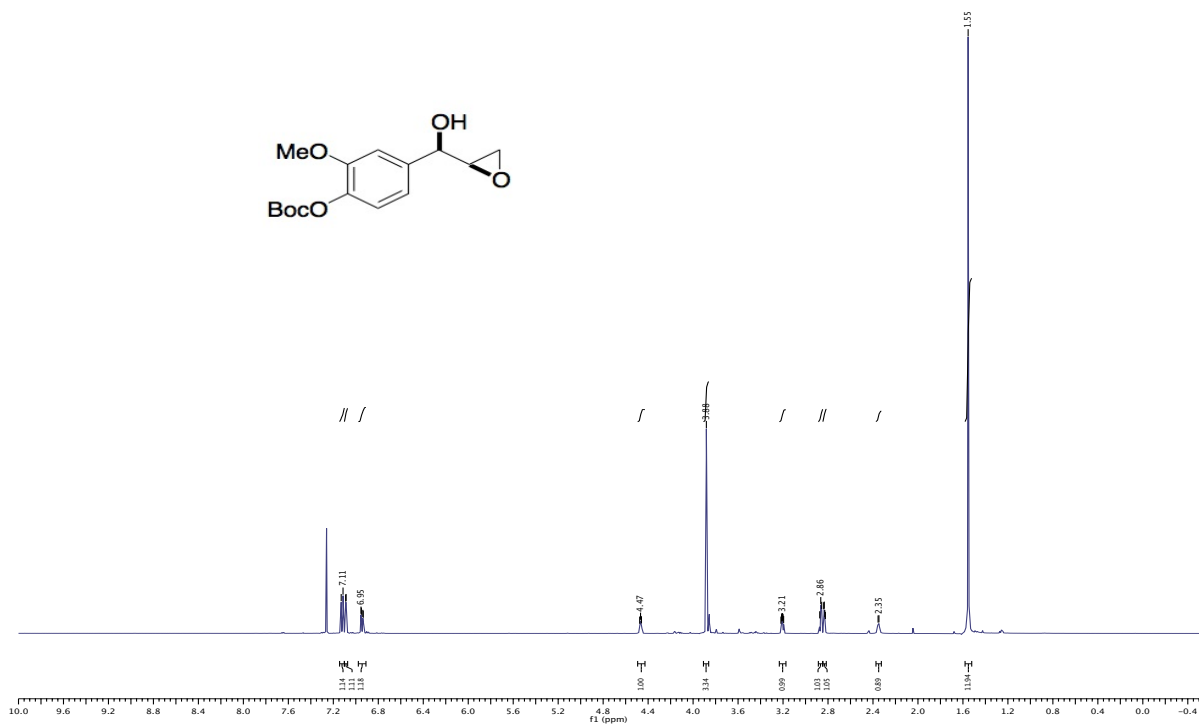


brm-05-triol.11.fid
NU_C13_5mg CDCl3 /home/walkon/data/Scheidt brm653 22

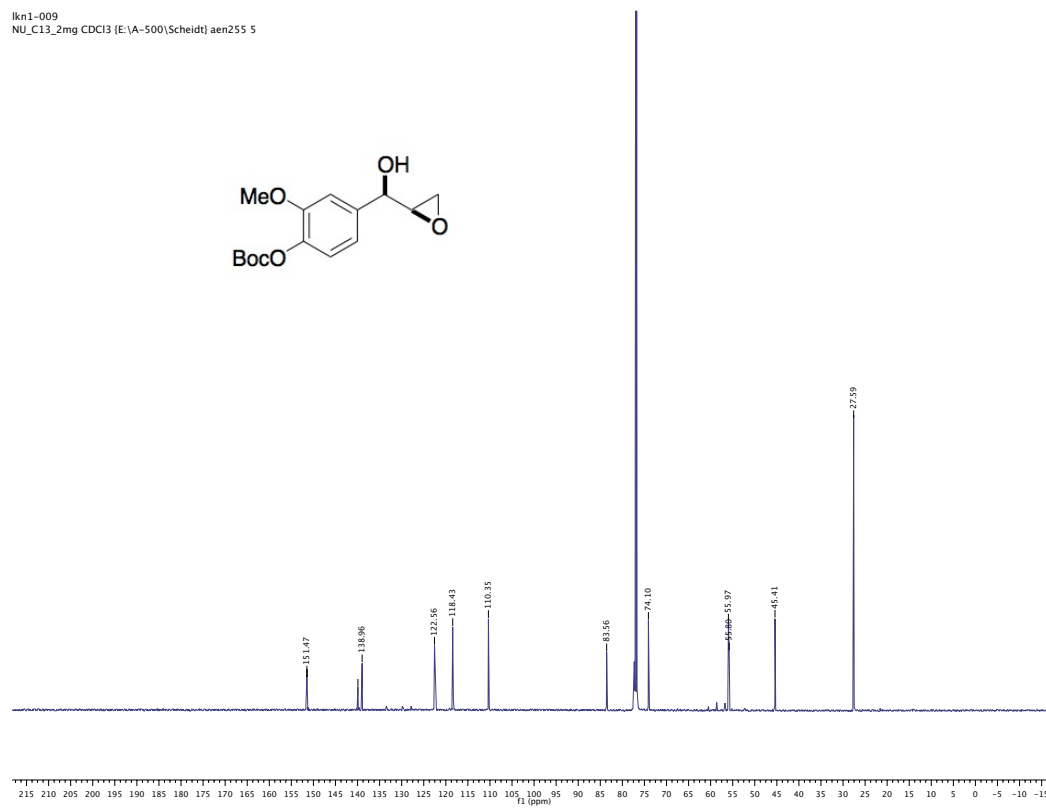




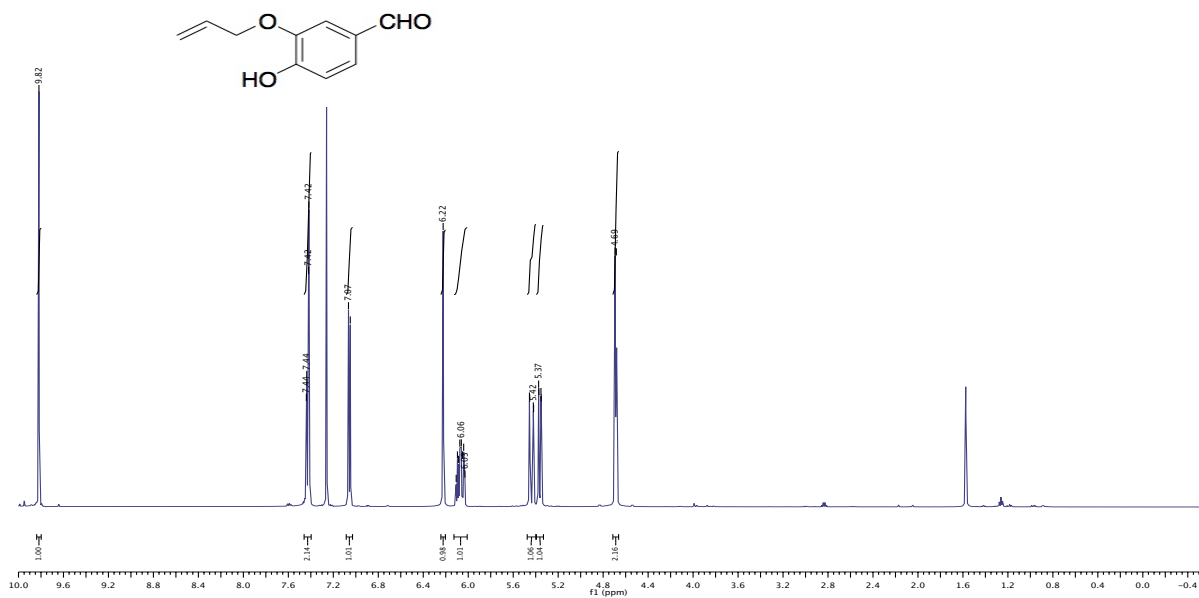
lkn1-009
PROTON CDCl3 (E:\A-500\Scheidt) aen255 5



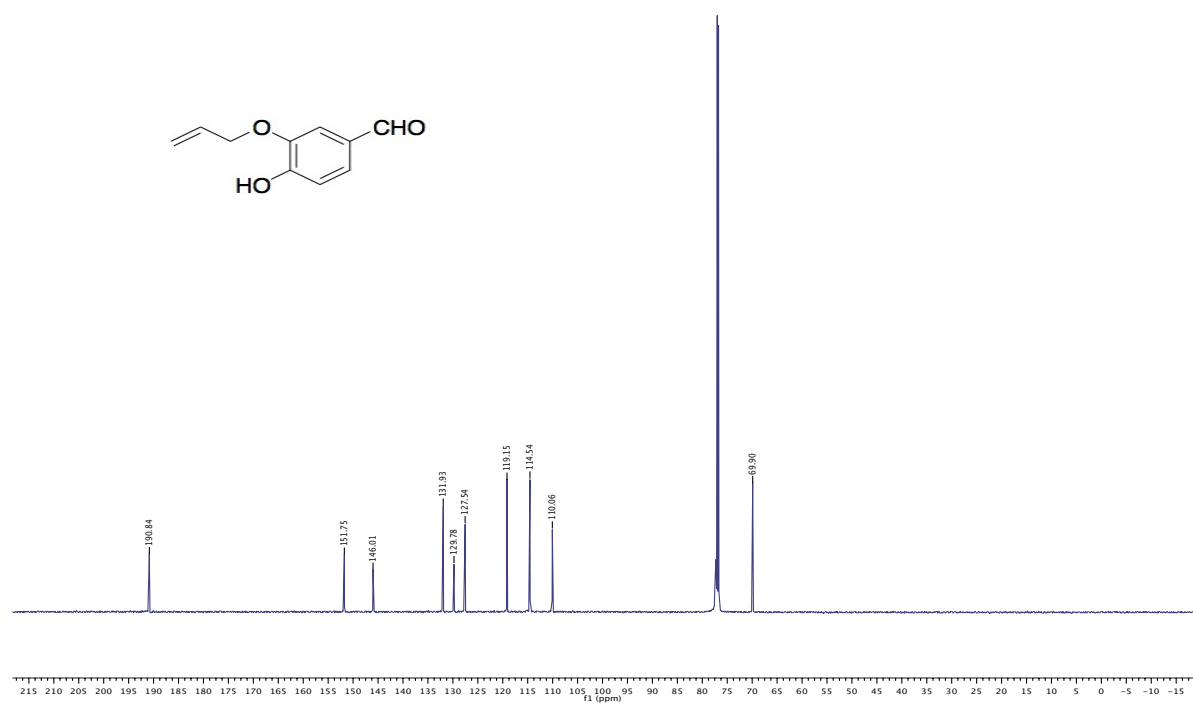
lkn1-009
NU_C13_2mg CDCl3 (E:\A-500\Scheidt) aen255 5



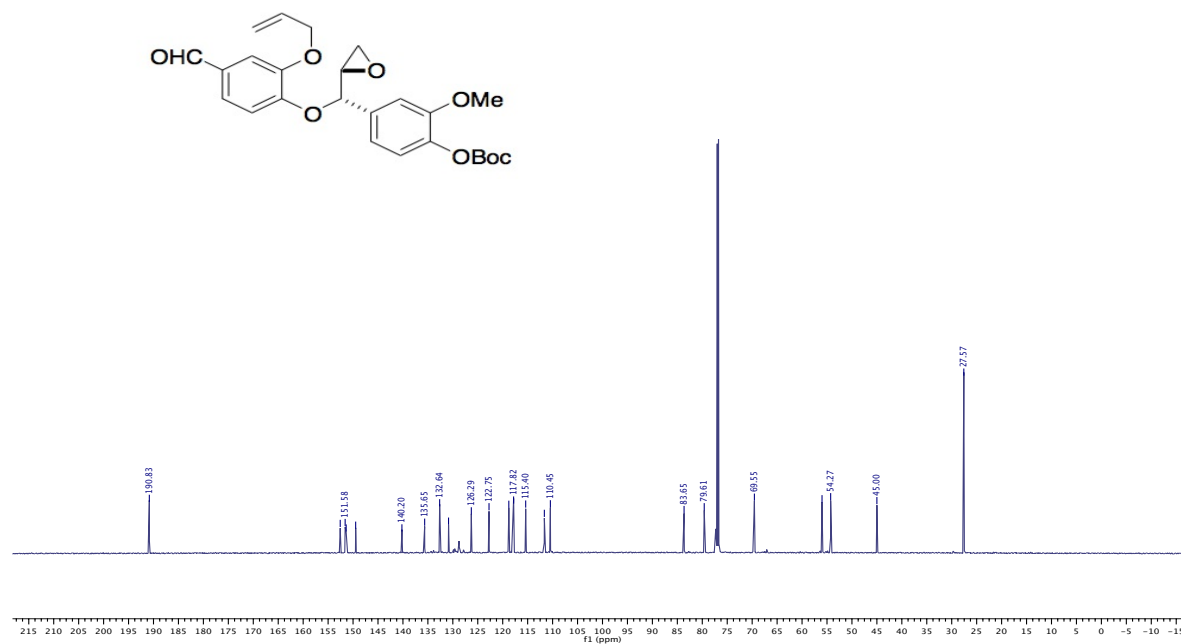
aen5287
PROTON CDCl3 [E:\A-500\Scheidt] aen255 3



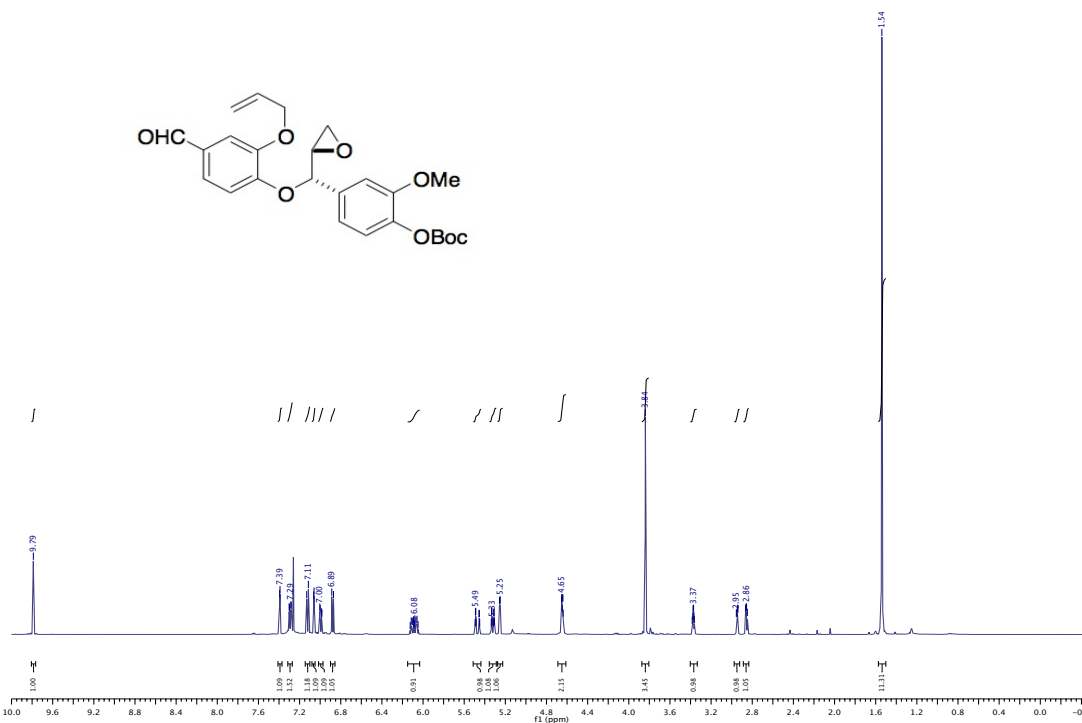
aen5287
NU_C13_2mg CDCl3 [E:\A-500\Scheidt] aen255 3



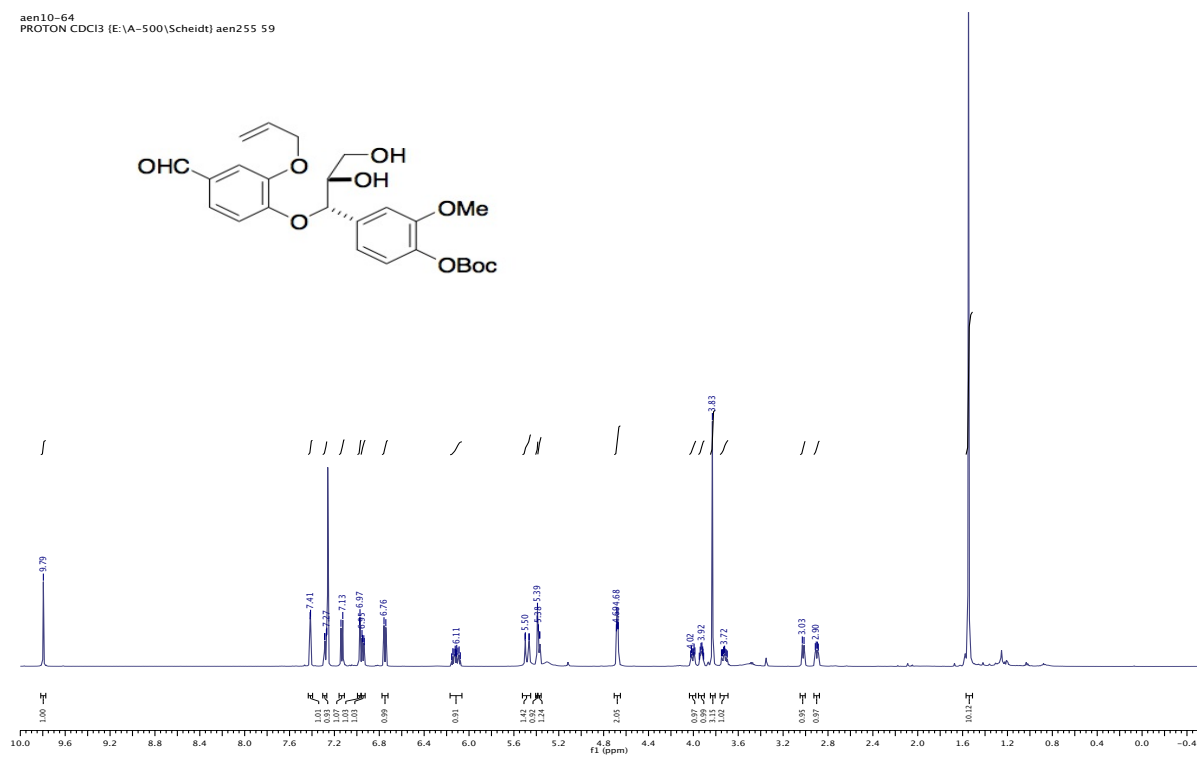
aen10-68
 NU_C13_5mg CDCl3 [E:\A-500\Scheidt] aen255 2



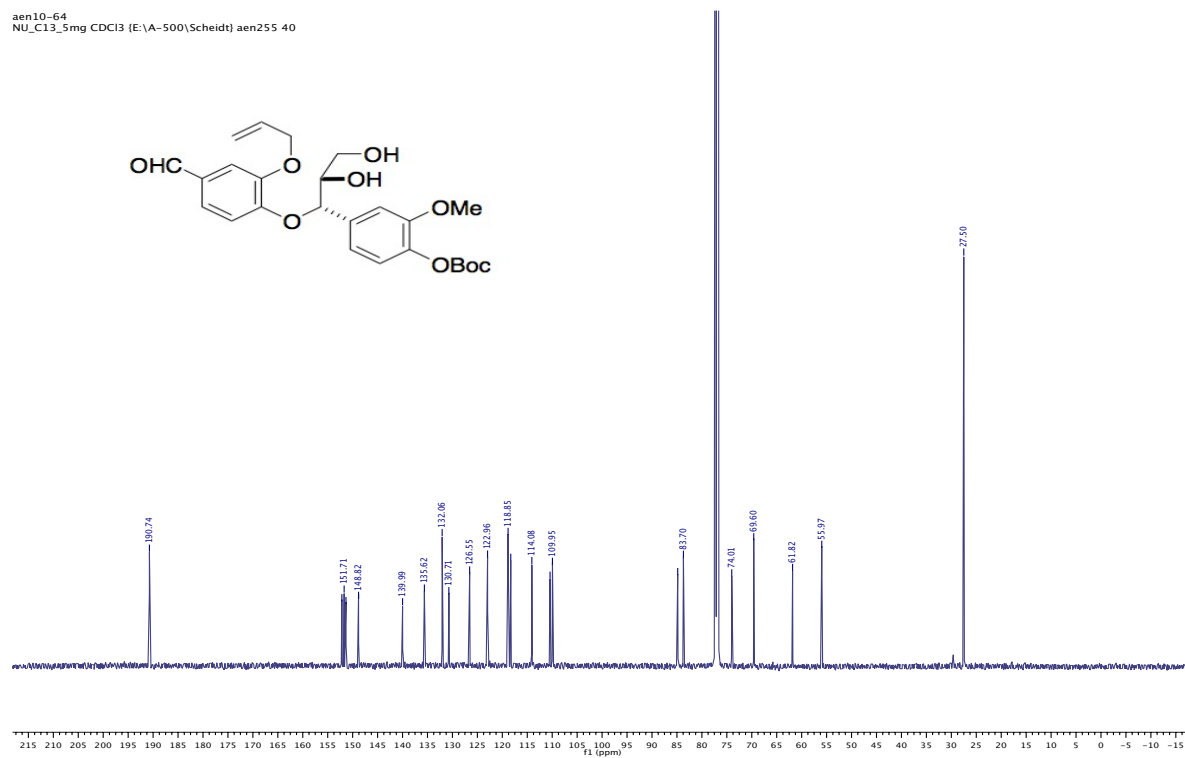
aen10-68
 PROTON CDCl3 [E:\A-500\Scheidt] aen255 2



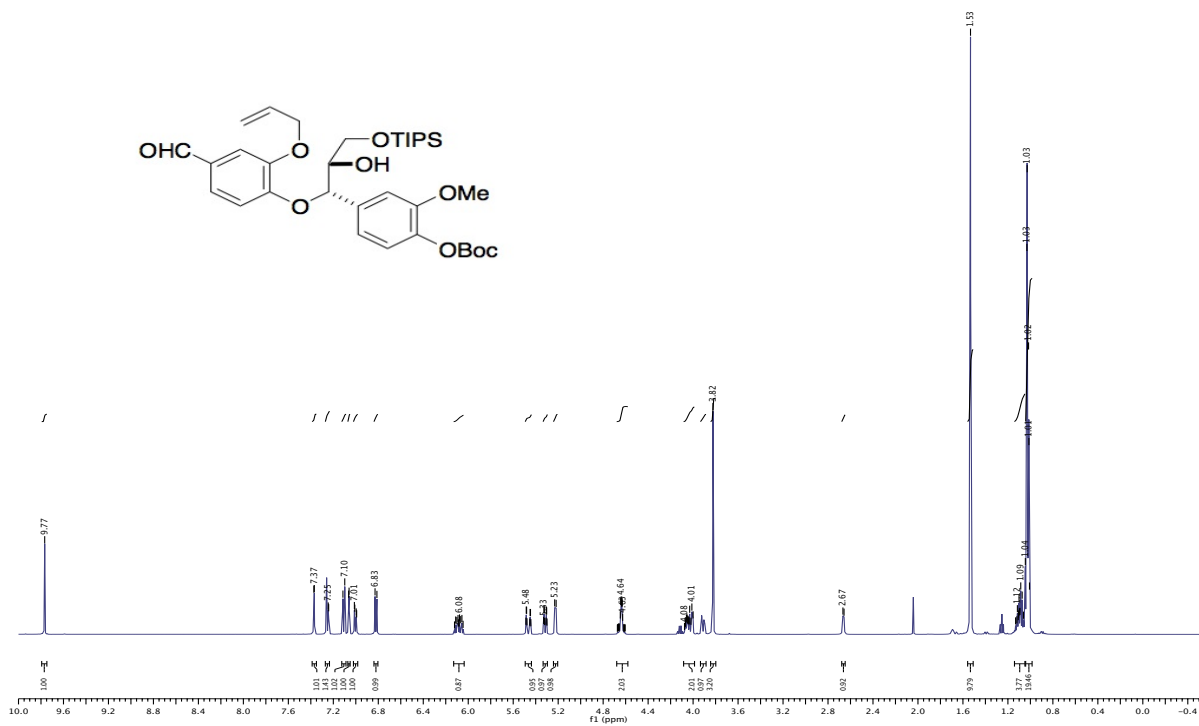
ae10-64
 PROTON CDCl3 [E:\A-500\Scheidt\ aen255 59



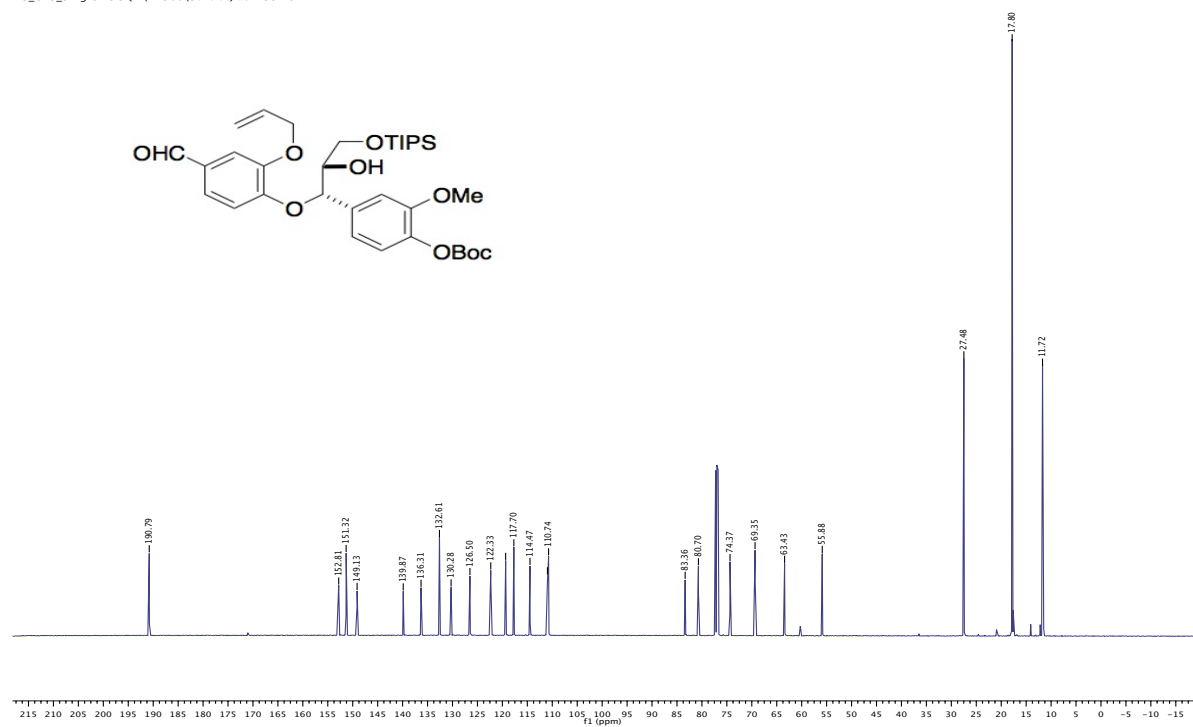
ae10-64
 NU_C13_5mg CDCl3 [E:\A-500\Scheidt\ aen255 40



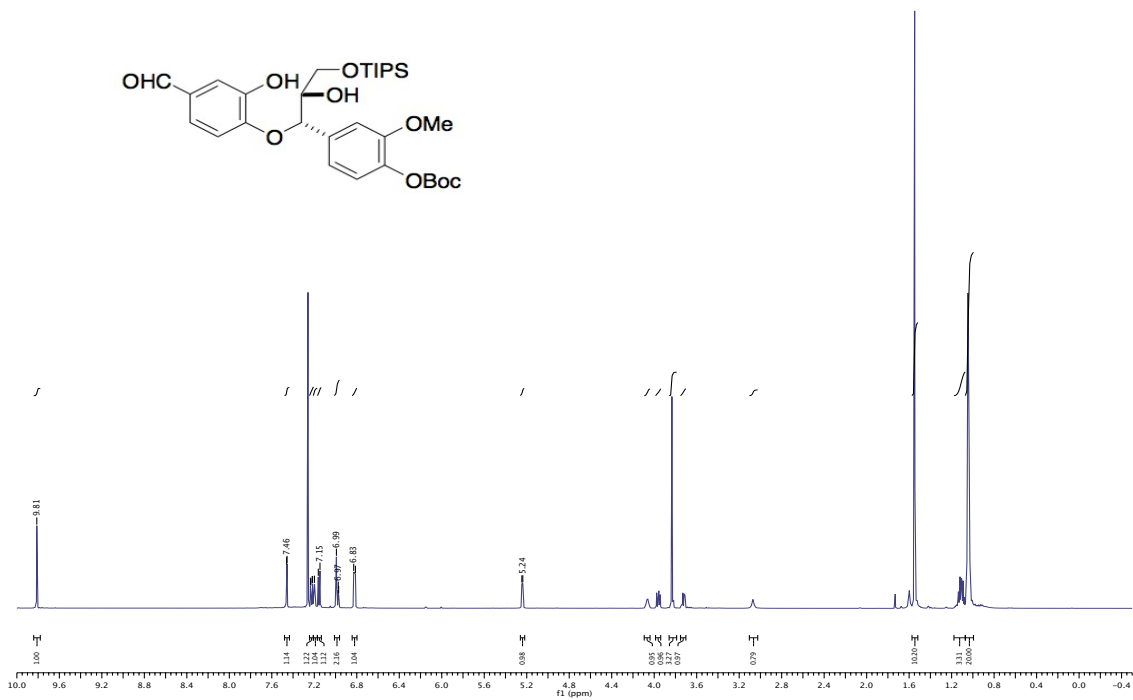
aen8-116
 PROTON CDCl3 [E:\A-500\Scheidt] aen255 43



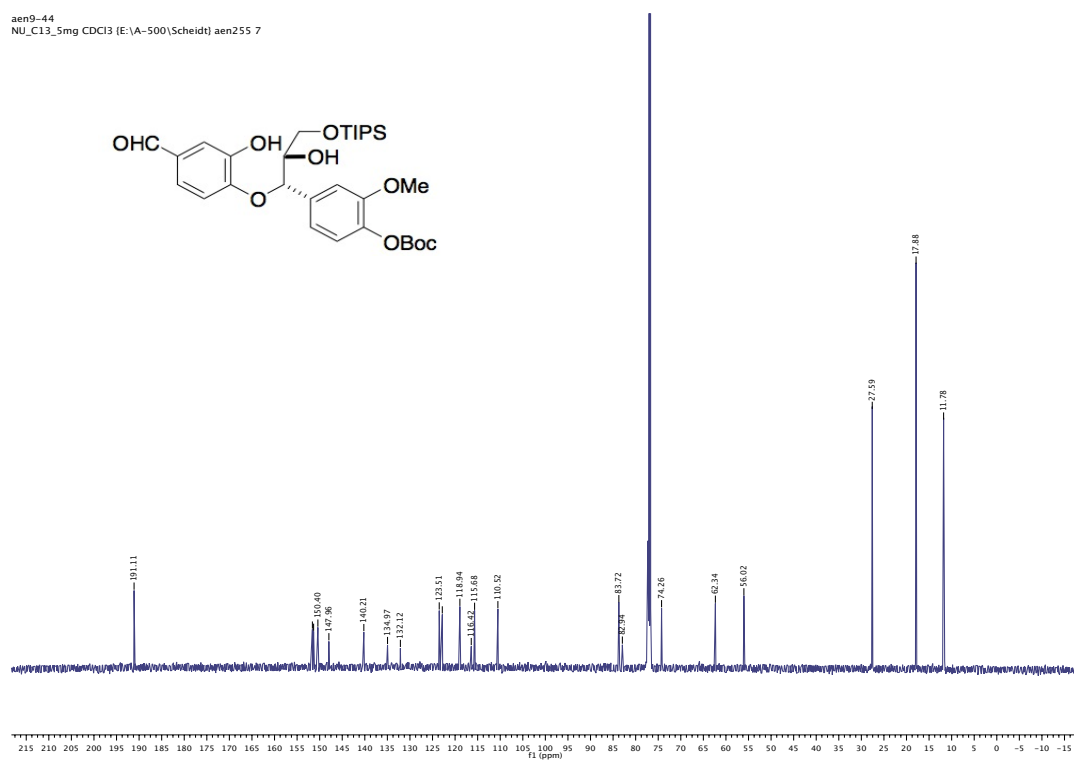
aen8-116
 NU_C13_5mg CDCl3 [E:\A-500\Scheidt] aen255 29



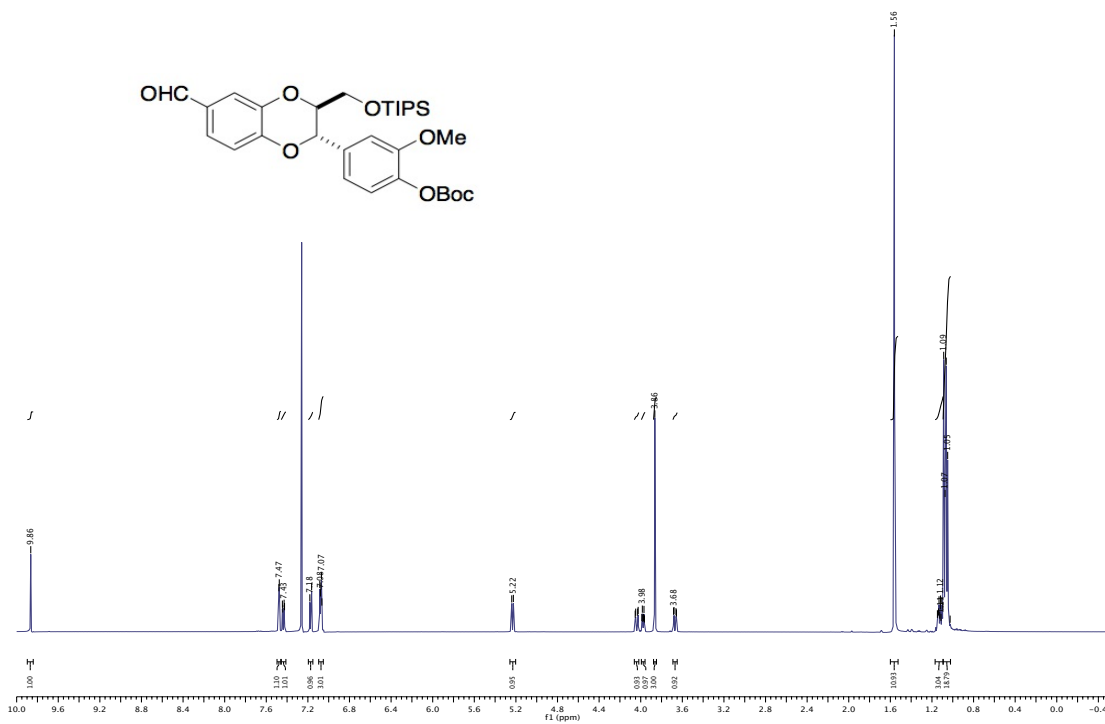
aen9-44
 PROTON CDCl3 [E:\A-500\Scheidt] aen255 59



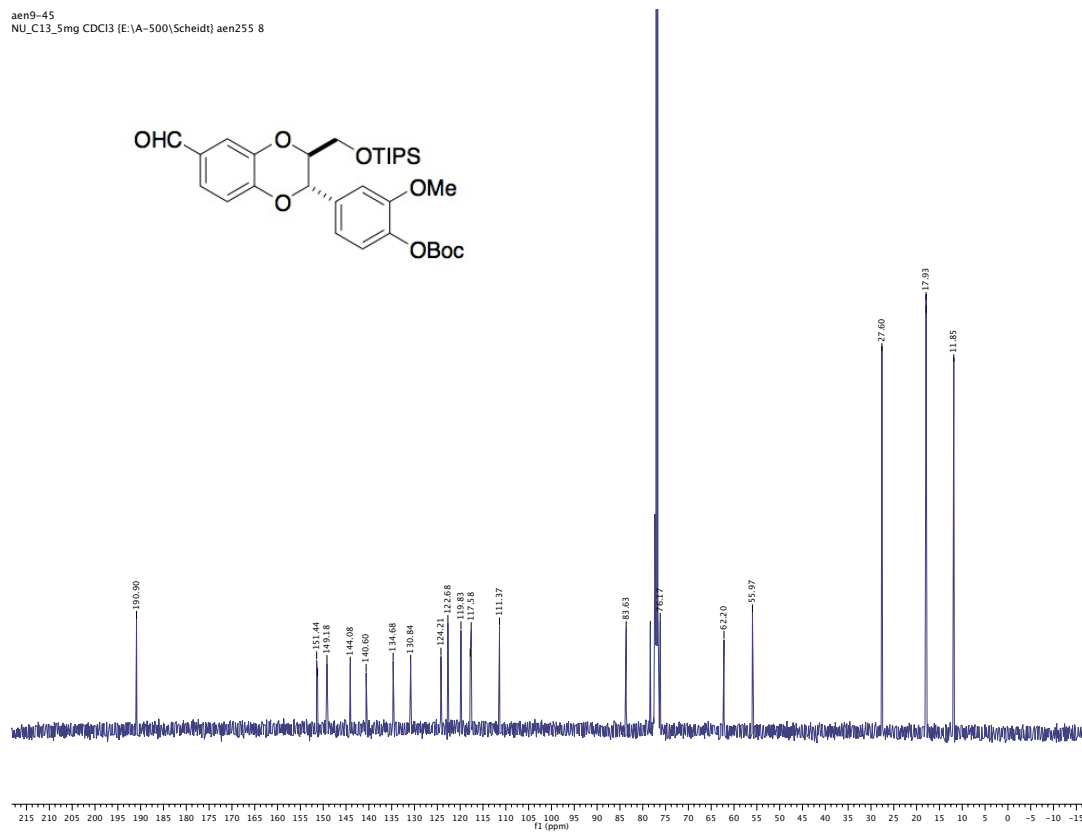
aen9-44
 NU_C13_5mg CDCl3 [E:\A-500\Scheidt] aen255 7



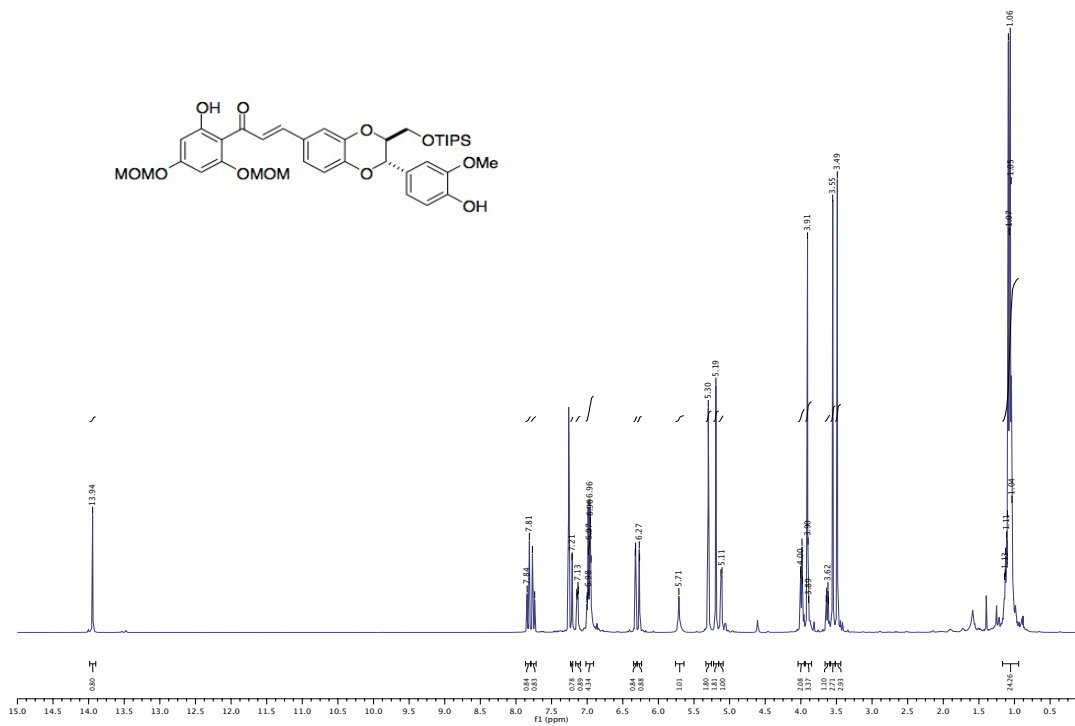
aen9-45
 PROTON CDCl3 [E:\A-500\Scheidt] aen255 8



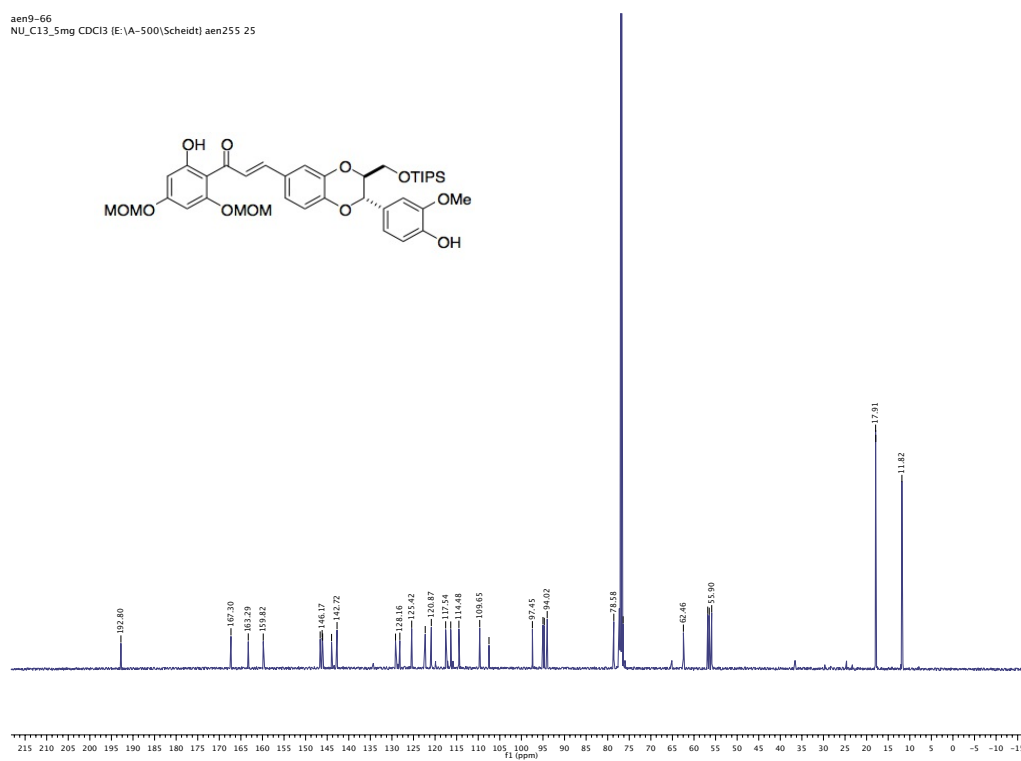
aen9-45
 NU_C13_5mg CDCl3 [E:\A-500\Scheidt] aen255 8



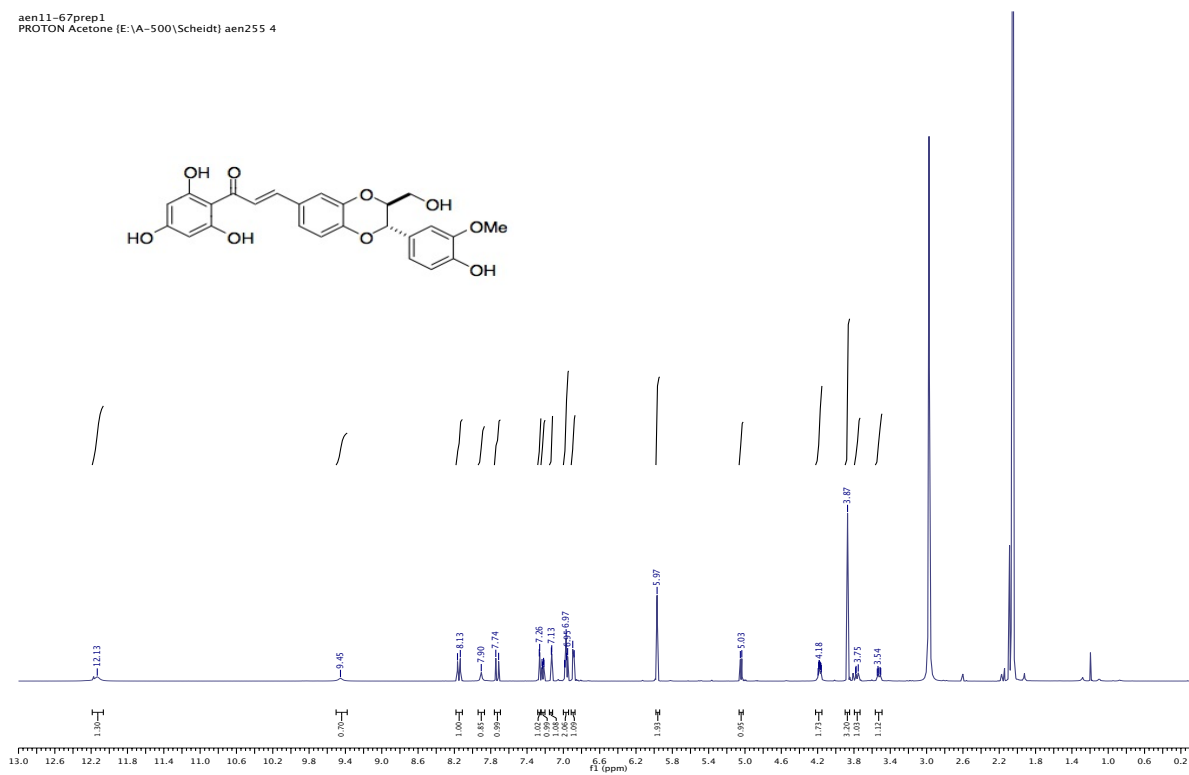
aen9-66
 PROTON CDCl3 [E:\A-500\Scheidt] aen255 25



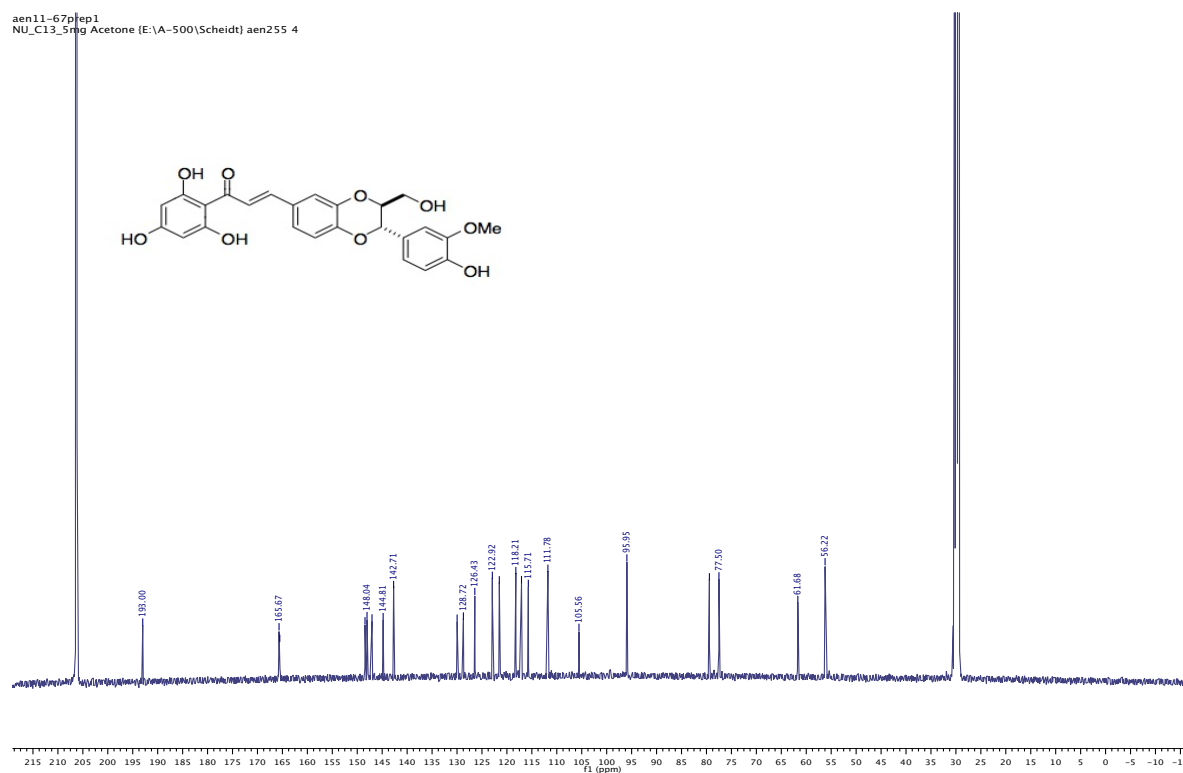
aen9-66
 NU_C13_5mg CDCl3 [E:\A-500\Scheidt] aen255 25

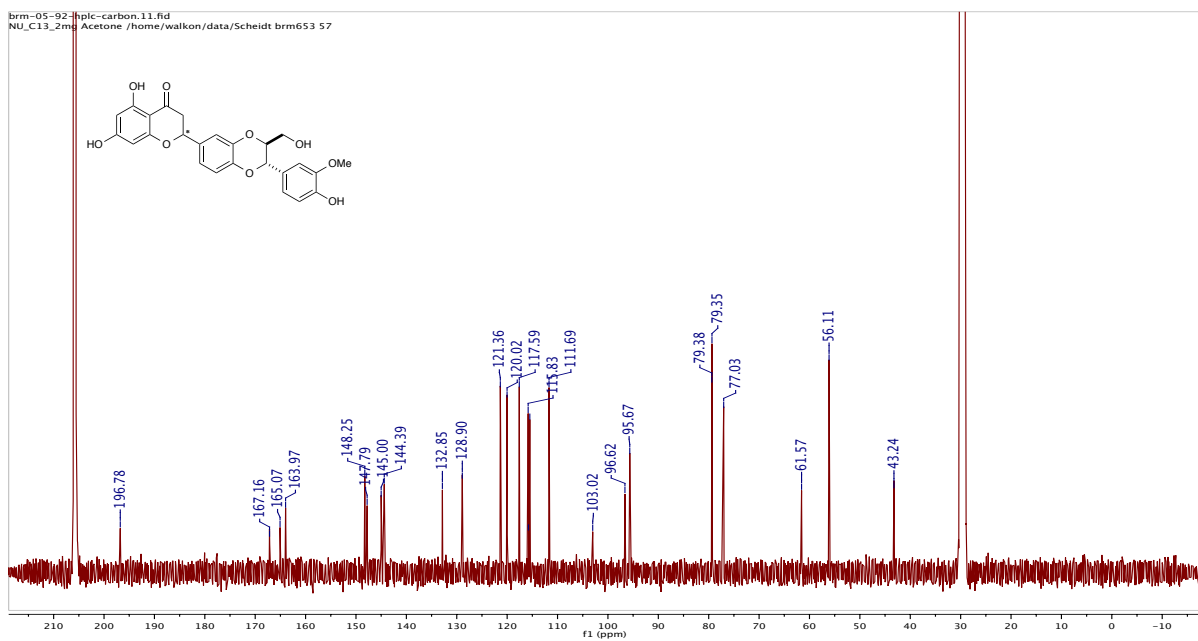
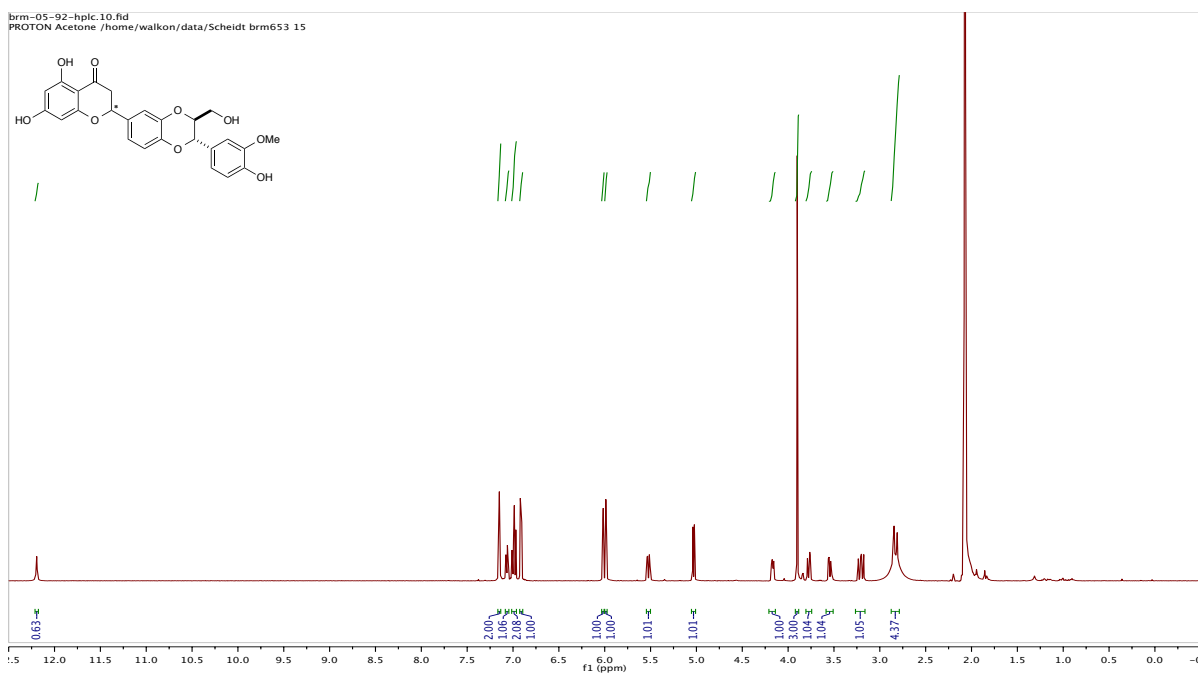


aen11-67prep1
 PROTON Acetone (E:\A-500\Scheidt) aen255 4

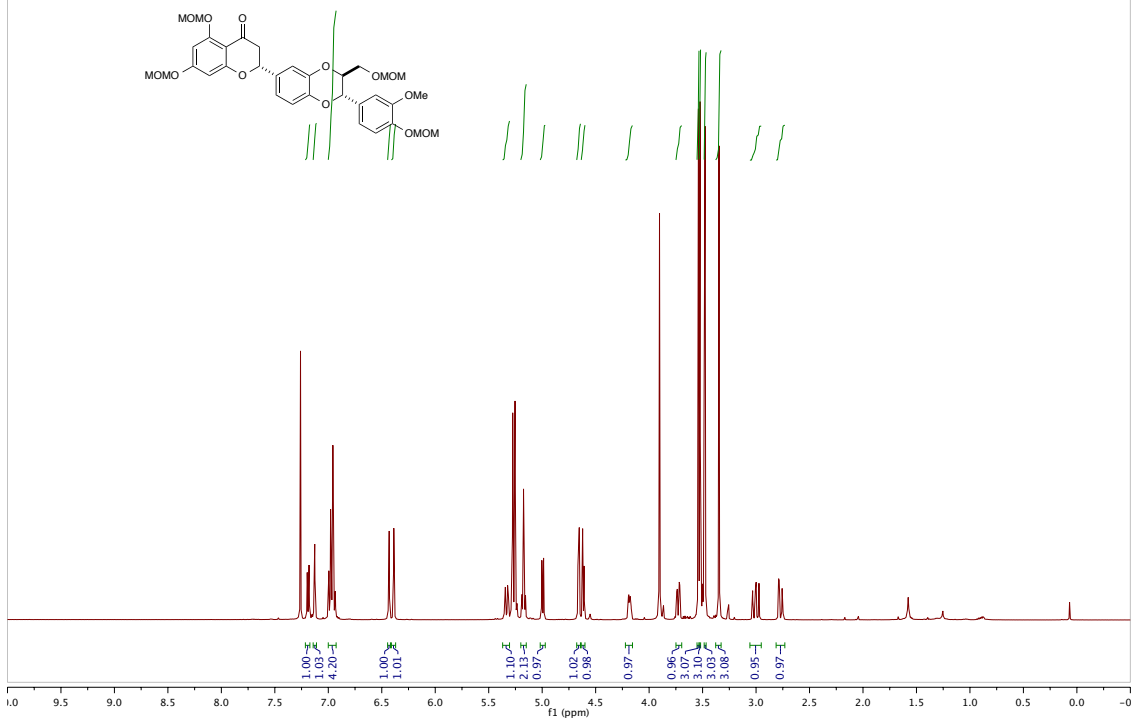


aen11-67prep1
 NU_C13_5mg Acetone (E:\A-500\Scheidt) aen255 4

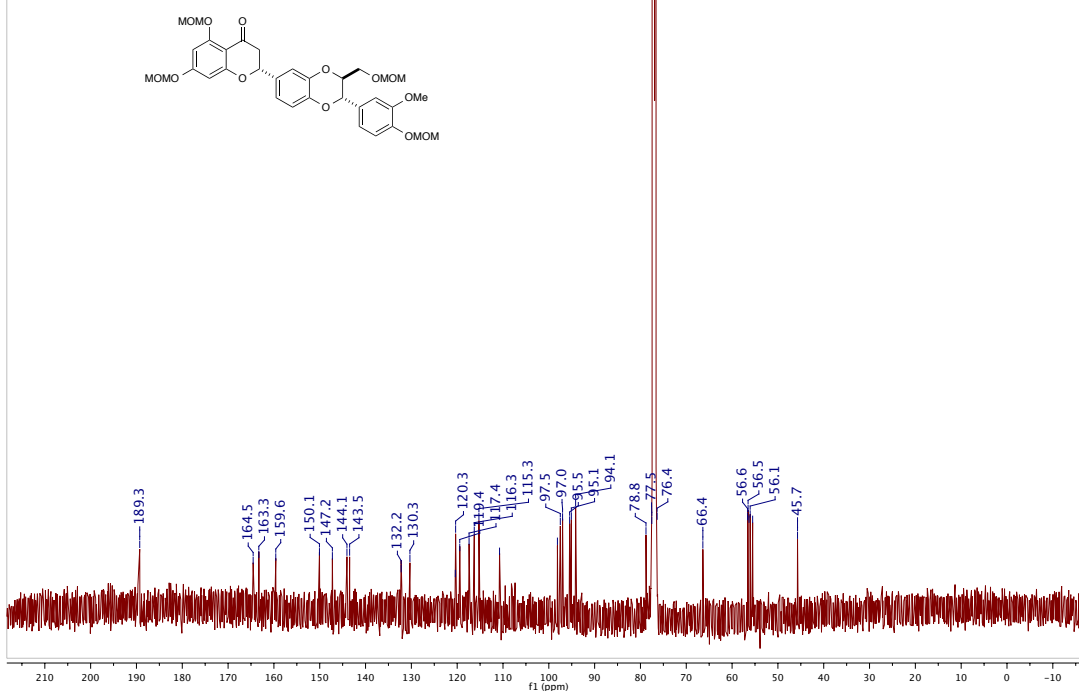


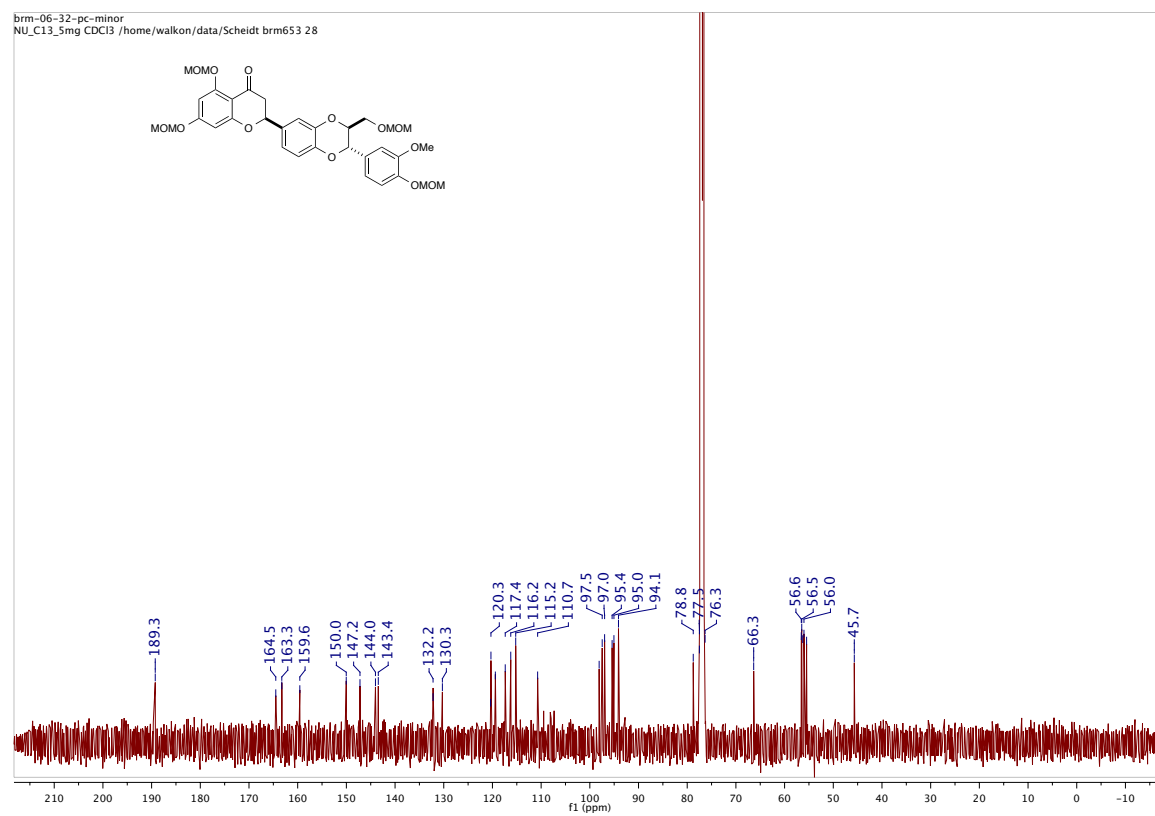
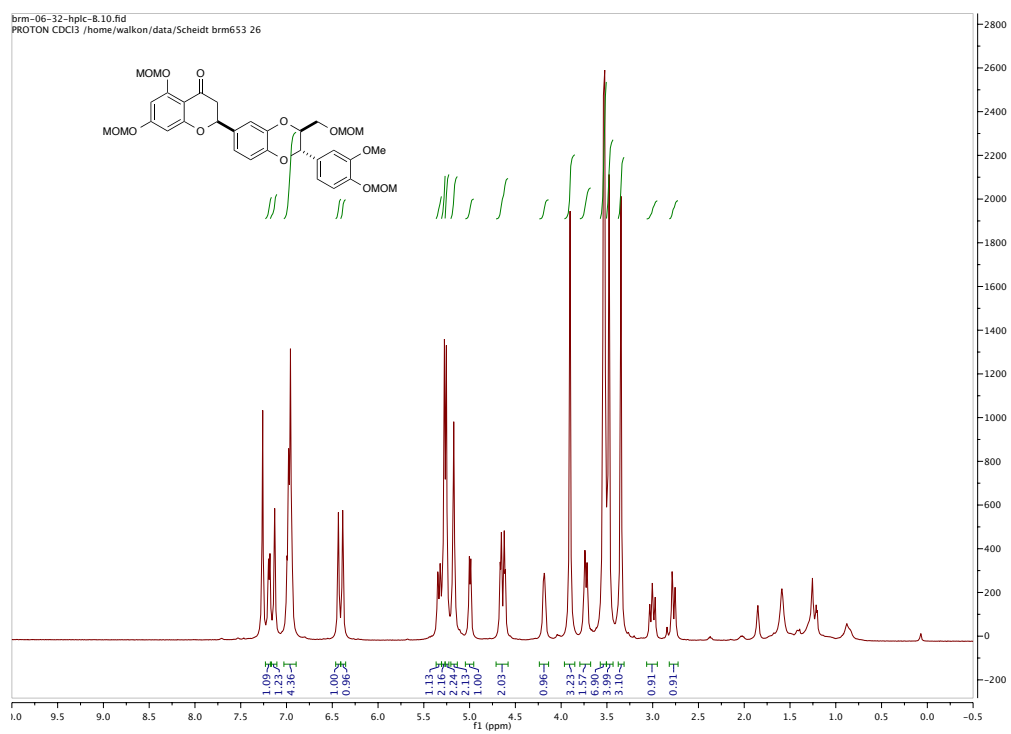


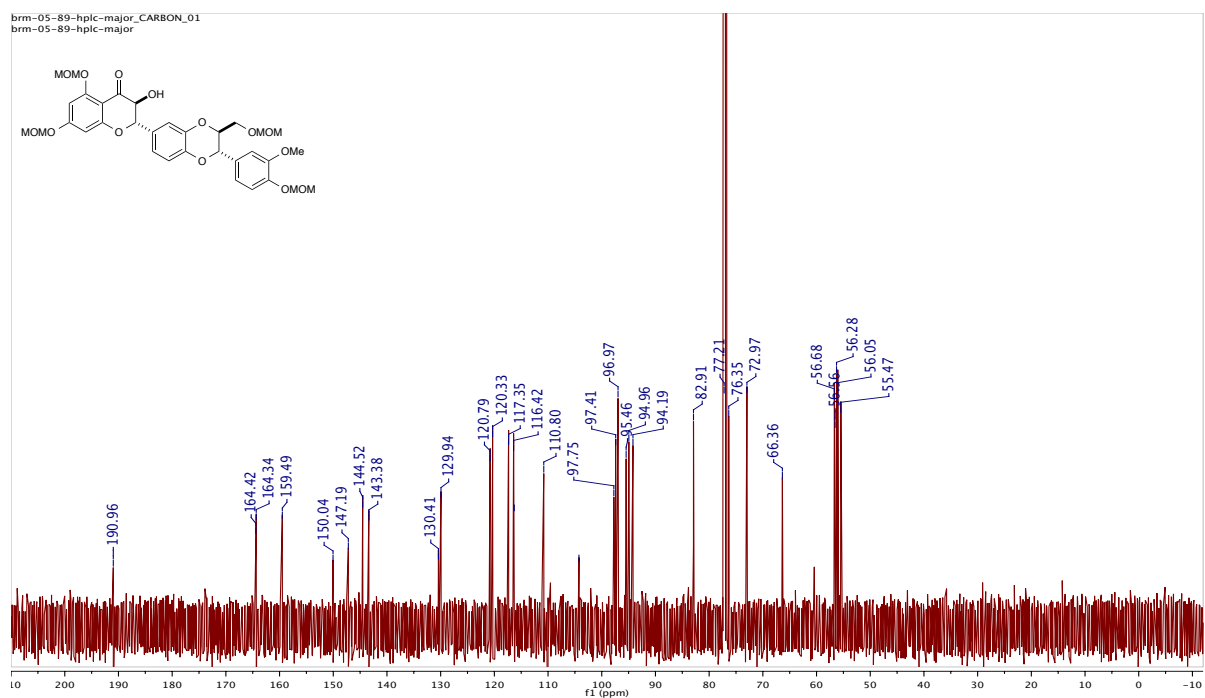
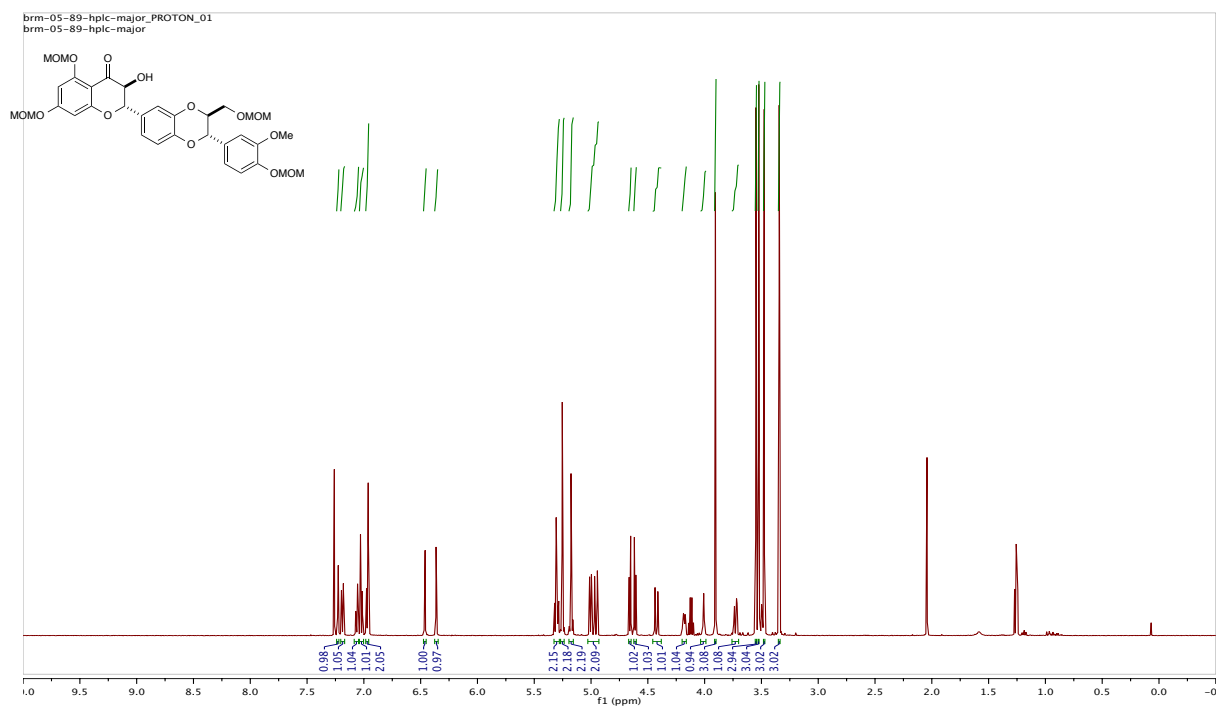
brm-06-32-hplc-major.10.fid
PROTON CDCl3 /home/walkon/data/Scheidt brm653 5



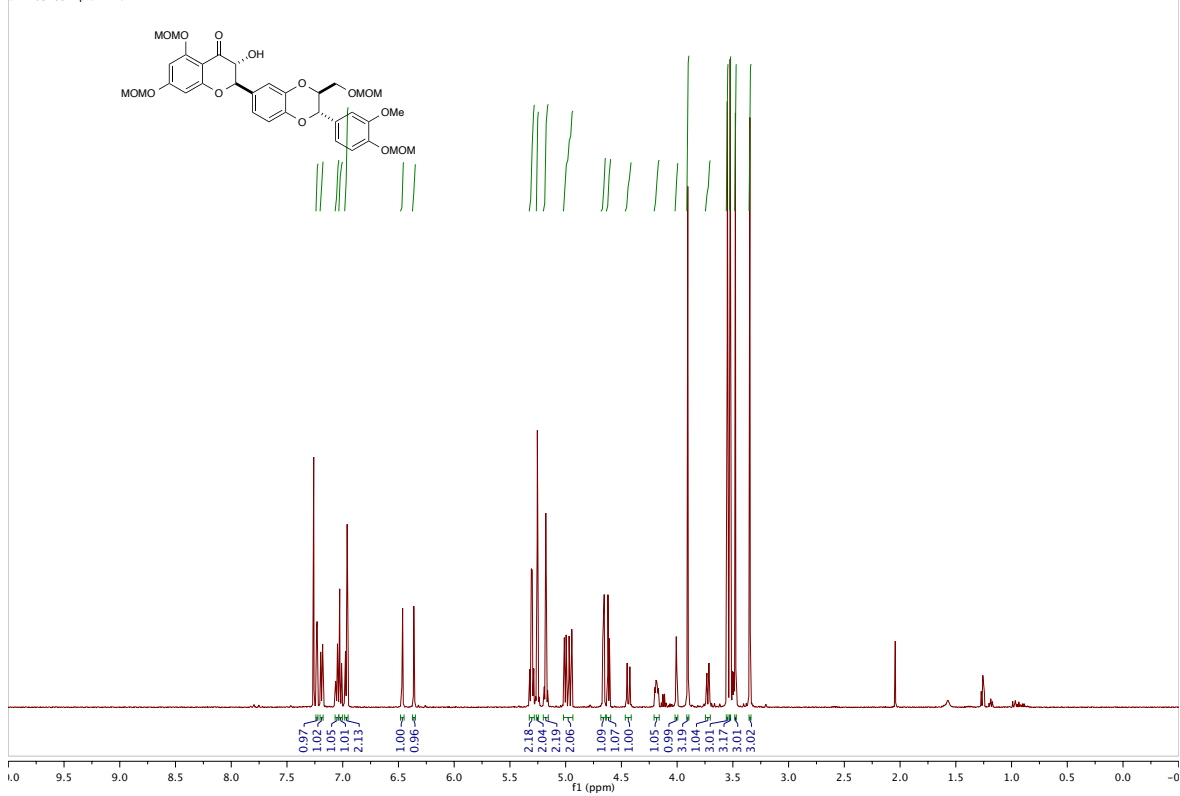
brm-06-32-pc.21.fid
NU_C13_5mg CDCl3 /home/walkon/data/Scheidt brm653 28



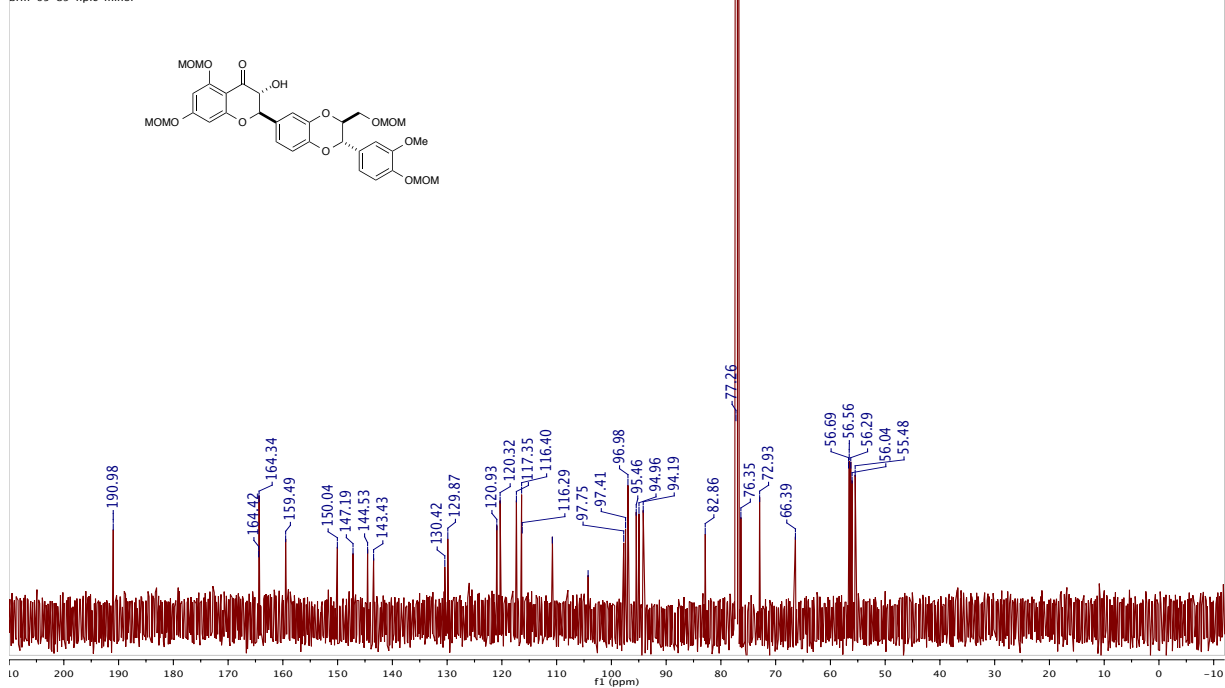


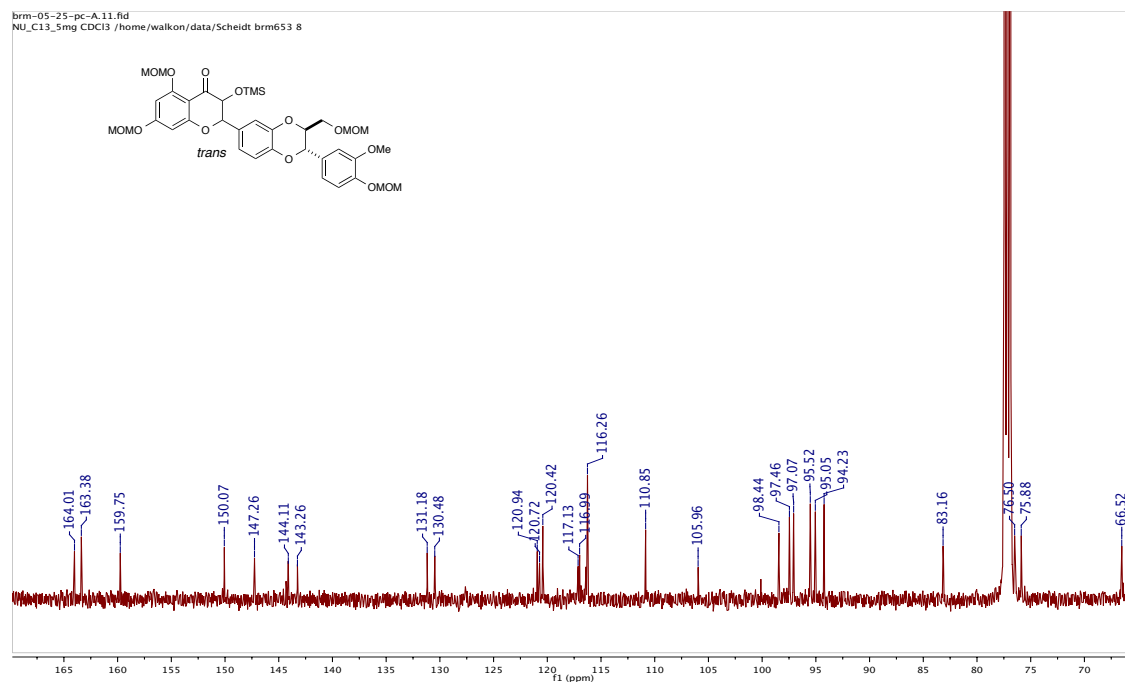
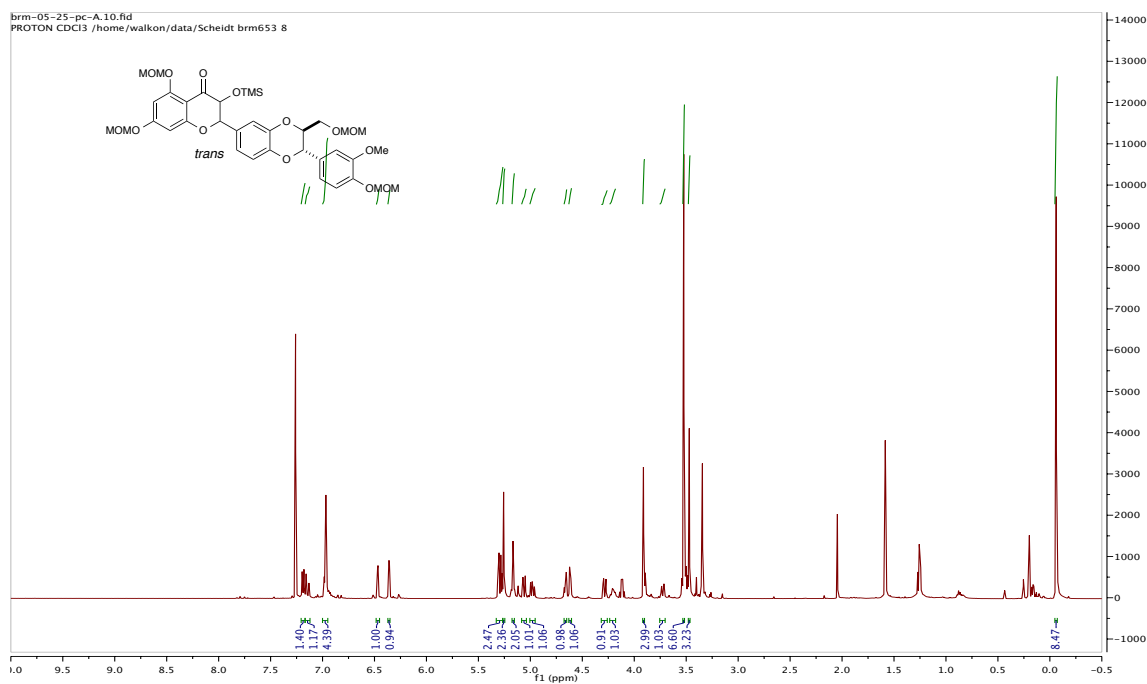


brm-05-89-hplc-minor PROTON_01
brm-05-89-hplc-minor

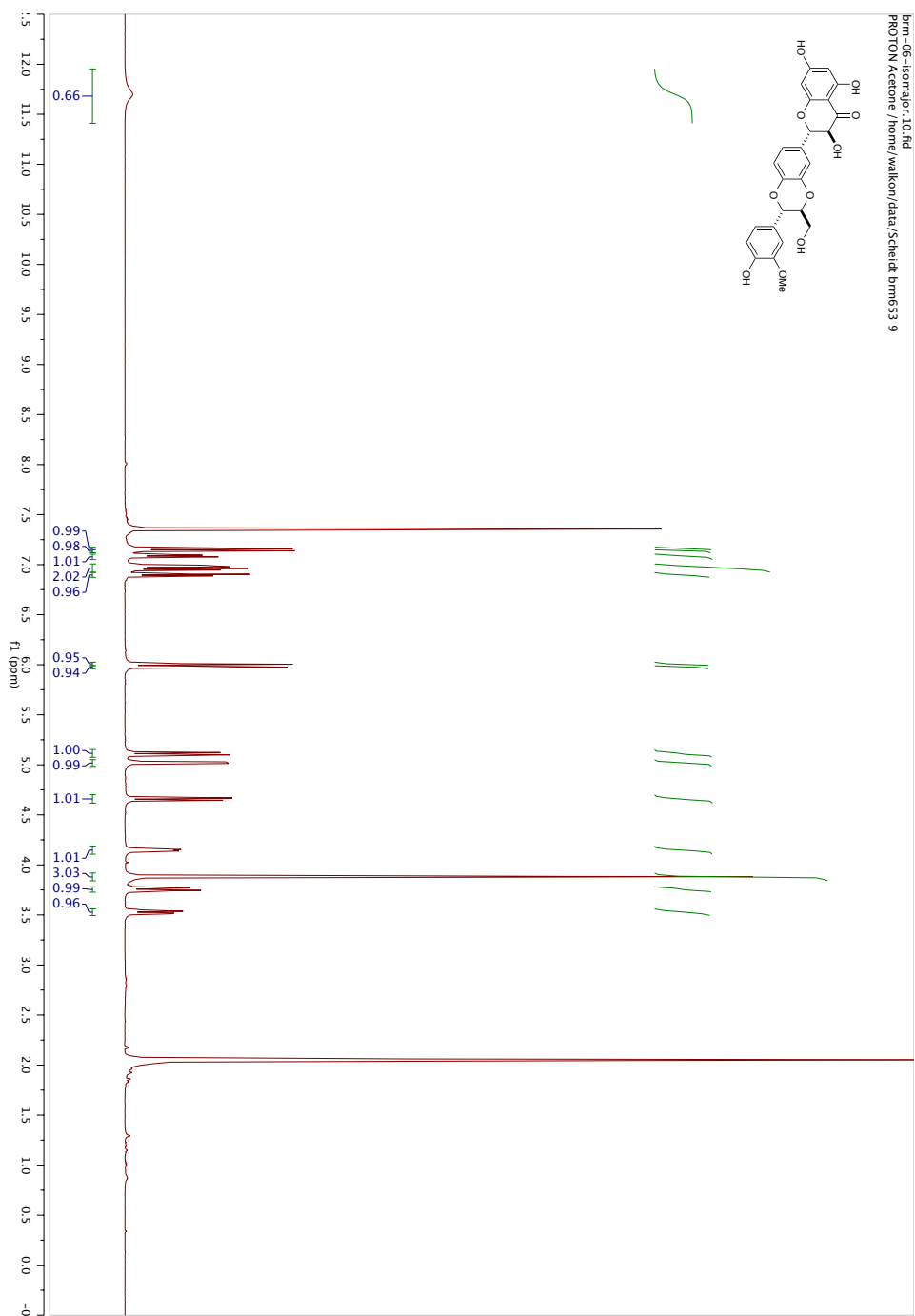


brm-05-89-hplc-minor CARBON_01
brm-05-89-hplc-minor

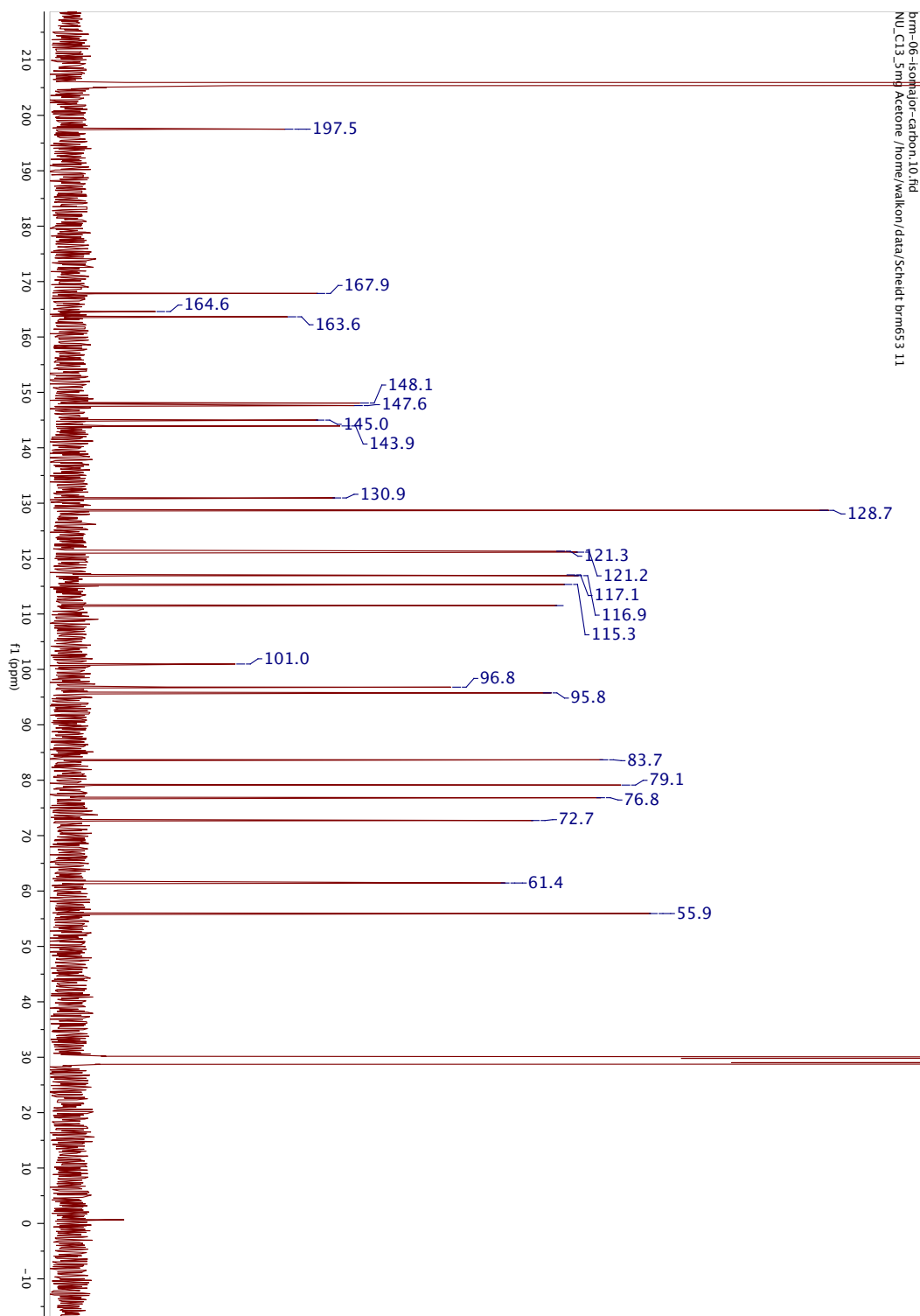




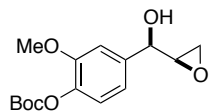
^1H NMR Spectra of (–)-isosilybin A (**1**) (500 MHz, $(\text{CD}_3)_2\text{CO}$):



^{13}C NMR Spectra of (-)-isosilybin A (1) (500 MHz, $(\text{CD}_3)_2\text{CO}$):

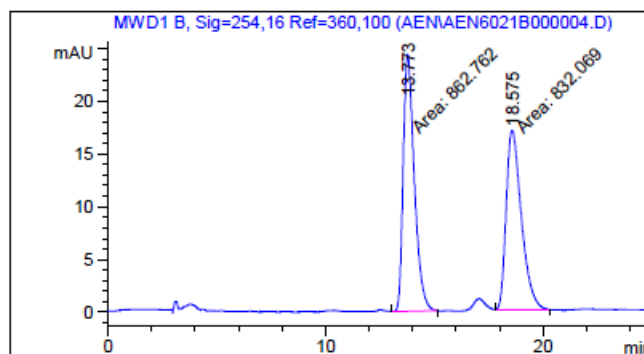


1.12.8 HPLC Traces of Selected Compounds



Racemic 7

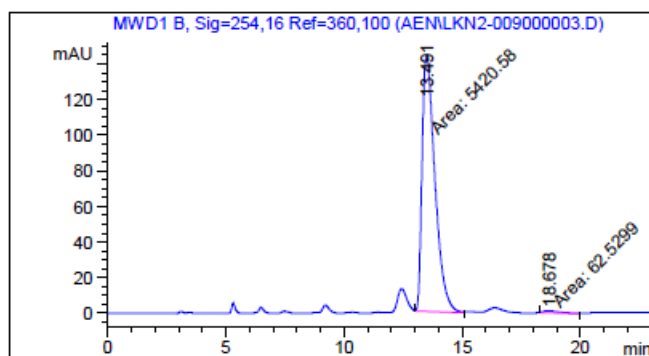
Chiralcel OD-H, 10% *i*-PrOH/hexanes, 1 mL/min:



Peak #	RetTime [min]	Type	Width [min]	Area [mAU*s]	Height [mAU]	Area %
1	13.773	MM	0.5919	862.76184	24.29473	50.9055
2	18.575	MM	0.8149	832.06915	17.01794	49.0945

Enantioenriched I-55 (99:1 er)

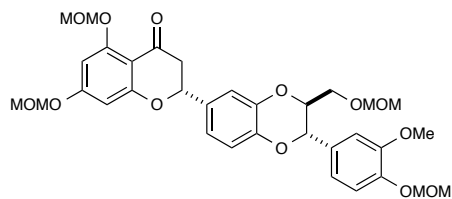
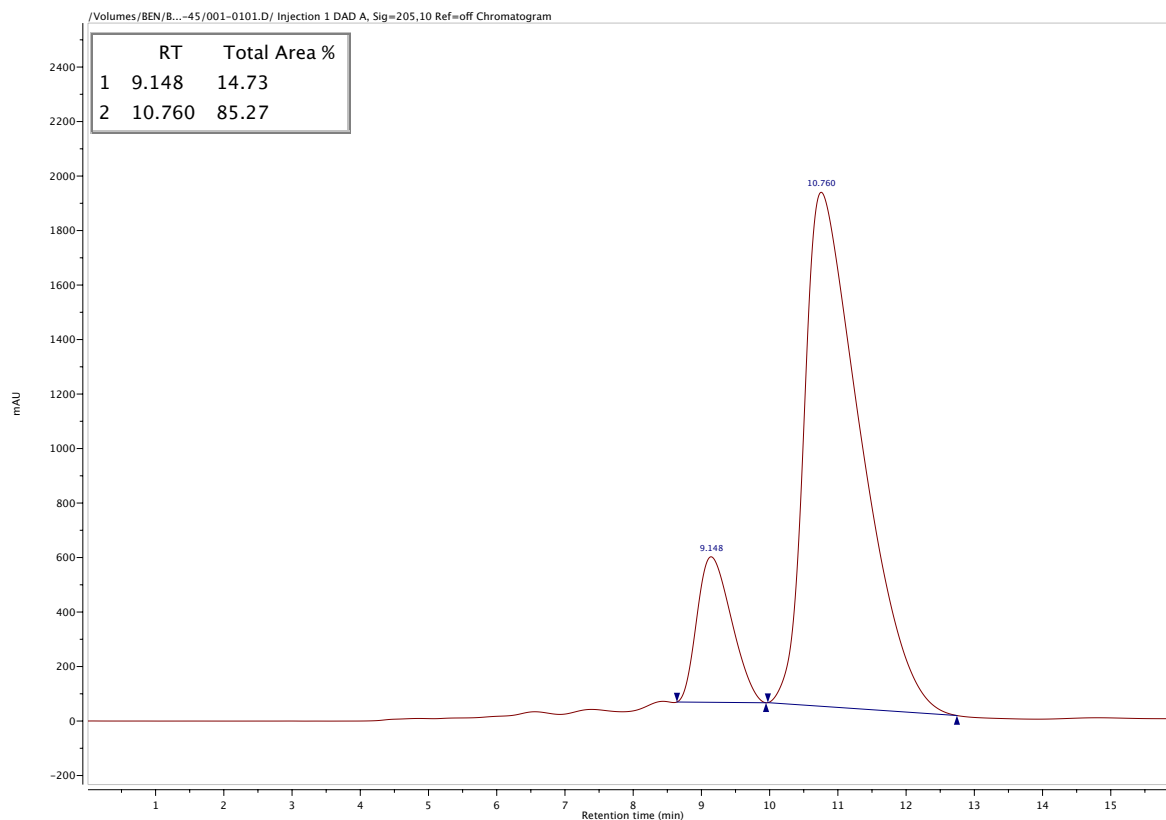
Chiralcel OD-H, 10% *i*-PrOH/hexanes, 1 mL/min:



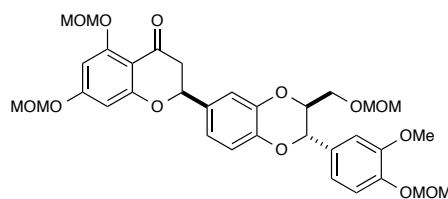
Peak #	RetTime [min]	Type	Width [min]	Area [mAU*s]	Height [mAU]	Area %
1	13.491	MM	0.6292	5420.57520	143.59250	98.8596
2	18.678	MM	0.8915	62.52987	1.16895	1.1404

1.12.9 Preparative Separation of Protected Flavanolignan SI-VIII Diastereomers

RegisPack, 80% EtOH/hexanes, 4 mL/min:



SI-9: Retention time: 10.8 min.

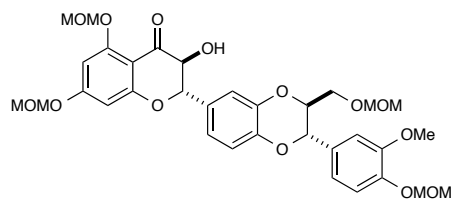
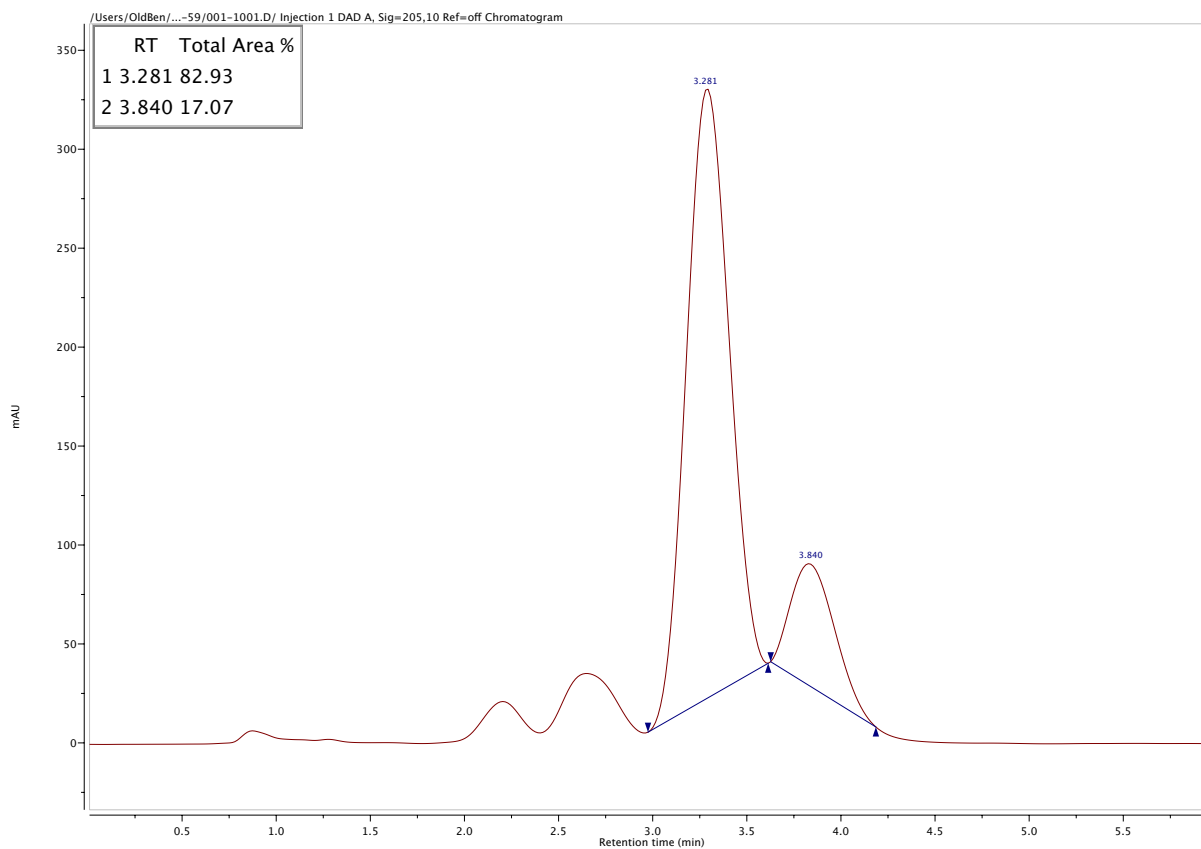


SI-10: Retention time: 9.1 min.

Isomers are identical by ^1H NMR. Separation confirmed by optical rotation and by analogy to the subsequent α -hydroxylated diastereomers.

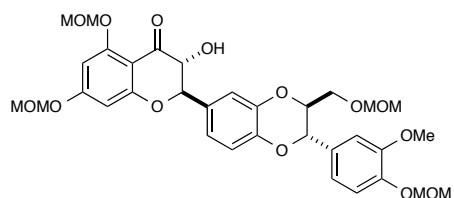
1.12.10 Preparative Separation of α -hydroxyflavanolignan SI-X Diastereomers

Regis (*S,S*)-Whelk-O 1, 100% MeOH, 10 mL/min:



I-80: Retention time: 3.3 min, purity confirmed by ^1H NMR spectroscopy.

Absolute configuration was determined by electronic circular dichroism (see above) and matches by analogy to final product.



I-79: Retention time: 3.8 min, purity confirmed by ^1H NMR spectroscopy.

Absolute configuration was determined by electronic circular dichroism (see above).

Chapter 2: Single-Electron Approaches to New Inverse Polarity Operators

2.1 Introduction

The study of new and underexplored reactive intermediates drives advances in carbon-carbon bond forming reactions, leading to atom/step-economical synthetic routes and access to previously to new molecular architectures. To this end, strategic bond disconnections opposite to standard polarity disconnections, termed *Umpolung*, have been a major focus of the synthetic organic community.¹²⁶⁻¹³²

2.1.1 Polarity Based-Bond Disconnections

Friedrich Whöhler's failed attempt to synthesize ammonium cyanate and resulting synthesis of urea effectively bridged the gap between "inorganic" and "organic" chemistries in 1828, and thus marked the beginning of modern synthetic organic chemistry.¹³³ Approximately 90 years later, Sir Robert Robinson's landmark single-step synthesis of tropinone conceptualized the practice of strategic bond disconnections in synthetic organic chemistry.^{134,135} The tropane alkaloids were a subject of great interest in the 19th due to their potent and broad biological activities, which had been known for centuries.¹³⁶ Notable members of this family are cocaine, hyoscyamine (antimuscarinic drug), and scopolamine (anticholinergic drug) (**Figure 2-1**).

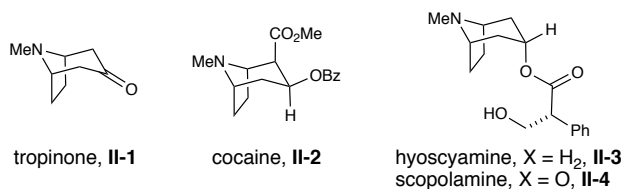
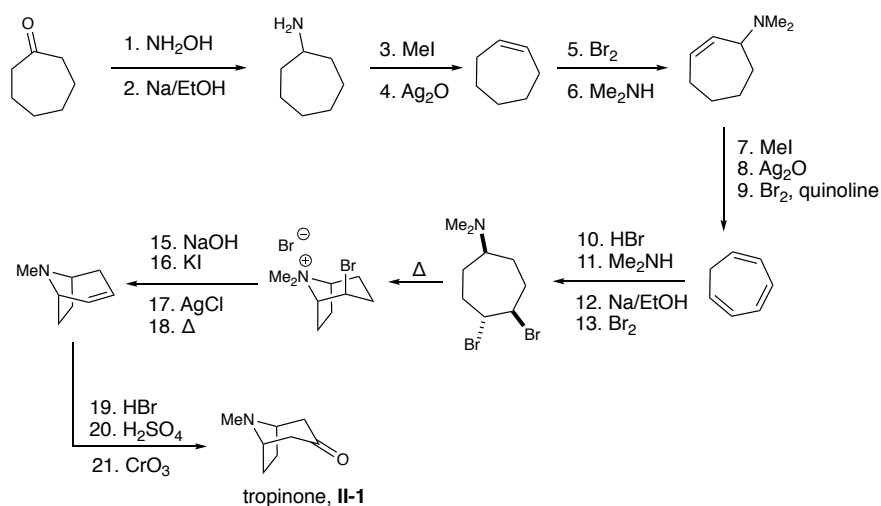


Figure 2-1. Selected Tropane Alkaloids.

The structure of these valuable alkaloids had been secured by laboratory synthesis, illustrated by the first synthesis of tropinone in 1901 by Willstätter (**Scheme 2-1**). This work while vital in its validation of structure and an early example of complex, multistep synthesis, is

highly inefficient from a practical synthetic point of view. The source of this inefficiency arises from the lack of functionalization on the starting cyclohexanone. A gap remained to be bridged, namely the strategic design of a synthetic route based upon the innate reactivity of functionalized carbon scaffolds.

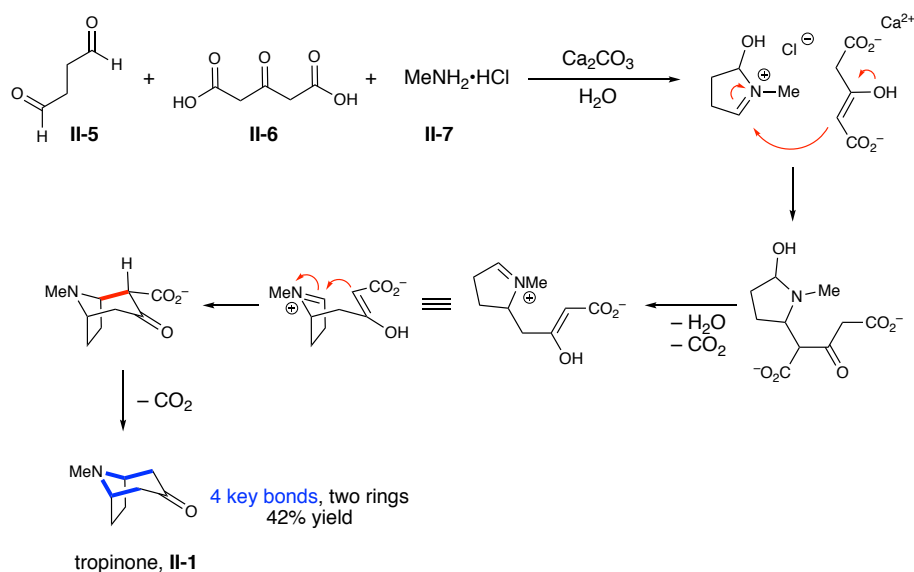
Scheme 2-1 The First Synthesis of Tropinone by Willstätter, 1901.



Just over a decade later, Robinson reported his single-step synthesis of tropinone. The strategic and conceptual advances in Robinson's approach are evidenced by the "hidden" complexity in his starting materials (**Scheme 2-2**), i.e., the inherent reactivity of the functionalized carbon frameworks. This remarkable transformation utilized succindialdehyde (**II-5**), methylamine hydrochloride (**II-6**), and acetone dicarboxylic acid (**II-7**) under physiological conditions (a mildly basic, aqueous environment). Beyond the impressive 42% single-step yield (in contrast to Willstätter's 21 step, >1% yield synthesis), the fundamental mechanistic understanding and exploitation of molecular symmetry renders this a landmark in synthetic organic chemistry. A total of four key bonds and two rings are formed in a single pot,

demonstrating the potential for chemists to deconstruct complex molecules into simple compounds through synthetic and what is now termed retrosynthetic logic.

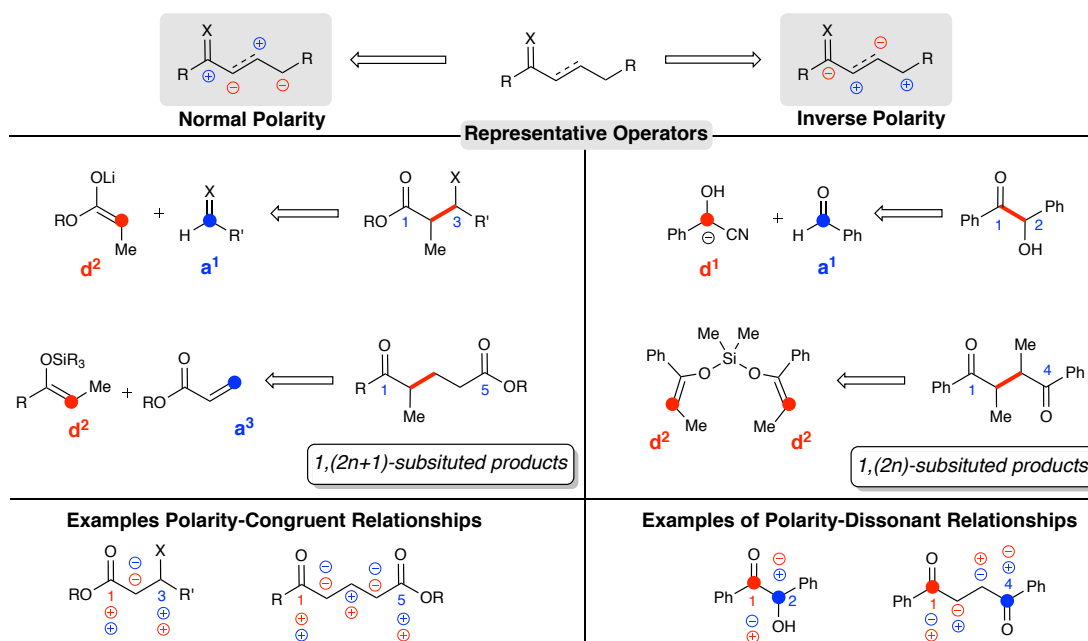
Scheme 2-2 Robinson's Biomimetic Synthesis of Tropinone.



In a contemporaneous manuscript, Robinson further advanced the hypothesis that the chemical transformations conducted by the machinery of biological systems were within reach of the synthetic chemist, a monumental hypothesis that has grown into the field of biomimetic synthesis. His hypothesis for the biosynthesis of tropinone is remarkably similar to his own synthetic route, but the causal relationship of these two schemes is unknown. However, this and his subsequent contributions to alkaloid synthesis were recognized with the 1947 Nobel Prize in Chemistry. This work ultimately laid the foundation for the work of luminaries R.B. Woodward and E.J. Corey, each of which have been recognized with subsequent Nobel Prizes in Chemistry. Corey, particularly is recognized for further codifying the general principles and guidelines for the design of synthetic routes by deconstructing target molecules to simple starting materials in an iterative fashion, a process termed retrosynthesis.¹³⁷

When considering the formation and thus retrosynthetic disconnection of chemical bonds in organic molecules, the standard logic is to create disconnections by heterolytic or 2-electron cleavage, assigning formally anionic and cationic atoms on the structures. The logic of these assignments is dictated by polarity, i.e. assigning what patterns of carbon and heteroatoms are able to support negative and positive charges based upon first principles (**Scheme 2-3**). Since heteroatoms are generally more electronegative than carbon, carbons attached to heteroatoms are thus formally positive and generally make electron acceptors (noted with an “a” designation) (**Scheme 2-3**). As a result, carbons adjacent to electropositive carbons, are able to support negative charge (noted with a “d” designation).¹²⁶ Thus, normal polarity disconnections can be made logically and systematically based placement of heteroatoms on a carbon scaffold, resulting in 1, (2n+1) heteroatom relationships, examples of which are seen in **Scheme 2-3**.

Scheme 2-3 Overview of Polarity-based Bond Disconnections.



Robinson's understanding of this logic (~70 years before Corey's Nobel Prize) enabled the designation of key bond disconnections and thus the identification of the starting materials required for the reaction (**Figure 2-2**).

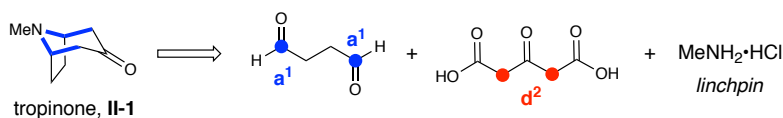


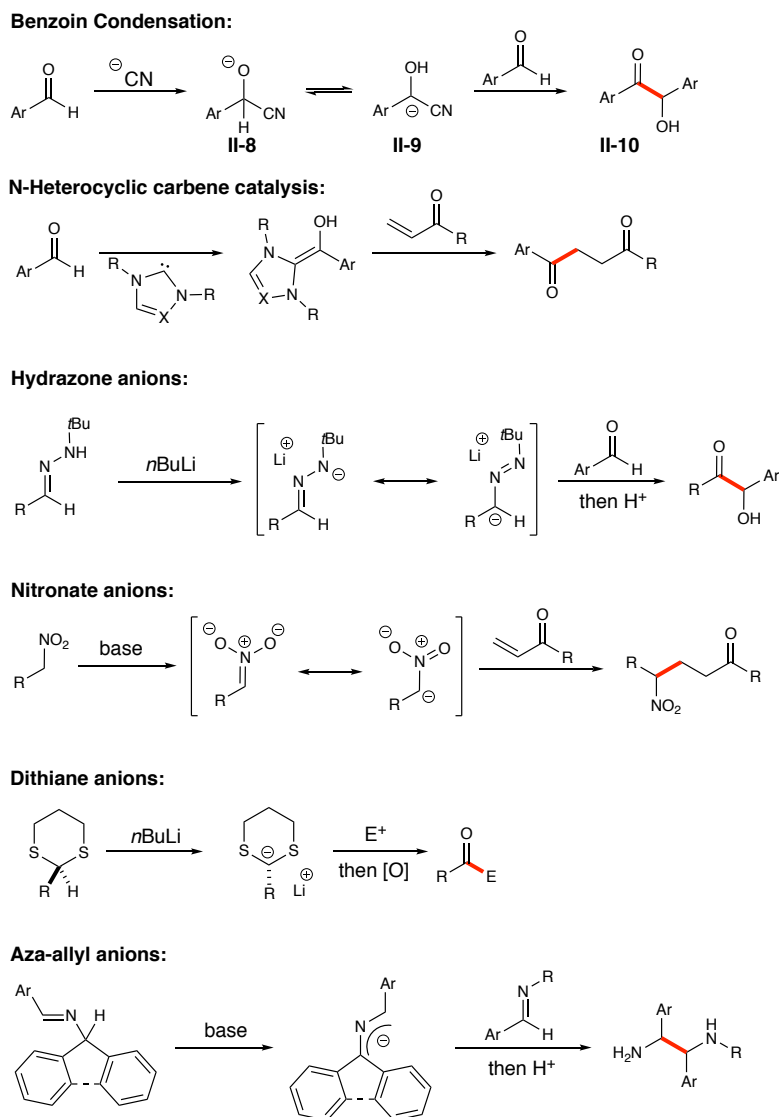
Figure 2-2. Polarity Analysis of Robinson's Tropinone Synthesis.

The reversal of standard polarity, termed *Umpolung* by Seebach in 1989, is generally required for the construction of polarity-dissonant heteroatom relationships (1, 2n)-substitution patterns. This concept has also been termed “charge affinity inversion” by Evans.¹³⁸ These are considered dissonant since polarity assignment based upon heteroatom relationship does not match, i.e. polarity assignments do not match when assignments from each heteroatom are made (**Scheme 2-3**). This makes the assignment of polarity-based disconnections more challenging, but these approaches enable new opportunities in molecular architecture and reaction design.

The polarity reversal of carbonyls (d^1 synthons) and enones (d^3 synthons) from electron acceptors to electron donors has been subject to considerable investigation for over half a century, but initial work began almost a century ago, with the benzoin condensation. The benzoin condensation, first discovered by Justus von Liebig and Friedrich Wöhler in 1832, is a dimerization of aromatic benzaldehydes.¹³⁹ The nucleophilic cyanide anion adds to aryl aldehydes to create an alkoxide (**II-8**), which tautomerizes to a resonance stabilized carbanion (**II-9**) (**Scheme 2-4**). **II-9** can then add to another equivalent of aldehyde, upon which expulsion of cyanide restores the ketone, yielding the acyloin **II-10**. Cyanide essentially installs a transient EWG to invert the carbonyl carbon's polarity. Just over a century later, in 1943 Ukai discovered

that this reactivity could be catalyzed by thiazolium salts under basic conditions.¹⁴⁰ The seminal report by Breslow¹⁴¹ in 1958 proposing the mechanism of the thiazolium catalyzed reaction provided the foundation for the field of NHC catalysis, one of the most active research areas of catalytic Umpolung reactivity.¹⁴²⁻¹⁴⁸ Interestingly, it was later discovered that nature uses a thiazolium-derived acyl anion equivalents in a variety of thiamine dependent enzymes.¹⁴⁹

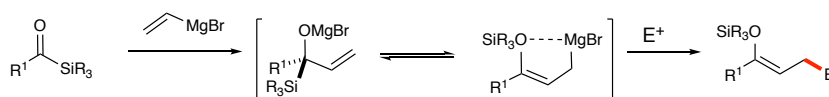
Scheme 2-4. Approaches to Acyl Anion Operators.



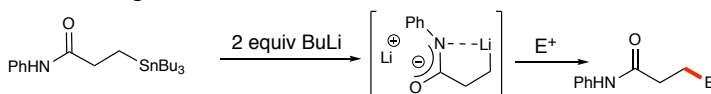
A variety of other methods towards acyl anions have followed (**Scheme 2-4**). Hydrazone anions^{150,151} (Baldwin) and 1,3-dithiane anions¹⁵²⁻¹⁵⁶ (Corey, Seebach) have been explored as stoichiometric entries to acyl anions. The intriguing, unique stability of lithiated 1,3-dithianes has been subject to stereoelectronic analysis by Alabugin.¹⁵⁷ Dithianes have further stimulated a number of advances, particularly the use of the Brook rearrangement (See Chapter 3 for an in-depth discussion of the Brook rearrangement) for the relay of reactive anions in domino processes to form multiple new bonds.¹⁵⁸⁻¹⁶³ Nitronate anions have been extensively explored, primarily due their broad success in asymmetric catalysis and the importance of chiral amine small molecules in medicinal chemistry.¹⁶⁴⁻¹⁶⁶ Finally, aza-allyl anions have recently become an area of interest for similar reasons as nitronate anions.¹⁶⁷⁻¹⁶⁹ Acyl anions are a thoroughly explored area of *Umpolung* synthetic chemistry. A considerably less developed area is the extension of *Umpolung* reactivity to the γ of carbonyl scaffolds, i.e. d^3 synthons (**Scheme 2-5**). Early work in this area focused on the use of metals to create anions at the γ position, known as homoenolates.¹⁷⁰⁻¹⁷⁴

Scheme 2-5. Approaches to Homoenolate Operators.

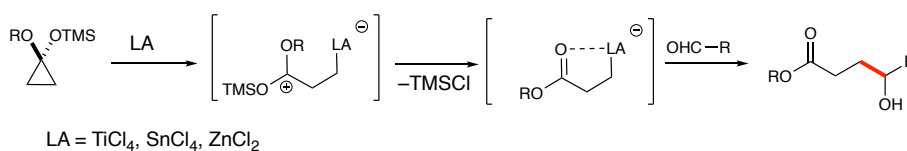
Brook rearrangement:



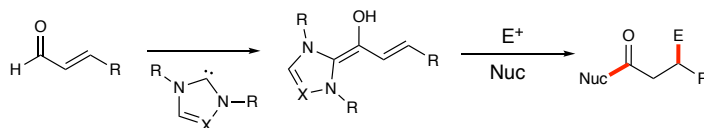
Metal exchange:



Cyclopropane opening:



N-Heterocyclic carbene catalysis:



These approaches included addition of vinyl Grignard reagents to acyl silanes, with the resulting Brook rearrangement creating the γ -anion.¹⁷⁵ Exchange of an alkyl tin group for lithium is another strategy investigated towards γ -anions.¹⁷⁶ Silylated ketals of cyclopropanones were thoroughly investigated as a variety of Lewis acids proved able to drive the open of these structures into homoenolates.¹⁷⁷⁻¹⁸² Notably, NHC catalysis is the only general catalytic approach to the generation of homoenolate equivalents.^{183,143,148} While the previous approaches require cryogenic temperatures and take place under harsh conditions, NHC reactions occur under mild conditions at room temperature. However, this increased stability comes at the cost of reduced reactivity, as NHC-homoenolates generally only react with activated electrophiles.

Interestingly, open-shell or free radical approaches are underexplored strategies in *Umpolung* reaction manifolds. Given the harsh conditions for reactive homoenolates as well as

some acyl anions, we were interested in expanding *Umpolung* disconnections in radical manifolds.

2.1.2 Open-Shell Reactive Intermediates

The first use of the term “radical” is believed to be by Lavoisier in the 18th century.¹⁸⁴ He used it to describe polyatomic fragments of a molecule that remained unchanged during chemical transformations to that molecule. It took until the establishment of carbon’s tetravalency for the term “radical” to be used in the modern, conventional sense. In 1900, Moses Gomber reported that a yellow color was obtained by shaking a benzene solution of chlorotriphenylmethane with mercury in the absence of oxygen yielded the triphenylmethyl radical **II-11** (**Figure 2-3**).

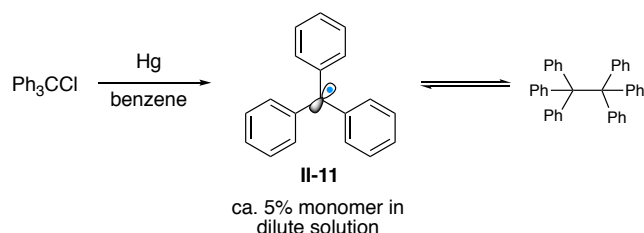


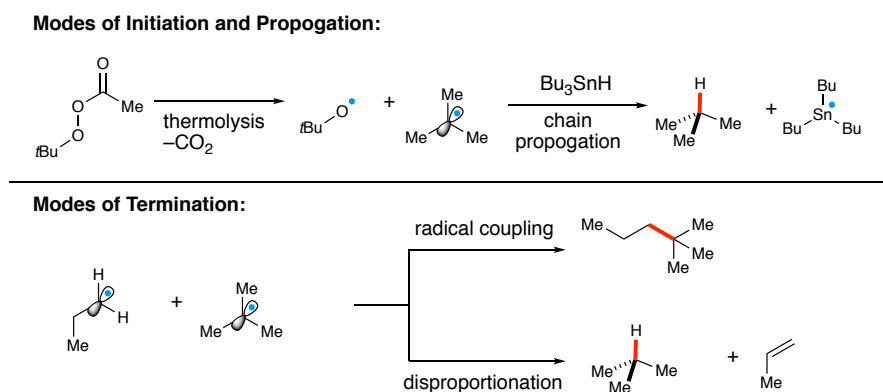
Figure 2-3. Gomburg’s Trityl Radical Synthesis.

Another important advance solution-phase radical chemistry was Morris Kharasch’s observation that the regiochemistry in the addition of hydrogen bromide to allyl bromide varied between the expected Markonikov and unexpected *anti*-Markonikov product correlated to the observed reaction rate, as the *anti*-Markonikov product was obtained when the reaction proceeded much more rapidly than normal. This rapid process was traced to peroxidic impurities (the “peroxide effect”) and was eventually attributed chain-radical processes.¹⁸⁴ Kharasch also went on to study radical polymerizations, making important advances in synthetic rubber, aiding the WWII effort, and laying the ground-work for much of the modern polymer industry.

2.1.3 Principles Governing the Reactivity of Radicals

To discuss the fate of radicals generated in these reactions, it is convenient to break the overall reactions into elementary steps, akin to catalytic reaction mechanisms. All radical reactions contain the steps of initiation and termination, with some also containing chain propagation. Initiation consists of the generation of a radical through the decomposition of a closed-shell species, either through thermolysis of weak bonds, photolytic cleavage, or redox chemistry (**Scheme 2-6**).

Scheme 2-6. Elementary Steps in Radical Reactions.



The two factors that dictate that outcome of radical reactions are the rates of reactions (kinetics) and heat of reaction (thermodynamics). A considerable challenge with open-shell intermediates are their high energy and the resulting the low barrier to their reactivity (1-2 kcal mol⁻¹) as well as the fact that they interact at the rate of diffusion in non-viscous solvents (10⁹-10¹⁰ M⁻¹s⁻¹).¹⁸⁵ Primary and secondary radicals typically react to provide dimerization products while tertiary whereas tertiary radicals tend to disproportionate. These considerations seem daunting if one wanted a radical (**A**) to react with another reagent or substrate in solution, **R-X** for example. However, factoring in the relative concentrations and rates of the substrate and

radical, one can understand how to make adjust conditions to favor the desired cross reaction (Figure 2-4).

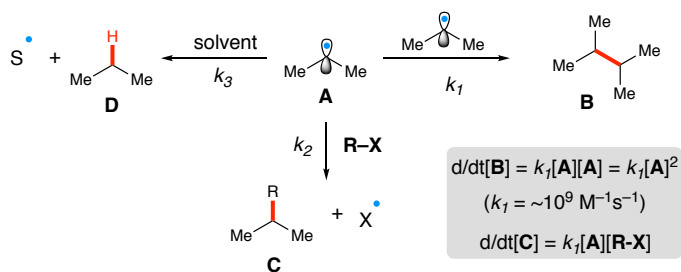


Figure 2-4. Competing Radical Reactions Depend on Radical Concentration.

From **Figure 2-4** it becomes apparent that the rate of radical dimerization is dependent on the *square* of radical concentration and thus, if the concentration of radical is kept at a small, steady-state concentration, cross-reactivity can be favored. If the concentration of radical is kept low, 10^{-8} M for example (roughly the concentration require for detection by ESR), using 10^9 for k_1 yields a rate of 10^{-7} M s^{-1} ($10^9[10^{-8}]^2$ M s^{-1}). If the concentration of R-X is 1 M, then the rate of cross-reaction is $k_2[10^{-8}][1]\text{M s}^{-1}$. If the rate of the cross-reaction must be greater than 10^{-7} M s^{-1} , then k_2 must be greater than $\text{M}^{-1}\text{s}^{-1}$.¹⁸⁵ Neglected in this simple analysis is k_3 , the rate of reaction with the solvent. To keep this term low, unreactive solvents, like benzene, must be used so that radical reactions with it are slow or undergo facile reverse reactions.¹⁸⁶

A considerable amount of data profiling the rate of radical additions to substrates has been collected. A particularly illuminating class of reaction is the addition of alkyl radicals to alkenes, as the effect of substituents on the fate of these reactions becomes readily apparent. In a landmark paper, Giese examined the effect of radical and alkene substituents on reaction rate and rationalized these outcomes based on frontier molecular orbital theory.¹⁸⁶ The conclusion was that since these reactions are exothermic, product stability was of limited importance, and that

polarity and steric effects dominated reaction outcomes. For electron-rich/nucleophilic radicals, the dominant interaction is the SOMO with the LUMO of the alkene while for electron-poor/electrophilic radicals, the dominant interaction is the SOMO with the HOMO of the alkene. These considerations starkly shown in the competition experiments to pi systems. Seen in **Figure 2-5** is a competition experiment recently conducted by Jui, in which they demonstrate the ability control alkene additions of pyridinyl radicals to alkenes based on reaction conditions.¹⁸⁷ Radical ions are a subset of radicals that have unique properties and reactivity that have recently begun to be exploited as new modes of catalysis have enabled the facile production (*vide infra*).^{188,189}

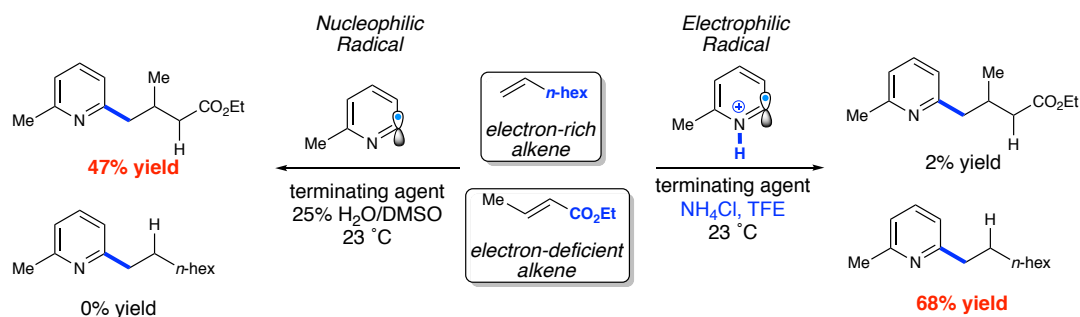


Figure 2-5. Radical-Alkene Addition Competition Experiment.

The exception to these general principles are a special subset, known as persistent radicals, stability leads to low reactivity and thus long life-spans.¹⁹⁰ The stability of these species is the result of their placement (surrounding bulk and localized on a heteroatom, e.g. TEMPO), but in the case of carbon-centered radicals it's is typical stabilization through delocalization. This results in unique reactivity, particularly highly selective radical cross-couplings when persistent radicals are combined with transient radicals.¹⁹¹ Since termination in persistent radicals is slow, even if a transient and persistent radical are generate at the rate, as the reaction progresses a build-up persistent radical occurs (since the transient radical undergoes a variety of termination

events) thus the cross-product becomes the dominant product. The design and creation of persistent or semi-persistent radicals will drive the future of highly efficient radical cross-couplings.

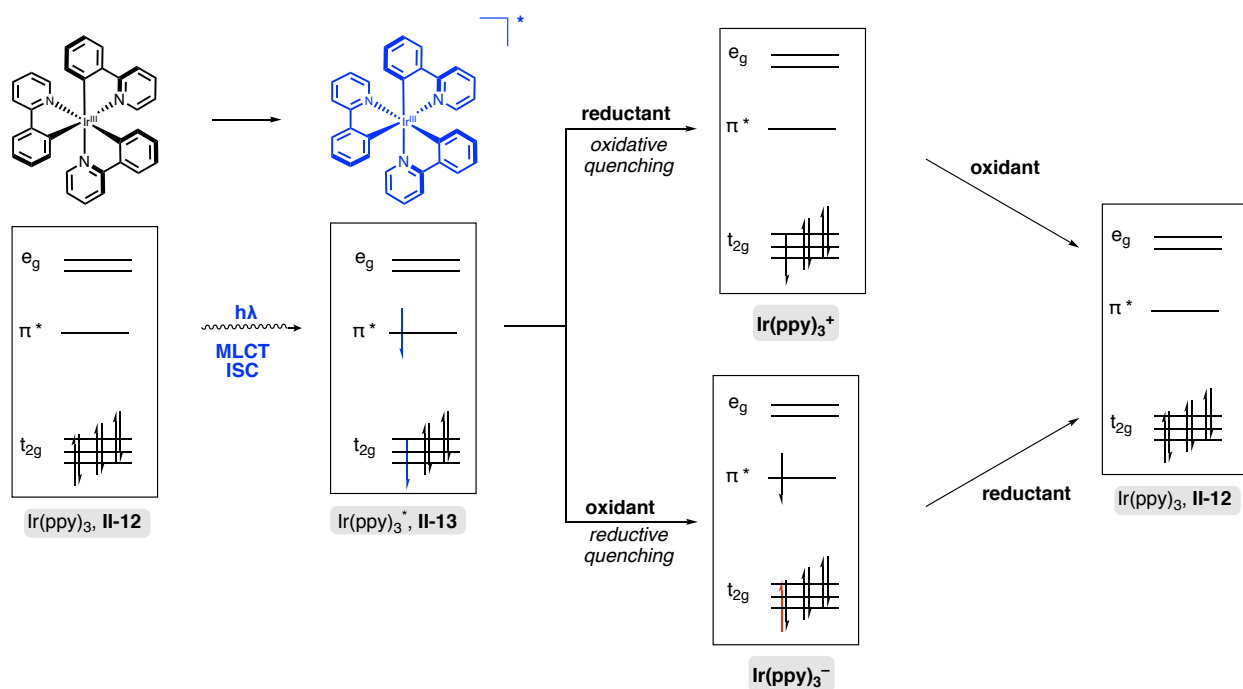
2.1.4 Photocatalysis for the Generation of Open-Shell Intermediates

The discovery and development of light-mediated chemistry, photocatalysis, has enabled a diverse new set of non-traditional bond constructions in organic chemistry. Photocatalysis broadly encompasses any reaction in which photonic energy is selectively input and specifically absorbed by a catalyst. Upon excitation, this catalyst is able to induce chemical reactions in an accompanying substrate, including an additional catalyst, reagent. The resulting reactions are often unique reaction pathways, not observed under thermally controlled conditions. Generally, photocatalysis is divided into two regimes, photosensitization and photoredox. Photosensitization is generally the transfer of the absorbed photonic energy to substrates, while photoredox is the light-driven transfer of an electron between catalyst and substrate. Over the past four decades, photoredox catalysis has found broad application in water splitting, carbon dioxide reduction, and the development of new solar cells. Recently, photoredox catalysis has expanded to the field of organic chemistry as mild and simple new entry in the initiation and termination of radical reactions.^{192,193} The insight that well-known and easily accessible metal complexes and organic dyes are able to convert visible light to chemical energy, thus creating reactive open-shell species under mild conditions has led to a veritable explosion in interest and reports of new reactions in the literature.

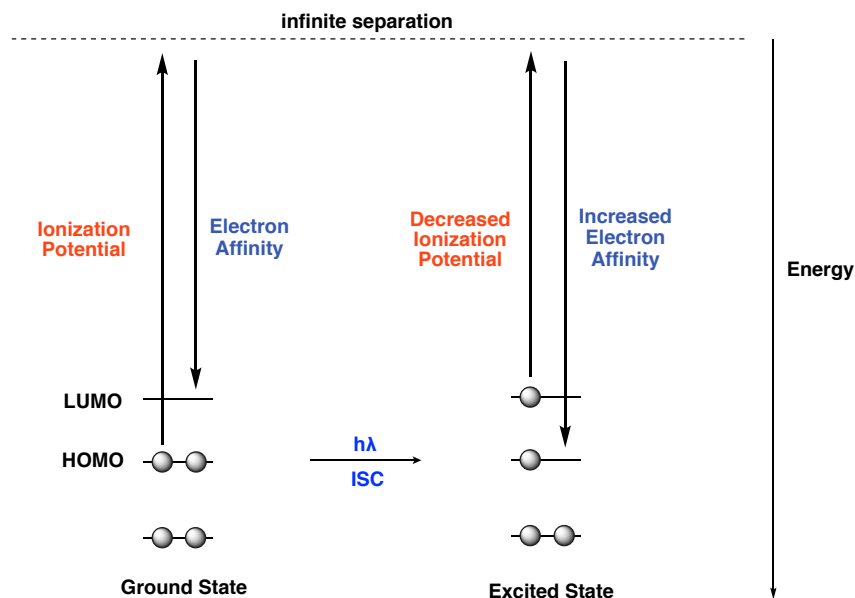
Polypyridyl metal complexes, like Ir(ppy)₃ (**II-12**) have been the primary impetus for the growth of organic photoredox chemistry, due to their long lived excited states (0.5-2.3 μs),

considerable energy in the photoexcited state (**II-13** possesses a triplet state energy of 56 kcal mol⁻¹ above its ground state),¹⁹⁴ as well as their stability in a variety of oxidation states.¹⁹⁵ An important characteristic of these complexes is their absorbance of visible light, wavelengths that common organic molecules do not absorb, enabling selective photoexcitation. This is in contrast to early efforts that employed UV light, resulting in unselective excitation and reactivity. Additionally, the photoexcited polypyridyl metal complexes can act as both oxidants and reductants, thereby creating a unique reaction environment (**Scheme 2-7**). This duality contrasts with traditional electrochemistry manifolds, in which the reaction medium is either oxidative or reductive (but not both), thus providing access to new opportunities in redox-neutral reactions.

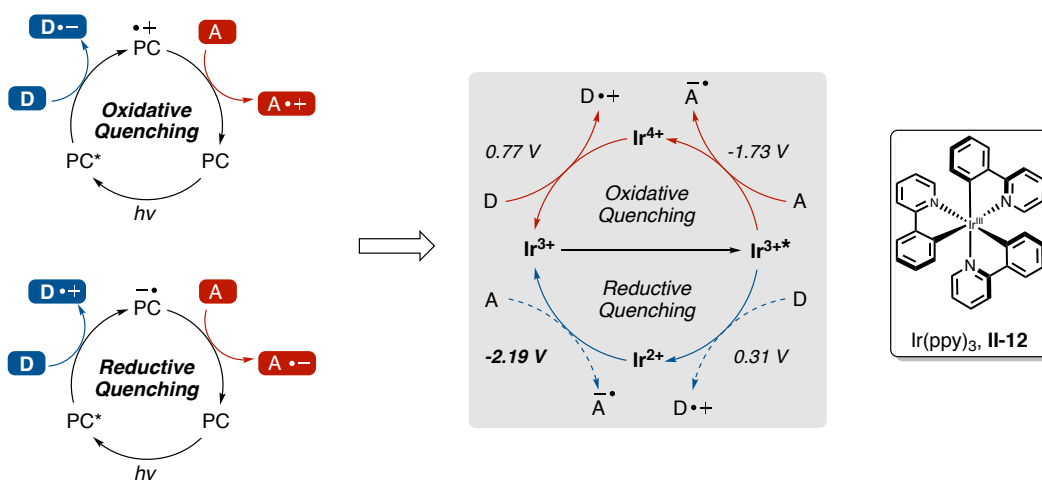
Scheme 2-7. Simplified Molecular Orbital Description of Photoredox Catalysis with Transition Metals



Depicted in **Scheme 2-7** is a simplified molecular picture of dual photoredox cycles possible with an polypyridyl iridium complex $\text{Ir}(\text{ppy})_3$, **II-12**. Upon photoexcitation, MLCT, and ISC, a triplet state **II-13** is obtained.¹⁹⁶ This triplet state can serve as a reductant, known as oxidative quenching or as an oxidant (reductive quenching). Subsequent reduction or oxidation, respectively, returns the paramagnetic ground-state to the starting diamagnetic state. The duality of these complexes, that they simultaneously become better oxidants and reductants upon photoexcitation, which may come as counter-intuitive. However, upon considering the electronic ramifications of photoexcitation to a high energy triplet state, the rationale becomes clear. Interestingly, this rationale is general to all diamagnetic atoms or molecules. As shown in **Scheme 2-8**, excitation to a triplet state creates two SOMOs. Comparing the ionization potentials (IPs) and electron affinities (EAs) of these two states shows that the EA of the excited molecule is higher than that of the ground state, while the IP is lower.¹⁹⁷ If we consider this in a thermodynamic sense, we observe that the addition of an electron to the half-filled HOMO of the excited molecule is more exothermic than its addition to the LUMO in the ground-state molecule. Furthermore, it also apparent that the removal of an electron from the excited-state molecule becomes less endothermic.

Scheme 2-8. Effect of Photoexcitation on the Molecular Orbitals of Small Molecules

Each of the described steps in the quenching cycle described has a redox potential associated with it. Thus every metal catalyst has two possible cycles, oxidative or reductive quenching cycles, associated with them (**Scheme 2-9**).

Scheme 2-9. Photoredox Catalyst Quenching Cycles

By modulating the electronic properties of the ligands, photocatalysts with unique potentials are thus created (**Figure 2-6**). Additionally, a host of organic dyes have been repurposed or developed as cost effective alternatives that can sometimes perform as well as the polypyridyl complexes (**Figure 2-6**).^{198,199} In the case of Mes-Acr (**II-21**), the oxidation potential of this catalysts far exceeds that of polypyridyl metal complexes and has been the centerpiece for the development of new oxidative pathways.²⁰⁰

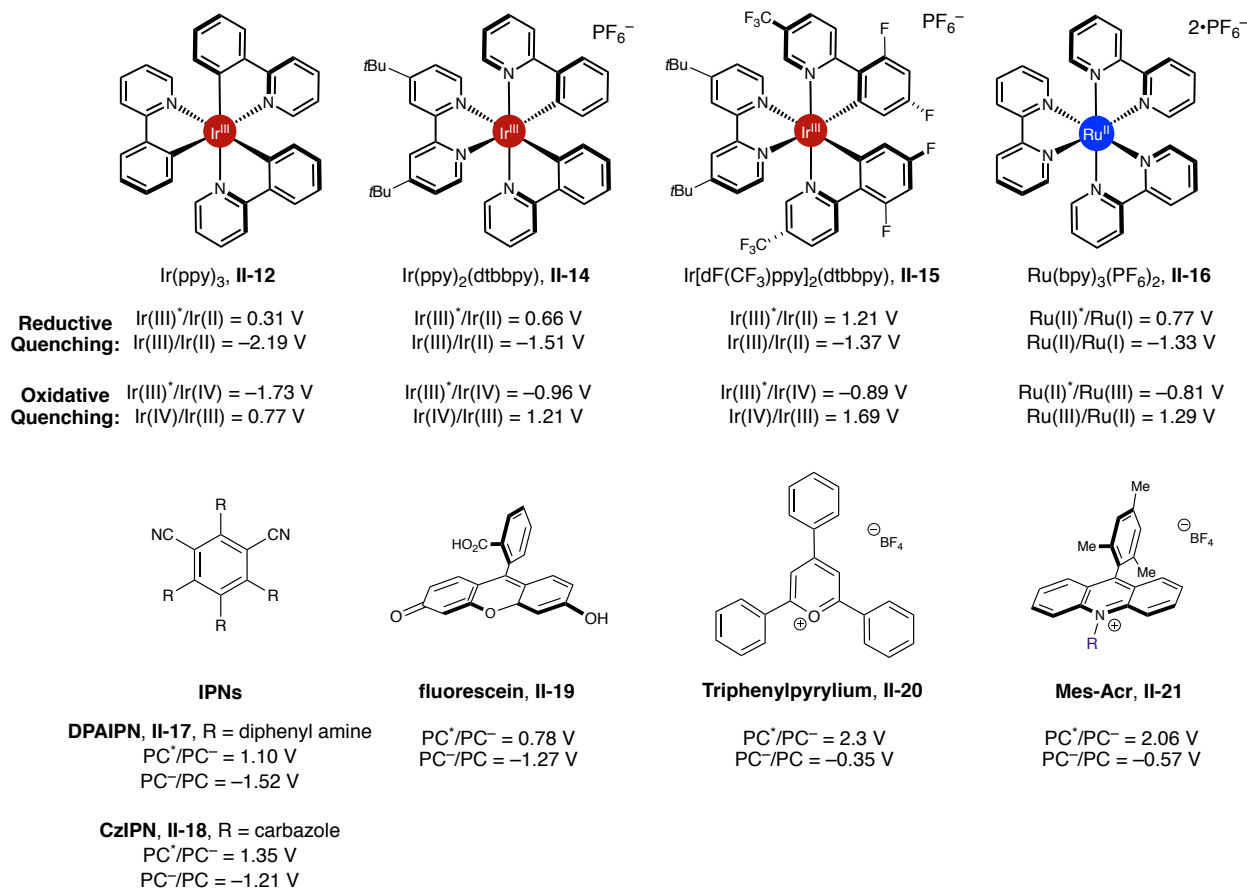


Figure 2-6. Commonly Employed Photoredox Catalysts.

Varying ligand type on the polypyridyl iridium complexes, homoleptic versus heteroleptic, different redox profiles are obtained (**Figure 2-6**) as well as differences in the

location of the HOMO and LUMO orbitals^{195,201} (**Figure 2-7**). The specific location of where outer-sphere electron transfer takes place on these complexes is important as substitution, particularly on the bipyridyl ligand of heteroleptic complexes like **II-14** and **II-15** (*t*butyl vs H vs CF₃), greatly affects the properties and hence reactivity of these complexes.

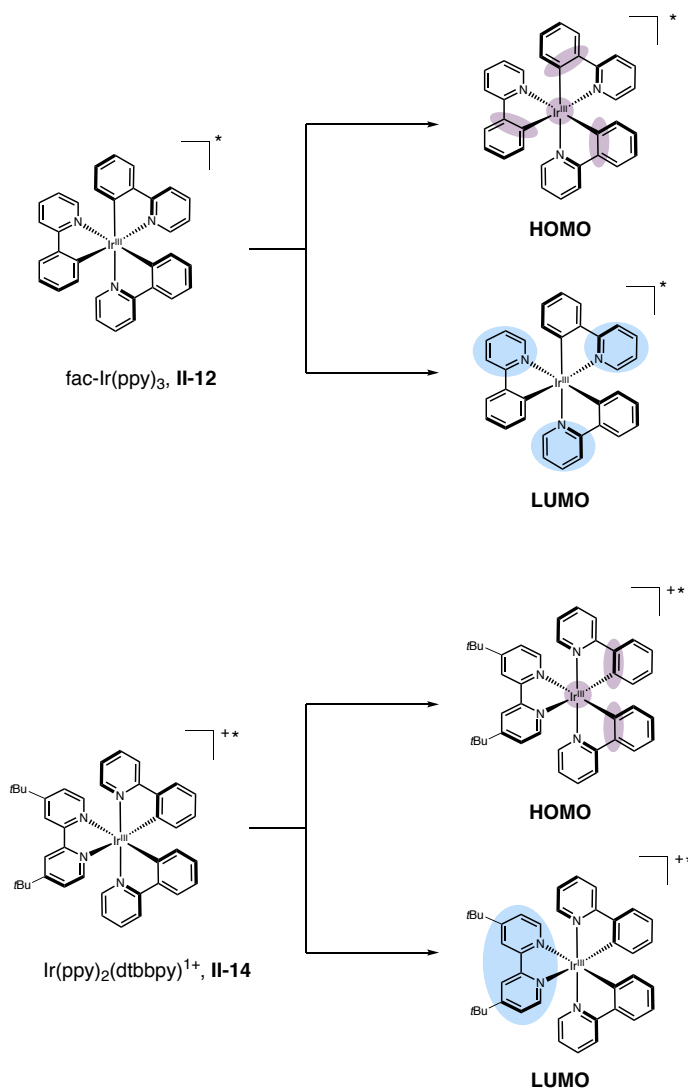
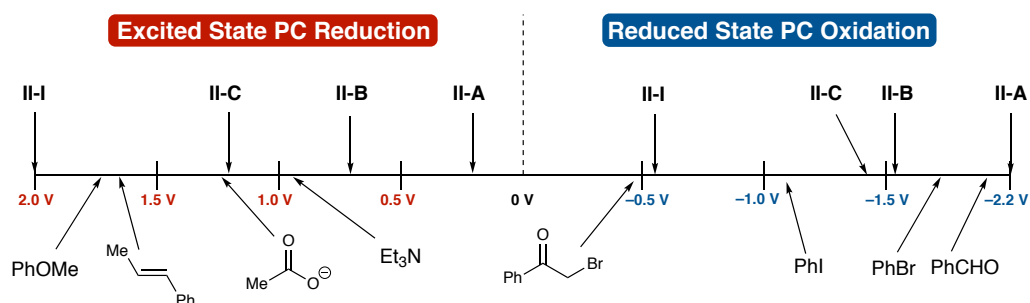


Figure 2-7. Location of Frontier Molecular Orbitals on Excited States of Homoleptic and Heteroleptic Polypyridyl Complexes.

Depicted in **Scheme 2-9** are the excited state oxidation of potentials and reduced state reduction potentials of some of the commonly used PCs compared with the respective oxidation or reduction potentials of common organic molecules. For a more comprehensive aggregation of electrochemical data of organic molecules see Nicewicz et al.²⁰²

Scheme 2-10. Scale of Electrochemical Data of Some Photocatalysts and Organic Compounds



A variety of co-catalytic approaches have been developed to extend the reactivity of photoredox systems. These include strategies to intercept intermediates, usually with transition metal co-catalysts, to mediate new bond forming reactions.^{192,203} Additionally, the use of co-catalysts to activate substrates for electron transfer have been explored.²⁰³ Yoon pioneered the merger of Lewis acid catalysis with photoredox catalysis to enable reduction of enone systems.²⁰⁴ Just as Lewis acids lower the LUMO of substrates to enable addition of electron rich nucleophiles, Lewis acids can facilitate the addition of an electron in the same fashion (**Figure 2-8**).

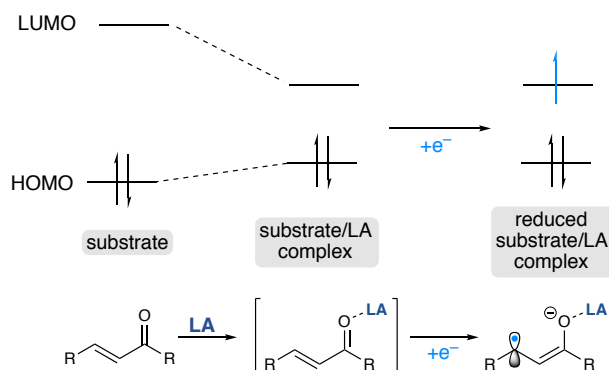


Figure 2-8. Lewis Acid Mediated Enone Reduction.

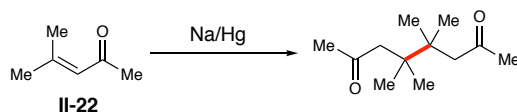
Recently, Knowles has formulated a paradigm of substrate activation around proton-coupled electron transfer (PCET).²⁰⁵ Using either Brønsted acids to activate substrates for reduction or Brønsted bases to activate substrates for oxidation, he has shown that reactivity of these cooperative catalytic systems can be predicted by comparing the calculated bond dissociation free energy (BDFE) for a given photocatalyst/HBD system to the bond energy of the newly formed bonds.²⁰⁶ With these significant theoretical and practical frameworks, we sought to build a cooperative catalytic approach to the generation of improved *Umpolung* operators.

2.1.5 β -Radical Enolates in Chemistry

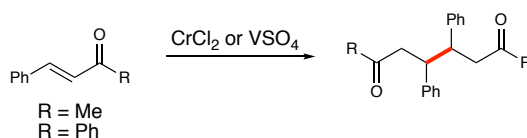
The reduction of enones to create β -radical enolates dates back to the late 19th century, when Claisen reported the reductive dimerization of mesityl oxide (**II-22**).²⁰⁷ The first use of homogenous reductants was carried out by Conant and Cutter in 1926.

Scheme 2-11. Stoichiometric Approaches to Enone Reduction.

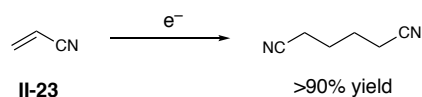
Claisen, 1876: Seminal report of reductive enone dimerization



Conant and Cutter, 1926: First use of homogenous metals



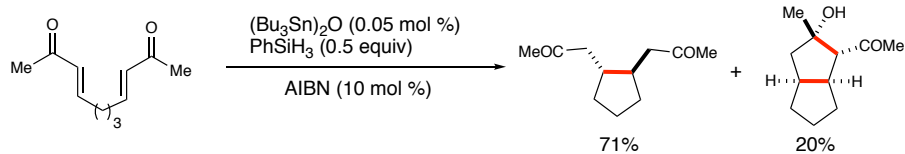
Monsanto, 1965: Large scale production of nylon precursor



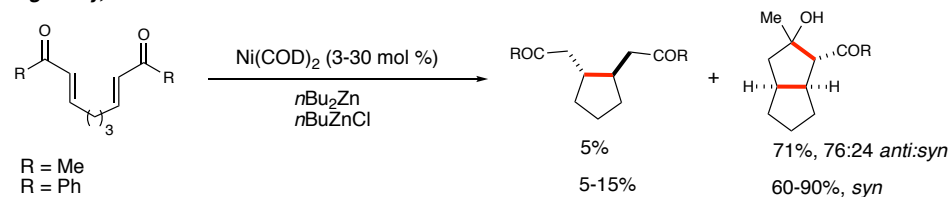
Further electrochemical approaches have been developed, with the Monsanto adiponitrile process being used to reductively dimerize acrylonitrile (**II-23**) on multi-ton scale, as part of the synthesis of polyamides.²⁰⁸ Interest in the reductive cyclization of enones was renewed in the late 1990's, with the use of transition metal catalysts. Transition-metal mediated reductive cyclizations were reported by Fu,²⁰⁹ Montgomery,²¹⁰ and Krische^{211,212} (**Scheme 2-12**). A decade later, Yoon pioneered the use of cooperative Lewis acid/photoredox catalysis access β -radical enolates.²¹³

Scheme 2-12. Approaches to Enone Reductive Cyclization.

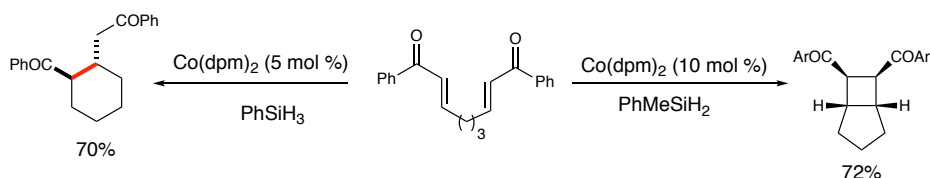
Fu, 1996:



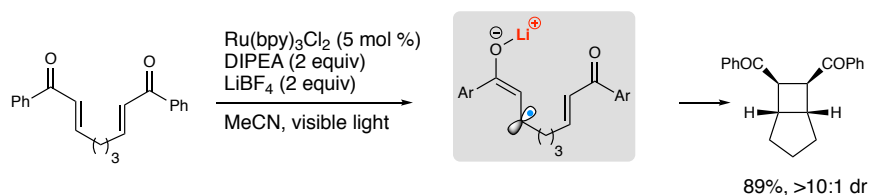
Montgomery, 1996:



Krische, 2001:



Yoon, 2008: Introduction of photoredox to reductive enone coupling



Interestingly, when these methods, including the photoredox method, are applied to the intermolecular reactions, homocoupling dominates.²¹⁴ It is only with the judicious choice of enone pro-nucleophile and enone electrophile that Streuff has been able to report reductive cross-coupling reactivity.^{215,216}

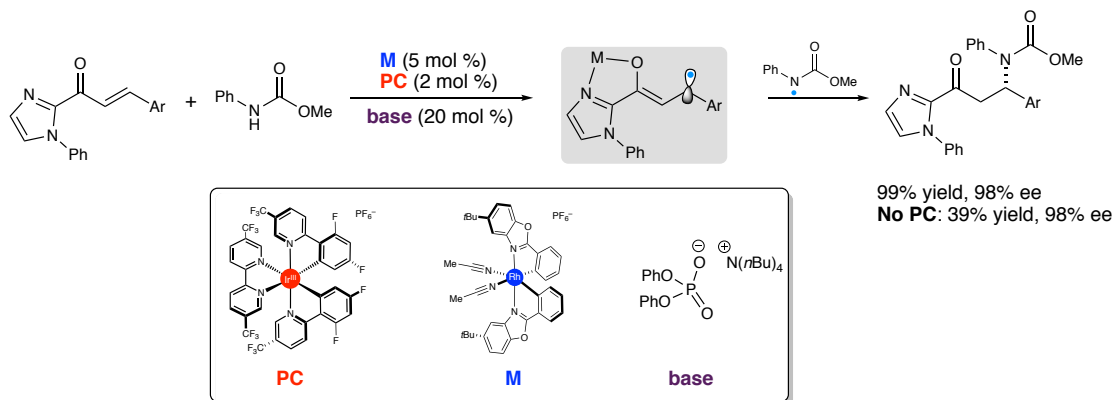
2.2 The Design of a New β -Radical Enolate

The lack of intermolecular cross-couplings in reductive enone reactions has been a long standing challenge, that has only begun to be addressed. In the last several years, bifunctional

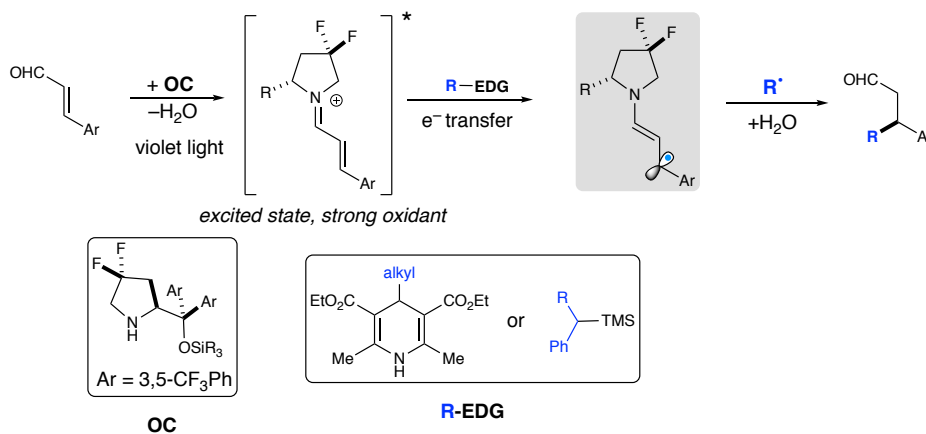
photoredox approaches from Meggers and Melchiorre have offered solutions to this challenge (Scheme 2-13).

Scheme 2-13. Approaches to Intermolecular Enone Reductive Reactivity.

Meggers, 2016: Bifunctional Lewis Acid/Photocatalyst



Melchiorre, 2017-18: Bifunctional organocatalytic approach



These approaches merge LUMO lowering catalysis with photoredox to create efficient, enantioselective cross-couplings. These reactions, particularly Melchiorre's system, likely succeed because the bifunctionality leads to rapid radical formation and coupling, likely within the solvent shell.¹⁸⁴ However, a pitfall of the bifunctional approach is that the functionality in both catalytic manifolds is inherently limited and thus reactivity is limited as well. We sought to design a new β -radical enolate species that would address the challenges of the conventional

approach and provide a flexible platform to moving forwards that would enable the discovery and development of new reactions.

2.2.1 Hypothesis Towards Stabilized β -Radical Enolate

In designing a new β -radical enolate species, we sought to identify the source of exclusive homo-coupling observed in intermolecular regimes. Our hypothesis was that the β -radical enolate species (e.g. **II-24**) were so reactive that dimerization was occurring through radical conjugate addition of the β -radical enolate to an equivalent of unreacted enone, rather than exclusive radical-radical coupling (**Figure 2-9**).²¹⁴ This would suggest that the energy of the species would need to be lowered, i.e. we needed to design a more persistent radical. We hypothesized that resonantly stabilizing the enolate would be a facile method of achieving this, in analogy to the relationship between enolates and deprotonated 1,3-carbonyl systems (**Figure 2-9**).

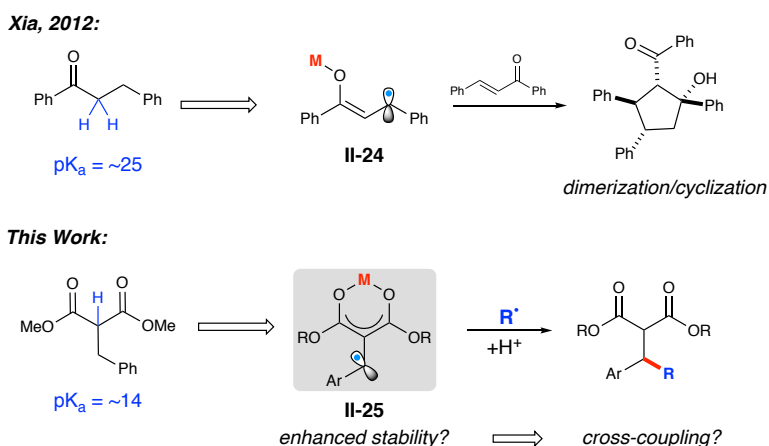


Figure 2-9. Hypothesis for Stabilization of β -Radical Enolate.

The corresponding enone would be a β -radical enolate (**II-25**) derived from an aryldiene malonate. Surprisingly, malonates, a canonical class of Lewis acid substrates, had not been explored in this context.

2.2.2 Redox Properties of Arylidene Malonates

The utility of bidentate systems in photoredox catalysis has been previously demonstrated by Meggers using bifunctional transition metal Lewis acidic/photocatalyst complexes, but these typically rely on N-carbonyl imidazoles as auxiliaries.²¹⁷⁻²²⁰ With desire to utilize arylidene malonates as a bidentate substrate, we first assessed the activation of arylidene malonates for single-electron reduction (**Figure 2-10**). A comparison of the reduction potential of benzylidene malonate (**II-26**) (literature reports -1.63 V, our measurement -1.57 V vs SCE)²²¹ and the corresponding cinnamate (-2.3 V)²²² suggests *a priori* that the arylidene malonate (AM) derived β -radical enolates is likely more stable than the previous enone-derived species. Previous literature reports that Lewis acids can dramatically shift the reduction potential of benzylidene malonate, with magnesium perchlorate reported to shift the reduction of phenyl AM to -0.64 V (vs SCE) in acetonitrile.²²¹ Our cyclic voltammetry studies showed a similarly significant shift (>1 V, -0.37 vs SCE, 100 mol % Sc(OTf)₃) of reduction potential when **II-26** was complexed with scandium triflate (**Figure 2-10**). This redox data as well as the robust and well-defined complexation of malonates with Lewis acids lead us to believe that the β -radical enolate species formed from arylidene malonates may be sufficiently persistent to enable challenging cross-coupling reactions.

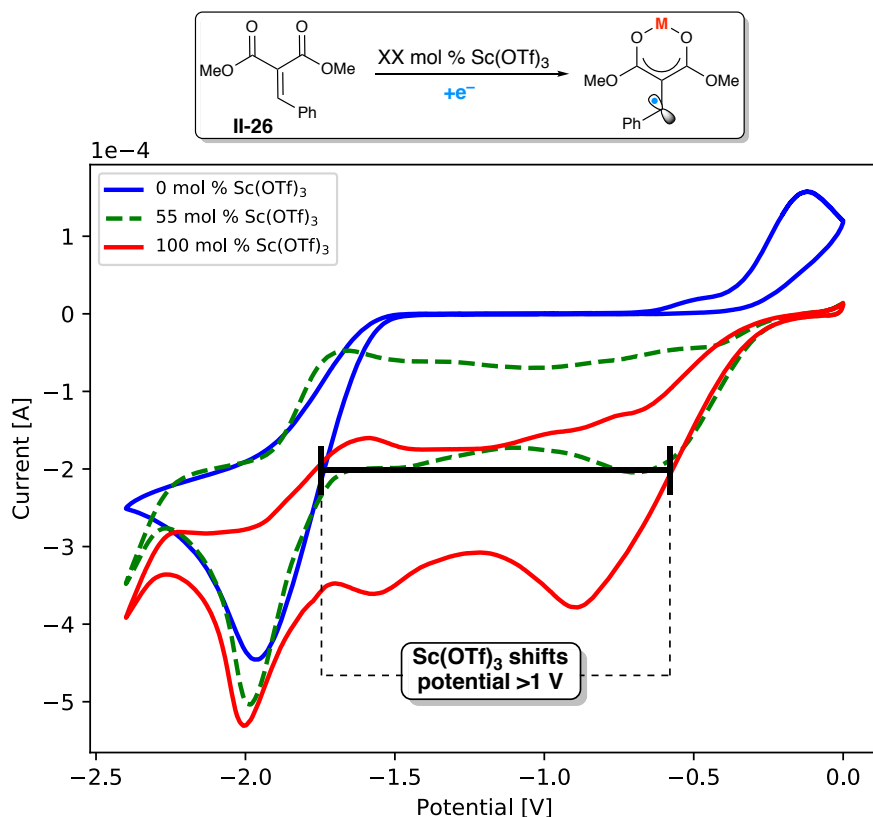


Figure 2-10. Effect of Scandium Triflate on the Reduction Potential of Ph Arylidene Malonate.

2.3 Transfer Hydrogenation of Arylidene Malonates

With this data, we sought to evaluate initial parameters like the scope of Lewis acids capable of activating AMs for reduction. A simple reaction that would provide the clearest initial data was desired and transfer hydrogenation was therefore chosen. Examining the rate of H-atom quenching vs the rate of dimerization AMs would serve as an initial benchmark of reactivity. Rueping et al. had previously disclosed that ketones, aldehydes, and imines underwent pinacol like dimerizations under photoredox conditions with tertiary amines as the terminal reductant and the Lewis acid (upon single-electron oxidation).²²³ This presented itself as a simple and useful launching point.

2.3.1 Initial Screening to Define Reaction Parameters

Examining three such tertiary amines, trimethylamine, tributylamine, and Hunig's base with three photocatalysts gratifyingly revealed that the transfer hydrogenation functioned well (**Figure 2-11**). It is believed that upon oxidation, the oxidized nitrogen can form a 2-center/3- e^- interaction²²⁴ or after a [1,2]-H shift, serve as a hydrogen-bond donor.^{225,226} In our follow-up studies (Section 2.4.1) we observed that only strongly acidic Brønsted acids like N-triflylphosphoramides were able to mediate the reduction, thus making the hydrogen-bond activation mode unlikely. Additionally, follow-up studies with organocatalysts indicated a dependence on photocatalyst reducing ability, indicating that this reaction was likely proceeding through reduction of the arylidene malonate (see **Scheme 2-14**). The transfer hydrogenation product **II-27** was isolated in 76% yield, when Hunig's base was used. The small amounts of dimer observed bolstered our belief in our hypothesis.

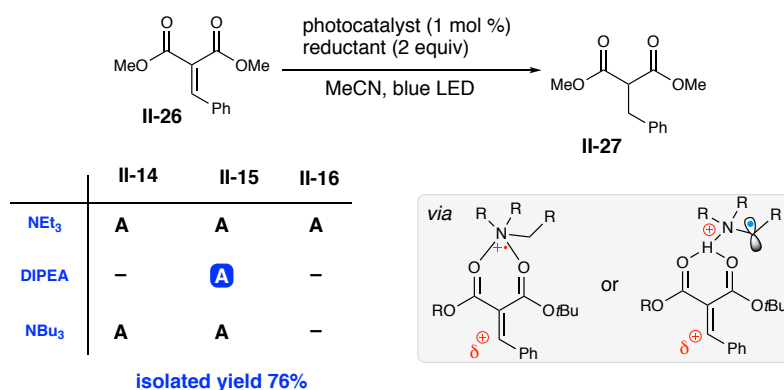


Figure 2-11. Transfer Hydrogenation of Arylidene Malonates with Tertiary Amines.

We next sought to briefly survey what Lewis acids could be used to activate arylidene malonates. A range of strong to mild Lewis acids were surveyed. Stronger Lewis acids like scandium triflate and magnesium bromide provided the hydrogenated product, while the milder

calcium methoxide only proved competent with the strongest reducing catalyst **II-14** (**Figure 2-12**). With this system, we found that the reaction proceeded normally, albeit in reduced yield, likely due to mismatch in radical termination by the oxidized HE (see **Scheme 2-17**, pg, 162, for more details). As a control, zinc triflate was used to observe how the reaction would progress if the Lewis acid was reducible by the photocatalyst (**Figure 2-12**). In all cases, formation of a metallic mirror on the vial was observed when zinc triflate was used.

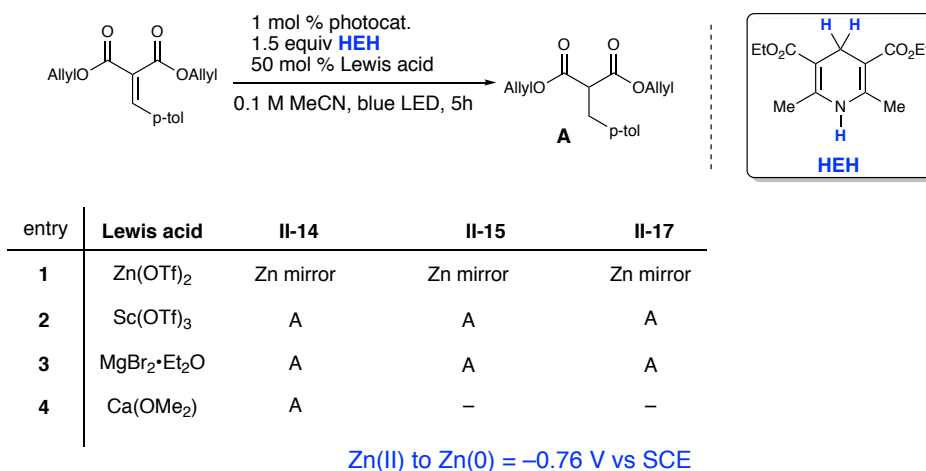
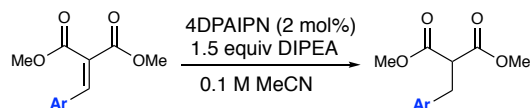


Figure 2-12. Transfer Hydrogenation of Arylidene Malonates with Lewis acids and Hantzsch Ester.

Since radical reactions are greatly affected by electronic factors, we sought to quickly survey the scope of aryldiene malonates compatible with this transfer hydrogenation reaction (**Table 2-1**). Pyridyl groups were not tolerated as no identifiable products were observed by UPLC/MS after submission to reaction conditions (**Table 2-1**, entries 1-2). Electron rich and bulky groups were well tolerated (**Table 2-1**, entries 4-7). Interestingly, the furyl and electron deficient 4-CF₃ aryl groups were not well tolerated (**Table 2-1**, entries 3, 8). Following this quick survey of reactivity we looked for a useful synthetic application of this reaction.

Table 2–1. Cursory Survey of Compatible Arylidene Malonates.

Entry	Aryl	Results
1	2-pyridyl	decomp
2	3-pyridyl	decomp
3	6-Me-2-furyl	SM, pdt, dimer
4	2-Bn-pyrrole	Full conversion to pdt
5	1-naphthyl	Full conversion to pdt
6	2-OBn	Full conversion to pdt
7	4-OMe	Full conversion to pdt
8	4-CF ₃	4 peaks, small pdt peak

2.3.2 Design of a One-Pot Homologation Reaction

As an application of the reaction to a more useful synthetic transformation, we designed a one-pot homologation of aryl-aldehydes (**Scheme 2-14**). Since the Knoevenagel condensation is highly efficient, with yields of 80-90% being obtained with only 10 mol % piperdinium aceate, in very concentrated (2-3 M) solutions, we believed that this condensation could be occur, then the mixture simply diluted and Hunig's base and photocatalyst added. Subjection to blue LEDs would then provide the saturated product. Additionally, if an easily cleavable, non-symmetrical malonate was used, the two-carbon homologated cinnanyl derivative could be obtained. Thus we settled on using the non-symmetric *t*Butyl ethyl malonate **II-28** (**Figure 2-13**).

The Knoevenagel condensation with *t*Butyl ethyl malonate needed examined, as conditions with cerium chloride had only been reported.²²⁷ Gratifyingly, the typical conditions of piperdinium aceate smoothly yielded the desired arylidene malonate **II-29** (**Figure 2-13**).

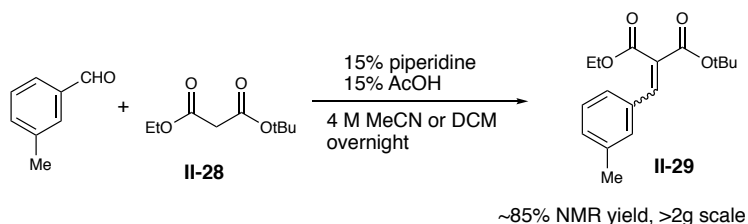
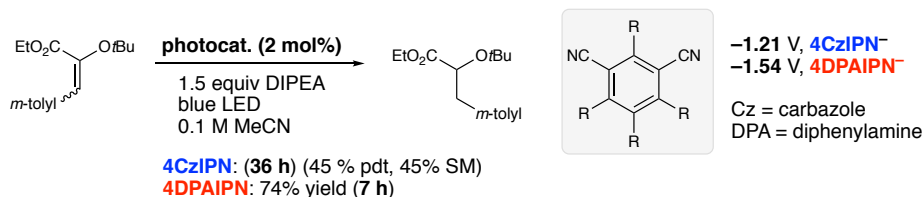
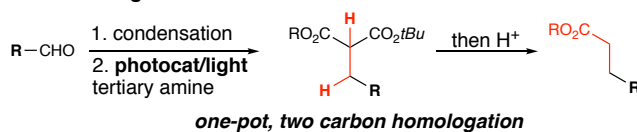


Figure 2-13. Knoevenagel condensation of *t*butyl ethyl malonate with *p*-tolylaldehyde.

Additionally, in order to enhance the utility of this reaction, a cheaper catalyst was needed. The recently disclosed carbazolyl dicyanobenzenes (**II-17** & **II-18**), preparable in a single step on multigram scale with no column chromatography, have similar properties to the reductive quenching cycles of the commonly used iridium catalysts (**Figure 2-6**, **II-14** & **II-15**).²²⁸ Interestingly when these catalysts were applied to the transfer hydrogenation reaction with Hunig's base, differential reactivity corresponding to the reducing power of the catalysts reduced state (-1.21 V, **II-18** vs -1.54 , **II-17**) was observed (**Scheme 2-14**). This dependence on catalyst reducing power supports a reaction mechanism proceeding through a LUMO-lowering catalyzed reduction of the arylidene malonate. The requirement of a strongly reducing catalyst further suggests that the activation arylidene malonate by the oxidized amine species isn't strong, as scandium triflate was observed to shift the potential to approximately -0.4 V vs SCE. Finally, with photocatalyst **II-17**, the same isolated yield was obtained as was with the iridium catalyst.

Scheme 2-14. Design of a One-Pot Reductive Homologation Reaction.

Reaction Design:



With the organo-photocatalysis identified as suitable catalysts, we again sought to understand Lewis acid compatibility (**Figure 2-14**). Interestingly, inexpensive and mild Lewis acids like lithium chloride and cerium chloride heptahydrate functioned just as well as scandium triflate, but yields were lower in all cases. These lower yields are attributed to the nature of the radical termination step, with oxidized HEH being less efficient than oxidized Hunig's base.

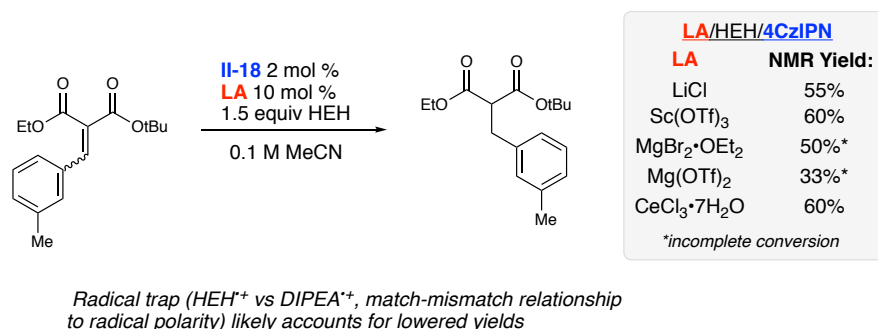


Figure 2-14. Organo-photocatalysis in Transfer Hydrogenation of Aryldiene Malonates.

Having defined the parameters for the condensation and transfer hydrogenation of the non-symmetric aryldiene malonate, testing the one-pot yield was in order. These conditions yielded the saturated product **II-29** in 64% NMR yield (**Figure 2-15**). With the initial application

of the unique reactivity of arylidene malonates under photoredox conditions, we sought to examine carbon-carbon bond forming reactions.

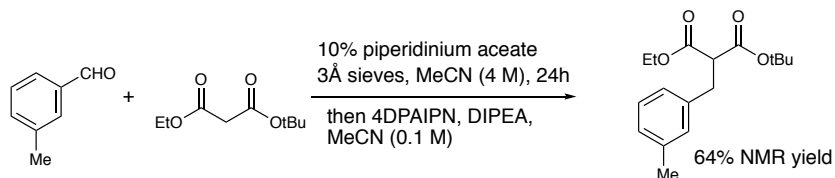


Figure 2-15. One-Pot Organocatalyzed Transfer Hydrogenation of Arylidene Malonates.

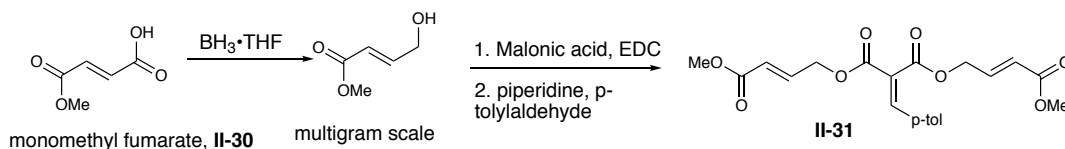
2.4 Intramolecular Cyclization Reactions of Arylidene Maloantes

2.4.1 Approaches towards δ -Lactones

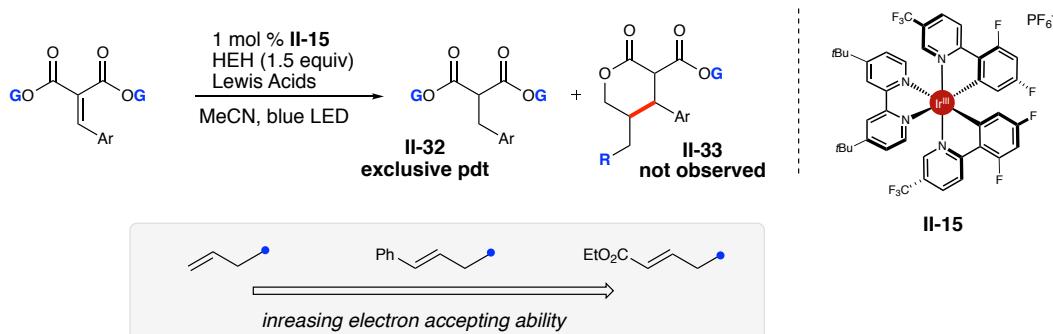
A reaction of the arylidene malonate derived β -radical enolate with an internal electron acceptor provides an opportunity to explore the fundamental reaction parameters in a reliable, controlled fashion. Since the ester groups of malonates can be easily modified, a new approach to δ -lactones seemed an ideal test reaction. A series of arylidene malonate substrates were prepared, with increasingly activated electron acceptors on the wingtips of the malonate (allyl, cinnamyl, crotonate). All of these substrates could be easily prepared by coupling of the appropriate alcohol with malonic acid. Interestingly, the crotonate derived malonate had not been previously prepared, but the could be easily prepared from the inexpensive monomethyl fumarate **II-30** (Scheme 2-15). A borane reduction followed by EDC coupling with malonic acid yielded the desired malonate. Finally, the standard piperinium acetate Knoevenagel conditions furnished the completed arylidene malonate **II-31**.

Scheme 2-15. Efforts Towards the Cyclization of Arylidene Malonate to δ -Lactones

Preparation of Cyclization Substrate:



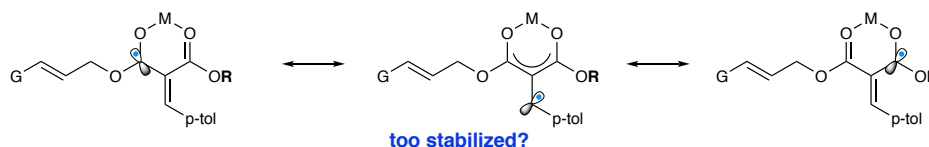
Attempted Cyclization:



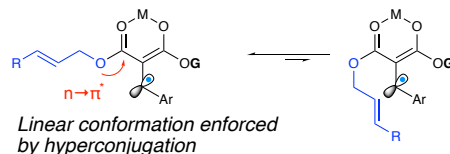
Frustratingly, regardless of wingtip group, photocatalyst, or terminal reductant the saturated, transfer hydrogenation product **II-32** was exclusive obtained with no evidence of cyclized product **II-33** (Scheme 2-15). We reasoned that there were two likely possible mechanistic explanations (Scheme 2-16).

Scheme 2-16. Two Possible Rationales for the Lack of Cyclization.

Explanation A:



Explanation B:



Either our β -radical enolate was too stabilized by the multiple sites for electron delocalization and was thus unable to undergo addition, or the ester group was locked in a

conformation unfavorable to cyclization by lone pair delocalization into the ester carbonyl. Before proceeding to investigating intermolecular reactivity, we wanted to have a clearer understanding and chose to design a new intramolecular substrate that would not be subject to these constraints.

2.4.2 Preparation of New Chroman Derivatives

We sought a different location for the electron accepting group on the arylidene malonate to probe our hypothesis that the lack of cyclization previously observed was a result of substrate limitations, not the fundamental reactivity of the AM-derived β -radical enolate. With the goal of maintaining the general arylidene malonate structure, the next logical position for the electron accepting group would be on the aryl ring (**Figure 2-16**). Additionally, the linkage would need to be through a conformationally flexible motif. With these design parameters in mind, salicylaldehyde derived systems were chosen since they could be easily assembled and would yield useful chroman derivatives.²²⁹ Simple alkylation of salicylaldehyde with a crotonate group followed by condensation with a malonate yields the desired system (**II-34**) in two simple steps.

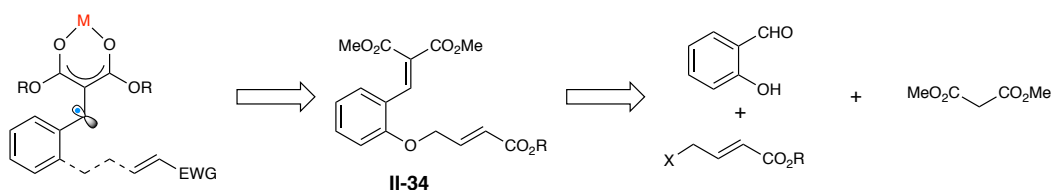


Figure 2-16. Design of a New Intramolecular Cyclization Substrate.

Using a scandium triflate or magnesium triflate with HEH as the terminal reductant, yielded **II-35** in 86-91% yield, albeit with low diastereoselectivity (**Figure 2-17**). Cyclization reactions templated by aryl rings rarely show diastereoselectivity as the planarity of the aryl ring

and ether linkage likely imposes minimal conformational restrictions on the pendant electron acceptor.^{206,230} Interestingly, when Hunig's base was used as the terminal reductant, the product was isolated in a much lower 57% yield, but with moderate diastereoselectivity (3:1). This unprecedented diastereoselectivity was intriguing.

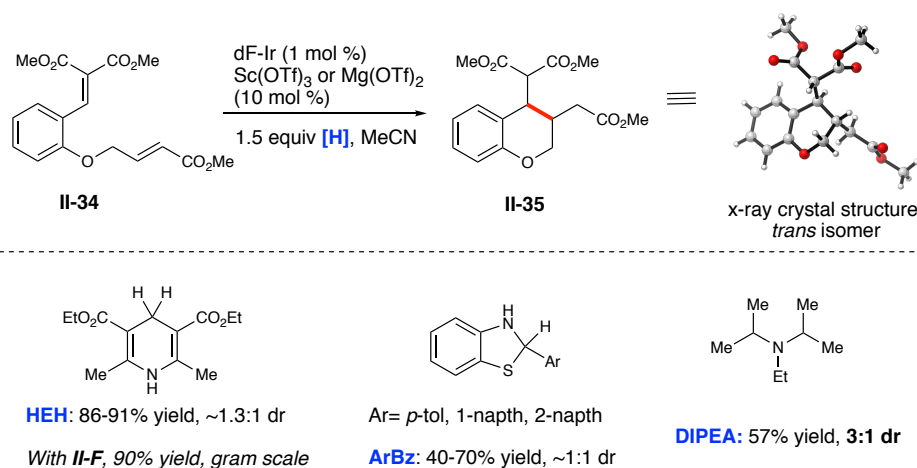
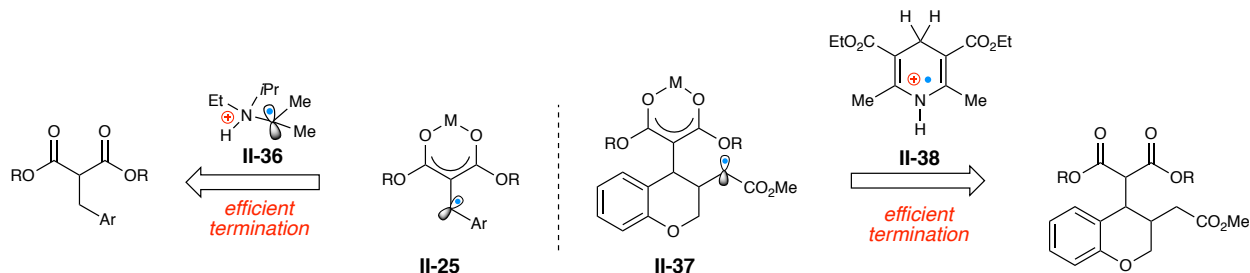
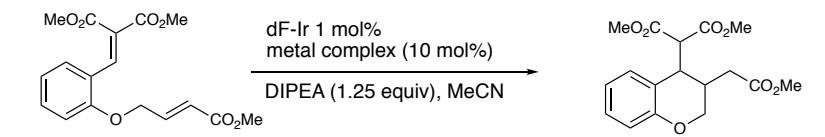


Figure 2-17. Optimization of Cyclization Reaction.

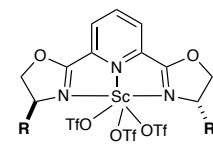
The lowered yield was attributed to the less efficient radical termination by the oxidized tertiary amine. A clear trend in H-atom transfer to terminate radicals has been established in our studies; HEH⁺ (**II-38**) is best at quenching electron deficient radicals (e.g. radicals adjacent to carbonyl systems, like **II-37**), while the radical cation species derived from tertiary amines (**II-36**) efficiently undergo H-atom transfer to more electron-rich radicals like the β -radical enolate (**II-25**) in the transfer hydrogenation reaction (**Scheme 2-17**). We also examined the substitution of the expensive iridium photocatalyst **II-15** and substituted it with the photo-organocatalyst **II-18**. With HEH as the terminal reductant, this system proved robust with the cyclization product obtained in 90% yield on gram-scale.

Scheme 2-17. Observed Trends in Radical Termination in this Work.

The result with Hunig's base was intriguing since this was a rare case of diastereoselectivity with these *ortho*-ether aryl substrates. Changing the malonate ester groups to the larger isopropyl substituents did not raise the diastereoselectivity in any of the conditions evaluated. Since we demonstrated that oxidized tertiary amines are able to catalyze this process, a variety of mechanistic possibilities exist to rationalize this observed reactivity. It is possible that the tertiary tertiary amine radical cation species is activating the malonate, rather than the Lewis acid or that the tertiary amine radical cation is activating the pendant crotonate group for reduction rather than the malonate. We examined the use of chiral Lewis acid complexes, to observe if there was any effect on the diastereoselectivity of the reaction. Using preformed PYBOX complexes^{231,232} of scandium triflate and BOX complexes²³³ of magnesium triflate, some improvement of diastereoselectivity was observed, but with no enantioselectivity (**Table 2–2**). The best dr was observed with magnesium triflate and indendol-fused BOX ligand (**Table 2–2**, entry 5).

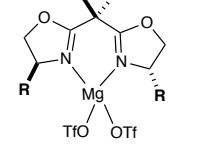
Table 2–2. Survey of Compatible Arylidene Malonates.


$\text{MeO}_2\text{C}-\text{C}(\text{CO}_2\text{Me})=\text{C}(\text{Ph})-\text{O}-\text{CH}_2-\text{CH}=\text{CH}-\text{CO}_2\text{Me}$
 $\xrightarrow[\text{DIPEA (1.25 equiv), MeCN}]{\text{dF-Ir 1 mol\% metal complex (10 mol\%)}}$
 $\text{MeO}_2\text{C}-\text{C}(\text{CO}_2\text{Me})-\text{C}(\text{Ph})-\text{O}-\text{CH}_2-\text{CH}(\text{CO}_2\text{Me})-\text{CH}_2-\text{CO}_2\text{Me}$



entry R yield* dr er

1	Ph	53	1.5:1	50:50
2	Inda	51	2:1	50:50
3	<i>i</i> Pr	50	2.5:1	50:50
4	Bn	10	1.5:1	50:50

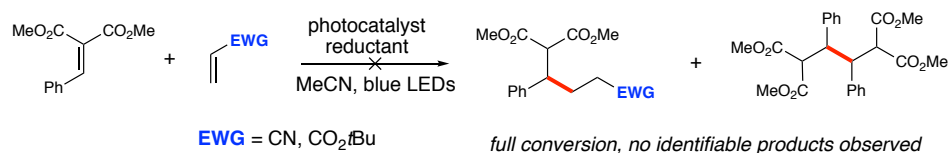


entry R yield dr er

5	Inda	52	4.8:1	50:50
6	<i>t</i> Bu	56	3:1	50:50

**all reactions showed incomplete conversion*

While further studies are needed to understand how to engender stereocontrol, we were happy to confirm that the new β -radical enolate underwent additions to electron acceptor groups. With this proof-of-concept, we set out to undertake more challenging intermolecular coupling reactions. Attempting the reductive cross-coupling of arylidene malonates and acrylates resulted in full conversion of the malonate, with no identifiable products (**Figure 2-18**). These results led to our decision to examine radical cross-couplings.

**Figure 2-18.** Attempted Reductive Enone Cross-Coupling.

2.5 Intermolecular Radical Cross-coupling Malonate Derived Radical Enolates

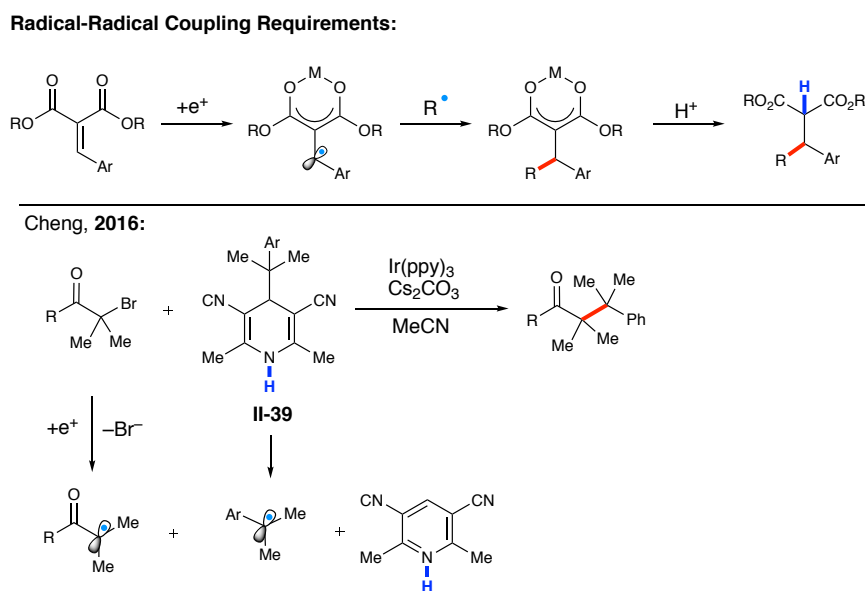
With our initial studies examining the fundamental reactivity of arylidene malonate derived β -radical enolate complete and our important observation that dimerization was not the

dominant reaction path for this species, a challenging radical-radical cross-coupling became our goal.

2.5.1 Reaction Design

Intermolecular radical-radical coupling reactions have some notoriety as being difficult to control due to the considerable number of possible outcomes. However, with the use of photoredox, it has become increasingly apparent that efficient radical-radical couplings can be achieved with judicious selection of radical partners.^{234,217,220,235,236} Our intended radical-radical coupling reaction had some key design features to consider if we were to use arylidene malonates (**Scheme 2-18**).

Scheme 2-18. Design of Radical-Radical Coupling Reaction.



Under the conditions, we would need to a) relay an electron from a substrate to our Lewis acid/AM complex; b) generate a radical to undergo coupling; and c) generate or have present a proton to turn over the Lewis acid (**Scheme 2-18**). We were particularly inspired by the radical

coupling reaction reported by Cheng et al, in which they coupled α -carbonyl radicals with a variety of benzylic radicals (**Scheme 2-18**). The use of a HE-derivative (**II-39**) that underwent mesolytic cleavage to yield a benzylic radical would be an ideal partner, since it meets all of the criteria outlined above. We set out to use the tertiary benzylic radical as the construction of quaternary centers is challenging as well the fact that this bulky, stable radical seemed more likely to undergo radical-radical coupling rather than Lewis acid mediated radical conjugate addition. Additionally, the synthesis of the HE derivatives is achieved in a straightforward two steps sequence (**Figure 2-19**).

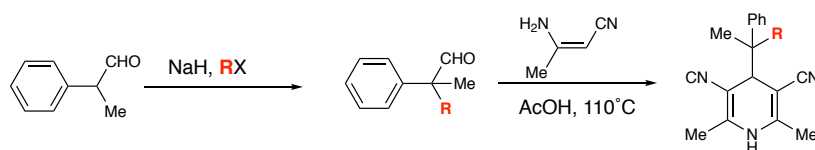
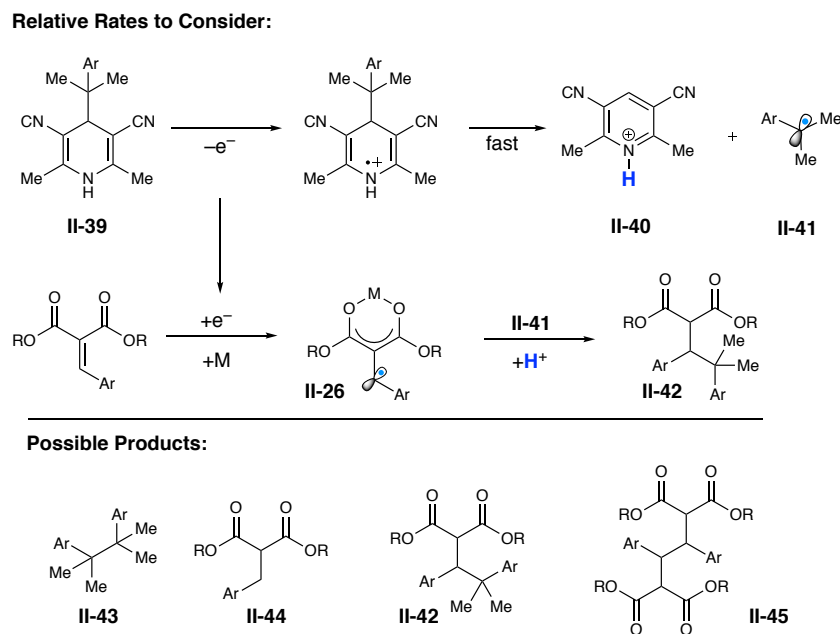


Figure 2-19. Preparation of HE-derivative Radical donor.

In executing this cross-coupling reaction, there are a variety of relative rates and possible products to consider (**Scheme 2-19**). The oxidation of **II-39** is believed to result in rapid fragmentation to protonated **II-40** and radical **II-41** due to the driving force of the pyridine aromatization. The resulting electron would then be relayed by the photocatalyst to the Lewis acid/arylidene malonate complex resulting in β -radical enolate **II-26**. This species will then be able to undergo a variety of reactions. Coupling with **II-41** would yield the desired cross-product **II-42**. However, a variety of coupling products are to be expected (**II-42-II-45**), which will be dictated by the relative rates of radical combination and proton transfer from **II-40**.

Scheme 2-19. Considerations of a Radical-Radical Coupling Reaction.

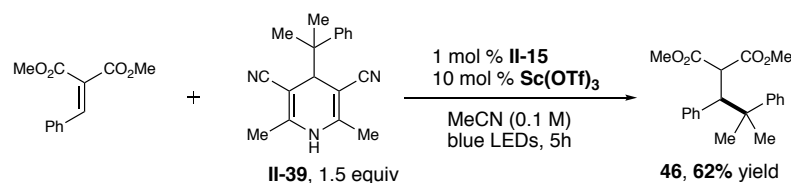


2.5.2 Reaction Optimization

Surprisingly, the first conditions examined provided the desired coupling product in the highest yield. Using 1.5 equivalents of the HE derivative **II-46**, 10 mol % scandium triflate, 1 mol % of **II-15** in acetonitrile (0.1 M) yielded the desired cross-coupling product **II-46** in 62% isolated yield. All deviations from these conditions led to decreased yield. A wide variety Lewis acids, including magnesium triflate (**Table 2-3**, entry 1), lanthanum triflate (**Table 2-3**, entry 2), and lithium chloride (**Table 2-3**, entry 3) were capable of facilitating the reaction. We confirmed that an excess of nitrile HE radical precursor (1.5 equivalents) was required to ensure full conversion of the malonate, as we observed by-products identified as tetramethyl bibenzyl HE-derived radical dimers, in addition to small amounts of saturated arylidene malonate. While photocatalysts **II-15** proved optimal, other photocatalysts such as $\text{Ru}(\text{bpy})_3(\text{PF}_6)_2$ and $\text{fac-Ir}(\text{ppy})_3$ resulted in greatly diminished yields (29% and <10% yield, respectively).

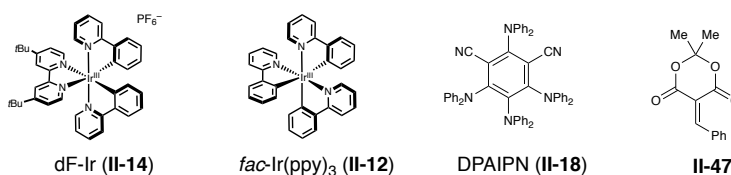
Organocatalysts of the dicyanobenzene family^{237,228} performed nearly as well as **II-15**, with diphenyl aniline organocatalyst DPAIPN (**II-17**) providing the coupling product in a similar 55% yield.

Table 2–3. Deviation from Optimal Conditions for Radical Cross-Coupling.



entry	Modification to Standard Conditions	Yield
1	10 mol % Mg(OTf)₂ instead of Sc(OTf) ₃	56 ^[a]
2	10 mol % La(OTf)₃ instead of Sc(OTf) ₃	54 ^[a]
3	50 mol % LiCl , MeCN (0.1 M)	0
4	10 mol % Yb(OTf)₃ , MeCN (0.1 M)	47
5	2 mol % DPAIPN instead of dF-Ir	55 ^[b]
6	1 mol % Ir(ppy)₃ instead of dF-Ir	trace
7	1 mol % Ru(bpy)₃(PF₆)₂ instead of dF-Ir	29
8	II-47 instead of malonate	NR
9	DCM instead of MeCN	5 ^[a]
10	1.5 equiv malonate, 1 equiv HEH	59 ^[a]
11	Sc 10%, 0.2 M , 0.5% dF-Ir	58 ^[a]
12	No Lewis acid	NR
13	No photocatalyst	NR
14	No light	NR

[a] Yield determined by GC with bibenzyl as internal standard. [b] Yield of isolated product.

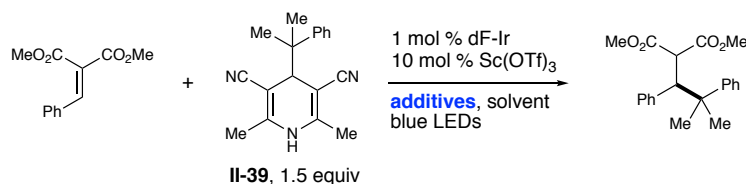


The importance of the malonate moiety was confirmed, as the conjugate acceptor **II-47** derived from Meldrum's acid showed no conversion under the optimized conditions. Additionally, when the alkylidene malonates were employed in place of arylidene malonates, no

reaction was observed. Finally, no reaction occurred with the omission of the Lewis acid, photocatalyst, or light

Acetonitrile proved to be a crucial solvent as other solvents such as THF and DCM showed minimal reaction (**Table 2–4**). In an attempt to control the rate of radical formation, the HE derivative was added in portionwise, but this only led to decreased yields (**Table 2–4**, entries 3-4). An additional possibility is that the β -radical enolate may be undergoing protonation before bond formation, thus greatly changing the nature of the radical and affecting the efficiency of the desired cross-coupling reaction. Hindered pyridine bases and NMI were employed in an attempt to buffer the reaction, but only minimally lowered the yield. Increasing the loading of the base beyond 10% (30%, 100%) resulted in minimal conversion.

Table 2–4. Effect of Modulation of Reaction Conditions.

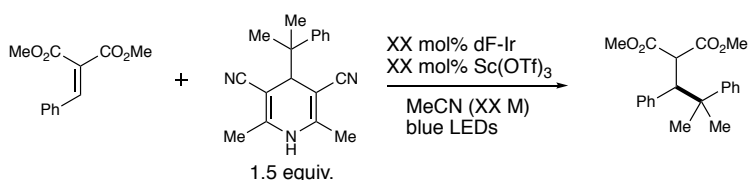


Entry:	Conditions:	GC Yield ^[a] :
1	DCM (0.1 M)	5
2	THF (0.1 M)	<5
3	4 portionwise additions of II-39, 30 min interval , MeCN (0.1 M)	42
4	4 portionwise additions of II-39, 20 min interval , MeCN (0.1 M)	40
5	10 mol % 2,6-tBu-4-Me-pyridine , MeCN (0.1 M)	56
6	10 mol % N-Me-imidazole , MeCN (0.1 M)	0
7	10 mol % 2,4,6-Me-pyridine , MeCN (0.1 M)	47
8	10 mol % 2,2'-bipyridine , MeCN (0.1 M)	47

[a] Yield determined by GC with bibenzyl as internal standard.

As discussed in **Figure 2-4**, the concentration of radical species likely plays a great role in the efficiency of radical reactions. As such there were several ways to control the relative and absolute concentration of the radical constituents. Cutting the photocatalyst loading in half and doubling the reaction concentration resulted in the same GC yield (**Table 2-5**). All other deviations resulted lowered yields.

Table 2-5. Effect of Concentration and Catalyst Loading on Coupling Reaction.



Entry:	mol % Sc(OTf) ₃ :	mol % dF-Ir:	Conc:	GC Yield ^[a] :
1	10	0.5	0.2 M	62
2	5	0.5	0.2 M	51
3	5	1	0.2 M	41
4	10	1	0.2 M	53
5	10	0.5	0.1 M	52
6	5	0.5	0.1 M	53
7	10	0.5	0.05 M	57
8	5	1	0.05 M	28

[a] Yield determined by GC with bibenzyl as internal standard.

With these promising results in hand, we explored the possibility employing chiral ligands with the Lewis acids (**Table 2-6**). Using the indenol derived PYBOX, promising 80:20 er was observed, but with very low conversion and yield (**Table 2-6**, entry 1). Raising the loading of the Lewis acid complex to 50 mol % resulted in increased conversion, but decreased enantioselectivity (**Table 2-6**, entry 4). Magnesium BOX complexes were employed and showed great reactivity, but low enantioinduction (**Table 2-6**, entries 9-10). Additionally, Feng's N-

oxide ligands²³⁸ were prepared and surveyed with a variety of Lewis acids. The best result was obtained with the ramipiril derived ligand, 41% yield, 35:65 er (**Table 2–6**, entry 5). Coupling the tertiary radical is indeed challenging, with the only comparable example being Melchiorre's bi-functional system coupled the same benzylic radical with cinnamaldehyde, obtaining the product in 46% yield, 85:15 er for the alkylation of cinnaldehyde.²³⁵

Table 2–6. Studies Towards Asymmetric Cross-Coupling Reaction.

Entry:	Conditions:	GC Yield ^[a] :	E.R.:
1	10 mol % Sc(OTf) ₃ , 12 mol % indenol-PYBOX	7	80:20
2	10 mol % Sc(OTf) ₃ , 12 mol % Ph-PYBOX	11	60:40
3	10 mol % Sc(OTf) ₃ , 12 mol % <i>i</i> Pr-PYBOX	NR	–
4	50 mol % Sc(OTf) ₃ , 55 mol % indenol-PYBOX	35	62:38
5	20 mol % Sc(OTf) ₃ , 22 mol % Ra-N-Ox	41 ^[b]	35:65
6	20 mol % Y(OTf) ₃ , 22 mol % Ra-N-Ox	59 ^[b]	51:49
7	20 mol % Gd(OTf) ₃ , 22 mol % Ra-N-Ox	45 ^[b]	53:47
8	10 mol % Mg(OTf) ₂ , 12 mol % <i>t</i> Bu-cyclopropyl-BOX	39	50.5:49.5
9	10 mol % Mg(OTf) ₂ , 12 mol % indenol-cyclopropyl-BOX	65	55:45
10	10 mol % Mg(OTf) ₂ , 12 mol % <i>t</i> Bu-cyclopentyl-BOX 3 equivs. HE	53	50.7:49.3

[a] Yield determined by GC with bibenzyl as internal standard. [b] Yield of product isolated after column chromatography

While follow-up studies are required to identify an optimal asymmetric system, we proceeded to examine the scope of enones that could serve as effective cross-coupling partners.

2.5.3 Scope of Malonate Coupling Partners

Since radical reactions are sensitive to the electronic nature of reaction partners (as seen in previous investigation of the transfer hydrogenation), we were pleased to observe that a variety of substituted AMs proved compatible with our optimized reaction conditions (**Figure**

2-20). The electron-deficient 4-trifluoromethyl substituted malonate proved the most efficient cross-coupling partner, with the product **II-48** obtained in 66% yield. We were also grateful to observe AMs possessing halogenation the 4- and 2-positions underwent coupling with no observed dehalogenation products (**II-50–II-53**, **II-55-56**, **II-59**). The selectivity for coupling in the presence of other radically labile bonds indicates enhanced stability of the β -radical enolate, likely due to complexation with the Lewis acid. The bulkier 2-methoxy and 1-naphthyl substituted AMs showed minimal reactivity, which could be attributed to reduced overlap between the enone and aryl π -systems.

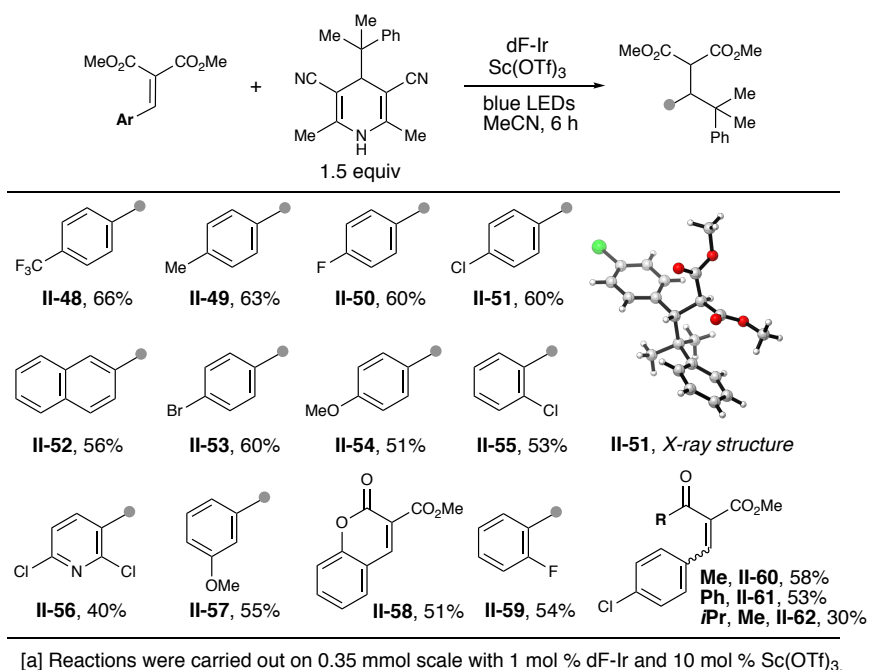


Figure 2-20. Scope of Malonate Coupling Partners.

Other electron rich substrates proved competent, with the 3- and 4-methoxy products obtained in 55% and 51% yield, respectively. We anticipated the potential for competitive reactivity at the ketone carbon, but we were pleased to observe that β -keto ester derived enones

were also competent enone substrates. The methyl ketone product (**II-60**) was isolated in a similar 60% yield, while the isopropyl derived product **II-62** was produced in greatly decreased yield (30%), likely due to the increased steric bulk on the ketone. Interested in probing the effect of locking the phenyl ring in a planar relationship to the enone system, the salicylaldehyde-derived arylidene malonate was tested, yielding **II-58** in 51% yield, thus indicating that this does not significantly enhance cross-coupling efficiency. Interestingly, replacing the aryl substituent with other aromatic heterocycles proved challenging. All unsubstituted (2-,3-,4-) pyridine and quinoline derived AMs resulted complete consumption of starting material with no observed product.²³⁹ However, coupling was observed with the 2,6-dichloropyridine malonate, with the product **II-56** obtained in a modest 40% yield. This could indicate competitive binding to the Lewis acid by the heterocycle, or instability of the β -radical enolate species. Further investigation is required to understand these observations.

Additionally, to understand the effect of steric bulk around the radical coupling partner, we subjected a variety of arylidene malonates to the same conditions, but with a HE-derivative that would yield the primary benzylic radical. Cheng et al. saw almost two-fold greater yields with the primary radical compared to the tertiary system.²³⁴ Interestingly, the yield and reactivity pattern trends observed on the tertiary system are mirrored with the primary radical coupling system. Notably, some conversion is observed with the primary radical in the absence of Lewis acid, but the yield and conversion is much lower, suggesting that this may proceed through a mixture of radical coupling and conjugate addition. This data suggests that electronic factors are more important than steric issues or that competing rates, such as dimerization (vide infra) are similar with both radicals.

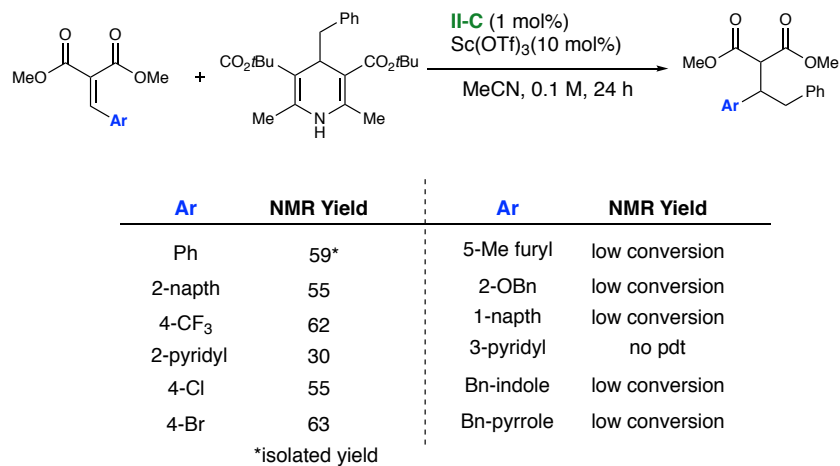


Figure 2-21. Scope of Malonate Coupling Partners with Primary Benzylic Radical.

2.5.4 Scope of Benzylic Radicals

With the enone scope explored, our attention turned to probing perturbations in the electronic character of the benzylic radical coupling partner (**Table 3**). A variety of aryl groups proved competent in the coupling reaction. Interestingly, the 4-fluoro substituted derivative proved most efficient, providing product **II-63** in 62% yield. Further work is needed to determine if this is the result of a faster rate of cross-coupling or a reduced rate of competing side reactions.

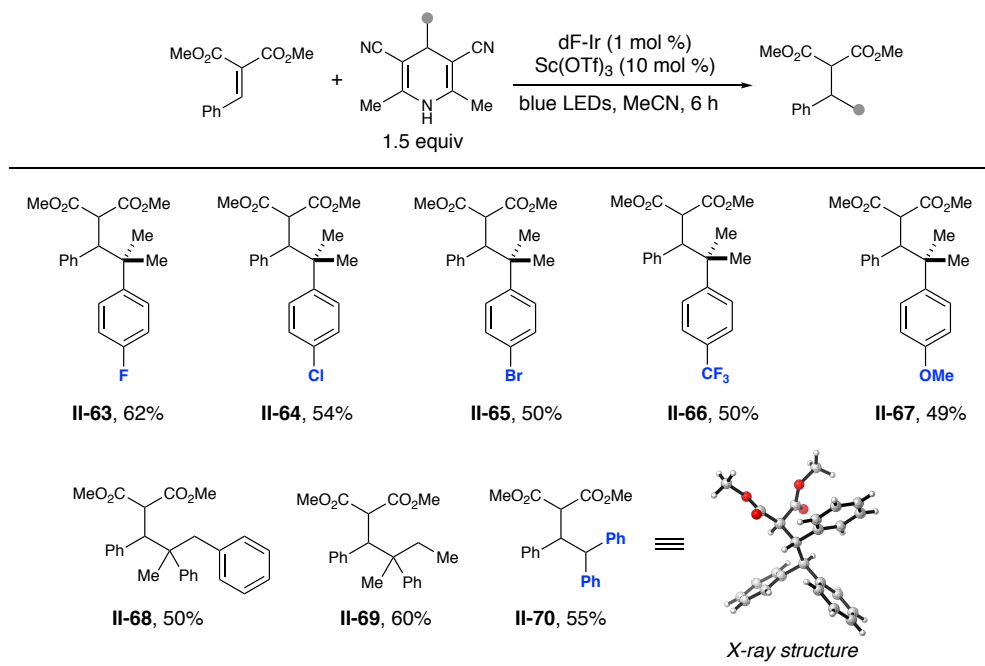


Figure 2-22. Scope of Malonate Coupling Partners with Primary Benzylic Radical.

Non-symmetric species with ethyl or benzyl substitution were tolerated, yielding the products **II-68** and **II-69** in 60% and 50% yield respectively, as a ~1:1 ratio of diastereomers. Interestingly, the stabilized, doubly benzylic species also proved competent in the reaction, with the product **70** isolated in 55% yield. A single-crystal x-ray structure to definitively confirmed its structure.

2.5.5 Proposed Mechanism For Radical Cross-Coupling Reaction

Addressing the possibility that the reaction might be proceeding via a radical conjugate addition pathway was a required. Cheng et al. established that substituted HE-derivatives are able to quench the excited state of iridium photocatalysts using Stern-Volmer quenching experiments.²³⁴ Given that the oxidation potential of a related benzyl nitrile HE has been reported as 1.08 V,²³⁴ our observation that only photocatalysts with matching oxidation

potentials (**Table 2–3**, entries 6-7) is consistent with initiation by reductive quenching with the HE. It is possible that the benzylic radical could undergo radical conjugate addition to the Lewis acid-AM complex, but alkylidene malonates, known to be more reactive in conjugate additions, yield no reaction under these conditions. This is indicative of a radical-radical coupling mechanism, as other photoredox/Lewis acid mediated radical conjugate additions have shown similar reactivity between alkyl and aryl substrates.^{240,218} Furthermore, a tail-to-tail dimer of phenyl AM (**II-71**), was isolated in ~30% yield as a side-product (1:1 ratio of diastereomers) and its structure confirmed by single-crystal x-ray analysis (**Figure 2-24**).²⁴¹ Notably, this intermediate has only been previously been reported in single-electron reductions of AMs, indicating that reduction of the arylidene malonate is an active mechanism in the reaction.^{241,242} Additionally, quantum yield experiments determined the quantum yield for the cross-coupling and dimeric product to be 1.0.

With this information, we propose the following mechanism for the radical cross-coupling reaction with HE derived benzylic radicals (**Figure 2-23**). Upon irradiation, the photoexcited iridium species oxidizes the nitrile HE **A**, yielding radical cation **B**. This species rapidly fragments into the tertiary radical coupling partner **C** and the protonated pyridine species **D**. Concurrently, the reduced iridium species transfers an electron to the Lewis acid-arylidene malonate complex, resulting in the β -radical enolate complex **G**. Radical-radical coupling of **C** and **G** yields the enolate complex **H**, which is then protonated by **D**, thus freeing the Lewis acid and providing the desired product **I**.

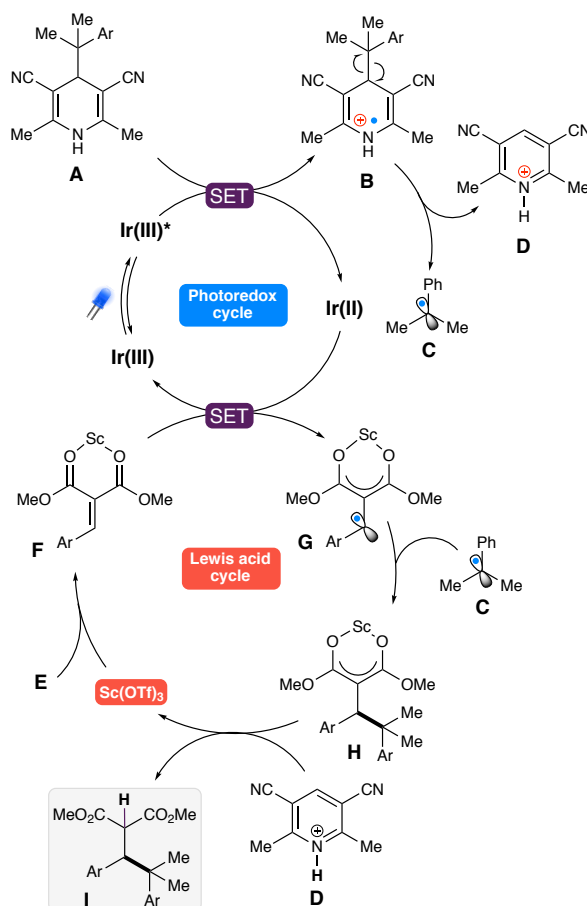


Figure 2-23. Proposed Mechanism for the Coupling of Arylidene Malonates with Benzylic Radicals.

2.6 Discovery of the Reductive Dimerization of Arylidene Malonates

As previously discussed, the isolation of the remaining material in the coupling reaction revealed that the remaining mass balance was accounted for by a dimer of the malonate **II-71**. To understand if this dimeric product originated from radical-radical coupling or radical conjugate addition, the reaction was run with inversion of the limiting reagent (using 1.5 equivalent of AM and 1 equivalent of HE). The result was a nearly identical yield of the desired cross-coupling product (59% vs 62% yield) (**Table 2-3**, entry 10). This would suggest that dimer (**71**) is

forming by dimerization of these species, not through addition of radical enolate (**II-25**) to unreacted AM or its Lewis acid complex. Switching the photocatalyst to fac-Ir(ppy)₃ would make not allow for reductive quenching (due to the low oxidation potential of the photoexcited species) and instead go through an oxidative quenching cycle (direct reduction of the AM-Lewis acid complex by the excited state of the photocatalyst). Employing tributylamine as the terminal reductant afforded significant quantities of the dimeric product (53% yield) with saturated malonate only observed in small quantities (**Figure 2-24**).

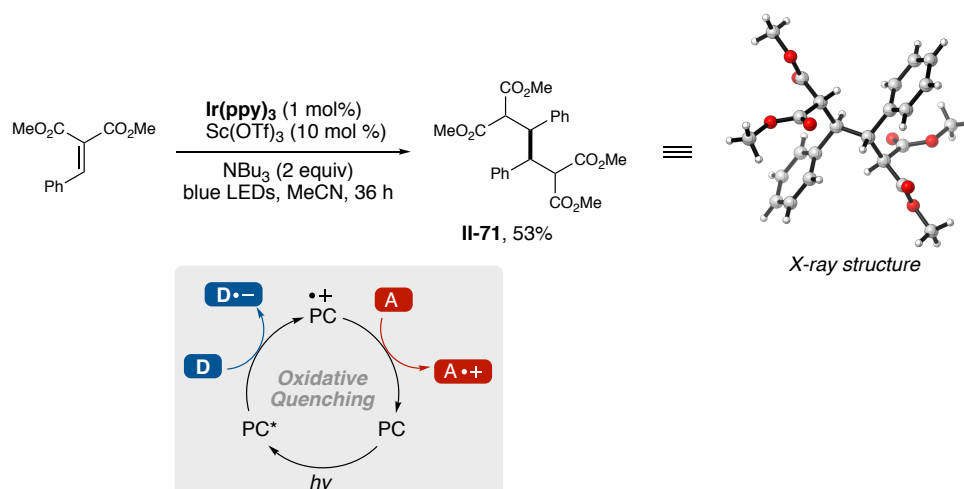


Figure 2-24. Reductive Dimerization of Arylidene Malonate through Oxidative Quenching.

2.6.1 Reaction Optimization

We sought to examine additives in the hope of suppressing side-reactions. A species containing 12 methyl ester groups and the mass of a trimer of the arylidene malonate was isolated in about 15% yield (**Figure 2-25**). The 12 methyl esters indicate that each carbonyl is unique, thus making structure **II-72** the likely structure.

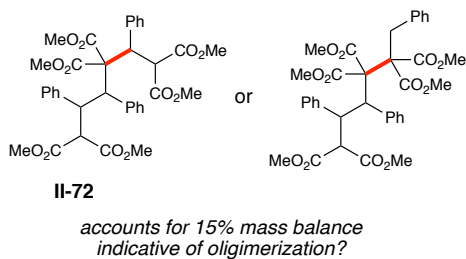


Figure 2-25. Possible Structure of Isolated Trimeric Species.

In an attempt to prevent reactivity at the malonate position, we examined acidic additives to buffer the reaction. Using a 96-well plate, we examined different Lewis acids and loadings, as well as different loadings of additives (**Figure 2-26**). Clear trends were not apparent from the data, with many of the reactions failing. Further work determined that this was likely due to solubility issues of photocatalyst Ir(ppy)₃. However, the reactions that did not show trimer, were not replicable upon scale up.

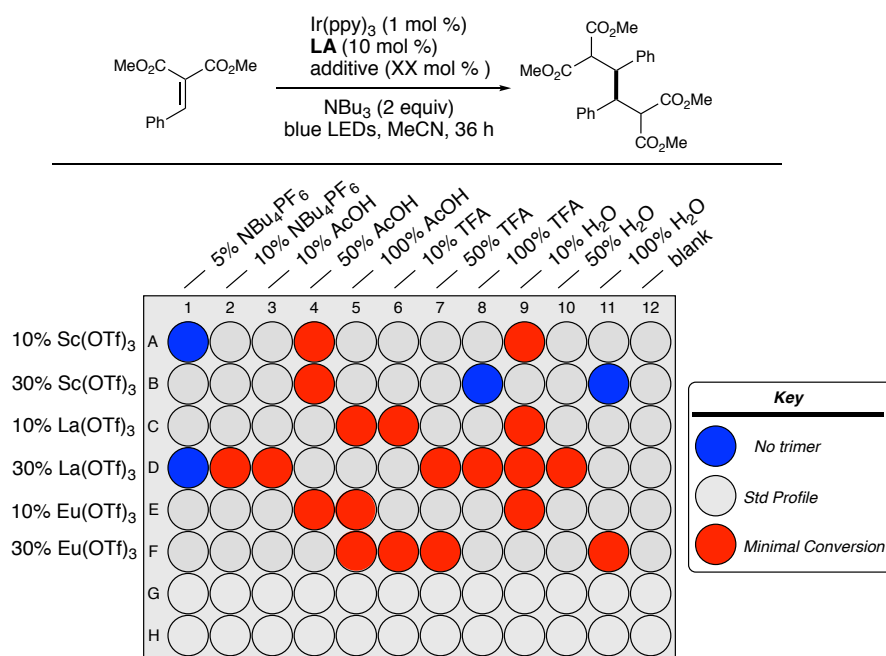


Figure 2-26. Optimization of Reductive Dimerization Conditions.

Unable to suppress the trimer formation, we decided to examine the scope of the reaction, as this issue may only be present for this or certain substrates.

2.6.2 Scope of Malonates

Interestingly, the trimer product was only observed for the Ph arylidene malonate substrate. The structural parameters of this dimerization were explored as they would provide contrast and valuable insight in the previously explored cross-coupling reaction (**Figure 2-27**). Generally, electron donating groups (4-OMe-Ph, 2-naphthyl) led to good yields of dimeric products **II-74** (74%), **II-76**, (76%). This could account for the lower yields seen in the cross-coupling with these substrates. The more electron neutral arene species (3-OMe, 4-F, 4-Br) performed similarly to the parent phenyl substrate (**II-77- II-79**). Surprisingly, the 4-Me dimeric product (**II-80**) was isolated in 74% yield, with no trimer product observed. Interestingly, the electron deficient 4-CF₃-Ph AM yielded minimal product (**II-75**), with the saturated AM obtained as the major product. This could account for its superior performance in the benzyl radical cross-coupling reaction and may suggest that this β -radical enolate is more unstable (less persistent) than those derived from other AMs. Interestingly, the salicylaldehyde substrate showed poor conversion, which could be attributed to rapid electron transfer back to the photocatalyst. The methyl keto-ester substrate also performed surprisingly poorly under these conditions, yielding only 40% isolated product (**II-81**). A reductive conjugate addition to arylidene malonate was attempted, resulting only in dimer **II-71**. This further indicates that the dimeric product is occurring via radical coupling. Finally, as seen in the cross coupling, 2-substituted substrates (2-OMe, 1-naphth) showed minimal conversion, confirming that this substitution hampers reduction, and likely results in rapid back-electron transfer. The data

collected in these studies will be important in the design of future reductive cross-coupling reactions with arylidene malonates.

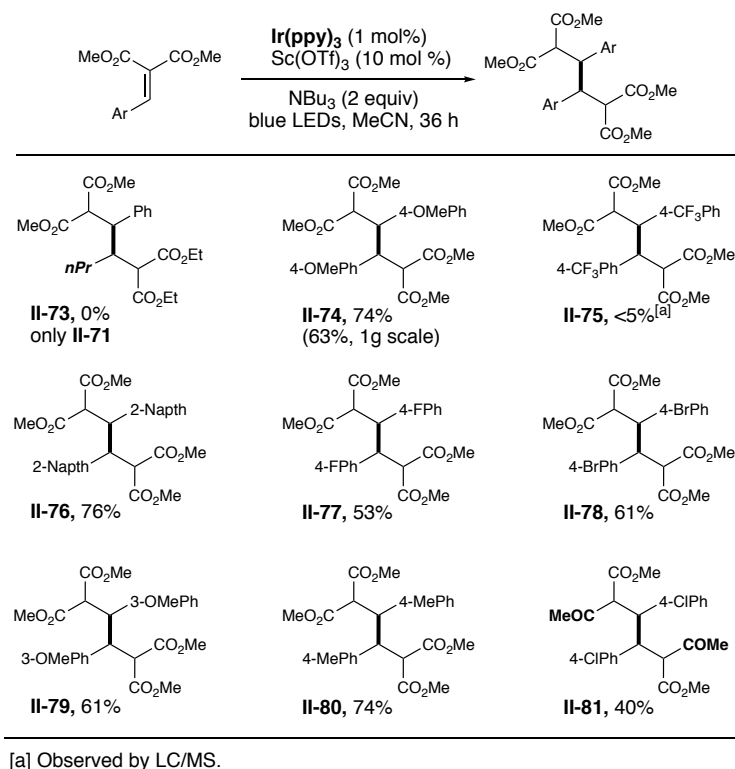


Figure 2-27. Scope of Malonate Dimerization.

2.7 Conclusion to Reductive Couplings of Arylidene Malonates.

Readily obtained arylidene malonates were demonstrated to form a stabilized β -radical enolate with reactivity divergent from high energy reductive species generated from cinnamates and chalcones. Initial studies demonstrated that these undergo efficient transfer hydrogenation and intramolecular cyclization reactions. The malonate derived β -radical enolate was further demonstrated to undergo challenging and productive reductive intermolecular radical-radical cross-coupling reactions, yielding vicinal tertiary and quaternary centers. The modularity of the cooperative catalytic approach enabled the use of a different photocatalytic pathway, thus

diverting the reactivity of the malonate derived β -radical enolates to 3,4-diaryl adipic ester derivatives via radical dimerization. This new platform sets the stage for the further development of d^3 or β -*Umpolung* reactivity via photoredox catalysis and investigations along those lines as well as enantioselective variants are ongoing.

2.8 Future Work

With significant progress made in both the areas so d^3 and d^1 open-shell operators there a considerable number of directions to take these chemistries.

2.8.1 Future Work on Reductive Arylidene Malonate Chemistry

Umpolung type couplings, chiefly enolate couplings (carbonyl α - α couplings), have played an important role in the advancement of carbon-carbon bond forming technologies enabling the preparation of important, polarity dissonant 1,4-carbonyl compounds.²⁴³⁻²⁴⁵ The homologous β - β coupling has not received the same level of attention, likely due to the difficulty of obtaining and controlling the requisite intermediates. Previous work by MacMillan has demonstrated that the oxidation and subsequent deprotonation of enamines yields transient β -radicals that will undergo couplings,²⁴⁶⁻²⁴⁸ Preliminary work (**Figure 2-28**) has demonstrated that this transient β -radical will couple with the AM β -radical, and producing **II-93** in approximately 15% yield.

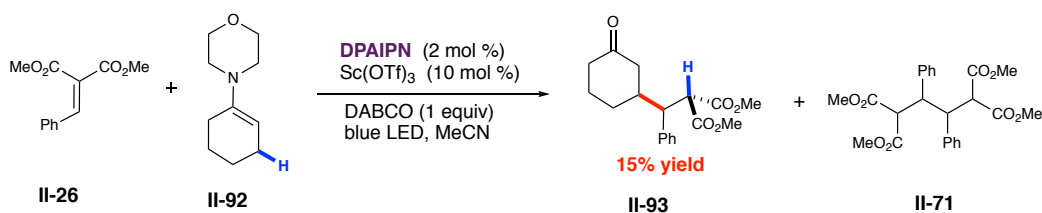
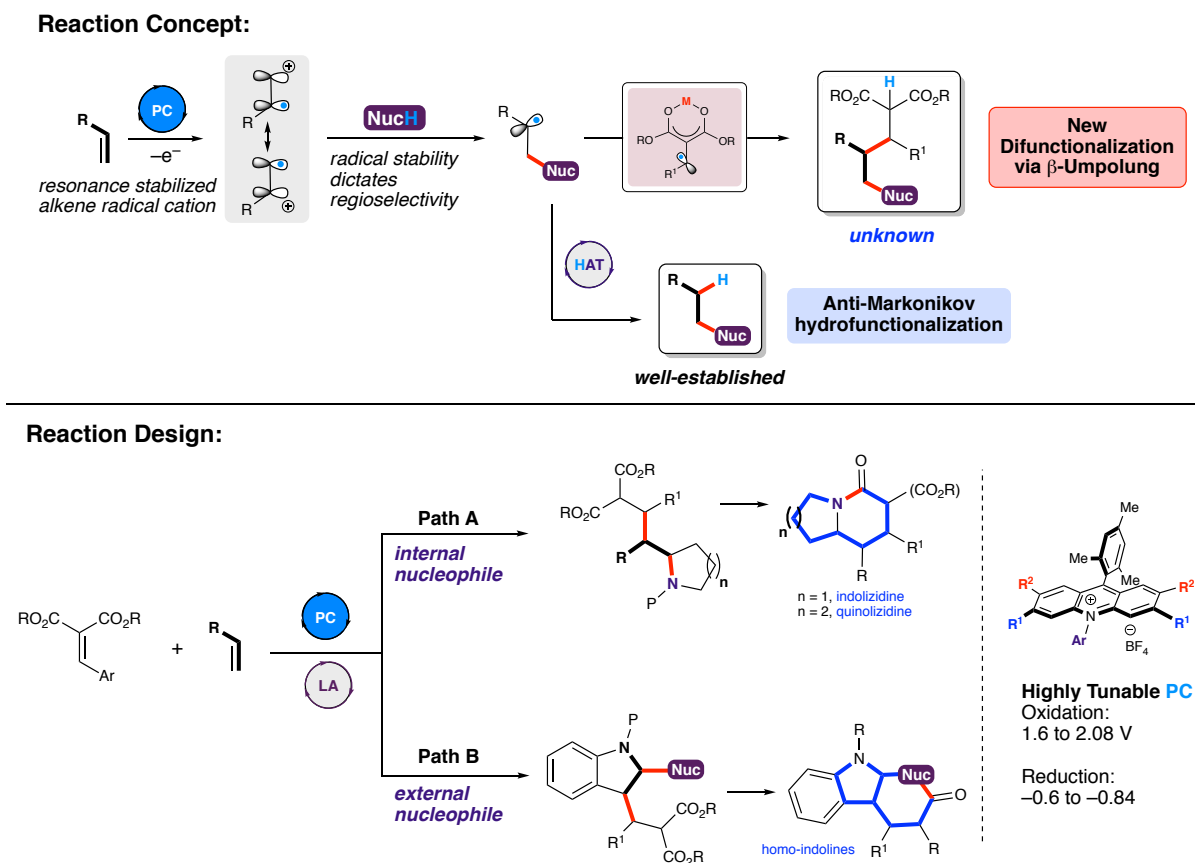


Figure 2-28. Initial Hit in β - β coupling of Enamine and Arylidene Malonate.

Well-established enamine catalysts^{249,250} could be employed in the reaction to perform an asymmetric coupling. If the diastereoselectivity of the reaction proves not be affected by a single catalyst, dual chiral systems could be explored to enable stereoselective preparation of each possible stereoisomer.^{251,252}

The regio- and stereoselective functionalization of alkenes are powerful tools towards the preparation of biologically and medicinally relevant small molecules. Nicewicz has demonstrated Mes-Acr-Me⁺ **II-21** and its derivatives can generate alkene radical-cations via photoexcited state quenching (**Scheme 2-20**).²⁵³⁻²⁶¹

Scheme 2-20. New Multi-Component Alkene Difunctionalizations.



This approach has been used to perform a variety of *anti-Markovnikov* alkene functionalizations via nucleophilic attack by internal and exogenous nucleophiles (**Scheme 2-20**). However, these reactions are terminated by hydrogen atom transfer, leaving a significant opportunity for new, powerful difunctionalization of alkenes. Cyclic voltammetry studies (*vide supra*) indicate that our LA/AM should be reducible by the reduced state of Mes-Acr family of photocatalysts (AM/Sc(OTf)₃ reduction potential approx. -0.5 V vs SCE, Mes-acridiums range -0.59 V to -0.84 V SCE)²⁶², thus enabling the merger of our radical enolate to create new redox neutral radical-polar cross-over reactions to rapidly build complexity from alkenes. The body of work on alkene radical-cations will serve as a foundation for the systematic investigation of coupling with our new β -radical enolate, starting with simple internal nucleophile substrates (**Scheme 2-20, path A**) and building to a multi-component coupling reaction (**Scheme 2-20, path B**). Preliminary work has shown that this Mes-Acridine is capable of reducing the scandium triflate/arylidene malonate system as AM dimer and product masses were observed via UPLC (). Future work will fully characterize and optimize this new reaction manifold.

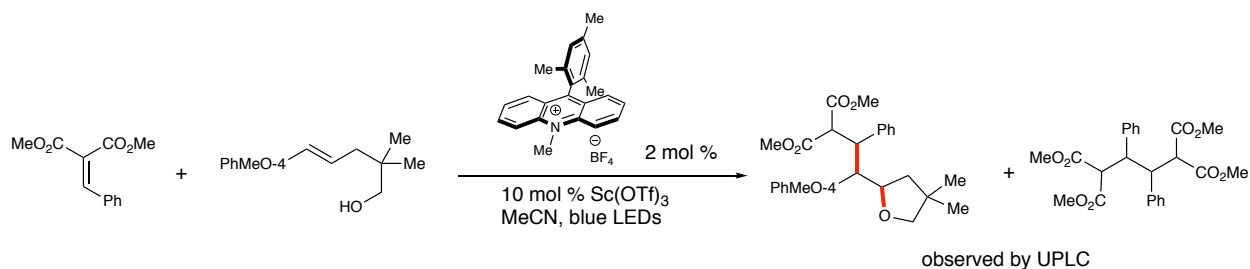


Figure 2-29. Initial Exploration of Merger with Mes-Acr Oxidative Pathway.

2.9 Summary

Significant progress has been made towards the access of *umpolung* operators through single electron chemistry. Approaches to both d^3 and d^1 operators were developed and each have

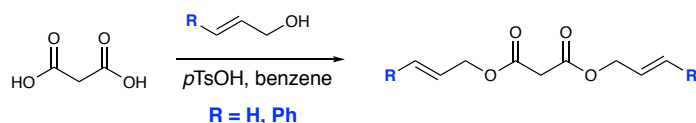
shown promising, new reactivity. The use of malonates as bidentate substrates for Lewis acid activation has resulted in a stabilized open-shell species capable of undergoing intermolecular cross-coupling reactions. The use of cooperative catalysis in the activation and reduction of arylidene malonates resulted in the discovery of divergent pathways, cross-coupling, dimerization, and transfer hydrogenation.

2.10 Experimental Section

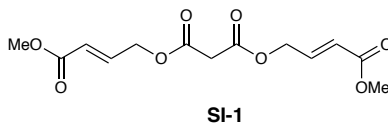
All reactions were carried out under an argon or nitrogen atmosphere in flame-dried glassware with magnetic stirring. Solvents used in reactions were purified by passage through a bed of activated alumina. Reagents were purified prior to use unless otherwise stated following the guidelines of Perrin and Armarego.¹²⁵ Purification of reaction products was carried out by flash chromatography on Biotage Isolera 4 systems with Ultra-grade silica cartridges. Analytical thin layer chromatography was performed on EM Reagent 0.25 mm silica gel 60-F plates. Visualization was accomplished with UV light. Infrared spectra were recorded on a Bruker Tensor 37 FT-IR spectrometer. ¹H NMR spectra were recorded on an AVANCE III 500 MHz with direct cryoprobe (500 MHz) spectrometer and Bruker Avance III 600 MHz (151 MHz) system. These are reported in ppm using solvent as an internal standard (CDCl₃ at 7.26 ppm). Data are reported as (s = singlet, d = doublet, t = triplet, q = quartet, quint = quintet, m = multiplet, br = broad; coupling constant(s) in Hz; integration.) Proton-decoupled ¹³C NMR spectra were recorded on an AVANCE III 500 MHz with direct cryoprobe (125 MHz) spectrometer and Bruker Avance III 600 MHz (151 MHz) system. These are reported in ppm using solvent as an internal standard (CDCl₃ at 77.16 ppm). Mass spectra were obtained on WATERS Acquity-H UPLC-MS with a single quad detector (ESI) Varian 1200 Quadrupole Mass Spectrometer. Gas chromatography experiments were run on Agilent 7890A/5975C GC/MS System. Enantioselectivity measurements were made on an Agilent 1290 Infinity SFC, using a Chiralpak ID-3 column. A Shimadzu UV-3600 spectrophotometer and a Horiba Fluoromax 4 (150 W Xe lamp) were used for quantum yield studies.

Iridium and Ruthenium photocatalysts were obtained from Strem Chemical and Sigma-Aldrich respectively and used as received. PYBOX and dimethyl-backbone BOX ligands were obtained from Sigma-Aldrich and used as received. The spirocyclic BOX ligands were prepared according to literature precedent.²⁶³ Ramipril derived N-oxide ligands were prepared according to Feng et al.²³⁸ Photocatalysts DPAIPN and CZIPN were synthesized according to Molander et al.²⁶⁴ The nitrile Hantzsch ester derivatives were prepared according to Cheng et al.²³⁴

2.10.1 Preparation of Substituted Malonates



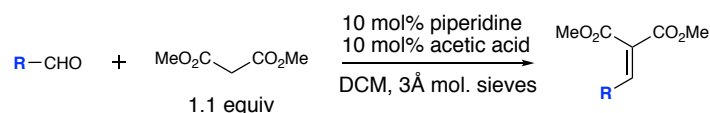
Condensation of allyl and cinnamyl alcohol was performed as reported by Kitamura et al.²⁶⁵ to yield known allyl²⁶⁶ and cinnamyl malonates.²⁶⁵



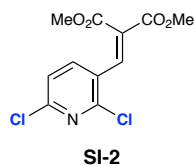
To a solution of malonic acid (728 mg, 1 equiv) in DCM (70 mL, 0.1 M) as added (E)-methyl 4-hydroxybut-2-enoate (1.8 g, 2.2 equiv) (prepared via borane•THF reduction of mono-methyl fumarate)²⁶⁷, HOBT (1.1 g, 1 equiv), DMAP (g, 43 mg, 0.05 equiv), and TEA (2.4 mL, 2.5 equiv). The solution was cooled to 0° C and stirred for 15 minutes before EDC•HCl (3.35 g, 2.5 equiv) was added in a single portion. The reaction was monitored via UPLC/MS for complete consumption of malonic acid. Upon complete consumption, the reaction was filtered, diluted with sat. NaHCO₃, and extracted with DCM three times. The organic layers were combined,

dried over sodium sulfate and concentrated. The resulting oil was purified via flash column chromatography (10-20% ethyl acetate/hexanes) to yield the malonate as a clear oil (840 mg, 40% yield). Analytical Data for **SI-1**: ^1H NMR (500 MHz, Chloroform-*d*) δ 6.93 (dt, $J = 15.8$, 4.7 Hz, 2H), 6.06 (dt, $J = 15.7$, 2.0 Hz, 2H), 4.83 (dd, $J = 4.7$, 2.0 Hz, 4H), 3.75 (s, 7H), 3.51 (s, 2H). ^{13}C NMR (126 MHz, CDCl_3) δ 166.1, 165.5, 140.4, 122.3, 63.6, 51.8, 41.0. LRMS (ESI): Mass calcd for $\text{C}_{13}\text{H}_{16}\text{O}_8$ $[\text{M}+\text{H}]^+$: 301.3; found 301.5

2.10.2 Preparation of Benzylidene Malonates and Ketoester Substrates

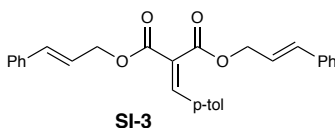


To a scintillation vial was added aldehyde (10 mmol). Dimethyl malonate or ketoester was added (11 mmol, 1.1 equiv) and 2 grams of activated 3Å molecular sieves (powder). A magnetic stirbar, 10 mL of DCM were added, followed by acetic acid (58 μL , 1 mmol, 0.1 equiv) and piperidine (99 μL , 1 mmol, 0.1 equiv). The mixture was stirred overnight. Silica was added and the reaction concentrated under reduced pressure. The resulting mixture was loaded onto a column of silica and purified via flash column chromatography (10-20% ethyl acetate/hexanes) to yield the desired product. Known compounds matched literature reported ^1H and ^{13}C spectra.

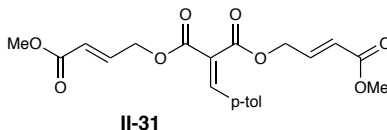


Prepared according to the general procedure. Obtained as a white solid (2.8 g, 80% yield). Analytical Data for **SI-2**: ^1H NMR (500 MHz, Chloroform-*d*) δ 7.87 (s, 1H), 7.71 (dd, $J = 8.2$,

0.7 Hz, 1H), 7.28 (dd, $J = 8.1, 0.6$ Hz, 1H), 3.88 (s, 3H), 3.77 (s, 3H). ^{13}C NMR (126 MHz, CDCl_3) δ 165.4, 163.4, 151.5, 150.2, 139.7, 136.8, 130.1, 127.3, 123.2, 53.1, 52.9. LRMS (ESI): Mass calcd for $\text{C}_{11}\text{H}_9\text{Cl}_2\text{NO}_4$ $[\text{M}+\text{H}]^+$: 290.0; found: 290.3. FTIR (ATR): 3095, 3052, 3016, 2961, 2854, 1730, 1710, 1637, 1574, 1544, 1454, 1440, 1426, 1368, 1347, 1274, 1228, 1195, 1140, 1077, 1069, 967, 939, 918, 873, 843, 831, 810, 768, 738, 701, 656, 621. LRMS (ESI): Mass calcd for $\text{C}_{21}\text{H}_{24}\text{O}_4$ $[\text{M}+\text{H}]^+$: 341.2; found 341.1

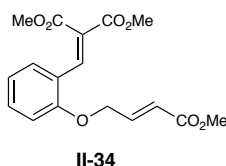


Prepared according to the general procedure (3.8 mmol scale). Obtained as a white solid (1.3 g, 76% yield). Analytical Data for **SI-3**: ^1H NMR (500 MHz, Chloroform-*d*) δ 7.78 (s, 1H), 7.41 – 7.26 (m, 10H), 7.10 (d, $J = 8.1$ Hz, 3H), 6.67 (dd, $J = 15.9, 11.6$ Hz, 3H), 6.29 (ddt, $J = 22.5, 15.9, 6.4$ Hz, 2H), 4.94 (dd, $J = 6.6, 1.3$ Hz, 2H), 4.91 (dd, $J = 6.3, 1.5$ Hz, 2H), 2.30 (s, 4H). LRMS (ESI): Mass calcd for $\text{C}_{29}\text{H}_{26}\text{O}_4$ $[\text{M}+\text{H}]^+$: 439.5; found 439.2.

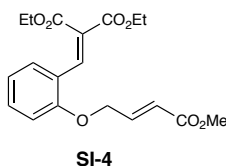


Prepared according to the general procedure (2.3 mmol). Obtained as a white solid (695 mg, 74% yield). Analytical Data for **II-31**: ^1H NMR (500 MHz, Chloroform-*d*) δ 7.81 (s, 1H), 7.32 (d, $J = 7.9$ Hz, 2H), 7.17 (d, $J = 7.9$ Hz, 2H), 6.94 (ddt, $J = 28.4, 15.8, 4.6$ Hz, 2H), 6.01 (ddt, $J = 29.0, 15.8, 2.0$ Hz, 2H), 4.91 (ddd, $J = 4.9, 3.4, 2.0$ Hz, 4H), 3.73 (s, 3H), 3.72 (s, 3H), 2.36 (s, 3H). ^{13}C NMR (126 MHz, CDCl_3) δ 166.1, 166.1, 165.9, 163.3, 144.5, 141.9, 140.7, 140.1, 129.8,

129.6, 123.4, 122.7, 122.2, 63.6, 63.5, 51.8, 51.7, 21.6. LRMS (ESI): Mass calcd for C₂₁H₂₂O₈ [M+H]⁺: 403.4; found 403.5.

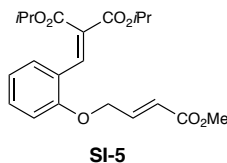


Prepared according to the general procedure. Obtained as a white solid (2.7 g, 81% yield). Analytical Data for **II-34**: ¹H NMR (500 MHz, Chloroform-*d*) δ 8.13 (s, 1H), 7.41 – 7.28 (m, 2H), 7.07 (dt, *J* = 15.8, 4.1 Hz, 1H), 6.94 (t, *J* = 7.6 Hz, 1H), 6.82 (d, *J* = 8.2 Hz, 1H), 6.14 (dt, *J* = 15.9, 2.1 Hz, 1H), 4.75 (dd, *J* = 4.2, 2.0 Hz, 2H), 3.84 (s, 3H), 3.76 (s, 3H), 3.74 (s, 3H). ¹³C NMR (126 MHz, CDCl₃) δ 167.1, 166.3, 164.6, 156.4, 141.9, 138.5, 132.1, 129.1, 125.9, 122.7, 122.0, 121.4, 112.1, 67.0, 52.6, 52.5, 51.8. Mass calcd for C₂₁H₂₆O₇ [M+H]⁺: 337.4; found 337.5

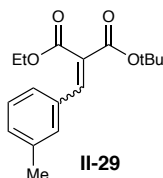


Prepared according to the general procedure (3.4 mmol scale). Obtained as a white solid (1.0 g, 83% yield). Analytical Data for **SI-1**: ¹H NMR (500 MHz, Chloroform-*d*) δ 8.13 (s, 1H), 7.42 (dd, *J* = 7.7, 1.6 Hz, 1H), 7.34 (ddd, *J* = 8.7, 7.6, 1.7 Hz, 1H), 7.09 (dt, *J* = 15.8, 4.0 Hz, 1H), 6.95 (t, *J* = 7.5 Hz, 1H), 6.84 (d, *J* = 8.3 Hz, 1H), 6.19 (dt, *J* = 15.8, 2.1 Hz, 1H), 4.77 (dd, *J* = 4.0, 2.1 Hz, 2H), 4.30 (dq, *J* = 19.3, 7.1 Hz, 5H), 3.76 (s, 3H), 1.35 (t, *J* = 7.1 Hz, 3H), 1.24 (t, *J* = 7.1 Hz, 3H). ¹³C NMR (126 MHz, CDCl₃) δ 166.6, 166.3, 164.2, 156.3, 142.0, 137.6, 131.9,

129.3, 126.7, 122.8, 121.9, 121.3, 112.0, 66.9, 61.6, 61.5, 51.7, 14.1, 13.9. Mass calcd for $C_{21}H_{26}O_7$ $[M+H]^+$: 363.1; found 363.2



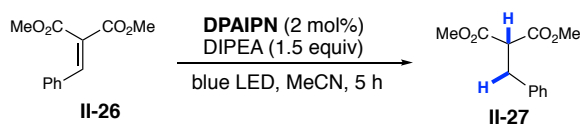
Prepared according to the general procedure (3.4 mmol scale). Obtained as a white solid (1.1 g, 84% yield). Analytical Data for **SI-5**: 1H NMR (500 MHz, Chloroform-*d*) δ 8.08 (s, 1H), 7.46 (dd, $J = 7.8, 1.7$ Hz, 1H), 7.33 (ddd, $J = 8.8, 7.5, 1.7$ Hz, 1H), 7.09 (dt, $J = 15.8, 4.0$ Hz, 1H), 6.97 – 6.90 (m, 1H), 6.86 – 6.80 (m, 1H), 6.20 (dt, $J = 15.8, 2.1$ Hz, 1H), 5.18 (dp, $J = 14.1, 6.3$ Hz, 2H), 4.76 (dt, $J = 5.0, 2.5$ Hz, 2H), 3.76 (s, 3H), 1.32 (d, $J = 6.3$ Hz, 6H), 1.26 – 1.22 (m, 6H). ^{13}C NMR (126 MHz, $CDCl_3$) δ 166.4, 166.2, 163.7, 156.3, 142.0, 136.6, 131.7, 129.2, 127.5, 122.8, 121.7, 121.2, 111.9, 69.1, 69.1, 66.8, 51.7, 21.8, 21.5. LRMS (ESI): Mass calcd for $C_{21}H_{26}O_7$ $[M+H]^+$: 391.2; found 391.3



Prepared according to the general procedure. Obtained as an off-white solid (2.0 g, 71% yield). Analytical Data for **II-29**: 1H NMR (500 MHz, Chloroform-*d*) δ 7.60 (d, $J = 3.8$ Hz, 1H), 7.37 – 7.24 (m, 2H), 7.19 (d, $J = 7.2$ Hz, 1H), 4.30 (dq, $J = 12.9, 7.2$ Hz, 2H), 2.34 (d, $J = 2.5$ Hz, 3H), 1.53 (d, $J = 6.4$ Hz, 8H), 1.32 (dt, $J = 16.1, 7.2$ Hz, 3H). ^{13}C NMR (126 MHz, $CDCl_3$) δ 167.0,

165.9, 164.5, 163.2, 141.1, 140.8, 138.3, 138.3, 133.1, 133.0, 131.2, 131.1, 130.1, 129.9, 128.6, 128.5, 127.8, 127.3, 126.9, 126.4, 82.5, 82.1, 61.4, 61.4, 28.0, 27.9, 27.9, 21.3, 14.1. Mass calcd for C₂₁H₂₆O₇ [M+H]⁺: 291.4; found 291.8

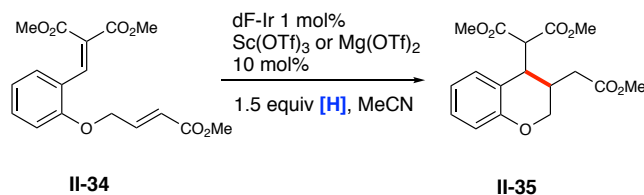
2.10.3 General Procedure for Transfer Hydrogenation



To a 2 dram vial was added phenyl arylidene malonate (77 mg, 0.35 mmol, 1 equiv). The reaction was equipped with magnetic stirbar, capped and taken in to a glovebox. DPAIPN (5.6 mg, 0.02 equiv) was added to the vial and the vial was removed from the glovebox and charged with 3.5 mL (0.1 M) of sparged acetonitrile (sparged for at least 20 minutes with argon) and stirred until homogenous. Sparged Hunig's base (92 uL, 1.5 equiv) was then added and the vial was then placed in between 3 Kessil blue LED lights and irradiated for 5 hours (with a small fan placed for cooling). Conversion of the malonate was monitored by UPLC/MS. Upon complete consumption of the benzylidene malonate, the reaction was concentrated under reduced pressure onto silica gel. This silica was loaded onto a column of silica gel and **II-27** isolated via flash column chromatography (2-20% ethyl acetate/hexanes) yield the product as a clear oil (58.6 mg, 75%).

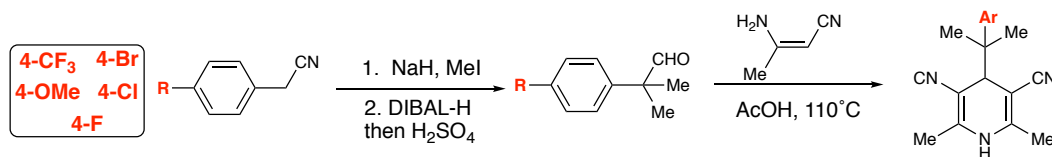
Collected ¹H and ¹³C NMR data matched literature reported data.²⁶⁸

2.10.4 General Procedure for Reductive Cyclization

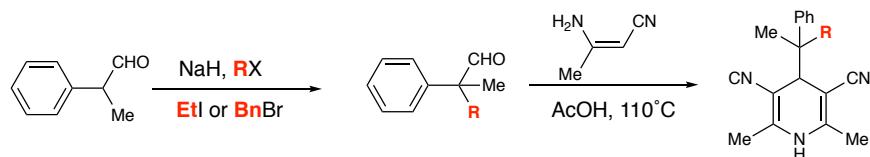


To a 2 dram vial was added arylidene malonate (67 mg, 0.2 mmol, 1 equiv). The reaction was equipped with magnetic stirbar, capped and taken in to a glovebox. dF-Ir (2.2 mg, 0.01 equiv) was added to the vial and the vial was removed from the glovebox. The vial was then charged with a solution of reductant (1.25 equiv) 2.0 mL (0.1 M) of sparged acetonitrile (sparged for at least 20 minutes with argon) and stirred until homogenous. The vial was then placed in between 3 Kessil blue LED lights and irradiated for 5 hours (with a small fan placed for cooling). Conversion of the malonate was monitored by UPLC/MS. Upon complete conversion, the reaction was concentrated under reduced pressure onto silica gel. This silica was loaded onto a column of silica gel and **II-35** isolated via flash column chromatography (2-20% ethyl acetate/hexanes) yield the product as a clear oil that slowly solidified (58.6 mg, 75%). Analytical Data for **II-35**: $^1\text{H NMR}$ (500 MHz, Chloroform-*d*) δ 7.13 (qd, $J = 8.1, 1.7$ Hz, 2H), 7.05 – 6.99 (m, 1H), 6.92 (dd, $J = 7.6, 1.6$ Hz, 1H), 6.84 – 6.75 (m, 3H), 4.24 (ddd, $J = 11.1, 3.6, 1.2$ Hz, 1H), 4.20 (d, $J = 2.0$ Hz, 1H), 4.11 (dd, $J = 11.1, 8.9$ Hz, 1H), 3.94 (dd, $J = 8.2, 4.1$ Hz, 1H), 3.79 (d, $J = 3.6$ Hz, 5H), 3.69 (d, $J = 5.3$ Hz, 5H), 3.58 (s, 2H), 3.47 (s, 3H), 2.71 (ddt, $J = 10.8, 5.4, 3.1$ Hz, 1H), 2.46 (dd, $J = 14.3, 6.6$ Hz, 1H), 2.22 (dd, $J = 16.4, 9.2$ Hz, 1H). Mass calcd for $\text{C}_{21}\text{H}_{26}\text{O}_7$ $[\text{M}+\text{H}]^+$: 337.3; found 337.1

2.10.5 Preparation of Nitrile Hantzsch Ester Derivatives

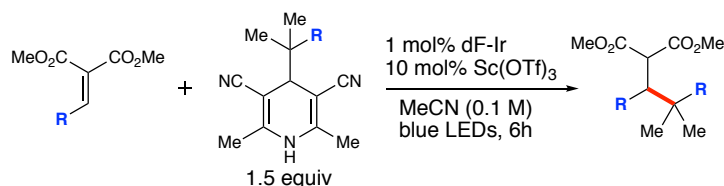


The dimethyl nitrile Hantzsch ester derivatives were prepared according to Cheng et al.²³⁴ The requisite aldehydes were prepared via dimethylation of the corresponding benzyl nitrile and reduced with DIBAL-H according to literature procedure.²⁶⁹ All of the aldehydes produced matched reported characterization data.

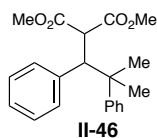


The ethyl methyl phenyl substituted and the benzyl methyl phenyl substituted aldehydes were prepared via alkylation of 2-phenylpropanal.²⁷⁰

2.10.6 General Procedure for Radical-Radical Coupling Reaction

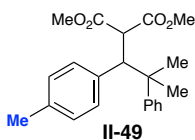


To a 2 dram vial was added desired benzylidene malonate (0.35 mmol, 1 equiv). The reaction was equipped with magnetic stirbar, capped and taken in to a glovebox. Scandium triflate (17 mg, 0.1 equiv), dF-Ir (4.4 mg, 0.01 equiv), and nitrile Hantzsch (1.5 equiv) were added to the vial. The vial was removed from the glovebox and charged with 3.5 mL (0.1 M) of sparged acetonitrile (sparged for at least 20 minutes with argon) and stirred until homogenous. The vial was then placed in between 3 Kessil blue LED lights and irradiated for 6 hours (with a small fan placed for cooling). Conversion of the malonate was determined by GC/MS or UPLC/MS. Upon complete consumption of the benzylidene malonate, the reaction was concentrated on silica gel under reduced pressure. If solids were present, DCM was added until these solids dissolved and the solution concentrated onto silica gel. This silica was loaded onto a column of silica gel and the desired product isolated via flash column chromatography (2-20% ethyl acetate/hexanes).

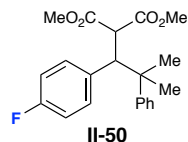


II-46: Prepared according to the general procedure using the corresponding benzylidene malonate (77.1 mg, 0.35 mmol). Isolated as a thick, clear oil that slowly became a solid (73.7 mg, 62%). Analytical Data for **II-46**: $^1\text{H NMR}$ (500 MHz, Chloroform-d) δ 7.37 - 7.33 (m,

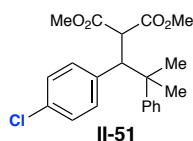
2H), 7.31 - 7.27 (m, 2H), 7.23 - 7.14 (m, 4H), 7.06 (dd, $J = 7.7, 1.8$ Hz, 2H), 4.05 (d, $J = 11.3$ Hz, 1H), 3.94 (d, $J = 11.3$ Hz, 1H), 3.29 (d, $J = 0.9$ Hz, 3H), 3.24 (s, 3H), 1.42 (s, 3H), 1.11 (s, 3H). ^{13}C NMR (126 MHz, CDCl_3) δ 168.6, 168.4, 146.9, 139.2, 129.8, 127.7, 127.4, 127.2, 126.7, 126.1, 55.4, 54.9, 52.4, 52.2, 41.0, 29.8, 23.5. FTIR (ATR): 3059, 3029, 2951, 2358, 1733, 1601, 1433, 1368, 1260, 1155, 1030, 776, 701, 582. LRMS (ESI): Mass calcd for $\text{C}_{21}\text{H}_{24}\text{O}_4$ $[\text{M}+\text{H}]^+$: 341.2; found 341.1



II-49: Prepared according to the general procedure using the corresponding benzylidene malonate (82 mg, 0.35 mmol). Isolated as a thick, clear oil that slowly became a crystalline solid (78.3 mg, 63%). Analytical Data for **II-49**: ^1H NMR (500 MHz, Chloroform- d) δ 7.38 - 7.34 (m, 2H), 7.28 (dd, $J = 7.1, 1.7$ Hz, 2H), 7.21 - 7.15 (m, 1H), 7.01 (d, $J = 7.9$ Hz, 2H), 6.95 (d, $J = 7.8$ Hz, 2H), 4.02 (d, $J = 11.3$ Hz, 1H), 3.91 (d, $J = 11.3$ Hz, 1H), 3.26 (d, $J = 1.5$ Hz, 6H), 2.28 (s, 3H), 1.41 (s, 3H), 1.09 (s, 3H). ^{13}C NMR (126 MHz, CDCl_3) δ 168.6, 168.5, 147.0, 136.2, 136.1, 129.7, 128.2, 127.7, 127.3, 126.1, 55.0, 55.0, 52.3, 52.2, 41.0, 30.1, 23.3, 21.0. FTIR (ATR): 3062, 3022, 2965, 1731, 1612, 1434, 1352, 1277, 1222, 1155, 1022, 997, 894, 805, 762, 701, 600. LRMS (ESI): Mass calcd for $\text{C}_{22}\text{H}_{26}\text{O}_4$ $[\text{M}+\text{H}]^+$: 355.18; found 355.28



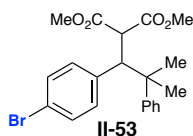
II-50: Prepared according to the general procedure using the corresponding benzylidene malonate (83.4 mg, 0.35 mmol). Isolated as a thick, clear oil that slowly crystallized into a solid (75.3 mg, 60%). Analytical Data for **II-50**: ^1H NMR (500 MHz, Chloroform- d) δ 7.35 - 7.27 (m, 4H), 7.24 - 7.13 (m, 1H), 6.98 (dd, J = 8.4, 5.1 Hz, 2H), 6.88 (td, J = 8.8, 1.3 Hz, 2H), 4.00 (dd, J = 11.2, 1.2 Hz, 1H), 3.93 (d, J = 11.2 Hz, 1H), 3.35 (d, J = 1.2 Hz, 3H), 3.27 (d, J = 1.2 Hz, 3H), 1.39 (s, 3H), 1.13 (s, 3H). ^{13}C NMR (126 MHz, CDCl_3) δ 168.5, 168.3, 161.6 (d, J = 245.5 Hz), 146.5, 135.0 (d, J = 3.5 Hz). 131.3, 127.8, 127.2, 126.3, 114.3, 114.2, 54.9, 54.7, 52.5, 52.3, 41.1, 29.0, 24.0. FTIR (ATR): 3061, 2958, 2851, 2361, 2262, 1761, 1498, 1433, 1255, 1196, 1156, 1133, 1110, 1018, 909, 842, 805, 771, 699, 595. LRMS (ESI): Mass calcd for $\text{C}_{21}\text{H}_{23}\text{FO}_4$ $[\text{M}+\text{H}]^+$: 359.16; found 359.27.



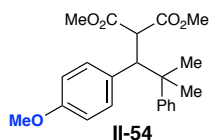
II-51: Prepared according to the general procedure using the corresponding benzylidene malonate (89.1 mg, 0.35 mmol). Isolated as a thick, clear oil that slowly crystallized into a solid (88.5 mg, 60%). Analytical Data for **II-51**: ^1H NMR (500 MHz, Chloroform- d) δ 7.31 - 7.25 (m, 4H), 7.19 - 7.11 (m, 3H), 6.92 (dd, J = 8.7, 2.2 Hz, 2H), 3.98 (d, J = 11.1 Hz, 1H), 3.90 (d, J = 11.2 Hz, 1H), 3.33 (s, 2H), 3.26 (s, 2H), 1.37 (s, 2H), 1.11 (s, 3H). ^{13}C NMR (126 MHz,

CDCl₃) δ 168.4, 168.2, 146.4, 137.8, 132.6, 131.1, 127.8, 127.6, 127.1, 126.3, 54.8, 54.7, 52.5, 52.3, 41.0, 29.1, 24.0.

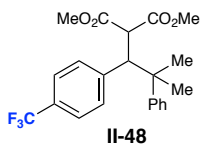
FTIR (ATR): 3029, 2951, 2841, 2360, 2256, 1761, 1732, 1492, 1433, 1255, 1196, 1156, 1133, 1091, 1014, 909, 839, 805, 751, 699, 594. LRMS (ESI): Mass calcd for C₂₁H₂₃ClO₄ [M+H]⁺: 375.1; found 375.2



II-53: Prepared according to the general procedure using the corresponding benzylidene malonate (104.9 mg, 0.35 mmol). Isolated as a thick, clear oil that slowly crystallized into a solid (88.1 mg, 60%). Analytical Data for **II-53**: ¹H NMR (500 MHz, Chloroform-d) δ 7.32 – 7.25 (m, 6H), 7.20 – 7.14 (m, 1H), 6.90 – 6.83 (m, 2H), 3.98 (d, J = 11.2 Hz, 1H), 3.89 (d, J = 11.1 Hz, 1H), 3.33 (d, J = 1.2 Hz, 3H), 3.27 (d, J = 1.2 Hz, 3H), 1.36 (s, 3H), 1.11 (s, 3H). ¹³C NMR (126 MHz, CDCl₃) δ 168.3, 168.2, 146.3, 138.3, 131.4, 130.5, 127.8, 127.1, 126.3, 120.7, 54.8, 54.6, 52.5, 52.3, 40.9, 29.1, 23.9. FTIR (ATR): 3057, 2970, 2951, 2883, 2841, 2359, 2255, 1761, 1732, 1600, 1488, 1432, 1255, 1195, 1074, 1029, 1009, 909, 837, 804, 767, 729, 699, 648, 591. LRMS (ESI): Mass calcd for C₂₁H₂₃BrO₄ [M+H]⁺: 419.1; found 419.2

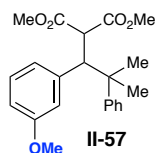


II-54: Prepared according to the general procedure using the corresponding benzylidene malonate (87.6 mg, 0.35 mmol). Isolated as a thick, clear oil that slowly crystallized into a white solid (66.2 mg, 51%). Analytical Data for **II-54**: ^1H NMR (500 MHz, Chloroform-*d*) δ 7.34 (dt, $J = 8.5, 1.9$ Hz, 2H), 7.28 (d, $J = 7.4$ Hz, 2H), 7.21 - 7.15 (m, 1H), 6.99 - 6.93 (m, 2H), 6.77 - 6.70 (m, 2H), 4.00 (d, $J = 11.3$ Hz, 1H), 3.89 (d, $J = 11.2$ Hz, 1H), 3.77 (s, 3H), 3.70 (s, 1H), 3.29 (s, 3H), 3.27 (s, 3H), 1.40 (s, 3H), 1.11 (s, 3H). ^{13}C NMR (126 MHz, CDCl_3) δ 168.7, 168.5, 158.2, 146.9, 131.2, 130.9, 127.7, 127.3, 126.1, 112.8, 55.1, 55.0, 54.7, 52.4, 52.2, 41.2, 29.7, 23.6. FTIR (ATR): 2952, 2837, 1732, 1610, 1582, 1512, 1433, 1231, 1179, 1155, 1031, 839, 701. LRMS (ESI): Mass calcd for $\text{C}_{22}\text{H}_{26}\text{O}_5$ $[\text{M}+\text{H}]^+$: 371.2; found 371.3

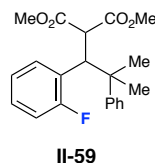


II-48: Prepared according to the general procedure using the corresponding benzylidene malonate (101 mg, 0.35 mmol). Isolated as a thick, clear oil that quickly solidified (94.9 mg, 66%). Analytical Data for **II-48**: ^1H NMR (500 MHz, Chloroform-*d*) δ 7.45 (d, $J = 8.1$ Hz, 2H), 7.34 - 7.27 (m, 4H), 7.23 - 7.17 (m, 1H), 7.14 (d, $J = 8.0$ Hz, 2H), 4.06 (d, $J = 11.1$ Hz, 1H), 4.01 (d, $J = 11.2$ Hz, 1H), 3.36 (s, 3H), 3.26 (s, 2H), 1.41 (s, 3H), 1.14 (s, 3H). ^{13}C NMR (126 MHz, CDCl_3) δ 168.3, 168.2, 146.2, 143.6, 130.1, 129.01 (q, $J = 32.4$ Hz), 127.9,

127.1, 126.4, 124.33 (q, $J = 3.9$ Hz), 124.1 (q, $J = 272$ Hz) 55.2, 54.6, 52.6, 52.3, 41.1, 29.1, 24.0. FTIR (ATR): 2974, 2954, 1757, 1726, 1619, 1436, 1327, 1230, 1155, 1121, 1067, 1015992, 850, 811, 765, 701, 661, 609. LRMS (ESI): Mass calcd for $C_{22}H_{23}F_3O_4$ $[M+H]^+$: 409.2; found 409.3

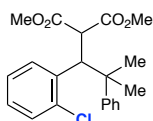


II-57: Prepared according to the general procedure using the corresponding benzylidene malonate (88 mg, 0.35 mmol). Isolated as a thick, clear oil (69.4 mg, 55%). Analytical Data for **II-57:** 1H NMR (500 MHz, Chloroform- d) δ 7.35 - 7.30 (m, 2H), 7.26 (dd, $J = 7.2, 1.8$ Hz, 2H), 7.21 - 7.13 (m, 1H), 7.09 (t, $J = 7.9$ Hz, 1H), 6.70 (ddd, $J = 8.2, 2.6, 0.9$ Hz, 1H), 6.65 (d, $J = 7.7$ Hz, 1H), 6.51 (t, $J = 2.1$ Hz, 1H), 4.02 (d, $J = 11.3$ Hz, 1H), 3.89 (d, $J = 11.2$ Hz, 1H), 3.68 (s, 3H), 3.29 (s, 3H), 3.26 (s, 3H), 1.40 (s, 3H), 1.11 (s, 3H). ^{13}C NMR (126 MHz, $CDCl_3$) δ 168.6, 168.4, 158.6, 146.9, 140.8, 128.3, 127.7, 127.3, 126.1, 112.4, 55.4, 55.1, 54.9, 52.4, 52.2, 41.1, 29.6, 23.8. FTIR (ATR): 2952, 2837, 1733, 1599, 1583, 1489, 1433, 1261, 1194, 1153, 1041, 1031, 781, 701. LRMS (ESI): Mass calcd for $C_{22}H_{26}O_5$ $[M+H]^+$: 371.2; found 371.3



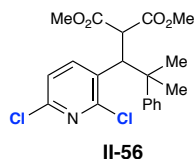
II-59: Prepared according to the general procedure using the corresponding benzylidene malonate (83.5 mg, 0.35 mmol). Isolated as a thick, clear oil that slowly crystallized into a colorless solid. Analytical Data for **II-59:** 1H NMR (500 MHz, Chloroform- d) δ 7.42 (d, $J =$

7.8 Hz, 2H), 7.30 (t, $J = 7.7$ Hz, 2H), 7.24 - 7.15 (m, 3H), 7.10 - 6.93 (m, 4H), 4.53 (s, 1H), 4.11 - 3.94 (m, 1H), 3.30 (s, 3H), 3.18 (s, 3H), 1.44 (s, 3H), 1.11 (s, 3H). ^{13}C NMR (126 MHz, CDCl_3) δ 168.3, 168.0, 161.37 (d, $J = 245.7$ Hz), 146.8, 128.40 (d, $J = 9.0$ Hz), 127.8, 127.3, 126.3, 123.26 (d, $J = 3.6$ Hz), 115.21 (d, $J = 24.5$ Hz), 54.7, 52.3, 52.3, 45.1, 41.2, 29.9, 22.3. FTIR (ATR): 3033, 2983, 2950, 2886, 1735, 1613, 1490, 1451, 1436, 1367, 1298, 1250, 1222, 1191, 1160, 1152, 1142, 1102, 1022, 981, 927, 851, 802, 778, 7601, 704673, 613, 587. LRMS (ESI): Mass calcd for $\text{C}_{21}\text{H}_{23}\text{FO}_4$ $[\text{M}+\text{H}]^+$: 359.2; found 359.2

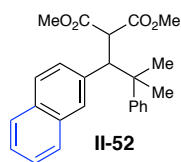


II-55

II-55: Prepared according to the general procedure using the corresponding benzylidene malonate (89.2 mg, 0.35 mmol). Isolated as a thick, clear oil (70.1 mg, 53%). Analytical Data for **II-55**: ^1H NMR (500 MHz, Chloroform-*d*) δ 7.52 - 7.47 (m, 2H), 7.46 - 7.40 (m, 1H), 7.32 (t, $J = 7.7$ Hz, 2H), 7.23 - 7.17 (m, 1H), 7.18 - 7.14 (m, 2H), 7.08 - 7.01 (m, 1H), 4.80 (d, $J = 11.6$ Hz, 1H), 4.02 (d, $J = 11.6$ Hz, 1H), 3.29 (s, 3H), 3.11 (s, 3H), 1.49 (s, 3H), 1.07 (s, 3H). ^{13}C NMR (151 MHz, CDCl_3) δ 168.2, 167.8, 147.2, 137.9, 136.6, 129.8, 128.5, 127.9, 127.8, 127.4, 126.3, 126.1, 55.5, 52.3, 49.0, 41.7, 30.3, 21.9. FTIR (ATR): 3088, 3060, 3023, 2952, 2886, 2848, 1764, 1736, 1496, 1474, 1434, 1389, 1369, 1280, 1255, 1202, 1159 1143, 1083, 1032, 772, 755, 701. LRMS (ESI): Mass calcd for $\text{C}_{21}\text{H}_{23}\text{ClO}_4$ $[\text{M}+\text{H}]^+$: 375.1; found 375.3

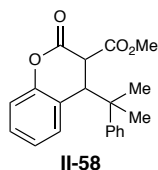


II-56: Prepared according to the general procedure using the corresponding benzylidene malonate (101.4 mg, 0.35 mmol). Isolated as a white powder (58.2 mg, 41%). Analytical Data for **17**: ^1H NMR (500 MHz, Chloroform- d) δ 7.42 - 7.36 (m, 2H), 7.33 (dd, J = 8.5, 7.0 Hz, 2H), 7.25 - 7.22 (m, 1H), 7.13 (d, J = 1.1 Hz, 2H), 4.67 (d, J = 11.4 Hz, 1H), 3.92 (d, J = 11.3 Hz, 1H), 3.36 (s, 3H), 3.28 (s, 3H), 1.43 (s, 3H), 1.17 (s, 3H). ^{13}C NMR (126 MHz, CDCl_3) δ 167.7, 167.4, 152.5, 148.3, 145.4, 139.3, 133.4, 128.1, 127.3, 126.8, 122.0, 55.0, 52.6, 49.0, 42.0, 29.5, 23.1. FTIR (ATR): 2953, 1731, 1573, 1548, 1497, 1423, 1370, 1344, 1277, 1135, 1052, 1031, 911, 841, 822, 784, 762, 731, 701, 661 LRMS (ESI): Mass calcd for $\text{C}_{20}\text{H}_{21}\text{Cl}_2\text{O}_4$ $[\text{M}+\text{H}]^+$: 410.1; found 410.3

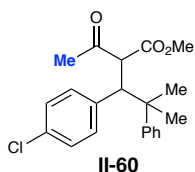


II-52: Prepared according to the general procedure using the corresponding benzylidene malonate (94.6 mg, 0.35 mmol). Isolated as a thick, clear oil that quickly crystallized into a solid (76.2 mg, 56%). Analytical Data for **II-52**: ^1H NMR (500 MHz, Chloroform- d) δ 7.79 - 7.76 (m, 1H), 7.75 - 7.71 (m, 1H), 7.67 (d, J = 8.5 Hz, 1H), 7.48 (s, 1H), 7.46 - 7.42 (m, 2H), 7.39 - 7.34 (m, 2H), 7.29 (dd, J = 8.5, 7.0 Hz, 2H), 7.23 - 7.18 (m, 2H), 4.18 (d, J = 11.2 Hz, 1H), 4.12 (d, J = 11.2 Hz, 1H), 3.32 (s, 3H), 3.16 (s, 3H), 1.47 (s, 3H), 1.15 (s, 3H). ^{13}C NMR (126 MHz,

CDCl₃) δ 168.6, 168.4, 146.8, 132.7, 132.3, 127.9, 127.8, 127.4, 127.3, 126.8, 126.2, 125.8, 125.7, 55.4, 55.1, 52.5, 52.2, 41.4, 29.8, 23.7. FTIR (ATR): 3055, 3022, 2951, 2841, 1761, 1735, 1600, 1497, 1432, 1263, 1226, 1194, 1154, 1133, 1030, 909, 861, 732, 700, 673, 647. LRMS (ESI): Mass calcd for C₂₂H₂₆O₅ [M+H]⁺: 391.2; found 391.3

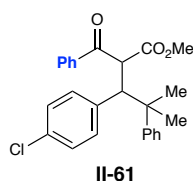


II-58: Prepared according to the general procedure using the corresponding benzylidene malonate (71.5 mg, 0.35 mmol). Isolated as a thick, clear oil that slowly crystallized into a white powder (58.2 mg, 51%). Analytical Data for **II-58**: ¹H NMR (500 MHz, Chloroform-*d*) δ 7.35 (d, *J* = 5.8 Hz, 4H), 7.34 – 7.26 (m, 2H), 7.07 (dt, *J* = 6.9, 3.0 Hz, 2H), 7.02 (dd, *J* = 7.9, 1.7 Hz, 1H), 3.69 (s, 1H), 3.60 (s, 1H), 3.54 (s, 3H), 1.36 (s, 3H), 1.28 (s, 3H). ¹³C NMR (126 MHz, CDCl₃) δ 168.0, 165.0, 151.7, 145.6, 131.2, 129.2, 128.7, 126.9, 126.2, 124.1, 120.5, 117.0, 53.2, 50.5, 48.5, 41.8, 28.1, 22.9. FTIR (ATR): 3087, 2969, 2883, 2359, 2161, 1753, 1734, 1612, 1587, 1489, 1457, 1435, 1388, 1352, 1300, 1276, 1221, 1171, 1116, 1031, 996, 944, 893, 848, 762, 700, 591, 571. LRMS (ESI): Mass calcd for C₂₀H₂₀O₄ [M+H]⁺: 325.1; found 325.2

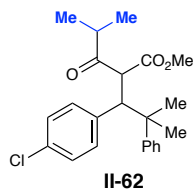


II-60: Prepared according to the general procedure using the corresponding benzylidene keto-malonate (83.4 mg, 0.35 mmol). Isolated as a thick, clear oil that slowly crystallized into a white

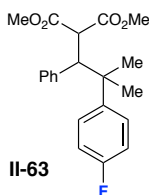
powder (74.7 mg, 60%, 11:1 dr). Analytical Data for **II-60**: ^1H NMR (500 MHz, Chloroform-*d*) δ 7.31 - 7.28 (m, 3H), 7.28 (s, 1H), 7.23 - 7.13 (m, 3H), 6.88 (d, $J = 8.0$ Hz, 2H), 4.11 (d, $J = 11.5$ Hz, 1H), 3.92 (d, $J = 11.5$ Hz, 1H), 3.35 (s, 3H), 1.78 (s, 3H), 1.37 (s, 3H), 1.14 (s, 3H). ^{13}C NMR (126 MHz, CDCl_3) δ 202.2, 169.0, 146.3, 137.4, 132.9, 127.9, 127.8, 127.2, 126.4, 63.6, 54.7, 52.5, 41.3, 28.6, 28.1, 24.1. FTIR (ATR): 3088, 3025, 2970, 2883, 2360, 2341, 1732, 1714, 1596, 1492, 1433, 1355, 1252, 1157, 1090, 1031, 1013, 911, 841, 806, 766, 731, 700, 600. LRMS (ESI): Mass calcd for $\text{C}_{21}\text{H}_{23}\text{ClO}_3$ $[\text{M}+\text{H}]^+$: 359.1; found 359.2.



II-61: Prepared according to the general procedure using the corresponding benzylidene malonate (105.2 mg, 0.35 mmol). Isolated as a thick, clear oil that slowly crystallized into a white powder (78.2 mg, 53%). Analytical Data for **II-61**: ^1H NMR (500 MHz, Chloroform-*d*) δ 7.82 - 7.76 (m, 2H), 7.53 - 7.47 (m, 1H), 7.43 - 7.34 (m, 4H), 7.31 (t, $J = 7.7$ Hz, 2H), 7.23 - 7.17 (m, 1H), 7.01 (d, $J = 8.1$ Hz, 2H), 6.90 - 6.81 (m, 2H), 5.16 (d, $J = 11.3$ Hz, 1H), 4.21 (d, $J = 11.3$ Hz, 1H), 3.22 (s, 3H), 1.49 (s, 3H), 1.14 (s, 3H). ^{13}C NMR (126 MHz, CDCl_3) δ 193.5, 168.6, 146.8, 138.5, 136.9, 133.4, 132.2, 128.6, 128.4, 127.8, 127.6, 127.3, 126.3, 56.4, 54.8, 52.5, 41.2, 29.9, 23.8. FTIR (ATR): 3088, 3058, 3029, 2971, 2883, 2841, 2582, 2257, 1743, 1688, 1596, 1580, 1492, 1447, 1434, 1410, 1389, 1369, 1277, 1253, 1210, 1184, 1149, 1111, 1091, 1014, 1001, 973, 909, 838, 809, 790, 765, 730, 700, 688, 660, 648, 625. LRMS (ESI): Mass calcd for $\text{C}_{26}\text{H}_{25}\text{ClO}_3$ $[\text{M}+\text{H}]^+$: 421.1; found 421.0

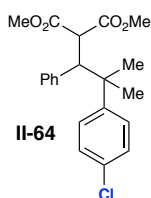


II-62: Prepared according to the general procedure using the corresponding benzylidene keto-malonate (93.4 mg, 0.35 mmol). Isolated as a thick, clear oil that slowly crystallized into a white powder (40.6 mg, 30%). Analytical Data for **II-62**: ^1H NMR (500 MHz, Chloroform- d) δ 7.36 – 7.30 (m, 2H), 7.30 – 7.27 (m, 1H), 7.21 – 7.12 (m, 3H), 6.92 (d, $J = 7.9$ Hz, 2H), 4.25 (d, $J = 11.4$ Hz, 1H), 3.98 (d, $J = 11.4$ Hz, 1H), 3.27 (s, 3H), 2.50 (hept, $J = 6.8$ Hz, 1H), 1.40 (s, 3H), 1.10 (s, 3H), 0.69 (d, $J = 6.8$ Hz, 3H), 0.57 (d, $J = 6.8$ Hz, 3H). ^{13}C NMR (126 MHz, CDCl_3) δ 207.8, 168.9, 146.7, 138.1, 132.6, 127.8, 127.7, 127.2, 126.2, 61.4, 54.5, 52.3, 41.1, 40.6, 29.4, 23.9, 19.1, 17.9. FTIR (ATR): 3058, 3029, 2971, 2874, 1742, 1710, 1600, 1492, 1467, 1434, 1411, 1383, 1368, 1348, 1264, 1193, 1157, 1091, 1014, 923. LRMS (ESI): Mass calcd for $\text{C}_{23}\text{H}_{27}\text{ClO}_3$ $[\text{M}+\text{H}]^+$: 387.2; found 387.4.

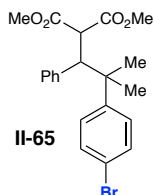


II-63: Prepared according to the general procedure using phenyl arylidene (77 mg, 0.35 mmol) and the corresponding 4-F HE derivative (155 mg, 0.525 mmol, 1.5 equivalents). Isolated as a thick, clear oil that slowly crystallized into a solid (78.1 mg, 62%). Analytical Data for **II-63**: ^1H NMR (500 MHz, Chloroform- d) δ 7.33 – 7.27 (m, 2H), 7.23 – 7.13 (m, 3H), 7.07 – 6.99 (m, 2H), 6.98 – 6.92 (m, 2H), 4.02 (d, $J = 11.3$ Hz, 1H), 3.89 (d, $J = 11.3$ Hz, 1H), 3.37 (d, $J = 1.6$

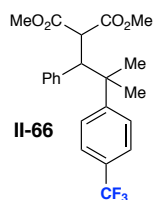
Hz, 3H), 3.24 (d, $J = 1.6$ Hz, 3H), 1.40 (s, 3H), 1.11 (s, 3H). ^{13}C NMR (126 MHz, CDCl_3) δ 168.6, 168.3, 161.2 (d, $J = 245.1$ Hz), 142.6 (d, $J = 3.2$ Hz), 139.0, 129.8, 128.8 (d, $J = 7.7$ Hz), 127.5, 126.8, 114.4, 114.3, 55.5, 54.8, 52.5, 52.2, 40.7, 29.5, 23.9. FTIR (ATR): 3054, 2982, 2956, 2884, 2845, 1759, 1728, 1599, 1509, 1479, 1434, 1388, 1369, 1354, 1306, 1281, 1263, 1221, 1205, 1178, 1167, 1136, 1108, 1033, 1015, 984, 972, 951, 939, 923, 910, 848, 821, 814, 794, 766, 759, 729, 699, 666, 645, 632. LRMS (ESI): Mass calcd for $\text{C}_{21}\text{H}_{23}\text{FO}_4$ $[\text{M}+\text{H}]^+$: 359.2; found 359.2



II-64: Prepared according to the general procedure using phenyl arylidene malonate (77 mg, 0.35 mmol) and the corresponding 4-Cl HE derivative (164 mg, 0.525 mmol, 1.5 equivalents). Isolated as a thick, clear oil that slowly crystallized into a white powder (69.9 mg, 54%). Analytical Data for **II-64**: ^1H NMR (500 MHz, Chloroform-*d*) δ 7.29 – 7.26 (m, 2H), 7.24 (d, $J = 8.8$ Hz, 2H), 7.20 (d, $J = 7.0$ Hz, 3H), 7.07 – 7.00 (m, 2H), 4.02 (d, $J = 11.2$ Hz, 1H), 3.89 (d, $J = 11.2$ Hz, 1H), 3.36 (s, 3H), 3.24 (s, 3H), 1.39 (s, 3H), 1.11 (s, 3H). ^{13}C NMR (126 MHz, CDCl_3) δ 168.6, 168.2, 145.4, 138.9, 132.0, 128.7, 127.7, 127.5, 126.9, 55.3, 54.8, 52.5, 52.2, 40.9, 29.4, 23.7. FTIR (ATR): 3061, 3030, 2952, 2362, 2336, 2336, 1763, 1734, 1493, 1453, 1433, 1400, 1368, 1302, 1261, 1206, 1157, 1133, 1102, 1026, 1012, 983, 913, 830, 777, 741, 706, 648. LRMS (ESI): $\text{C}_{21}\text{H}_{23}\text{ClO}_4$ $[\text{M}+\text{H}]^+$: 375.1; found 375.2

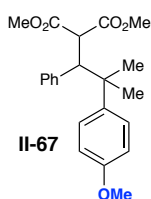


II-65: Prepared according to the general procedure using phenyl arylidene malonate (77 mg, 0.35 mmol) and the corresponding 4-Br HE derivative (187 mg, 0.525 mmol, 1.5 equivalents). Isolated as a thick, clear oil that slowly crystallized into a white powder (72.8 mg, 50%). Analytical Data for **II-65**: ^1H NMR (500 MHz, Chloroform-d) δ 7.42 - 7.34 (m, 2H), 7.20 (ddd, $J = 8.1, 4.5, 2.0$ Hz, 5H), 7.07 - 6.96 (m, 2H), 4.01 (d, $J = 11.3$ Hz, 1H), 3.89 (d, $J = 11.2$ Hz, 1H), 3.35 (s, 3H), 3.24 (s, 3H), 1.38 (s, 3H), 1.10 (s, 3H). ^{13}C NMR (126 MHz, CDCl_3) δ 168.6, 168.2, 146.0, 138.9, 130.7, 129.2, 127.5, 126.9, 120.2, 55.3, 54.9, 52.5, 52.2, 41.0, 29.4, 23.6. FTIR (ATR): 3041, 2965, 2359, 2255, 1758, 1725, 1599, 1486, 1430, 1260, 1199, 1078, 1029, 1010, 911, 831, 801, 771, 729, 700, 647, 592. LRMS (ESI): Mass calcd for $\text{C}_{21}\text{H}_{23}\text{BrO}_4$ $[\text{M}+\text{H}]^+$: 419.1; found 419.2

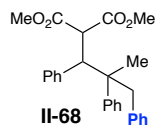


II-66: Prepared according to the general procedure using phenyl arylidene malonate (77 mg, 0.35 mmol) and the corresponding 4- CF_3 HE derivative (181 mg, 0.525 mmol, 1.5 equivalents). Isolated as a thick, clear oil that slowly crystallized into a solid (69.4 mg, 49%). Analytical Data for **II-66**: ^1H NMR (500 MHz, Chloroform-d) δ 7.53 (d, $J = 8.3$ Hz, 2H), 7.47 (d, $J = 8.2$ Hz, 2H), 7.24 - 7.17 (m, 3H), 7.08 - 7.02 (m, 2H), 4.03 (d, $J = 11.3$ Hz, 1H), 3.94 (d, $J = 11.3$ Hz,

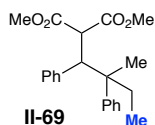
¹H), 3.27 (s, 3H), 3.25 (s, 3H), 1.44 (s, 3H), 1.13 (s, 3H). ¹³C NMR (126 MHz, CDCl₃) δ 168.5, 168.1, 151.2, 138.7, 127.7, 127.6, 127.0, 124.6 (q, J = 3.8 Hz), 124.6, 124.6, 124.5, 55.1, 54.8, 52.4, 52.3, 41.3, 29.5, 23.4. FTIR (ATR): 2976, 2952, 1754, 1722, 1620, 1435, 1324, 1230, 1155, 1124, 1069, 1011, 848, 810, 762, 700, 658, 609. Mass calcd for C₂₂H₂₃F₃O₄ [M+H]⁺: 409.2; found 409.2



II-67: Prepared according to the general procedure using phenyl arylidene malonate (77 mg, 0.35 mmol) and the 4-OMe HE derivative (161 mg, 0.525 mmol, 1.5 equivalents). Isolated as a thick, clear oil that slowly crystallized into a white powder (63.5 mg, 49%). Analytical Data for **II-67**: ¹H NMR (500 MHz, Chloroform-*d*) δ 7.31 – 7.27 (m, 3H), 7.25 – 7.17 (m, 3H), 7.08 – 7.01 (m, 2H), 4.03 (d, *J* = 11.3 Hz, 1H), 3.91 (d, *J* = 11.2 Hz, 1H), 3.37 (s, 3H), 3.26 (s, 3H), 1.41 (s, 3H), 1.12 (s, 3H). ¹³C NMR (126 MHz, CDCl₃) δ 168.7, 168.5, 157.8, 139.3, 138.8, 129.9, 128.4, 127.4, 126.7, 113.0, 55.7, 55.2, 55.0, 52.5, 52.2, 40.5, 29.8, 23.9. FTIR (ATR): 3061, 3030, 2951, 2837, 2361, 2339, 1762, 1734, 1700, 1696, 1685, 1653, 1646, 1636, 1610, 1576, 1559, 1540, 1513, 1456, 1432, 1388, 1367, 1296, 1250, 1223, 1187, 1156, 1132, 1032, 983, 914, 831, 801, 764, 733, 705, 668, 645. LRMS (ESI): Mass calcd for C₂₂H₂₆O₅ [M+H]⁺: 371.2; found 371.2

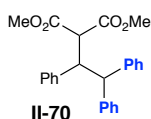


II-68: Prepared according to the general procedure using phenyl arylidene malonate (77 mg, 0.35 mmol) and the corresponding HE derivative (185 mg, 0.525 mmol, 1.5 equivalents). Isolated a 1:1 mixture of diastereomers, as a thick, clear oil that slowly crystallized into a white solid (72.5 mg, 50%). Analytical Data for **II-68**: ^1H NMR (500 MHz, Chloroform-*d*) δ 7.43 – 7.35 (m, 3H), 7.33 (t, $J = 7.1$ Hz, 2H), 7.28 (t, $J = 6.4$ Hz, 2H), 7.22 – 7.10 (m, 8H), 7.08 – 6.93 (m, 10H), 6.92 – 6.85 (m, 2H), 6.82 – 6.77 (m, 3H), 6.72 – 6.64 (m, 3H), 6.40 – 6.34 (m, 2H), 4.27 (dd, $J = 10.9, 6.3$ Hz, 2H), 4.20 (d, $J = 10.8$ Hz, 1H), 4.08 (d, $J = 11.0$ Hz, 1H), 3.81 (s, 4H), 3.40 (d, $J = 13.1$ Hz, 1H), 3.28 (s, 3H), 3.22 (s, 4H), 3.07 (d, $J = 13.6$ Hz, 1H), 3.05 (s, 3H), 2.64 (d, $J = 13.0$ Hz, 1H), 2.17 (d, $J = 13.1$ Hz, 1H). ^{13}C NMR (126 MHz, CDCl_3) δ 170.0, 168.5, 168.4, 168.2, 143.6, 143.4, 139.3, 138.6, 138.0, 137.6, 130.7, 130.4, 130.4, 128.8, 128.1, 127.9, 127.6, 127.5, 127.4, 127.2, 127.1, 126.9, 126.4, 126.4, 126.2, 125.9, 125.7, 55.8, 55.4, 55.2, 54.8, 53.1, 52.3, 52.2, 52.1, 49.1, 46.6, 45.6, 45.5, 19.4, 17.5. FTIR (ATR): 3088, 3060, 3029, 3000, 2951, 2888, 2841, 2362, 2337, 1762, 1734, 1653, 1601, 1496, 1453, 1433, 1381, 1304, 1256, 1196, 1156, 1132, 1089, 1030, 911, 778, 731, 701, 668, 648. LRMS (ESI): Mass calcd for $\text{C}_{27}\text{H}_{28}\text{O}_4$ $[\text{M}+\text{H}]^+$: 417.2; found 417.3



II-69: Prepared according to the general procedure using phenyl arylidene malonate (77 mg, 0.35 mmol) and the corresponding HE derivative (181 mg, 0.525 mmol, 1.5 equivalents). Isolated a

1:1 mixture of diastereomers as a thick, clear oil (73.8 mg, 60%). Analytical Data for **II-69**: ^1H NMR (500 MHz, Chloroform-*d*) δ 7.40 – 7.33 (m, 2H), 7.30 (t, $J = 7.6$ Hz, 2H), 7.26 – 7.13 (m, 7H), 7.13 – 7.10 (m, 2H), 7.09 – 7.02 (m, 3H), 6.81 – 6.72 (m, 2H), 4.08 (d, $J = 11.0$ Hz, 1H), 4.05 (d, $J = 11.0$ Hz, 1H), 3.95 (d, $J = 11.0$ Hz, 1H), 3.88 (d, $J = 11.0$ Hz, 1H), 3.65 (s, 3H), 3.22 (s, 3H), 3.18 (s, 3H), 3.14 (s, 3H), 2.08 (dq, $J = 14.5, 7.3$ Hz, 1H), 1.82 (dq, $J = 14.6, 7.4$ Hz, 1H), 1.54 (dq, $J = 14.4, 7.2$ Hz, 1H), 1.41 (s, 3H), 1.27 (s, 3H), 1.02 (dq, $J = 14.4, 7.3$ Hz, 1H), 0.67 (t, $J = 7.3$ Hz, 3H), 0.36 (t, $J = 7.3$ Hz, 3H). ^{13}C NMR (126 MHz, CDCl_3) δ 169.5, 168.5, 168.5, 168.3, 144.1, 143.8, 139.4, 138.9, 130.3, 128.3, 128.0, 127.7, 127.7, 127.6, 126.9, 126.8, 126.4, 126.1, 126.0, 56.6, 56.2, 55.1, 54.7, 52.8, 52.2, 52.1, 52.1, 45.3, 44.6, 34.8, 30.1, 21.3, 17.7, 8.9, 8.3. FTIR (ATR): 3089, 3059, 3029, 2951, 2881, 2841, 2362, 2337, 1763, 1734, 1601, 1497, 1453, 1433, 1384, 1304, 1263, 1195, 1154, 1131, 1032, 914, 792, 777, 759, 732, 702, 648. LRMS (ESI): Mass calcd for $\text{C}_{22}\text{H}_{26}\text{O}_4$ $[\text{M}+\text{H}]^+$: 355.2; found 355.3

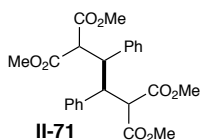


II-70: Prepared according to the general procedure using phenyl arylidene malonate (77 mg, 0.35 mmol) and the corresponding HE derivative (171 mg, 0.525 mmol, 1.5 equivalents). Isolated as a thick, clear oil that slowly crystallized into a white powder (74.8 mg, 55%). Analytical Data for **II-70**: ^1H NMR (500 MHz, Chloroform-*d*) δ 7.43 (dt, $J = 8.4, 1.8$ Hz, 2H), 7.33 – 7.24 (m, 5H), 7.22 – 7.16 (m, 3H), 7.12 (dd, $J = 8.4, 6.9$ Hz, 2H), 7.09 – 7.02 (m, 3H), 7.00 – 6.93 (m, 1H), 4.63 (d, $J = 11.7$ Hz, 1H), 4.43 (dd, $J = 11.7, 6.5$ Hz, 1H), 3.76 (d, $J = 6.5$ Hz, 1H), 3.39 (s, 2H), 3.38 (s, 3H). ^{13}C NMR (126 MHz, CDCl_3) δ 168.9, 168.3, 142.4, 142.3, 139.0, 129.5,

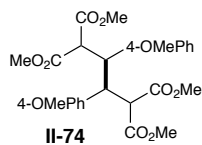
128.8, 128.6, 128.4, 128.1, 127.8, 126.8, 126.8, 126.0, 56.3, 55.5, 52.2, 52.0, 48.9. FTIR (ATR): 3062, 3005, 2952, 2922, 1755, 1721, 1597, 1494, 1449, 1432, 1310, 1268, 1208, 1197, 1171, 1074, 1052, 1033, 1019, 923, 912, 841, 791, 779, 752, 740, 699, 602, 577. LRMS (ESI): Mass calcd for $C_{25}H_{24}O_4$ $[M+H]^+$: 389.2; found 389.2

2.10.7 General Procedure for Radical Dimerization

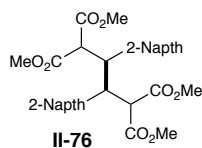
To a 2 dram vial was added desired benzylidene malonate (0.30 mmol, 1 equiv). The reaction was equipped with magnetic stirbar, capped and taken in to a glovebox. Scandium triflate (0.1 equiv) and Ir(ppy)₃ (0.01 equiv) were added to the vial. The vial was removed from the glovebox and charged with 3.5 mL (0.1 M) of sparged acetonitrile (sparged for at least 20 minutes with argon) and stirred until homogenous. Sparged tributylamine (1.5 equiv) was then added and the vial was then placed in between 3 Kessil blue LED lights and irradiated for 36 hours (with a small fan placed for cooling). Conversion of the malonate was monitored by UPLC/MS. Upon complete consumption of the benzylidene malonate, the reaction was concentrated under reduced pressure. If solids were present, DCM was added until these solids dissolved and the solution concentrated onto silica gel. This silica was loaded onto a column of silica gel and the desired product isolated via flash column chromatography (5-55% ethyl acetate/hexanes).



II-71: Prepared according to the general procedure using the corresponding benzylidene malonate (66.2 mg, 0.30 mmol). Isolated as a white powder (78.1 mg, 62%). ¹H and ¹³C matched reported data.²⁴¹

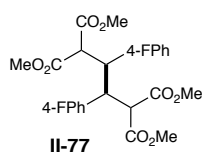


II-74: Prepared according to the general procedure using the corresponding benzylidene malonate (75.1 mg, 0.30 mmol). Isolated as a 1:1 mixture of diastereomers; white powder (57.3 mg, 74%). Analytical Data for **II-74**: ^1H NMR (500 MHz, Chloroform-*d*) δ 7.23 (d, $J = 8.4$ Hz, 2H), 6.81 (d, $J = 8.5$ Hz, 2H), 6.71 (s, 2H), 4.03 (dd, $J = 5.1, 2.2$ Hz, 1H), 3.93 (s, 3H), 3.79 (s, 3H), 3.78 (s, 3H), 3.74 (d, $J = 4.6$ Hz, 2H), 3.62 (dd, $J = 5.1, 2.2$ Hz, 1H), 3.46 (s, 3H), 3.40 (s, 3H), 3.32 (s, 3H). ^{13}C NMR (126 MHz, CDCl_3) δ 168.8, 168.4, 168.2, 167.7, 158.8, 158.8, 131.0, 129.8, 127.4, 113.5, 113.0, 55.6, 55.5, 55.2, 55.1, 53.1, 52.3, 52.3, 52.1, 47.9, 46.0. FTIR (ATR): 3002, 2954, 2840, 2362, 2337, 1734, 1611, 1583, 1513, 1434, 1294, 1250, 1180, 1158, 1032, 916, 840, 791, 731, 668, 648. LRMS (ESI): Mass calcd for $\text{C}_{26}\text{H}_{30}\text{O}_{10}$ $[\text{M}+\text{H}]^+$: 503.2; found 503.4.



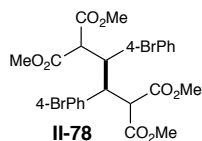
II-76: Prepared according to the general procedure using the corresponding benzylidene malonate (81.1 mg, 0.30 mmol). Isolated as white powders (28.9 mg **II-76-A**, 28.5 mg **II-76-B**, 76% total yield). Analytical Data for **II-76-A**: ^1H NMR (600 MHz, Chloroform-*d*) δ 7.84 – 7.78 (m, 8H), 7.54 – 7.50 (m, 2H), 7.48 (dt, $J = 6.2, 3.4$ Hz, 4H), 4.40 (dd, $J = 5.3, 2.3$ Hz, 2H), 3.79 (dd, $J = 5.2, 2.3$ Hz, 2H), 3.29 (s, 6H), 3.27 (s, 6H). ^{13}C NMR (151 MHz, CDCl_3) δ 168.5, 168.0, 135.4, 133.1, 132.8, 128.0, 127.9, 127.6, 126.1, 55.7, 52.3, 52.1, 48.7. FTIR (ATR): 3060, 3022, 2995, 2948, 2842, 1752, 1733, 1601, 1509, 1433, 1351, 1312, 1264, 1234, 1208, 1169, 1159,

1134, 1019, 966, 949, 908, 869, 837, 814, 781, 751, 731, 668, 639. LRMS (ESI): Mass calcd for $C_{32}H_{30}O_8$ $[M+H]^+$: 543.2; found 543.0 Analytical Data for **II-76-B**: 1H NMR (600 MHz, Chloroform-*d*) δ 7.79 (d, $J = 8.0$ Hz, 2H), 7.50 – 7.41 (m, 3H), 4.14 – 4.09 (m, 2H), 4.01 (s, 6H), 3.95 (s, 2H), 3.22 (s, 6H). ^{13}C NMR (151 MHz, $CDCl_3$) δ 168.4, 167.5, 133.2, 132.7, 128.0, 127.5, 126.0, 53.2, 52.3 FTIR (ATR): 3056, 3024, 3006, 2953, 2843, 2362, 2336, 2260, 1756, 1734, 1600, 1508, 1434, 1253, 1228, 1193, 1156, 1019, 910, 864, 802, 732, 648. LRMS (ESI): Mass calcd for $C_{32}H_{30}O_8$ $[M+H]^+$: 543.2; found 543.1.

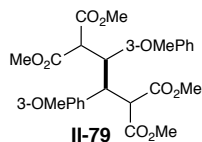


II-77: Prepared according to the general procedure using the corresponding benzylidene malonate (71.5 mg, 0.30 mmol). Isolated as white powders (18.9 mg **II-77-A**, 19.3 mg **II-77-B**, 53% total yield). Analytical Data for **II-77-A**: 1H NMR (500 MHz, Chloroform-*d*) δ 7.32 – 7.27 (m, 4H), 6.98 (t, $J = 8.6$ Hz, 4H), 4.14 – 4.04 (m, 2H), 3.60 (dd, $J = 5.1, 2.3$ Hz, 2H), 3.48 (s, 6H), 3.41 (s, 6H). ^{13}C NMR (126 MHz, $CDCl_3$) δ 168.4, 167.9, 162.2 (d, $J = 246.9$ Hz), 133.4 (d, $J = 3.4$ Hz), 131.5 (d, $J = 6.9$ Hz), 115.3, 115.1, 55.2, 52.5, 52.2, 47.7. FTIR (ATR): 3077, 2999, 2953, 2843, 2362, 2331, 1749, 1749, 1749, 1604, 1510, 1434, 1359, 1317, 1256, 1222, 1192, 1159, 1141, 1099, 1013, 961, 921, 847, 785, 728, 638. LRMS (ESI): Mass calcd for $C_{24}H_{24}F_2O_8$ $[M+H]^+$: 479.1; found 479.2. Analytical Data for **II-77-B**: 1H NMR (500 MHz, Chloroform-*d*) δ 6.88 (s, 6H), 3.94 (s, 6H), 3.80 (d, $J = 11.6$ Hz, 2H), 3.72 (d, $J = 11.6$ Hz, 2H), 3.35 (s, 6H). ^{13}C NMR (126 MHz, $CDCl_3$) δ 168.1, 167.3, 162.1 (d, $J = 246.9$ Hz), 131.2 (d, $J = 3.5$ Hz), 114.9, 114.7, 55.3, 53.2, 52.4, 46.0. FTIR (ATR): 3007, 2956, 2846, 1734, 1605, 1511, 1435, 1289,

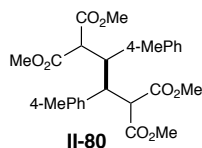
1228, 1193, 1163, 1106, 1025, 915, 837, 805, 733, 648. LRMS (ESI): Mass calcd for $C_{24}H_{24}F_2O_8$ $[M+H]^+$: 479.1; found 479.2.



II-78: Prepared according to the general procedure using the corresponding benzylidene malonate (89.8 mg, 0.30 mmol). Isolated as white powders (27.8 mg **II-78-A**, 27.0 mg **II-78-B**, 61% total yield). Analytical Data for **II-78-A**: 1H NMR (500 MHz, Chloroform-*d*) δ 7.42 (d, J = 8.2 Hz, 4H), 7.17 (d, J = 8.2 Hz, 4H), 4.06 (dd, J = 5.3, 2.1 Hz, 2H), 3.59 (dd, J = 5.2, 2.2 Hz, 2H), 3.50 (s, 6H), 3.42 (s, 6H). ^{13}C NMR (126 MHz, $CDCl_3$) δ 168.3, 167.7, 136.6, 131.5, 131.4, 121.9, 54.9, 52.6, 52.3, 47.7. FTIR (ATR): 3011, 2951, 2840, 2362, 2336, 2258, 1751, 1723, 1490, 1432, 1358, 1310, 1239, 1208, 1158, 1071, 1012, 976, 917, 843, 810, 737, 725, 648. LRMS (ESI): Mass calcd for $C_{24}H_{24}Br_2O_8$ $[M+H]^+$: 600.0; found 601.1. Analytical Data for **II-78-B**: 1H NMR (500 MHz, Chloroform-*d*) δ 7.31 (s, 5H), 3.91 (s, 6H), 3.77 (d, J = 11.7 Hz, 2H), 3.72 – 3.65 (m, 2H), 3.34 (s, 6H). ^{13}C NMR (151 MHz, $CDCl_3$) δ 167.9, 167.2, 134.4, 131.4 (broad), 131.0, 121.9, 55.0, 53.3, 52.5, 46.0. FTIR (ATR): 3011, 2951, 2840, 2362, 2336, 2258, 1751, 1723, 1490, 1432, 1358, 1310, 1239, 1208, 1158, 1071, 1012, 976, 917, 843, 810, 737, 725, 648. LRMS (ESI): Mass calcd for $C_{24}H_{24}Br_2O_8$ $[M+H]^+$: 600.0; found 601.1.

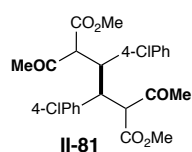


II-79: Prepared according to the general procedure using the corresponding benzylidene malonate (75.1 mg, 0.30 mmol). Isolated as a 1:1 mixture of diastereomers, white semi-solid (45.6 mg, 61%). Analytical Data for **II-79**: ^1H NMR (600 MHz, Chloroform-*d*) δ 7.18 (t, $J = 7.9$ Hz, 2H), 6.85 (t, $J = 5.6$ Hz, 4H), 6.76 (ddd, $J = 14.5, 8.2, 2.4$ Hz, 4H), 4.06 (dd, $J = 5.5, 2.3$ Hz, 2H), 3.93 (s, 6H), 3.83 (s, 2H), 3.80 (d, $J = 12.6$ Hz, 2H), 3.77 (s, 6H), 3.69 (dd, $J = 5.5, 2.3$ Hz, 2H), 3.49 (s, 6H), 3.39 (s, 6H), 3.34 (s, 6H). ^{13}C NMR (151 MHz, CDCl_3) δ 168.6, 168.3, 168.0, 167.6, 159.3, 139.5, 137.1, 129.1, 113.5, 55.4, 55.2, 55.2, 55.0, 53.1, 52.4, 52.4, 52.1, 48.5, 46.6. FTIR (ATR): 3003, 2954, 2838, 1753, 1734, 1600, 1584, 1490, 1454, 1434, 1257, 1194, 1154, 1041, 913, 782, 732, 704, 648. LRMS (ESI): Mass calcd for $\text{C}_{26}\text{H}_{30}\text{O}_{10}$ $[\text{M}+\text{H}]^+$: 503.2; found 503.4.



II-80: Prepared according to the general procedure using the corresponding benzylidene malonate (70.3 mg, 0.30 mmol). Isolated as a 1:1 mixture of diastereomers as white solids (26.3 mg **II-80-A**, 25.8 mg **II-80-B**, 74% total yield). Analytical Data for **II-80-A**: ^1H NMR (600 MHz, Chloroform-*d*) δ 7.24 – 7.18 (m, 2H), 7.10 (d, $J = 7.8$ Hz, 2H), 4.08 (dd, $J = 5.1, 2.3$ Hz, 1H), 3.67 (dd, $J = 5.1, 2.3$ Hz, 1H), 3.47 (s, 3H), 3.41 (s, 3H), 2.33 (s, 3H). ^{13}C NMR (151 MHz, CDCl_3) δ 168.7, 168.1, 137.1, 134.8, 129.7, 128.9, 55.6, 52.3, 52.0, 48.2, 21.1. FTIR (ATR): 3025, 3007, 2952, 2863, 2845, 1731, 1731, 1731, 1731, 1515, 1434, 1308, 1285, 1192, 1155,

1057, 1022, 911, 833, 728, 648. LRMS (ESI): Mass calcd for C₂₆H₃₀O₈ [M+H]⁺: 471.2; found 471.1. Analytical Data for **II-80-B**: ¹H NMR (600 MHz, Chloroform-*d*) δ 6.96 (s, 4H), 3.92 (s, 6H), 3.81 – 3.77 (m, 2H), 3.77 – 3.73 (m, 2H), 3.30 (s, 6H), 2.29 (s, 6H). ¹³C NMR (151 MHz, CDCl₃) δ 168.4, 167.7, 137.0, 132.4, 129.9, 128.3, 55.4, 53.0, 52.2, 46.2, 21.1. FTIR (ATR): 3026, 3010, 2954, 2925, 2865, 2845, 2362, 1757, 1734, 1515, 1433, 1285, 1251, 1228, 1193, 1157, 1119, 1022, 914, 823, 786, 730, 647. LRMS (ESI): Mass calcd for C₂₆H₃₀O₈ [M+H]⁺: 471.2; found 471.1.



II-81: Prepared according to the general procedure using the corresponding benzylidene malonate (71.6 mg, 0.30 mmol). Isolated as a 1:1 mixture of diastereomers (at 3,4 bond) and a complex mixture of tautomers. Confirmed pure by LC/MS analysis. Obtained as an off-white solid (29 mg, 40%). Analytical Data for **II-81**: ¹H NMR (500 MHz, Chloroform-*d*) δ 7.26 – 7.15 (m, 2H), 7.12 – 7.01 (m, 4H), 5.14 (dd, *J* = 57.4, 1.8 Hz, 1H), 4.16 – 4.06 (m, 0H), 4.01 (tdd, *J* = 17.0, 7.8, 4.7 Hz, 2H), 3.86 (s, 1H), 3.81 – 3.71 (m, 2H), 3.65 (d, *J* = 8.0 Hz, 2H), 3.56 (d, *J* = 3.2 Hz, 3H), 3.39 (d, *J* = 2.0 Hz, 2H), 2.02 (d, *J* = 6.0 Hz, 2H), 1.82 (d, *J* = 11.9 Hz, 3H). ¹³C NMR (101 MHz, CDCl₃) δ 206.7, 201.5, 201.4, 201.1, 172.4, 170.2, 169.8, 169.1, 168.7, 168.1, 168.0, 139.0, 138.9, 137.1, 137.0, 136.2, 136.1, 133.7, 132.8, 131.3, 131.1, 130.9, 130.6, 129.6, 129.5, 129.0, 128.8, 128.7, 128.6, 128.6, 128.4, 128.3, 84.4, 82.0, 63.0, 62.9, 62.6, 59.4, 59.2, 57.4, 56.1, 55.8, 53.2, 52.7, 52.7, 52.6, 52.3, 52.0, 51.9, 48.5, 47.8, 47.5, 46.6, 30.7, 30.1, 29.8, 29.6, 29.6, 29.5, 25.4, 24.7. FTIR (ATR): 3486, 3030, 2999, 2952, 2848, 2362, 2337, 2257,

1739, 1716, 1492, 1434, 1412, 1356, 1245, 1221, 1196, 1158, 1090, 1014, 910, 835, 731, 668,

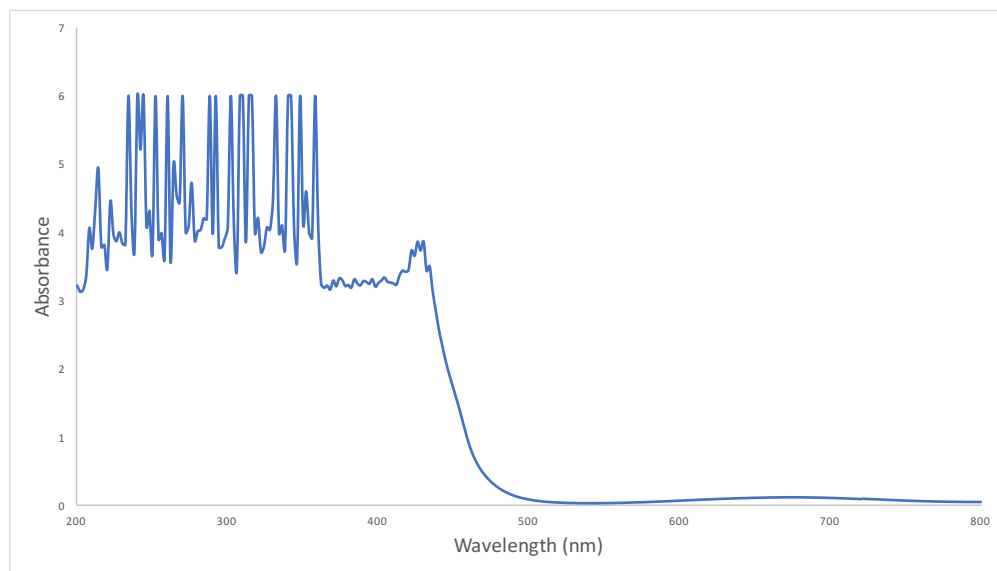
649. LRMS (ESI): Mass calcd for $C_{24}H_{24}Cl_2O_6$ $[M+H]^+$: 479.1; found 479.2.

2.10.8 Procedure for Determination of Quantum Yield of Cross-Coupling Reaction

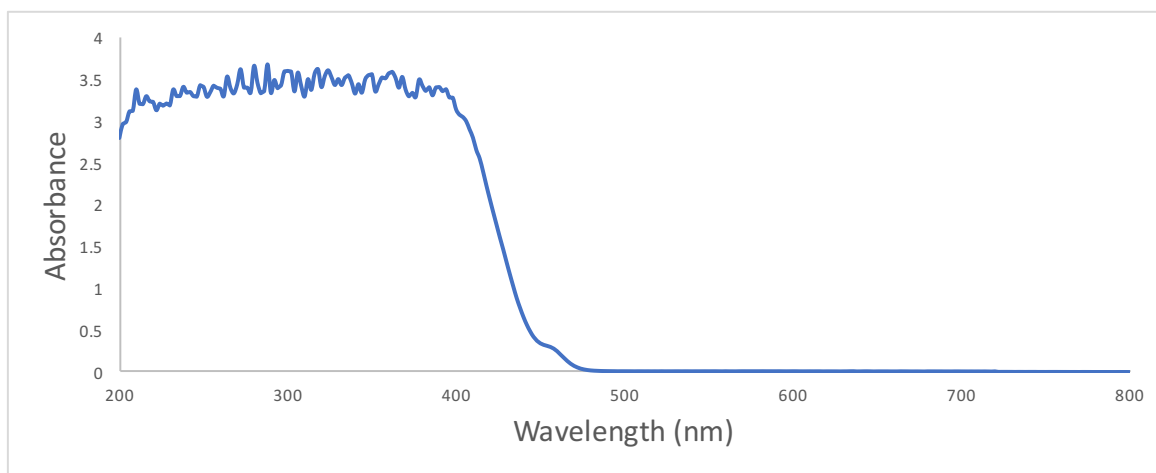
The photon flux of the fluorimeter was determined using a ferrioxolate Hatchard–Parker actinometer as described by Yoon et al.^{271,272} Based on the average of three experiments, the photon flux at 420 nm (10 nm slit width) was determined to be 5.27712E-09 einsteins s⁻¹. UV/Vis absorbance spectra of dF-Ir in MeCN (0.1 M) showed that essentially all light was absorbed at 420 nm ($f = 0.99148$) (*vide infra*).



A screw-top quartz cuvette with Teflon septa was taken into a glovebox. 4-Me phenylidene methyl malonate (47.0 mg, 0.2 mmol, 1 equiv), dF-Ir (2.2 mg, 0.0020 mmol, 1 mol %), scandium triflate (9.8 mg, 0.020 mmol, 10 mol %), and HEH derivative (83.2 mg, 0.3 mmol, 1.5 equiv) and a small teflon coated magnetic stirbar. The cuvette was sealed and removed from glovebox. The cuvette was then capped with a PTFE stopper and 2 mL sparged MeCN added. The solution was stirred until homogenous. The sample placed in the fluorimeter and irradiated ($\lambda = 420$ nm, slit width = 10.0 nm) for 5400 s (3 hours). The yield of product formed was determined by ¹H NMR based on a trimethoxybenzene standard. The combined yield of the cross-coupling product and the dimeric product was 14% and 15% in two experiments. The average quantum yield of the two experiments was determined to be 1.0.

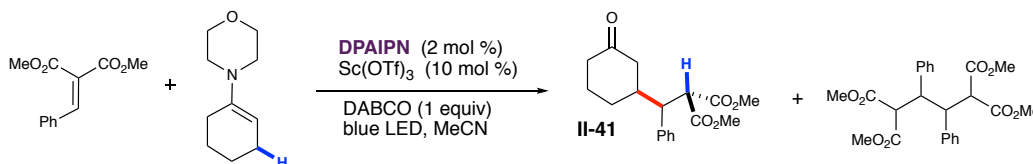


UV/Vis spectra of ferrioxolate solution before irradiation. The absorbance at 420 nm was 3.45053. The fraction of light absorbed was calculated using the equation $f = 1 - 10^{-A}$, yielding 0.99966. Hatchard and Parker report the quantum yield at 420 nm to be 1.13.²⁷¹



UV/Vis spectra of dF-Ir in MeCN (0.1 M). Absorbance at 420 nm is 2.06945. The fraction of light absorbed was calculated using the equation $f = 1 - 10^{-A}$, yielding 0.99148.

2.10.9 Procedure for Coupling of Arylidene Malonate and Enamine

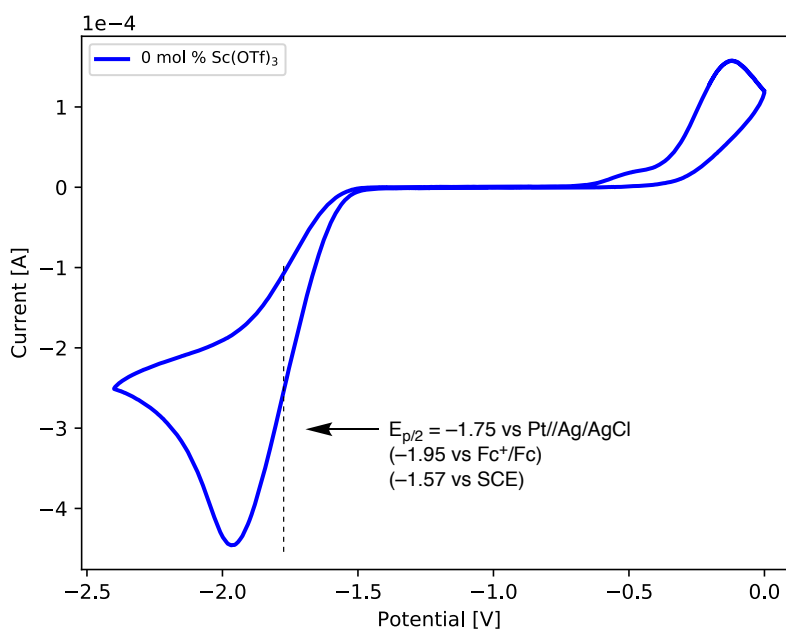


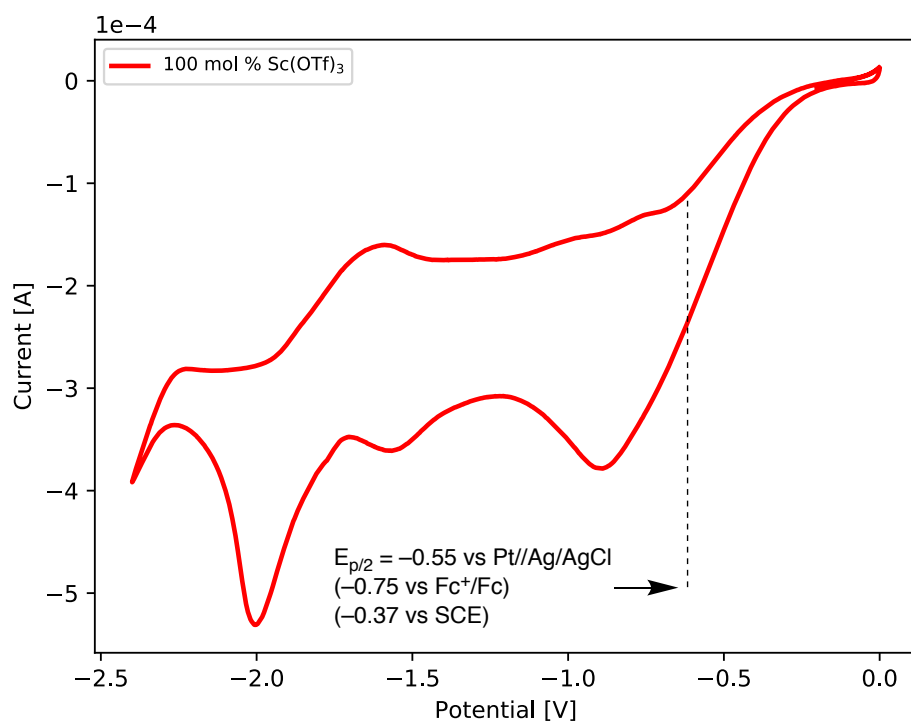
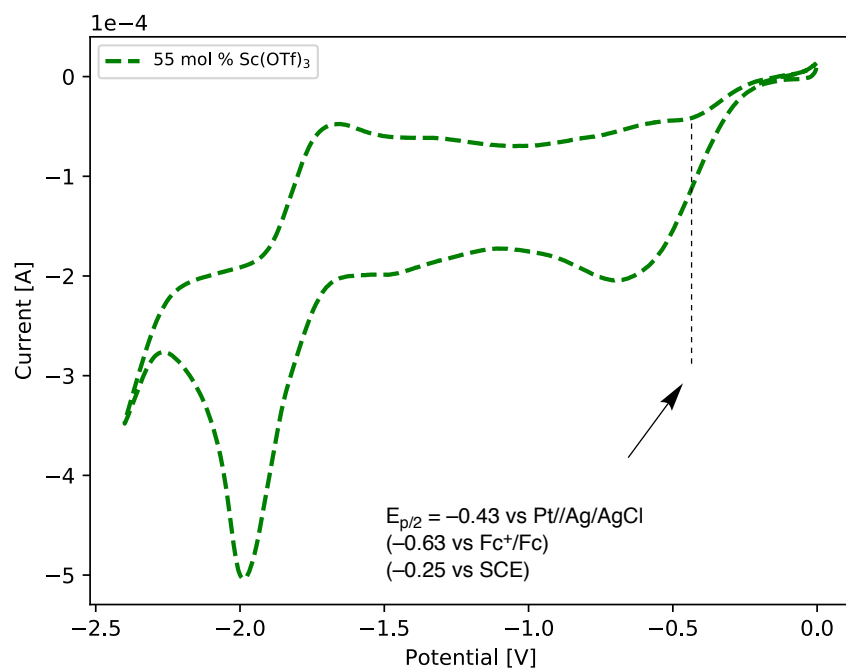
To a 100 mL flask fitted with magnetic stirbar was added benzylidene malonate (1000 mg, 4.5 mmol, 1 equiv). The reaction was equipped with magnetic stirbar, capped and taken in to a glovebox. Scandium triflate (220 mg, .45 mmol, 0.1 equiv), DABCO (509 mg, 4.5 mmol, 1 equiv), DPAIPN (73.4 mg, .09 mmol, 0.02 equiv) were added to the vial. The vial was removed from the glovebox and charged with 45 mL (0.1 M) of sparged acetonitrile (sparged for at least 20 minutes with argon) and stirred until homogenous. Cyclohexyl morpholine enamine (1.5 g, 0.9 mmol, 2 equiv) was then added. The flask was then placed in between 3 Kessil blue LED lights and irradiated for 12 hours (with a small fan placed for cooling) with positive pressure nitrogen atmosphere. The reaction was concentrated under reduced pressure. DCM was added to form a homogenous solution and the solution was concentrated onto silica gel. This silica was loaded onto a column of silica gel and the desired product was isolated as a mixture with the malonate dimer via flash column chromatography (2-40% ethyl acetate/hexanes). The desired compound was separated from malonate dimer by preparative HPLC to yield 1:1 mixture of diastereomers as a thick clear oil (132 mg, 9 % yield). Analytical Data for **41**: ¹H NMR (500 MHz, Chloroform-*d*) δ 7.32 – 7.20 (m, 5H), 7.11 (dd, *J* = 12.5, 7.4 Hz, 5H), 4.01 (d, *J* = 11.3 Hz, 1H), 3.91 (d, *J* = 11.3 Hz, 1H), 3.78 – 3.72 (m, 6H), 3.69 – 3.65 (m, 1H), 3.56 (dd, *J* = 11.3, 4.9 Hz, 1H), 3.39 (d, *J* = 2.4 Hz, 6H), 2.33 (dd, *J* = 13.7, 3.1 Hz, 3H), 2.29 – 2.22 (m, 2H), 2.03 (qd, *J* = 14.8, 13.9, 6.8 Hz, 5H), 1.95 – 1.81 (m, 4H), 1.58 (ddt, *J* = 13.1, 9.1, 4.3 Hz, 1H), 1.53 – 1.43

(m, 1H), 1.25 – 1.15 (m, 2H). ^{13}C NMR (126 MHz, CDCl_3) δ 210.9, 210.8, 168.8, 168.6, 168.0, 167.9, 137.2, 137.1, 129.3, 129.2, 128.2, 128.2, 127.4, 54.9, 54.5, 52.9, 52.9, 52.4, 50.0, 49.9, 47.1, 43.8, 41.3, 41.1, 41.1, 41.0, 30.3, 26.6, 25.0.

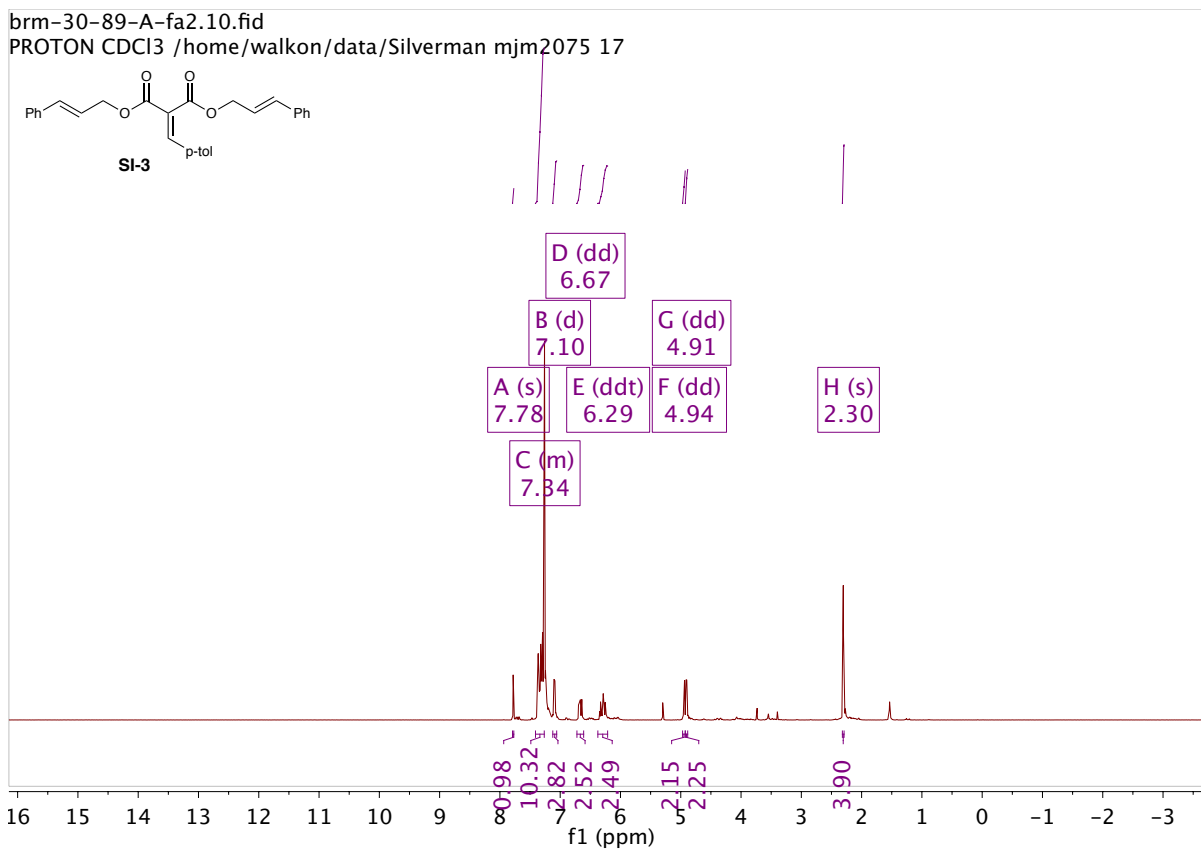
2.10.10 Electrochemical Measurements

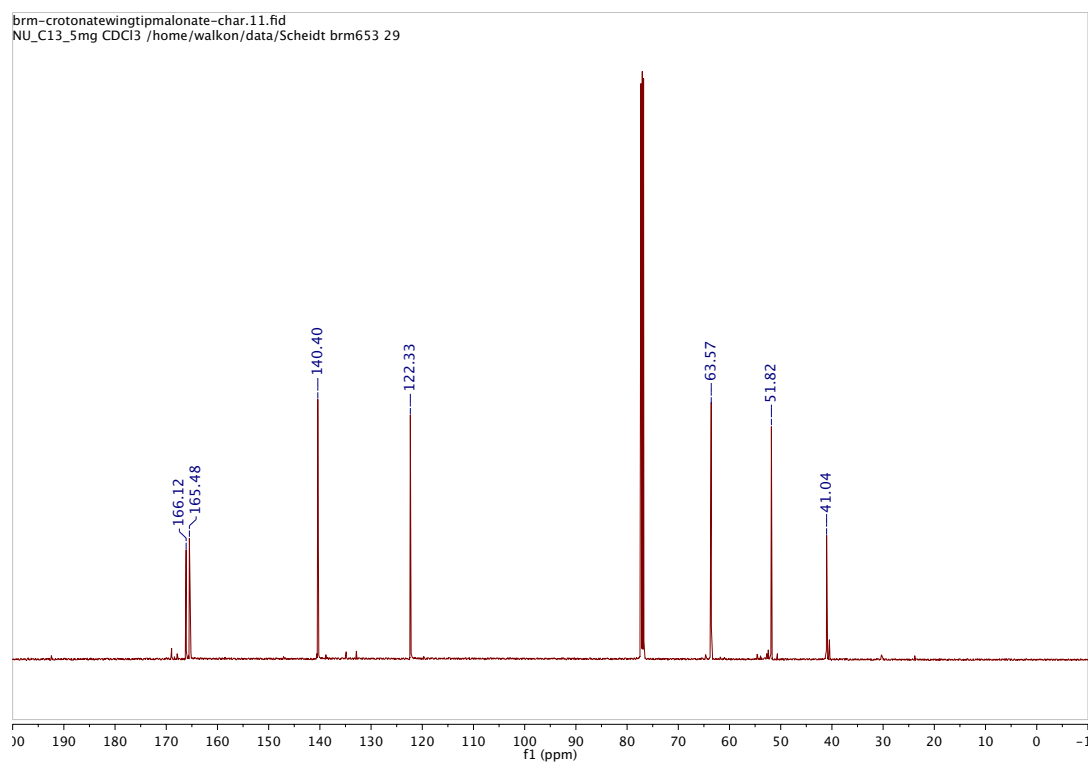
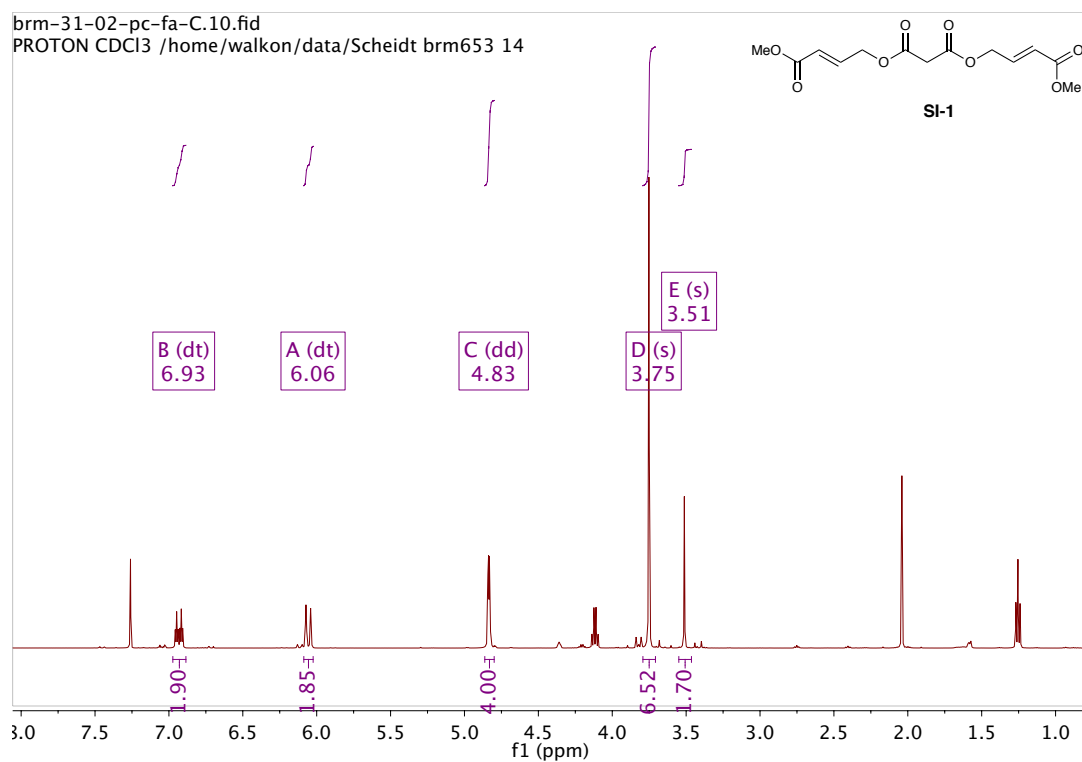
Electrochemical potentials were obtained with a standard set of conditions to main internal consistency. Cyclic voltammograms were collected with a Nuvant Ezstat Pro potentiostat/galvanostat. Samples were prepared with 0.05 mmol of substrate in 5 mL of 0.1 M tetra-*n*-butylammonium hexafluorophosphate (freshly recrystallized) in dry, degassed acetonitrile. Measurements employed a platinum working electrode, platinum wire counter electrode, a Pt/ Ag/AgCl pseudo reference electrode²⁷³ and a scan rate of 250 mV/s. Ferrocene was used as an internal standard. Two cycles were performed on each sample. Measurements reported are of the second scan cycle.²⁷⁴

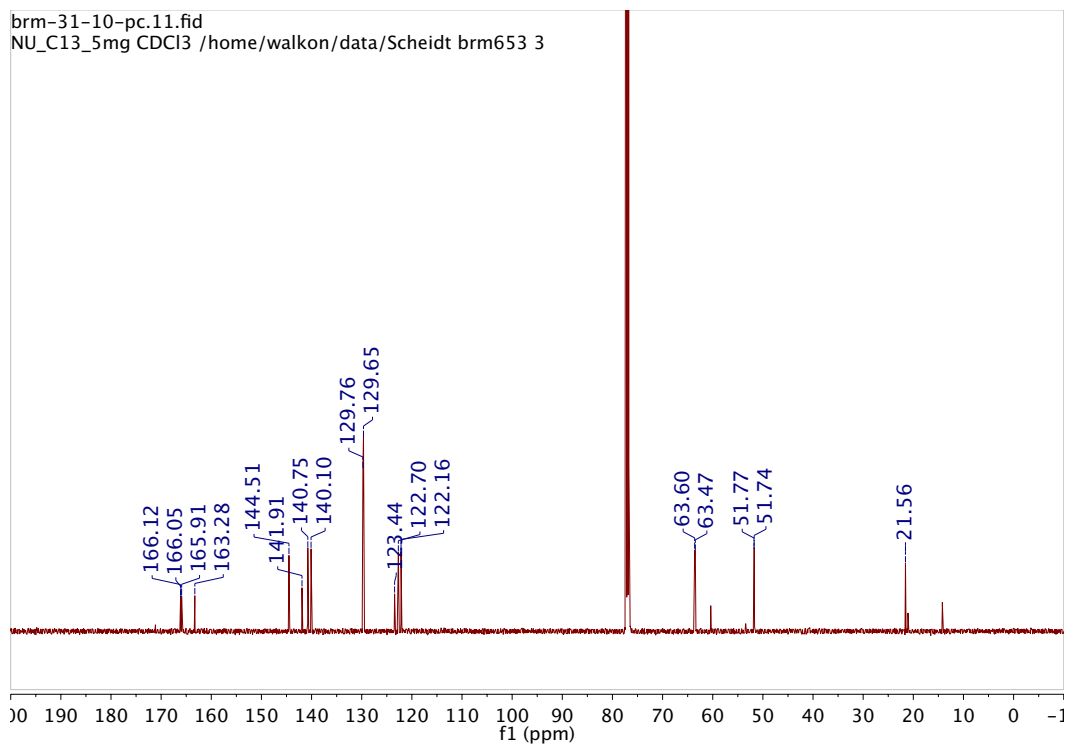
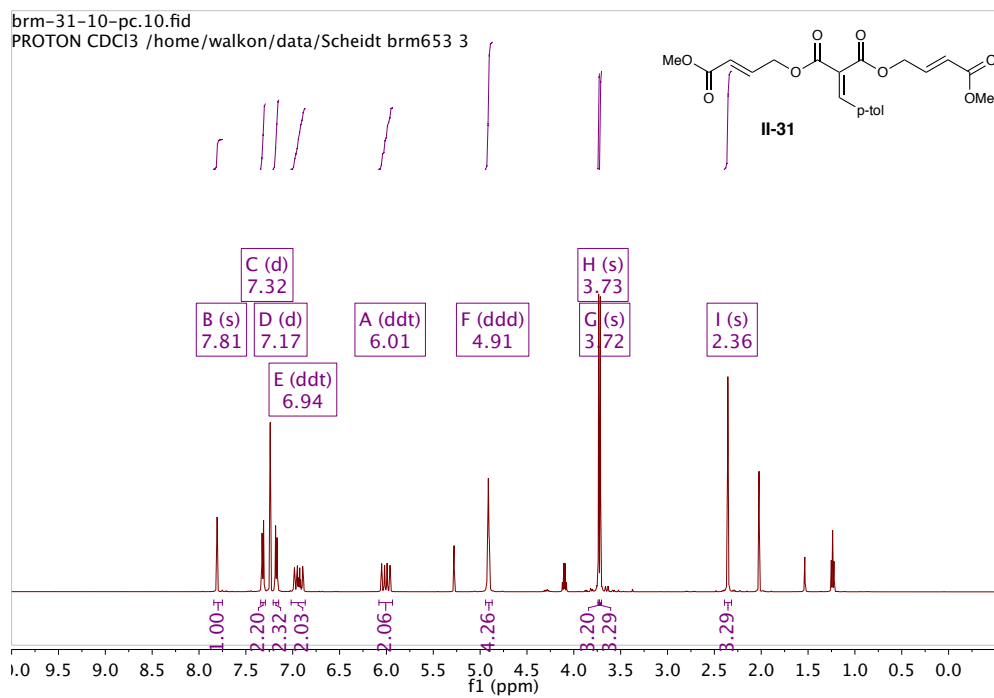


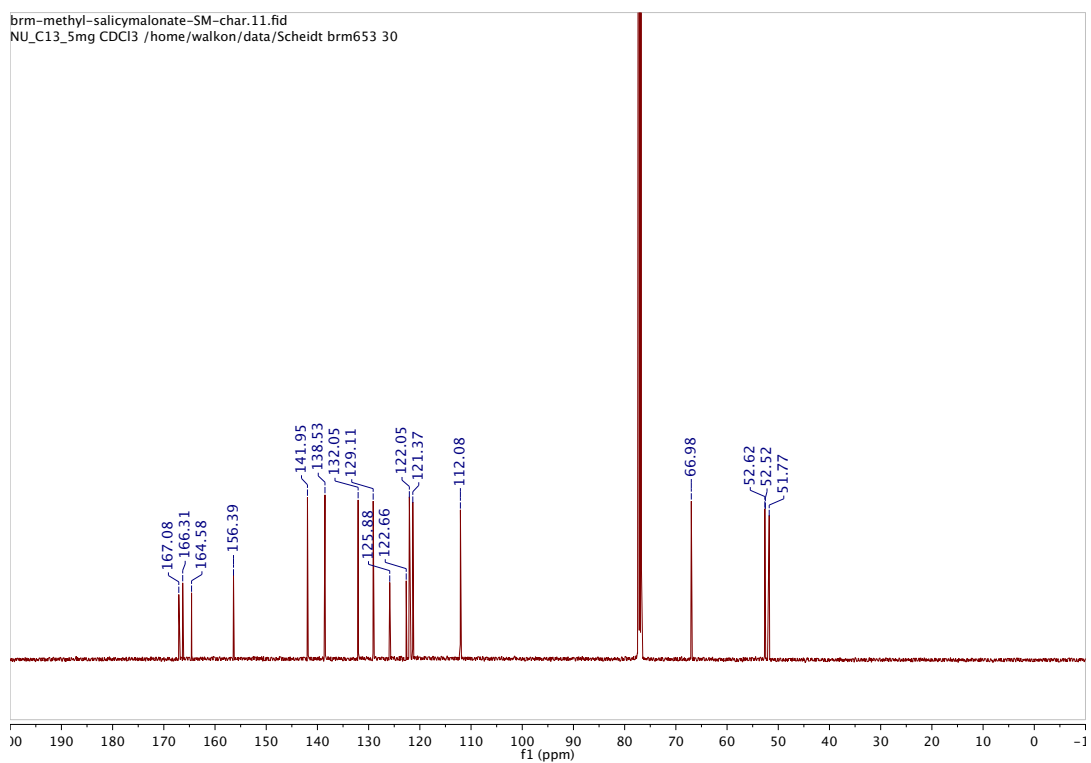
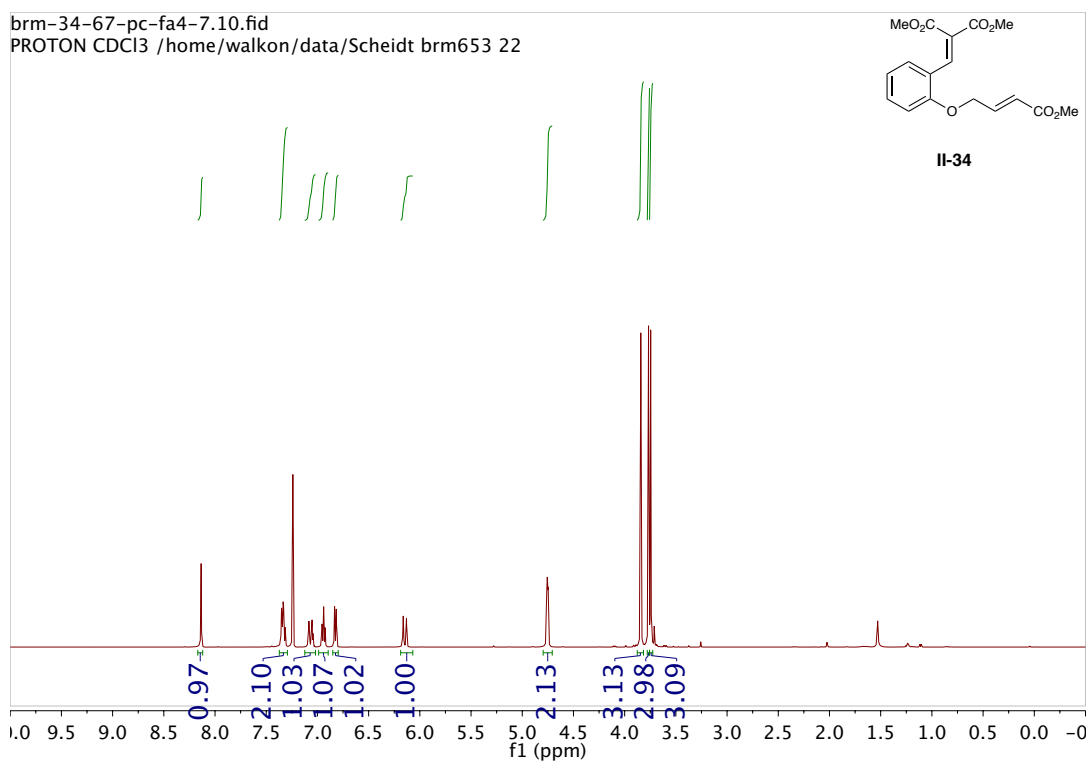


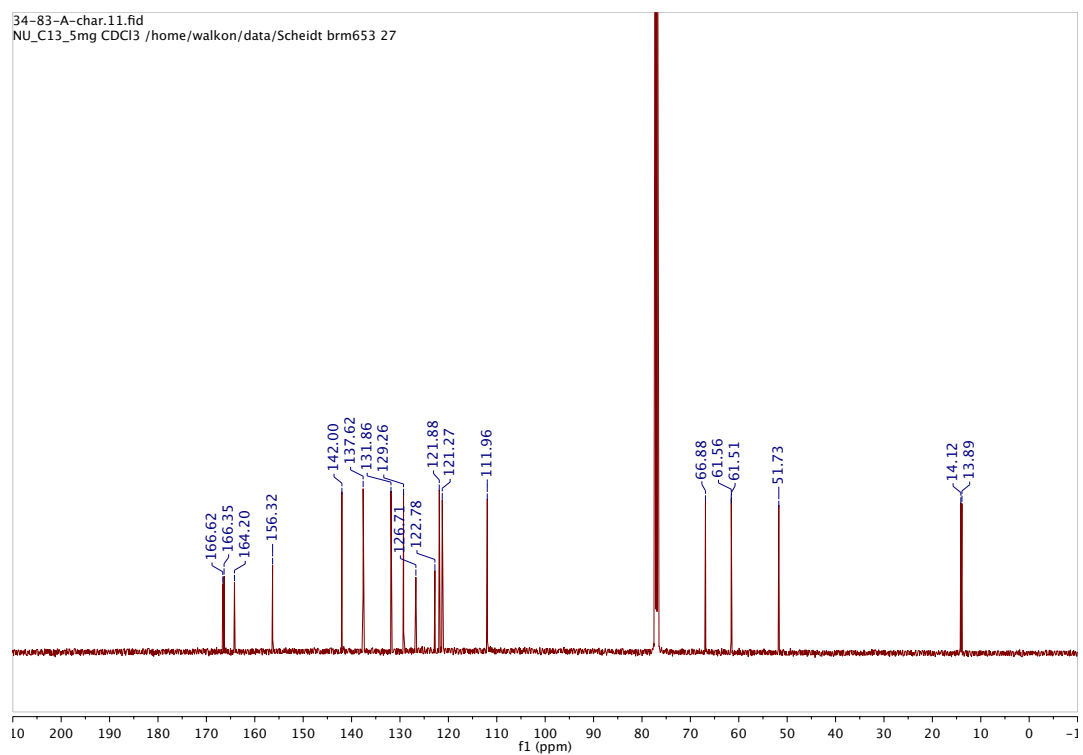
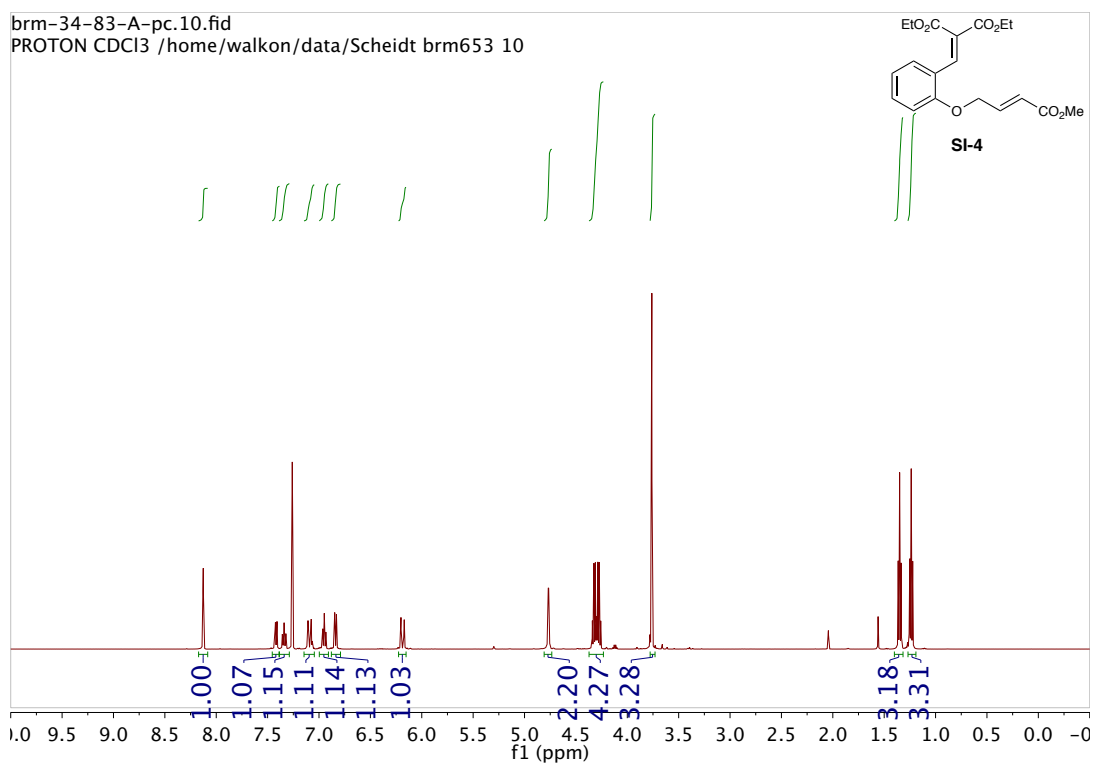
2.10.11 Selected NMR Spectra

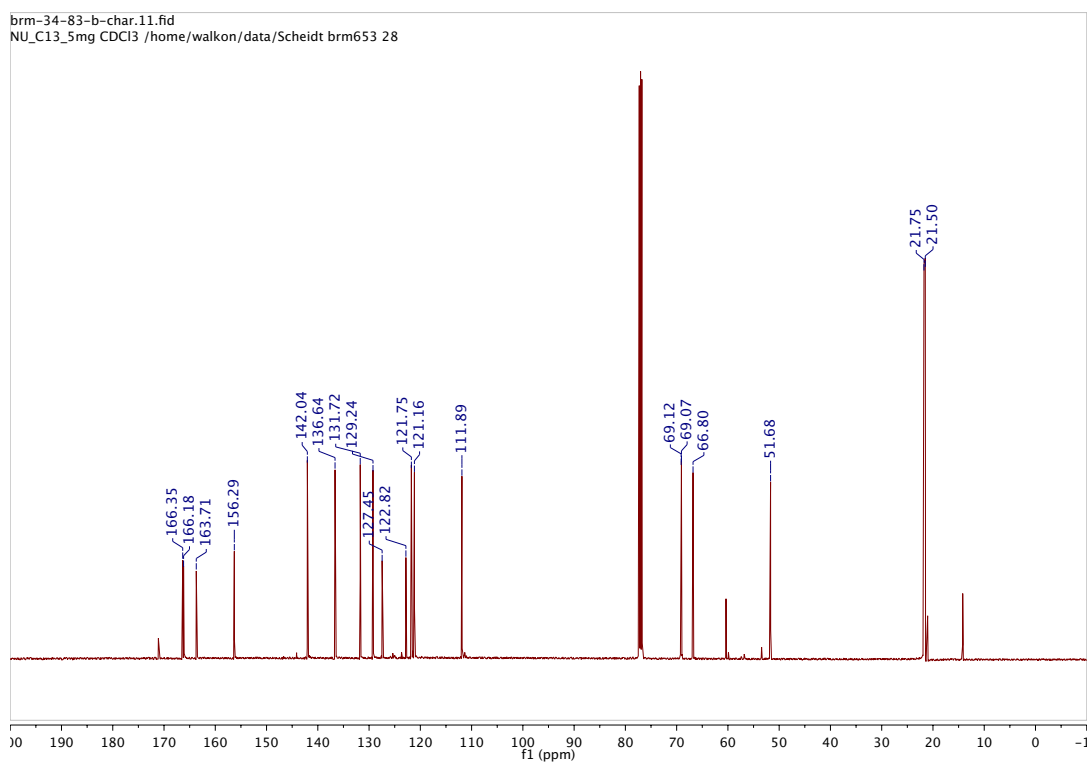
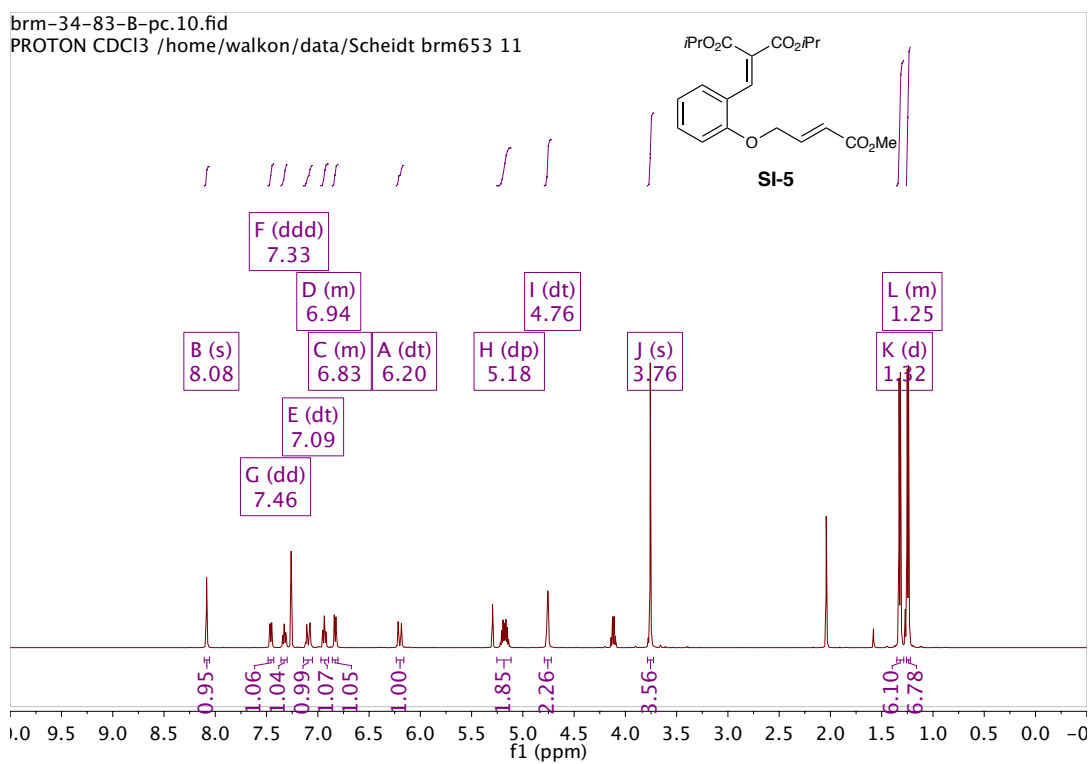


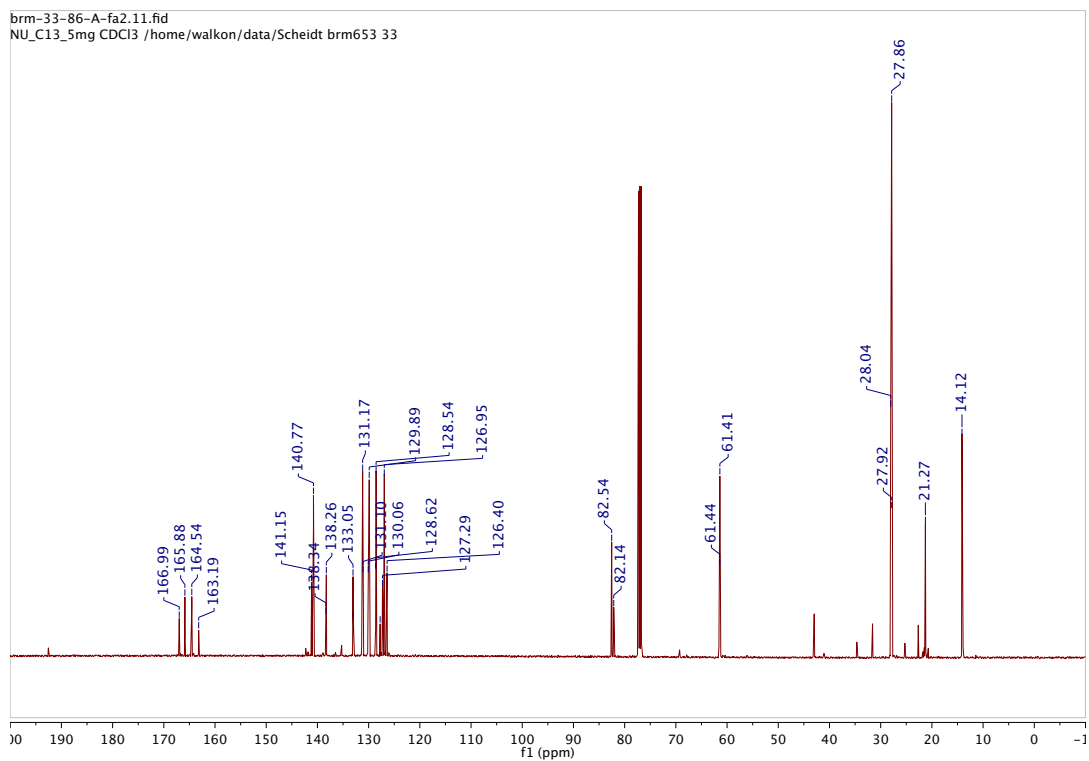
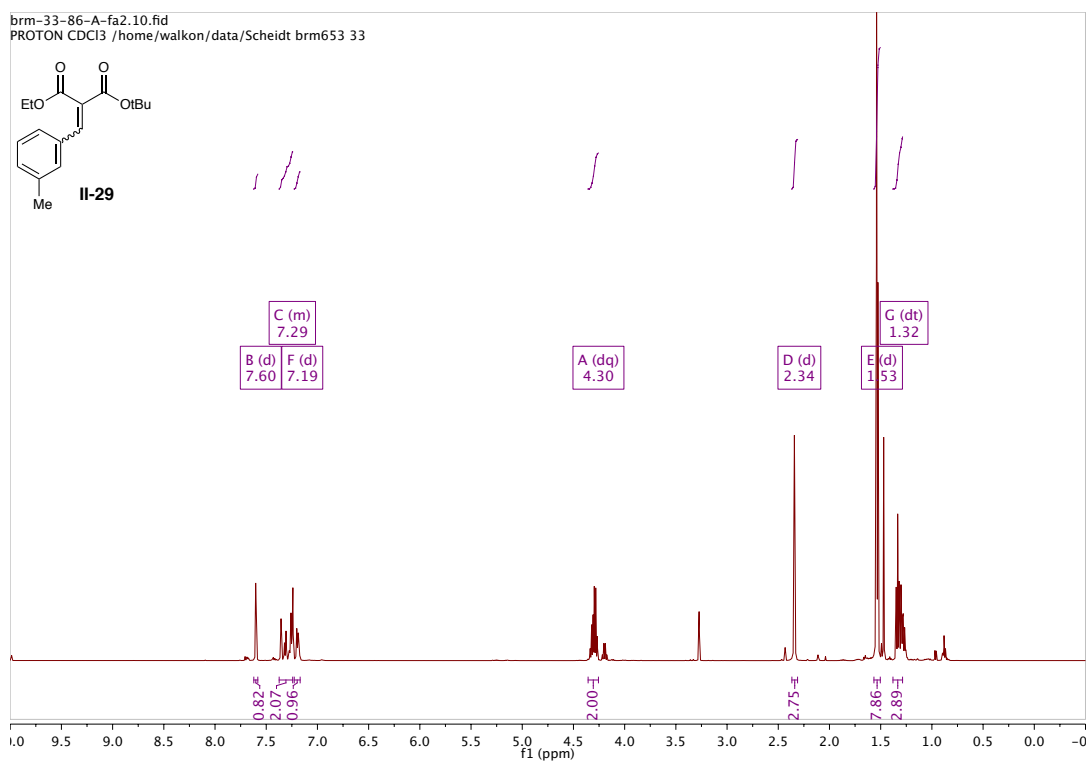


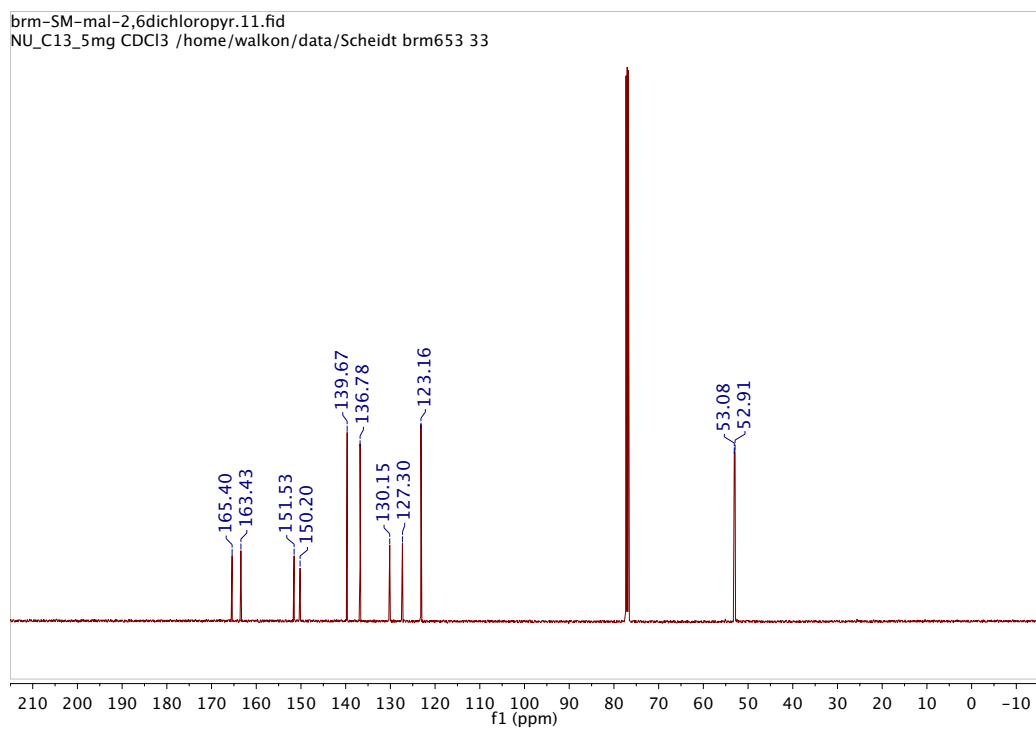
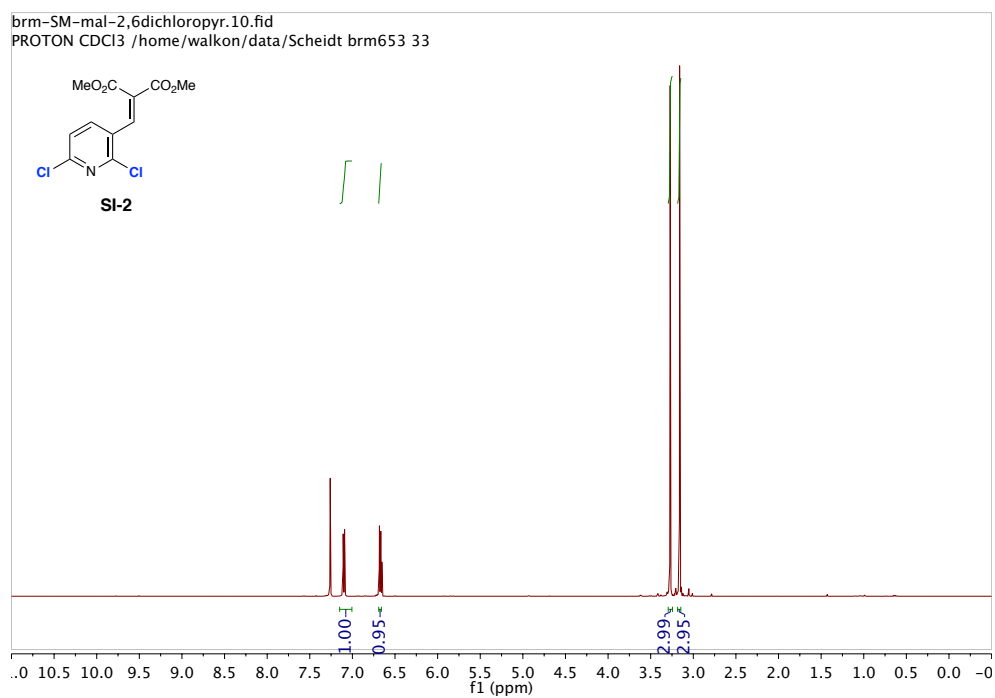






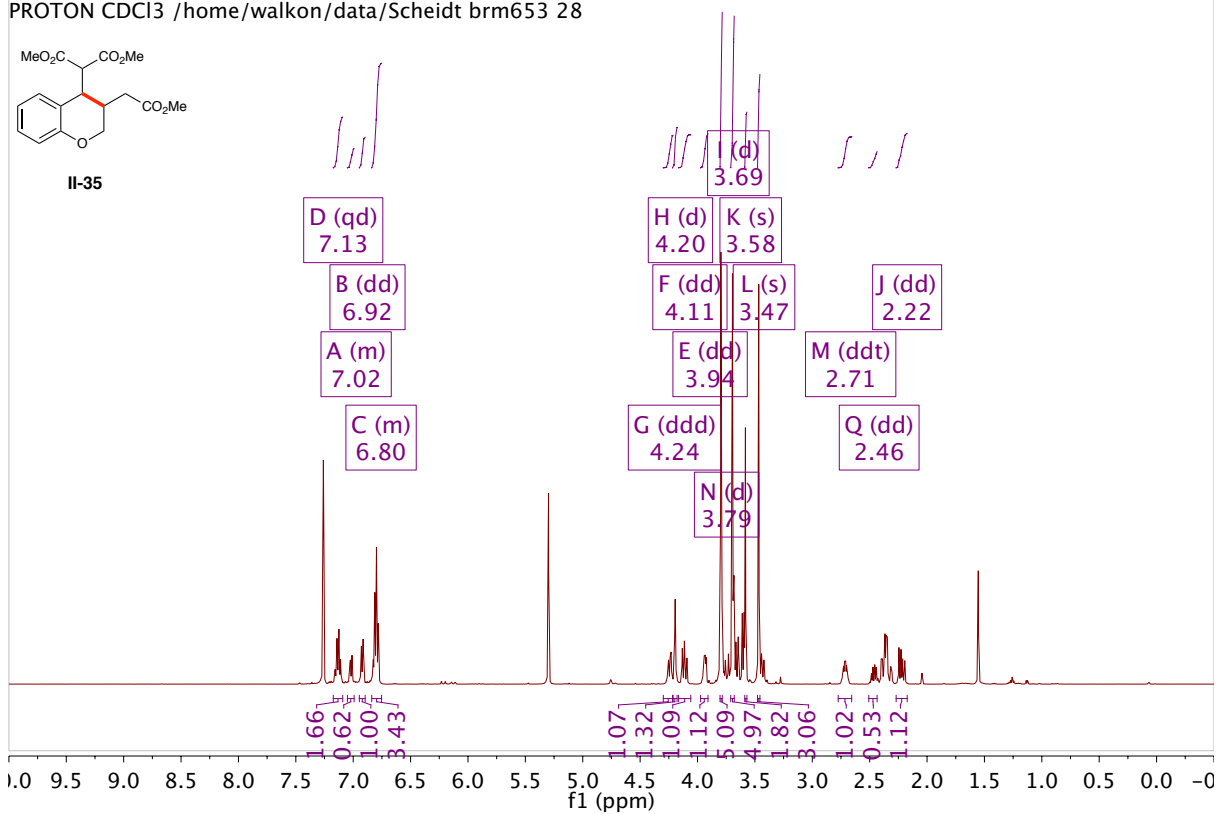
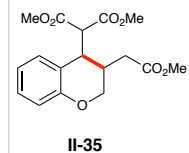


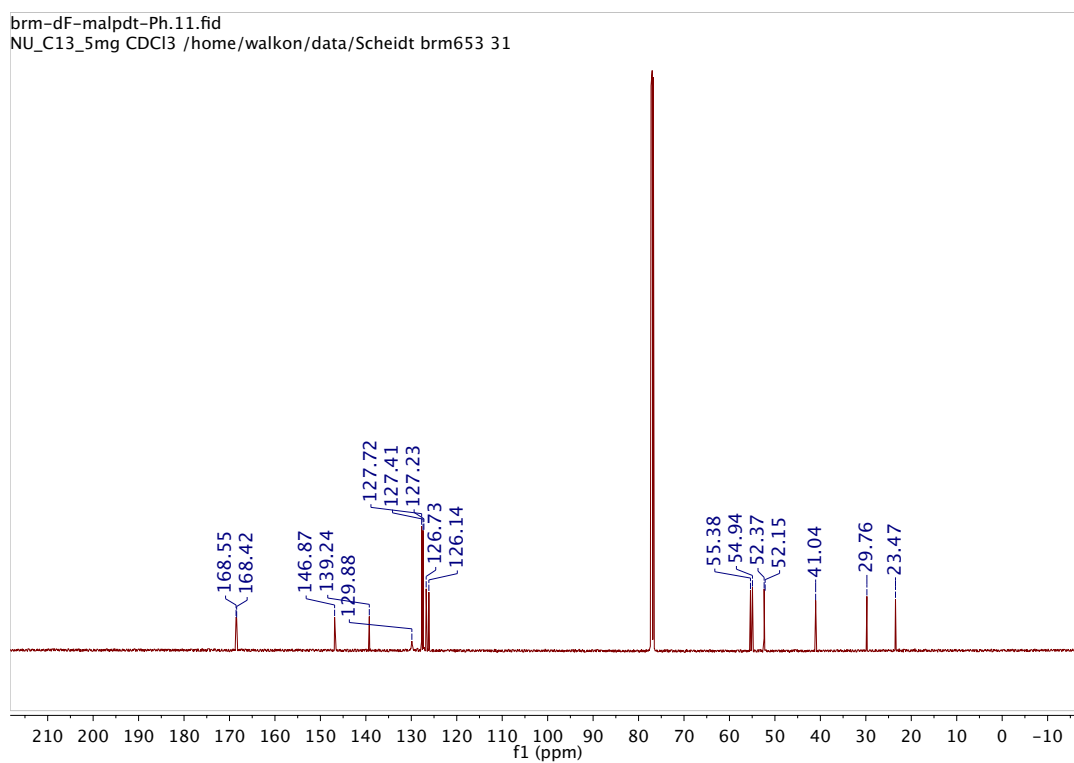
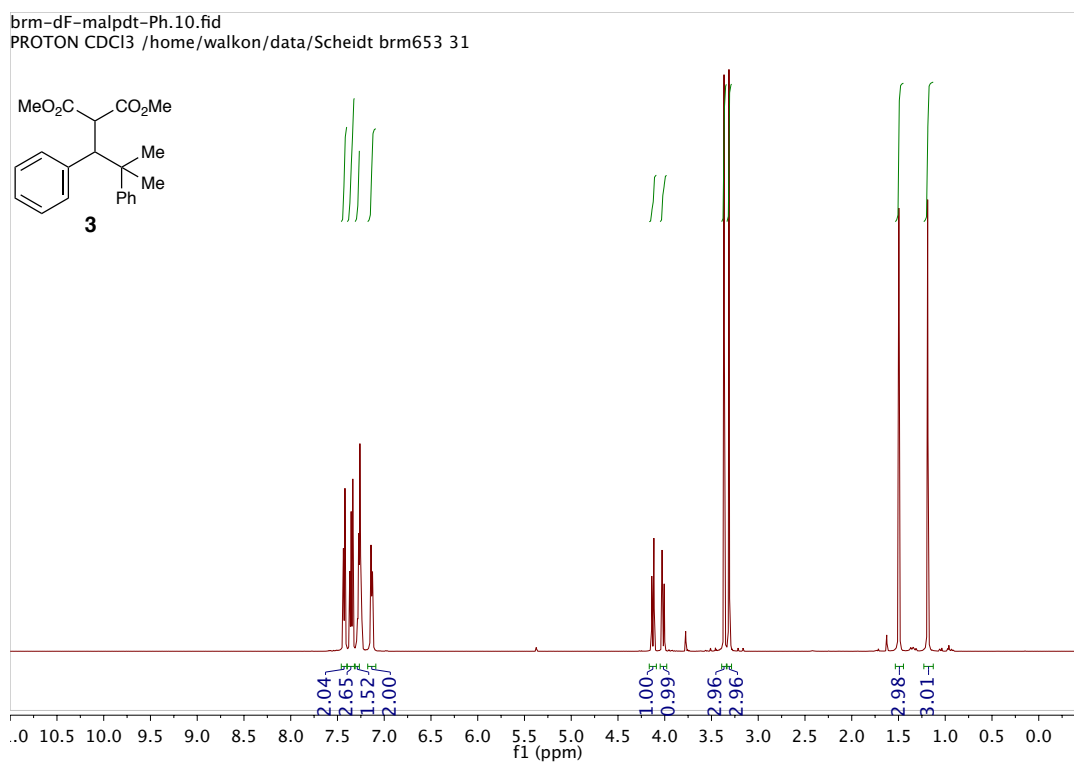


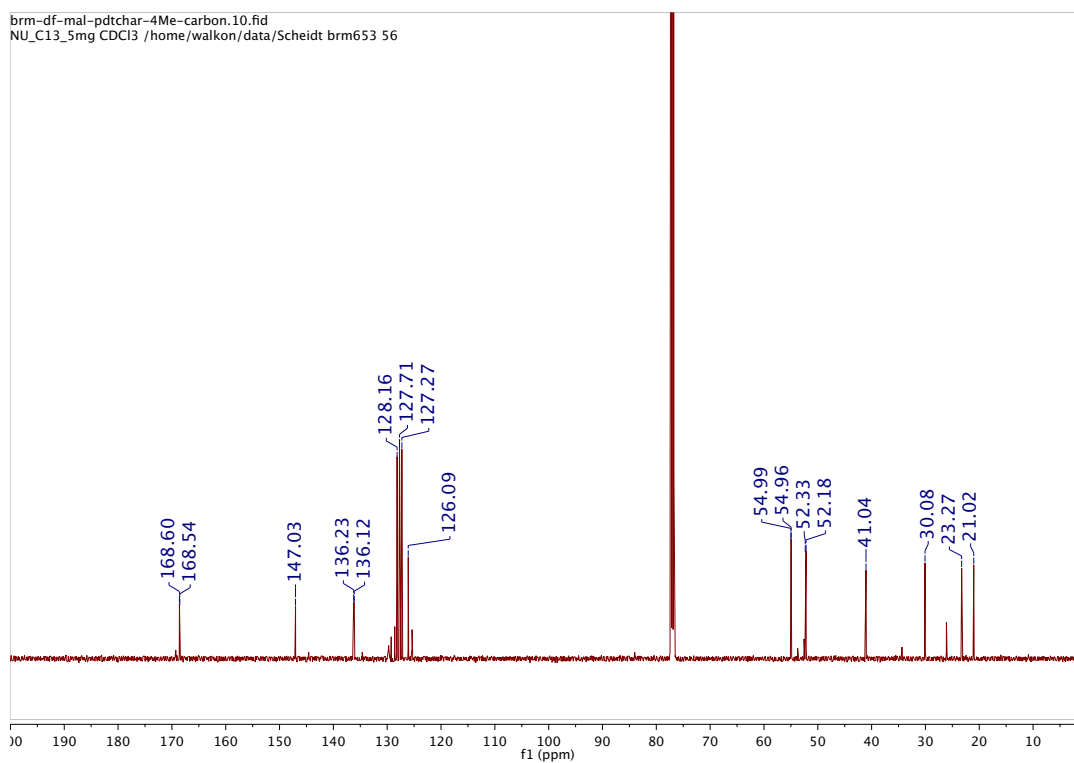
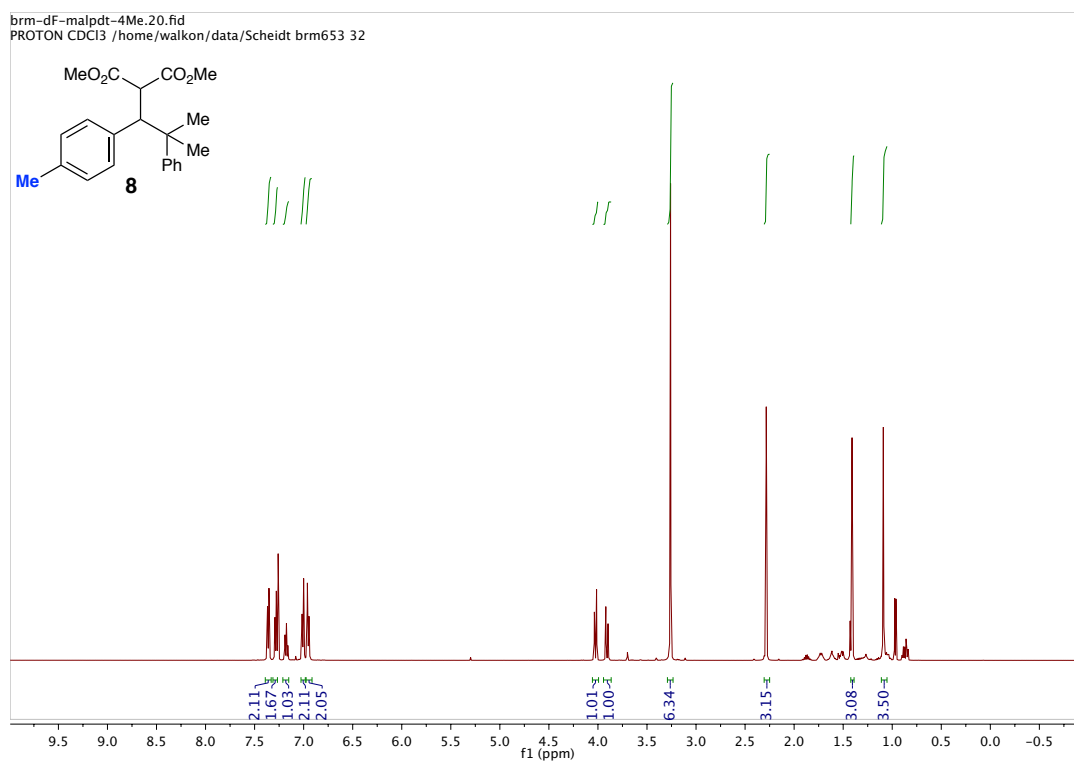


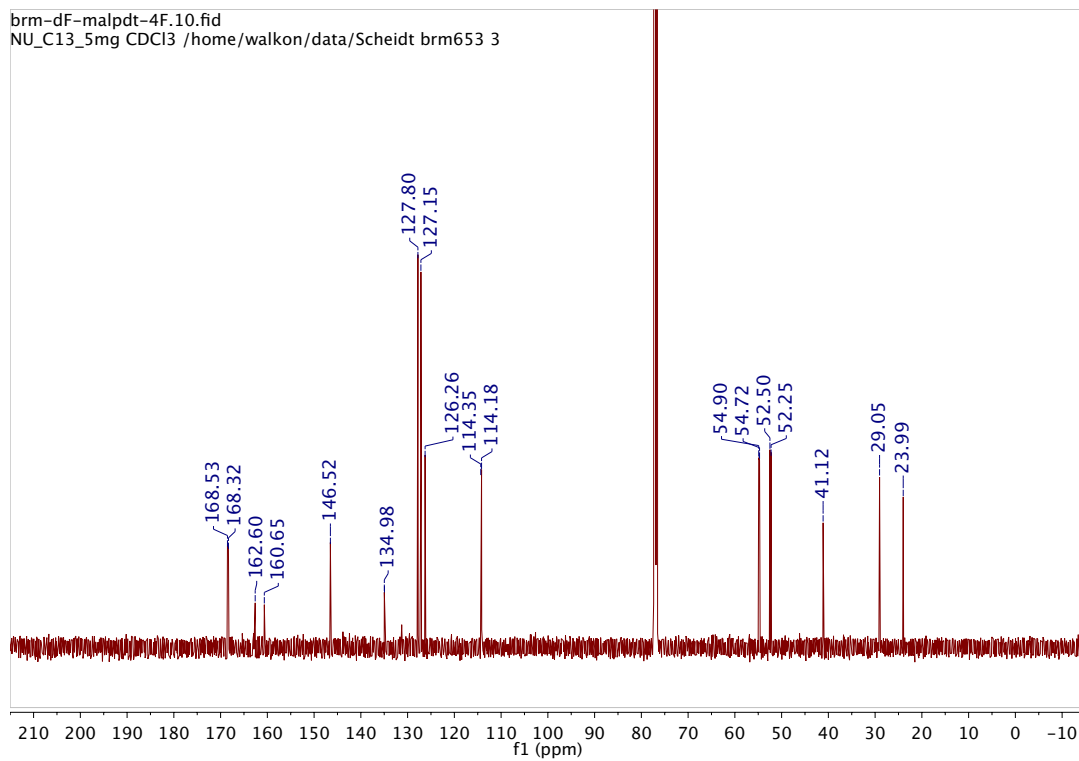
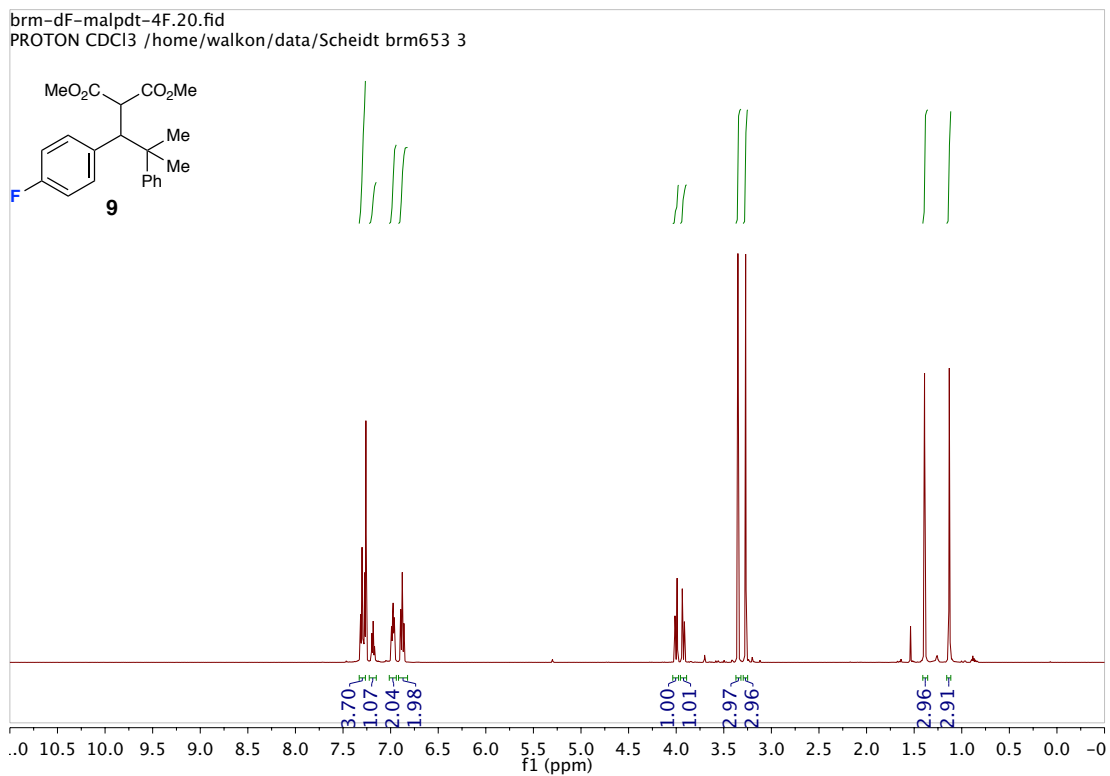
brm-34-70-pc-A.10.fid

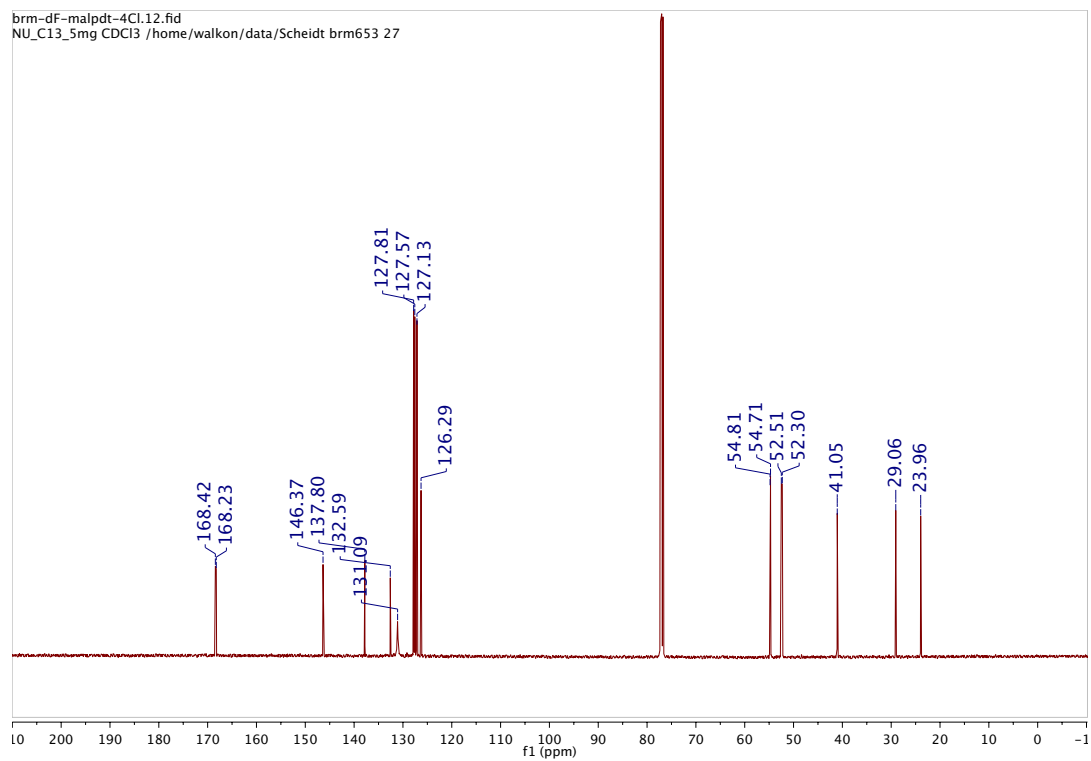
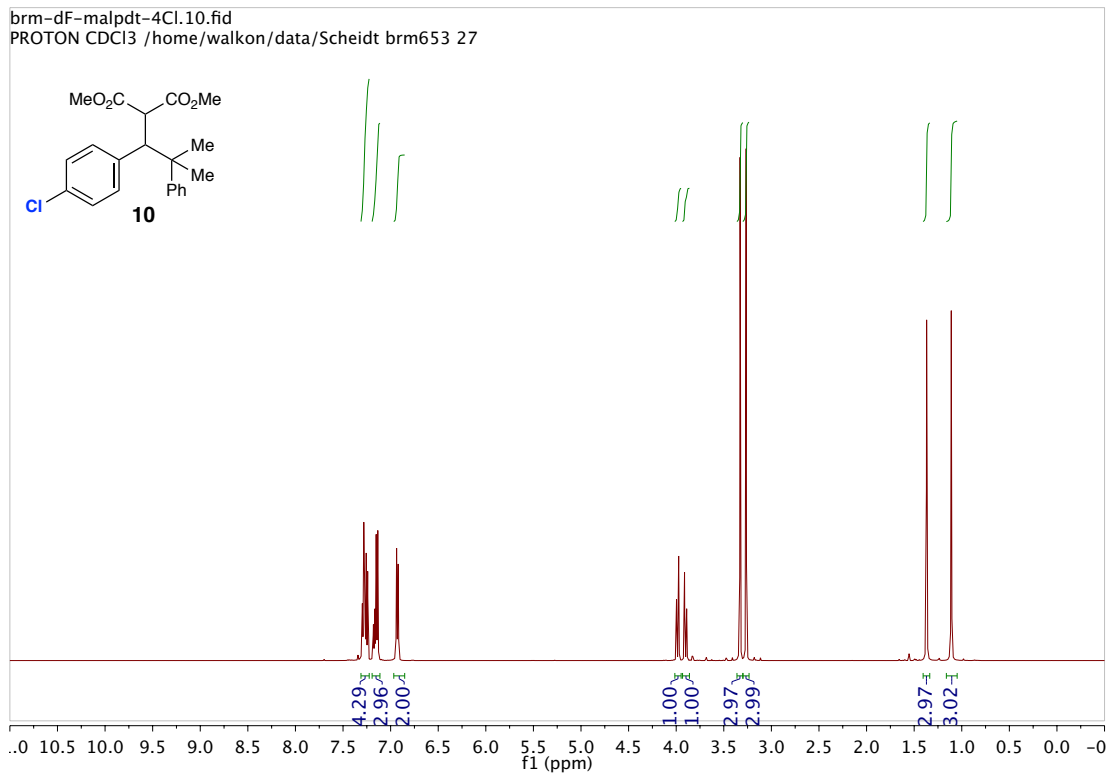
PROTON CDCl3 /home/walkon/data/Scheidt brm653 28

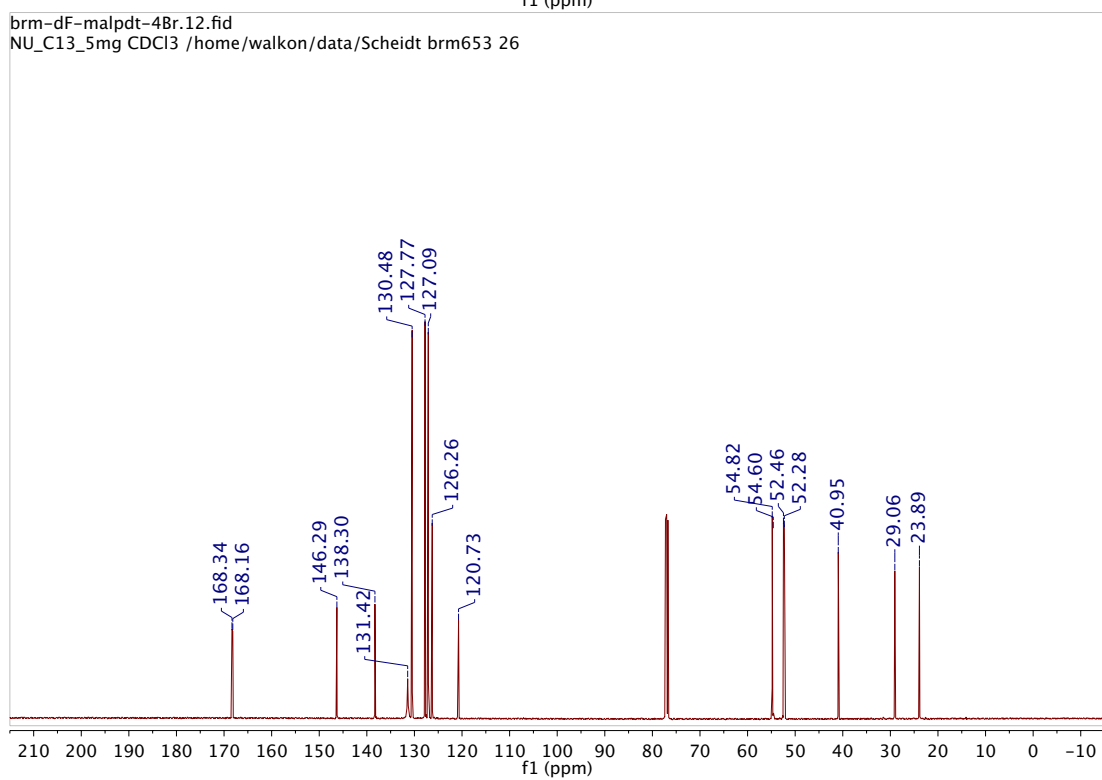
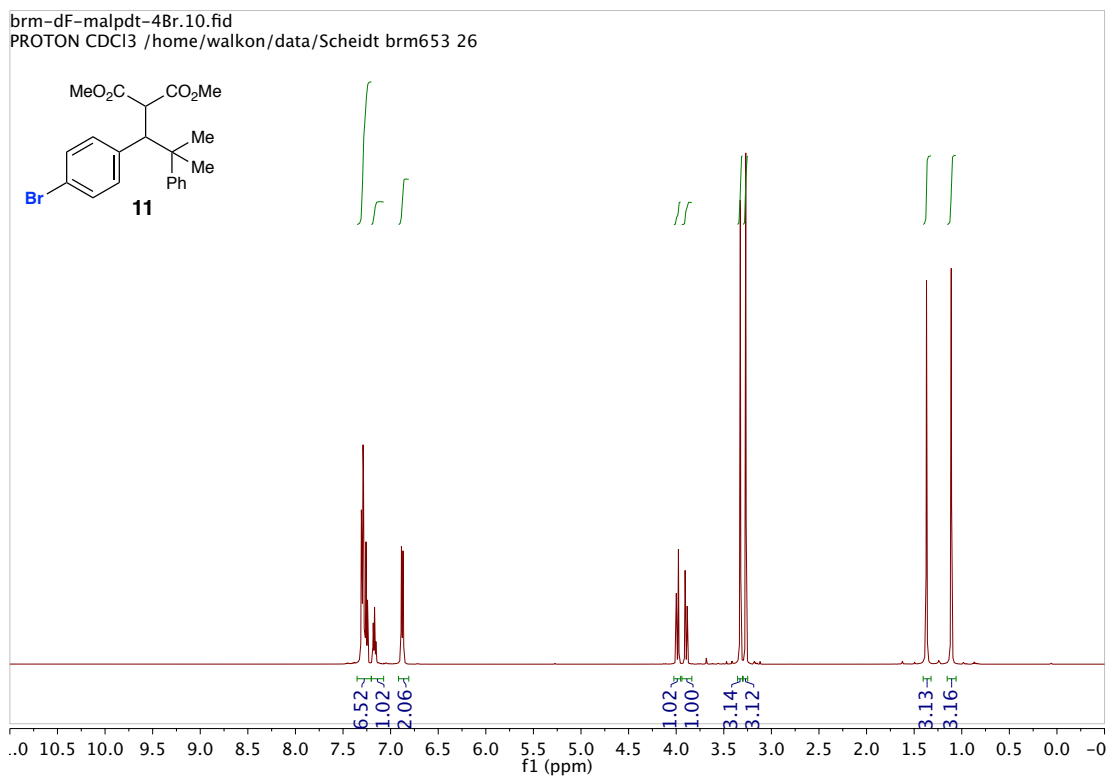


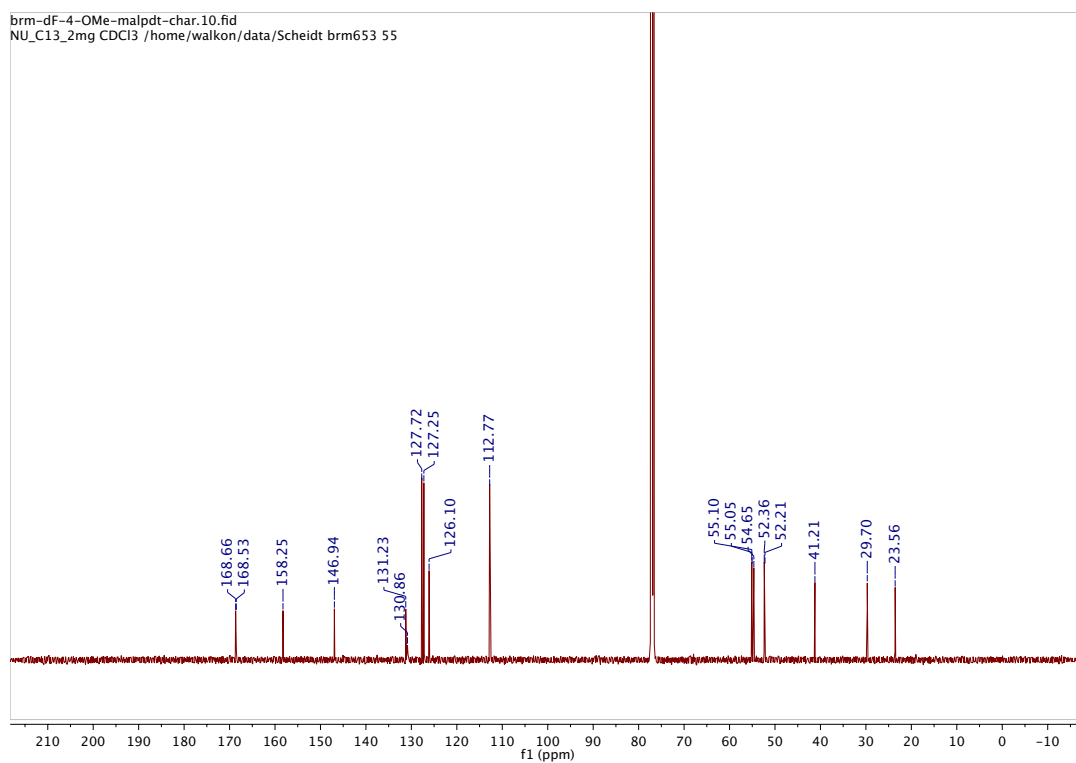
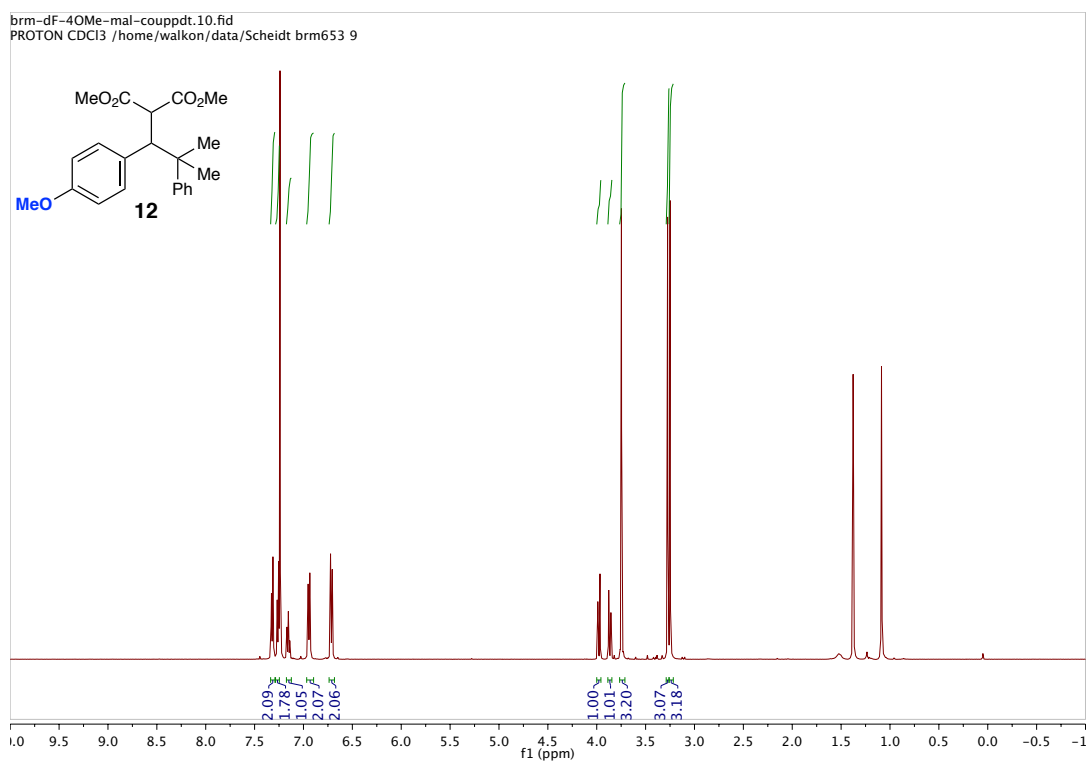


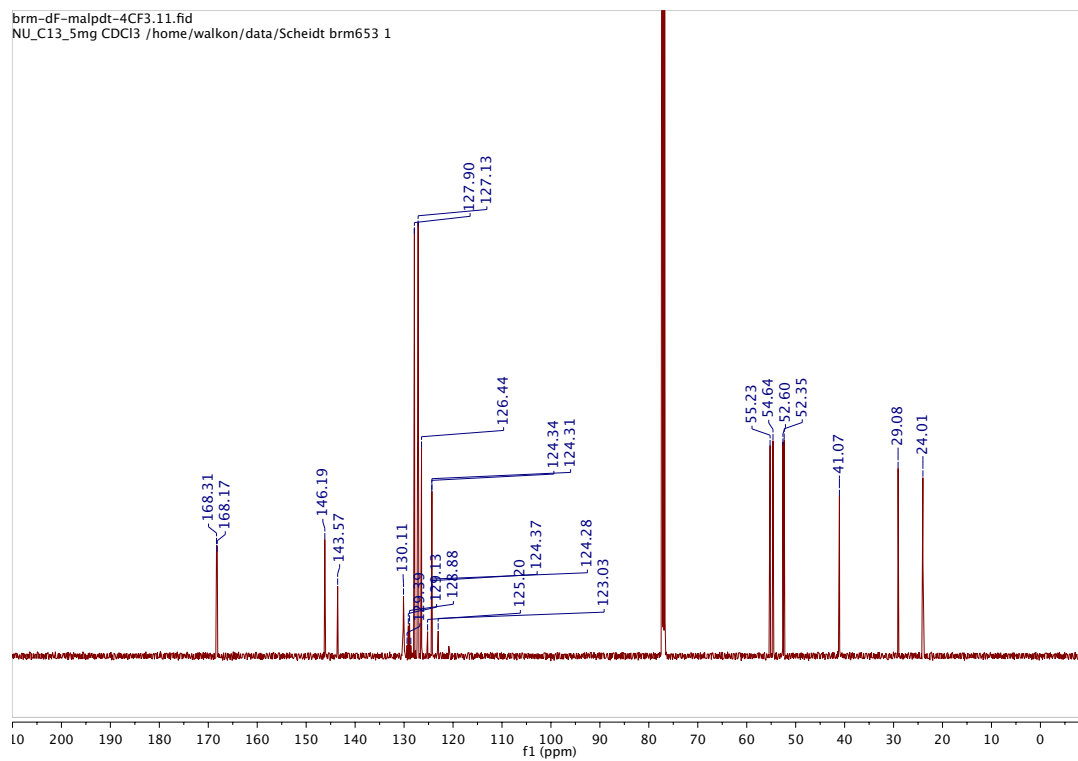
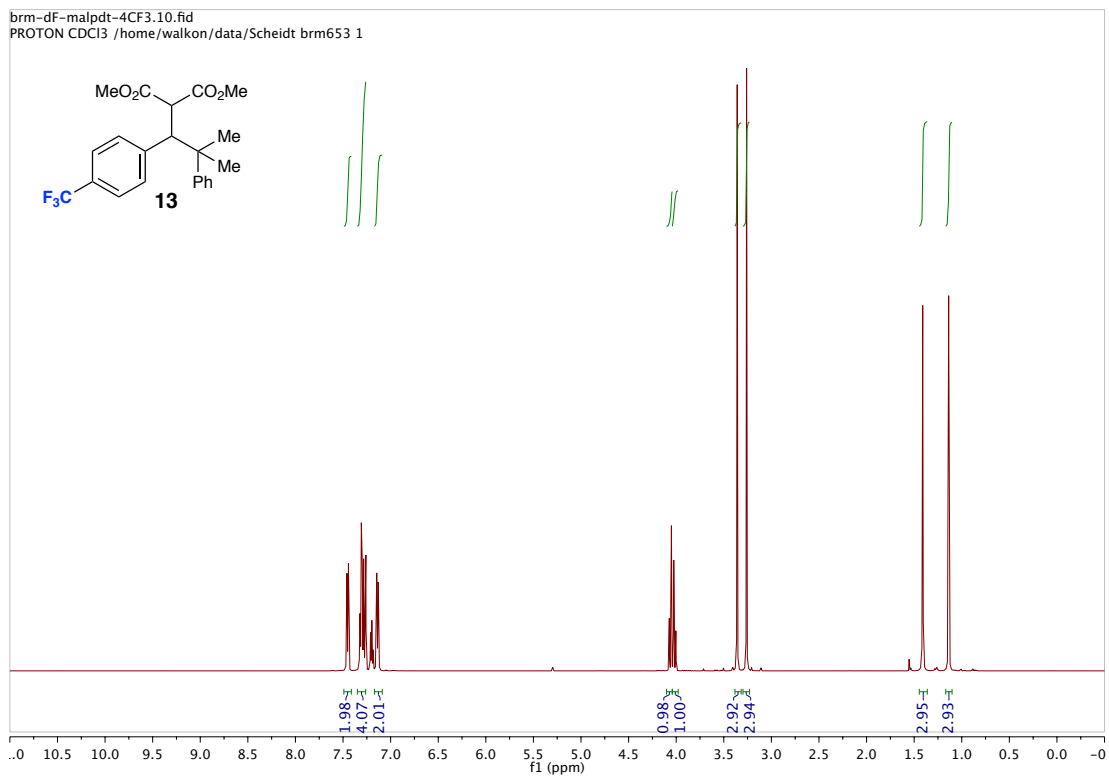


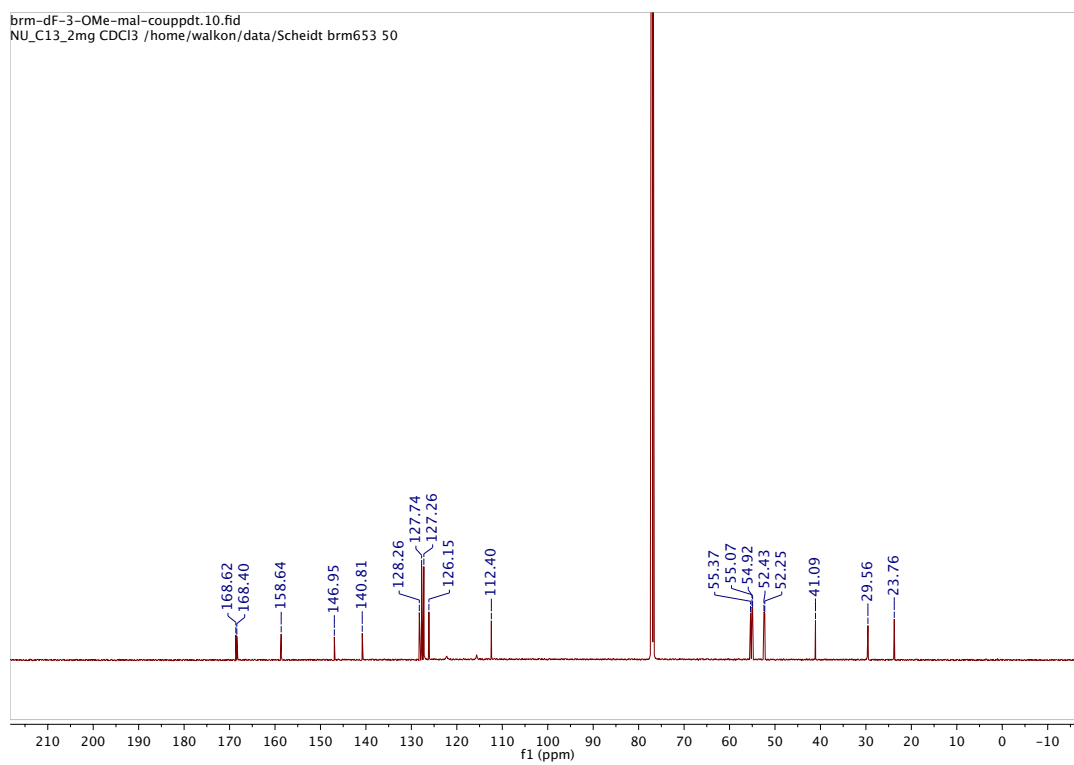
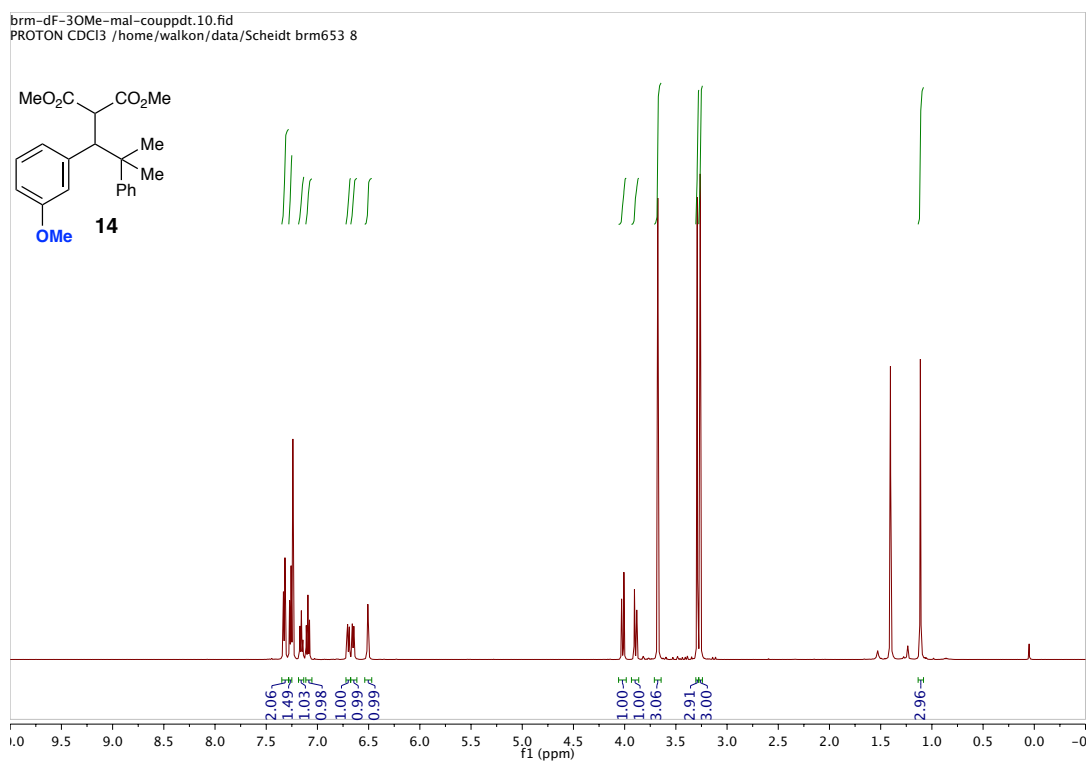


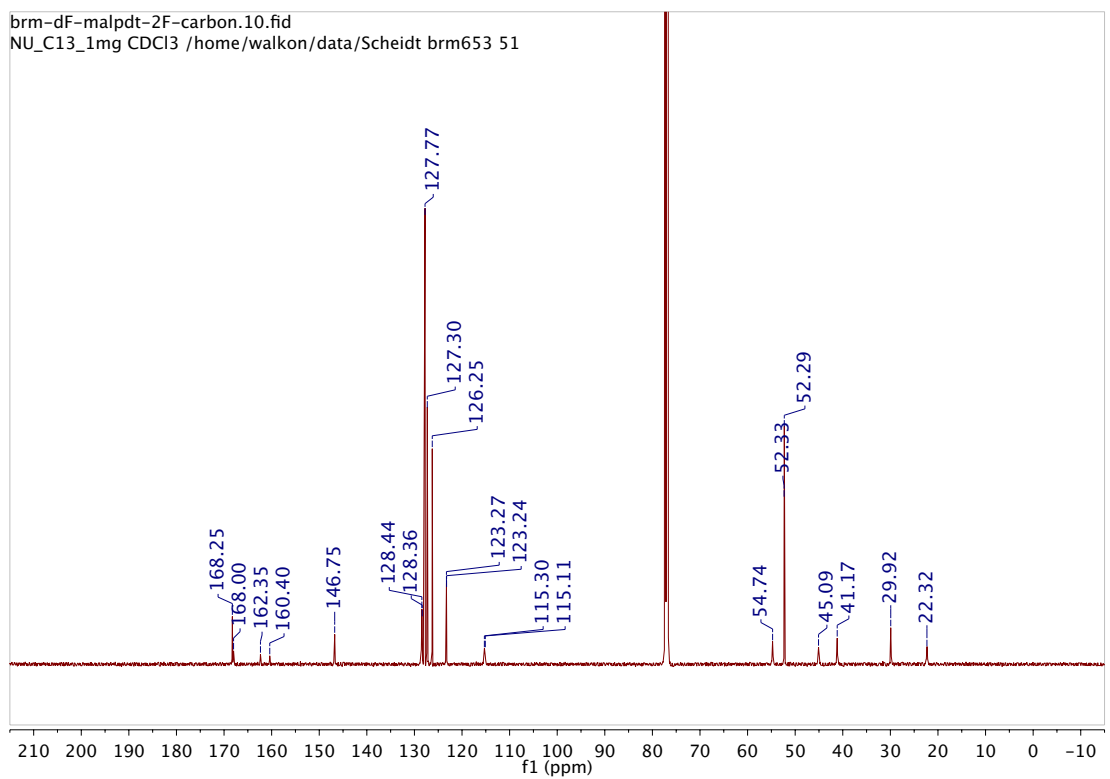
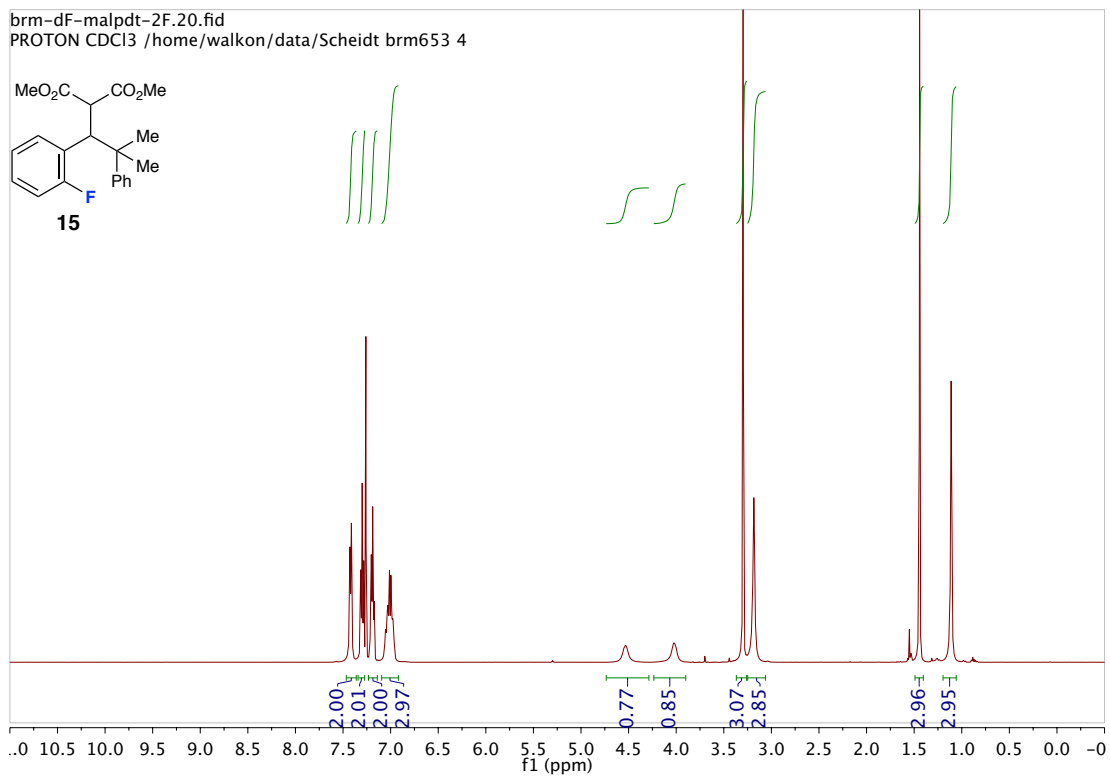


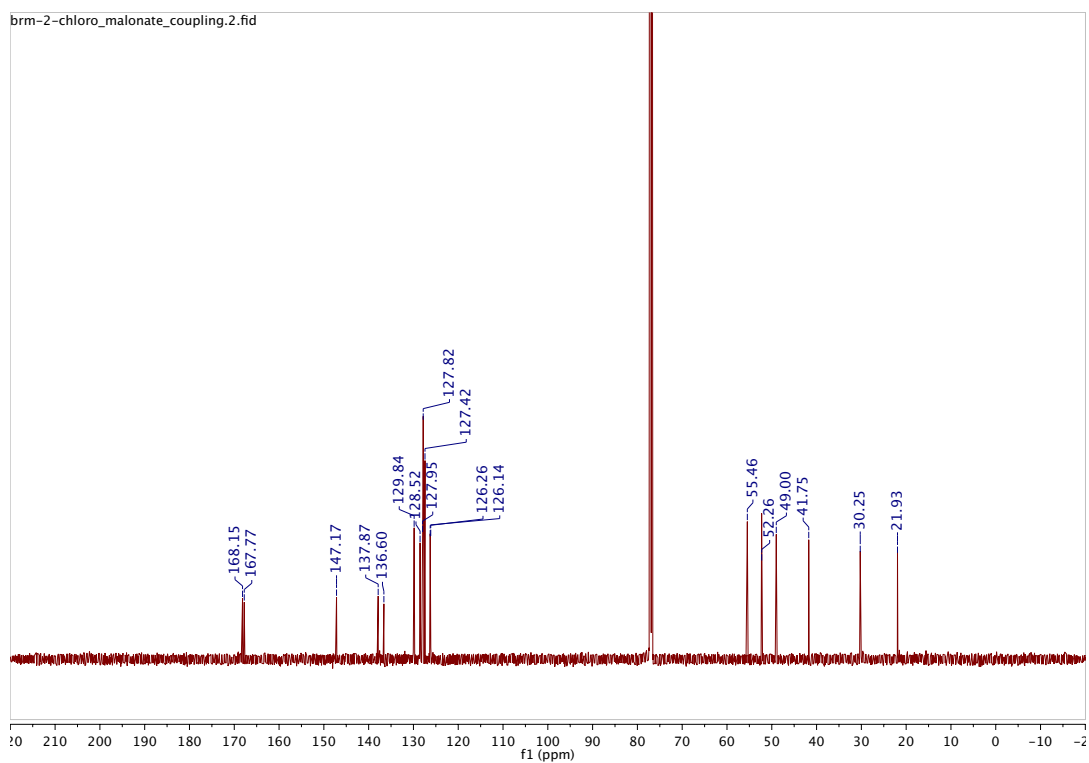
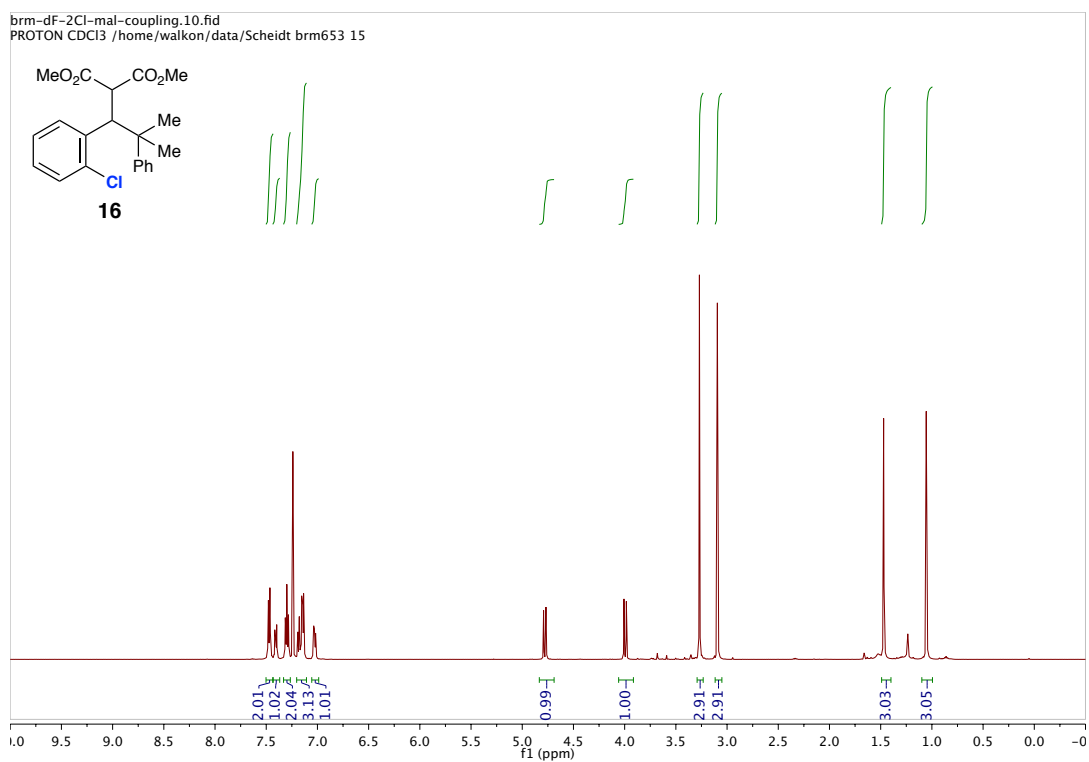


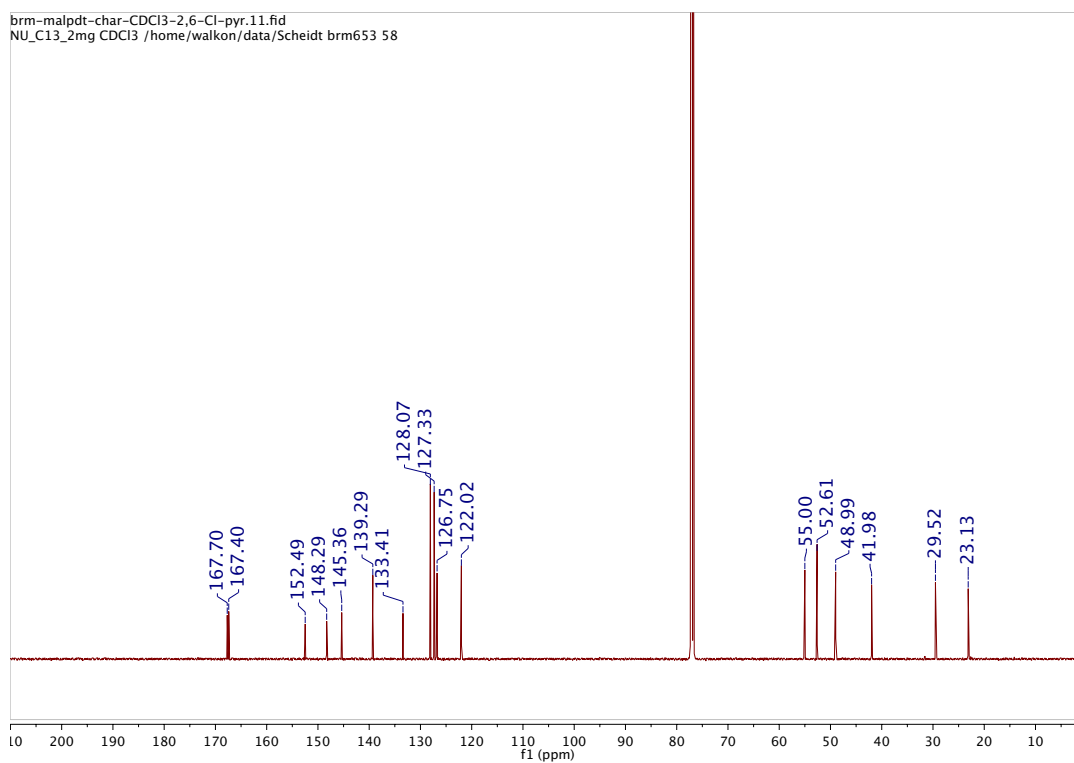
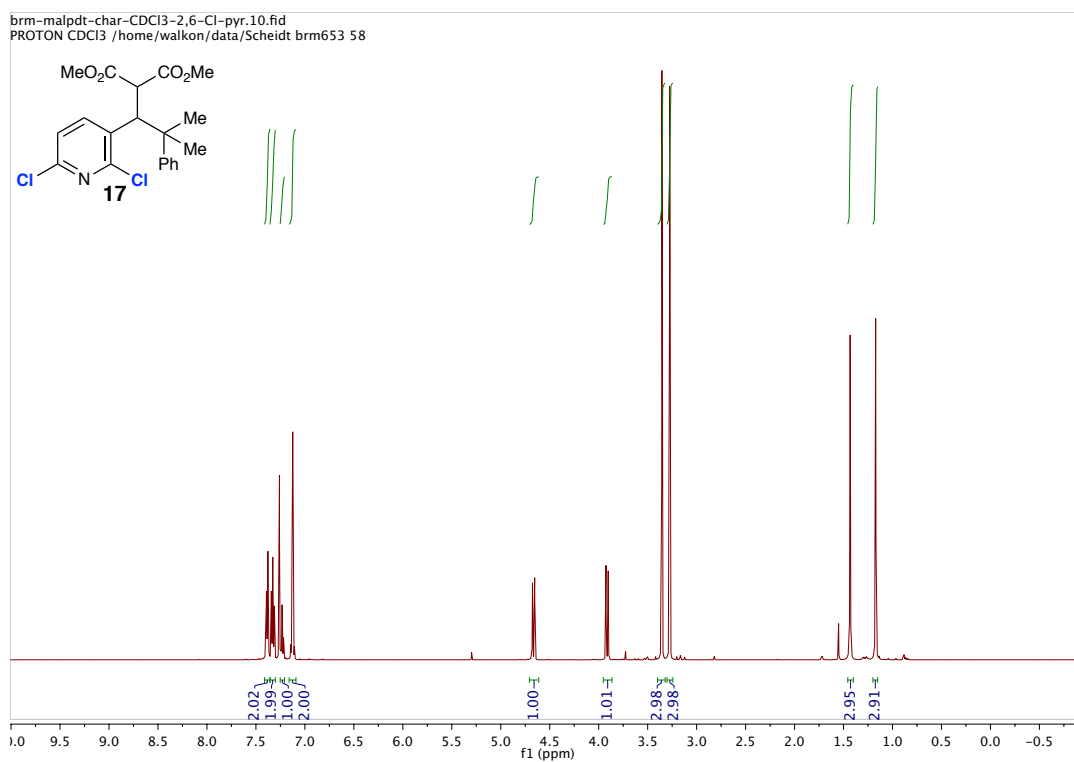


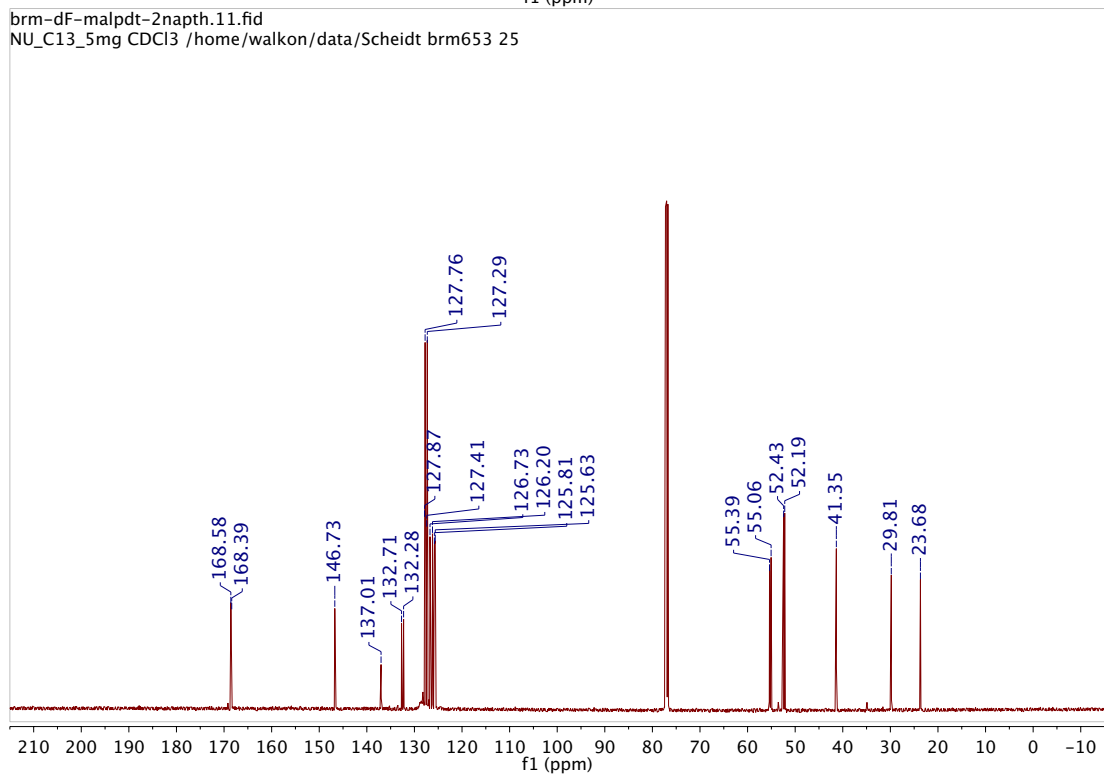
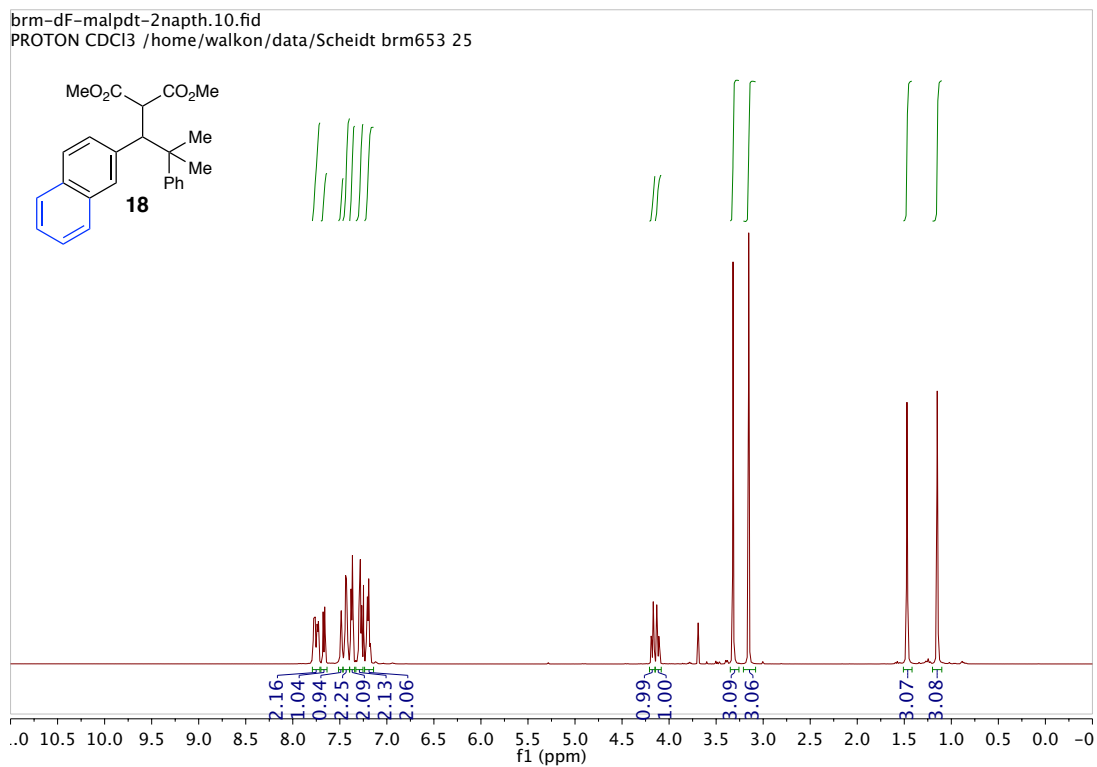


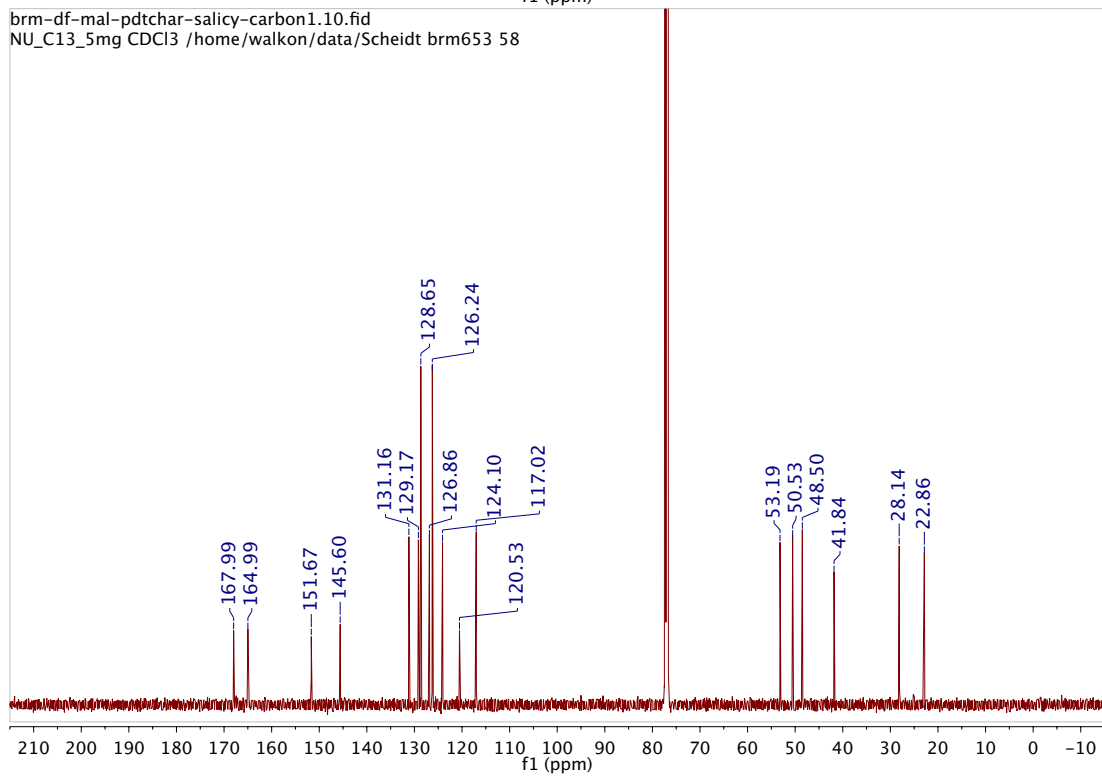
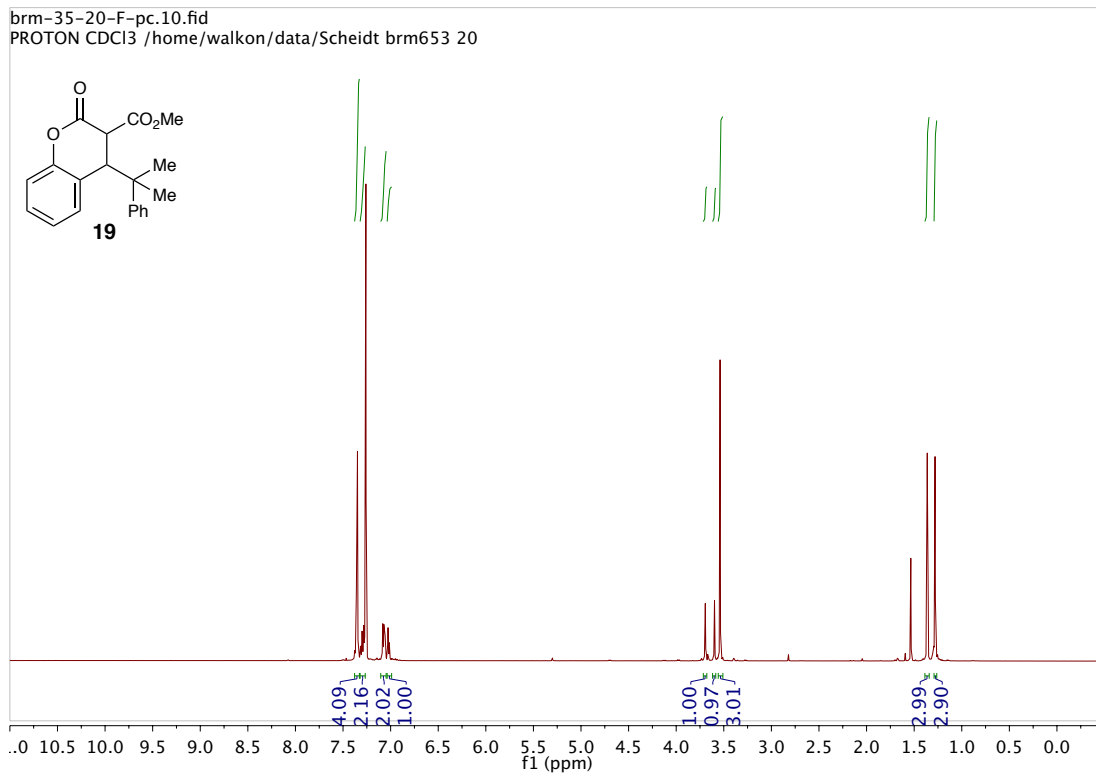


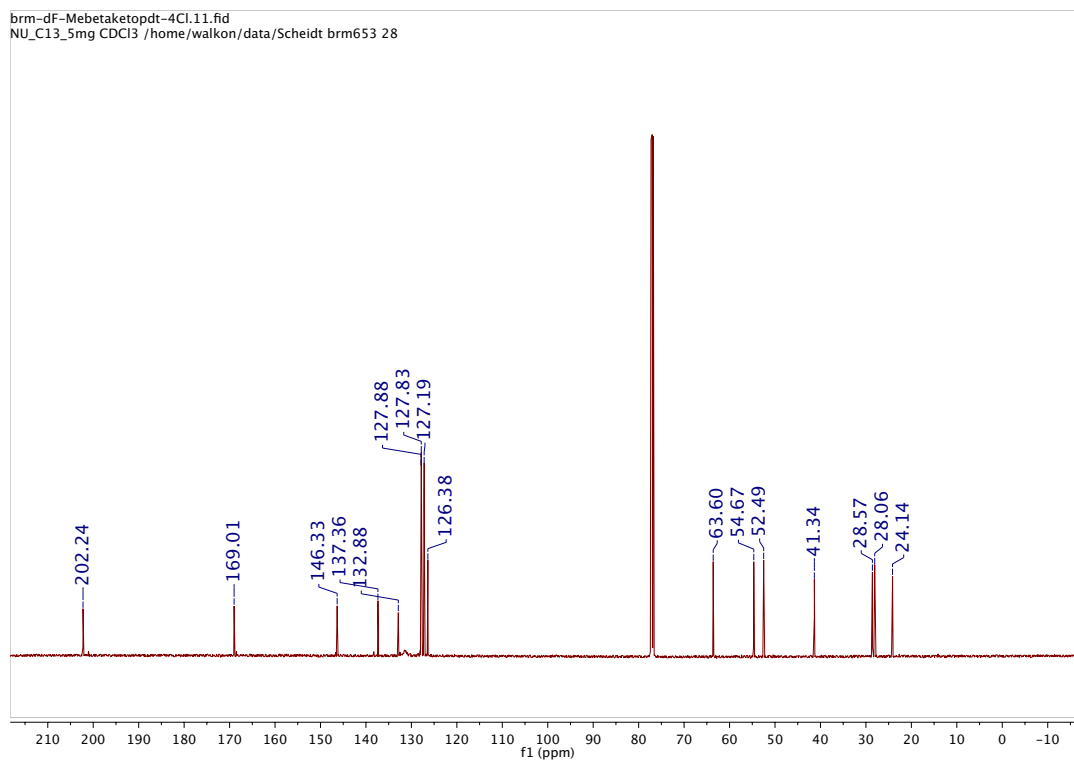
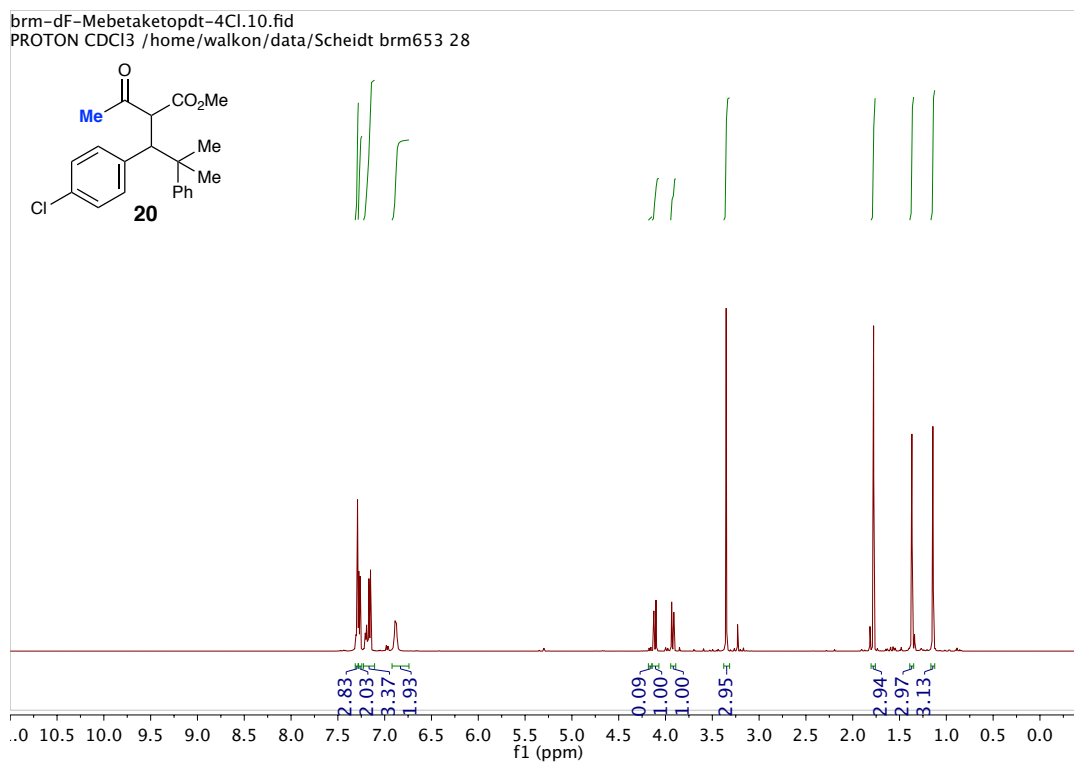


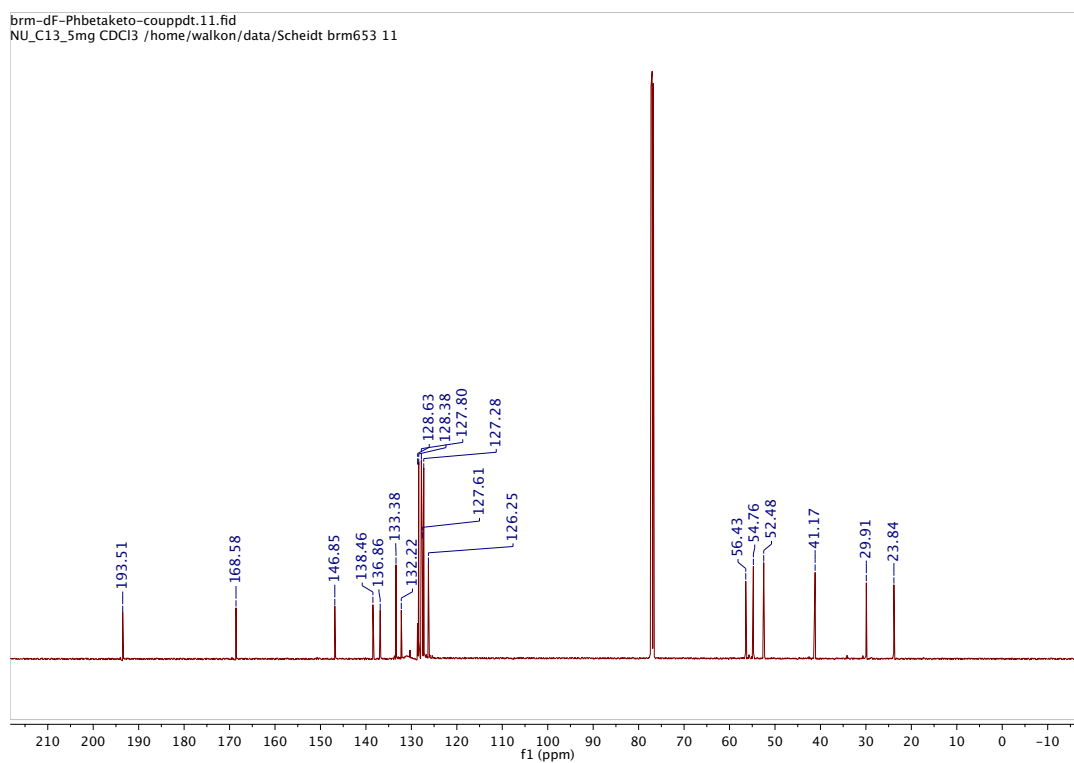
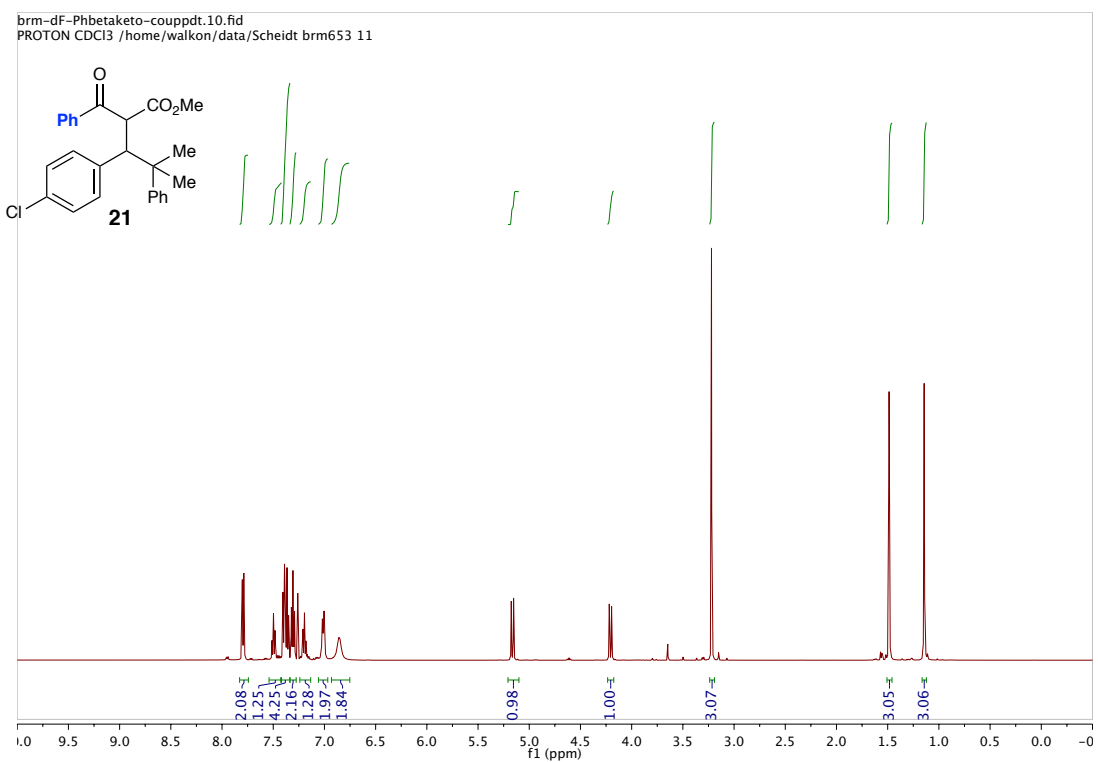


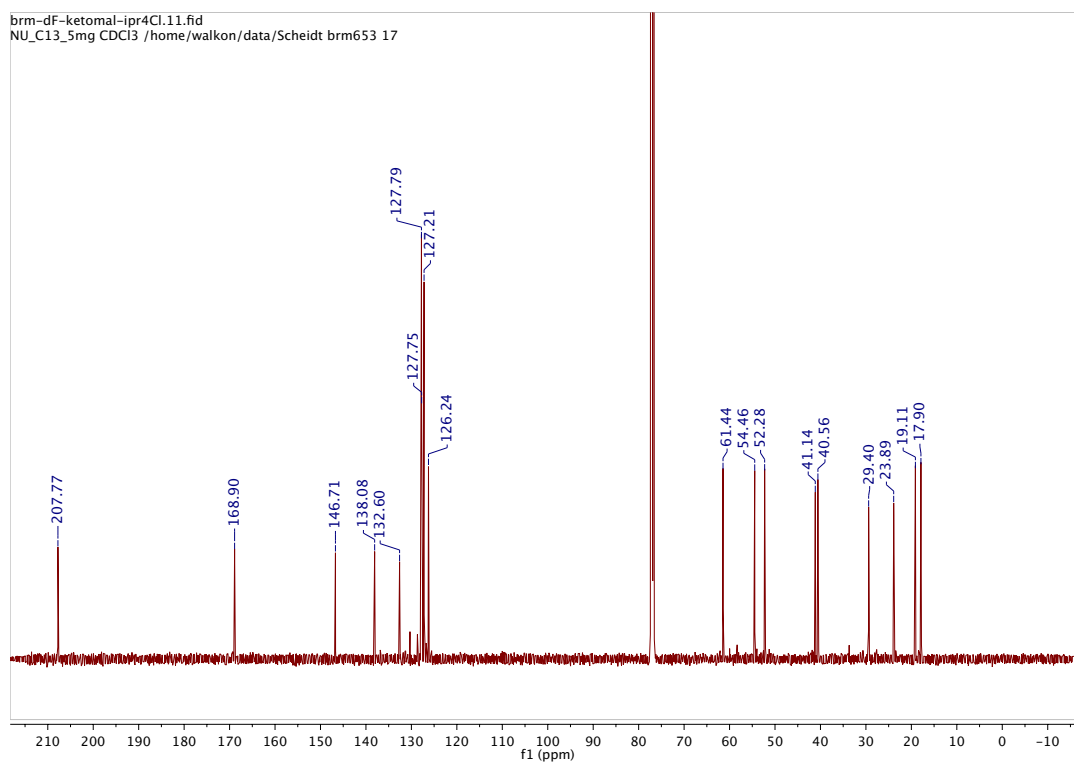
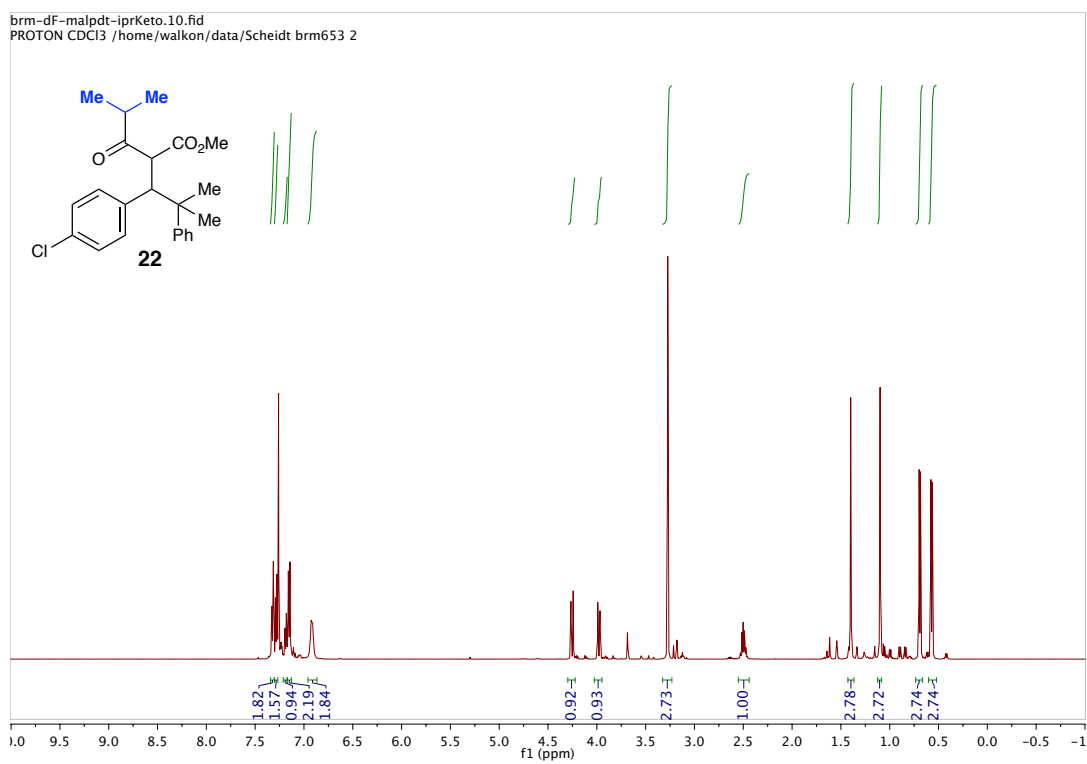


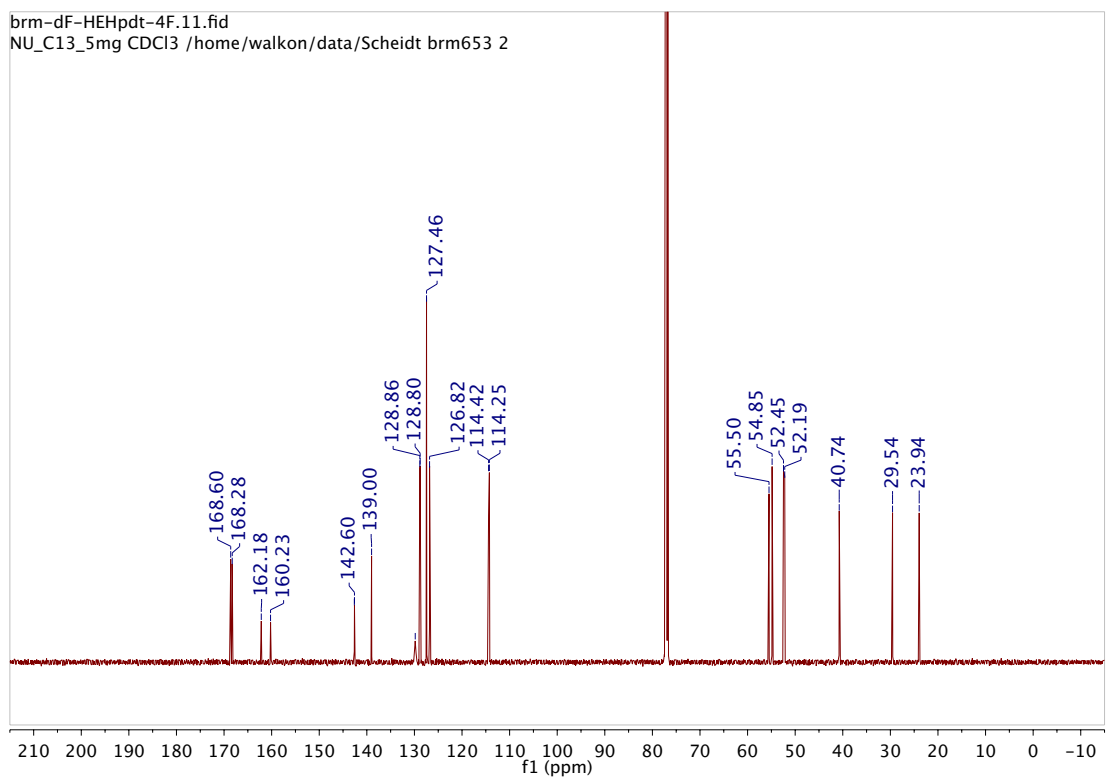
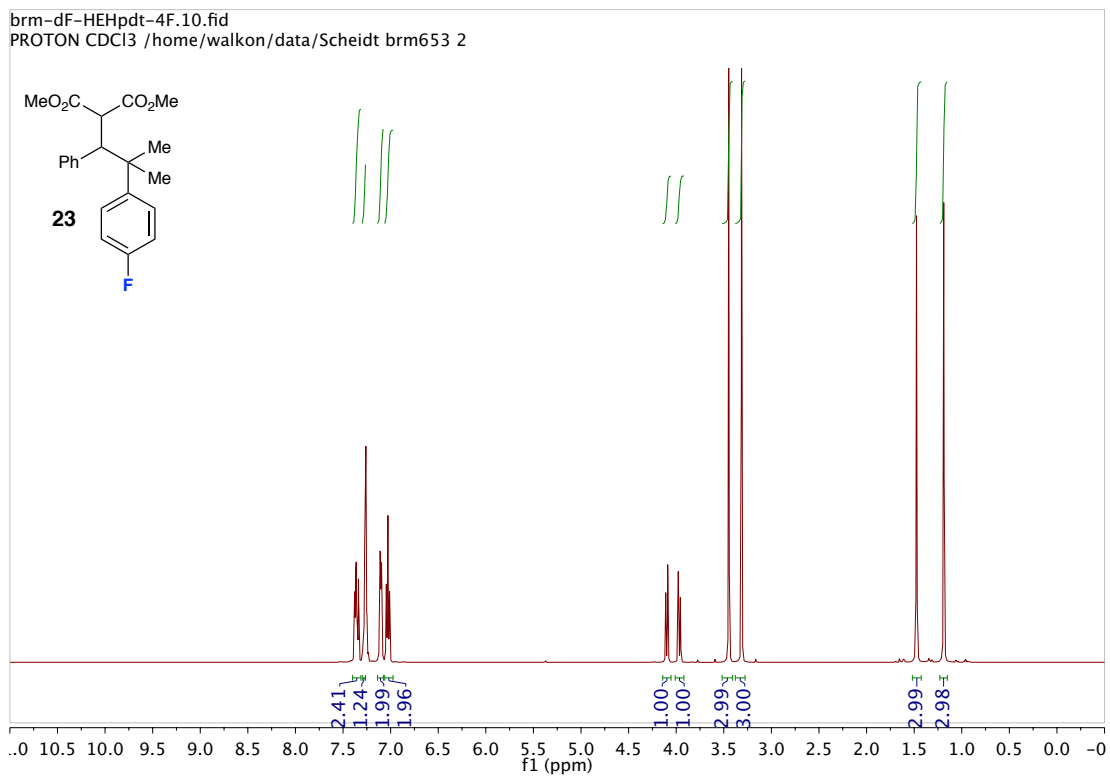


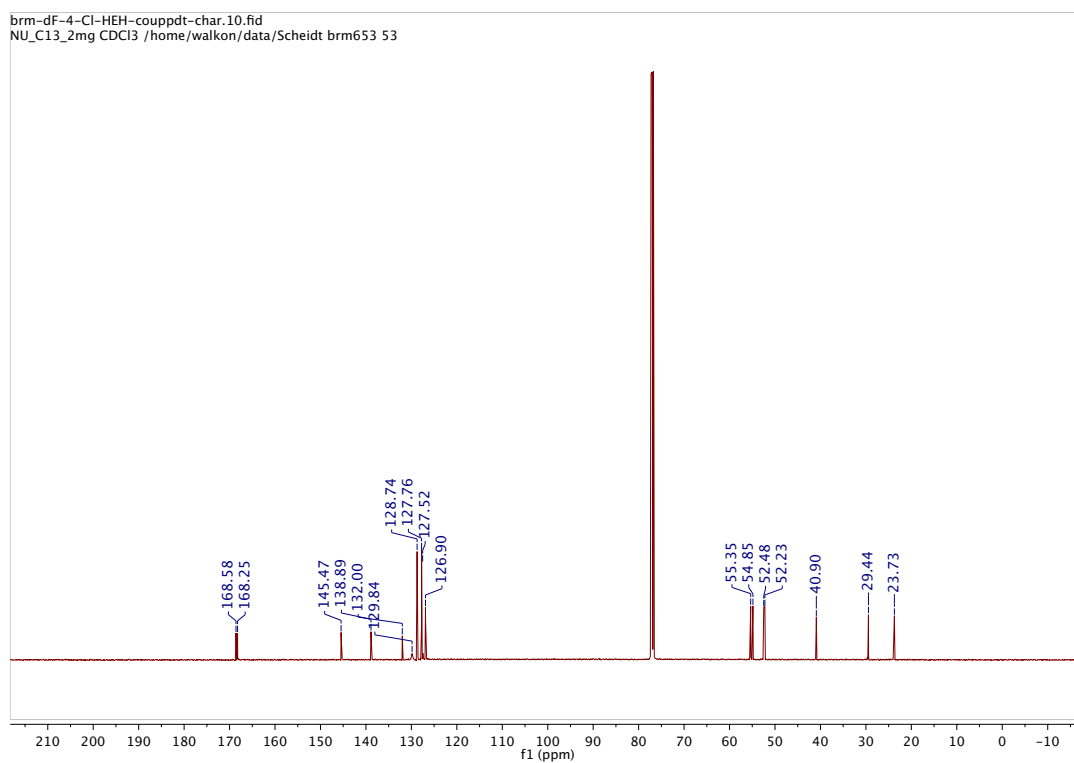
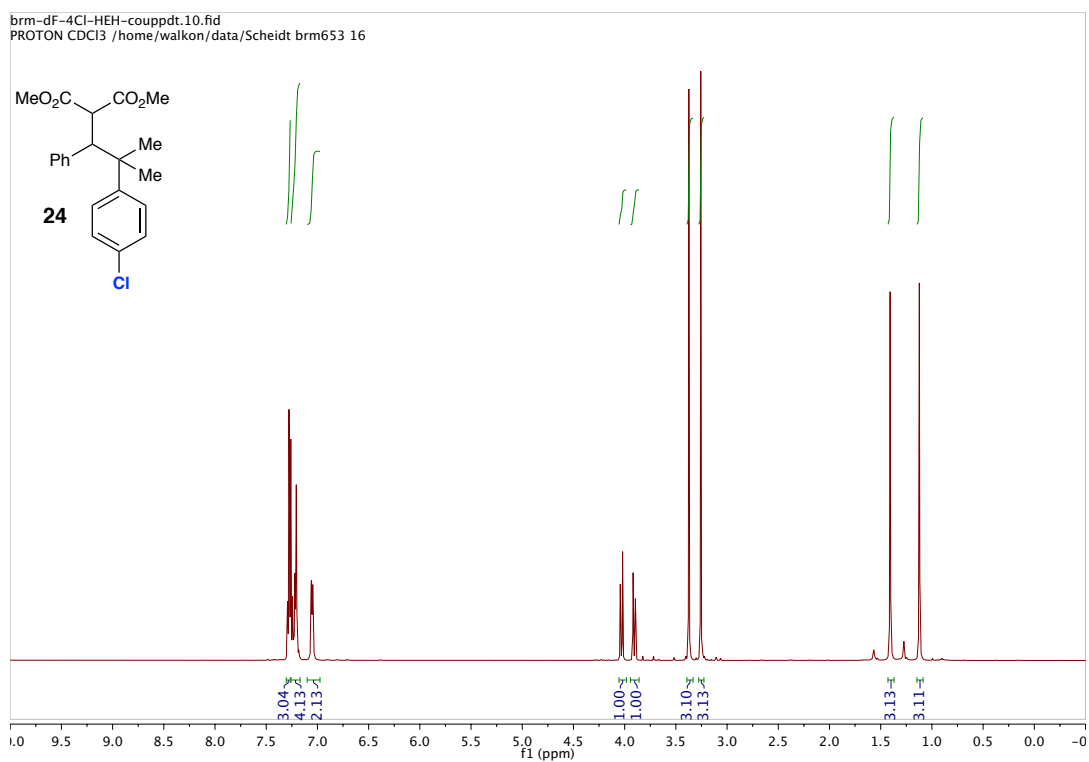


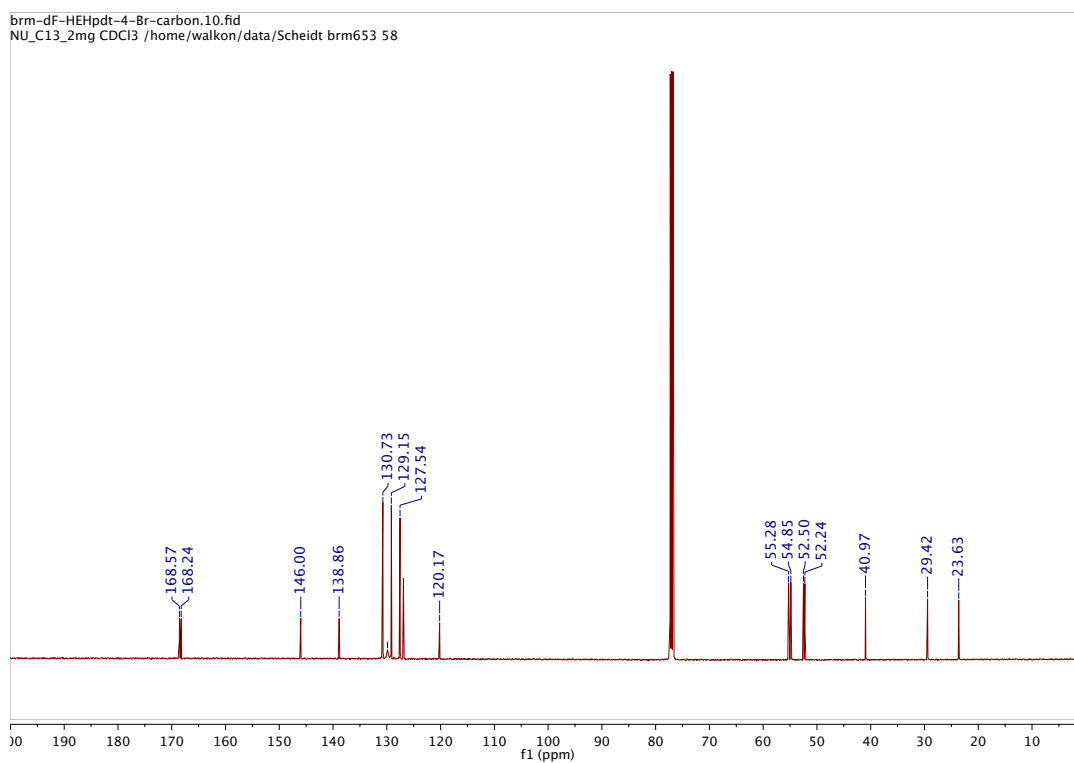
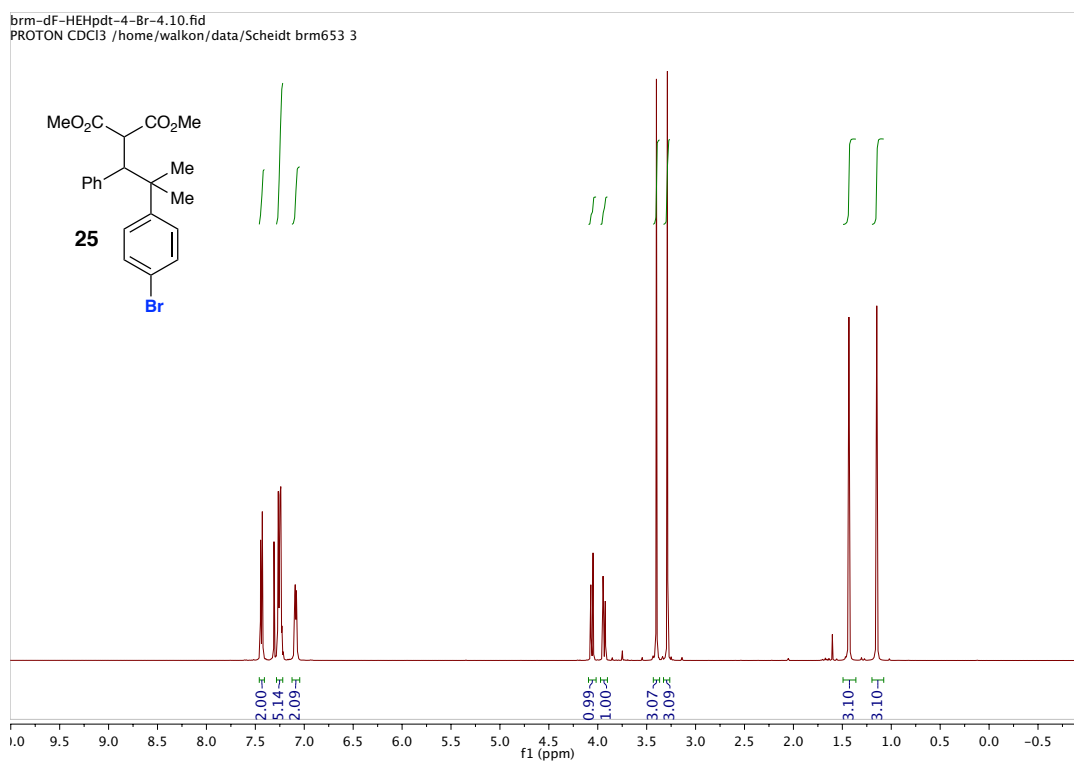


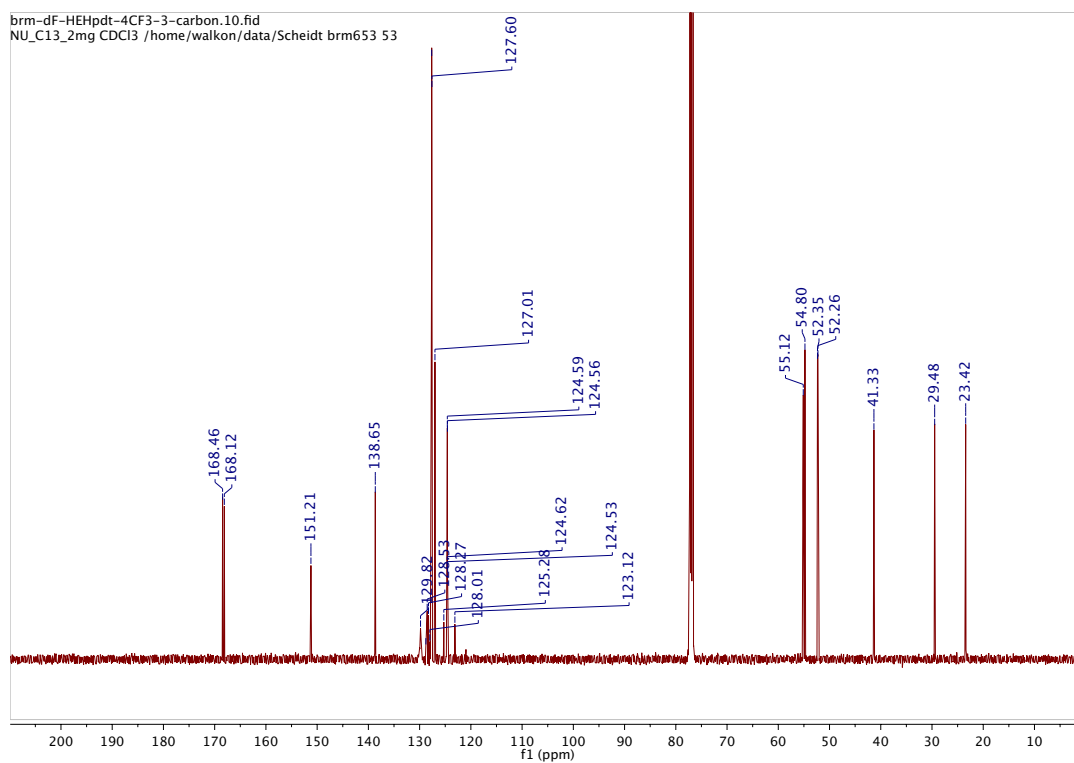
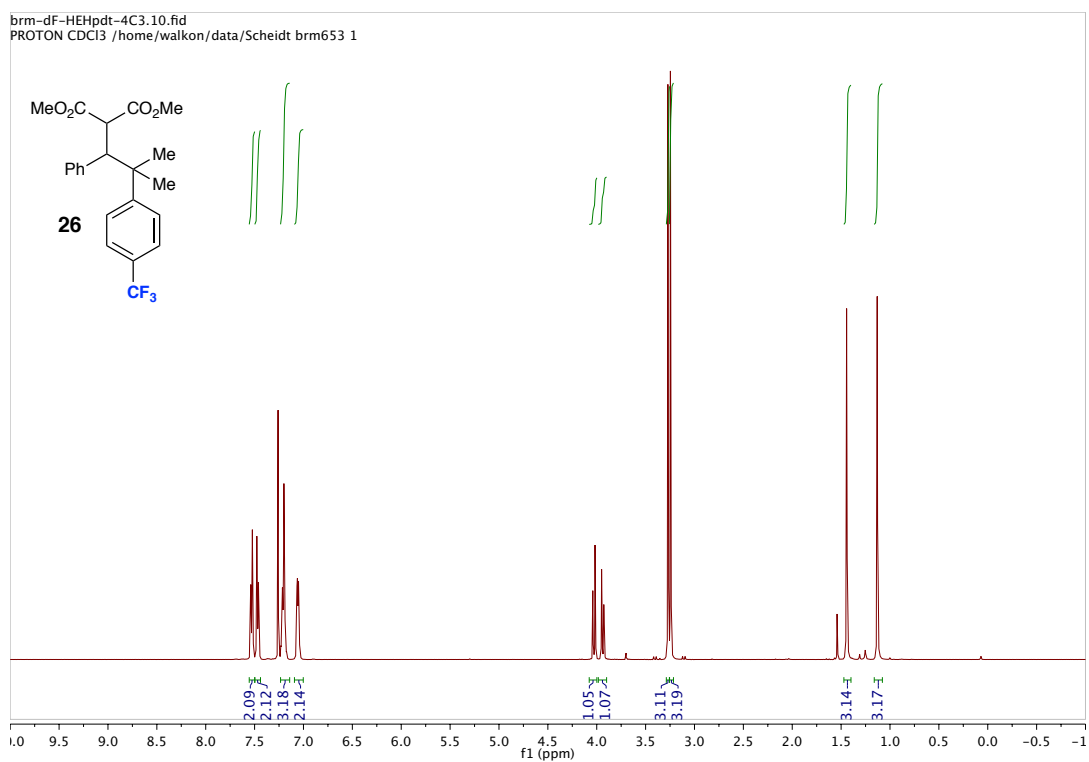


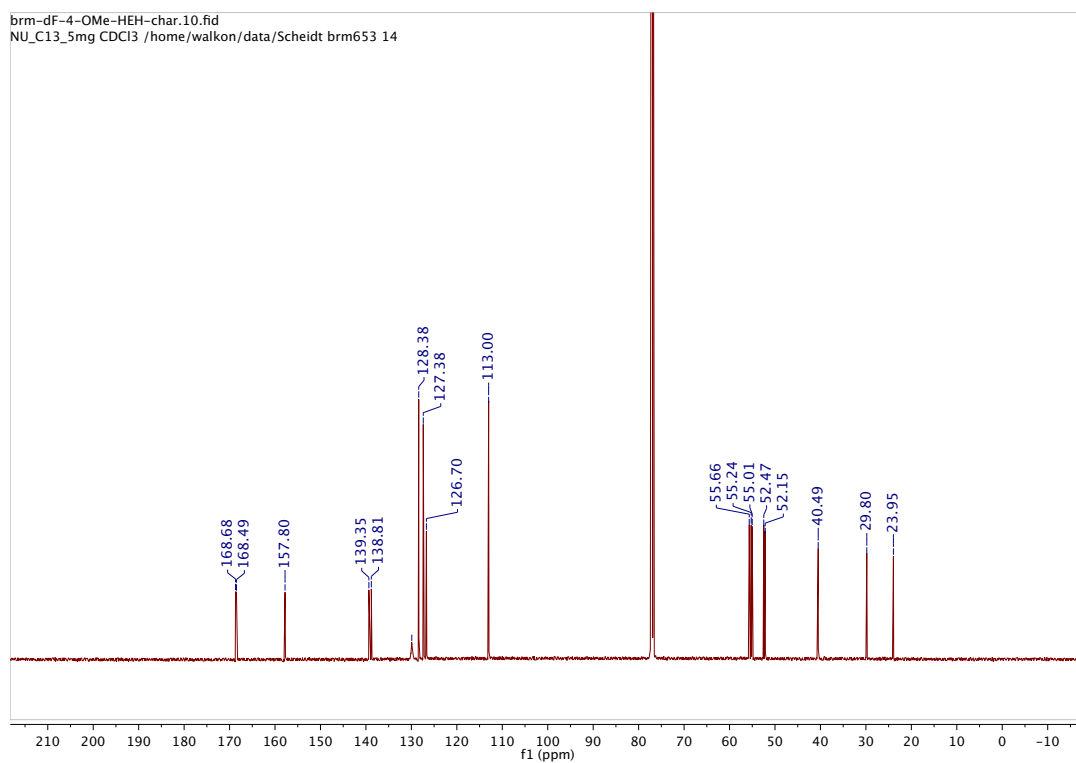
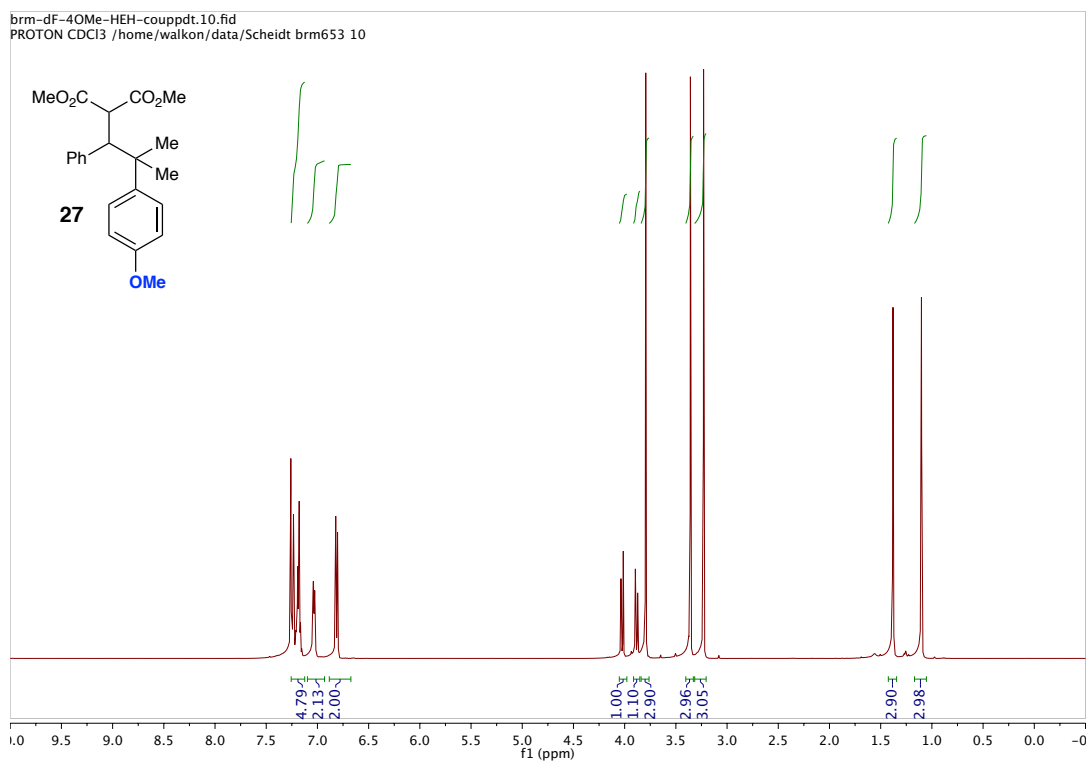


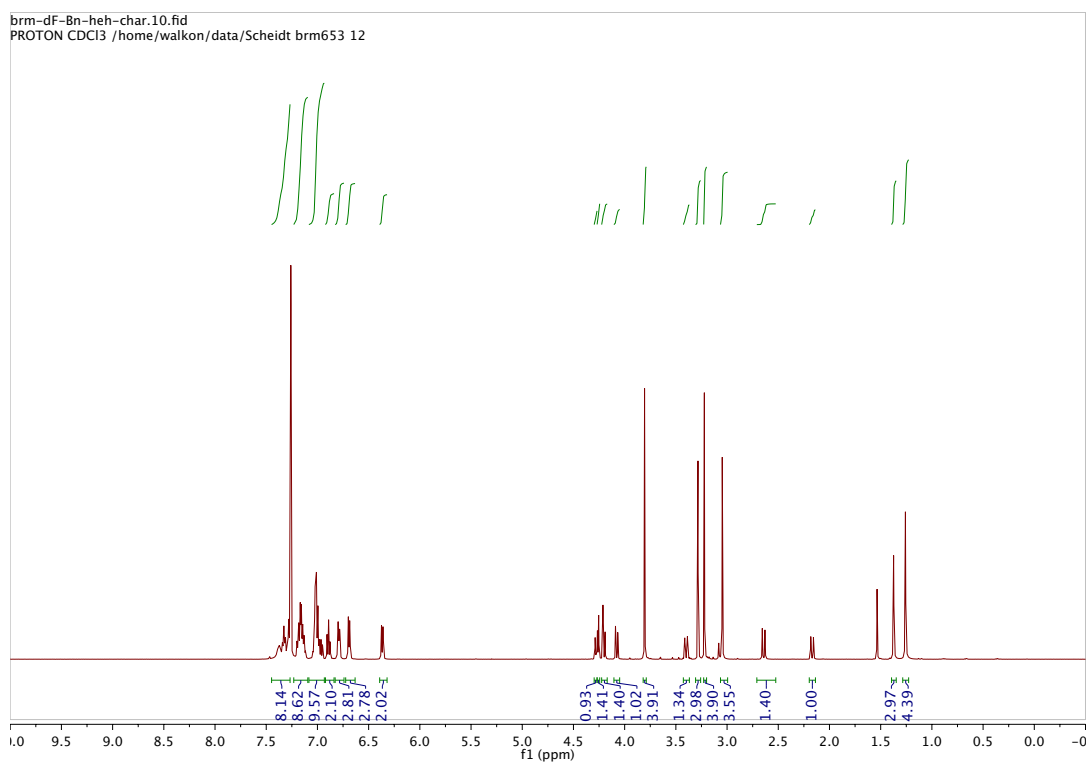
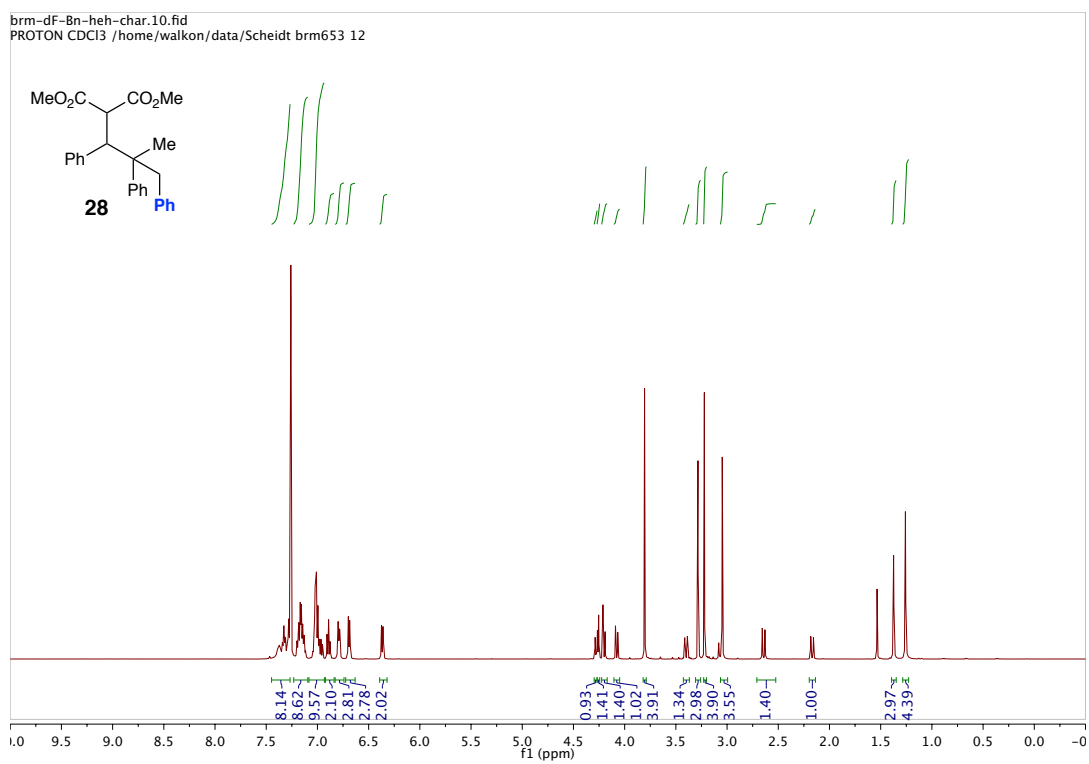


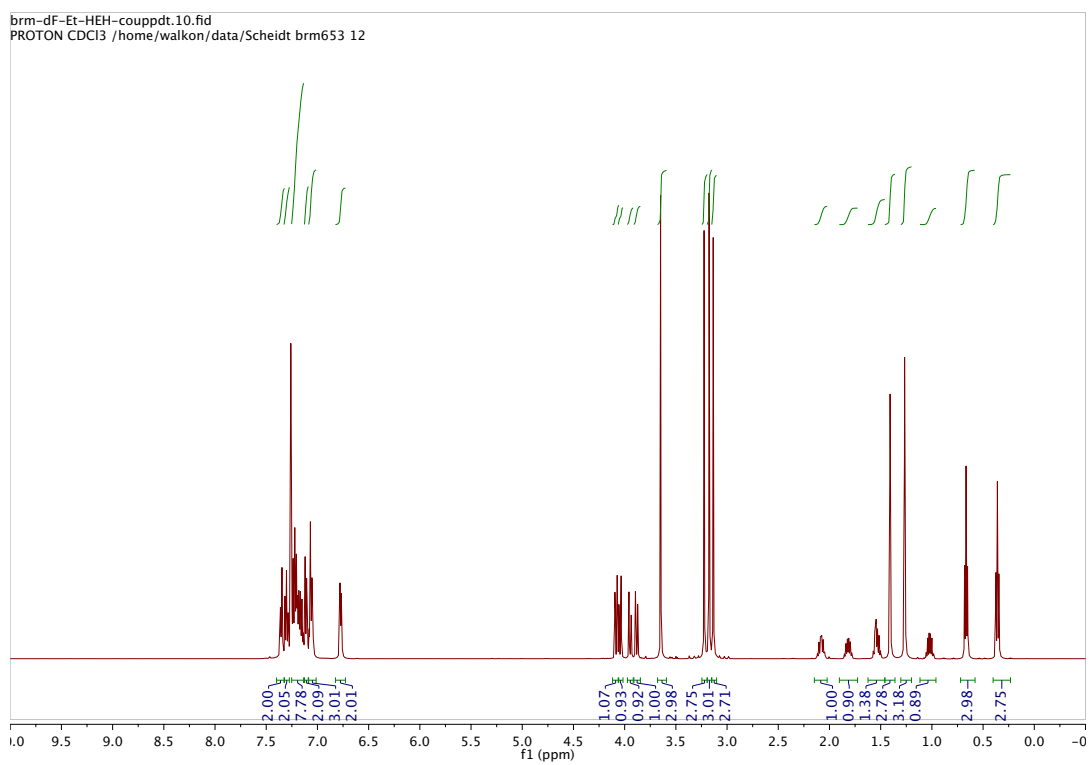
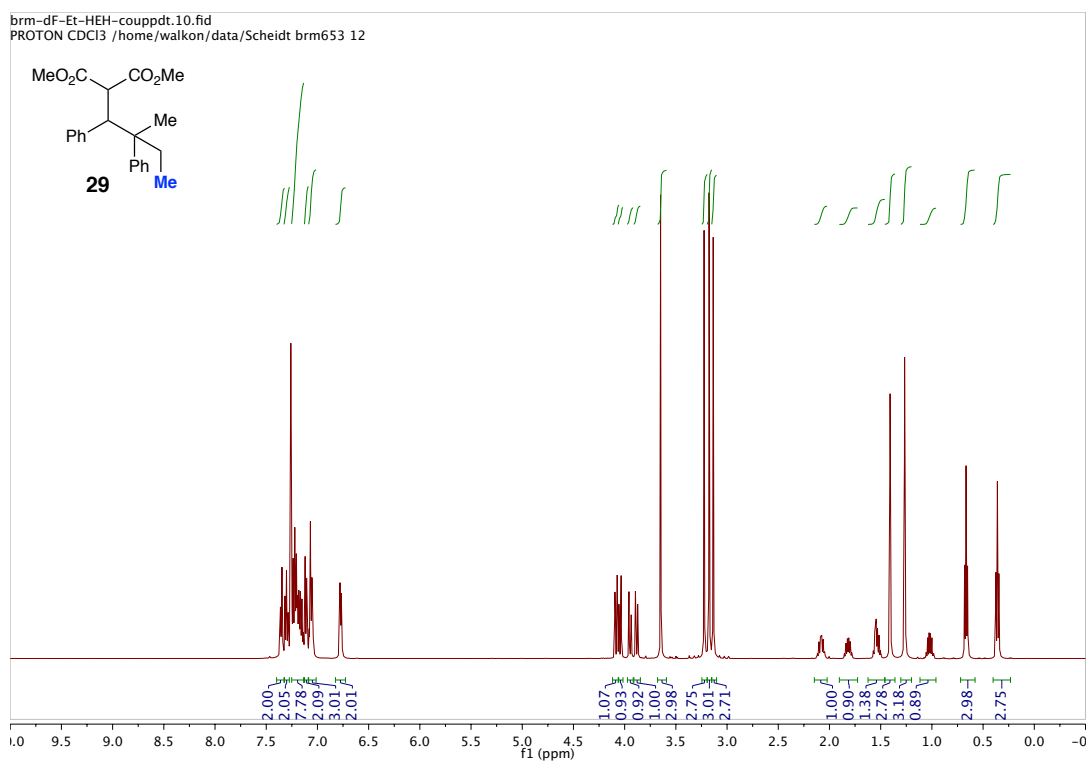


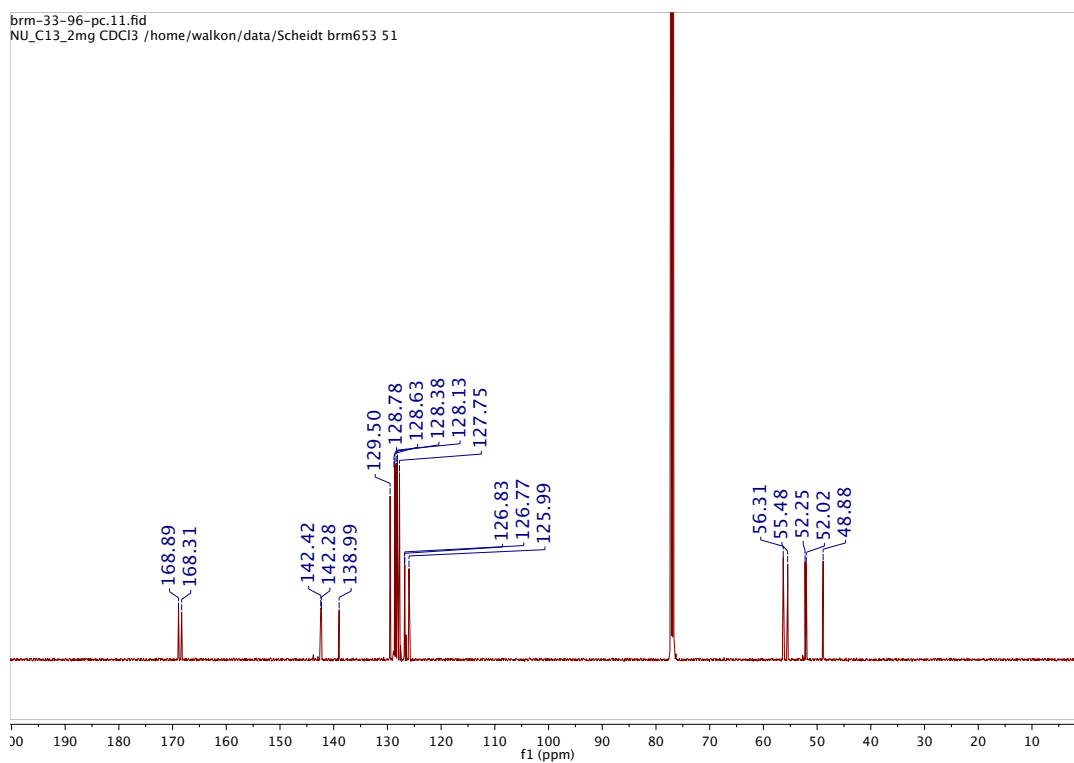
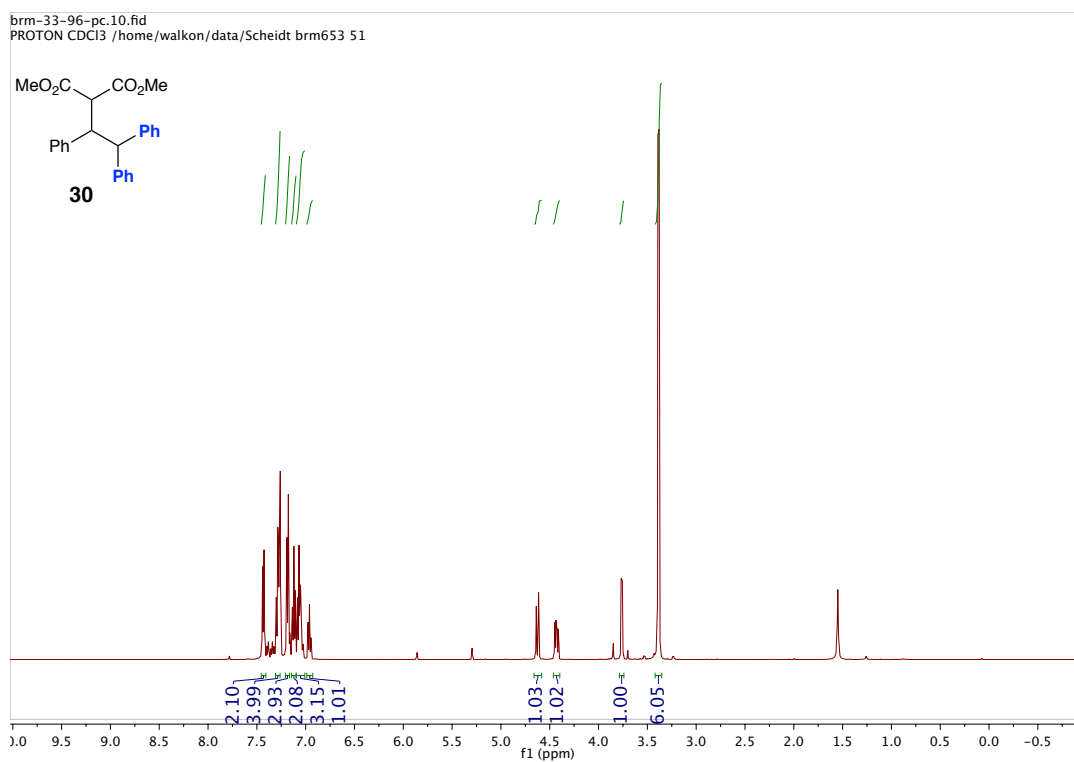


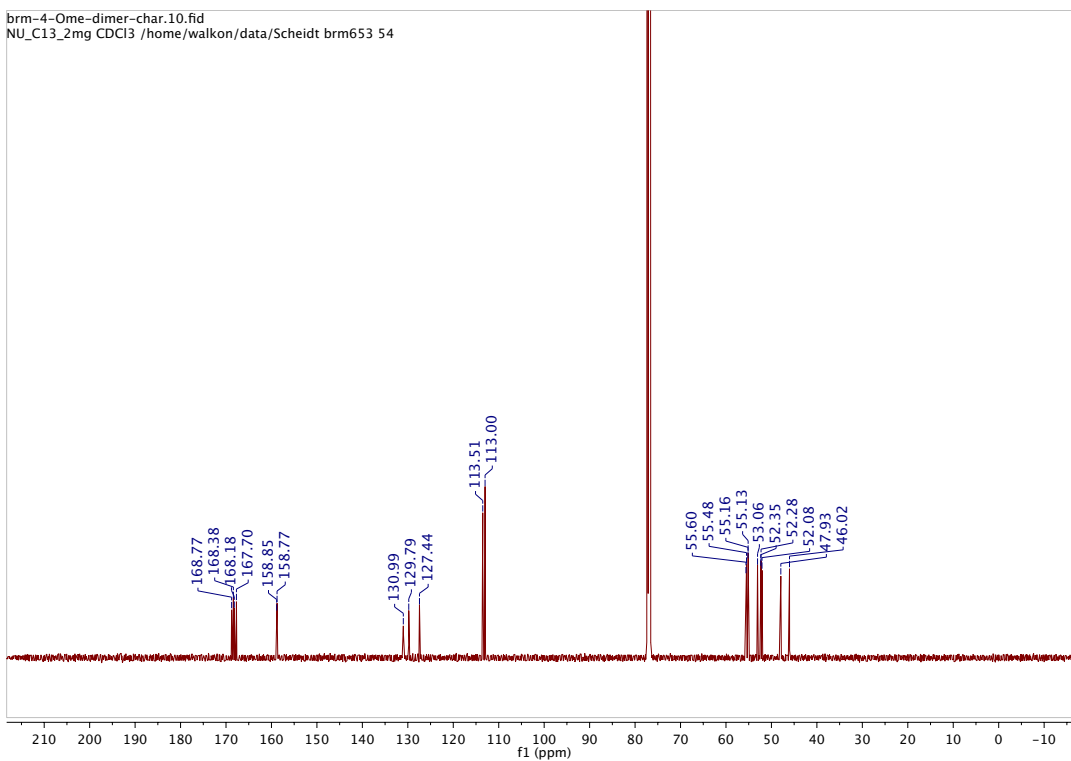
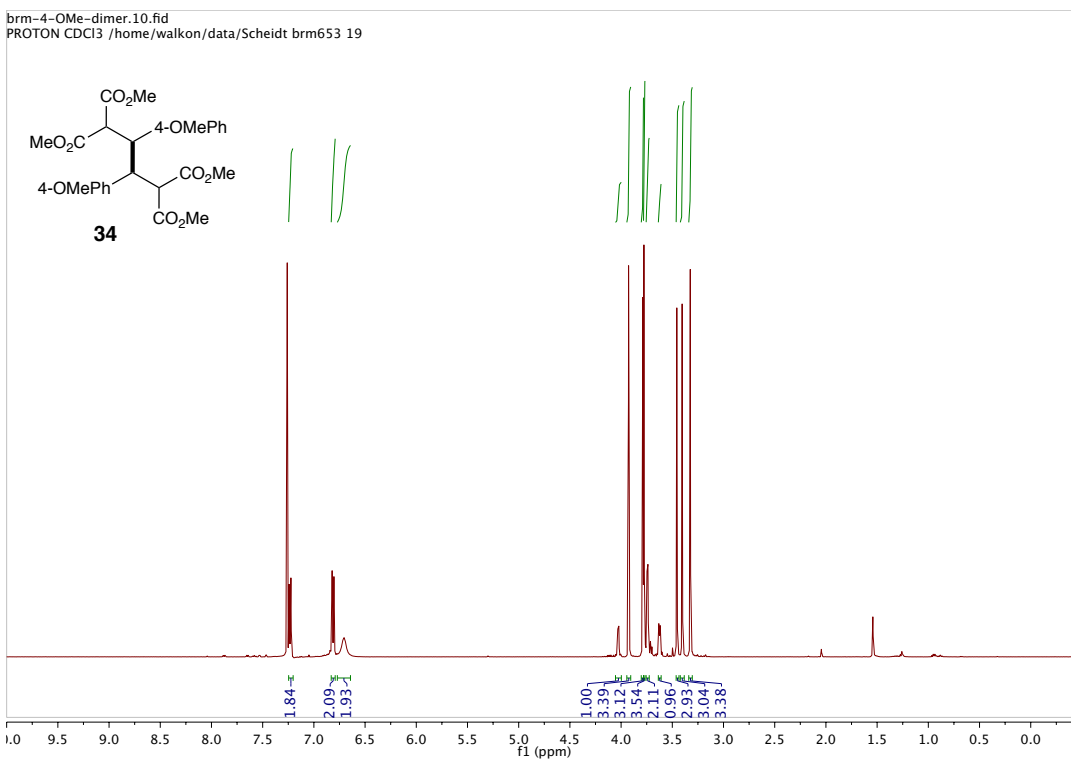


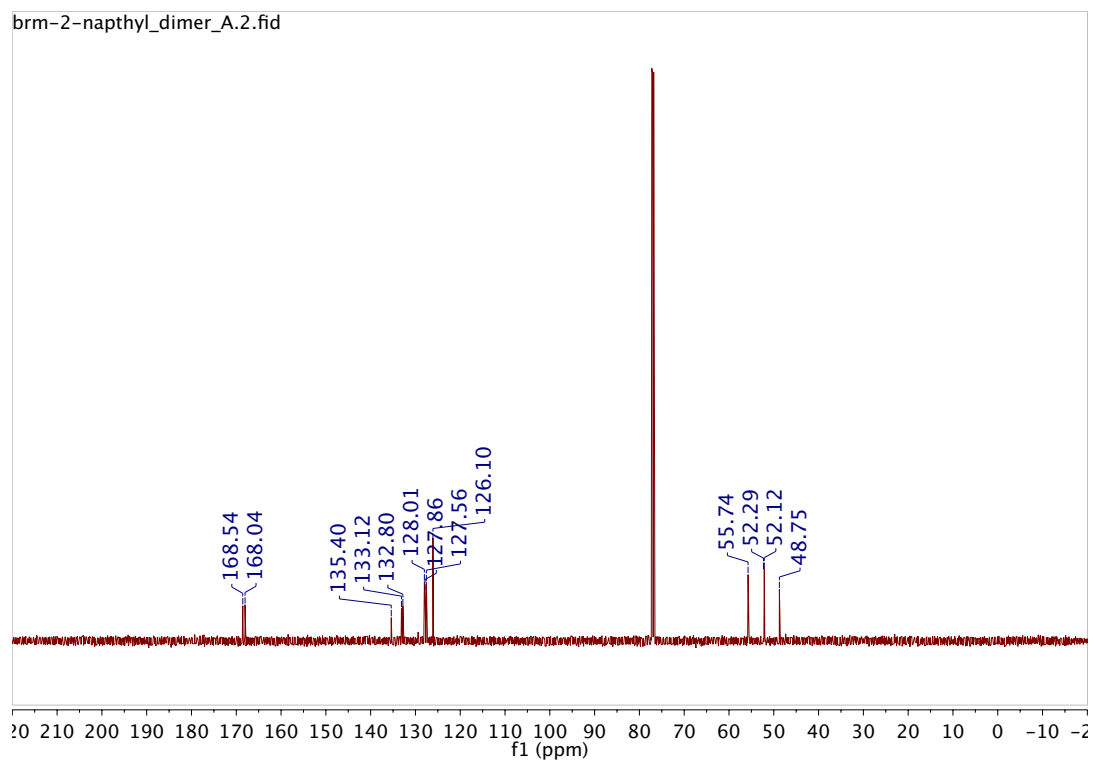
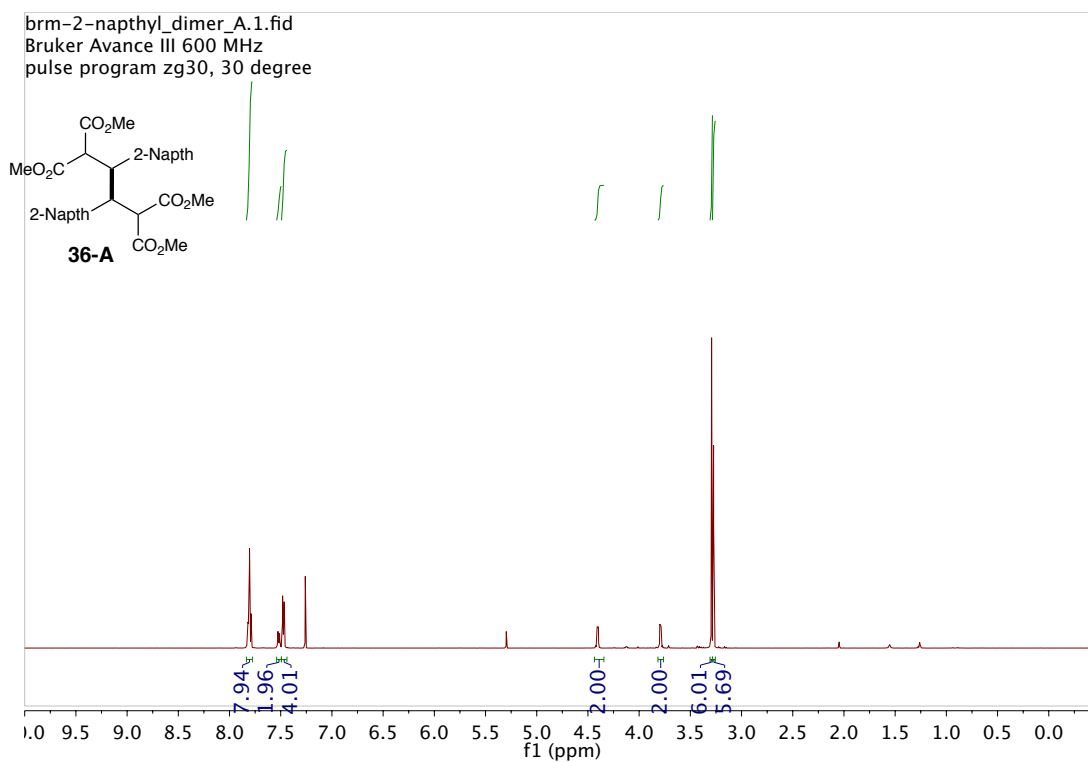


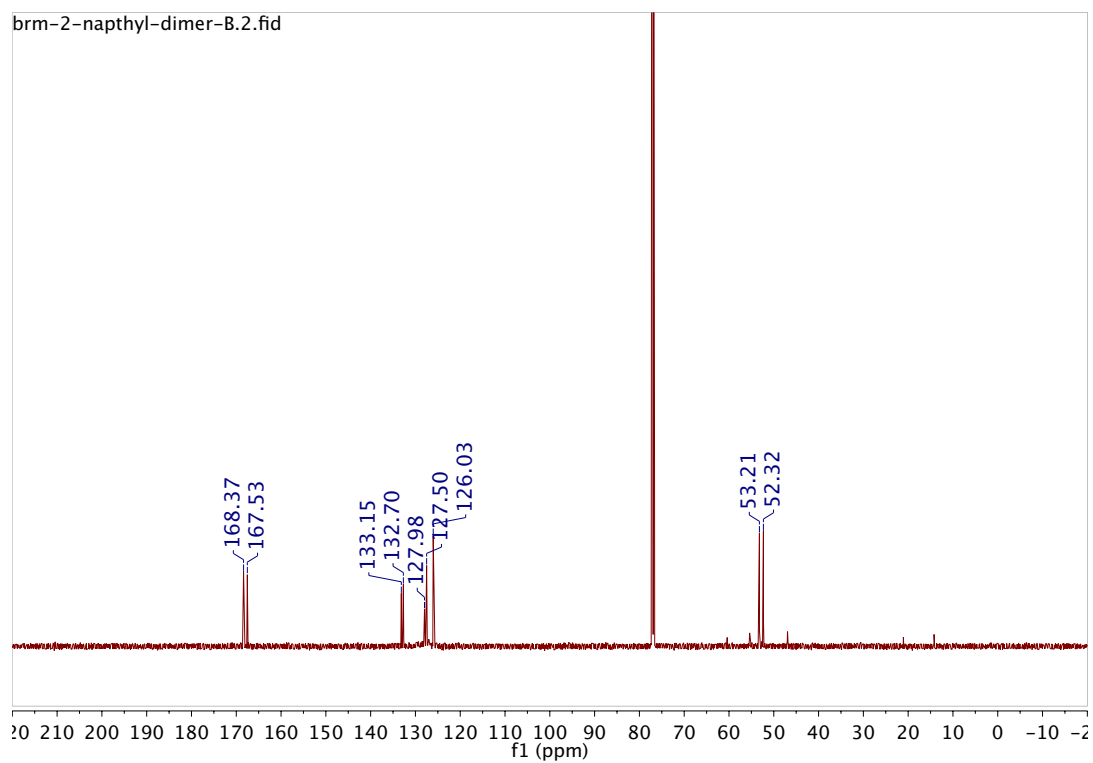
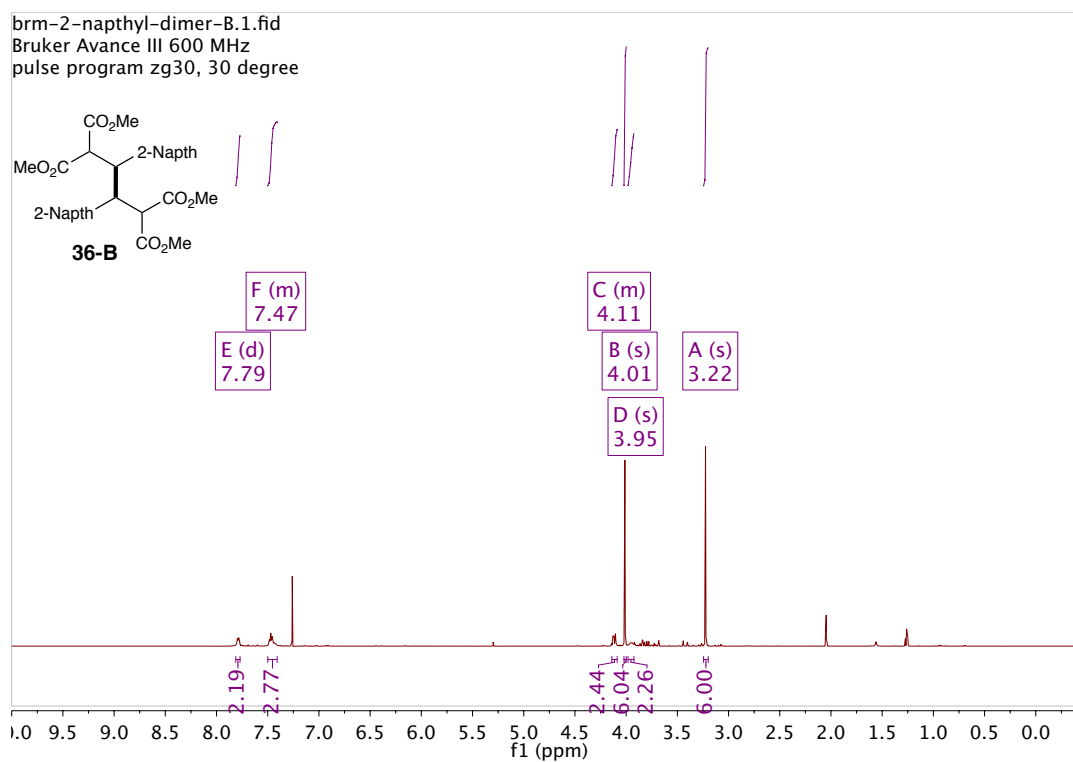


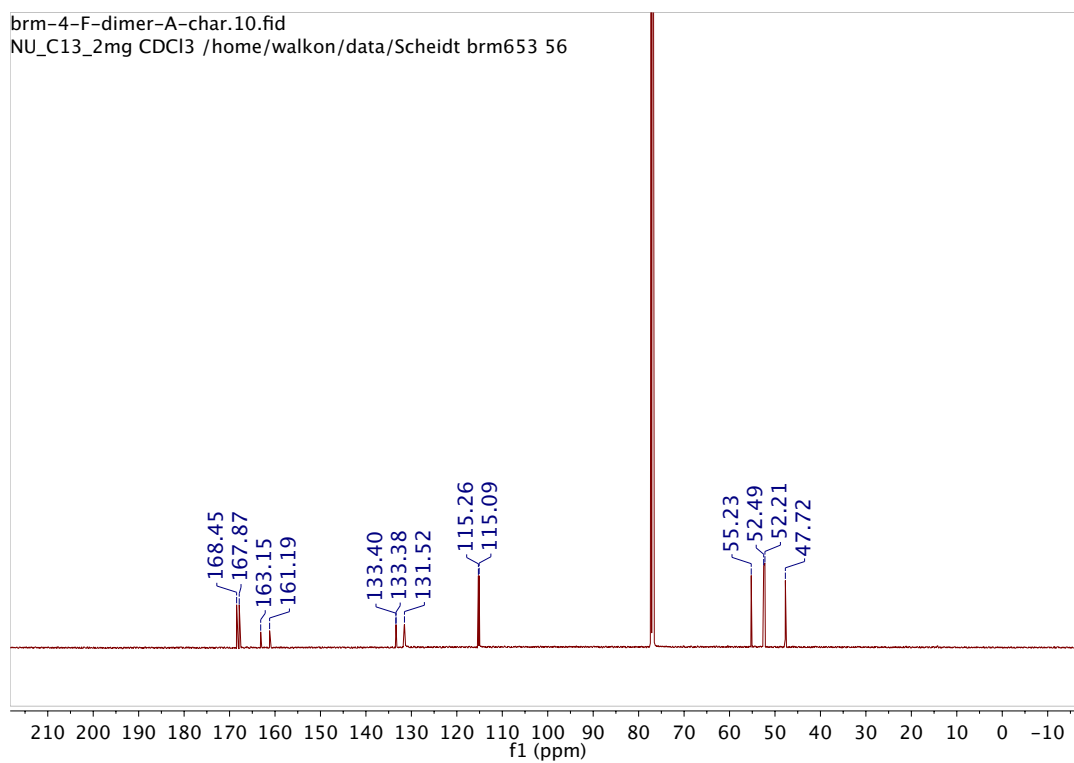
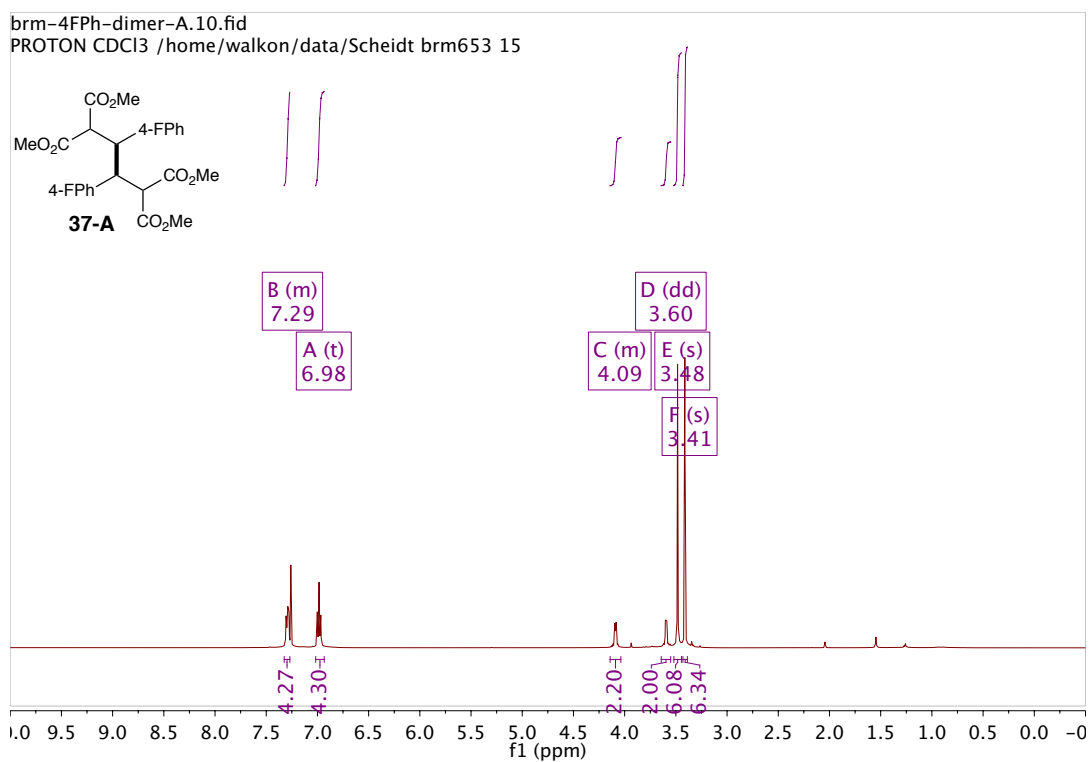


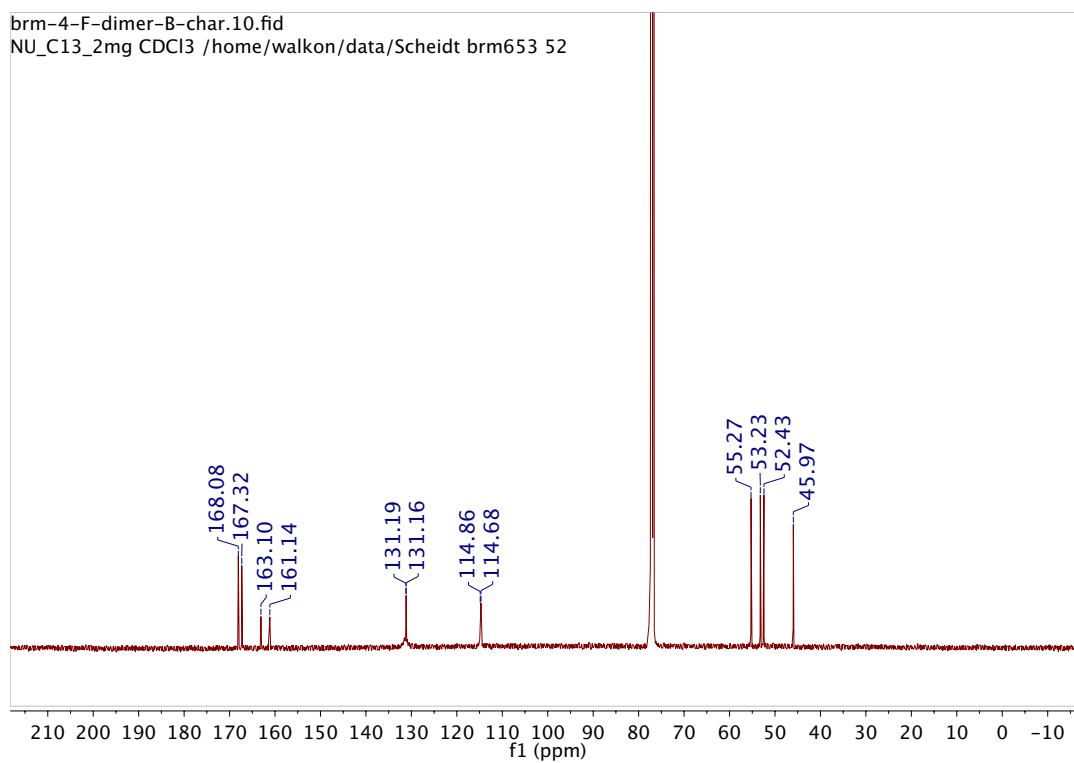
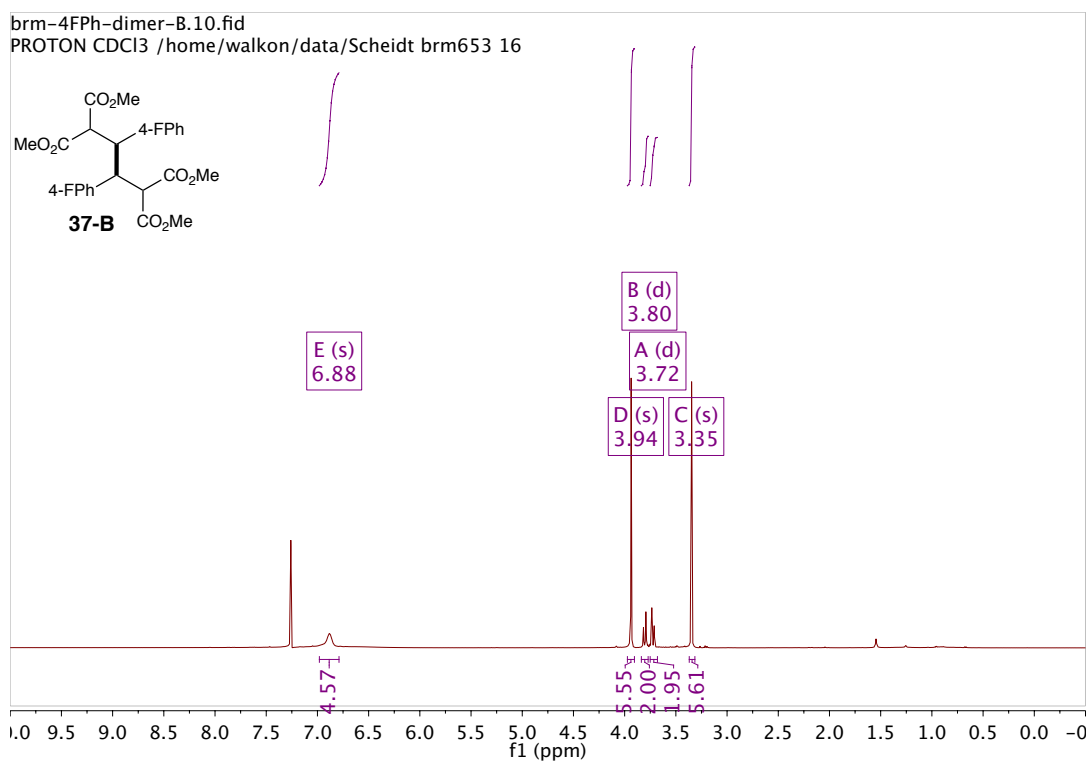


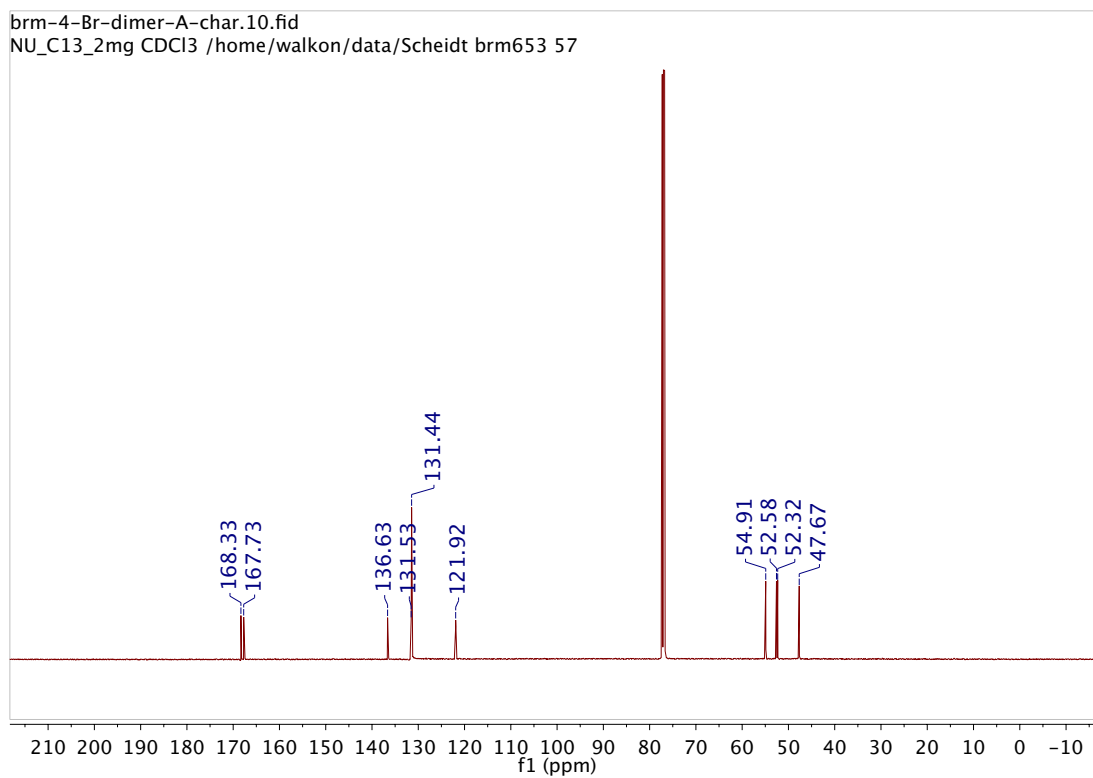
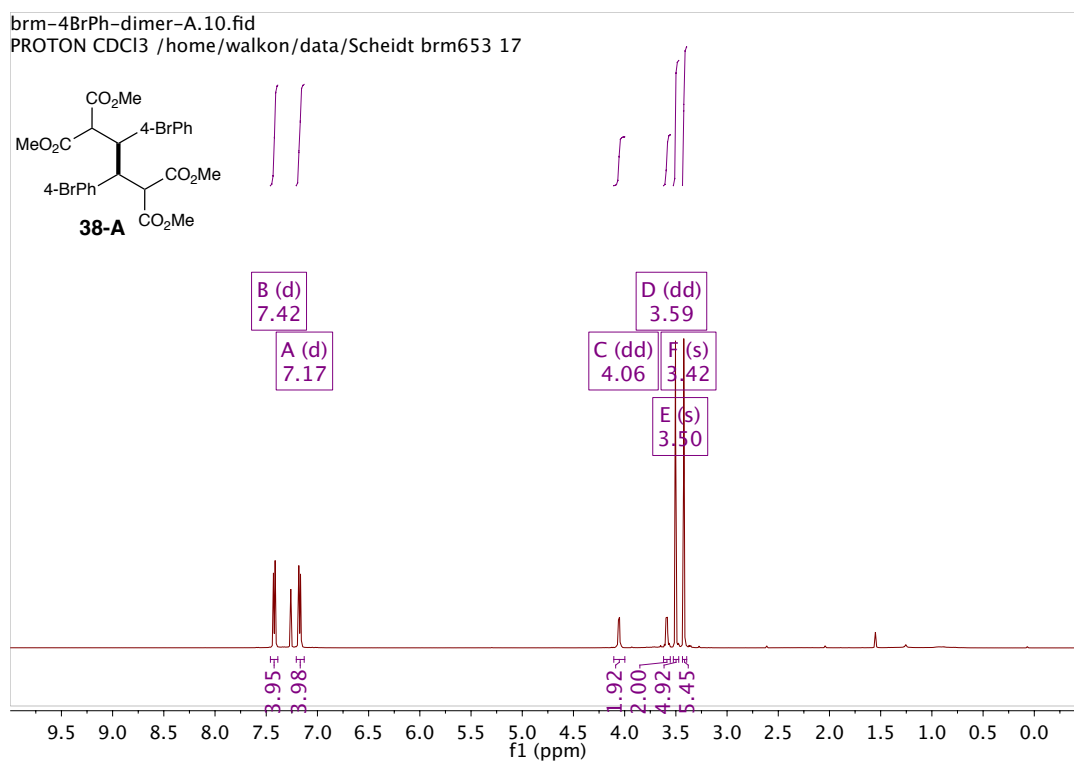


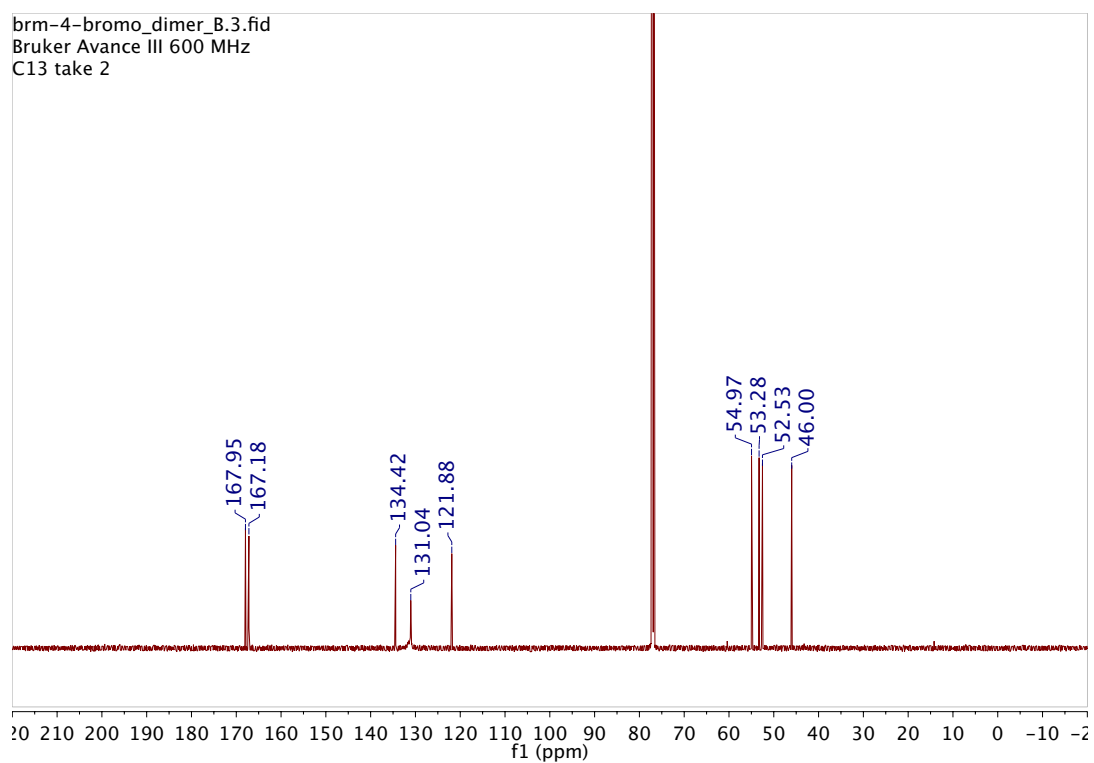
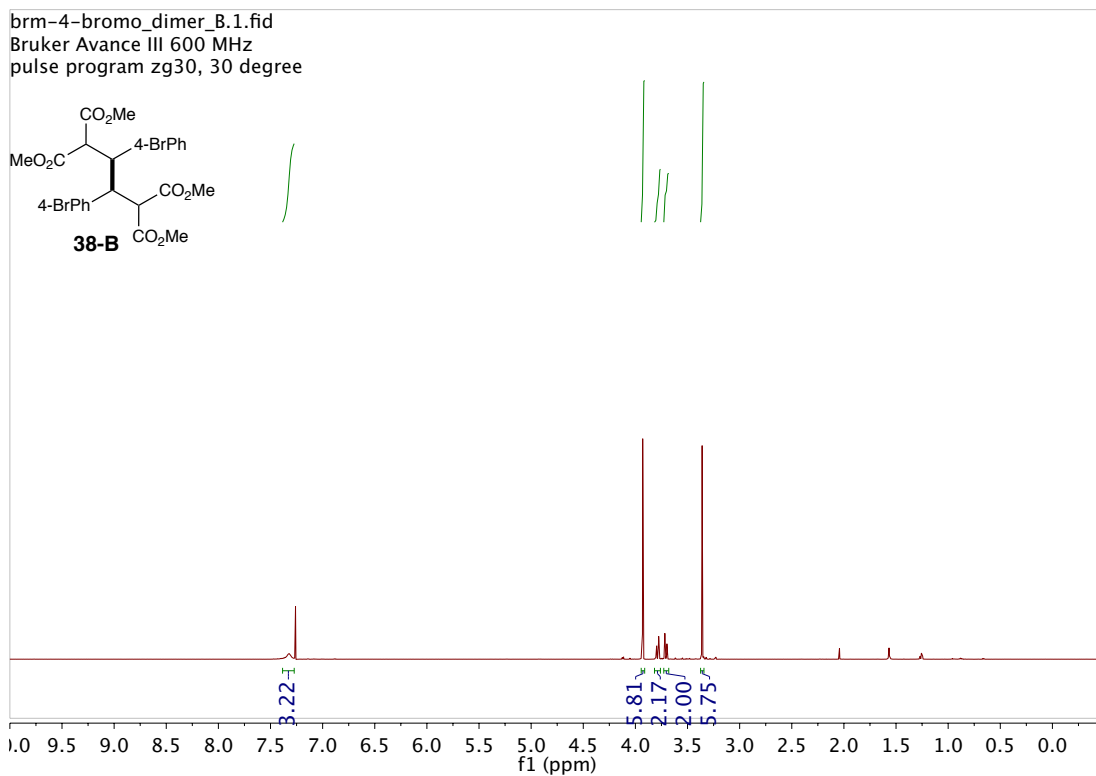


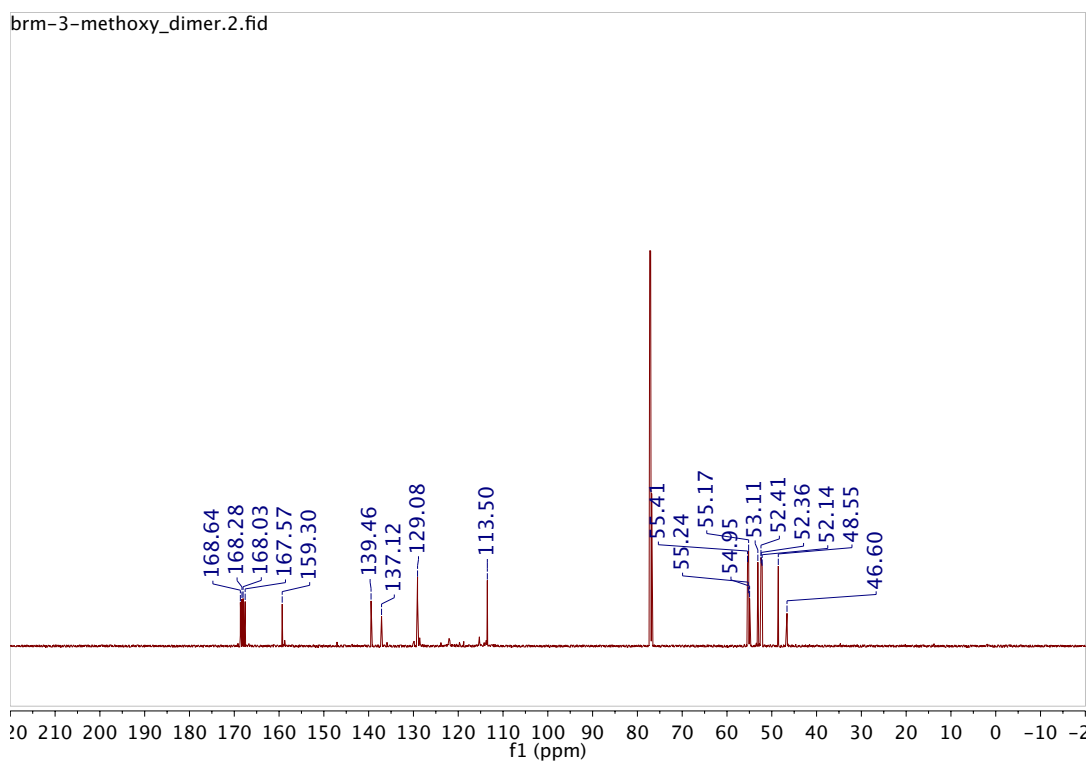
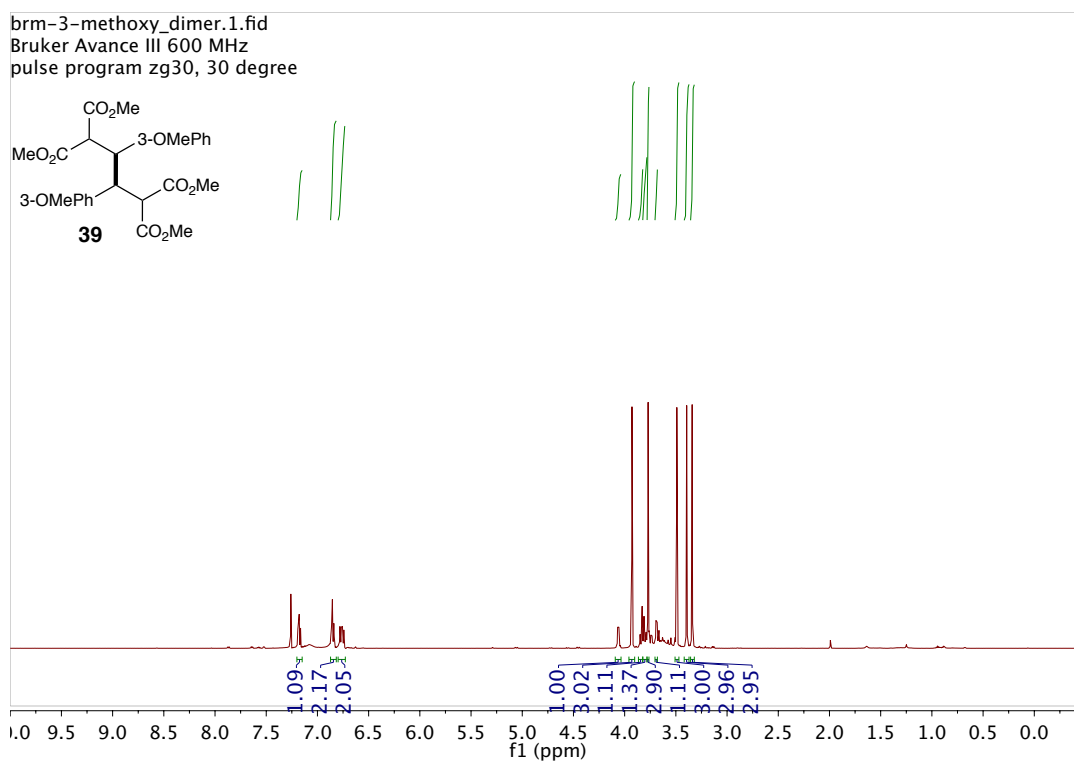


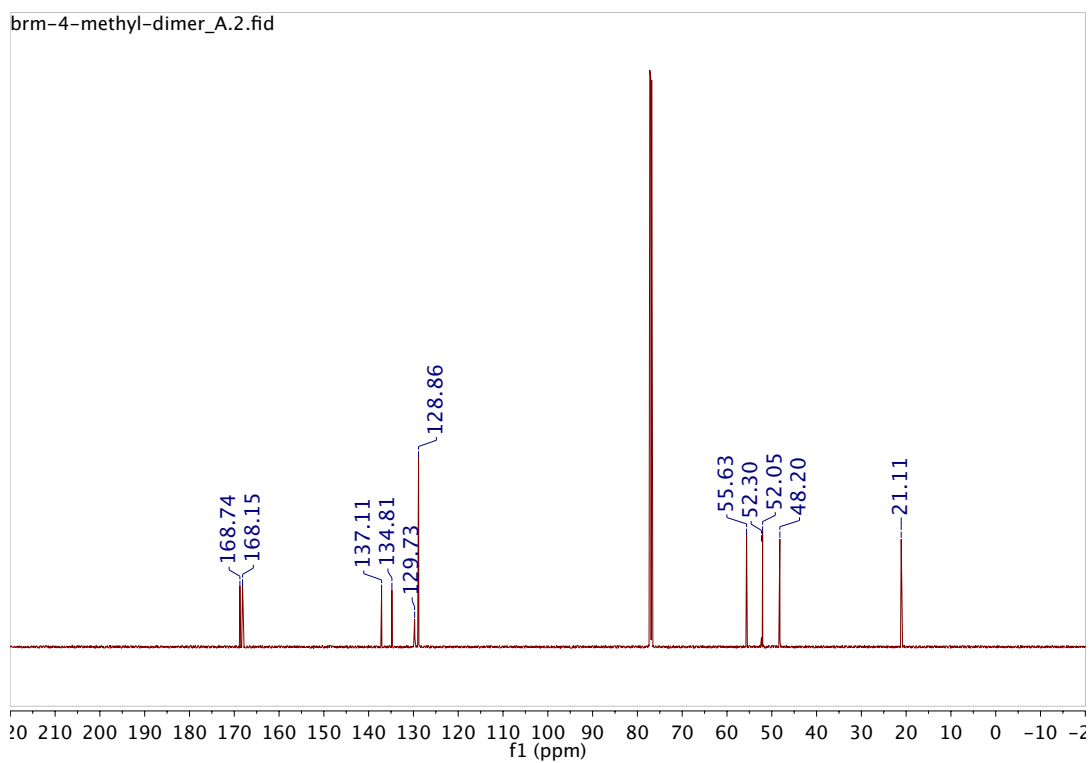
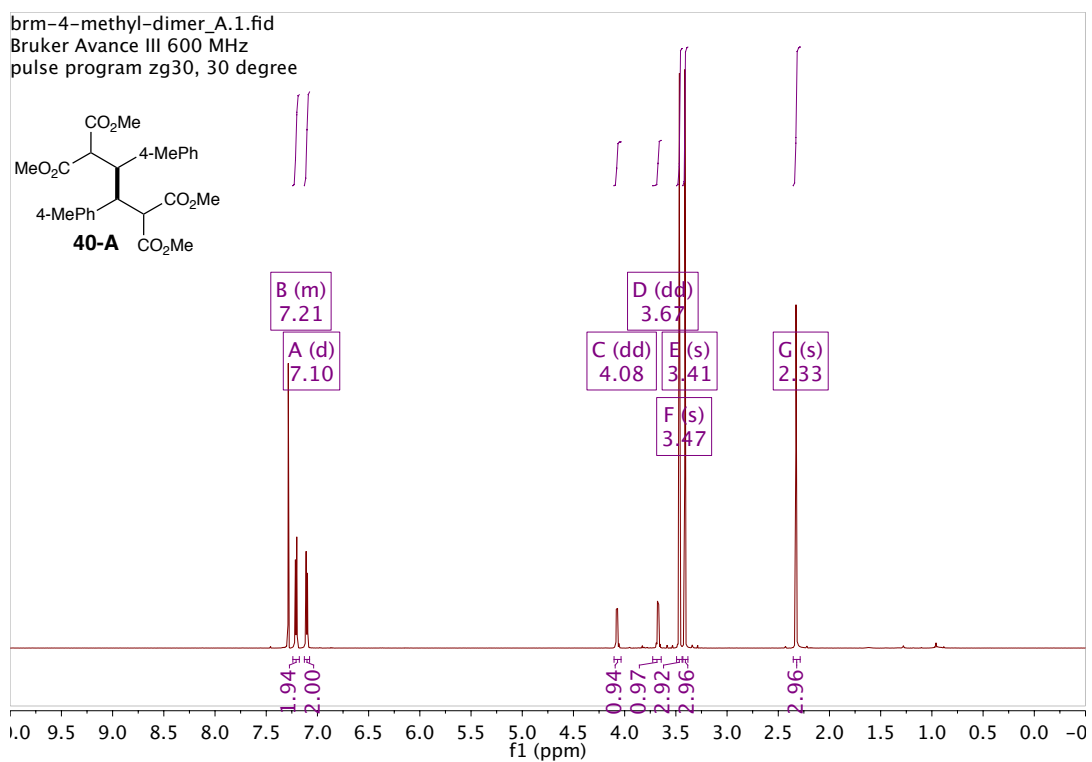


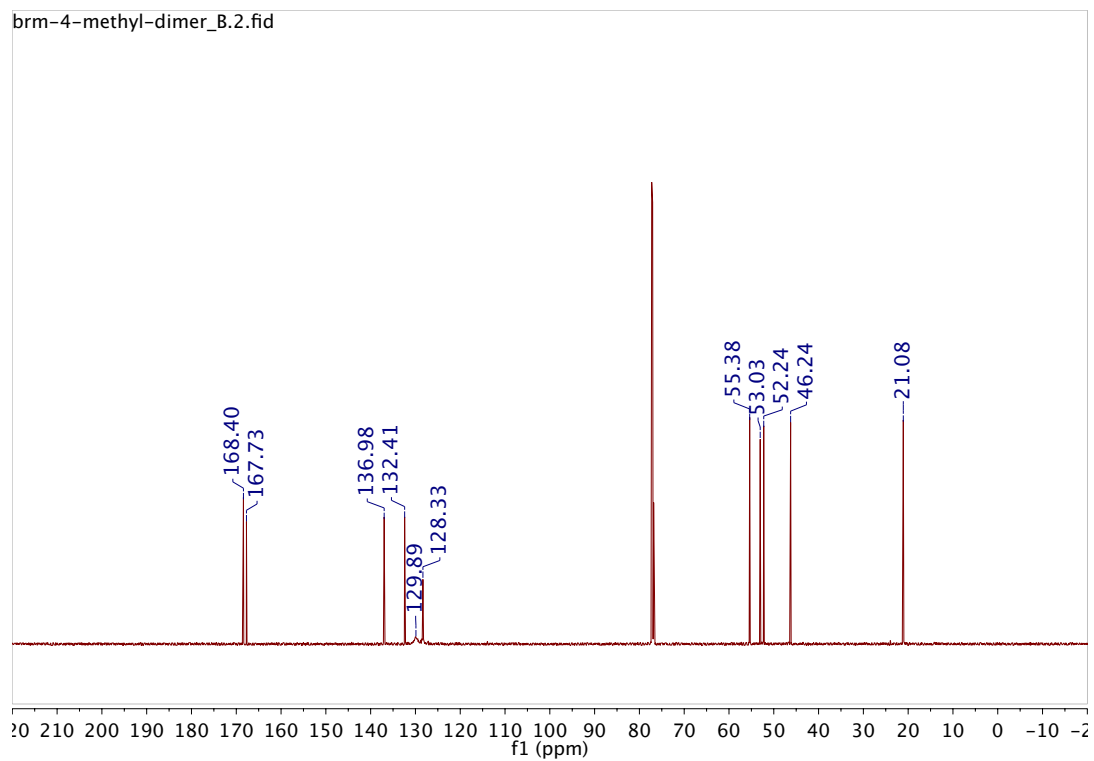
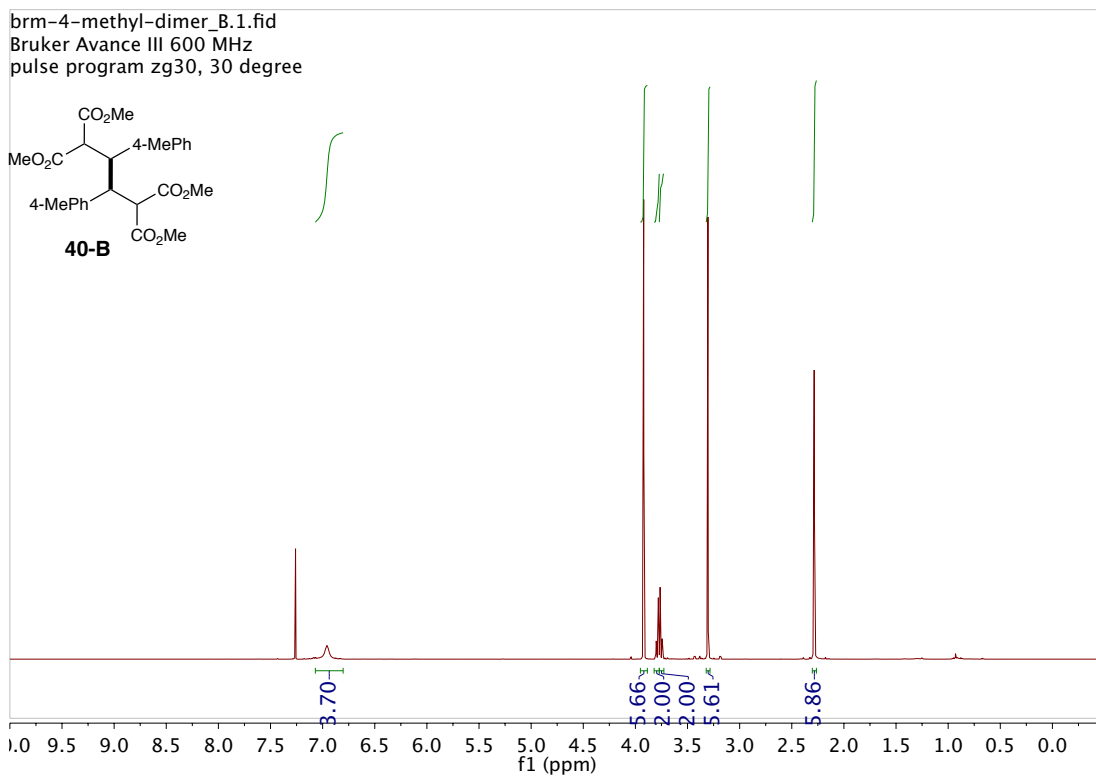


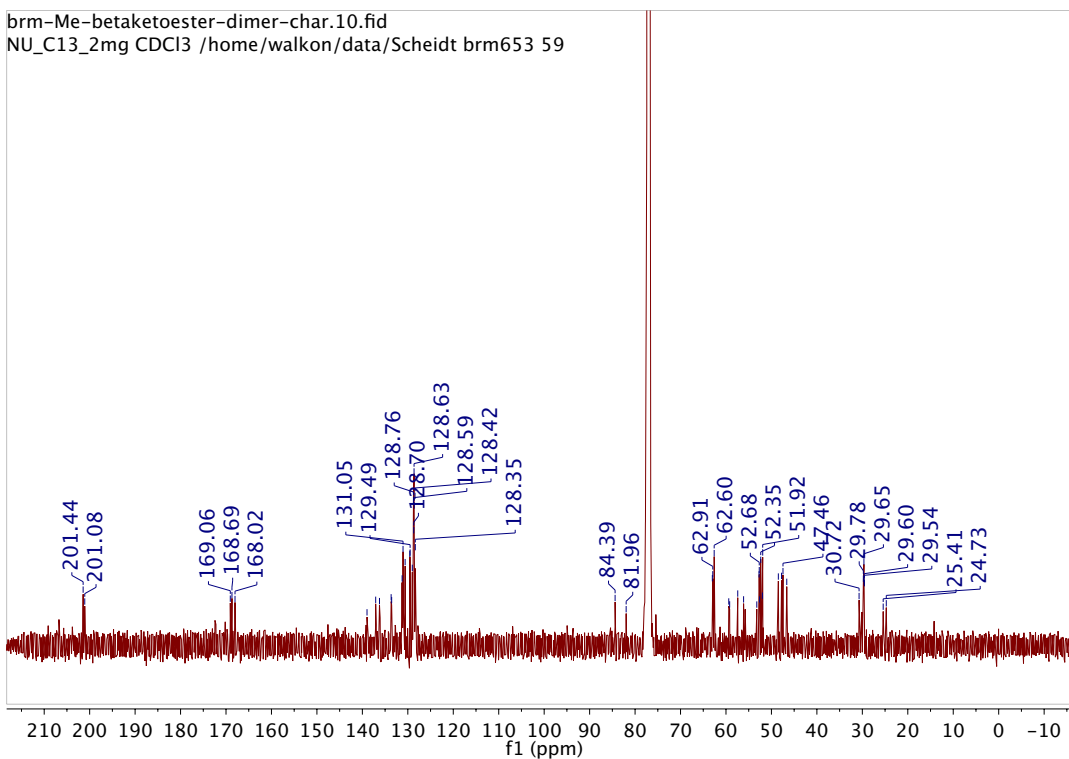
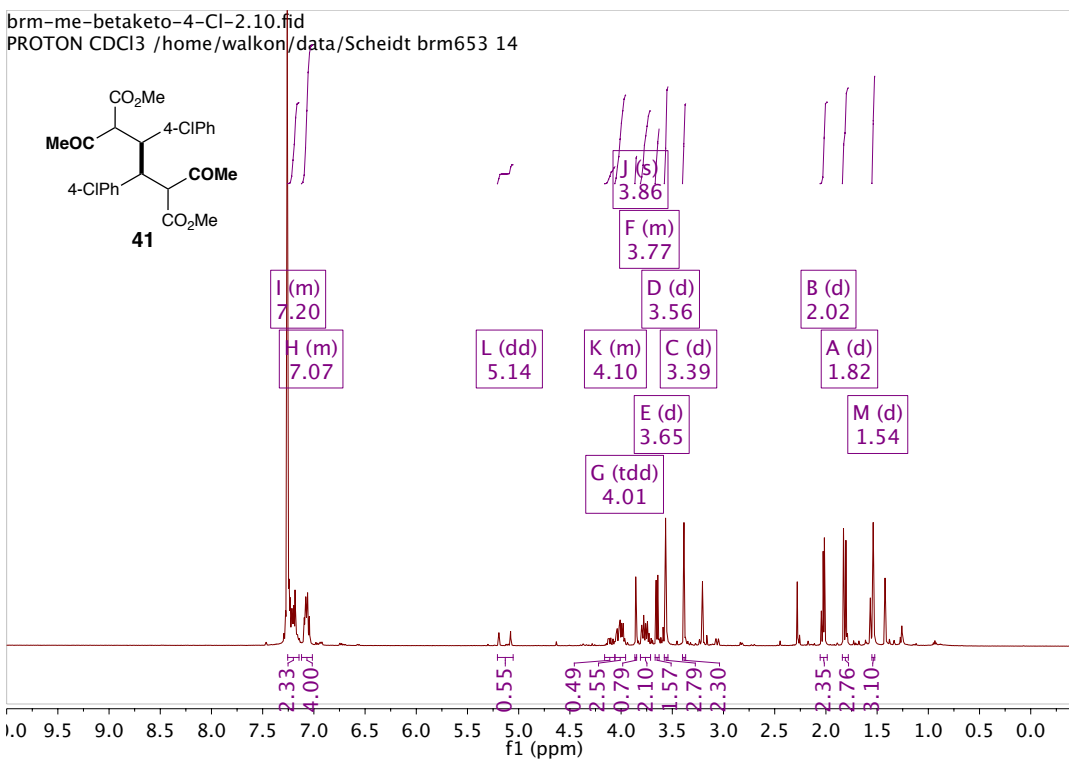


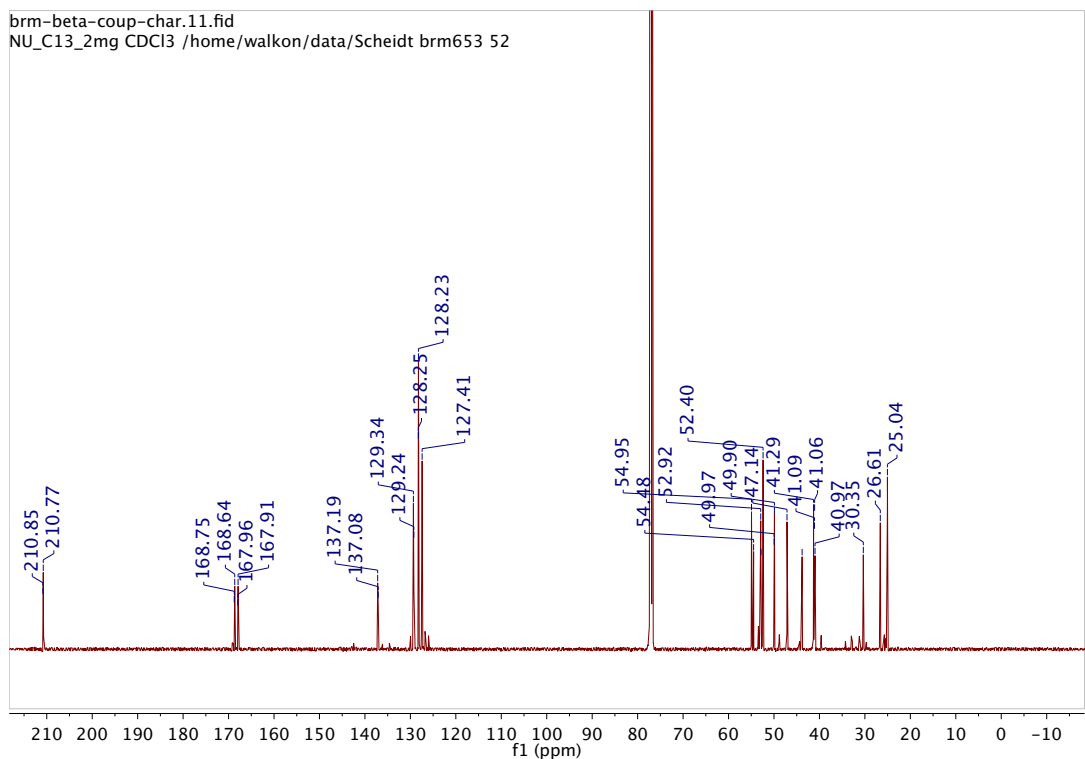
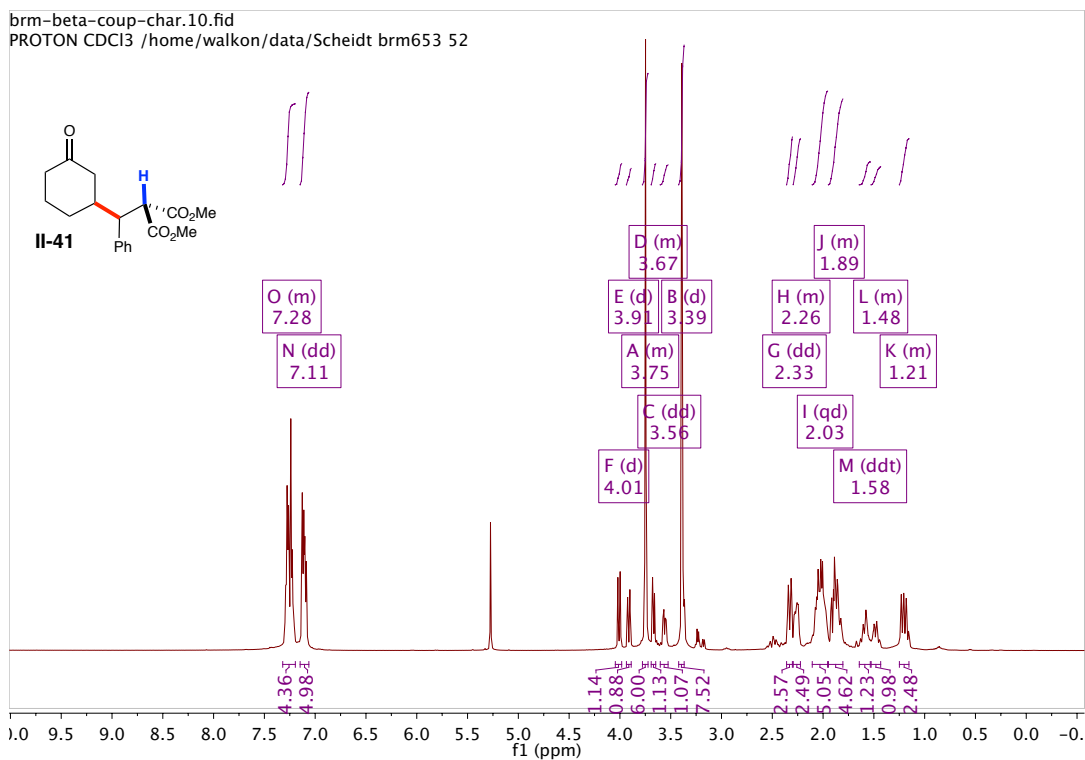


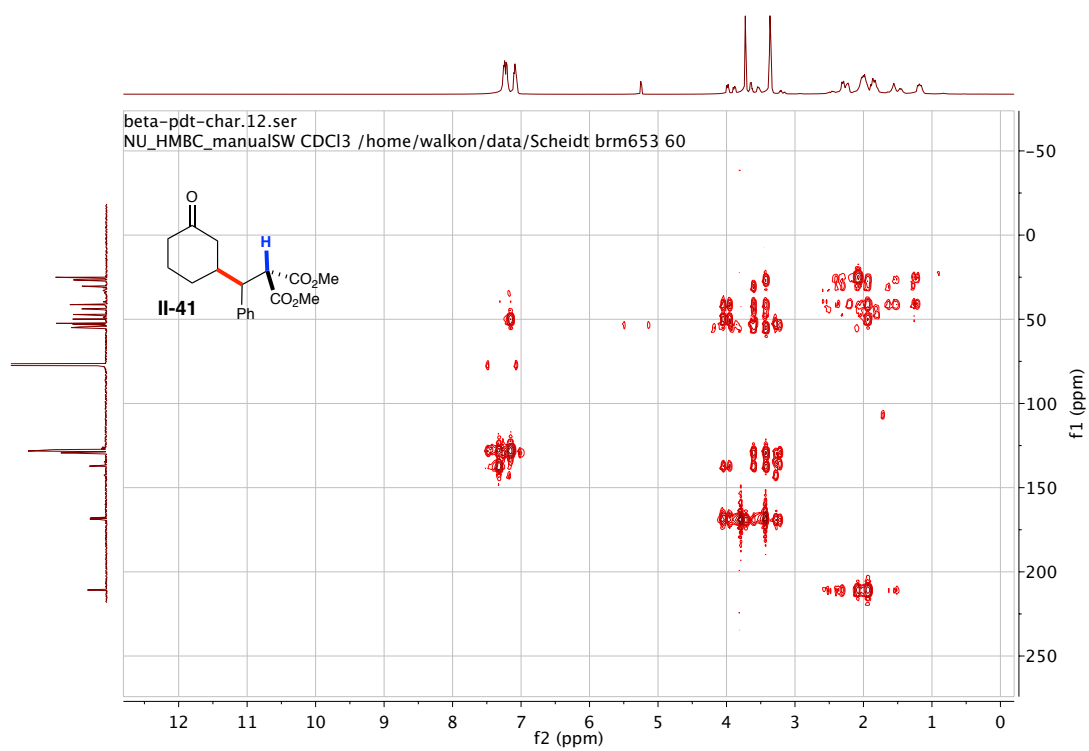
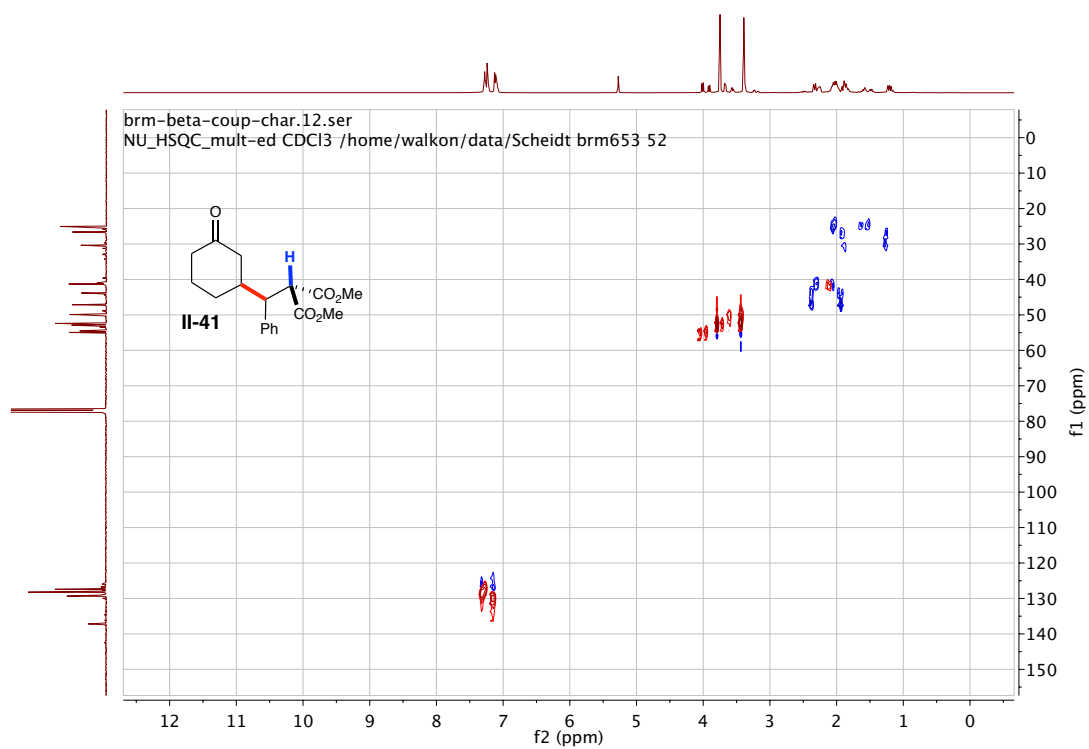


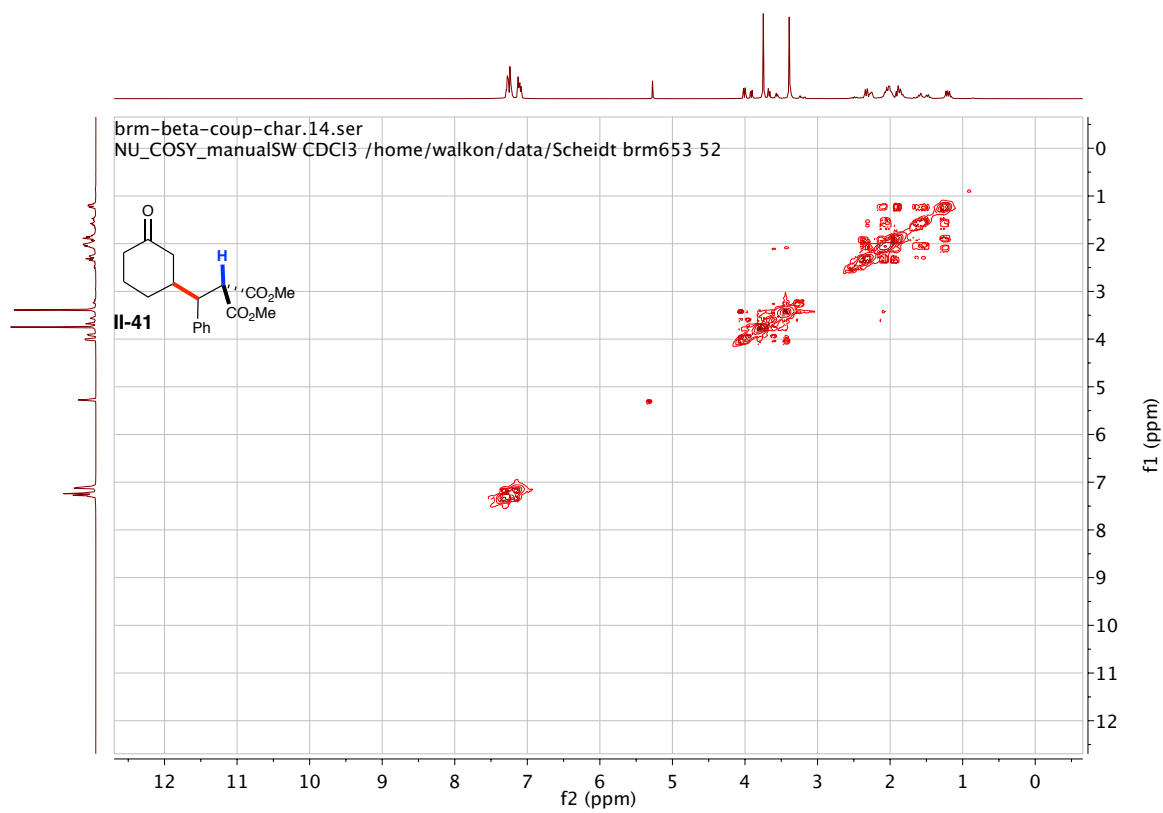












Racemate for Table 2-6, Entry 5, (column conditions shifted)

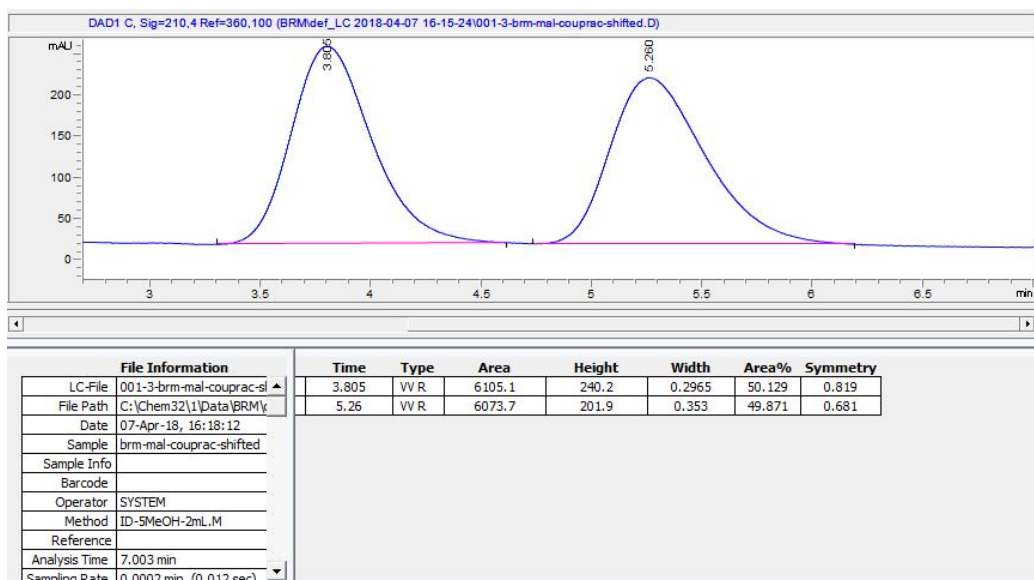


Table 2-6, Entry 5

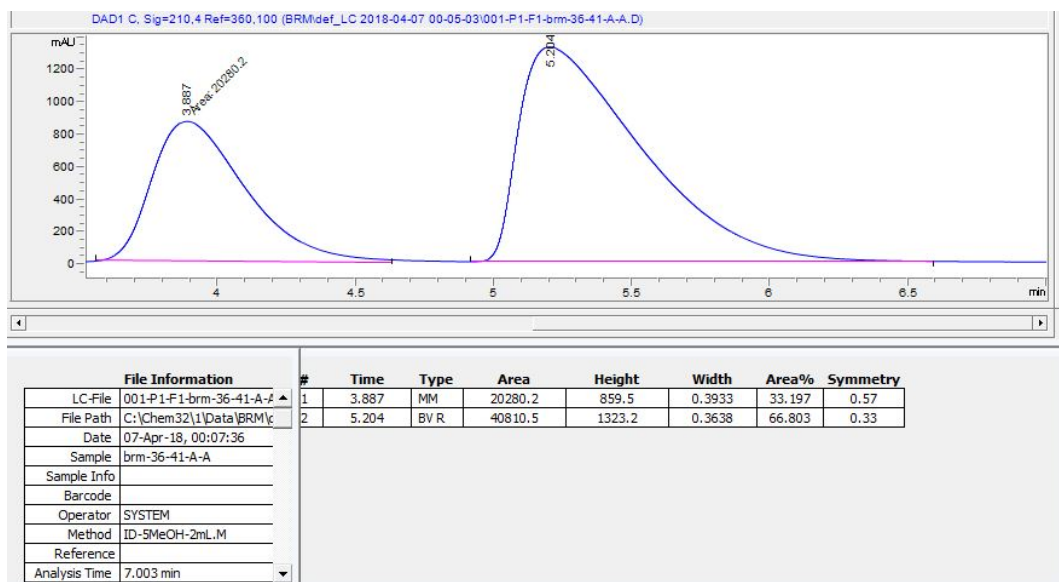
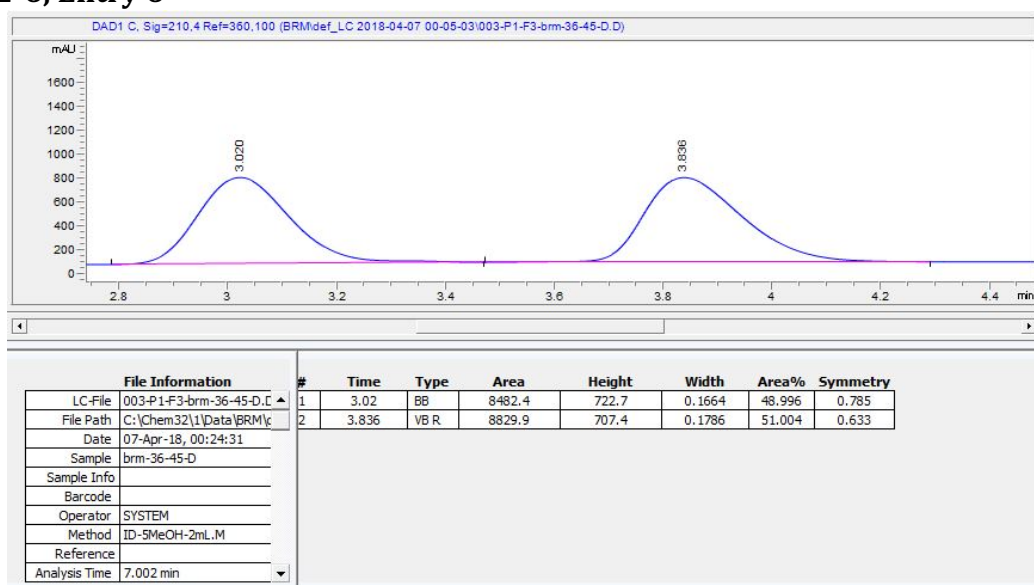
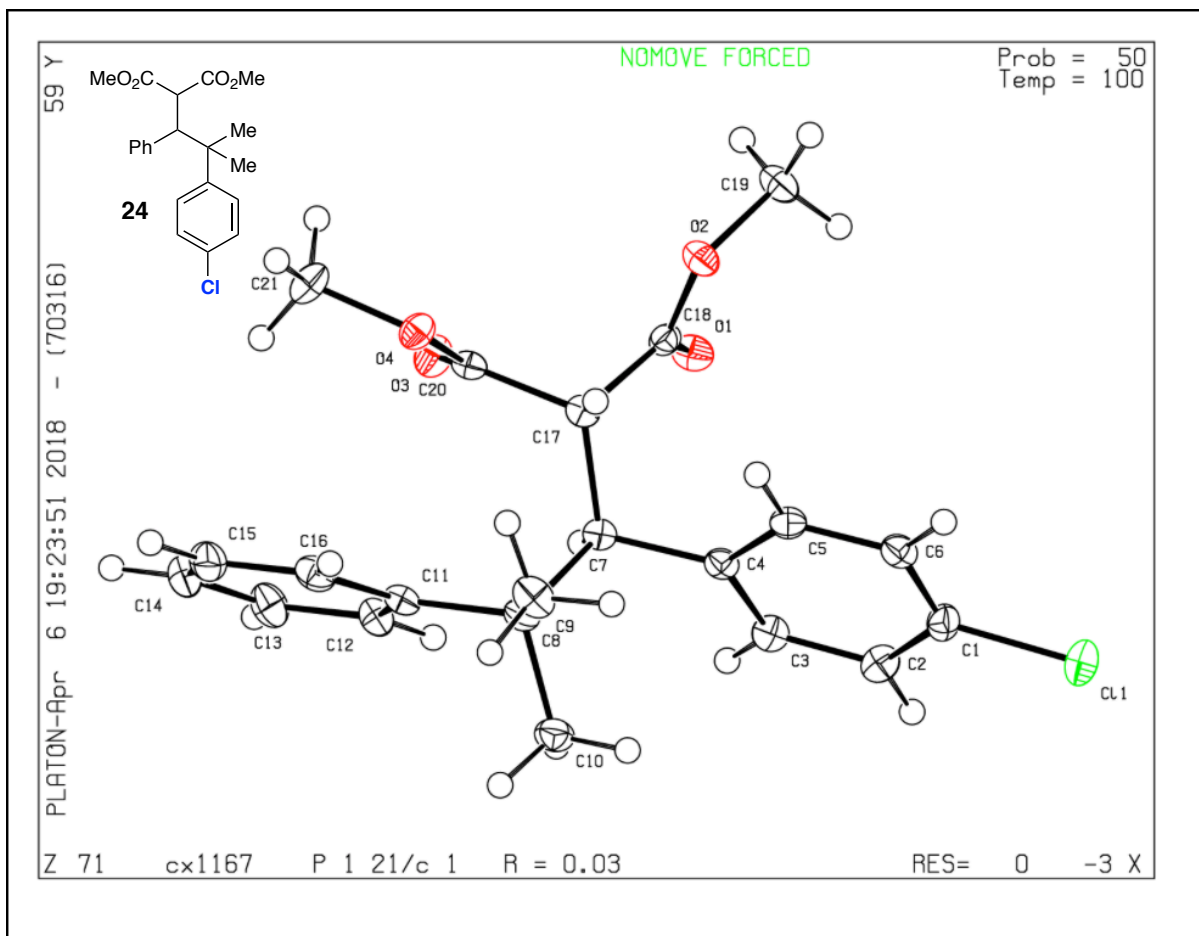
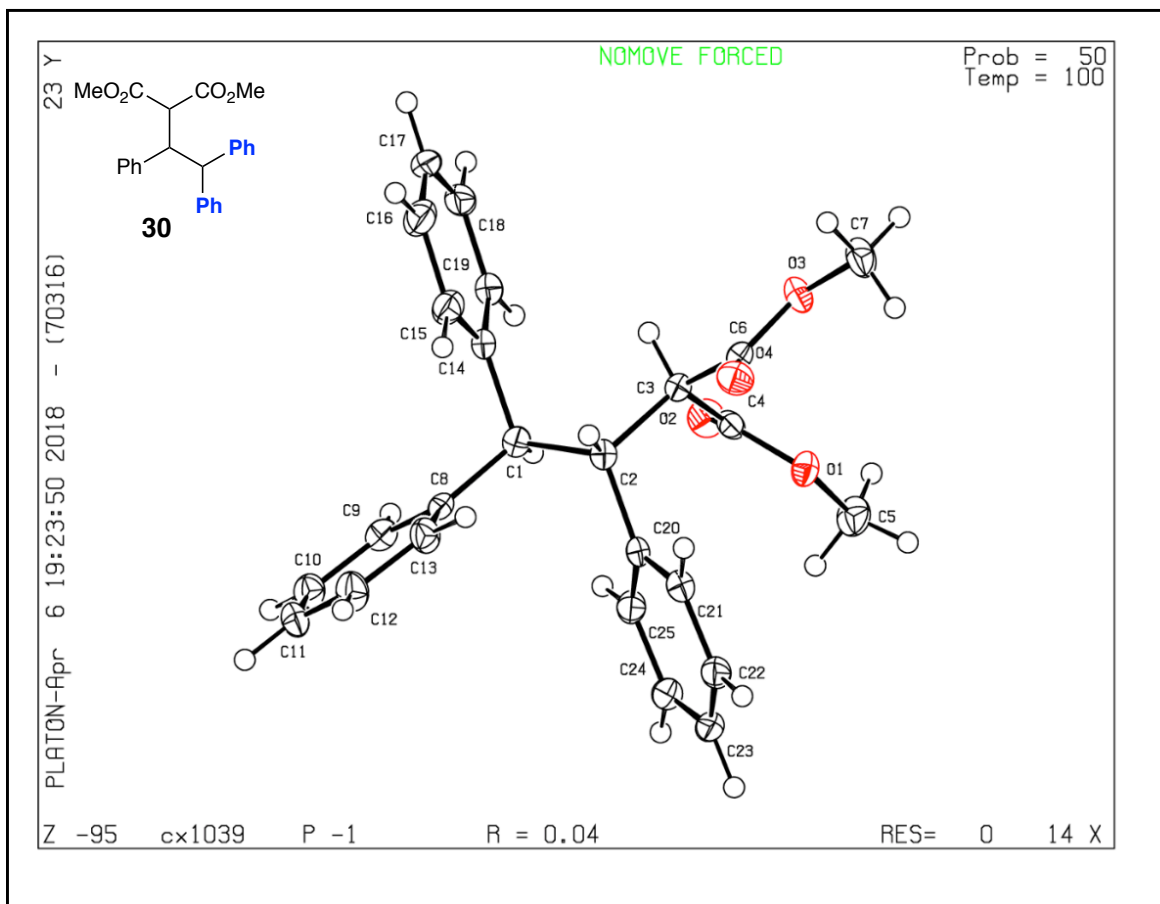


Table 2-6, Entry 6

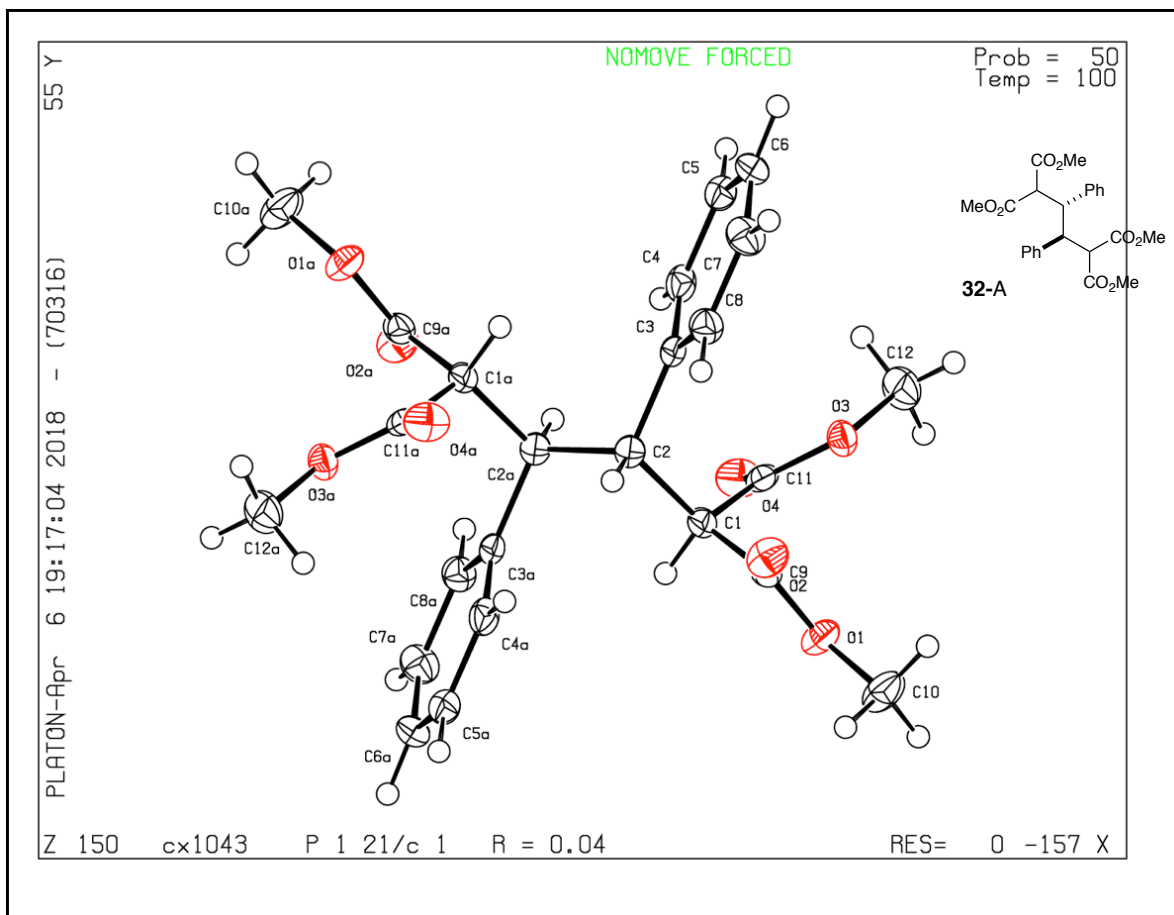




A single crystal of **24** was grown by evaporative diffusion in dichloromethane with hexanes as the anti-solvent at room temperature. This crystal structure was deposited in the Cambridge Crystallographic Data Centre and assigned as CCDC 1835357. Further information can be found in the CIF file.



A single crystal of **30** was grown by evaporative diffusion in dichloromethane with hexanes as the anti-solvent at room temperature. This crystal structure was deposited in the Cambridge Crystallographic Data Centre and assigned as CCDC 1835355. Further information can be found in the CIF file.



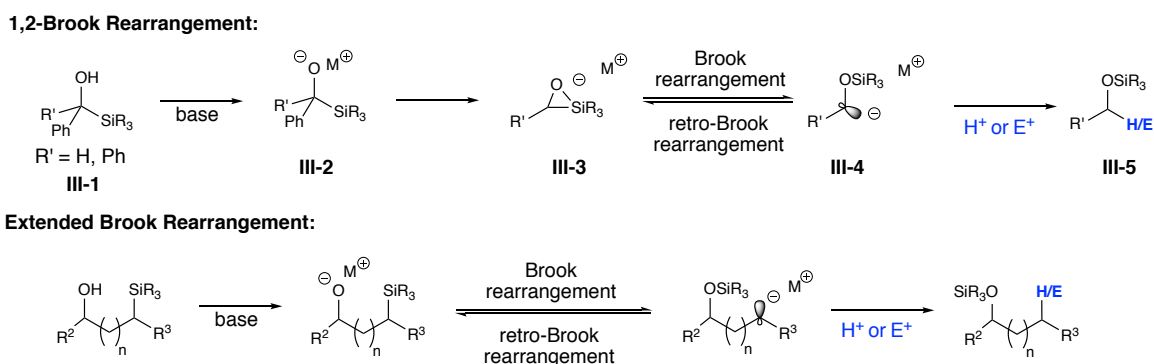
A single crystal of **32-A** was grown by evaporative diffusion (from a 1:1 mixture of **32-A** and **32-B**) in dichloromethane with hexanes as the anti-solvent at room temperature. This crystal structure was deposited in the Cambridge Crystallographic Data Centre and assigned as CCDC 1835353. Further information can be found in the CIF file.

**Chapter 3: The Application of the 1,2-Brook Rearrangement Towards Inverse Polarity
Carbonyl Operators**

3.1 The Brook Rearrangement

The 1,2-anionic migration of a silyl group from a carbon to an oxygen atom was discovered by Brook in the late 1950s. This migration has been further demonstrated to be a general (1,n)-carbon to oxygen rearrangement (**Scheme 3-1**). Since this migration results in a nucleophilic carbon, this is an important approach to both normal and inverse polarity carbon nucleophiles (See Chapter 2 for introduction to polarity disconnections).^{275,158,159,276}

Scheme 3-1. The Brook Rearrangement



The 1,2-anionic Brook rearrangement has been subject to mechanistic inquiry, with the migration of the silicon group demonstrated to be a reversible, equilibrium process. Assuming the migration of the silicon has a low barrier, the position of the equilibrium is thus dictated by the thermodynamic stabilities of the competing species.²⁷⁵ When sub-stoichiometric amounts of base are employed, the relative energies of the silyl carbinol **III-1** and silyl ether **III-5** dictate the equilibrium position. The significant difference between the carbon-silicon bond (75-85 kcal mol⁻¹) and oxygen-silicon bond (120-130 kcal mol⁻¹) provides a strong driving force, resulting in a rapid and essentially irreversible silicon migration and protonation.²⁷⁷ However, under anionic conditions, the energy difference between anionic species **III-2** and **III-4** are the dominant considerations. The major factors are basicity of the carbanion and the identity of counter-ion.

Substituents on the carbanion capable of accepting electron density stabilize the carbanion, favoring migration, while the identity of the counter ion correlates to stability of the alkoxide.²⁷⁸ Highly aggregated states with tight ion pairing, characteristic of lithium alkoxides, result in the favoring of **III-2**, while weaker interactions with cations such as sodium and potassium favor silicon migration. Additionally the alkoxide can be destabilized by the use of metal chelators such as crown ethers and TMEDA, or the use of polar aprotic solvents.²⁷⁵

The effect of substituents on the rate of 1,2-Brook rearrangement has been studied (**Figure 3-1**). Brook demonstrated that substitution on the carbon and silicon have significant effects on the rate of the reaction.²⁷⁷

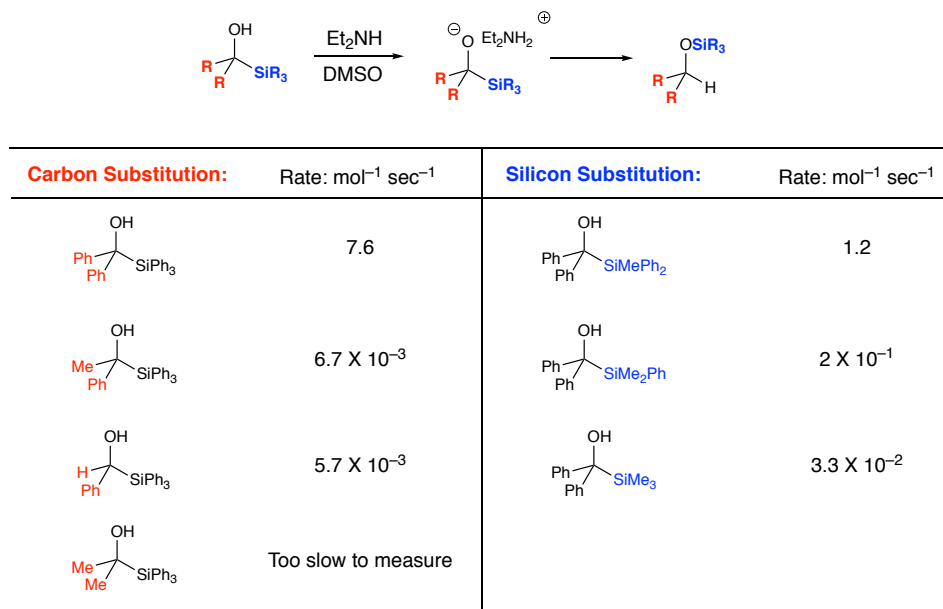


Figure 3-1. Substituent Effects on the Rate of the 1,2-Brook Rearrangement.

The dramatic effect of carbinol substitution on the rate of 1,2-silyl migration indicates that carbanion stability is a key factor in the rate of the 1,2-Brook rearrangement. At least one aryl group must be present for the reaction to occur and the difference in rate between the

benzylic and doubly benzylic substrates is 3 orders of magnitude. Interestingly, substitution on the silicon has a significant effect as well, with aryl substitution being heavily favored. This, along with observations of stereospecific inversion of chiral carbon centers resulted in the proposal of **III-3**, characterized by a hypervalent silicon center, as the operative intermediate in this rearrangement.²⁷⁹

While the orbital considerations accounting for this stereochemical fidelity have not been explicitly outlined in the literature, it is unlikely that full carbanions like **III-4** exist in solution, but rather silicate intermediate **III-6** (**Figure 3-2**). To account for the stereochemical inversion, the new bond formed at carbon would occur by the flow of electron density through the backside of the silicon-carbon bond. An analogous mechanism has been proposed by Aggarwal et al. in the stereoinvertive borylation of lithiated carbinols.²⁸⁰

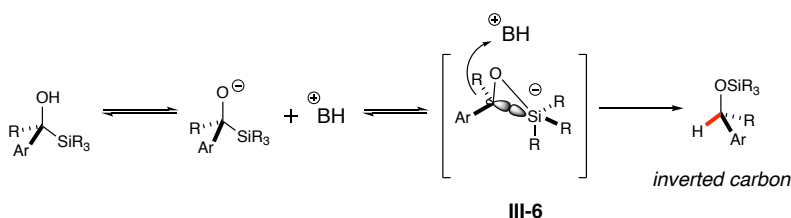


Figure 3-2. Inversion Process in the 1,2-Brook Rearrangement.

Due to the nature of hypervalent silicon, the benzylic carbon-silicon bond is not a typical sp^3 bond.²⁸¹ While early work advanced rehybridization of the silicon center to sp^3d , subsequent computational analyses have indicated the d orbitals of silicon are too high in energy to favor this configuration. Instead, it is proposed that pentacoordinate silicon complexes are trigonal bipyramidal structures with a sp^2 hybridized silicon center (**Figure 3-3**).²⁸² In this arrangement, the equatorial ligands are engaged in sp^2 bonding interactions while the axial ligands are

involved in a 3-center, 4-electron bonding arrangement with the silicon p-orbital while the equatorial.^{283,284} Further experimental work and computational analysis is required to provide more explicit and concrete structural information on intermediate **III-6**.

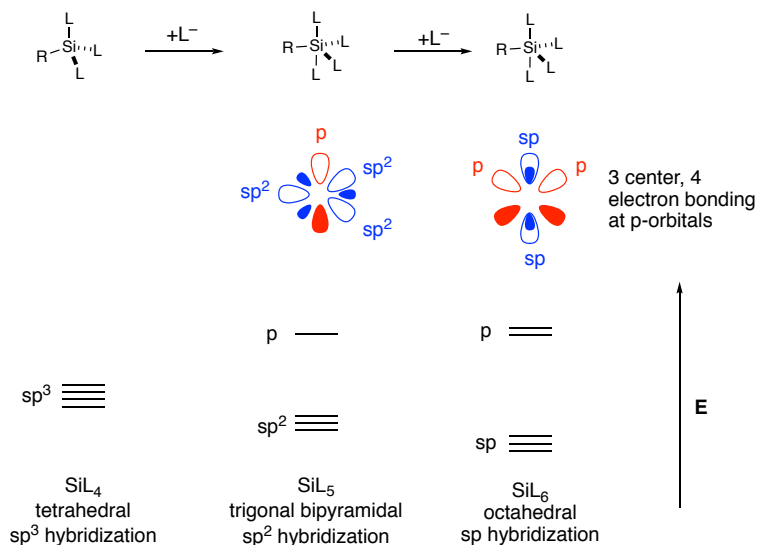
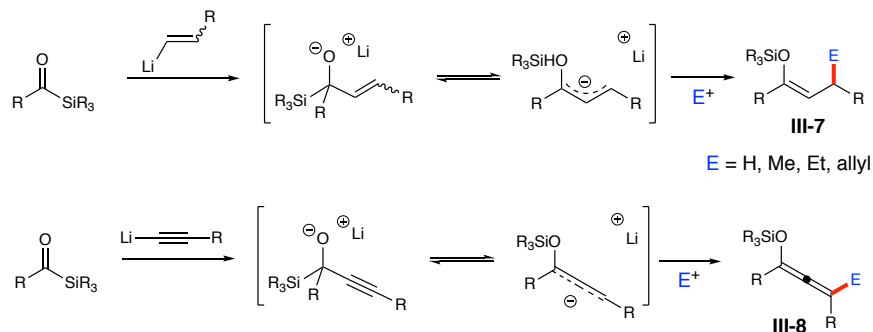


Figure 3-3. Hybridization and Molecular Orbital Schemes of Silicon Complexes.

3.2 Applications of the Brook Rearrangement in Carbon-Carbon Bond Forming Reactions

While Brook performed foundational studies characterizing the mechanistic aspects of this silicon migration, a number of applications to carbon-carbon bond formation have been developed utilizing the Brook rearrangement in tandem and cascade reactions.²⁷⁵ It was recognized that acyl silanes could be used with nucleophiles to generate conditions for the anionic 1,2-Brook rearrangement to take place (**Scheme 3-2**).²⁸⁵ Reich and co-workers reported that the addition of alkenyl and alkynyl lithiates results in silyl enol ethers (**III-7**) and siloxyallenes, respectively (**III-8**).

Scheme 3-2. Addition of Unsaturated Nucleophiles to Acyl Silanes.



This acyl silane addition strategy has been further applied to cyclization cascades. Takeda et al. utilized and extended the concepts demonstrated by Reich to the addition of lithium enolates to unsaturated acyl silanes (**Figure 3-4**).²⁸⁶ The earliest example utilized the addition of an enolate to generate a 1,3-alkoxy ketone **III-9** that upon 1,2-Brook rearrangement resulted in an allyl stabilized carbanion **III-10**. This carbanion then undergoes addition to the ketone, yielded cyclopentanols **III-11** in good yield. Treatment with TBAF yield, cyclopentenones **III-12**. This cascade was applied to the synthesis of anti-tumore marine prostanoids clavulones II and III.^{286,287}

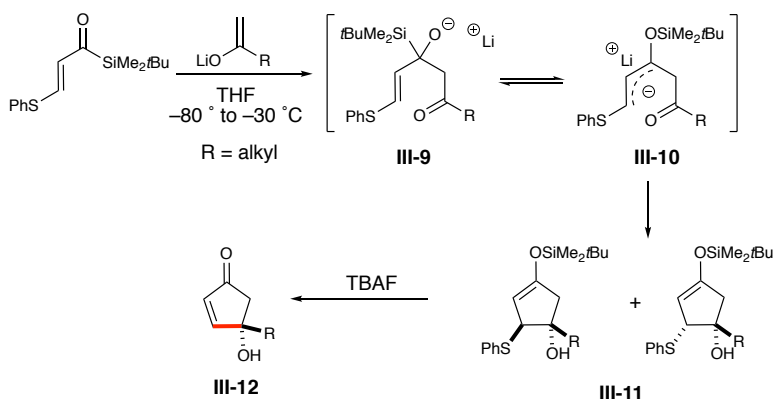


Figure 3-4. Cyclopentenone Synthesis By 1,2-Brook Cascade.

The use of an unsaturated enolate results in a formal 4+3 annulation (**Figure 3-5**). Rather than the allylic anion undergoing addition at the β -position, it is proposed that addition to the ketone at the carbinol position yields the alkoxy-cyclopropane **III-13** that undergoes an oxyanion-accelerated Cope rearrangement.^{288,287}

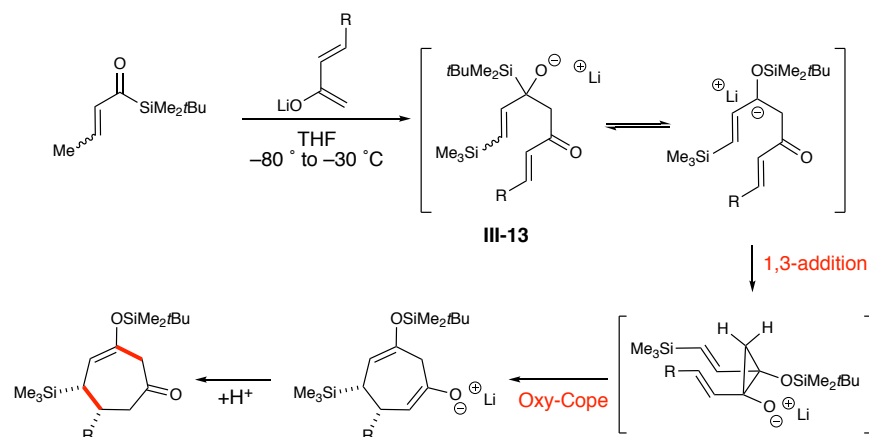


Figure 3-5. Cycloheptanone Synthesis By 1,2-Brook/Oxy-Cope Cascade.

This 4+3 annulation strategy has been employed in the preparation of complex polycyclic systems. Takeda et al. applied this strategy to the synthesis of the tricyclic core of Cyanthin natural products.²⁸⁹ The addition of enolates to acyl silanes to create homoenolates (**III-14**) has been conducted by Scheidt et al. Notably, aryl silanes must be used to stabilize the carbanion for the desired alkylation to take place (**Figure 3-6**).

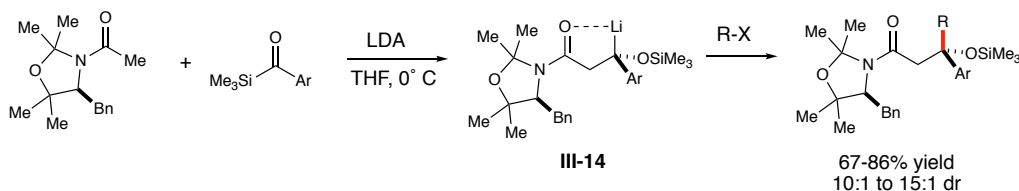
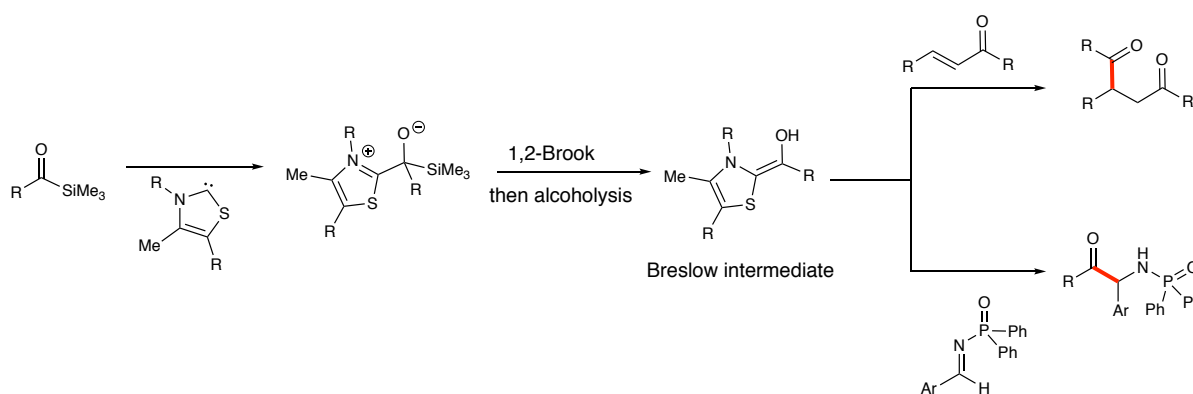


Figure 3-6. Diastereoselective Homoenolate Alkylation via Enolate Addition to Acyl Silanes.

The Scheidt laboratory has also integrated acyl silanes into NHC catalysis, using them as aldehydes surrogates in cross-coupling reactions (**Scheme 3-3**). Since acyl silanes do not undergo addition by the Breslow intermediate, cross-reactivity was thus enabled, overcoming a serious limitation of the conventional reactivity of aldehydes in NHC manifolds.²⁹⁰⁻²⁹²

Scheme 3-3. Integration of 1,2-Brook Rearrangement into NHC Catalysis.



3.3 New Brønsted Base Mediated 1,2-Brook Rearrangement Coupling Reactions

While acyl silanes has served as useful electrophiles for the development of 1,2-Brook rearrangement cascades, investigation of fundamental reactivity has been limited. With reactions like the deprotonation of α -silyl alcohols such as alkylations of carbanion have never been reported. Since Brook reported that α -silyl alkoxides underwent stereospecific rearrangements, opportunities to prepare valuable enantioenriched substituted alcohols were yet unrealized. The Scheidt laboratory attempted the stereoselective addition of 1,2-Brook based d¹ operators into imines to stereoselectively provide 1,2-amino alcohol products. Promising reactivity was observed by a post-doctoral worker that I later found to be unreproducible (**Figure 3-7**).

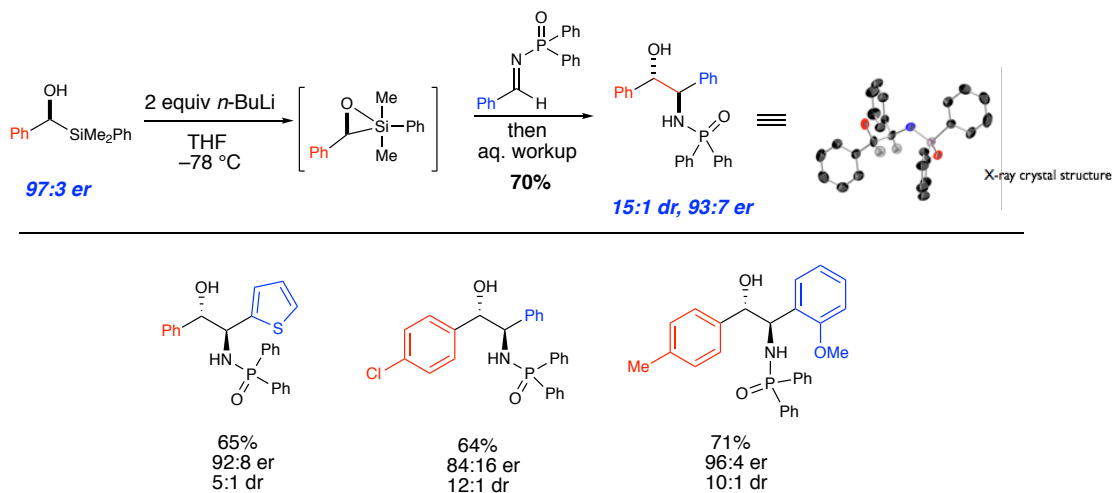


Figure 3-7. 1,2-Brook Mediated Stereoselective Synthesis of 1,2-Aminoalcohols Initially Reported by Dr. Dmitrijs Cernaks

Careful attempts to examine order of addition, ageing of lithiated species, base/counter ions, temperature, source of THF, and electrophile never resulted in recovery of the desired reactivity. Stabilized substrates were designed and tested in an attempt to favor the carbanion species (**Figure 3-8**). Interestingly, when these fluorinated analogs were lithiated, a persistent deep red color was observed, similar to the reports of West et al. in which the lithiation of silylated benzylic ethers *t*-BuLi resulted in a deep red solution.²⁹³ The addition of imine to this solution did not result in the observation of product.

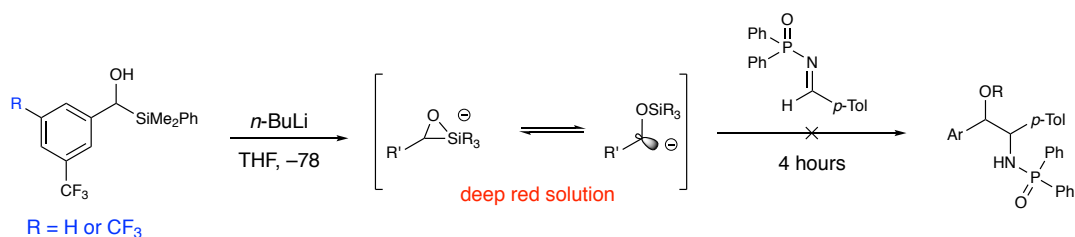


Figure 3-8. Testing Stabilized Carbanions in the Imine Addition Reaction

The addition of fluoride additives was investigated in the hope of creating a more reactive silicate intermediate, since a pentacoordinate silicon centers are more Lewis acidic than the corresponding tetracoordinate center.^{281,282} Upon addition of TBAF, a similar deep red solution was observed, however this color dissipated after several seconds, likely due to the water in the TBAF solution (**Figure 3-9**). Unfortunately, no other anhydrous sources of fluoride showed the same reactivity nor did other Lewis bases such as MeLi or Grignard reagents. With Brønsted base approaches not yielding significant progress, efforts turned to the Lewis base mediated 1,2-Brook rearrangement.

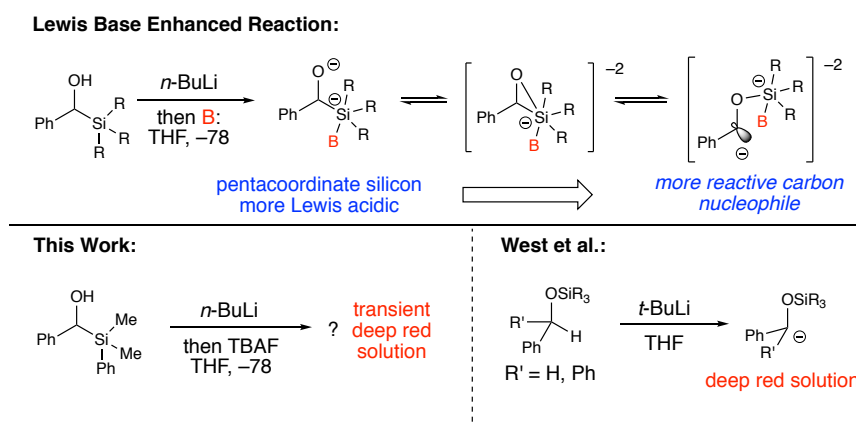


Figure 3-9. Lewis Base Enhanced 1,2-Brook Rearrangement

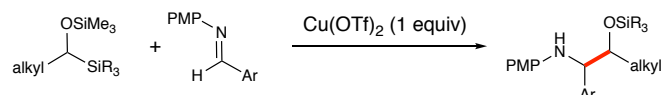
3.4 Lewis Base Mediated 1,2-Brook Coupling Reactions

Another entry point to d^1 operators from the 1,2-Brook rearrangement is the desilylation of α -silyl, silyl ethers. These and related compounds have seen a variety of uses in synthesis in Lewis acid mediated reactions, as chiral auxiliaries,²⁹⁴ in allylic transpositions,²⁹⁵ Prins reactions,²⁹⁶ as well as other capacities.²⁹⁷⁻³⁰⁰ However, their use as nucleophiles via the 1,2-Brook rearrangement is rare (**Scheme 3-4**).³⁰¹⁻³⁰³ The Scheidt laboratory demonstrated that α -silyl, silyl ethers underwent the 1,2-Brook rearrangement and alkylation upon exposure to

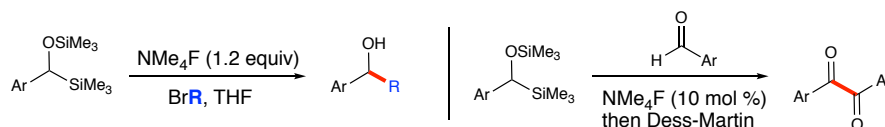
fluoride. Additionally, they were shown to add to aldehydes in good yield, albeit with low diastereoselectivity.

Scheme 3-4. Use of α -Silyl, Silyl Ethers as Nucleophiles.

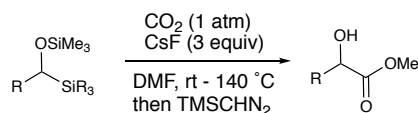
Yonezawa et al. 2005:



Scheidt et al. 2012:



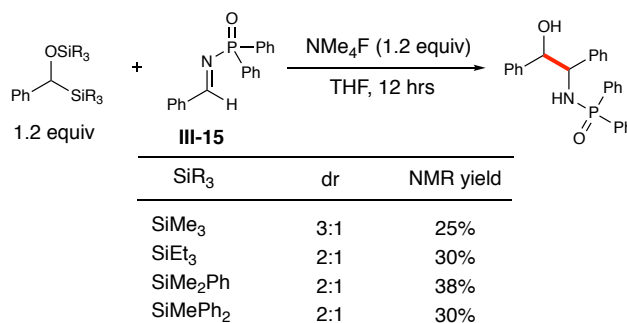
Sato et al. 2014:



3.4.1 Addition to Imines

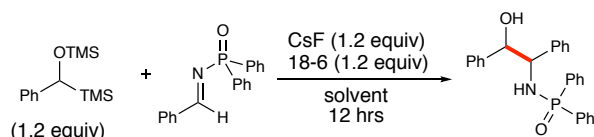
Following up upon our efforts to use the Brønsted mediated 1,2-Brook to add d^1 operators to imines, the application of fluoride initiated 1,2-Brook was investigated. Screening several aldimines (Boc, tosyl, diphenyl phosphoryl) with the conditions previously established revealed that only the diphenyl phosphoryl imine **III-15** showed competent reactivity. Subsequently, silicon groups on the α -silyl, silyl ether nucleophile were evaluated (**Table 3-1**).

Table 3-1. Effect of Silicon Group on Addition to Diphenyl Phosphoryl Aldimine.



The greatest diastereoselectivity was observed with trimethyl silyl (3:1 dr) while the best yield was observed with the dimethylphenyl silyl group (38%). Further attempts to improve yield with tetramethyl ammonium fluoride, by modulation of solvent and temperature, did not yield significant improvements. Cesium fluoride and phase transfer catalyst 18-crown-6 were then evaluated as the fluoride source. A range of solvents were evaluated, with toluene showing promising diastereoselectivity. Further attempts to replicate this reaction were unsuccessful (**Table 3–2**).

Table 3–2. Effect of Solvent Upon Addition to Diphenyl Phosphoryl Aldimine.



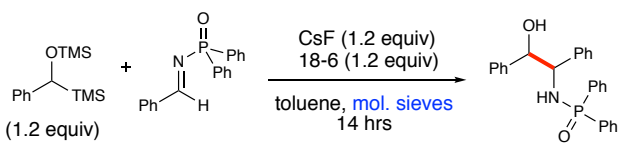
solvent	dr	NMR yield	conversion
THF	3:1	<5%	70%
MeCN	2:1	17%	>90%
trifluorotoluene	-	-	-
toluene	10:1*	10%	75%

*result not reproduced

An additional concern was the high conversion of aldimine observed, with relatively little product formation. Exposure of the diphenyl phosphoryl aldimine to the reaction conditions without the α -silyl, silyl ether resulted in little to no change to the imine. We hypothesized that the degradation of aldimine in the presence of the alkoxide as well as the inconsistent diastereoselectivity was potentially occurring due to varying water content in the reaction solvent. 3 and 4 Å molecular sieves along with varying amounts of α -silyl, silyl ether nucleophile and fluoride equivalents examined (**Table 3–3**). With 3 Å sieves 7:1 diastereoselectivity was observed, but the yield (NMR yield) remained low (25%) with >90% of the aldimine consumed.

Attempting slow addition of α -silyl, silyl ether nucleophile did not enhance the yield. With efforts to increase the yield of the reaction unsuccessful, attention was turned to other electrophiles.

Table 3–3. Optimization of Biomimetic Arylidene Malonate Cyclization



sieves	TMS equiv	F ⁻ equiv	dr	NMR yield	conversion
3Å	2.4	3.6	7:1	25%	>90%
4Å	2.4	3.6	3:1	25%	>90%
3Å	4	6	3:1	16%	>90%
4Å	4	6	4:1	16%	>90%

3.4.2 Addition to Arylidene Malonates

The addition of the α -silyl, silyl ether d¹ operator (**III-16**) to arylidene malonates was next explored. This addition would result in silyl ether **III-17** that could be easily converted to γ -butyrolactones, a privileged motif. Interestingly, a preliminary screen of solvents and fluoride sources revealed that the γ -butyrolactone product **III-18** was directly formed (**Figure 3-10**). The structure was confirmed by Krapcho decarboxylation to a known γ -butyrolactone structure **III-19**. Cesium fluoride and 18-crown-6 in acetonitrile proved to be the lead conditions, furnishing the lactone product in approximately 20% yield.

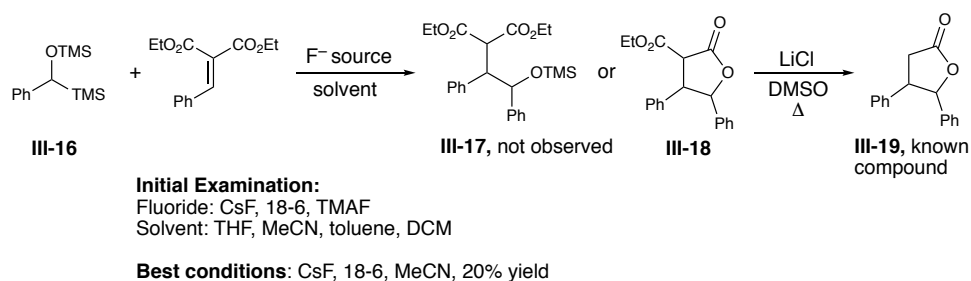


Figure 3-10. Investigation of Addition to Arylidene Malonates.

The transfer of stereochemical information was also evaluated, using the coupling/decarboxylation sequence to yield a γ -butyrolactone that could be analyzed with chiral HPLC (**Figure 3-11**). Unfortunately, all efforts resulted in racemic product. This is likely due to the reaction to be conducted at room temperature. Frustratingly, all attempts to run this reaction at temperatures lower than 0 °C resulted in no reaction.

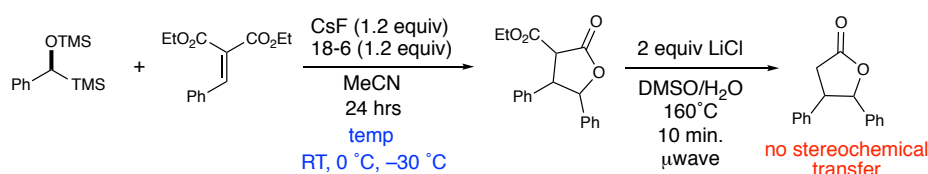


Figure 3-11. Investigation of Stereochemical Transfer in Fluoride Mediated 1,2-Brook

Enhancement of reactivity with Lewis acids was also attempted. However, in all case the initial desilylation of the the α -silyl, silyl ether was observed, but no product or malonate dimer (**Figure 3-12**).

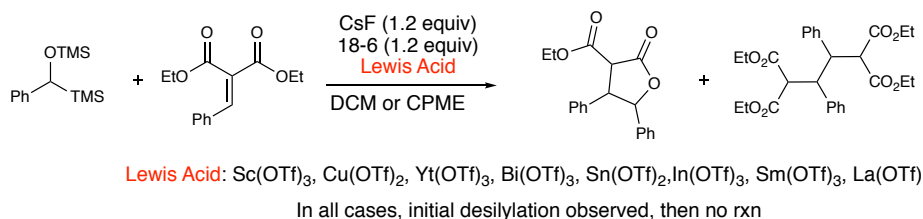


Figure 3-12. Screen of Lewis Acids as Additives in Addition to Arylidene Malonates.

While the initial conditions provided product **III-18** in an isolated yield of 20%, further optimization raised the isolated yield to 48% by the use of a mixed solvent system acetonitrile/tetrahydrofuran (**Figure 3-13**). Additionally, the mass balance of the aryldiene malonate was determined to be the dimeric diastereomers **III-20** and **III-21**.²⁴²

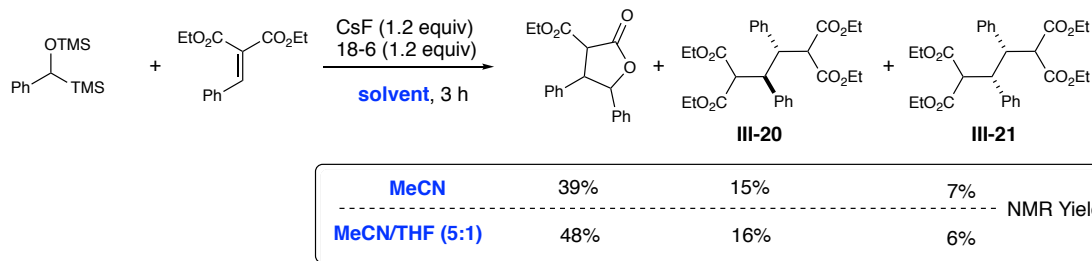


Figure 3-13. Product Distribution in Addition to Aryldiene Malonate.

With other efforts to improve the reaction failing, we sought to probe the origin of the dimeric species. At the time, these dimers had only been reported in obscure electrochemical papers, but later as reported in Chapter 2, we developed a photoredox approach towards the efficient preparation of these structures. Interestingly, unlike our photoredox reaction, the diastereomers of this dimer were formed in a ~2:1 ratio. This could indicate that these dimers are forming through a different pathway. Radical traps were added to the reaction to probe whether open-shell species were implicated in this dimerization. Three such radical traps were tested and all showed desilylation, but no formation of desired product (**Figure 3-14**). Additionally, silver triflate resulted in a silver mirror, indicating that the α -silyl alkoxide is able to undergo electron transfer reactions.

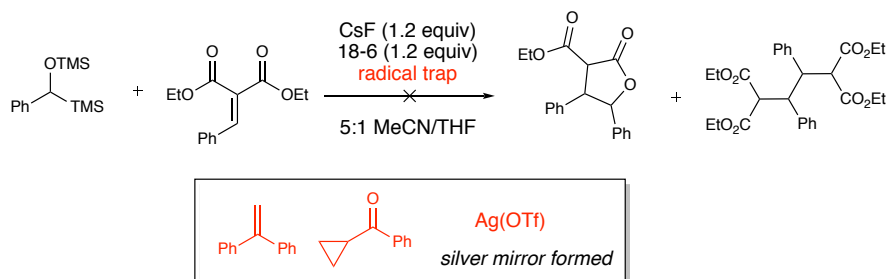


Figure 3-14. Investigation of Radical Traps on the Addition to Aryldiene Malonates

Salts of *tert*-butoxide have been implicated in single electron reactions and further shown to be weakly reducing.³⁰⁴ This reducing ability has been shown to correlate to counter ion as lithium salts show no single-electron reactivity while the more ionic and less coordinating sodium and potassium counter ions result in single electron reactions. This reaction uses cesium that is further coordinated by a crown ether, meaning that the reduction potential of this system could be even higher. Additionally, this reaction works best in acetonitrile a solvent known for supporting electron transfer.³⁰⁵ Finally, under the Brønsted base mediated 1,2-Brook conditions, no bond formed products were observed (**Figure 3-15**).

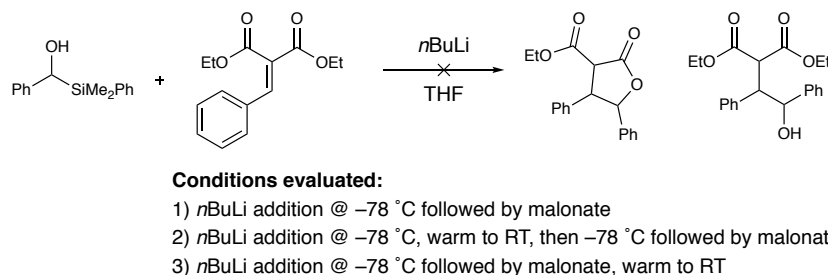
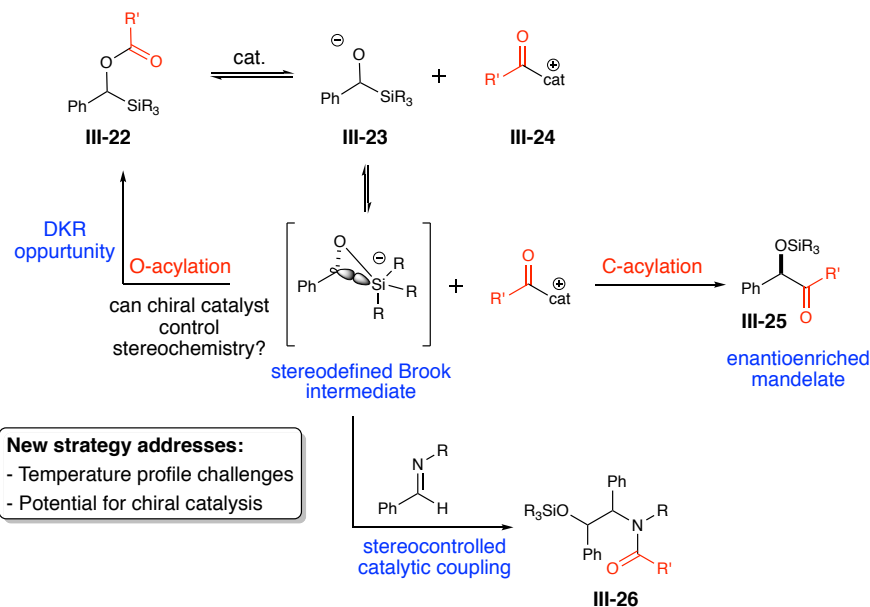


Figure 3-15. Investigation of Brønsted Base Mediated Addition to Arylydene Malonates

3.4.3 Studies Towards Acyl Transfer Initiated 1,2-Brook

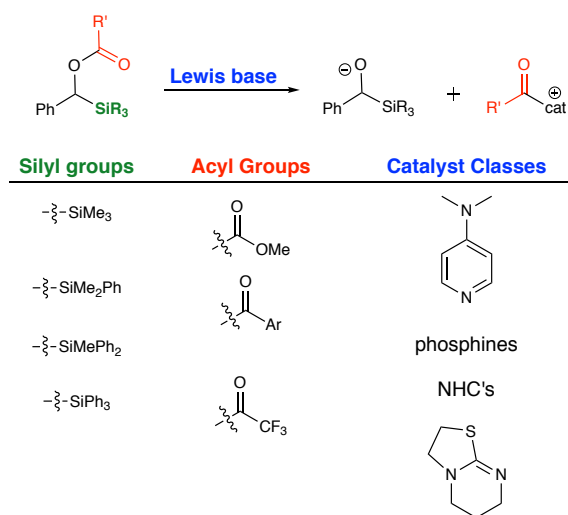
With the challenges associated with the fluoride initiated 1,2-Brook rearrangement proving difficult to surmount, an alternate strategy towards Lewis base reaction initiation was considered. We hypothesized that other strategies to create the requisite α -silyl alkoxide could enable a more controllable reaction, particularly since the fluoride sources shown to initiate the reaction prove insoluble in organic solvents at low temperatures. Acyl transfer was identified as an attractive alternate strategy, since a variety of Lewis bases, particularly chiral variants, are well established (**Scheme 3-5**).²⁸²

Scheme 3-5. Acyl Transfer Initiated 1,2-Brook Rearrangement.

The use of a chiral counter ion to create stereoconvergent processes with the 1,2-Brook rearrangement had never been reported, with an example only being published recently on the rearrangement of acyl silanes to enantioenriched secondary alcohols.³⁰⁶ Given that we had shown erosion of stereochemistry at room temperature of the α -silyl alkoxide, we believed it possible to create a new, stereoconvergent process. A number of possible pathways were identified upon acyl transfer, depending on relative rates of several pathways possible after acyl transfer. Rapid acylation of the α -silyl alkoxide **III-23** could result in a dynamic kinetic resolution of the secondary acylated species **III-22**. If the Brook intermediate was able to undergo acylation, mandelate products **III-25** would be formed. Alternatively, if this C-acylation process was slow, addition to another electrophile could occur, followed by acyl transfer (e.g. product **III-26**) to regenerate the catalyst or generate another equivalent of α -silyl alkoxide. With this framework outlined, possible silyl groups, acyl groups and classes of catalysts were mapped out. We

believed that based on the rate studies of the 1,2-Brook, the rate silicon migration could be controlled by silicon substitution, while acyl group and catalyst could control turnover of the system (**Scheme 3-6**).

Scheme 3-6. Investigation of Acyl Transfer Driven 1,2-Brook Rearrangement.



Preparation of these acylated systems was straightforward. Simply quenching the retro-Brook reaction of silylated benzyl alcohols with acylating agents provided a simple, practical entry to the carbonate analogs (**Figure 3-16**).

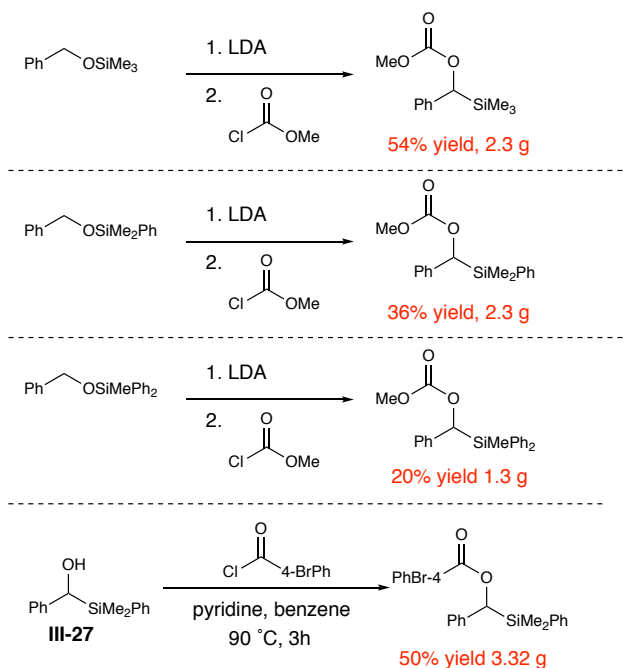


Figure 3-16. Preparation of Acylated α -Silyl Alcohols.

Additionally, the α -silyl alcohol **III-27** could be acylated under mild conditions as previously demonstrated by Brook.³⁰⁷ It is interesting to note that the yield of the process generally correlated to the rate of silicon migration previously shown by Brook. Product with quenching by TFAA showed no sign of product, but further studies are needed to fully evaluate how to prepare this compound. A point of entry for follow-up studies would be the application of the mild acylation conditions of α -silyl alcohol **III-27** with TFAA.

With a preliminary set of acylated α -silyl alcohols prepared, investigation of this system began by evaluating the rate at which free carbenes underwent acyl transfer.³⁰⁸⁻³¹⁰ This was accomplished by mixing stoichiometric amounts of free carbenes **III-29** and **III-30** with acylated substrate **III-28** and quenching with methanol. Yield of the resulting silyl ether **III-31** was obtained by comparison to an NMR standard. With the N,N-diisopropyl carbene (**III-29**), full

conversion was observed at 2.5 minutes, while the triazole NHC showed minimal conversion, which was attributed to its low solubility in THF.

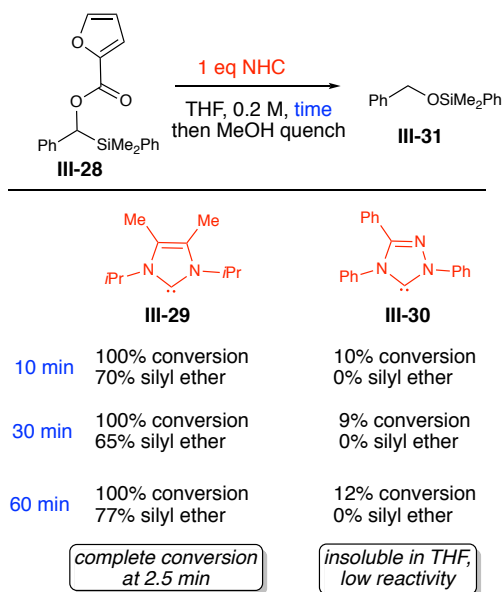


Figure 3-17. Investigation of 1,2-Brook Rearrangement of Acylated α -Silyl Alcohols.

Excited by these results, we sought to perform a cross-coupling reaction. Since our laboratory had previously shown efficient reactivity between the α -silyl nucleophile and aryl aldehydes, this was chosen as our initial point of investigation (**Figure 3-18**).

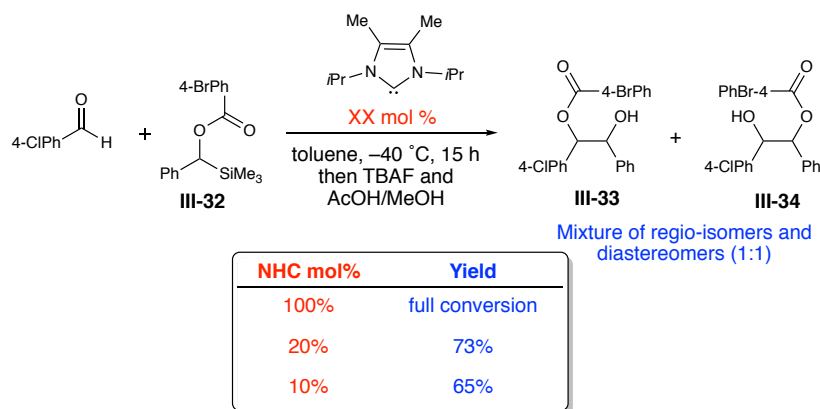


Figure 3-18. NHC Transesterification Catalyzed Addition to an Aryl Aldehyde.

Further guided by the previous experiment that demonstrated complete acylation of the NHC in 2.5 minutes, the α -silyl ester **III-32** and the NHC **III-29** were premixed (for 10 minutes) to ensure complete acylation (and avoid NHC addition to the aryl aldehyde) followed by addition of 4-Cl benzaldehyde. We were pleased to observe the formation of the cross-coupling product, even when the NHC loading was reduced to 20 or 10 mol %. Subsequent treatment of the reaction mixture by a buffered TBAF solution yielded the alcohol products (**III-33** & **III-34**) as a mixture of diastereomers (1:1) and regio-isomers, as the acyl and silyl groups likely underwent considerable exchange and transfer under the alkoxide conditions. Notably, no benzoin dimer corresponding to the 4-Cl benzaldehyde used were observed. To further understand this reaction, a cross-over reaction was performed. 4-BrPh α -silyl ester **III-32** was mixed with NHC **III-29** to form an initial alkoxide (**Figure 3-19**). Furyl α -silyl ester **III-28** and 4-Cl benzaldehyde were subsequently added and the reaction allowed to proceed. Only the coupled product with furyl acyl group **III-35** was observed. No product with the 4-BrPh acyl group **III-36** was detected. This indicates acyl transfer is not occurring at the carbene center, with the reaction propagating through acyl transfer to the alkoxide product. The NHC remaining acylated is also important as alternate as concerns that conventional NHC reactivity with aldehydes to form nucleophiles are obviated.

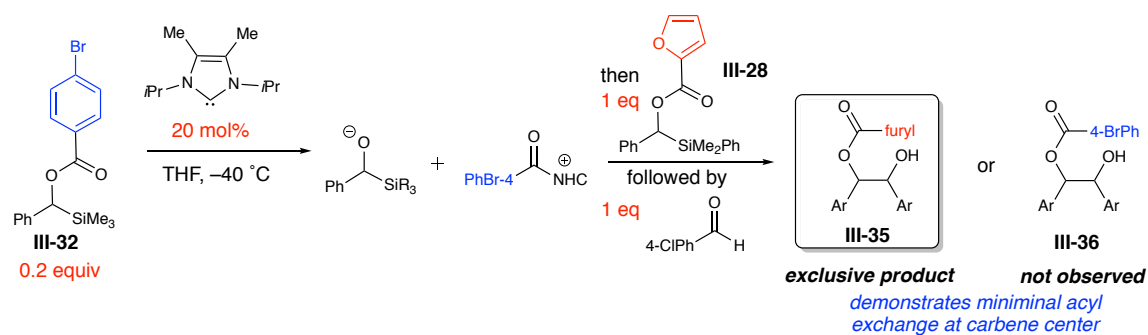
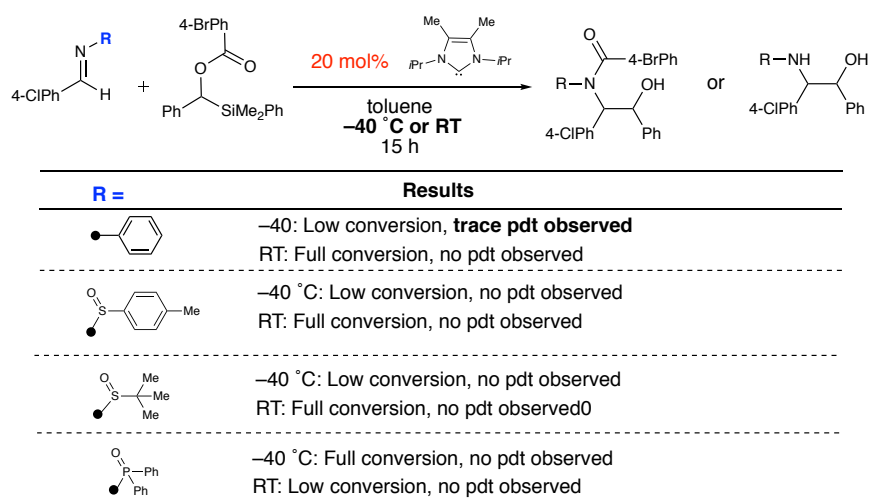


Figure 3-19. Acyl Cross-Over Experiment.

Excited by these promising results, attempts to extend this reactivity to imines was attempted. A variety of aldimines were screened under the previous conditions, but trace product was only observed in a single case (**Figure 3-20**). Frustrated by the lack of electrophile diversity, the decision was made to move to other 1,2-Brook rearrangement manifolds.

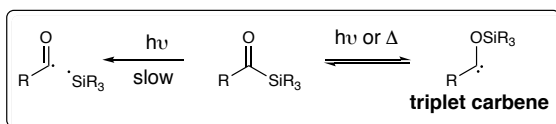
**Figure 3-20.** NHC Transesterification Catalyzed Addition to Aryl Aldimines.

3.5 Photo-triggered 1,2-Brook Rearrangement of Acyl Silanes

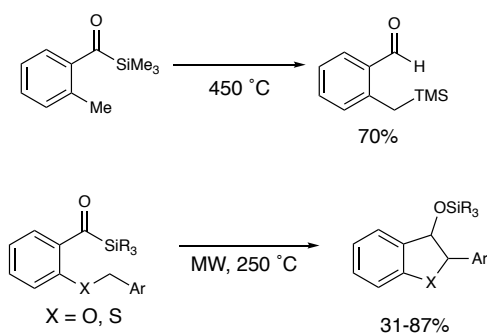
While silyl carbinols undergo a variety of 1,2-Brook Rearrangements, acyl silanes also undergo a 1,2-migration to yield a triplet carbene.³¹¹ This can occur under high heat, or irradiation with light. Acyl silanes possess an abnormally large n to π^* (380-420 nm) and a large extinction coefficient.³¹² Depending on the structure of the acyl silane, both carbene and radical intermediates are active under photochemical reaction conditions. Brook first reported the photolysis of acyl silanes and their resulting insertion into a variety of polarized X-H bonds.³¹³ While the photolysis of alkyl acyl silanes often results in radical reactions, Bolm and co-workers

have shown a number of photochemical reactions of acyl silanes.³¹⁴⁻³¹⁷ With only limited examples of intermolecular reactivity, we set out to establish new reactivity.

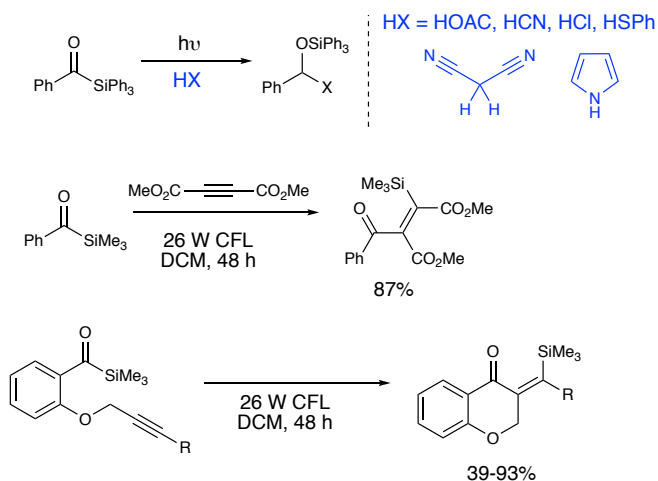
Scheme 3-7. 1,2-Brook Rearrangement of Acyl Silanes.



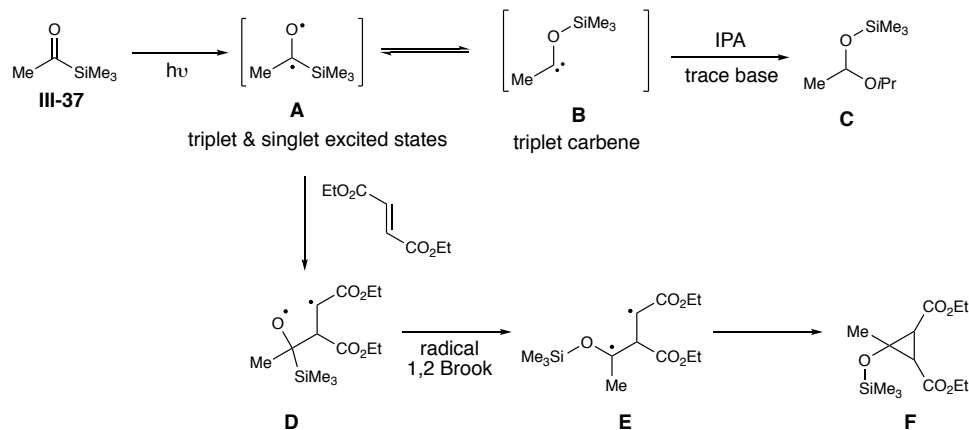
Thermal Reaction Examples:



Photolytic Reaction Examples:



Kinetic studies have been carried out on the acyl silane photochemical system with some key observations regarding the addition to polar X-H bonds and unsaturated pi systems (**Scheme 3-8**).^{318,319} Dalton and co-workers demonstrated that for acetyltrimethyl silane **III-37** the cycloaddition to activated olefins does not involve a carbene intermediate, but is a result of the interaction of the alkenes with the triplet & singlet states of the photoexcited acyl silane. Interestingly, they also demonstrated that the reactivity with polarized X-H bonds does go through a carbene intermediate (derived from the triplet state).

Scheme 3-8. Proposed Mechanism of Photo-Cyclopropanation of Activated Alkenes.

Regarding reactivity with polarized olefins, the following key observations were made: Stern-Volmer quenching studies showed that 1,2-dicyanoethylene quenches the excited singlet state of the acylsilane at the diffusion-controlled limit; triplet lifetime is not affected by concentration of isopropanol; up to 10 M isopropanol has no effect on quantum yield of cycloaddition process. An additional important observation was that only alkenes with triplet energies ($E_T = 61 \text{ kcal mol}^{-1}$) matching the triplet energy of the acyl silane quench it. **Thus 1,3-cyclohexadiene ($E_T = 54 \text{ kcal mol}^{-1}$) only partially quenches the triplet state and is unreactive.** Previous studies of photoreactions of alkanones has demonstrated that biradicals like **D** are plausible intermediates. Additionally, Turro et al. have demonstrated that these intermediates react stereospecifically.^{320,321} Dalton et al. invoked that intermediate, followed by a radical 1,2-Brook migration to give biradical **E**, that closes to yield the cyclopropanated product **F**.

3.5.1 Lewis Acid Mediated Cyclopropanation of Arylidene Malonates

Since the cycloaddition of acyl silanes to olefins is limited to highly polarized systems, we sought to explore whether Lewis acids could engender the required polarization. A screen of

Lewis acids complexed with *t*-butyl BOX revealed that magnesium bromide uniquely catalyzed the addition of acyl silane **III-38** to acrylidene malonate **III-39** under irradiation with blue lights (**Figure 3-21**). Given the carbene addition-like products Bolm had shown these photoreactions to undergo, we believed that the malonate was getting cyclopropanated (**III-41**) then cleaving under silica conditions to yield the d¹ addition product **III-40**.

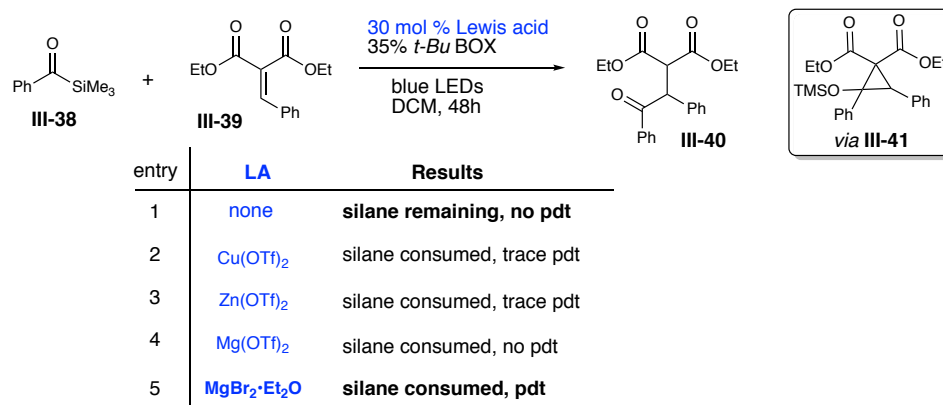
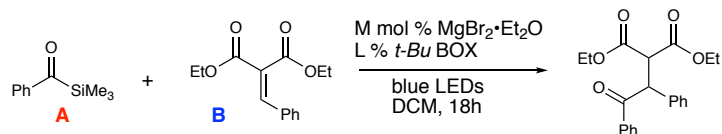


Figure 3-21. Initial Investigation of Lewis Acid Mediated Photoaddition of Acyl Silanes.

Follow-up investigations showed that stoichiometric Lewis acid was required to enable the transformation (**Table 3-4**). Additionally, either excess acyl silane or acrylidene malonate were required if complexed magnesium bromide was used.

Table 3–4. Optimization of Lewis Acid Mediated Photoaddition of Acyl Silanes.

entry	M, L mol %	A : B	NMR Yield
1	30, 35	1:1	10%
2	100, 105	1:1	3%
3	100, 0	1:1	40%
4	30, 35	2:1	10%
5	100, 105	2:1	50%
6	100, 0	2:1	40%
7	30, 35	1:2	10%
8	100, 105	1:2	0%
9	100, 0	1:2	40%

The best results were observed with 1 equivalent of magnesium bromide-BOX complex with a 2:1 ratio of acyl silane to malonate (entry 5). Further screening with BOX ligands show inconsistent reaction outcomes (**Table 3–5**). Using *i*Pr-PYBOX, promising enantioselectivity 70:30 was observed in 50% yield. However, the same reaction run on a different day showed racemic product, but 70% yield.

Table 3–5. Investigation of Magnesium Lewis Acids in Photoaddition of Acyl Silanes

MgX ₂	L	NMR yield	ER
MgBr ₂ ·Et ₂ O	A	50%	50:50
MgI ₂	A	25%	40:60
Mg(OTf) ₂	A	—	—
MgBr ₂ ·Et ₂ O	B	70%	50:50
MgBr ₂ ·Et ₂ O	B	50%	70:30

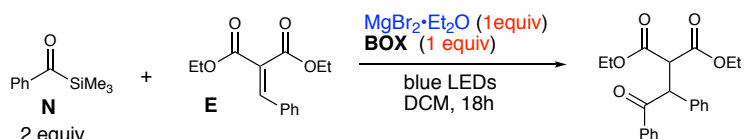
inconsistent reactivity

t-Bu-BOX (A)

i-Pr-PyBOX (B)

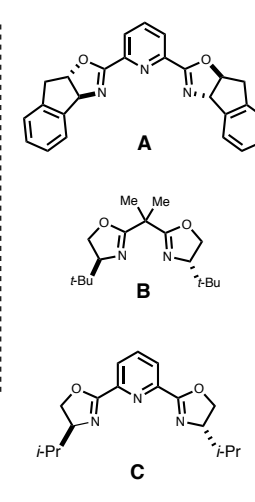
Examining reaction set-up closely still revealed inconsistent reactivity. The order of addition and complexation with the Lewis acid were investigated. Premixing the acyl silane and the malonate with the Lewis acid, versus the malonate alone greatly changed the outcome of the reaction (entries 1-4). Again in the case *i*Pr-PYBOX (ligand **C**), inconsistent reactivity was observed when the reactions were set-up identically in parallel. With these frustrating inconsistencies, attention was turned to a different substrate.

Table 3–6. Investigation of Operational Parameters of Lewis Acid Mediated Photoaddition.



entry	BOX	Premix	ER	Conversion %	Yield %
1	A	E + N	52:48	>80	<20
2	A	E	–	–	–
3	B	E + N	50:50	>80	23
4	B	E	42:58	43	~20
5	C	E	54:46	>80	42
6	C	E	52:48	60	<20

SAME REACTION HEAD TO HEAD



3.5.2 Cyclopropanation of Maleimides

Maleimides were targeted next as cycloaddition substrates. Subjecting benzyl maleimide **III-42** to the photolytic conditions with acyl silanes revealed that acyl silanes added efficiently, with good diastereoselectivity in 79% total yield (**Figure 3-22**). Hydrolysis upon silica was observed, with no ketone product **III-44** observed in the unpurified reaction mixture.

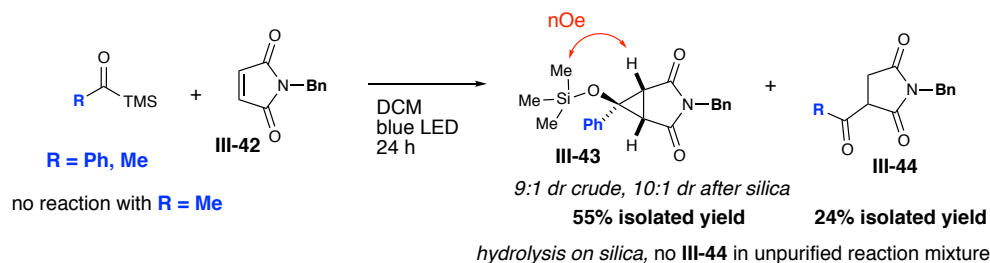


Figure 3-22. Initial Investigation of Lewis Acid Mediate Photoaddition of Acyl Silanes.

We sought a more challenging reaction with a methyl substituted maleimide **III-45** to explore the preparation of quaternary centers. This added substitution proved to hamper reactivity, with the reaction taking 60 hours and five equivalents of acyl silane. Additionally, considerable amounts of maleimide dimer **III-48** were isolated and the use of a chiral maleimide **III-45** resulted in no observed diastereoselectivity (**Figure 3-23**). While maleimides are known to undergo photoreactions, UV light typically is used in these reactions.^{322,323} Without acyl silane, no dimerization was observed so energy transfer from the photoexcited acyl silane to the maleimide must be taking place.

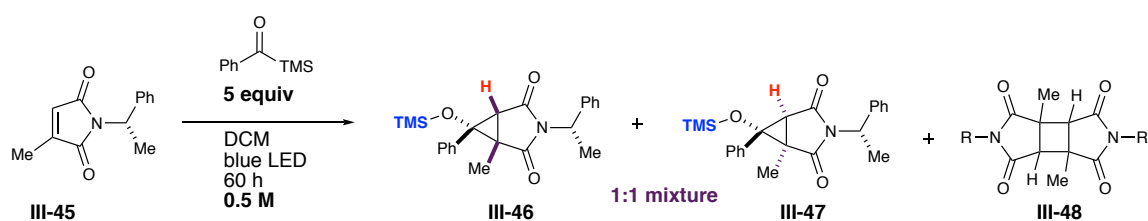


Figure 3-23. Photoaddition to Substituted Maleimides.

In an attempt to favor addition of the acyl silane, LUMO activating catalysts were screened (**Figure 3-24**). However, the reaction proved to only be compatible with lithium hexafluorophosphate, but showed the same profile. With the substrate scope for cycloadditions

of acyl silanes frustratingly limited, we suspended the pursuit of novel photoreactions with acyl silanes.

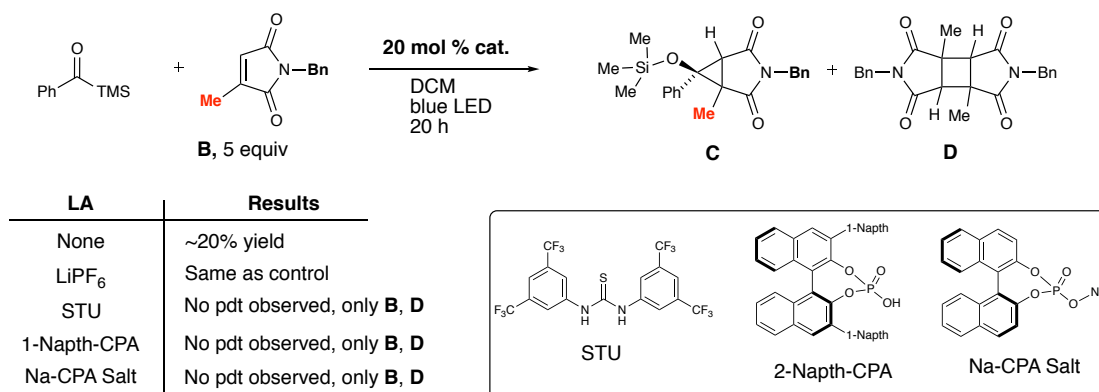


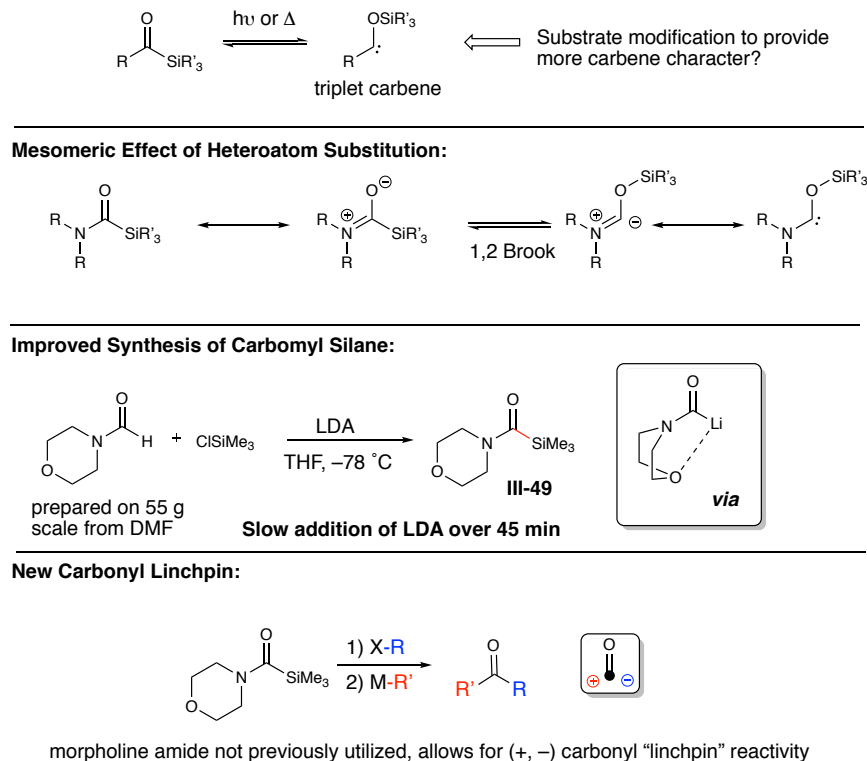
Figure 3-24. Application of LUMO Lowering Catalysts to Photoaddition to Maleimides.

3.6 Future Work

Promising results have been obtained in the area of the 1,2-Brook rearrangement. Follow-up work in alternative Lewis base-mediated reaction initiation should be conducted. It was shown that under the reaction conditions, acylated N,N-diisopropyl imidazolium species does not undergo acyl transfer. Variants of this species could be employed as a chiral counter ion with silyl, silyl systems, as silyl group transfer may be more facile than acyl transfer. Additional electrophiles should be explored with this catalytic system as well. Finally, the use of allylic species were underexplored in these studies and could result in a new approach to homoenolate operators.

A class of compounds related to acyl silanes are carbamoyl silanes. With the carbon substituent an acyl silane replaced by nitrogen, the resulting amide-like structure possesses its own unique characteristics and reactivity due to contributions from the nitrogen lone pair (**Scheme 3-9**).

Scheme 3-9. 1,2-Brook Rearrangement of Carbamoyl Silanes.



Preliminary work conducted has shown that the morpholinyl derivative **III-49** is much simpler and easier to prepare. Rather than syringe-pumping base for 8 hours, base can be slowly added to a mixture of morpholinyl formamide and trimethyl silane (**Scheme 3-9**). Simply concentrating the resulting solution and switching solvent to DCM, allows for lithium chloride to be filtered (under inert conditions), yielding clean material. This analog has yet to be reported and could be exploited as a new carbonyl linchpin. Cunico has studied the addition of these species to conjugate acceptors and demonstrated that their integration into transition metal catalysis, these d^1 operators remain poised to be further explored in transition metal reactions beyond simple arylations.³²⁴⁻³³¹ Merger with Fu³³² and Reisman³³³ type stereoconvergent nickel reactions are one such area.³³⁴

3.7 Conclusion

Broad investigations in the area of d^1 operators derived from the 1,2-Brook rearrangement were conducted. Long term goals for this work are the development of catalytic asymmetric reactions that use catalyst chirality to drive stereoconvergent bond forming reactions. Additionally, the utility of carbamoyl silanes in transition metal reactions has only been investigated in simple coupling reactions, with opportunities in stereospecific and stereoconvergent couplings still unrealized .

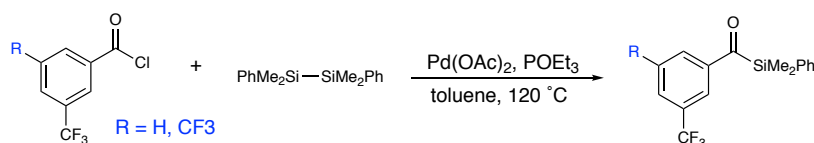
3.8 Experimental Section

3.8.1 General Information

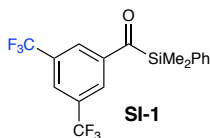
All reactions were carried out under an argon or nitrogen atmosphere in flame-dried glassware with magnetic stirring. Solvents used in reactions were purified by passage through a bed of activated alumina. Reagents were purified prior to use unless otherwise stated following the guidelines of Perrin and Armarego.¹²⁵ Purification of reaction products was carried out by flash chromatography on Biotage Isolera 4 systems with Ultra-grade silica cartridges. Analytical thin layer chromatography was performed on EM Reagent 0.25 mm silica gel 60-F plates. Visualization was accomplished with UV light. Infrared spectra were recorded on a Bruker Tensor 37 FT-IR spectrometer. ¹H NMR spectra were recorded on an AVANCE III 500 MHz with direct cryoprobe (500 MHz) spectrometer and Bruker Avance III 600 MHz (151 MHz) system. These are reported in ppm using solvent as an internal standard (CDCl₃ at 7.26 ppm). Data are reported as (s = singlet, d = doublet, t = triplet, q = quartet, quint = quintet, m = multiplet, br = broad; coupling constant(s) in Hz; integration.) Proton-decoupled ¹³C NMR spectra were recorded on an AVANCE III 500 MHz with direct cryoprobe (125 MHz) spectrometer and Bruker Avance III 600 MHz (151 MHz) system. These are reported in ppm using solvent as an internal standard (CDCl₃ at 77.16 ppm). Mass spectra were obtained on WATERS Acquity-H UPLC-MS with a single quad detector (ESI) Varian1200 Quadrupole Mass Spectrometer. Gas chromatography experiments were run on Agilent 7890A/5975C GC/MS System.

Diphenyl phosphoryl aldimines,³³⁵ tosyl aldimines,³³⁶ and Boc aldimines³³⁷ were prepared according to literature procedure. α -Silyl, silyl ethers were prepared according to Brekan et al.³³⁸ Free carbenes **III-29** and **III-30** were prepared according to Sanford³³⁹ and Enders³⁴⁰. Methyl substituted maleimides were prepared as reported by Hayashi et al.³⁴¹ Morpholine formamide was prepared according Nguyen et al.³⁴²

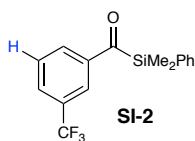
3.8.2 Preparation of α -Silyl, Silyl Alcohols



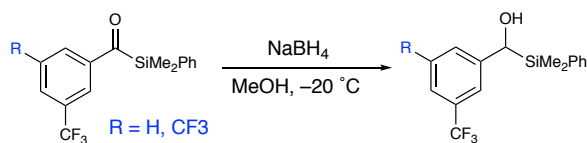
In a syn-vial were placed diacetoxypalladium (0.067 g, 0.300 mmol) and triethyl phosphite (0.103 ml, 0.600 mmol) under nitrogen atmosphere. 1,1,2,2-tetramethyl-1,2-diphenyldisilane (0.832 ml, 3.00 mmol) in toluene (Volume: 2.5 ml) was added, and the mixture was stirred magnetically for 5 min at room temperature, during which time the mixture became a yellowish suspension. The corresponding freshly distilled benzoyl chloride (3 mmol) was then added and the mixture was heated at 110 °C for 20 h. After complete conversion of the benzoyl chloride (usually a palladium mirror formed), the reaction mixture was cooled and subjected directly to column chromatographic separation (3-5% Ethyl Acetate/Hexanes).



Prepared according to the method described above. Purification yielded a yellow oil (553 mg, 49%). Analytical data for **SI-1**: ^1H NMR (500 MHz, Chloroform-*d*) δ 8.13 – 8.06 (m, 2H), 7.96 – 7.89 (m, 1H), 7.64 – 7.56 (m, 2H), 7.49 – 7.38 (m, 3H), 0.66 (s, 6H).

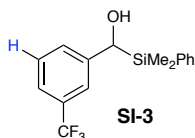


Prepared according to the method described above. Purification yielded a yellow oil (407 mg, 44%). Analytical data for **SI-1**: ^1H NMR (500 MHz, Chloroform-*d*) δ 7.98 (d, $J = 1.8$ Hz, 1H), 7.88 (d, $J = 7.9$ Hz, 1H), 7.73 – 7.68 (m, 1H), 7.61 – 7.56 (m, 2H), 7.56 – 7.52 (m, 1H), 7.49 (t, $J = 7.8$ Hz, 1H), 7.45 – 7.37 (m, 2H), 7.37 – 7.32 (m, 1H), 0.64 (s, 6H).

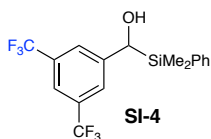


A solution of acyl silane (0.5 mmol) in methanol (1.25 ml) was added to a solution of sodium borohydride (0.25 mmol) in methanol (1.25 ml) at -20 °C under an argon atmosphere. The reaction mixture was stirred at -20 °C for 45 min, quenched with saturated NH_4Cl solution, and extracted with ethyl acetate (x2). The combined organic layers were washed with brine, dried over MgSO_4 , and filtered. The filtrate was concentrated under reduced pressure. The residue was

purified by flash column chromatography on silica gel (5% Ethyl Acetate/Hexanes) to yield a clear oil.

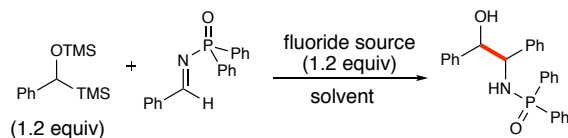


Prepared according to the method described above. Purification yielded a thick clear oil (124 mg, 84%). Analytical data for **SI-3**: ^1H NMR (500 MHz, Chloroform-*d*) δ 7.42 (ddd, $J = 10.8, 6.8, 1.8$ Hz, 4H), 7.39 – 7.31 (m, 4H), 7.23 (d, $J = 7.9$ Hz, 2H), 4.76 (s, 1H), 0.31 (s, 3H).



Prepared according to the method described above (1.4 mmol scale). Purification yielded a thick clear oil (450 mg, 86%). Analytical data for **SI-4**: ^1H NMR (500 MHz, Chloroform-*d*) δ 7.62 (s, 1H), 7.40 (p, $J = 1.3$ Hz, 3H), 7.37 – 7.31 (m, 4H), 4.80 (d, $J = 3.5$ Hz, 1H), 0.32 (s, 3H), 0.28 (s, 3H). ^{13}C NMR (126 MHz, CDCl_3) δ 147.8, 135.8, 135.7, 132.7 (q, $J = 33.1$ Hz), 131.7, 129.7, 126.5, 126.5, 125.0 (q, $J = 271.5$ Hz), 121.1 (p, $J = 3.9$ Hz), 71.1, -4.7, -4.7.

3.8.3 General Procedure for the Fluoride Triggered Addition to Imines



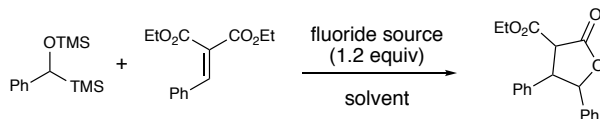
Two 1 dram vial was brought into a glovebox. To it was added silane (1.2 equiv) and imine (1 equiv). To a second vial with stirbar was added fluoride source. Sealed and removed from glovebox. Added solvent (0.2 M) to the silane/imine and stirred until homogenous. Transferred

solution to vial with stir bar and allowed to stir until the aldimine was consumed. TBAF (1 equiv) was added via syringe and the reaction stirred for 1 hour. The reaction mixture was concentrated under vacuum and subjected to column chromatography (2.5-5% MeOH/CHCl₃).



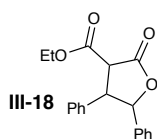
Prepared according to the method described above. Purification yielded a white solid. Analytical data for **SI-5**: ¹H NMR (500 MHz, Chloroform-*d*) δ 7.79 (ddt, *J* = 12.2, 6.9, 1.4 Hz, 2H), 7.69 (ddt, *J* = 12.2, 6.8, 1.3 Hz, 2H), 7.56 – 7.45 (m, 2H), 7.39 (dtd, *J* = 13.7, 7.7, 3.4 Hz, 4H), 7.21 – 7.17 (m, 3H), 7.17 – 7.12 (m, 3H), 7.09 – 7.03 (m, 2H), 6.98 – 6.92 (m, 2H), 4.95 (s, 1H), 4.83 (d, *J* = 7.4 Hz, 1H), 4.25 – 4.08 (m, 1H), 3.72 (dd, *J* = 10.6, 7.5 Hz, 1H). ¹³C NMR (126 MHz, CDCl₃) δ 140.8, 140.2, 132.8, 132.7, 132.2, 132.2, 131.8, 131.7, 128.7, 128.7, 128.6, 128.5, 127.9, 127.6, 127.4, 127.0, 127.0, 79.1, 79.1, 64.0.

3.8.4 General Procedure for the Fluoride Triggered Addition to Arylidene Malonate

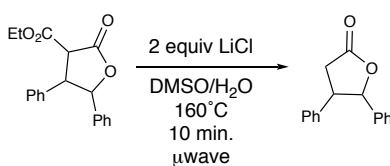


A flame-dried 1 dram vial containing a magnetic stirring bar was brought into a glove box. To the vial was added α -silyl silylether (1.2 equiv), arylidene malonate (1 equiv) and solvent (0.2 M) followed by fluoride source (1.2 equiv). The vial was capped and stirred until complete conversion of the arylidene malonate. The reaction mixture was quenched with 1-%

AcOH/MeOH and concentrated under vacuum and subjected to flash chromatography (10% Ethyl Acetate/Hexanes) to yield a white solid.



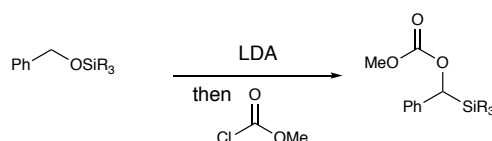
Prepared according to the method described above. Purification yielded a white solid (150 mg, 48%). Analytical data for **III-18**: ^1H NMR (500 MHz, Chloroform-*d*) δ 7.23 – 7.17 (m, 4H), 7.14 (s, 1H), 7.11 – 7.07 (m, 1H), 7.08 – 6.96 (m, 6H), 6.76 – 6.65 (m, 4H), 5.82 (d, $J = 7.5$ Hz, 1H), 5.30 (d, $J = 9.7$ Hz, 1H), 4.36 (dd, $J = 8.7, 7.5$ Hz, 1H), 4.22 – 4.04 (m, 3H), 3.94 (dd, $J = 12.1, 9.7$ Hz, 1H), 3.89 – 3.85 (m, 2H), 1.16 (dt, $J = 10.7, 7.1$ Hz, 4H). ^{13}C NMR (126 MHz, CDCl_3) δ 171.6, 169.9, 166.8, 166.6, 136.2, 135.2, 134.8, 134.6, 129.1, 128.9, 128.5, 128.3, 128.2, 128.0, 127.9, 127.9, 127.7, 127.5, 126.0, 125.5, 85.4, 83.5, 62.3, 62.2, 54.9, 54.0, 51.3, 50.6, 13.9.



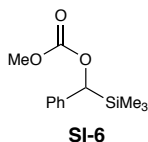
To microwave vial with magnetic stir bar was added unpurified lactone **III-18** in DMSO/ H_2O (50:1). Lithium chloride (2 equiv) were added and the vial sealed. Heated to 160 °C for 10 minutes in microwave. The resulting solution was diluted with DI water and extracted with ethyl acetate (3 x). The organic extracts were washed with water (5 x). The organic extracts were

concentrated and subjected to flash chromatography (10% Ethyl Acetate/Hexanes) to yield a clear residue (10 mg, 20% over two steps). ^1H and ^{13}C matched reported data.

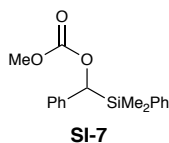
3.8.5 General Procedure Preparation of α -Silyl Carbonates



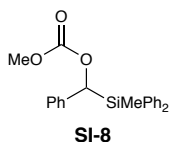
To a flame-dried round bottom flask containing a magnetic stirring bar under nitrogen was added freshly distilled diisopropyl amine (1.3 equiv) and THF (0.2 M). The solution was cooled to -78°C and freshly titrated n-butyl lithium in hexane (1.3 equiv) was added. The solution was warmed to room temperature for 15 minutes and then cooled to -78°C . To the stirred solution was added the corresponding benzyl silyl ether (1 equiv) in THF dropwise. The reaction was warmed to rt or until disappearance of the benzyl silyl ether by TLC. The solution was then cooled to -78°C and methyl chloroformate (1.1 equivalents) was added. The reaction was stirred at -78°C 0.5 hours and warmed to room temperature. The reaction was quenched with saturated ammonium chloride. The mixture was extracted with ethyl acetate (3 x). The aqueous layer was discarded and the resulting ether layer was dried over anhydrous MgSO_4 , filtered, and concentrated in vacuo. The product was purified by flash chromatography (2-5% EtOAc/hexanes,) on silica gel to afford a white solid.



Prepared according to the method described above to provide a thick clear oil that slowly solidified into a white solid. (2.3 g, 53%). Analytical data for **SI-6**: ^1H NMR (500 MHz, Chloroform-*d*) δ 7.24 – 7.18 (m, 2H), 7.12 – 7.03 (m, 3H), 5.34 (s, 1H), 3.66 (s, 3H), -0.06 (s, 9H).



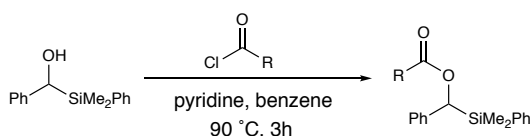
Prepared according to the method described above. The resulting material was further recrystallized from hexanes to provide a white crystalline material. (2.3 g, 36%). Analytical data for **SI-7**: ^1H NMR (500 MHz, Chloroform-*d*) δ 7.45 – 7.40 (m, 2H), 7.38 (dt, $J = 6.0, 1.4$ Hz, 1H), 7.36 – 7.30 (m, 2H), 7.25 – 7.20 (m, 2H), 7.20 – 7.12 (m, 1H), 7.01 (dd, $J = 7.3, 1.7$ Hz, 2H), 5.60 (s, 1H), 3.72 (s, 3H), 0.36 (s, 3H), 0.29 (s, 3H). ^{13}C NMR (126 MHz, CDCl_3) δ 156.2, 139.0, 134.7, 134.3, 129.7, 128.6, 128.5, 128.3, 128.1, 128.1, 127.7, 126.5, 125.4, 75.5, 54.9, -5.5, -5.8.



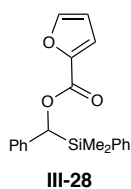
Prepared according to the method described above. The resulting material was further recrystallized from hexanes to provide a white crystalline material. (2.3 g, 36%). Analytical data for **SI-8**: ^1H NMR (500 MHz, Chloroform-*d*) δ 7.53 (dt, $J = 6.8, 1.4$ Hz, 2H), 7.43 – 7.38 (m,

3H), 7.35 (dt, $J = 8.1, 6.4$ Hz, 3H), 7.30 (dd, $J = 7.8, 6.6$ Hz, 2H), 7.18 – 7.11 (m, 3H), 6.99 – 6.92 (m, 2H), 5.94 (s, 1H), 3.67 (s, 3H), 0.53 (s, 3H). ^{13}C NMR (126 MHz, CDCl_3) δ 156.1, 138.5, 135.3, 135.1, 133.3, 132.8, 129.9, 129.8, 128.1, 127.9, 127.8, 126.7, 126.0, 74.5, 54.9, - 6.5.

3.8.6 General Procedure Preparation of α -Silyl Esters

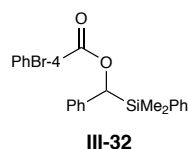


Dimethyl phenyl α -silyl alcohol (1.3 g, 5.36 mmol, 1 equiv) and the corresponding acyl chloride (1.5 equiv) were dissolved in a mixture of benzene and pyridine (4 mL benzene, 1.5 mL pyridine, 2.7/1 ratio, 1.0 M). The mixture was heated to 90 °C for 3.5 h. The solvent was removed under vacuum and the residue purified by flash chromatography (1-5% Ethyl Acetate/Hexanes).



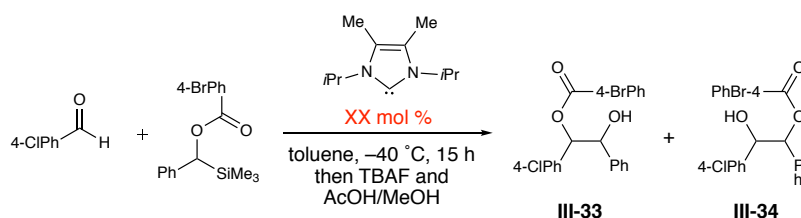
Prepared according to the method described above to provide a white crystalline material. (). Analytical data for **III-28**: ^1H NMR (500 MHz, Chloroform- d) δ 7.59 (dd, $J = 1.7, 0.9$ Hz, 1H), 7.44 (dt, $J = 7.9, 1.3$ Hz, 2H), 7.41 – 7.36 (m, 1H), 7.35 – 7.30 (m, 2H), 7.23 – 7.18 (m, 1H), 7.17 – 7.12 (m, 1H), 7.04 (dd, $J = 7.9, 1.6$ Hz, 2H), 6.52 (dd, $J = 3.5, 1.8$ Hz, 1H), 6.05 (s, 1H), 5.30 (s, 1H), 0.38 (d, $J = 1.0$ Hz, 3H), 0.34 (d, $J = 1.1$ Hz, 3H). ^{13}C NMR (126 MHz, CDCl_3) δ

157.6, 145.4, 144.1, 138.3, 133.9, 133.5, 128.8, 127.2, 126.8, 125.4, 124.6, 116.8, 110.9, 70.6, -6.2, -6.4.



Prepared according to the method described above to provide a white crystalline material. (3.32 g, 50%). Analytical data for **III-32**: ^1H NMR (500 MHz, Chloroform-*d*) δ 8.02 – 7.97 (m, 1H), 7.91 – 7.86 (m, 2H), 7.72 – 7.66 (m, 1H), 7.61 – 7.56 (m, 2H), 7.43 – 7.40 (m, 2H), 7.39 – 7.36 (m, 1H), 7.34 – 7.29 (m, 2H), 7.25 – 7.20 (m, 2H), 7.18 – 7.13 (m, 1H), 7.07 – 7.01 (m, 2H), 6.06 (s, 1H), 0.38 (s, 3H), 0.35 (s, 3H). ^{13}C NMR (126 MHz, CDCl_3) δ 165.5, 139.3, 134.7, 134.3, 132.4, 131.9, 131.8, 131.1, 129.7, 129.4, 128.2, 128.0, 127.8, 126.4, 125.4, 72.0, -5.3, -5.5.

3.8.7 General Procedure for the Acyl Transfer Mediated Addition to Aldehydes



In a 1 dram vial with magnetic stir bar, silyl ester **III-32** (1 equiv) was dissolved in toluene (1 M) and added to vial containing NHC **III-29** (20 mol %) and magnetic stir bar at room temperature. Stirred for 10 minutes. The solution was cooled to $-40\text{ }^\circ\text{C}$ and 4-Cl benzaldehyde (1 equiv) was slowly added as a solution in toluene (1 M). Stirred for 18 hrs at $-40\text{ }^\circ\text{C}$ in a cryocool. The

reaction was quenched with 10% AcOH/MeOH and subject to flash chromatography to yield **III-33** and **III-34** as an inseparable mixture.

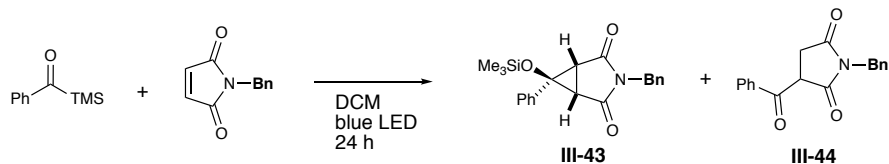
Analytical data for **III-33/III-34**: ^1H NMR (500 MHz, Chloroform-*d*) δ 7.99 – 7.90 (m, 2H), 7.90 – 7.81 (m, 2H), 7.66 – 7.55 (m, 4H), 7.40 – 7.27 (m, 5H), 7.25 – 7.15 (m, 7H), 7.15 – 7.09 (m, 2H), 6.10 (dd, $J = 10.4, 5.7$ Hz, 1H), 6.06 (t, $J = 7.6$ Hz, 1H), 5.12 (ddd, $J = 9.1, 5.6, 3.6$ Hz, 1H), 5.06 (ddd, $J = 10.4, 7.2, 3.1$ Hz, 1H), 2.52 (dd, $J = 34.1, 3.4$ Hz, 1H), 2.19 (dd, $J = 27.1, 3.7$ Hz, 1H). Assigned in analogy to related aryl ester products.³⁴³

3.8.8 General Procedure for the Photoaddition of Aryl Silanes to Arylidene Malonates



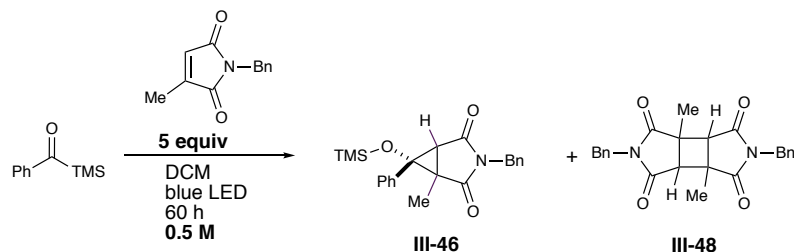
Magnesium bromide diethyl etherate (26 mg, 0.1 mmol, 1 equiv), aryl silane (36 mg, 0.2 mmol, 2 equiv), arylidene malonate (25 mg, 0.1 mmol, 1 equiv) and the corresponding BOX ligand (1.05 equiv) were stirred in 0.5 mL of DCM for 30 minutes in a foil wrapped vial. The heterogenous mixture was then subject to irradiation under blue LEDs and fan cooling for 18 h. The homogenous solution was concentrated and purified by flash chromatography (1-10% Ethyl Acetate/Hexanes) to yield a clear residue (14.8 mg, 42% yield). Analytical data for **III-40**: ^1H NMR (500 MHz, Chloroform-*d*) δ 7.96 – 7.90 (m, 2H), 7.46 – 7.38 (m, 1H), 7.32 (dd, $J = 8.4, 7.1$ Hz, 2H), 7.28 – 7.23 (m, 2H), 7.24 – 7.18 (m, 2H), 7.17 – 7.11 (m, 1H), 5.25 (d, $J = 11.4$ Hz, 1H), 4.38 (d, $J = 11.3$ Hz, 1H), 4.11 (qd, $J = 7.1, 4.8$ Hz, 2H), 3.87 (q, $J = 7.1$ Hz, 2H), 1.15 (t, $J = 7.1$ Hz, 3H), 0.89 (t, $J = 7.1$ Hz, 3H). ^{13}C NMR (126 MHz, CDCl_3) δ 197.3, 168.2, 168.1, 135.9, 134.5, 133.1, 129.0, 129.0, 128.9, 128.5, 128.0, 61.9, 61.4, 56.0, 52.9, 14.0, 13.8.

3.8.9 General Procedure for the Photoaddition of Acyl Silanes to Maleimides



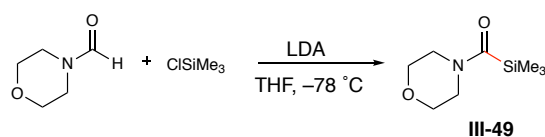
Acyl silane (1 equiv) and maleimide (2 equiv) were dissolved in dichloromethane (0.1 M) (sparged with nitrogen for 30 minutes) and irradiated under blue LEDs until the solution was no longer yellow (18-24 h) Concentrated and purified by flash column chromatography, 1-5% Ethyl Acetate/Hexanes). Analytical data for **III-43**: ¹H NMR (500 MHz, Chloroform-*d*) δ 7.37 – 7.32 (m, 2H), 7.21 – 7.16 (m, 1H), 7.16 – 7.07 (m, 3H), 7.07 – 7.00 (m, 2H), 6.89 – 6.78 (m, 2H), 4.07 (s, 2H), 2.91 (s, 2H), -0.13 (s, 9H). ¹³C NMR (126 MHz, CDCl₃) δ 171.9, 134.5, 132.8, 129.2, 129.0, 128.2, 127.9, 127.8, 126.7, 41.3, 33.9, 0.0. Analytical data for **III-44**: ¹H NMR (500 MHz, Chloroform-*d*) δ 8.10 (ddd, *J* = 7.8, 3.3, 1.3 Hz, 2H), 7.69 – 7.63 (m, 1H), 7.53 (t, *J* = 7.8 Hz, 2H), 7.50 – 7.42 (m, 1H), 7.41 – 7.27 (m, 6H), 4.85 (dd, *J* = 8.9, 4.0 Hz, 1H), 4.80 – 4.70 (m, 1H), 4.70 – 4.59 (m, 2H), 3.42 (dd, *J* = 18.2, 4.0 Hz, 1H), 2.87 (dd, *J* = 18.2, 8.9 Hz, 1H). ¹³C NMR (126 MHz, CDCl₃) δ 192.3, 175.3, 172.5, 135.4, 135.3, 134.3, 129.8, 128.8, 128.7, 128.1, 48.5, 43.0, 31.7.

3.8.10 General Procedure for the Photoaddition of Acyl Silanes to Maleimides



Acyl silane (1 equiv) and maleimide (5 equiv) were dissolved in dichloromethane (0.1 M) (sparged with nitrogen for 30 minutes) and irradiated under blue LEDs until the solution was no longer yellow (18-24 h) Concentrated and purified by flash column chromatography, 1-5% Ethyl Acetate/Hexanes). **III-46** was not stable to silica and assigned based on analogy to **III-43**. Analytical data for **III-48**: ^1H NMR (500 MHz, Chloroform- d) δ 7.42 – 7.36 (m, 4H), 7.34 – 7.26 (m, 6H), 4.71 (d, J = 13.9 Hz, 2H), 4.64 (d, J = 13.8 Hz, 2H), 2.81 (s, 2H), 1.06 (s, 6H). ^{13}C NMR (126 MHz, CDCl_3) δ 176.4, 174.5, 135.3, 129.0, 128.8, 128.4, 49.2, 43.9, 43.0, 15.9.

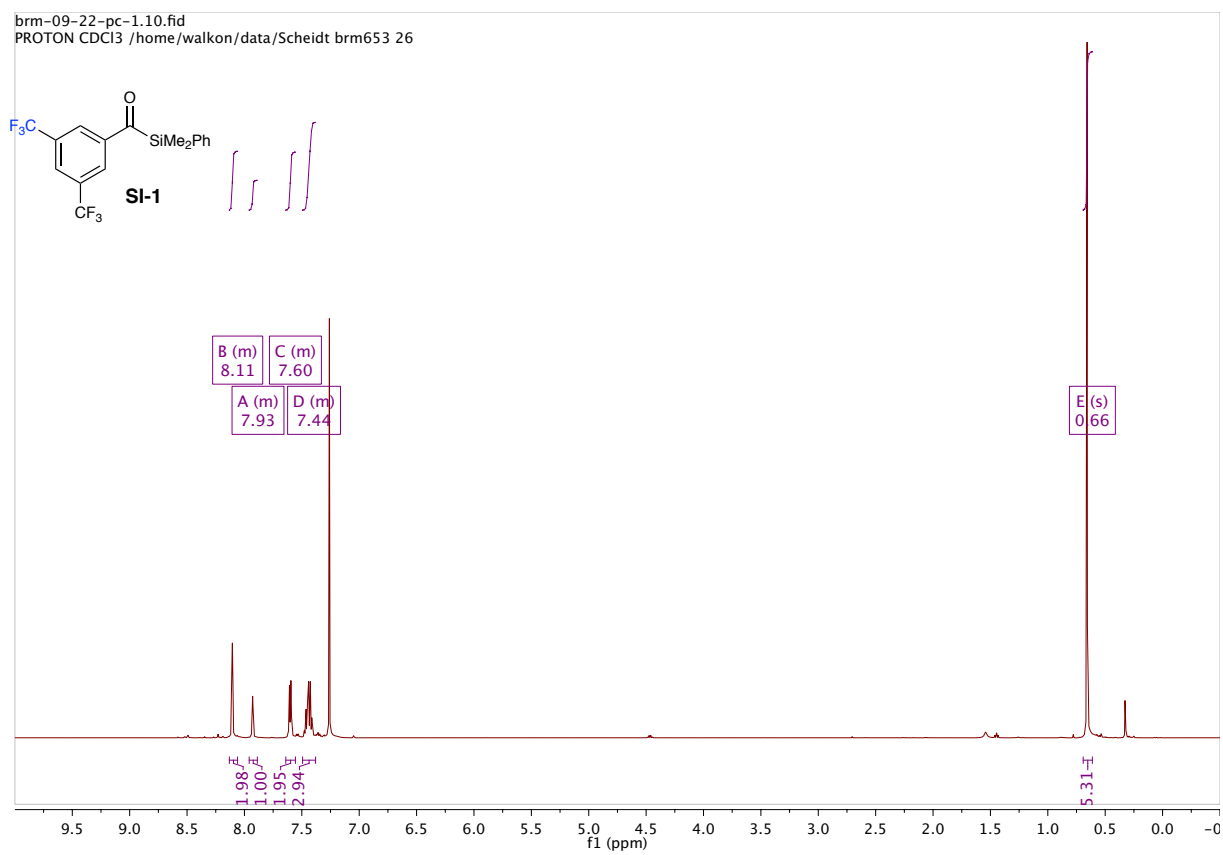
3.8.11 General Procedure for Preparation of Morpholinyl Carbamoyl Silane

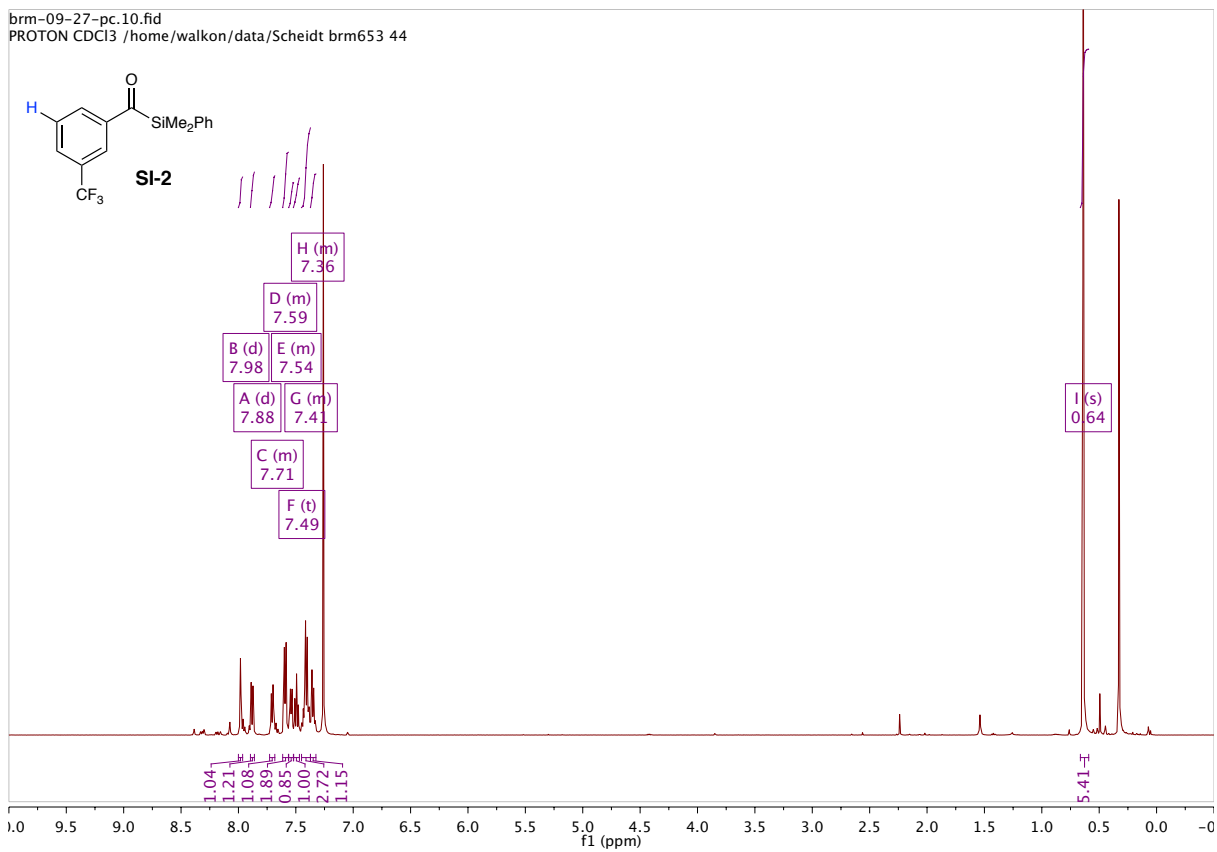


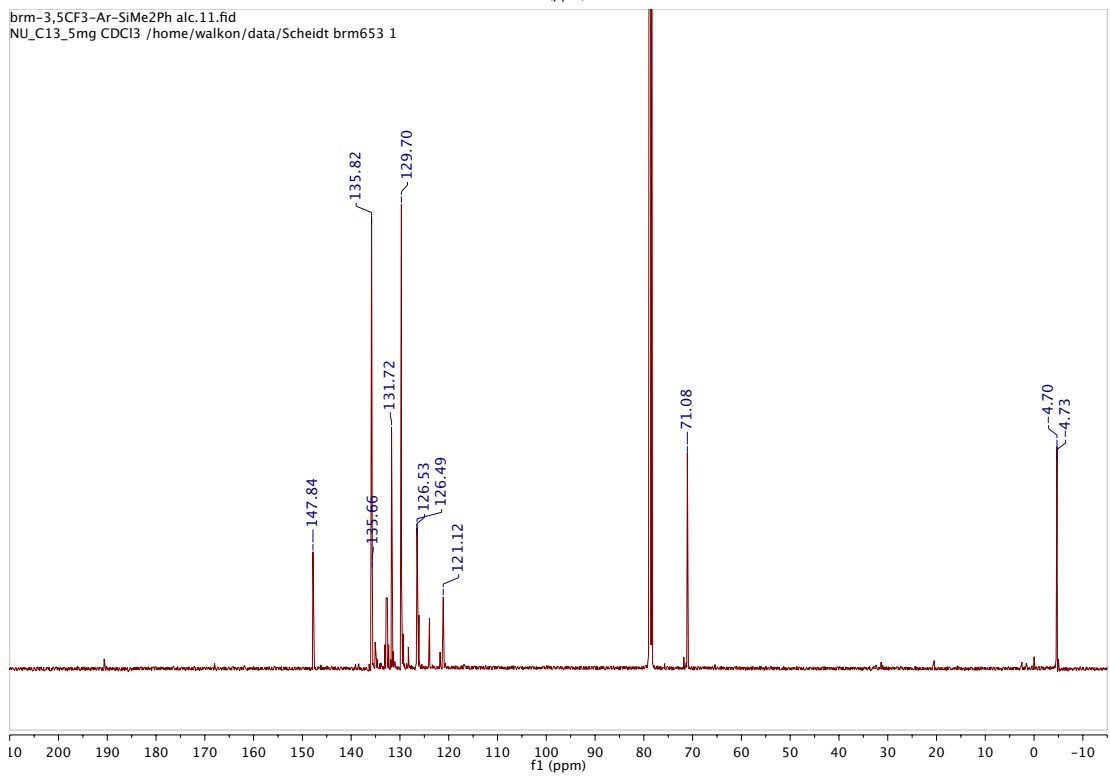
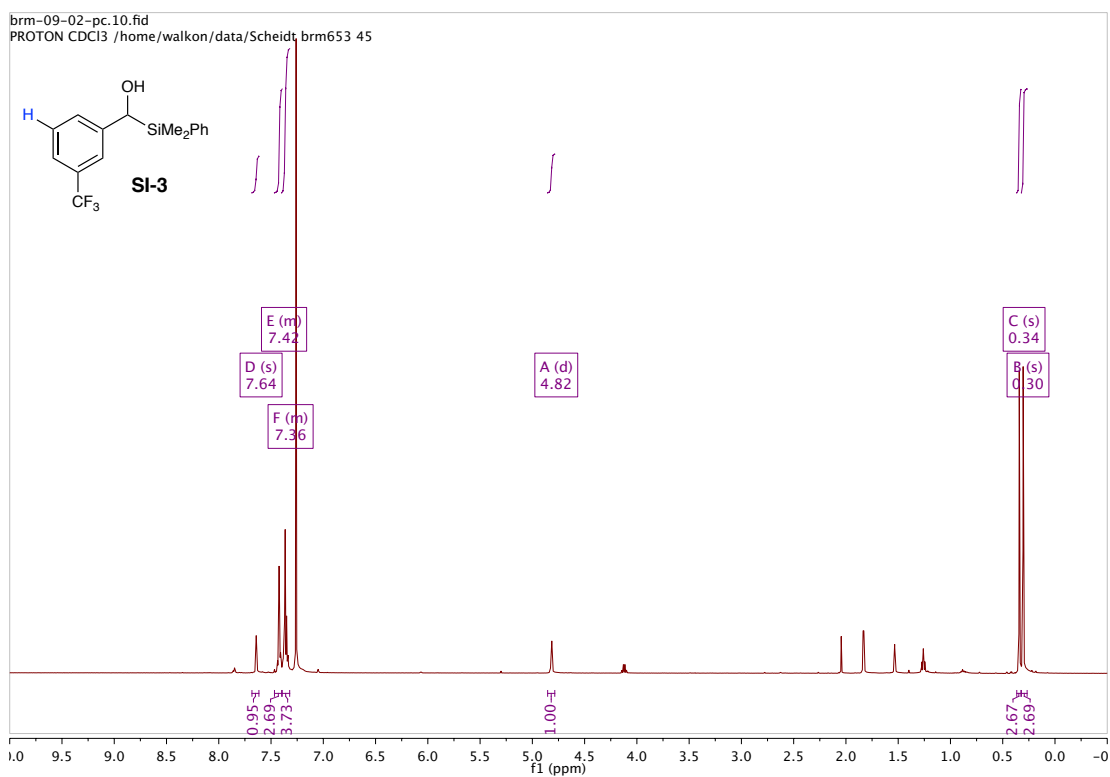
LDA was prepared by dropwise addition of $n\text{BuLi}$ (2.4 M) (5.43 ml, 13.03 mmol, 1.0 equiv) to a stirred solution of diisopropylamine (1.894 ml, 13.29 mmol, 1.02 equiv) in THF (9.5 ml) at -78°C . After warming to room temperature, the LDA solution was added down the side of flask by cannula to a stirred mixture of morpholine-4-carbaldehyde (1.5 g, 13.03 mmol, 1 equiv) over 45 minutes, chlorotrimethylsilane (2.232 ml, 17.59 mmol, 1.35 equiv) and THF (Volume: 19 ml) held at -78°C . The reaction mixture was allowed to slowly warm to room temperature and

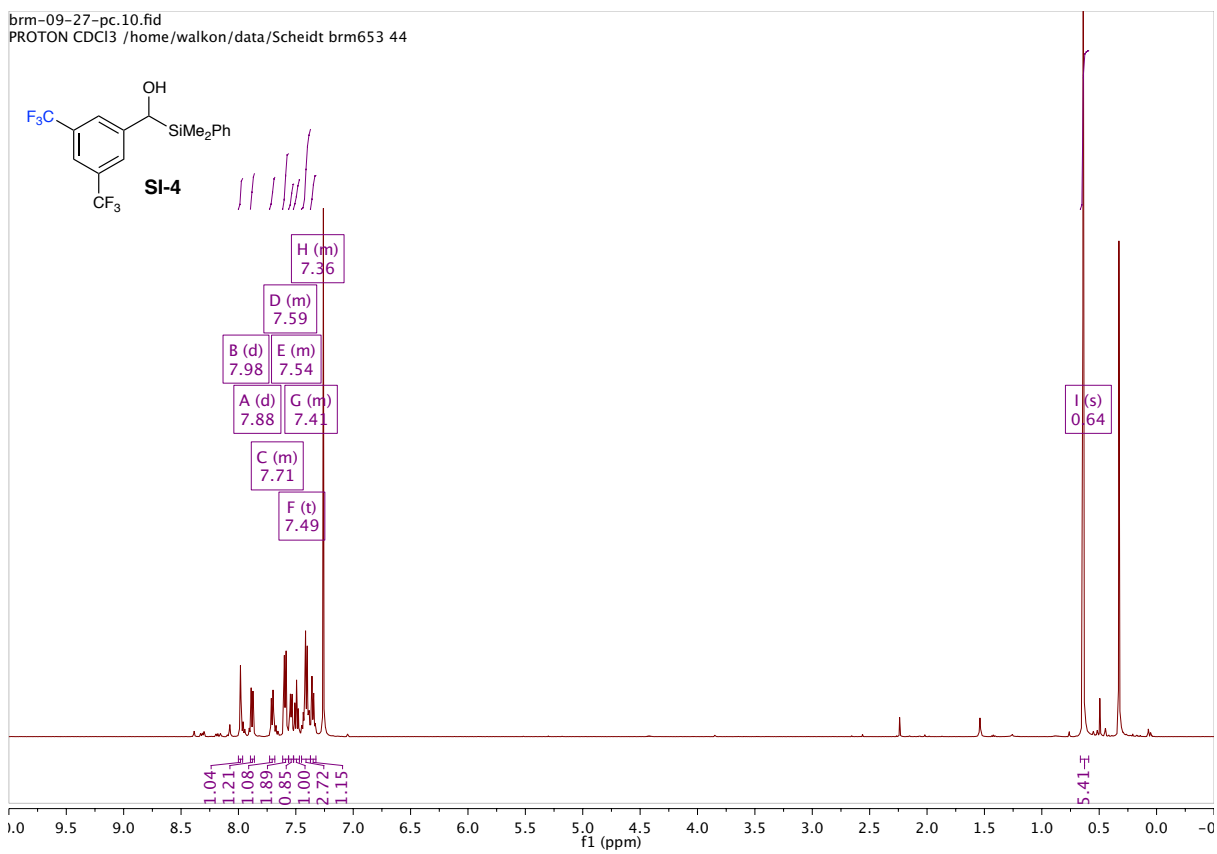
volatiles removed under vacuum. Treatment to hi-vac yielded an off-white foam. Dissolved in dry DCM and brought into glovebox. Filtered milky-white solution through syringe filter to yield clear solution which was concentrated to afford the product as an off-white solid (1.49 g, 62% yield). **III-49**: ^1H NMR (500 MHz, Chloroform-*d*) δ 3.77 – 3.65 (m, 2H), 3.64 (s, 4H), 3.59 – 3.49 (m, 2H), 0.30 (s, 9H). ^{13}C NMR (126 MHz, CDCl_3) δ 186.8, 69.2, 68.5, 68.3, 68.1, 54.6, 47.8, 41.3, 26.8, 0.0.

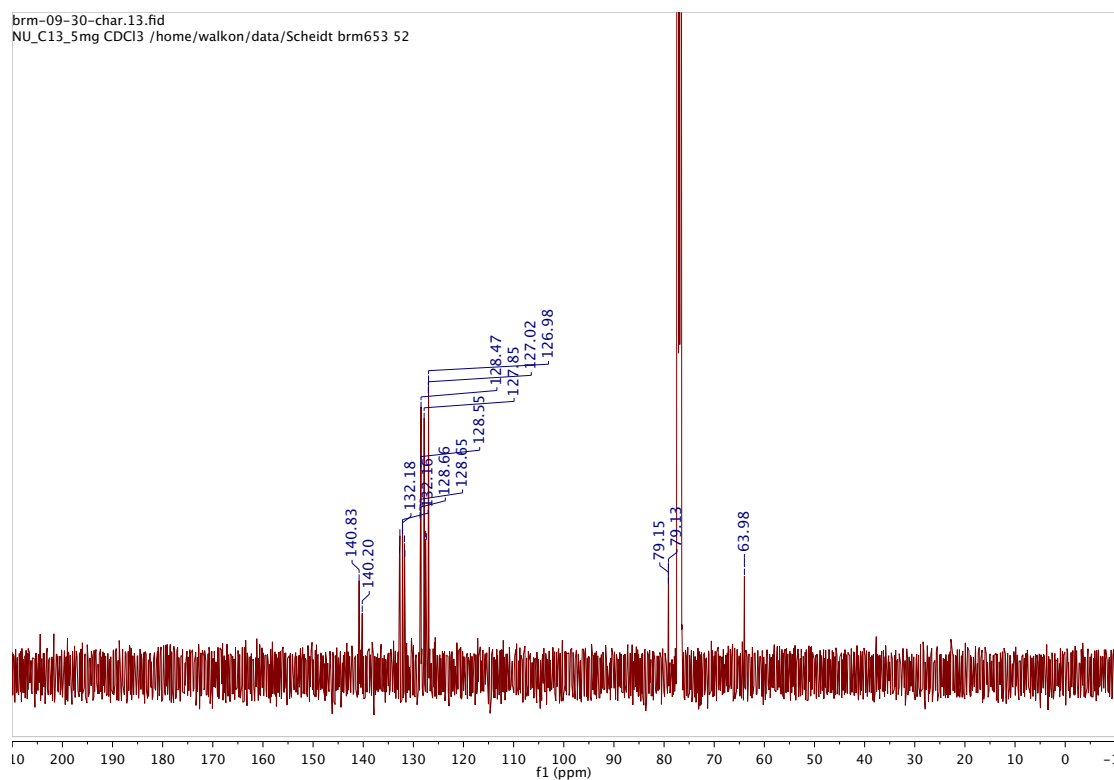
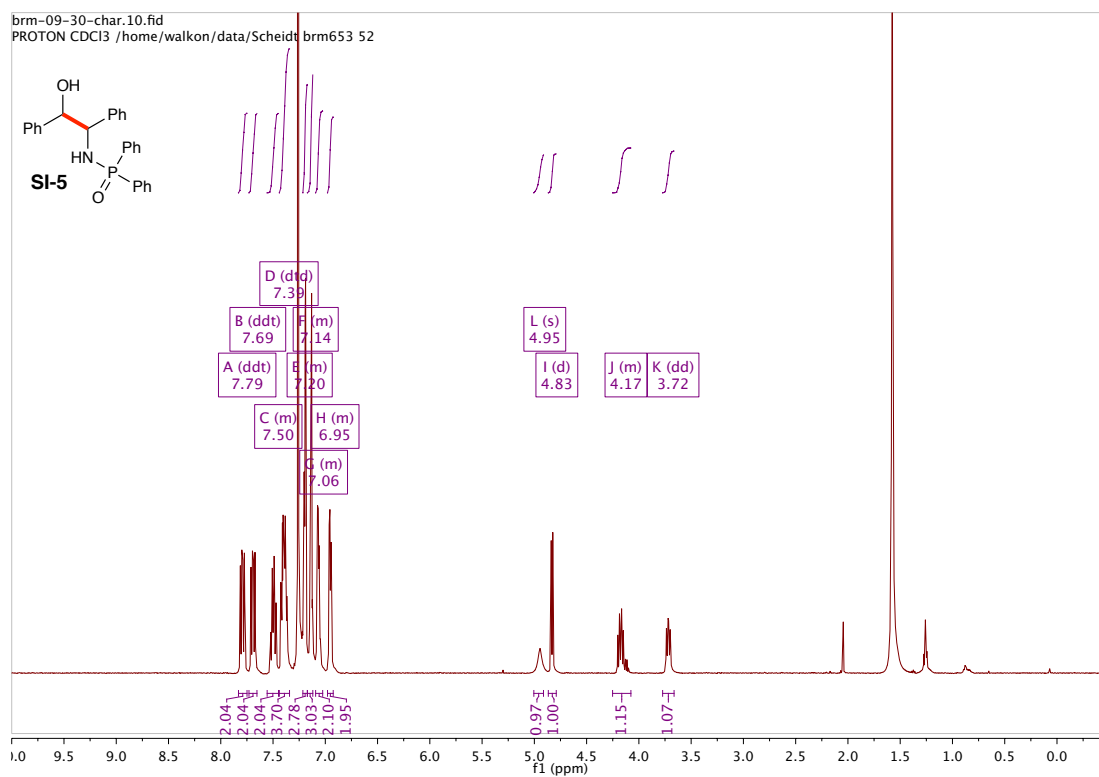
3.8.12 Selected NMR Spectra

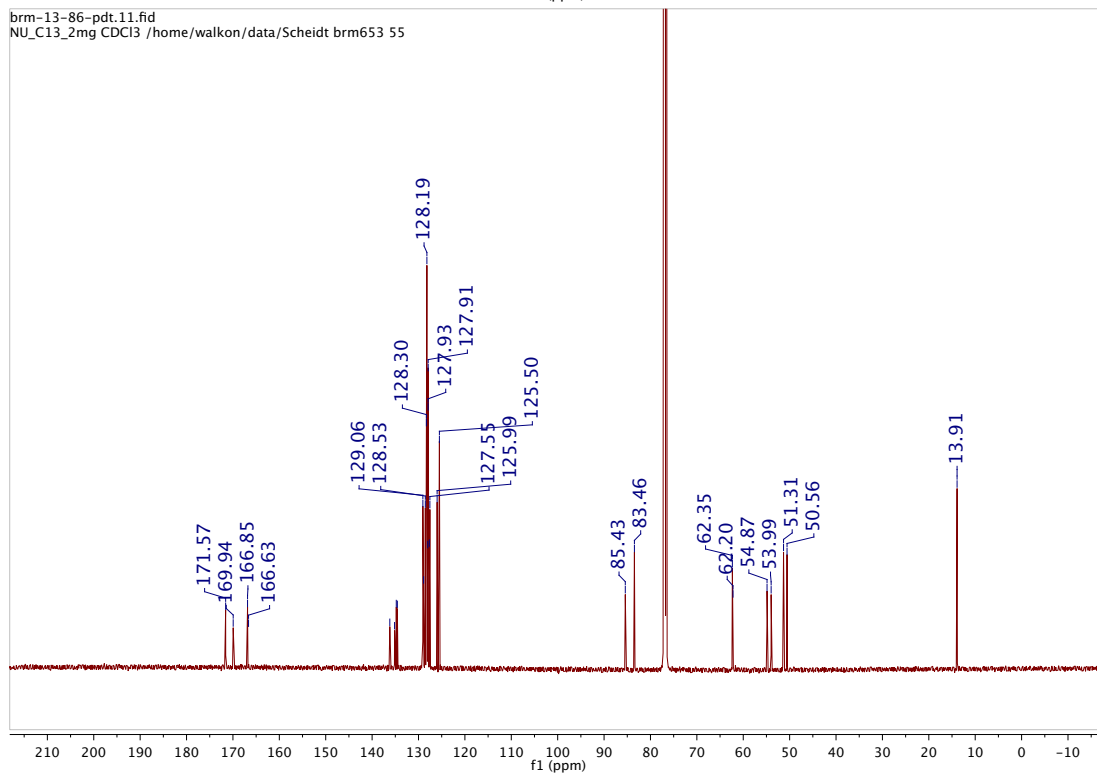
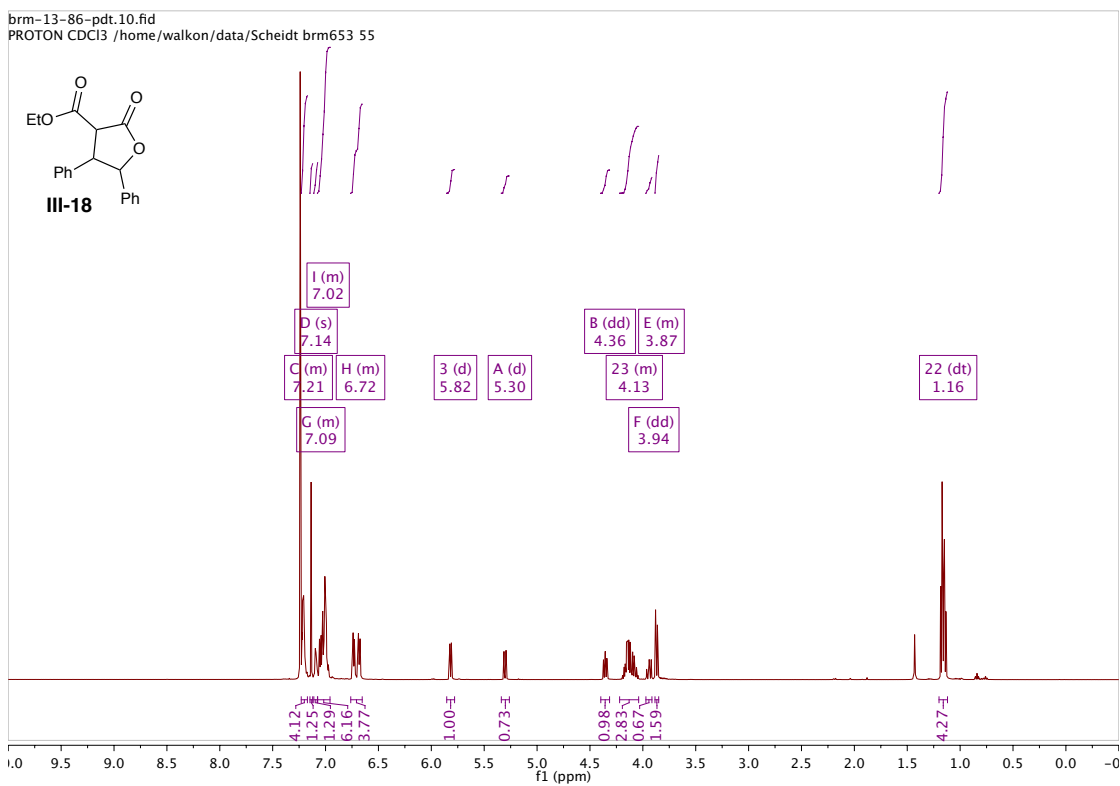


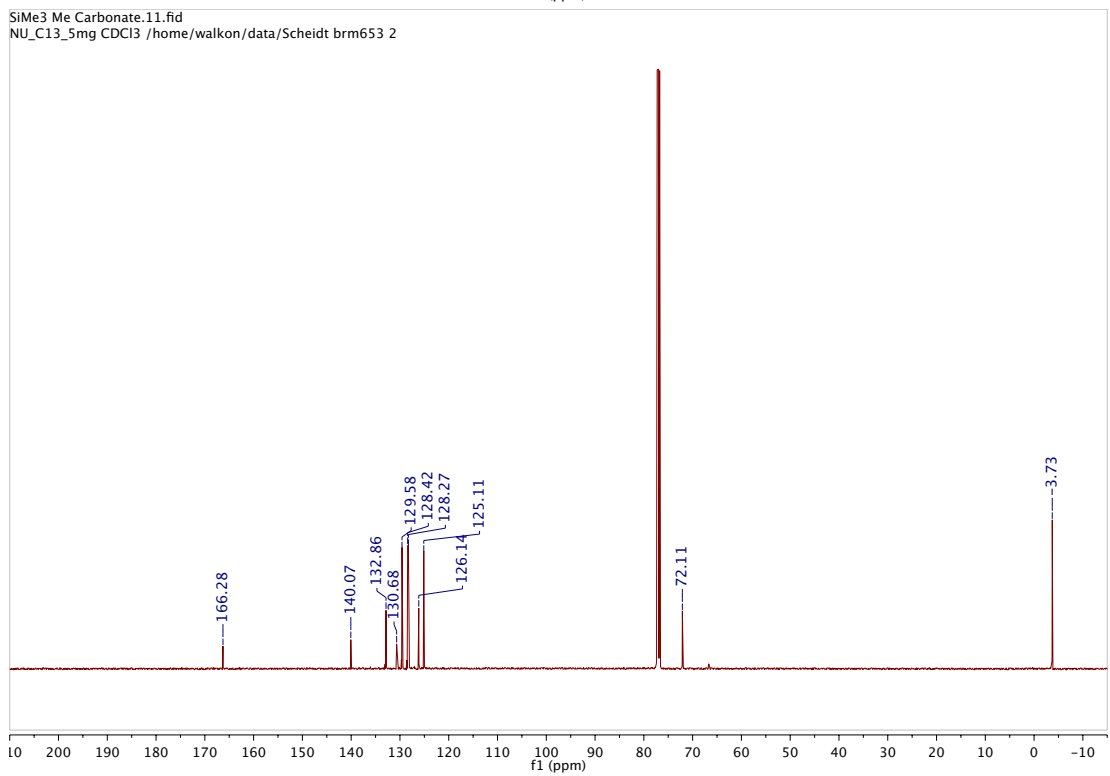
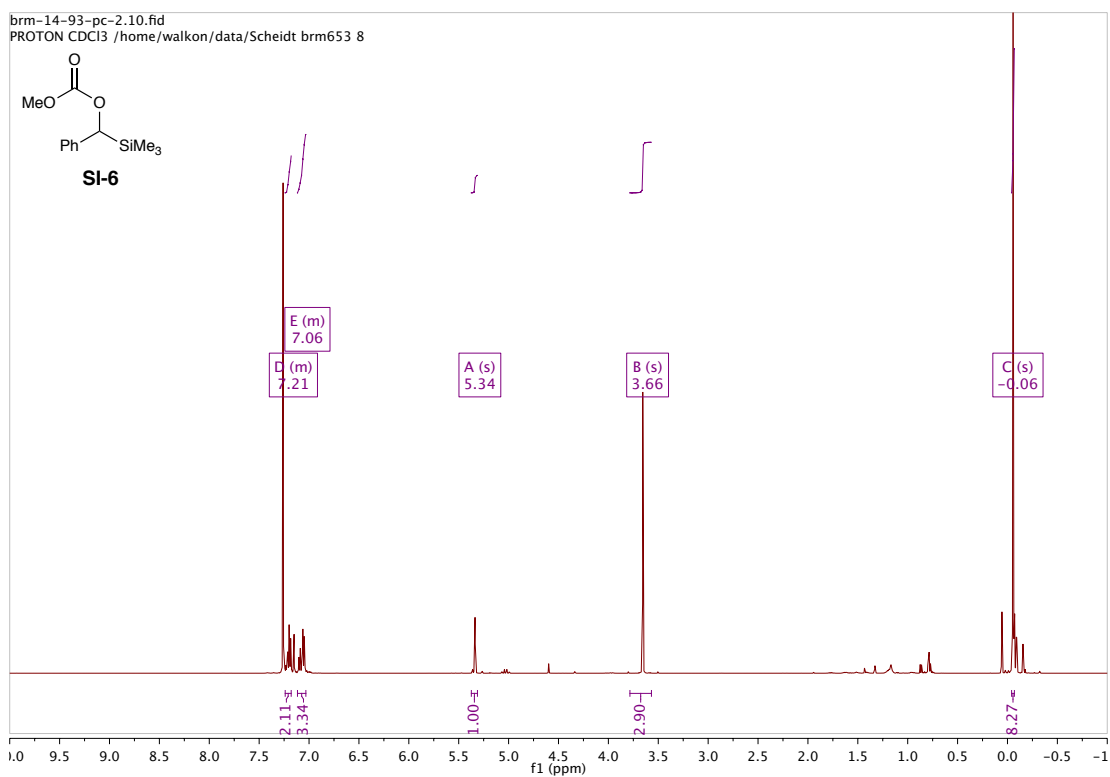


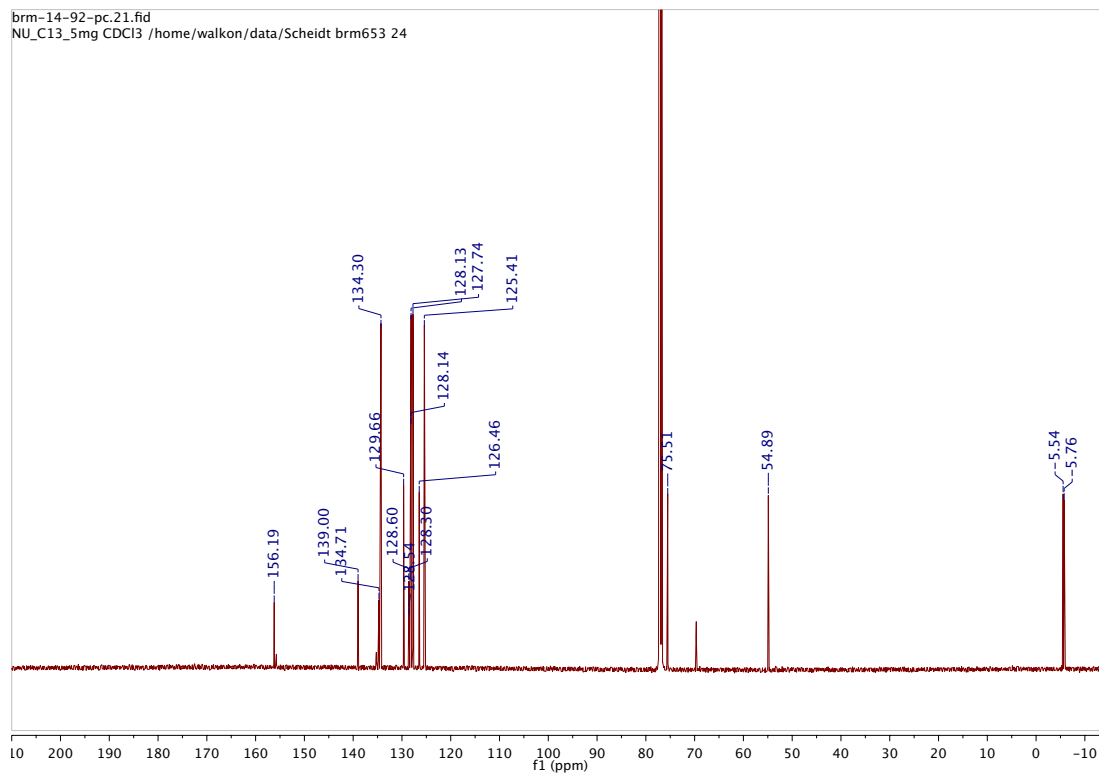
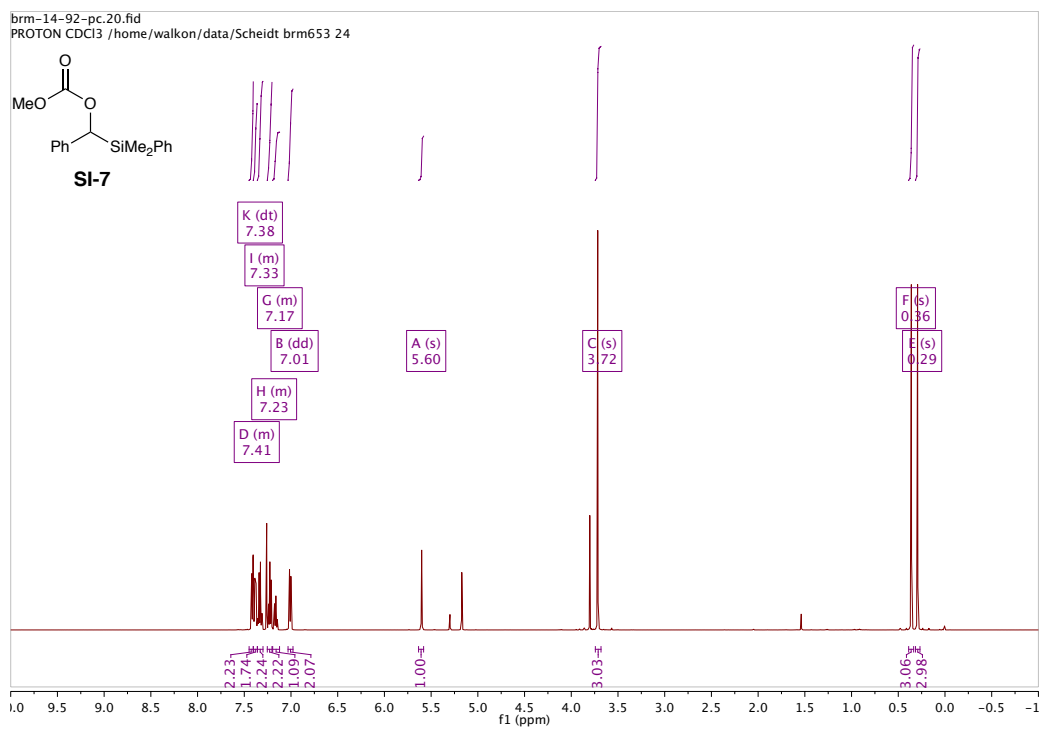


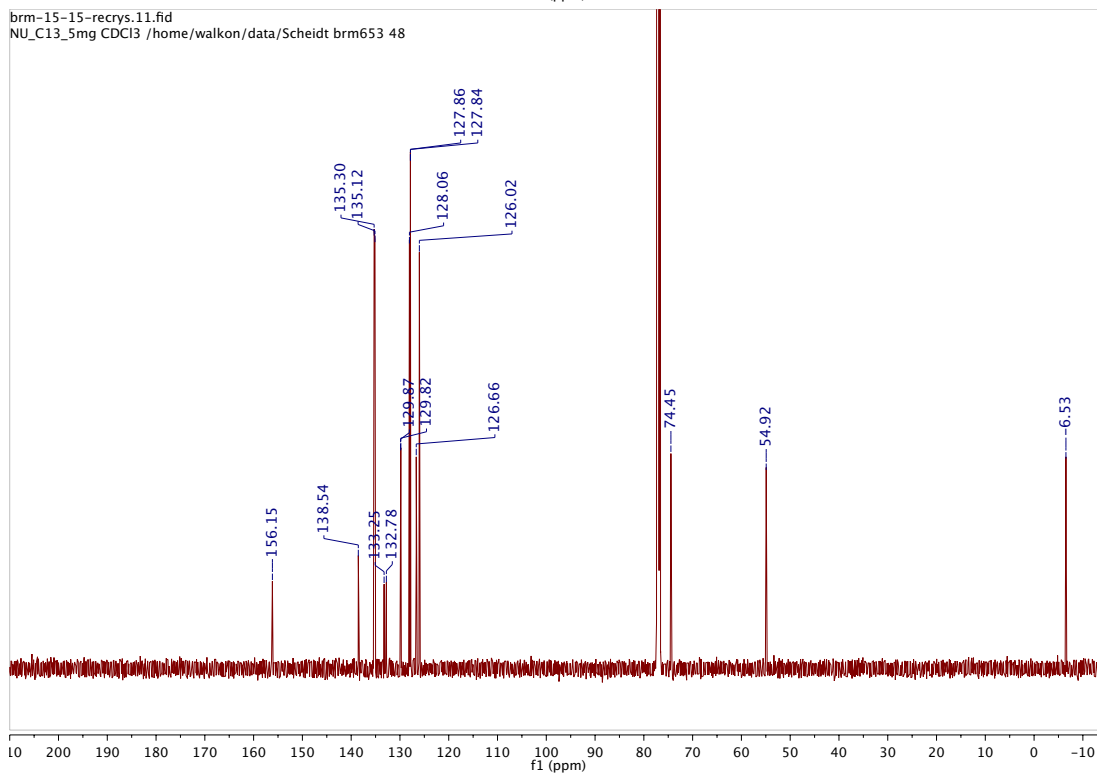
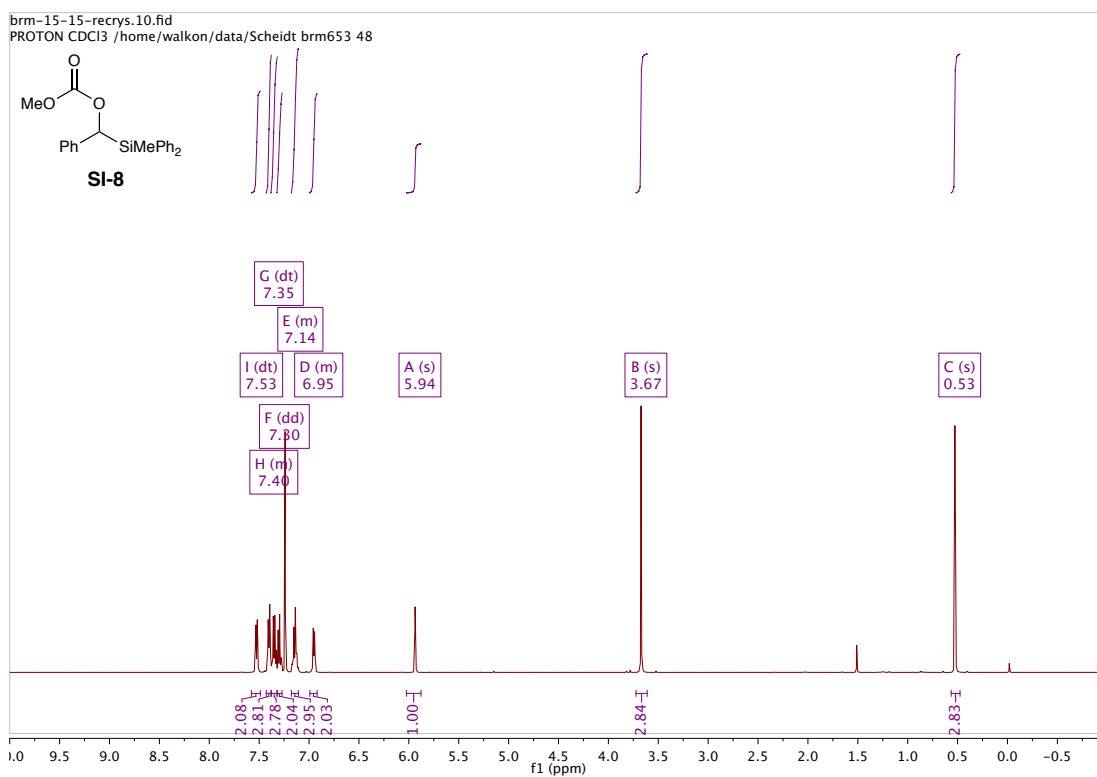


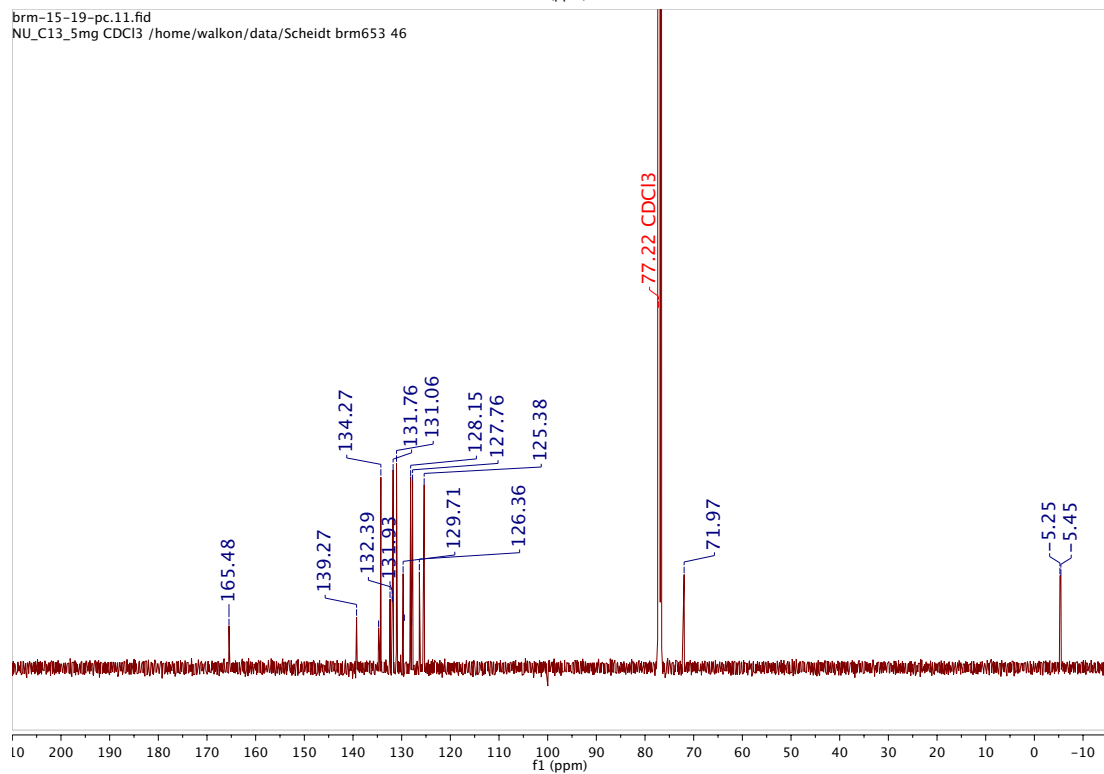
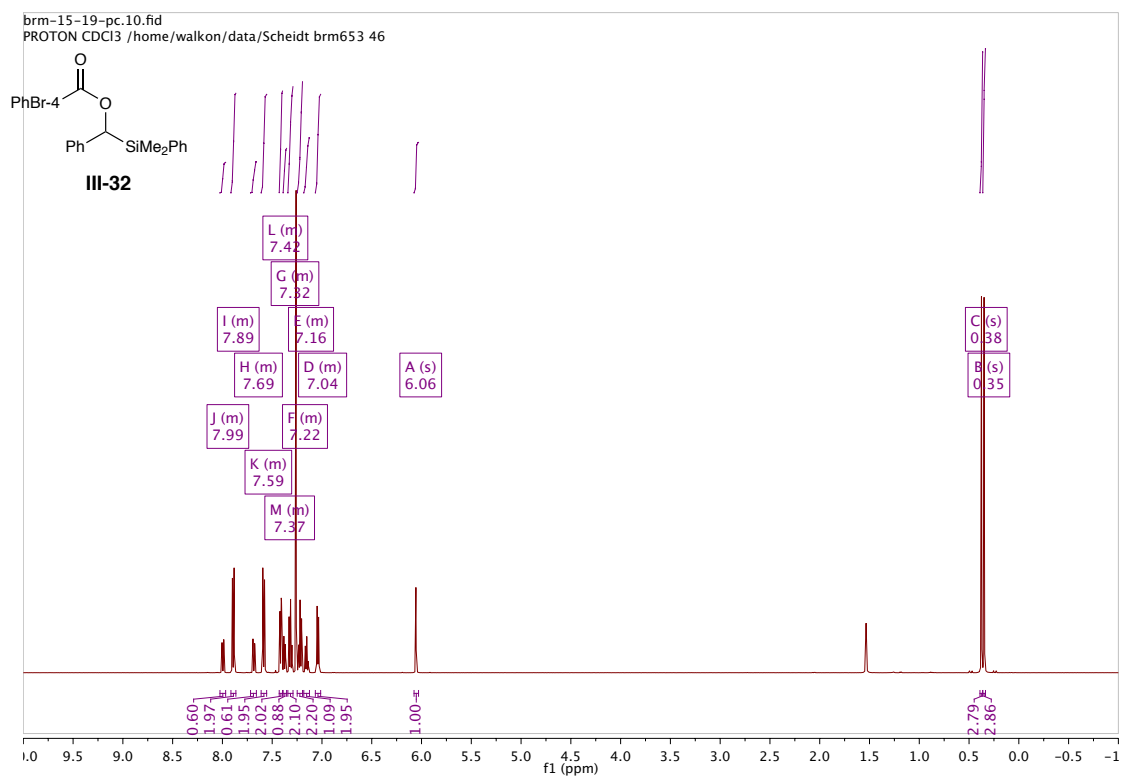


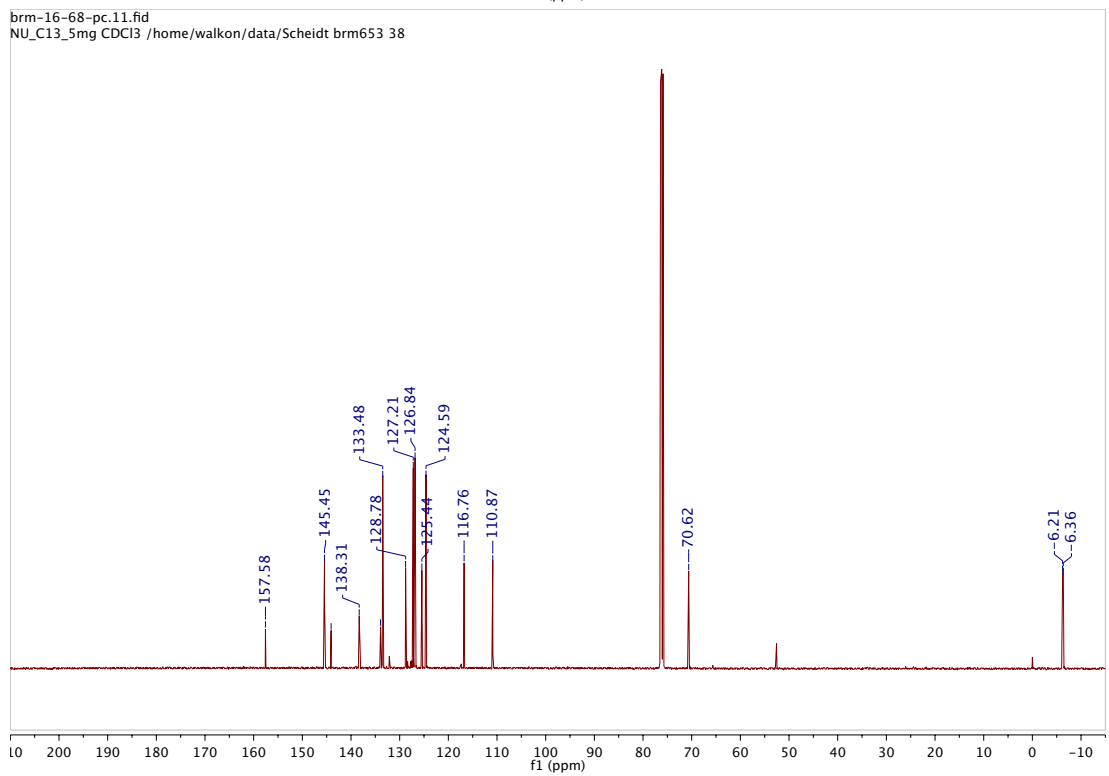
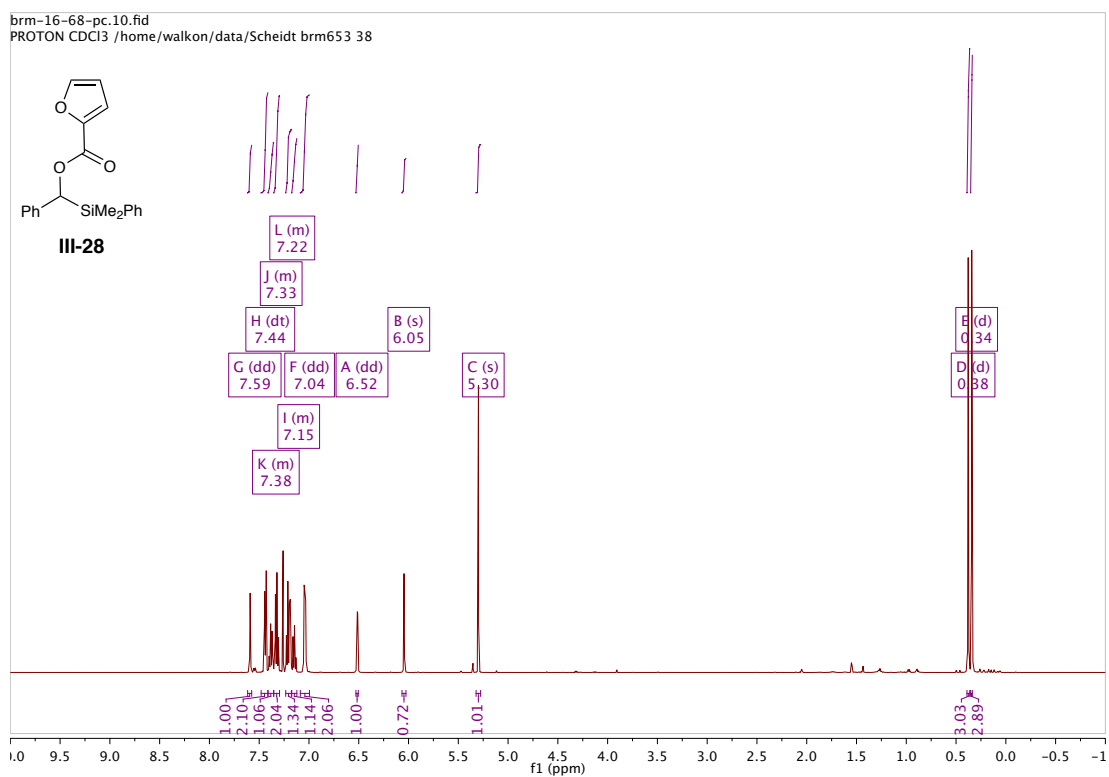


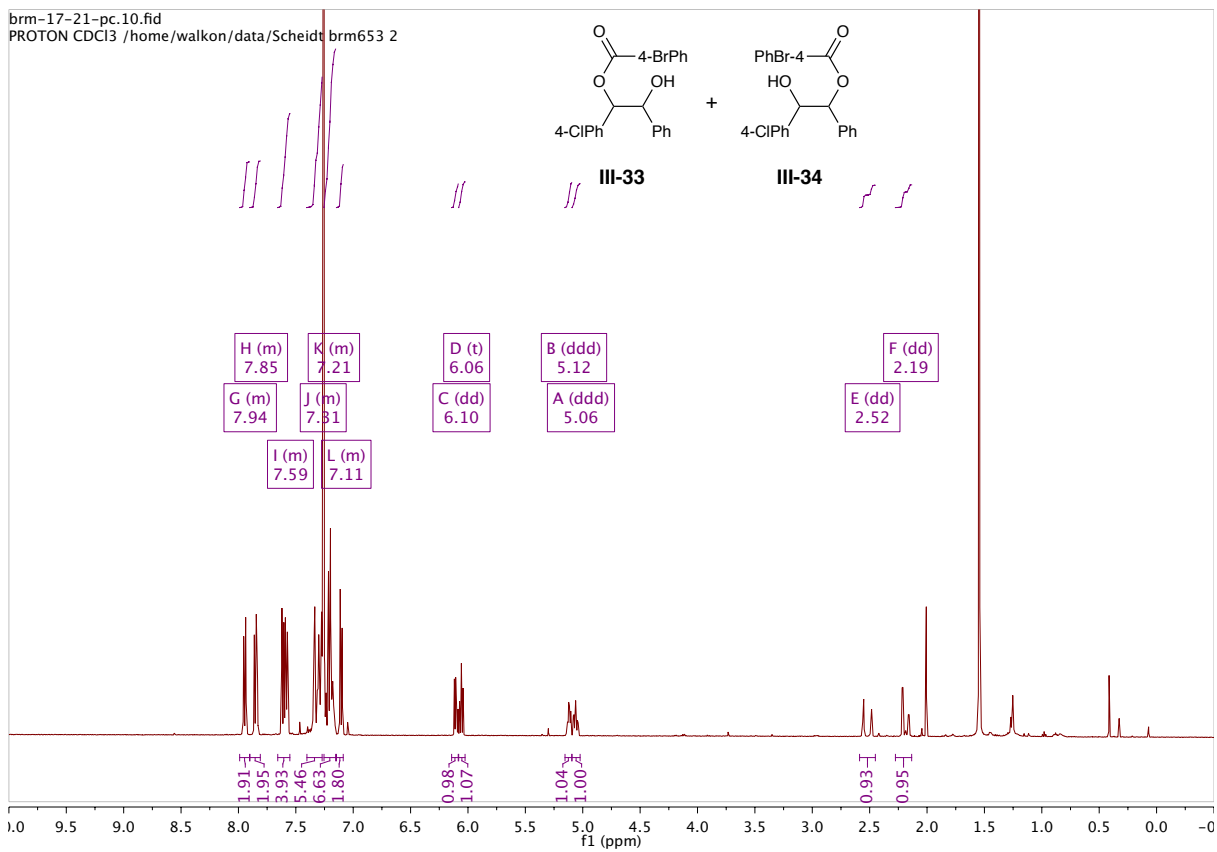




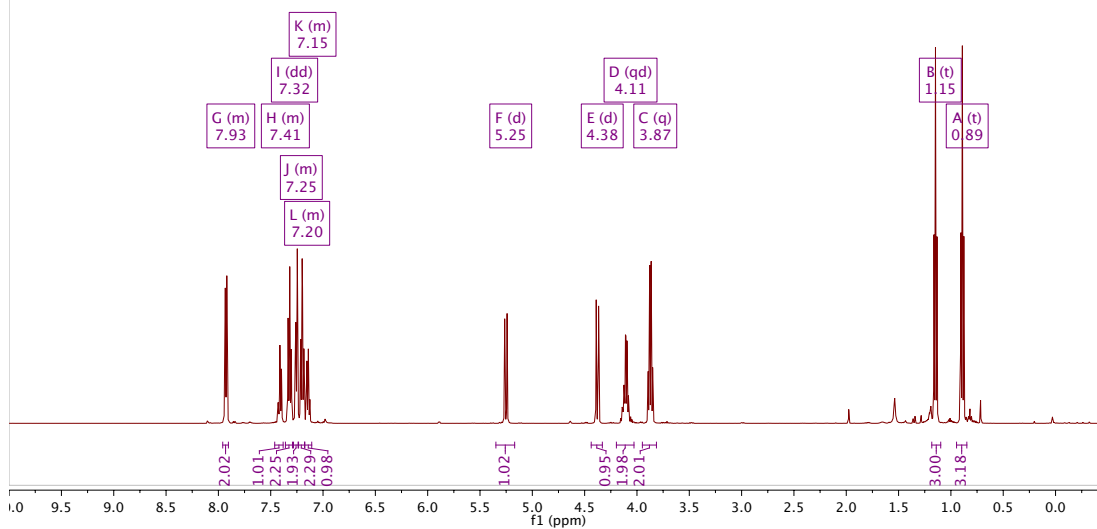
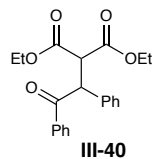




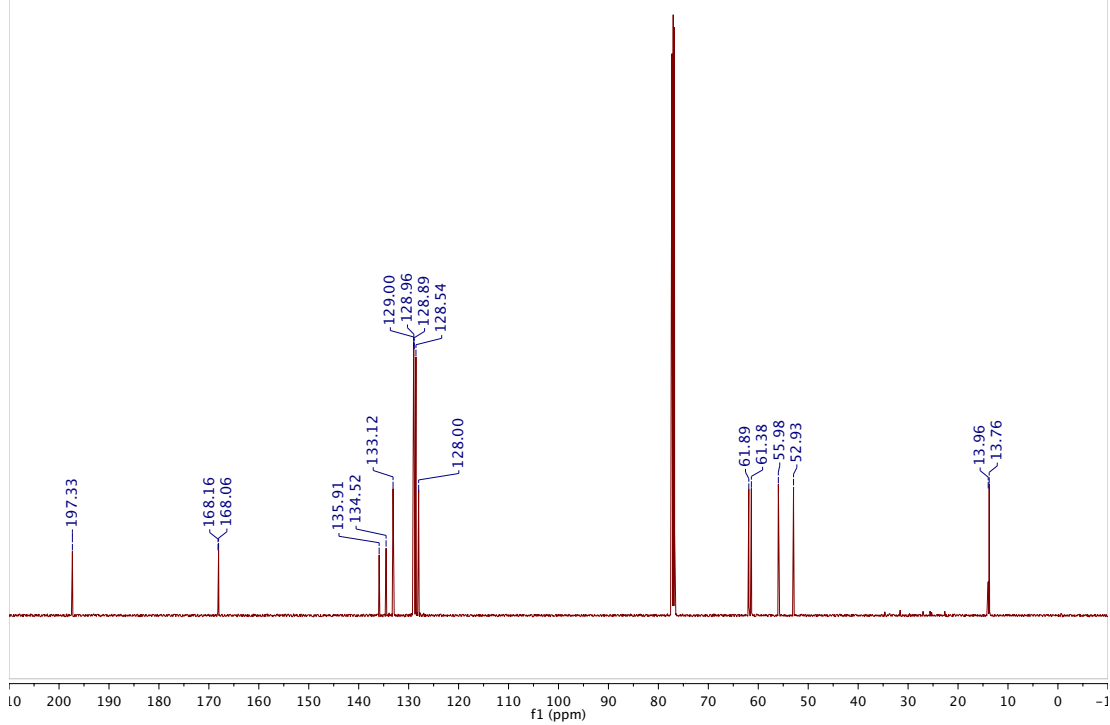


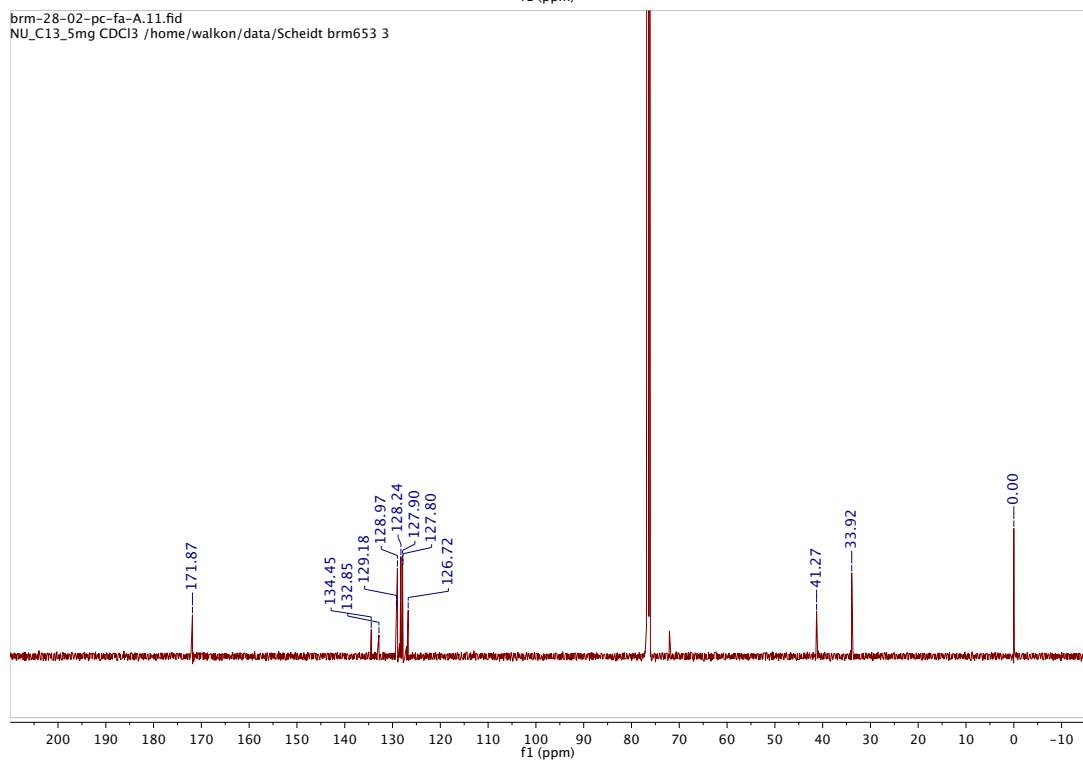
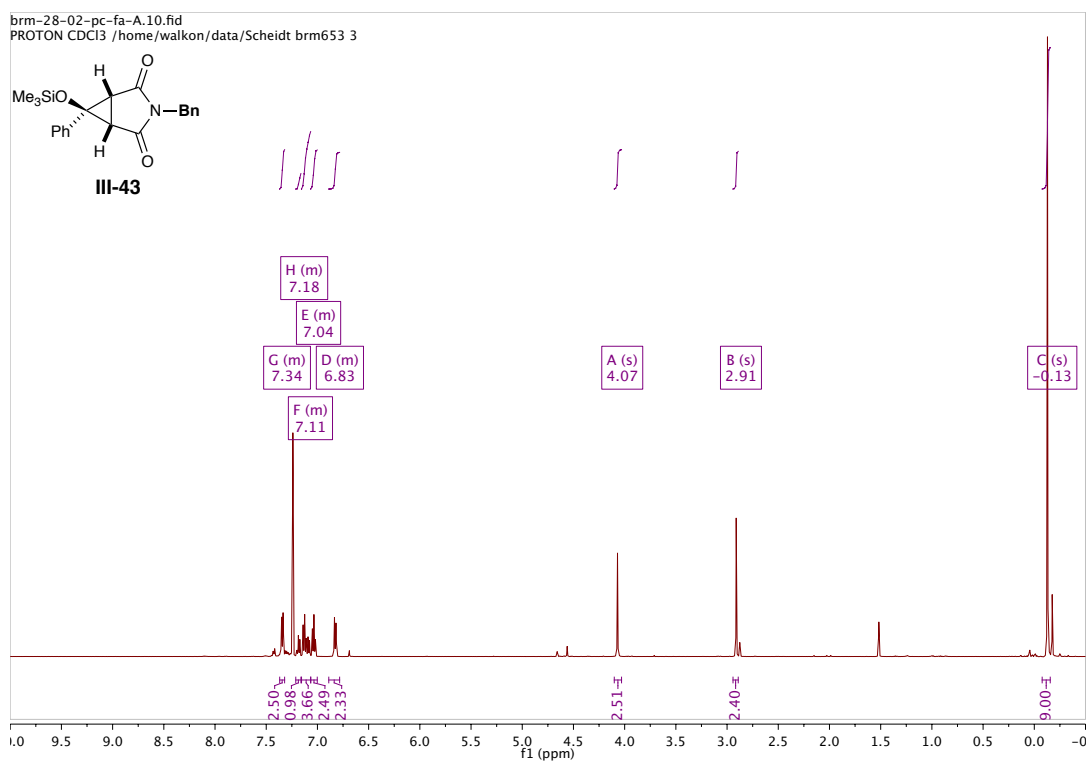


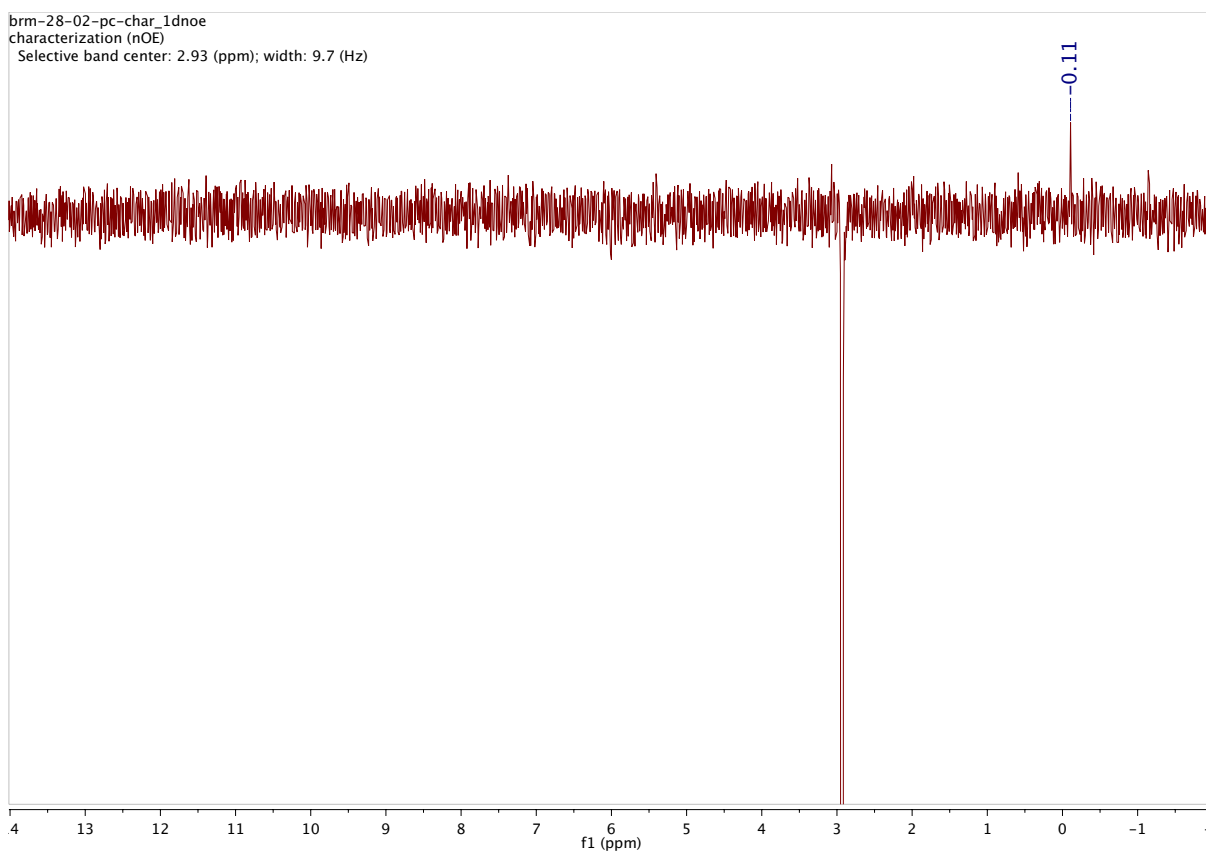
brm-27-42-PC-FA-2.10.fid

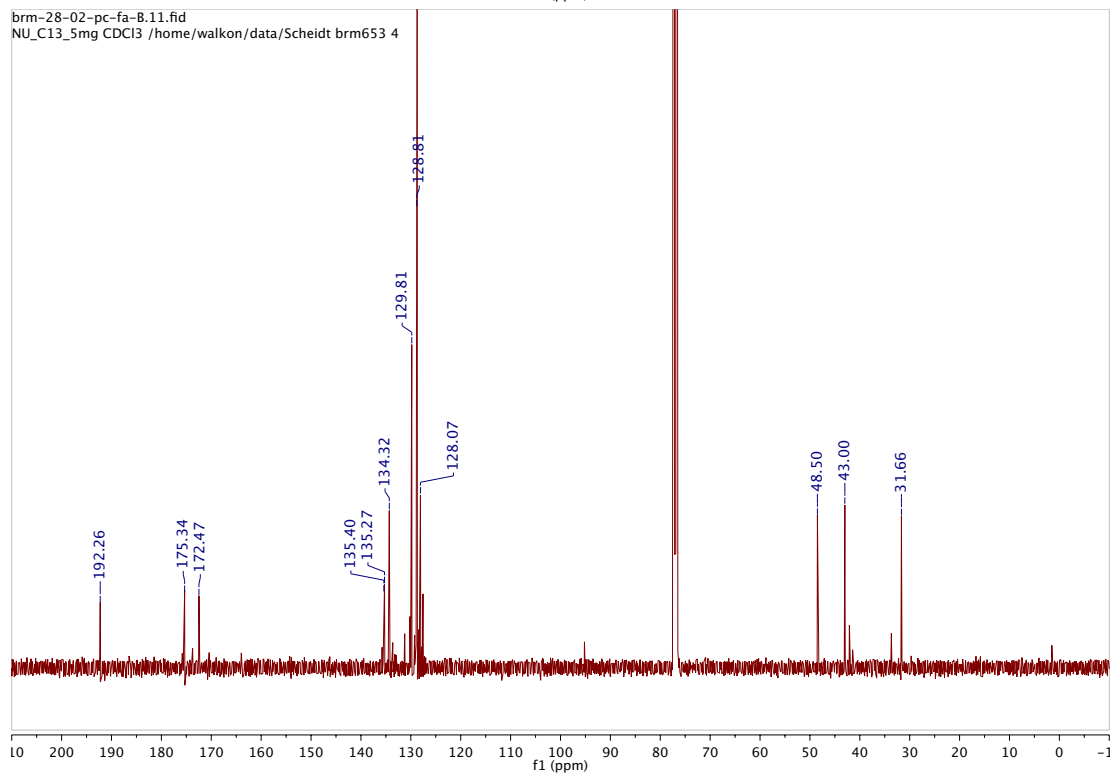
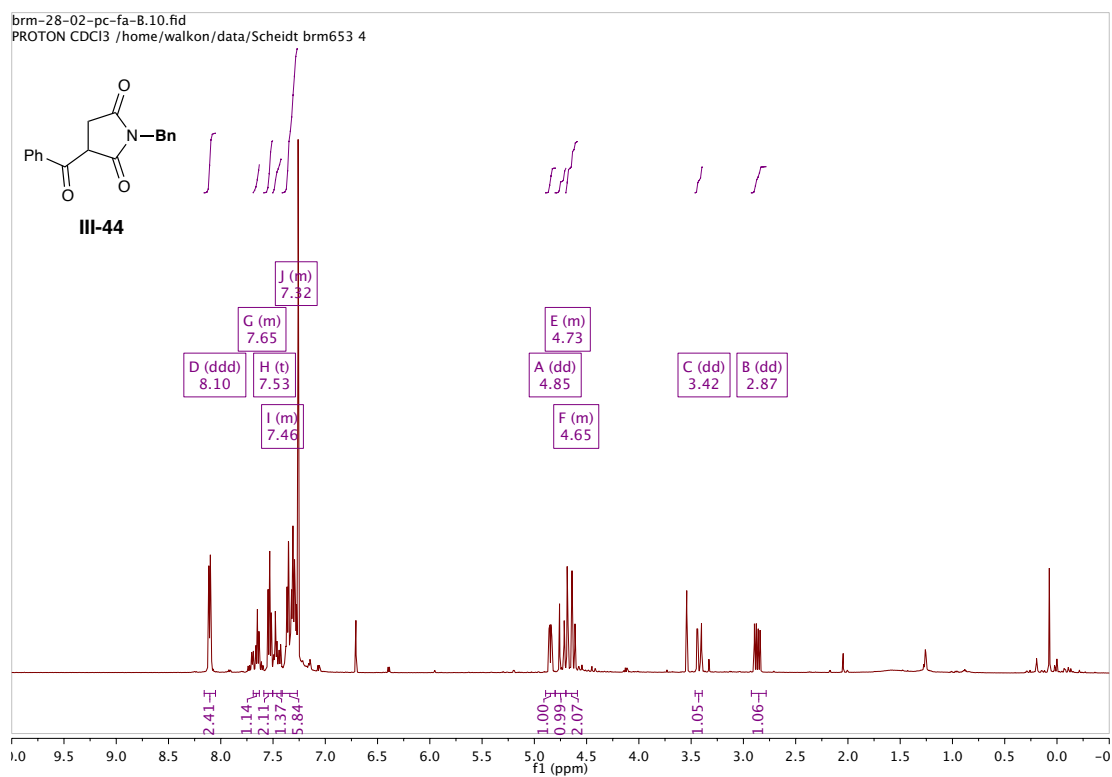
PROTON CDCl₃ /home/walkon/data/Scheidt brm653 21

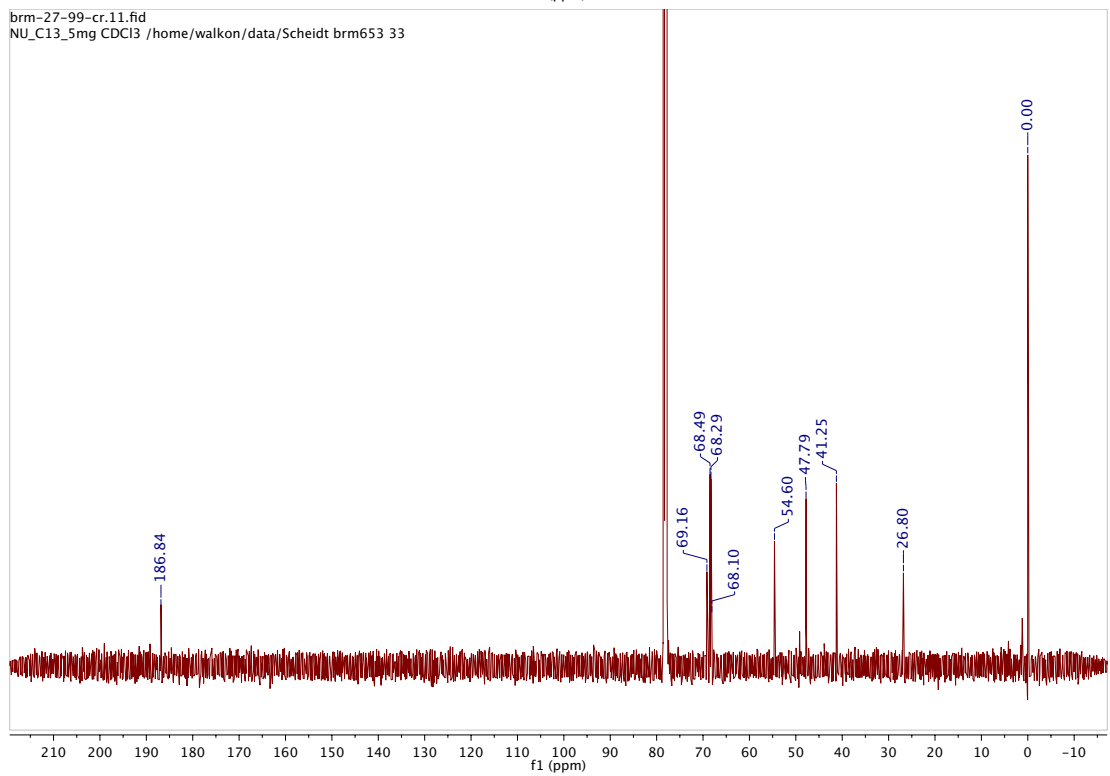
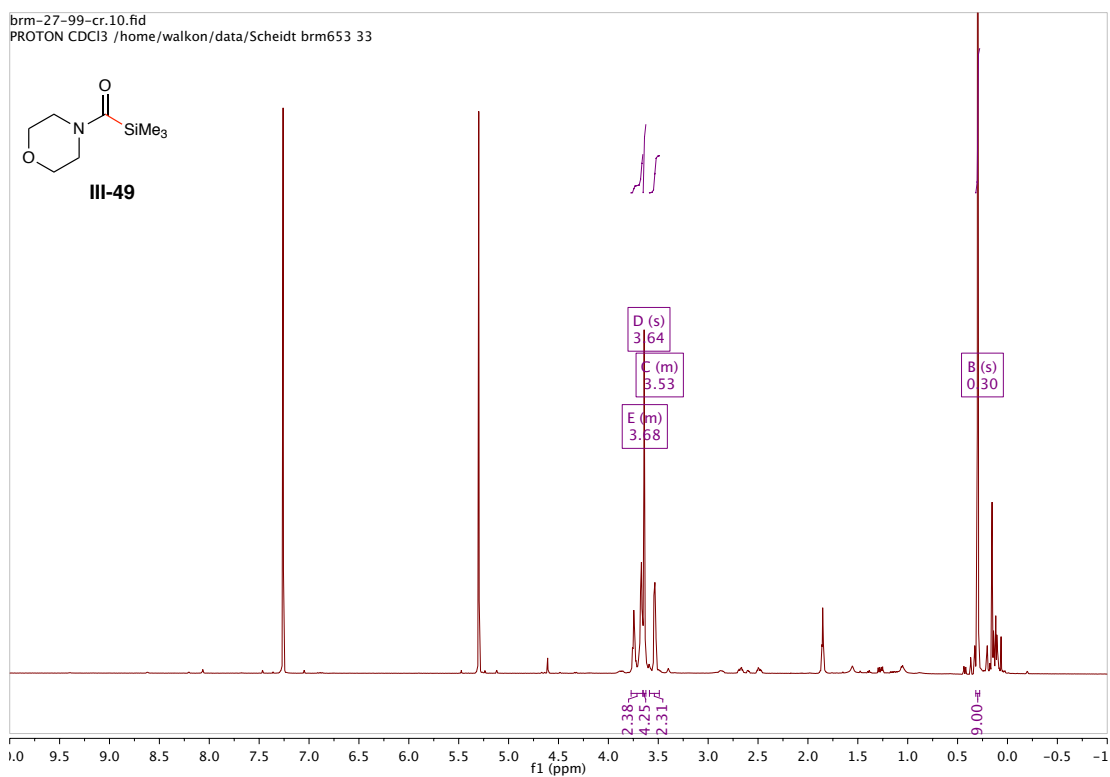
brm-27-42-PC-FA-2.11.fid

NU_C13_5mg CDCl₃ /home/walkon/data/Scheidt brm653 21









References:

1. Borchardt, J. K. *Drug News Perspect* **2002**, *15*, 187.
2. Retief, F. P.; Cilliers, L. *Samj S Afr Med J* **2007**, *97*, 27.
3. Gurib-Fakim, A. *Molecular Aspects of Medicine* **2006**, *27*, 1.
4. Tse, H. Y. G.; Li, V. W. T.; Hui, M. N. Y.; Chan, P. K.; Cheng, S. H. *J Biomol Screen* **2008**, *13*, 390.
5. Liu, X. M.; Zou, J. Q.; Sheng, Z. X.; Su, G. Q.; Chen, S. L. *Phytother. Res.* **2009**, *23*, 1493.
6. Kapoor, L. D. *CRC handbook of ayurvedic medicinal plants*; CRC Press: Boca Raton, Fla., 1990.
7. Krebs, R. E.; Krebs, C. A. *Groundbreaking scientific experiments, inventions, and discoveries of the ancient world*; Greenwood Press: Westport, Conn., 2003.
8. Iwu, M. M.; Wootton, J. C. *Ethnomedicine and drug discovery*; 1st ed.; Elsevier: Amsterdam ; New York, 2002.
9. Chattopadhyay, D. *Ethnomedicine : a source of complementary therapeutics*; Research Signpost: Trivandrum, 2010.
10. Cordell, G. A.; Colvard, M. D. *J. Nat. Prod.* **2012**, *75*, 514.
11. O'Neil, M. J.; Heckelman, P. E.; Dobbelaar, P. H.; Roman, K. J.; Kenny, C. M.; Karaffa, L. S.; Royal Society of Chemistry (Great Britain) *The Merck index : an encyclopedia of chemicals, drugs, and biologicals*; 15th ed.; Royal Society of Chemistry: Cambridge, UK, 2013.

12. Schultes, R. E.; Raffauf, R. F. *The healing forest : medicinal and toxic plants of the northwest Amazonia*; Dioscorides Press: Portland, Or., 1990.
13. Farnsworth, N. R.; Akerele, O.; Bingel, A. S.; Soejarto, D. D.; Guo, Z. *Bulletin of the World Health Organization* **1985**, *63*, 965.
14. Harvey, A. L. *Drug Discovery Today* **2008**, *13*, 894.
15. Newman, D. J.; Cragg, G. M.; Snader, K. M. *Nat. Prod. Rep.* **2000**, *17*, 215.
16. Koehn, F. E.; Carter, G. T. *Nat. Rev. Drug Discovery* **2005**, *4*, 206.
17. Dias, D. A.; Urban, S.; Roessner, U. *Metabolites* **2012**, *2*.
18. Gould, K. J. *Antimicrob. Chemother.* **2016**, *71*, 572.
19. Newman, D. J.; Cragg, G. M. *J. Nat. Prod.* **2012**, *75*, 311.
20. Newman, D. J.; Cragg, G. M.; Snader, K. M. *J. Nat. Prod.* **2003**, *66*, 1022.
21. Altmann, K. H.; Gertsch, J. *Nat. Prod. Rep.* **2007**, *24*, 327.
22. Molinski, T. F.; Dalisay, D. S.; Lievens, S. L.; Saludes, J. P. *Nat. Rev. Drug Discovery* **2009**, *8*, 69.
23. Majumdar, K. C.; Chattopadhyay, S. K. *Heterocycles in natural product synthesis*; Wiley-VCH Verlag: Weinheim, 2011.
24. Kumar, D.; Sharma, P.; Singh, H.; Nepali, K.; Gupta, G. K.; Jain, S. K.; Ntie-Kang, F. *Rsc Advances* **2017**, *7*, 36977.
25. Kang, E. J.; Lee, E. *Chem. Rev.* **2005**, *105*, 4348.
26. Nakata, T. *Chem. Rev.* **2005**, *105*, 4314.
27. Yeung, K.-S.; Paterson, I. *Chem. Rev.* **2005**, *105*, 4237.
28. Adams, D. R.; Bhatnagar, S. P. *Synthesis* **1977**, 661.

29. Snider, B. B. In *Comprehensive Organic Synthesis*; Trost, B. M., Fleming, I., Eds.; Pergamon Press: Oxford, 1991; Vol. 2.
30. Cloninger, M. J.; Overman, L. E. *J. Am. Chem. Soc.* **1999**, *121*, 1092.
31. Hart, D. J.; Bennett, C. E. *Org. Lett.* **2003**, *5*, 1499.
32. Jasti, R.; Vitale, J.; Rychnovsky, S. D. *J. Am. Chem. Soc.* **2004**, *126*, 9904.
33. Pastor, I. M.; Yus, M. *Curr. Org. Chem.* **2007**, *11*, 925.
34. Boger, D. L.; Weinreb, S. L. *Hetero Diels-Alder Methodology in Organic Synthesis*; Academic Press: San Diego, 1987; Vol. 47.
35. Clarke, P. A.; Santos, S. *Eur. J. Org. Chem.* **2006**, 2045.
36. Larrosa, I.; Romea, P.; Urpi, F. *Tetrahedron* **2008**, *64*, 2683.
37. Imai, H. S.; Suzuki, K. I.; Morioka, M.; Numasaki, Y.; Kadota, S.; Nagai, K.; Sato, T.; Iwanami, M.; Saito, T. *J. Antibiot.* **1987**, *40*, 1475.
38. Imai, H. S.; Kaniwa, H.; Tokunaga, T.; Fujita, S.; Furuya, T.; Matsumoto, H.; Shimizu, M. *J. Antibiot.* **1987**, *40*, 1483.
39. Nakai, R.; Kakita, S.; Asai, A.; Chiba, S.; Akinaga, S.; Mizukami, T.; Yamashita, Y. *J. Antibiot.* **2001**, *54*, 836.
40. Nakai, R.; Ishida, H.; Asai, A.; Ogawa, H.; Yamamoto, Y.; Kawasaki, H.; Akinaga, S.; Mizukami, T.; Yamashita, Y. *Chem. Biol.* **2006**, *13*, 183.
41. Cunningham, A. P.; Love, W. K.; Zhang, R. W.; Andrews, L. G.; Tollefsbol, T. O. *Curr. Med. Chem.* **2006**, *13*, 2875.
42. Takeda, K.; Shimotani, a.; Yoshii, E.; Yamaguchi, K. *Heterocycles* **1992**, *34*, 2259.
43. Paquette, L. A.; Boulet, S. L. *Synthesis* **2002**, 888.

44. Boulet, S. L.; Paquette, L. A. *Synthesis* **2002**, 895.
45. Smith, A. B.; Basu, K.; Bosanac, T. *J. Am. Chem. Soc.* **2007**, *129*, 14872.
46. Alder, R. W.; Harvey, J. N.; Oakley, M. T. *J. Am. Chem. Soc.* **2002**, *124*, 4960.
47. Crane, E. A.; Scheidt, K. A. *Angew. Chem. Int. Ed.* **2010**, *49*, 8316.
48. Lolkema, L. D. M.; Hiemstra, H.; Semeyn, C.; Speckamp, W. N. *Tetrahedron* **1994**, *50*, 7115.
49. Roush, W. R.; Dilley, G. J. *Synlett* **2001**, 955.
50. Jasti, R.; Rychnovsky, S. D. *J. Am. Chem. Soc.* **2006**, *128*, 13640.
51. Rychnovsky, S. D.; Marumoto, S.; Jaber, J. J. *Org. Lett.* **2001**, *3*, 3815.
52. Jasti, R.; Anderson, C. D.; Rychnovsky, S. D. *J. Am. Chem. Soc.* **2005**, *127*, 9939.
53. Jasti, R.; Rychnovsky, S. D. *Org. Lett.* **2006**, *8*, 2175.
54. Grunwell, J. R.; Karipides, A.; Wigal, C. T.; Heinzman, S. W.; Parlow, J.; Surso, J. A.; Clayton, L.; Fleitz, F. J.; Daffner, M.; Stevens, J. E. *J. Org. Chem.* **1991**, *56*, 91.
55. Seebach, D.; Misslitz, U.; Uhlmann, P. *Chem. Ber.* **1991**, *124*, 1845.
56. Teerhuis, N. M.; Hiemstra, H.; Speckamp, W. N. *Tetrahedron Lett.* **1997**, *38*, 159.
57. Betori, R. C.; Miller, E. R.; Scheidt, K. A. *Adv. Synth. Catal.* **2017**, *359*, 1131.
58. Morris, W. J.; Custar, D. W.; Scheidt, K. A. *Org. Lett.* **2005**, *7*, 1113.
59. Tenenbaum, J. M.; Morris, W. J.; Custar, D. W.; Scheidt, K. A. *Angew. Chem. Int. Ed.* **2011**, *50*, 5892.
60. Custar, D. W.; Zabawa, T. P.; Scheidt, K. A. *J. Am. Chem. Soc.* **2008**, *130*, 804.
61. Custar, D. W.; Zabawa, T. P.; Hines, J.; Crews, C. M.; Scheidt, K. A. *J. Am. Chem. Soc.* **2009**, *131*, 12406.

62. Crane, E. A.; Zabawa, T. P.; Farmer, R. L.; Scheidt, K. A. *Angew. Chem. Int. Ed.* **2011**, *50*, 9112.
63. *Flavanoids: Chemistry, Biochemistry and Applications*; Andersen, O. M.; Markham, K. R., Eds.; CRC Press: Boca Raton, 2006.
64. Jez, J. M.; Bowman, M. E.; Dixon, R. A.; Noel, J. P. *Nat. Struc. Mol. Biol.* **2000**, *7*, 786.
65. Ngaki, M. N.; Louie, G. V.; Philippe, R. N.; Manning, G.; Pojer, F.; Bowman, M. E.; Li, L.; Larsen, E.; Wurtele, E. S.; Noel, J. P. *Nature* **2012**, *485*, 530.
66. Bednar, R. A.; Hadcock, J. R. *J. Biol. Chem.* **1988**, *263*, 9582.
67. Nibbs, A. E.; Scheidt, K. A. *Eur. J. Org. Chem.* **2012**, 449.
68. Miles, C. O.; Main, L. *J Chem Soc Perk T 2* **1985**, 1639.
69. Biddle, M. M.; Lin, M.; Scheidt, K. A. *J. Am. Chem. Soc.* **2007**, *129*, 3830.
70. Marcelli, T.; Hiemstra, H. *Synthesis* **2010**, 1229.
71. Vakulya, B.; Varga, S.; Csampai, A.; Soos, T. *Org. Lett.* **2005**, *7*, 1967.
72. Marcelli, T.; van der Haas, R. N. S.; van Maarseveen, J. H.; Hiemstra, H. *Angew. Chem. Int. Ed.* **2006**, *45*, 929.
73. Abenavoli, L.; Capasso, R.; Milic, N.; Capasso, F. *Phytother. Res.* **2010**, *24*, 1423.
74. Davis-Searles, P. R.; Nakanishi, Y.; Kim, N. C.; Graf, T. N.; Oberlies, N. H.; Wani, M. C.; Wall, M. E.; Agarwal, R.; Kroll, D. J. *Cancer Res.* **2005**, *65*, 4448.
75. Sy-Cordero, A.; Graf, T. N.; Nakanishi, Y.; Wani, M. C.; Agarwal, R.; Kroll, D. J.; Oberlies, N. H. *Planta Med.* **2010**, *76*, 644.
76. Kroll, D. J.; Shaw, H. S.; Oberlies, N. H. *Integr Cancer Ther* **2007**, *6*, 110.

77. Nyiredy, S.; Samu, Z.; Szucs, Z.; Gulacsi, K.; Kurtan, T.; Antus, S. *J. Chromatogr. Sci.* **2008**, *46*, 93.
78. Althagafy, H. S.; Meza-Avina, M. E.; Oberlies, N. H.; Croatt, M. P. *J. Org. Chem.* **2013**, *78*, 7594.
79. Rambaldi, A.; Jacobs, B. P.; Iaquinto, G.; Gluud, C. *Am J Gastroenterol* **2005**, *100*, 2583.
80. Ball, K. R.; Kowdley, K. V. *J Clin Gastroenterol* **2005**, *39*, 520.
81. Flora, K.; Hahn, M.; Rosen, H.; Benner, K. *Am. J. Gastro.* **1998**, *93*, 139.
82. Tamayo, C.; Diamond, S. *Integr Cancer Ther* **2007**, *6*, 146.
83. Loguercio, C.; Festi, D. *World J. Gastro.* **2011**, *17*, 2288.
84. Agarwal, R.; Agarwal, C.; Ichikawa, H.; Singh, R. P.; Aggarwal, B. B. *Anticancer Res.* **2006**, *26*, 4457.
85. Singh, R. P.; Agarwal, R. *Curr. Cancer Drug Tar.* **2004**, *4*, 1.
86. Ramasamy, K.; Agarwal, R. *Cancer Letters* **2008**, *269*, 352.
87. Singh, R. P.; Agarwal, R. *Mutat. Res., Fundam. Mol. Mech. Mutagen.* **2004**, *555*, 21.
88. Deep, G.; Singh, R. P.; Agarwal, C.; Kroll, D. J.; Agarwal, R. *Oncogene* **2006**, *25*, 1053.
89. Flaig, T. W.; Gustafson, D. L.; Su, L. J.; Zirrolli, J. A.; Crighton, F.; Harrison, G. S.; Pierson, A. S.; Agarwal, R.; Glode, L. M. *Invest. New Drugs* **2007**, *25*, 139.
90. Deep, G.; Raina, K.; Singh, R. P.; Oberlies, N. H.; Kroll, D. J.; Agarwal, R. *Int. J. Cancer* **2008**, *123*, 2750.
91. Deep, G.; Oberlies, N. H.; Kro, D. J.; Agarwal, R. *Int. J. Cancer* **2008**, *123*, 41.
92. Zhou, Y.; Bolton, E. C.; Jones, J. O. *J. Mol. Endocrinol.* **2015**, *54*, R15.
93. Deep, G.; Oberlies, N. H.; Kroll, D. J.; Agarwal, R. *Oncogene* **2008**, *27*, 3986.

94. Marker, P. C.; Donjacour, A. A.; Dahiya, R.; Cunha, G. R. *Dev. Biol.* **2003**, *253*, 165.
95. Yuan, X.; Cai, C.; Chen, S.; Chen, S.; Yu, Z.; Balk, S. P. *Oncogene* **2014**, *33*, 2815.
96. Deep, G.; Oberlies, N. H.; Kroll, D. J.; Agarwal, R. *Carcinogenesis* **2007**, *28*, 1533.
97. Kim, N. C.; Graf, T. N.; Sparacino, C. M.; Wani, M. C.; Wall, M. E. *Org. Biomol. Chem.* **2003**, *1*, 1684.
98. Graf, T. N.; Wani, M. C.; Agarwal, R.; Kroll, D.; Oberlies, N. H. *Planta Med.* **2007**, *73*, 1495.
99. Sy-Cordero, A. A.; Day, C. S.; Oberlies, N. H. *J. Nat. Prod.* **2012**, *75*, 1879.
100. Merlini, L.; Zanarotti, A.; Pelter, A.; Rochefort, M. P.; Hansel, R. *J. Chem. Soc., Perkin Trans. 1* **1980**, 775.
101. Yang, L. X.; Huang, K. X.; Li, H. B.; Gong, J. X.; Wang, F.; Feng, Y. B.; Tao, Q. F.; Wu, Y. H.; Li, X. K.; Wu, X. M.; Zeng, S.; Spencer, S.; Zhao, Y.; Qu, J. *J. Med. Chem.* **2009**, *52*, 7732.
102. Gu, W. X.; Chen, X. C.; Pan, X. F.; Chan, A. S. C.; Yang, T. K. *Tetrahedron-Asymmetr* **2000**, *11*, 2801.
103. Chen, X. C.; Ren, X. F.; Peng, K.; Pan, X. F.; Chan, A. S. C.; Yang, T. K. *Tetrahedron-Asymmetr* **2003**, *14*, 701.
104. Martinelli, M. J.; Nayyar, N. K.; Moher, E. D.; Dhokte, U. P.; Pawlak, J. M.; Vaidyanathan, R. *Org. Lett.* **1999**, *1*, 447.
105. O'donnell, C. J.; Burke, S. D. *J. Org. Chem.* **1998**, *63*, 8614.
106. Lipshutz, B. H.; Chung, D. W.; Rich, B.; Corral, R. *Org. Lett.* **2006**, *8*, 5069.
107. Tokunaga, M.; Larrow, J. F.; Kakiuchi, F.; Jacobsen, E. N. *Science* **1997**, *277*, 936.

108. Dittmer, C.; Raabe, G.; Hintermann, L. *Eur. J. Org. Chem.* **2007**, *35*, 5886.
109. Schreiner, P. R. *Chem. Soc. Rev.* **2003**, *32*, 289.
110. Masamune, S.; Choy, W.; Petersen, J. S.; Sita, L. R. *Angew. Chem., Int. Ed. Engl.* **1985**, *24*, 1.
111. Paterson, I.; Watson, C.; Yeung, K.-S.; Wallace, P. A.; Ward, R. A. *J. Org. Chem.* **1997**, *62*, 452.
112. Napolitano, J. G.; Lankin, D. C.; Graf, T. N.; Friesen, J. B.; Chen, S. N.; McAlpine, J. B.; Oberlies, N. H.; Pauli, G. F. *J. Org. Chem.* **2013**, *78*, 2827.
113. Adam, W.; Muller, M.; Prechtel, F. *J. Org. Chem.* **1994**, *59*, 2358.
114. Johnson, F. *Chem. Rev.* **1968**, *68*, 375.
115. Olah, G. A.; Narang, S. C.; Gupta, B. G. B.; Malhotra, R. *J. Org. Chem.* **1979**, *44*, 1247.
116. Atkins, P. W.; De Paula, J. *Elements of physical chemistry*; 6th ed.; Oxford University Press: Oxford, 2013.
117. Gaffield, W. *Tetrahedron* **1970**, *26*, 4093.
118. Slade, D.; Ferreira, D.; Marais, J. P. J. *Phytochemistry* **2005**, *66*, 2177.
119. Tomita, D.; Wada, R.; Kanai, M.; Shibasaki, M. *J. Am. Chem. Soc.* **2005**, *127*, 4138.
120. Coombs, J. R.; Haeffner, F.; Kliman, L. T.; Morken, J. P. *J. Am. Chem. Soc.* **2013**, *135*, 11222.
121. Lam, H. W. *Synthesis* **2011**, 2011.
122. Zeng, B. S.; Yu, X. Y.; Siu, P. W.; Scheidt, K. A. *Chem. Sci.* **2014**, *5*, 2277.

123. Ingólfsson, H. I.; Thakur, P.; Herold, K. F.; Hobart, E. A.; Ramsey, N. B.; Periole, X.; de Jong, D. H.; Zwama, M.; Yilmaz, D.; Hall, K.; Maretzky, T.; Hemmings, H. C.; Blobel, C.; Marrink, S. J.; Koçer, A.; Sack, J. T.; Andersen, O. S. *ACS Chem. Biol.* **2014**, *9*, 1788.
124. Pangborn, A. B.; Giardello, M. A.; Grubbs, R. H.; Rosen, R. K.; Timmers, F. J. *Organometallics* **1996**, *15*, 1518.
125. Perrin, D. D.; Armarego, W. L. F. *Purification of Laboratory Chemicals*; 3rd ed.; Pergamon Press: Oxford, 1988.
126. Seebach, D. *Angew. Chem. Int. Ed.* **1979**, *18*, 239.
127. Hoppe, D.; Hense, T. *Angew. Chem. Int. Ed.* **1997**, *36*, 2283.
128. Reissig, H. U.; Zimmer, R. *Chem. Rev.* **2003**, *103*, 1151.
129. Smith, A. B.; Adams, C. M. *Acc. Chem. Res.* **2004**, *37*, 365.
130. Ballini, R.; Bosica, G.; Fiorini, D.; Palmieri, A.; Petrini, M. *Chem. Rev.* **2005**, *105*, 933.
131. Chatterjee, A.; Joshi, N. N. *Tetrahedron* **2006**, *62*, 12137.
132. Guo, F.; Clift, M. D.; Thomson, R. J. *Eur. J. Org. Chem.* **2012**, 4881.
133. Hopkins, F. G. *Biochem. J.* **1928**, *22*, 1341.
134. Robinson, R. *Journal of the Chemical Society, Transactions* **1917**, *111*, 762.
135. Medley, J. W.; Movassaghi, M. *Chem. Commun. (Cambridge, U. K.)* **2013**, *49*, 10775.
136. Scholz, U.; Winterfeldt, E. *Nat. Prod. Rep.* **2000**, *17*, 349.
137. Corey, E. J. *The logic of chemical synthesis*; New York : Wiley: New York, 1989.
138. Evans, D. A.; Andrews, G. C. *Acc. Chem. Res.* **1974**, *7*, 147.
139. Wöhler, n.; Liebig, n. *Annalen der Pharmacie* **2006**, *3*, 249.
140. Menon, R. S.; Biju, A. T.; Nair, V. *Beilstein J. Org. Chem.* **2016**, *12*, 444.

141. Breslow, R. *J. Am. Chem. Soc.* **1958**, *80*, 3719.
142. Nair, V.; Bindu, S.; Sreekumar, V. *Angew. Chem. Int. Ed.* **2004**, *43*, 5130.
143. Nair, V.; Vellalath, S.; Babu, B. P. *Chem. Soc. Rev.* **2008**, *37*, 2691.
144. Nair, V.; Menon, R. S.; Biju, A. T.; Sinu, C. R.; Paul, R. R.; Jose, A.; Sreekumar, V. *Chem. Soc. Rev.* **2011**, *40*, 5336.
145. Grossmann, A.; Enders, D. *Angew. Chem. Int. Ed.* **2012**, *51*, 314.
146. Hopkinson, M. N.; Richter, C.; Schedler, M.; Glorius, F. *Nature* **2014**, *510*, 485.
147. Flanigan, D. M.; Romanov-Michailidis, F.; White, N. A.; Rovis, T. *Chem. Rev.* **2015**, *115*, 9307.
148. Menon, R. S.; Biju, A. T.; Nair, V. *Chem. Soc. Rev.* **2015**, *44*, 5040.
149. Pohl, M.; Sprenger, G. A.; Muller, M. *Curr. Opin. Biotechnol.* **2004**, *15*, 335.
150. Adlington, R. M.; Baldwin, J. E.; Bottaro, J. C.; Perry, M. W. D. *J Chem Soc Chem Comm* **1983**, 1040.
151. Baldwin, J. E.; Adlington, R. M.; Bottaro, J. C.; Kolhe, J. N.; Perry, M. W. D.; Jain, A. *U. Tetrahedron* **1986**, *42*, 4223.
152. Corey, E. J.; Seebach, D. *Angew. Chem., Int. Ed. Engl.* **1965**, *4*, 10750.
153. Corey, E. J.; Seebach, D.; Freedman, R. *J. Am. Chem. Soc.* **1967**, *89*, 434.
154. Seebach, D.; Corey, E. J. *J. Org. Chem.* **1975**, *40*, 231.
155. Page, P. C. B.; van Niel, M. B.; Prodger, J. C. *Tetrahedron* **1989**, *45*, 7643.
156. Yus, M.; Najera, C.; Foubelo, F. *Tetrahedron* **2003**, *59*, 6147.
157. Alabugin, I. V. *J. Org. Chem.* **2000**, *65*, 3910.
158. Smith, A. B.; Xian, M.; Kim, W. S.; Kim, D. S. *J. Am. Chem. Soc.* **2006**, *128*, 12368.

159. Smith, A. B.; Xian, M. *J. Am. Chem. Soc.* **2006**, *128*, 66.
160. Smith, A. B.; Wuest, W. M. *Chem. Commun. (Cambridge, U. K.)* **2008**, 5883.
161. Devarie-Baez, N. O.; Kim, W. S.; Smith, A. B.; Xian, M. *Org. Lett.* **2009**, *11*, 1861.
162. Montgomery, T. D.; Smith, A. B. *Org. Lett.* **2017**, *19*, 6216.
163. Han, H.; Smith, A. B. *Angew. Chem. Int. Ed.* **2017**, *56*, 14102.
164. Adams, H.; Anderson, J. C.; Peace, S.; Pennell, A. M. K. *J. Org. Chem.* **1998**, *63*, 9932.
165. Westermann, B. *Angew. Chem. Int. Ed.* **2003**, *42*, 151.
166. Noble, A.; Anderson, J. C. *Chem. Rev.* **2013**, *113*, 2887.
167. Wu, Y. W.; Hu, L.; Li, Z.; Deng, L. *Nature* **2015**, *523*, 445.
168. Liu, J.; Cao, C. G.; Sun, H. B.; Zhang, X.; Niu, D. W. *J. Am. Chem. Soc.* **2016**, *138*, 13103.
169. Li, M. Y.; Gutierrez, O.; Berritt, S.; Pascual-Escudero, A.; Yesilcimen, A.; Yang, X. D.; Adrio, J.; Huang, G.; Nakamaru-Ogiso, E.; Kozlowski, M. C.; Walsh, P. J. *Nat. Chem.* **2017**, *9*, 997.
170. Nickon, A.; Lambert, J. L. *J. Am. Chem. Soc.* **1962**, *84*, 4604.
171. Werstiuk, N. H. *Tetrahedron* **1983**, *39*, 205.
172. Kuwajima, I.; Nakamura, E. In *Comprehensive Organic Synthesis*; Trost, B. M., Fleming, I., Eds.; Pergamon Press: Oxford, 1991; Vol. 2, p 441.
173. Crimmins, M. T.; Nantermet, P. G. *Org. Prep. Proced. Int.* **1993**, *25*, 41.
174. Ahlbrecht, H.; Beyer, U. *Synthesis* **1999**, 365.
175. Kuwajima, I.; Kato, M. *J. Chem. Soc. Chem. Comm.* **1979**, 708.
176. Goswami, R. *J. Am. Chem. Soc.* **1980**, *102*, 5973.

177. Nakamura, E.; Kuwajima, I. *J. Am. Chem. Soc.* **1983**, *105*, 651.
178. Nakamura, E.; Oshino, H.; Kuwajima, I. *Heterocycles* **1984**, *21*, 599.
179. Nakamura, E.; Kuwajima, I. *J. Am. Chem. Soc.* **1984**, *106*, 3368.
180. Nakamura, E.; Shimada, J.; Kuwajima, I. *Organometallics* **1985**, *4*, 641.
181. Nakamura, E.; Oshino, H.; Kuwajima, I. *J. Am. Chem. Soc.* **1986**, *108*, 3745.
182. Cozzi, P. G.; Carofiglio, T.; Floriani, C.; Chiesivilla, A.; Rizzoli, C. *Organometallics* **1993**, *12*, 2845.
183. Maki, B. E.; Chan, A.; Scheidt, K. A. *Synthesis* **2008**, 1306.
184. Perkins, M. J. *Radical chemistry : the fundamentals*; Oxford ; New York : Oxford University Press: Oxford ; New York, 2000.
185. Zard, S. Z. *Radical reactions in organic synthesis*; Oxford New York : Oxford University Press: Oxford New York, 2003.
186. Giese, B. *Angew Chem Int Edit* **1983**, *22*, 753.
187. Boyington, A. J.; Riu, M. L. Y.; Jui, N. T. *J. Am. Chem. Soc.* **2017**, *139*, 6582.
188. Donoghue, P. J.; Wiest, O. *Chem. - Eur. J.* **2006**, *12*, 7019.
189. Ischay, M. A.; Yoon, T. P. *Eur. J. Org. Chem.* **2012**, 3359.
190. Fischer, H. *Chem. Rev.* **2001**, *101*, 3581.
191. Studer, A. *Chem. - Eur. J.* **2001**, *7*, 1159.
192. Shaw, M. H.; Twilton, J.; MacMillan, D. W. C. *J. Org. Chem.* **2016**, *81*, 6898.
193. Matsui, J. K.; Lang, S. B.; Heitz, D. R.; Molander, G. A. *Acs Catal* **2017**, *7*, 2563.
194. Hofbeck, T.; Yersin, H. *Inorg. Chem.* **2010**, *49*, 9290.

195. Tamayo, A. B.; Alleyne, B. D.; Djurovich, P. I.; Lamansky, S.; Tsyba, I.; Ho, N. N.; Bau, R.; Thompson, M. E. *J. Am. Chem. Soc.* **2003**, *125*, 7377.
196. Tucker, J. W.; Stephenson, C. R. J. *J. Org. Chem.* **2012**, *77*, 1617.
197. Pitre, S. P.; McTiernan, C. D.; Scaiano, J. C. *Acc. Chem. Res.* **2016**, *49*, 1320.
198. Nicewicz, D. A.; Nguyen, T. M. *Acs Catal* **2014**, *4*, 355.
199. Romero, N. A.; Nicewicz, D. A. *Chem. Rev.* **2016**, *116*, 10075.
200. Margrey, K. A.; Nicewicz, D. A. *Acc. Chem. Res.* **2016**, *49*, 1997.
201. Lowry, M. S.; Goldsmith, J. I.; Slinker, J. D.; Rohl, R.; Pascal, R. A.; Malliaras, G. G.; Bernhard, S. *Chem. Mater.* **2005**, *17*, 5712.
202. Roth, H. G.; Romero, N. A.; Nicewicz, D. A. *Synlett* **2016**, *27*, 714.
203. Skubi, K. L.; Blum, T. R.; Yoon, T. P. *Chem. Rev.* **2016**, *116*, 10035.
204. Ischay, M. A.; Anzovino, M. E.; Du, J.; Yoon, T. P. *J. Am. Chem. Soc.* **2008**, *130*, 12886.
205. Gentry, E. C.; Knowles, R. R. *Acc. Chem. Res.* **2016**, *49*, 1546.
206. Tarantino, K. T.; Liu, P.; Knowles, R. R. *J. Am. Chem. Soc.* **2013**, *135*, 10022.
207. Streuff, J. *Synthesis* **2013**, *45*, 281.
208. Danly, D. E. *J. Electrochem. Soc.* **1984**, *131*, C435.
209. Hays, D. S.; Fu, G. C. *J. Org. Chem.* **1996**, *61*, 4.
210. Savchenko, A. V.; Montgomery, J. *J. Org. Chem.* **1996**, *61*, 1562.
211. Baik, T.-G.; Luis, A. L.; Wang, L.-C.; Krische, M. J. *J. Am. Chem. Soc.* **2001**, *123*, 6716.
212. Wang, L.-C.; Jang, H.-Y.; Roh, Y.; Lynch, V.; Schultz, A. J.; Wang, X.; Krische, M. J. *J. Am. Chem. Soc.* **2002**, *124*, 9448.
213. Ischay, M. A.; Anzovino, M. E.; Du, J.; Yoon, T. P. *J. Am. Chem. Soc.* **2008**, *130*, 12886.

214. Zhao, G.; Yang, C.; Guo, L.; Sun, H.; Lin, R.; Xia, W. *J. Org. Chem.* **2012**, *77*, 6302.
215. Streuff, J. *Chem. - Eur. J.* **2011**, *17*, 5507.
216. Bichovski, P.; Haas, T. M.; Keller, M.; Streuff, J. *Org. Biomol. Chem.* **2016**, *14*, 5673.
217. Wang, C. Y.; Qin, J.; Shen, X. D.; Riedel, R.; Harms, K.; Meggers, E. *Angew. Chem. Int. Ed.* **2016**, *55*, 685.
218. Huo, H.; Harms, K.; Meggers, E. *J. Am. Chem. Soc.* **2016**, *138*, 6936.
219. Ma, J. J.; Rosales, A. R.; Huang, X. Q.; Harms, K.; Riedel, R.; Wiest, O.; Meggers, E. *J. Am. Chem. Soc.* **2017**, *139*, 17245.
220. Zhou, Z. J.; Li, Y. J.; Han, B. W.; Gong, L.; Meggers, E. *Chem. Sci.* **2017**, *8*, 5757.
221. Deng, G.; Yu, J.; Yang, X. P.; Xu, H. J. *Tetrahedron* **1990**, *46*, 5967.
222. Shono, T.; Nishiguchi, I.; Ohmizu, H. *J. Am. Chem. Soc.* **1977**, *99*, 7396.
223. Nakajima, M.; Fava, E.; Loescher, S.; Jiang, Z.; Rueping, M. *Angew. Chem. Int. Ed.* **2015**, *54*, 8828.
224. Humbel, S.; Cote, I.; Hoffmann, N.; Bouquant, J. *J. Am. Chem. Soc.* **1999**, *121*, 5507.
225. Schuster, T.; Kurz, M.; Göbel, M. W. *J. Org. Chem.* **2000**, *65*, 1697.
226. Akalay, D.; Dürner, G.; Bats, J. W.; Bolte, M.; Göbel, M. W. *J. Org. Chem.* **2007**, *72*, 5618.
227. Bartoli, G.; Beleggia, R.; Giuli, S.; Giuliani, A.; Marcantoni, E.; Massaccesi, M.; Paoletti, M. *Tetrahedron Lett.* **2006**, *47*, 6501.
228. Luo, J.; Zhang, J. *Acs Catal* **2016**, *6*, 873.
229. Nakano, S.; Kakugawa, K.; Nemoto, T.; Hamada, Y. *Adv. Synth. Catal.* **2014**, *356*, 2088.
230. Fava, E.; Nakajima, M.; Nguyen, A. L. P.; Rueping, M. *J. Org. Chem.* **2016**, *81*, 6959.

231. Desimoni, G.; Faita, G.; Quadrelli, P. *Chem. Rev.* **2003**, *103*, 3119.
232. Desimoni, G.; Faita, G.; Jorgensen, K. A. *Chem. Rev.* **2006**, *106*, 3561.
233. Rasappan, R.; Laventine, D.; Reiser, O. *Coord. Chem. Rev.* **2008**, *252*, 702.
234. Chen, W. X.; Liu, Z.; Tian, J. Q.; Li, J.; Ma, J.; Cheng, X.; Li, G. G. *J. Am. Chem. Soc.* **2016**, *138*, 12312.
235. Silvi, M.; Verrier, C.; Rey, Y. P.; Buzzetti, L.; Melchiorre, P. *Nat. Chem.* **2017**, *9*, 868.
236. Verrier, C.; Alandini, N.; Pezzetta, C.; Moliterno, M.; Buzzetti, L.; Hepburn, H. B.; Vega-Penaloza, A.; Silvi, M.; Melchiorre, P. *Acs Catal* **2018**, *8*, 1062.
237. Uoyama, H.; Goushi, K.; Shizu, K.; Nomura, H.; Adachi, C. *Nature* **2012**, *492*, 234.
238. Liu, X. H.; Lin, L. L.; Feng, X. M. *Org Chem Front* **2014**, *1*, 298.
239. Full conversion of these heteroarylidene malonates was observed with no identifiable products observed.
240. Espelt, L. R.; McPherson, I. S.; Wiensch, E. M.; Yoon, T. P. *J. Am. Chem. Soc.* **2015**, *137*, 2452.
241. Elinson, M. N.; Feducovich, S. K.; Zakharenkov, A. A.; Ugrak, B. I.; Nikishin, G. I.; Lindeman, S. V.; Struchkov, J. T. *Tetrahedron* **1995**, *51*, 5035.
242. Yamashita, M.; Okuyama, K.; Kawasaki, I.; Nakamura, S.; Nagamine, R.; Tsujita, T.; Ohta, S. *Chem. Pharm. Bull.* **2000**, *48*, 1799.
243. Csaky, A. G.; Plumet, J. *Chem. Soc. Rev.* **2001**, *30*, 313.
244. Yeung, C. S.; Dong, V. M. *Chem. Rev.* **2011**, *111*, 1215.
245. Guo, F. H.; Clift, M. D.; Thomson, R. J. *Eur. J. Org. Chem.* **2012**, 4881.

246. Petronijevic, F. R.; Nappi, M.; MacMillan, D. W. C. *J. Am. Chem. Soc.* **2013**, *135*, 18323.
247. Pirnot, M. T.; Rankic, D. A.; Martin, D. B. C.; MacMillan, D. W. C. *Science* **2013**, *339*, 1593.
248. Jeffrey, J. L.; Petronijevic, F. R.; MacMillan, D. W. C. *J. Am. Chem. Soc.* **2015**, *137*, 8404.
249. Mukherjee, S.; Yang, J. W.; Hoffmann, S.; List, B. *Chem. Rev.* **2007**, *107*, 5471.
250. Erkkilä, A.; Majander, I.; Pihko, P. M. *Chem. Rev.* **2007**, *107*, 5416.
251. Krautwald, S.; Sarlah, D.; Schafroth, M. A.; Carreira, E. M. *Science* **2013**, *340*, 1065.
252. Beletskaya, I. P.; Nájera, C.; Yus, M. *Chem. Rev.* **2018**, *118*, 5080.
253. Hamilton, D. S.; Nicewicz, D. A. *J. Am. Chem. Soc.* **2012**, *134*, 18577.
254. Grandjean, J. M. M.; Nicewicz, D. A. *Angew. Chem. Int. Ed.* **2013**, *52*, 3967.
255. Perkowski, A. J.; Nicewicz, D. A. *J. Am. Chem. Soc.* **2013**, *135*, 10334.
256. Nguyen, T. M.; Nicewicz, D. A. *J. Am. Chem. Soc.* **2013**, *135*, 9588.
257. Nguyen, T. M.; Manohar, N.; Nicewicz, D. A. *Angew. Chem. Int. Ed.* **2014**, *53*, 6198.
258. Wilger, D. J.; Grandjean, J. M. M.; Lammert, T. R.; Nicewicz, D. A. *Nat. Chem.* **2014**, *6*, 720.
259. Morse, P.; Nicewicz, D. *Abstracts of Papers of the American Chemical Society* **2014**, 248.
260. Gesmundo, N. J.; Grandjean, J. M. M.; Nicewicz, D. A. *Org. Lett.* **2015**, *17*, 1316.
261. Margrey, K. A.; McManus, J. B.; Bonazzi, S.; Zecri, F.; Nicewicz, D. A. *J. Am. Chem. Soc.* **2017**, *139*, 11288.

262. Joshi-Pangu, A.; Levesque, F.; Roth, H. G.; Oliver, S. F.; Campeau, L. C.; Nicewicz, D.; DiRocco, D. A. *J. Org. Chem.* **2016**, *81*, 7244.
263. Denmark, S. E.; Stiff, C. M. *J. Org. Chem.* **2000**, *65*, 5875.
264. Lin, K.; Wiles, R. J.; Kelly, C. B.; Davies, G. H. M.; Molander, G. A. *Acs Catal* **2017**, *7*, 5129.
265. Miyata, K.; Kutsuna, H.; Kawakami, S.; Kitamura, M. *Angew. Chem. Int. Ed.* **2011**, *50*, 4649.
266. Muthusamy, S.; Azhagan, D. *Eur. J. Org. Chem.* **2014**, 363.
267. Jimenez, J.; Ramirez, J.; Huelgas, G.; Melendrez, R.; Cabrera-Vivas, B. M.; Sansinenea, E.; Ortiz, A. *Tetrahedron* **2015**, *71*, 4590.
268. Guyon, C.; Duclos, M. C.; Sutter, M.; Metay, E.; Lemaire, M. *Org. Biomol. Chem.* **2015**, *13*, 7067.
269. Doi, R.; Abdullah, I.; Taniguchi, T.; Saito, N.; Sato, Y. *Chem. Commun. (Cambridge, U. K.)* **2017**, *53*, 7720.
270. Dudnik, A. S.; Schwier, T.; Gevorgyan, V. *Org. Lett.* **2008**, *10*, 1465.
271. Hatchard, C. G.; Parker, C. A. *Proc R Soc Lon Ser-A* **1956**, *235*, 518.
272. Cismesia, M. A.; Yoon, T. P. *Chem. Sci.* **2015**, *6*, 5426.
273. Beati, A. A. G. F.; Reis, R. M.; Rocha, R. S.; Lanza, M. R. V. *Ind. Eng. Chem. Res.* **2012**, *51*, 5367.
274. Pavlishchuk, V. V.; Addison, A. W. *Inorg. Chim. Acta* **2000**, *298*, 97.
275. Moser, W. H. *Tetrahedron* **2001**, *57*, 2065.
276. Sanchez, L.; Smith, A. B. *Org. Lett.* **2012**, *14*, 6314.

277. Brook, A. G. *Acc. Chem. Res.* **1974**, *7*, 77.
278. Lautens, M.; Delanghe, P. H. M.; Goh, J. B.; Zhang, C. H. *J. Org. Chem.* **1995**, *60*, 4213.
279. Brook, A. G.; Warner, C. M.; Limburg, W. W. *Can. J. Chem.* **1967**, *45*, 1231.
280. Leonori, D.; Aggarwal, V. K. *Acc. Chem. Res.* **2014**, *47*, 3174.
281. Rendler, S.; Oestreich, M. *Synthesis* **2005**, 1727.
282. Denmark, S. E.; Beutner, G. L. *Angew. Chem. Int. Ed.* **2008**, *47*, 1560.
283. Corriu, R. J. P. *Journal of Organometallic Chemistry* **1990**, *400*, 81.
284. Chuit, C.; Corriu, R. J. P.; Reye, C.; Young, J. C. *Chem. Rev.* **1993**, *93*, 1371.
285. Reich, H. J.; Olson, R. E.; Clark, M. C. *J. Am. Chem. Soc.* **1980**, *102*, 1423.
286. Takeda, K.; Fujisawa, M.; Makino, T.; Yoshii, E.; Yamaguchi, K. *J. Am. Chem. Soc.* **1993**, *115*, 9351.
287. Takeda, K.; Nakajima, A.; Yoshii, E. *Synlett* **1997**, 1997, 255.
288. Takeda, K.; Takeda, M.; Nakajima, A.; Yoshii, E. *J. Am. Chem. Soc.* **1995**, *117*, 6400.
289. Takeda, K.; Nakane, D.; Takeda, M. *Org. Lett.* **2000**, *2*, 1903.
290. Mattson, A. E.; Bharadwaj, A. R.; Scheidt, K. A. *J. Am. Chem. Soc.* **2004**, *126*, 2314.
291. Mattson, A. E.; Scheidt, K. A. *Org. Lett.* **2004**, *6*, 4363.
292. Mattson, A. E.; Bharadwaj, A. R.; Zuhl, A. M.; Scheidt, K. A. *J. Org. Chem.* **2006**, *71*, 5715.
293. Wright, A.; West, R. *J. Am. Chem. Soc.* **1974**, *96*, 3214.
294. Cossrow, J.; Rychnovsky, S. D. *Org. Lett.* **2002**, *4*, 147.
295. Kim, A. I.; Kimmel, K. L.; Romero, A.; Smitrovich, J. H.; Woerpel, K. A. *J. Org. Chem.* **2007**, *72*, 6595.

296. Gandhamsetty, N.; Jee, S.; Chang, S. *Eur. J. Org. Chem.* **2017**, 933.
297. Curran, D. P.; Gothe, S. A. *Tetrahedron* **1988**, *44*, 3945.
298. Cunico, R. F.; Zaporowski, L. F.; Rogers, M. J. *J. Org. Chem.* **1999**, *64*, 9307.
299. Romero, A.; Woerpel, K. A. *Org. Lett.* **2006**, *8*, 2127.
300. Nakazaki, A.; Nakai, T.; Tomooka, K. *Angew. Chem. Int. Ed.* **2006**, *45*, 2235.
301. Kagoshima, H.; Yonezawa, K. *Synth. Commun.* **2006**, *36*, 2427.
302. Brekan, J. A.; Chernyak, D.; White, K. L.; Scheidt, K. A. *Chem. Sci.* **2012**, *3*, 1205.
303. Mita, T.; Higuchi, Y.; Sato, Y. *Org. Lett.* **2014**, *16*, 14.
304. Barham, J. P.; Coulthard, G.; Emery, K. J.; Doni, E.; Cumine, F.; Nocera, G.; John, M. P.; Berlouis, L. E. A.; McGuire, T.; Tuttle, T.; Murphy, J. A. *J. Am. Chem. Soc.* **2016**, *138*, 7402.
305. Foley, J. K.; Korzeniewski, C.; Pons, S. *Canadian Journal of Chemistry-Revue Canadienne De Chimie* **1988**, *66*, 201.
306. Cao, W.; Tan, D.; Lee, R.; Tan, C.-H. *J. Am. Chem. Soc.* **2018**, *140*, 1952.
307. Brook, A. G.; Pascoe, J. D. *J. Am. Chem. Soc.* **1971**, *93*, 6224.
308. Nyce, G. W.; Lamboy, J. A.; Connor, E. F.; Waymouth, R. M.; Hedrick, J. L. *Org. Lett.* **2002**, *4*, 3587.
309. Singh, R.; Kissling, R. M.; Letellier, M. A.; Nolan, S. P. *J. Org. Chem.* **2004**, *69*, 209.
310. Kano, T.; Sasaki, K.; Maruoka, K. *Org. Lett.* **2005**, *7*, 1347.
311. Zhang, H. J.; Priebbenow, D. L.; Bolm, C. *Chem. Soc. Rev.* **2013**, *42*, 8540.
312. Brook, A. G.; Duff, J. M. *J. Am. Chem. Soc.* **1967**, *89*, 454.
313. Duff, J. M.; Brook, A. G. *Canadian Journal of Chemistry-Revue Canadienne De Chimie* **1973**, *51*, 2869.

314. Zhang, H. J.; Becker, P.; Huang, H.; Pirwerdjan, R.; Pan, F. F.; Bolm, C. *Adv. Synth. Catal.* **2012**, *354*, 2157.
315. Becker, P.; Priebbenow, D. L.; Zhang, H. J.; Pirwerdjan, R.; Bolm, C. *J. Org. Chem.* **2014**, *79*, 814.
316. Becker, P.; Priebbenow, D. L.; Pirwerdjan, R.; Bolm, C. *Angew. Chem. Int. Ed.* **2014**, *53*, 269.
317. Becker, P.; Pirwerdjan, R.; Bolm, C. *Angew. Chem. Int. Ed.* **2015**, *54*, 15493.
318. Bourque, R. A.; Davis, P. D.; Dalton, J. C. *J. Am. Chem. Soc.* **1981**, *103*, 697.
319. Dalton, J. C.; Bourque, R. A. *J. Am. Chem. Soc.* **1981**, *103*, 699.
320. Turro, N. J.; Dalton, J. C.; Dawes, K.; Farrington, G.; Hautala, R.; Morton, D.; Niemczyk, M.; Schore, N. *Acc. Chem. Res.* **1972**, *5*, 92.
321. Yang, N. C.; Man Him, H.; Shold, D. M.; Turro, N. J.; Hautala, R. R.; Dawes, K.; Dalton, J. C. *J. Am. Chem. Soc.* **1977**, *99*, 3023.
322. Yoon, U. C.; Oh, S. W.; Lee, S. M.; Cho, S. J.; Gamlin, J.; Mariano, P. S. *J. Org. Chem.* **1999**, *64*, 4411.
323. von Sonntag, J.; Knolle, W.; Naumov, S.; Mehnert, R. *Chem. - Eur. J.* **2002**, *8*, 4199.
324. Cunico, R. F. *Tetrahedron Lett.* **2001**, *42*, 2931.
325. Chen, J. X.; Cunico, R. F. *Tetrahedron Lett.* **2002**, *43*, 8595.
326. Cunico, R. F. *Tetrahedron Lett.* **2002**, *43*, 355.
327. Cunico, R. F.; Maity, M. C. *Org. Lett.* **2002**, *4*, 4357.
328. Chen, H. X.; Cunico, R. F. *Tetrahedron Lett.* **2003**, *44*, 8025.
329. Cunico, R. F.; Maity, B. C. *Org. Lett.* **2003**, *5*, 4947.

330. Cunico, R. F.; Pandey, R. K. *J. Org. Chem.* **2005**, *70*, 9048.
331. Cunico, R. F.; Motta, A. R. *Org. Lett.* **2005**, *7*, 771.
332. Fischer, C.; Fu, G. C. *J. Am. Chem. Soc.* **2005**, *127*, 4594.
333. Cherney, A. H.; Kadunce, N. T.; Reisman, S. E. *J. Am. Chem. Soc.* **2013**, *135*, 7442.
334. Tasker, S. Z.; Standley, E. A.; Jamison, T. F. *Nature* **2014**, *509*, 299.
335. Yamada, K.; Harwood, S. J.; Groger, H.; Shibasaki, M. *Angew. Chem. Int. Ed.* **1999**, *38*, 3504.
336. Lee, K. Y.; Lee, C. G.; Kim, J. N. *Tetrahedron Lett.* **2003**, *44*, 1231.
337. Vyas, D. J.; Fröhlich, R.; Oestreich, M. *Org. Lett.* **2011**, *13*, 2094.
338. Brekan, J. A.; Chernyak, D.; White, K. L.; Scheidt, K. A. *Chem. Sci.* **2012**, *3*, 1205.
339. Ryan, S. J.; Schimler, S. D.; Bland, D. C.; Sanford, M. S. *Org. Lett.* **2015**, *17*, 1866.
340. Enders, D.; Breuer, K.; Kallfass, U.; Balensiefer, T. *Synthesis* **2003**, 1292.
341. Shintani, R.; Duan, W.-L.; Hayashi, T. *J. Am. Chem. Soc.* **2006**, *128*, 5628.
342. Nguyen, T. B.; Sorres, J.; Tran, M. Q.; Ermolenko, L.; Al-Mourabit, A. *Org. Lett.* **2012**, *14*, 3202.
343. Nakamura, D.; Kakiuchi, K.; Koga, K.; Shirai, R. *Org. Lett.* **2006**, *8*, 6139.